

# **BASS STRAIT OIL COMPANY LTD**



## **MOBY-1 WELL COMPLETION REPORT**

---

## **INTERPRETIVE DATA**

---

**OCTOBER 2005**

VOLUME 1 OF 1

This Page is Left Blank Intentionally



**MOBY-1**

**WELL COMPLETION REPORT**

VOLUME 1 OF 1

(INTERPRETIVE DATA)

Vic/P47  
GIPPSLAND BASIN

OFFSHORE  
VICTORIA

Date: October 2005  
Compiled by: R. Fisher  
Reviewed by: Ian Reid

Controlled Copy No: \_\_\_\_\_

This Page is Left Blank Intentionally

## TABLE OF CONTENTS

### Volume 1 of 1

<b>1.1</b>	<b>INTRODUCTION AND SUMMARY .....</b>	<b>1</b>
<b>1.2</b>	<b>Geological and Formation Evaluation Summary .....</b>	<b>5</b>
1.2.1	Prospect Summary .....	5
1.2.2	Geological and Formation Evaluation Summary .....	5
<b>1.3</b>	<b>Drilling Summary .....</b>	<b>8</b>
<b>2.</b>	<b>WELL HISTORY .....</b>	<b>10</b>
<b>2.1</b>	<b>Well Data Summary .....</b>	<b>10</b>
<b>2.2</b>	<b>Operations Summary .....</b>	<b>11</b>
<b>3.</b>	<b>GEOLOGY .....</b>	<b>12</b>
<b>3.1</b>	<b>Summary of Previous Exploration .....</b>	<b>12</b>
3.1.1	Seismic Data .....	12
3.1.2	Well Data .....	14
<b>3.2</b>	<b>Regional Structure and Geology .....</b>	<b>15</b>
3.2.1	Geological Evolution .....	15
3.2.2	Tectonic History .....	15
<b>3.3</b>	<b>Stratigraphy .....</b>	<b>19</b>
3.3.1	Gippsland Limestone Seafloor – 510.4mMD RT (53-488.9mTVDSS) .....	20
3.3.2	Lakes Entrance Formation 510.4 – 553.0mMD RT (488.9 – 531.5mTVDSS) .....	21
3.3.3	‘Early Oligocene Wedge’ (EOW) 553 – 555.5mMD RT (531.5- 534mTVDSS) .....	22
3.3.4	Gurnard Formation 555.5 – 587mMD RT (534 – 565.5mTVDSS) .....	22
3.3.5	Kingfish Formation 587 – 589.5mMD RT (565.5 - 568mTVDSS) .....	24
3.3.6	Strzelecki Group 589.5 – 660mMDRT (568 – 638.5mTVDSS) .....	25
<b>3.4</b>	<b>Structure and Seal .....</b>	<b>26</b>
<b>3.5</b>	<b>Source and Migration .....</b>	<b>30</b>
<b>3.6</b>	<b>Relevance to the Occurrence of Hydrocarbons .....</b>	<b>30</b>
3.6.1	Gas Readings .....	30
3.6.2	Hydrocarbon Shows Recorded in Ditch Cuttings .....	31
3.6.3	Hydrocarbon Shows recorded in Sidewall Core Samples .....	31
<b>3.7</b>	<b>Formation Evaluation .....</b>	<b>32</b>
3.7.1	Borehole Temperature Data .....	32
3.7.2	Wireline Testing .....	36
3.7.3	DST Testing .....	36
3.7.4	Porosity, Permeability and Formation Fluids .....	38
3.7.5	Geochemical Analysis .....	41
<b>3.8</b>	<b>Conclusions and Contributions To Geological Knowledge .....</b>	<b>43</b>
<b>4.</b>	<b>REFERENCES .....</b>	<b>43</b>

## Volume 1 of 1 (Continued)

### TABLES

<i>Table 1: Moby-1 Stratigraphic Table.</i> .....	19
<i>Table 2. Summary of Gas Readings Recorded for All Lithology Intervals</i> .....	31
<i>Table 3: Hydrocarbon Shows Recorded in Sidewall Core Samples</i> .....	32

### FIGURES:

<i>Figure-1 VIC/P47 Location Map</i> .....	2
<i>Figure 2 Moby-1 Location Map</i> .....	3
<i>Figure 3 Tectonic Elements map (modified after Wong D., Bernecker T. &amp; Moore D., 2001.)</i> .....	4
<i>Figure 4 Generalised Stratigraphic Column of the gippsland basin (after Bernecker, T., Thomas, H. &amp; Driscoll, J., 2003.</i> .....	18
<i>Figure 5 Post-Drill Structural Interpretation of Moby Fault Block</i> .....	28
<i>Figure 6 Seismic Inline 601 Displaying Post-Drill Interpretation</i> .....	29
<i>Figure 7 Horner Extrapolated BHT</i> .....	34
<i>Figure 8 Geothermal Gradient Plot</i> .....	35
<i>Figure 9: RCI Plot of Pressure Data in Moby-1</i> .....	37
<i>Figure 10: Image of Very Fine Grained Lithic Arkose typical of Gurnard Formation; SWC-11 from 575.7mMD</i> .....	38
<i>Figure 11: SEM of SWC-11 showing details of fine grain size of Lithic Arkose lithology in Gurnard Formation and development of chlorite and smectite blocking pore throats and reducing permeability.</i> .....	39

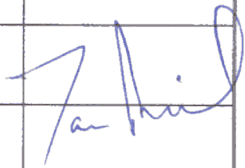
### APPENDICES:

<i>Appendix 1</i>	<i>Well Card (Bass Strait Oil Company Limited)</i>
<i>Appendix 2</i>	<i>Petrophysical Report – (The Saros Group Pty Ltd)</i>
<i>Appendix 3</i>	<i>Palynology Report: Sample Interval- 538-630m. – (Dr Alan Partridge)</i>
<i>Appendix 4</i>	<i>Petrographic Analysis of Six samples selected from the Well Moby-1 – (Core Laboratories Australia Pty Ltd.)</i>
<i>Appendix 5</i>	<i>RCI Analysis: Pressure, Mobility and Gradient Report for Well Moby-1 – (Baker Atlas Geoscience)</i>
<i>Appendix 6</i>	<i>Hydrocarbon Characterization Study: Moby-1 (GeoTechnical Services Pty Ltd)</i>

### ENCLOSURES:

<i>Enclosure 1</i>	<i>Composite Well Log (1:500 Scale)</i>
<i>Enclosure 2</i>	<i>Petrophysical Summary Plot (1:200 Scale)</i>

<b>DOCUMENT NO.:</b>	BAS_WCR_001
<b>TITLE:</b>	BASS STRAIT OIL COMPANY LTD WELL COMPLETION REPORT FOR MOBY-1 (VIC/P47) <i>INTERPRETIVE DATA</i>

DOCUMENT REVISION RECORD					
Rev. No.	Date	Description	Prepared	Reviewed	Approved
0	July 2005	Well Completion Report- Interpretive Data	R Fisher	I. Reid	
1	October 2005	Well Completion Report- Interpretive Data	R. Fisher	I. Reid	

CONTROLLED DISTRIBUTION LIST	
Copy No.	Recipient
001	Bass Strait Oil Company Ltd: Ian Reid – General Manager - Exploration (Melbourne, Vic) Hard Copy + CD
002	Eagle Bay Resources NL: Tony Rechner – Director (Perth, WA) Hard Copy + CD
003	Moby Oil & Gas Limited: Geoffrey Albers – Chairman (Melbourne, Vic) Hard Copy + CD
004	Labrador Petro-Management Pty Ltd: Tom Brand -Project Advisor (Perth, WA) Hard Copy + CD
005	Victorian Department of Primary Industries; Minerals & Petroleum Division: Kourosh Mehin - Manager, Petroleum Resources (Melbourne, Vic) CD Only
006	GeoScience Australia: Trevor Powell – Chief Petroleum & Marine Division (Canberra, ACT) CD Only

## 1.1 INTRODUCTION AND SUMMARY

The Moby-1 well is located in Commonwealth waters within Permit Vic/P47 approximately 350km east of Port Melbourne (Figure 1) and 5 km east of the Patricia/Baleen producing gas field. This location is covered by the SJ 55 1:1,000,000 Melbourne Map Sheet; Graticular Block 1783. Vic/P47 is located offshore on the northern margin of the Gippsland Basin straddling the Northern Platform and Northern Terrace. The southern or 'neck' portion of the permit that incorporates Moby-1 lies to the south of the Lake Wellington Fault System that separates the Northern Platform from the Northern Terrace.

The Moby-1 well was designed to test the Moby Prospect, primarily to target a seismic amplitude anomaly identified on the Baleen 3D survey, interpreted to represent gas within reservoirs of the Gurnard Formation. Although the Moby Prospect is located on a significant anticline with over 70km<sup>2</sup> areal closure, the structure had previously been drilled by Flathead-1 and Whale-1 in a crestal location and which both failed to encounter suitable reservoirs within the Gurnard Formation. It was anticipated that Moby-1 would encounter improved reservoir development in a downdip location.

Moby-1 was drilled in 53 metres (174') (MSL) of water by the DOGC 'Ocean Patriot' semi-submersible drilling unit and spudded on the 7<sup>th</sup> October 2004 at 16:45 hrs. The well reached a total depth of 660 m MD on the 11<sup>th</sup> October 2004 at 20:30 hrs in the Early Cretaceous Strzelecki Group. Wireline logs were acquired at this depth and the well was subsequently plugged and abandoned as a new field gas discovery in the Gurnard Formation and the rig released at 13:00 hrs 17th October 2004. There were no lost time accidents and no environmental accidents during the drilling of Moby-1.

The Well Card (Appendix 1) summarises pertinent data from the Moby-1 well.

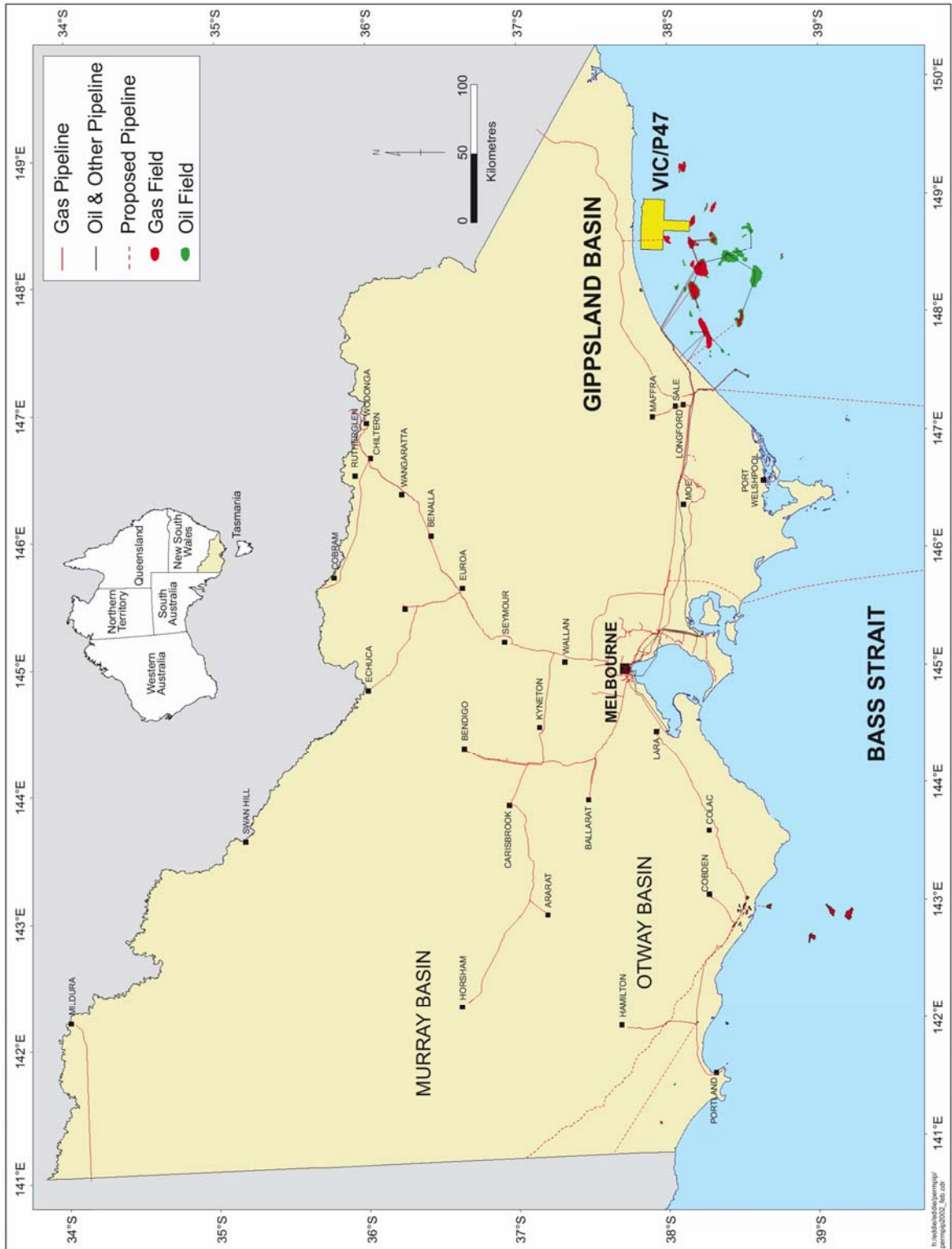


FIGURE-1 VIC/P47 LOCATION MAP

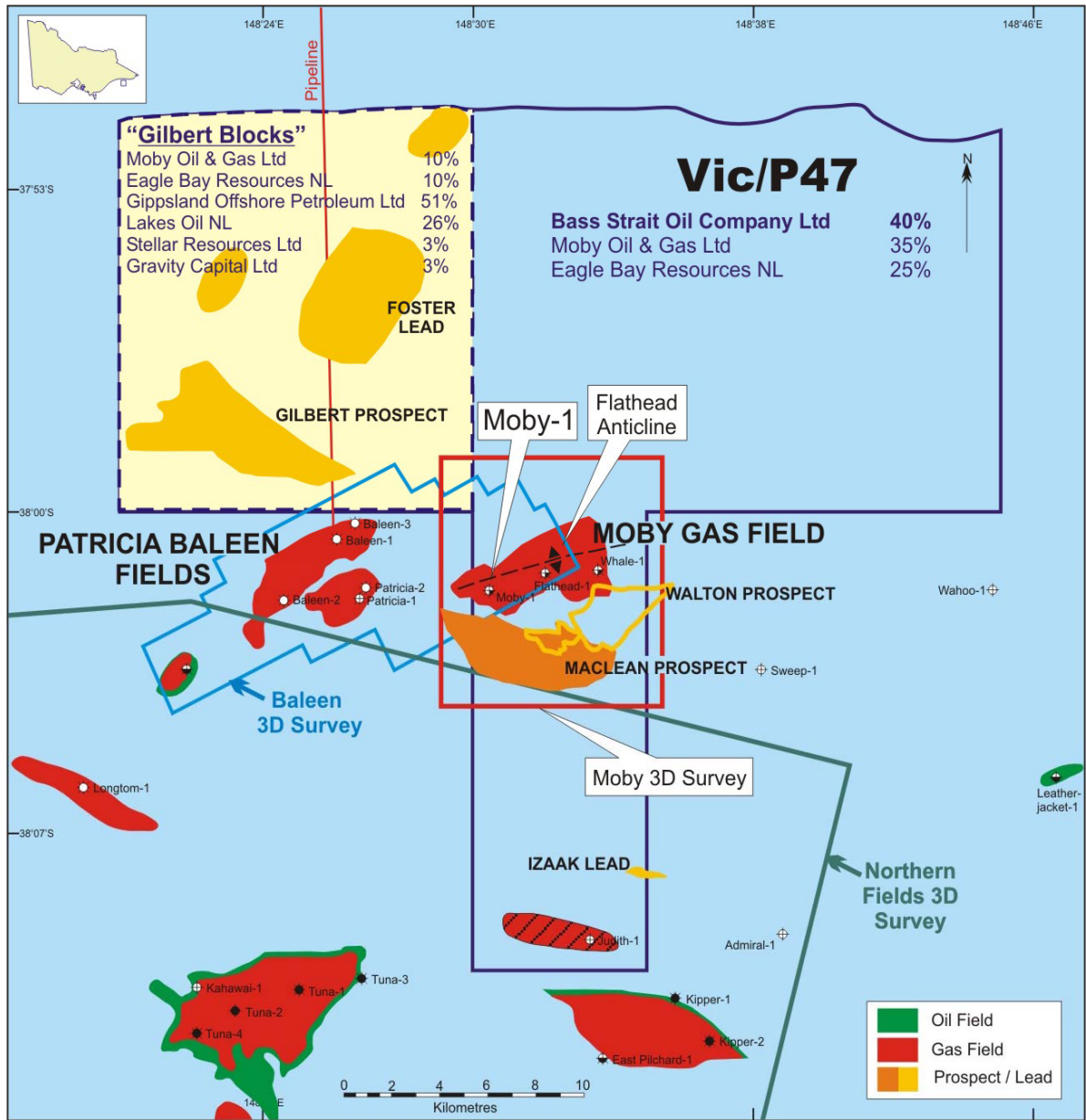
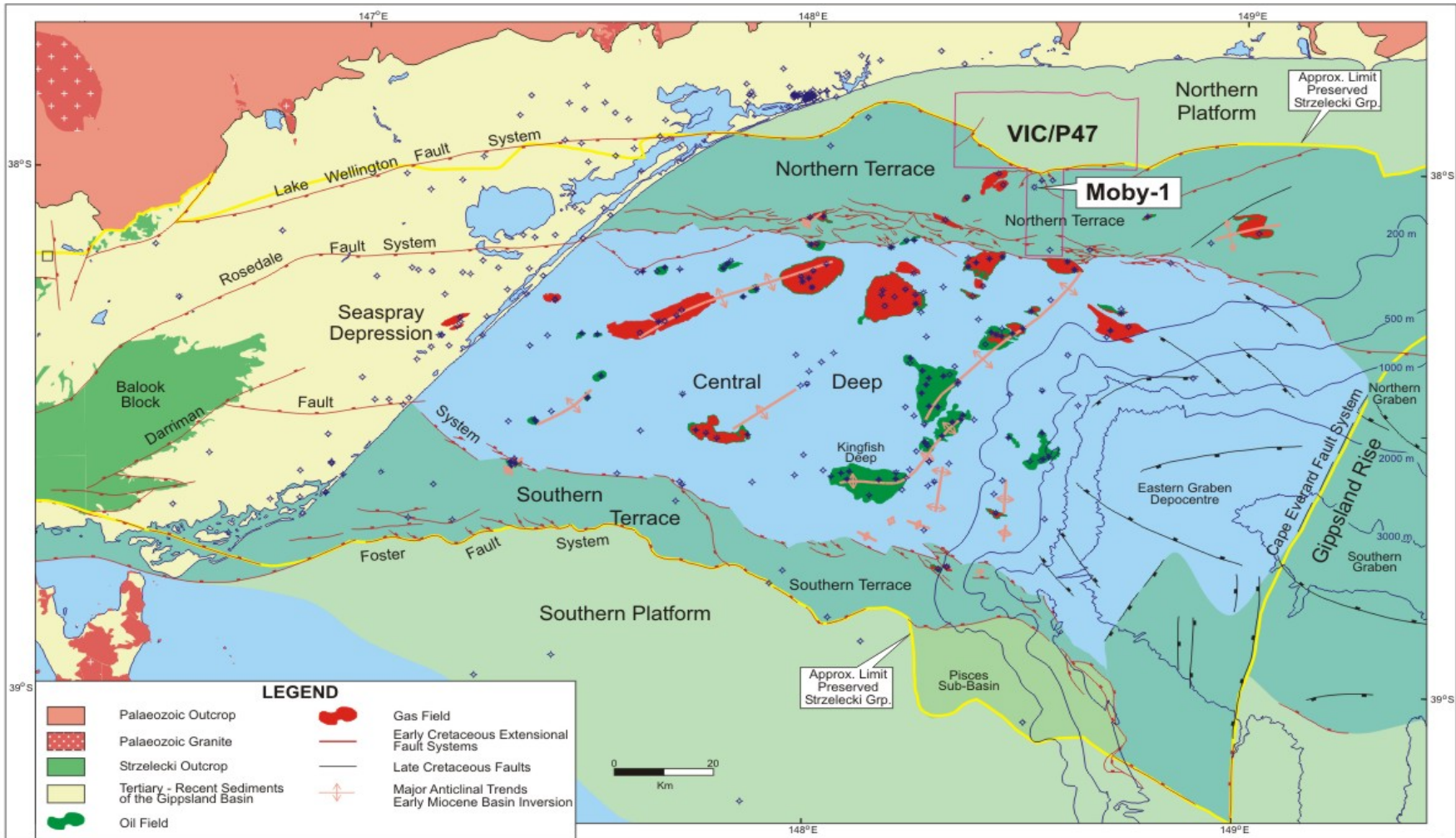


FIGURE 2 MOBY-1 LOCATION MAP



After Woollands & Wong (Eds), 2001

FIGURE 3 TECTONIC ELEMENTS MAP (MODIFIED AFTER WONG D., BERNECKER T. & MOORE D., 2001.)

## 1.2 GEOLOGICAL AND FORMATION EVALUATION SUMMARY

### 1.2.1 Prospect Summary

The Moby-1 exploration well is located at CDP 4403 on the Baleen 3D INLINE 601 and proposed to be drilled to a Projected Total Depth of 603 metres TVD subsea. The Moby-1 well was designed to test the Moby Prospect, primarily to target the seismic amplitude anomaly identified on the Baleen 3D survey, interpreted to represent gas within reservoirs of the Gurnard Formation. Although the Moby Prospect is present on a significant anticline with over 70km<sup>2</sup> areal closure, the structure was previously drilled in a crestal location by Flathead-1 and Whale-1 which both failed to encounter suitable reservoirs within the Gurnard Formation. Better reservoir development was interpreted from well and seismic data to exist downdip at the Moby-1 location.

Pre-drill evaluation of Moby-1 identified key geological issues relating to the economic success of Moby-1 as being reservoir quality and gas composition. Gas was likely, although an oil leg may also have occurred. Oil quality was perceived as potentially being too poor for economic flow rates to exist.

The reservoir quality at the crest of the structure at Flathead-1 was very poor within the Gurnard Formation (where excellent gas shows suggest it is part of the downdip accumulation) with only minor fine grained sandstones and siltstones. Within the Kingfish Formation, 6m of coarse sandstones were encountered with good oil shows. It is not known if this oil is live or residual and if these sandstones are in communication with the Barracouta or Gurnard formations downdip at the Moby-1 location. Oil extracted from core at Flathead-1 was severely biodegraded and quality and likely flow rates posed a risk for any oil development on Moby.

The well was a test of a seismic amplitude anomaly at top Gurnard Formation reservoir level (outside of the area of a small four-way dip closure to the west) to ensure that the broader Moby Structure entrapment mechanism can be shown to be valid. It was designed to test the hydrocarbon saturation and nature of the amplitude anomaly and to confirm that it was not 'fizz gas'. It was also designed to determine reservoir quality in the Gurnard Formation, the underlying Latrobe Group Kingfish Formation and the upper part of the Strzelecki Group. It was designed to determine if potential seals exist between Gurnard Formation, Kingfish Formation and Strzelecki Group reservoirs and whether any gas pay in the Gurnard is in communication with the Kingfish Formation.

Gas and any oil pay was to be sampled for analysis to determine composition and economic value. The well was sited so as to intersect the gas-fluid contact interpreted from seismic and hence an oil leg within the Gurnard Formation. Any oil pay in the Latrobe or Strzelecki groups was to be identified and sampled to determine if a larger oil accumulation exists in communication with the oil encountered in Flathead-1. Oil quality posed a risk as it was most likely biodegraded and productive flow rates may not occur.

### 1.2.2 Geological and Formation Evaluation Summary

Moby-1 was spudded at 16:45 Hrs 7<sup>th</sup> October 2004 and penetrated a sedimentary section ranging in age from Tertiary to Late Cretaceous. The stratigraphic section encountered was

essentially as predicted with all of the formation tops slightly high to prognosis. The geological formations and data encountered for each hole section are discussed below.

The Miocene to Pliocene Gippsland Limestone was encountered at seafloor (possibly covered by a veneer of Recent sediments) at 74.5mMD RT (53mTVDSS), the upper part of which down to a depth of 325mMD RT was drilled riserless in the 914mm (36") and 445mm (17 1/2") hole sections. Intermediate 340mm (13 3/8") casing was subsequently run to 321.8mMD RT and the BOP's and marine riser nipped up, below which 311mm (12 1/4") hole was drilled to 328mMD RT and 216mm (8 1/2") hole was drilled to total depth at 660mMD RT (638.5mTVDSS). The main hole sections to total depth were logged with the benefit of wireline logs after reaching TD and which provide the depth control for the stratigraphic sub-divisions included herein, together with the assistance of biostratigraphic control.

The lower part of the Gippsland Limestone below 325mMD RT consists of argillaceous calcilutite with minor calcarenite and argillaceous calcisiltite. The base Gippsland Limestone/Top Lakes Entrance Formation is identified at 510.4mMD RT (-488.9mTVDSS). It was encountered 63.9 metres low to prognosis, based upon the appearance of marl in the section. The Oligocene to early Miocene Lakes Entrance Formation consists of marl grading to and interbedded with argillaceous calcilutite, calcilutite and calcareous claystone. The basal part of the Lakes Entrance Formation is differentiated at 553mMD RT (-531.5mTVDSS) and defined herein as the Early Oligocene Wedge.

The primary objective Middle to Late Eocene Gurnard Formation was intersected at 555.5mMD RT (534mTVDSS), 16m high to prediction and consists of argillaceous and silty sandstone, siltstone with minor greensand and claystone. All lithologies are generally rich in glauconite. The Early Eocene Kingfish Formation was intersected at 587mMD RT (565.5mTVDSS), 9.5m high to prognosis. The interval which is only 2.5m thick and consists of feldspathic lithic sandstone, rests unconformably on the Early Cretaceous (Late Albian) Strzelecki Group at 589.5mMD RT (568.0mTVDSS), 17m high to prognosis. The Strzelecki Group consists predominantly of argillaceous lithic sandstone.

The well reached TD within the Strzelecki Group at 660mMD RT (-638.5mTVDSS), which was reached at 20:34 Hrs 11<sup>th</sup> October 2004. This is 35 metres below the originally programmed total depth of the well. BakerAtlas wireline logs were run at this depth. The primary wireline log recorded was the DLL-MLL-MAC-DSL-ZDL-CN-TTRM-4401 which was logged from 659 metres to 321.5 metres, after which the GR-MAC were logged up through casing to the seafloor. This log represents the primary depth control for Moby-1. TD was shallow to driller's TD by 1m owing to possible fill on bottom and the 340mm (13 3/8") casing shoe was found 0.25m shallower than driller's depth. The second logging run was with the RCI-GR tool for formation pressures and samples and which was logged from 613 metres to 558.5 metres MD after being tied into the first logging run for depth control. A total of 40 pre-test levels were attempted for formation pressures which included thirteen (13) repeat tests and four (4) tests were tight. Also collected two (2) gas samples at 568.8m within the Gurnard Formation and one (1) formation water sample with a scum of oil was collected at 588.5mMD RT from the Kingfish Formation.

The third run in the hole was for a VSP/checkshot survey with the SLR tool across the interval 650-90 metres and the fourth run was to acquire percussion sidewall cores (SWC-GR). Twenty five (25) shots attempted and 25 cores were successfully recovered (100%).

Trace to minor amounts of total gas consisting entirely of methane (C<sub>1</sub>) were recorded upon commencement of first drilling returns in the 311mm (12 ¼") hole section below 325mMD RT and which continued in the 216mm (8 ½") hole section. Trace amounts of ethane (C<sub>2</sub>), pentane (C<sub>3</sub>), iso-butane (iC<sub>4</sub>) and n-butane (nC<sub>4</sub>) were recorded below approximately 468mMD RT. Background gas levels increased slightly below 515mMD RT, increasing further to low to moderate levels of methane (C<sub>1</sub>) and ethane (C<sub>2</sub>) and continuing trace C<sub>3</sub> to C<sub>5</sub> below 556mMD RT. The maximum total gas recorded was 1.64% at 570mMD RT, consisting of 18,184ppm C<sub>1</sub>, 178ppm C<sub>2</sub>, 23ppm C<sub>3</sub>, 6ppm iC<sub>4</sub>, 4ppm nC<sub>4</sub> and 5ppm iC<sub>5</sub> and 3ppm nC<sub>5</sub>. Background levels remained moderately uniform to 587mMD RT, decreasing progressively below this depth to TD.

Sandstone cuttings over the gross interval 562–574mMD RT exhibited 5-20% dull – moderately bright yellow fluorescence, with a slow to moderately fast blue-white cut and solid blue-white ring residue. At 568–571mMD RT, fluorescence increased to 60% dull to moderately bright yellow fluorescence, with an instantaneous blue-white cut and a solid blue-white residue. Nil to trace fluorescence only occurred below 574mMD RT. Weak to moderate fluorescence was exhibited in eleven sidewall core samples over the gross interval 555.9-586mMD RT, entirely within the Gurnard Formation.

Log evaluation, analysis of the RCI pressure and sampling data and core analysis confirms the likely presence of a 21m gross column of gas within the Gurnard Formation, with an estimated free water level at approximately 555mTVDSS. Core measured porosities through the Gurnard Formation average 36.8% (31.6-39.2%), while measured permeabilities are in the range of 102-1850md (average 543 md). These latter figures are some 30% higher than those recorded from petrographic analyses and do not reconcile with the low mobilities observed with the RCI tool and with the general log response expected from gas-filled sands of such high permeability and porosity.

Moby-1 was plugged and abandoned as a new field gas discovery and the rig released at 13:00 hrs 17<sup>th</sup> October 2004. A composite well log of the lithology and biostratigraphy intersected in Moby-1 is included as Enclosure 1, while a petrophysical summary plot is included as Enclosure 2.

### 1.3 DRILLING SUMMARY

The Diamond Offshore General Company MODU “Ocean Patriot” was mobilised from the TAP Oil Tawatawa-1 location off the east coast of New Zealand and towed across the Tasman Sea by two AHSV’s (Far Grip & Pacific Wrangler). Moby-1 operations commenced at 02:45 Hrs 5<sup>th</sup> October 2004 when the first anchor was dropped at the Moby-1 location. Anchor handling operations were delayed by bad weather, while additional delays were caused by having to re-run a number of anchors. Positioning the rig on location was completed by 05:30 Hrs 7<sup>th</sup> October 2004 at which time the rig was ballasted down to drilling draft. The final location for Moby-1 was confirmed as being 2.4m from the proposed location on a bearing of 270.28<sup>o</sup> True. The final fix for Moby-1 was:

Latitude: 38<sup>o</sup> 01’ 44.25” S  
Longitude: 148<sup>o</sup> 30’ 27.40” E  
Easting: 632, 316.41m  
Northing: 5, 789, 884.86m  
DATUM: AGD 66.

The TGB was run and landed at 74.5mMD RT. Made up 914mm (36”) BHA and ran in hole with ROV assisting through TGB and tagged seafloor at 74.5m corrected to Mean Sea Level (MSL). The water depth at Mean Sea Level was recorded as 53.0m, with a drill floor elevation of 21.5m. The well was spudded at 16:45 Hrs 7<sup>th</sup> October 2004 with a 914mm (36”) hole drilled from seafloor (74.5mMD RT) to a depth of 101mMD RT, pumping 50 bbl gel sweeps every 9m. Ran 762mm (30”) casing and cemented with 758.8 sacks (160.8 bbl), cement slurry at 15.8 ppg.

Made up 445mm (17 ½”) BHA and installed guide ropes to BHA and guide lines. Ran in hole and tagged cement at 96.7mMD RT. Drilled cement and casing shoe from 96.7mMD RT to 98mMD RT and continued drilling to 325mMD RT, pumping 40 bbl guar gum sweeps every 15m and 50 bbl gel sweeps before very connection. Pumped 100 bbl hi-vis sweep at 1100gpm and conducted wiper trip to 762mm (30”) casing shoe. Took weight at 315mMD RT and reamed back to 325mMD RT. Circulated bottoms up at 1100 gpm and displaced hole to 350 bbl hi-vis mud. Dropped single shot survey tool and pulled out of hole to 203mMD RT. Recovered survey tool and continued pulling out of hole, jetting 762mm (30”) housing on the way out of hole.

Ran 340mm (13 ⅜”) casing to 321.8mMD RT and cemented with 140 bbls (295 sacks) of 12.5 ppg Class G Lead cement followed by 71 bbls (335 sacks) of 15.8 ppg Class G Tail cement. Displaced cement with 116 bbls of seawater. Bumped plugs and pressure tested casing to 2000 psi. Observed returns to seabed throughout cementing. Ran BOP’s while testing choke and kill lines to 300 psi for 5 minutes and 3000 psi for 10 minutes and marine riser. Landed BOP’s and pressure tested wellhead connection to 300 psi for 5 minutes and 3000 psi for 10 minutes.

Made up 311mm (12 ¼”) bit and ran in hole. Washed down from 286mMD RT and tagged top of cement at 295.5mMD RT. Drilled plugs, cement and shoe track and cleaned rat hole to 325mMD RT. Drilled ahead in 311mm (12 ¼”) hole from 325m to 328mMD RT. Displaced well to 10 ppg KCL/Polymer mud system, displacing choke and kill lines. Pressure tested lines to 1000 psi and performed FIT to 1.7 SG (14.16 ppg), OK. Pulled out of hole laying down 311mm (12 ¼”) BHA.

Made up 216mm (8 ½”) BHA and ran in hole to 328mMD RT and drilled ahead to 660mMD RT (TD), taking Anderdrift survey every connection. Circulated hole clean and dropped multi-shot and pulled out of hole from 660m to 248mMD RT, working tight spots between 612m and 560mMD RT. Finished pulling out of hole and retrieved EMS tool.

Rigged up BakerAtlas for running wireline logs and ran the following logs; RUN#1: DLL-MLL-MAC-ZDL-CNL-DSL-TTRM over the interval 659-321.5m with GR-MAC through casing to 75mMD RT; RUN#2: RCI-GR over the interval 558.3-612.8m for pressures and samples; RUN#3: SLR-GR (VSP survey) over the interval 659-80m and RUN#4: SWC-GR over the interval 651.5-538m; shot 25 cores, recovered 25 cores; rigged down BakerAtlas.

Commenced plug and abandonment operations at 22:30 Hrs 13th October 2004. Picked up and ran in hole with 73mm (2 7/8") tubing cement stinger on 127mm (5") drill pipe to 650mMD RT and pumped 42.8 bbls of 15.8 ppg Class G cement slurry setting Plug#1 from 660mMD RT to 505mMD RT. Pulled out of hole to 370mMD RT and pumped 43 bbls of 15.8 ppg Class G cement slurry setting Plug#2 from 370mMD RT to 270mMD RT. Ran in hole with 127mm (5") open ended drill pipe and tagged top of cement Plug#2 at 259mMD RT. Pressure tested casing against lower annular to 500 psi, OK. Picked up 340mm (13 3/8") cement retainer and ran in hole to 160mMD RT and set same. Pumped 30 bbls of 15.8 ppg Class G cement slurry, setting cement Plug#3 from 160m to 100mMD RT.

Picked up wellhead jetting tool and wear bushing retrieval tool and ran in hole to 74m while jetting stack and wellhead. Landed out wear bushing retrieval tool and pulled out of hole. Pulled riser and BOP's and secured same. Picked up 508mm x 762mm (20" x 30") spear and cutting assembly and ran in hole stabbing into 18 3/4" wellhead and cut 508mm (20") casing at 77.39mMD RT and pulled out of hole with casing cut-off stub and housing. Re-dressed spear and RIH, stabbing into 762mm (30") housing, cutting 762mm (30") casing at 76.84mMD RT.

Commenced anchor handling operations at 18:00 Hrs 16<sup>th</sup> October 2004. Last anchor racked at 13:00 Hrs 17<sup>th</sup> October 2004 and the rig was released to Santos. Total time on Moby-1 location was 12.427 days.

A more comprehensive summary of the drilling may be found in the Moby-1 Well Completion Report –Basic Data issued under separate cover.

## 2. WELL HISTORY

### 2.1 WELL DATA SUMMARY

<b>Well Name</b>	Moby-1										
<b>Operator</b>	Bass Strait Oil Company Ltd Bass Strait Oil Company Ltd. (40%)										
<b>Equity Partners</b>	Eagle Bay Resources NL (25%) Moby Oil & Gas Limited (35%)										
<b>Permit</b>	Vic/P47										
<b>Basin</b>	Gippsland Basin										
<b>Type of Well</b>	Exploration										
<b>Well Status</b>	Plugged & Abandoned as New Field Gas Discovery										
<b>Surface Well Location</b>	<table> <tr> <td><b>Easting</b></td> <td>632316.41m E</td> </tr> <tr> <td><b>Northing</b></td> <td>5,789,884.86m N</td> </tr> <tr> <td><b>Latitude</b></td> <td>38° 01' 44.25" S</td> </tr> <tr> <td><b>Longitude</b></td> <td>148° 30' 27.40" E</td> </tr> <tr> <td><b>Datum</b></td> <td>AGD 66</td> </tr> </table>	<b>Easting</b>	632316.41m E	<b>Northing</b>	5,789,884.86m N	<b>Latitude</b>	38° 01' 44.25" S	<b>Longitude</b>	148° 30' 27.40" E	<b>Datum</b>	AGD 66
<b>Easting</b>	632316.41m E										
<b>Northing</b>	5,789,884.86m N										
<b>Latitude</b>	38° 01' 44.25" S										
<b>Longitude</b>	148° 30' 27.40" E										
<b>Datum</b>	AGD 66										
<b>Map Reference</b>	SJ 55 1:1,000,000 Melbourne Map Sheet; Graticular Block 1783										
<b>Objectives</b>	<table> <tr> <td><i>Primary</i></td> <td>Gurnard Formation</td> </tr> <tr> <td><i>Secondary</i></td> <td>Kingfish Formation</td> </tr> </table>	<i>Primary</i>	Gurnard Formation	<i>Secondary</i>	Kingfish Formation						
<i>Primary</i>	Gurnard Formation										
<i>Secondary</i>	Kingfish Formation										
<b>Total Depth</b>	<table> <tr> <td><b>mMD RT</b></td> <td>660mMD RT</td> </tr> <tr> <td><b>mTVD SS</b></td> <td>638.5mTVD SS</td> </tr> </table>	<b>mMD RT</b>	660mMD RT	<b>mTVD SS</b>	638.5mTVD SS						
<b>mMD RT</b>	660mMD RT										
<b>mTVD SS</b>	638.5mTVD SS										
<b>Elevations</b>	<table> <tr> <td><b>Water Depth</b></td> <td>53m (MSL)</td> </tr> <tr> <td><b>Rotary Table</b></td> <td>+21.5m</td> </tr> </table>	<b>Water Depth</b>	53m (MSL)	<b>Rotary Table</b>	+21.5m						
<b>Water Depth</b>	53m (MSL)										
<b>Rotary Table</b>	+21.5m										
<b>Rig on Contract</b>	5 <sup>th</sup> October 2004; 02:45 hours										
<b>Spud Date</b>	7 <sup>th</sup> October 2004; 16:45 hours										
<b>Well Reach TD</b>	11 <sup>th</sup> October 2004; 20:30 hours										
<b>Rig Released</b>	17 <sup>th</sup> October 2004; 13:00 hours										
<b>AFE Number</b>											
<b>Budget Well Cost</b>	A\$4,557,231										
<b>Estimated Actual Well Cost</b>	A\$5,285,107										

## **2.2 OPERATIONS SUMMARY**

Detailed information on drilling and engineering data may be found in the Moby-1 Final Well Report - Basic Data, Volume 1 of 2.

### 3. GEOLOGY

#### 3.1 SUMMARY OF PREVIOUS EXPLORATION

Permit Vic/P47 which covers an area of 718 km<sup>2</sup> in water depths of 20-75 m in Bass Strait near the Patricia Baleen gas fields, was granted to Eagle Bay Resources NL (100%) pursuant to the PSLA by the Designated Authority for an initial six year period commencing on the 28<sup>th</sup> May 2001. On the 15<sup>th</sup> March 2004 Year 2 was suspended so that the Year 2 anniversary date is the 27<sup>th</sup> February 2005. Year 2 and Year 3 anniversary dates are now the common date of 27<sup>th</sup> February 2005.

By a farm-in agreement made between Bass Strait Oil Company Ltd (BAS) and Eagle Bay Resources on the 13<sup>th</sup> June 2003 (pursuant to an option agreement between BAS and Eagle Bay dated 8<sup>th</sup> April 2002, as amended), BAS acquired a 75% interest in permit Vic/P47 and became operator. BAS agreed to earn the 75% farm-in interest by meeting the Year 2 work commitment by drilling Moby-1. The drilling of the Moby-1 well met BAS's obligation to Eagle Bay Resources. By a further farm-in agreement made between Moby Oil & Gas Limited (MOG) and BAS, MOG acquired a 35% interest in a portion of permit Vic/P47 by contributing to the cost of drilling Moby-1. Pursuant to this later agreement, the participating interests in Vic/P47 are as follows:

Bass Strait Oil Company Ltd (BAS) - 40.0%; Moby Oil & Gas Limited (MOG) - 35.0% and Eagle Bay Resources NL - 25.0%.

##### 3.1.1 Seismic Data

Seismic coverage varies over Vic/P47. Where full-fold 3D coverage exists, such as over the Baleen and Esso Northern Fields surveys, data coverage is excellent. The fold of coverage for the Esso 3D area drops away to zero some 2.3 km from the north eastern boundary of that 3D seismic survey. Hence data quality in this north eastern zone of the Moby feature where this occurs, is quite poor. Seismic coverage of the Moby Prospect varies; over the western edge downdip of Flathead-1, data is excellent, with evidence of direct hydrocarbon indicators ("DHI's"). The southern edge of the prospect has low fold coverage from the Northern Fields 3D seismic survey and data quality is fair to poor. On the crest of the Moby Anticline coverage, from the few 2D seismic lines available, is sparse, although data quality on these lines is fair. Seismic over the Moby feature in Vic/P55 to the east is not available digitally. Since drilling Moby-1, BAS acquired 148sq. km of 3D seismic over the discovery with the GAP04A survey in January 2005 (see Figure 2). The following significant seismic events and markers were correlated by BAS from all relevant wells to seismic data and were interpreted over the entire 3D and 2D dataset: namely Top Gurnard Formation Reservoir, Top Volador Formation and the Top of the Strzelecki Group.

The following significant seismic events and markers were correlated from well to seismic:

- Top Gurnard Formation Reservoir from Baleen-1 and Patricia-1
- Top Volador Formation after Judith-1
- Top Strzelecki Group in all wells (equals Top Emperor in Judith-1)

In addition, an event at the base of the Gippsland Limestone was interpreted from the northern wells, but does not correlate with the event as encountered in Judith-1.

These seismic events were correlated from the wells into the seismic and were interpreted on every tenth or 20th in-line and crossline, and on the 2D seismic. The data was autotracked to remaining 3D bins using extended and interpolated tracking, with typically over 25% quality factors. Faults were interpreted on every tenth in-line and crossline and correlated across time slices and between vertical sections.

A significant top Latrobe 'coarse clastics' event was not apparent in the northern wells due to the thin reservoir section encountered, and could not be mapped separately.

The most significant observation on the Baleen 3D dataset is that the top Gurnard Formation reservoir sequence is nearly always marked by a decrease in acoustic impedance contrast relative to its overburden. When the Gurnard reservoir is gas bearing, as in the Patricia and Baleen Fields, the event experiences a sharp drop in acoustic impedance compared to water filled sands. This significantly increases the confidence in its interpretation and identifies areas most likely to be gas filled.

The interpretation of the Gurnard Formation reservoir became problematic towards the South into Judith 1, as the sequence diverges. There were significant misties between the 2D and 3D data sets, which could be due to 'out of plain' reflections on the 2D data.

The top Volador Formation, tied to Judith-1, only exists in Vic/P47 south of Flathead-1 towards the Central Deep and can be mapped with some difficulty through the Northern Fields 3D area. It was selected as it marks a major 'intra-Latrobe' reservoir sequence, and is at base of the regional Kate Shale seal. The top Strzelecki Group seismic event is always recognisable due to the existence of a steep angular unconformity and resulting event terminations.

The base Gippsland Limestone Formation was mapped to assist in-depth conversion as it is known that high velocity material often exists in submarine canyon fill sequences. It was eventually not used for depth conversion purposes, however, during mapping it was also noted that this sequence erodes top Latrobe Group reservoirs and so is critical for assessing prospectivity. A correlation of the base Gippsland Limestone in Whale 1 towards Judith 1 shows these events cannot be correlated and may represent two separate sequences of submarine canyon incision.

The Moby-1 well was designed to test the Moby Prospect, primarily to target the seismic amplitude anomaly identified on the Baleen 3D survey, interpreted to represent gas within reservoirs of the Gurnard Formation. Although the Moby Prospect is present on a significant anticline with over 70km<sup>2</sup> areal closure, it was drilled in a crestal location by Flathead-1 and Whale-1 which both failed to encounter suitable reservoirs within the Gurnard Formation. Better reservoir development was interpreted from well and seismic data to exist downdip at the Moby-1 location.

The Moby Prospect is a compressional anticline drilled on the crest by wells Whale-1 and Flathead-1. Reservoir development on the crest is minimal due to erosion or non-deposition and reservoir thickness is interpreted to thicken significantly downdip to the south within closure. It is also not known if the thin reservoirs on the crest are in communication with any downdip. The mapped areal closure for Moby extends into permit Vic/L21 to the west and V02-3 to the east. The mapped gross reservoir sequence is bound by the Top Gurnard Formation reservoir event and the Top Strzelecki Group event. The likely gas fluid contact

is believed marked by the downdip extent of amplitude anomalies from the Baleen 3D at around 560-565m bmsl. Current mapping does not identify the structural spill point, but regional mapping e.g. reference VIMP 56 (Megallaa *et al.*, 1998 - encl. 4 – not included) and reference Shell 1985 suggest that mapped TWT fault closure at Top Gurnard would extend beneath the gas in the Patricia Field. As oil is not identified in Patricia-1 this would indicate closure cannot extend below the depth of the structural spill point between the Moby and Patricia structures, which is identified at approximately 700m – 710m bmsl.

### 3.1.2 Well Data

To date, only three other wells have been drilled in the area now covered by permit Vic/P47 prior to Moby-1, while a number of other key wells have been drilled immediately adjacent to the permit and are currently within Vic/L21.

Four wells are relevant in assessing the Moby-1 prospect. These are Flathead-1 and Whale-1 in Vic/P47 and Patricia-1 and Baleen-1 in Vic/L21. All wells intersected the Top Latrobe as their target and bottomed in sediments of the Strzelecki Group. In addition to these four wells, a well drilled in the south of Vic/P47 in 1989, Judith-1, is interpreted to have encountered gas in the Emperor Subgroup although it was never tested.

Flathead-1 which was drilled by Esso Australia in 1969, was drilled in a crestal position on the Moby Anticline, 2km NE of Moby-1. The well reached a total depth of 1066 m MD in the Strzelecki Formation and it was plugged and abandoned as a potential oil discovery in the Kingfish Sandstone, with good gas shows in the Gurnard Formation siltstone. Oil was extracted from Kingfish Formation core with an API gravity of 14.6° and 50 centipoise.

Whale-1 was drilled by Hudbay Oil (Australia) Ltd in 1981, also in a crestal position on the Moby Anticline, 5 km NE of Moby-1. The well reached a total depth of 810 m MD in the Strzelecki Formation and it was plugged and abandoned with excellent oil shows in Latrobe Group sandstone and Gurnard Formation, with some minor gas shows, although testing failed to recover fluids. Oil extracted from a sidewall core sample from the Gurnard Formation had an API gravity of 19.9-22.3°.

Patricia-1 and Baleen-1 are located 5 km and 7 km west of Moby-1 and were drilled in 1987 and 1981 respectively. These wells were drilled on closed structures and intersected gas-bearing sandstones in the Gurnard Formation. The Patricia Baleen gas project is now on stream through a pipeline which joins the fields extending through the western portion of Vic/P47 to the main trunkline to New South Wales.

Judith-1 which was drilled by Shell Australia in 1989 is located 17.5 km south of Moby-1. The well reached a total depth of 2958 m MD in the Emperor Sub-Group. This well was drilled within the Rosedale Fault System and was designed primarily to test alluvial fan reservoir objectives in the lower part of the Golden Beach Sub-Group within a rotated fault block. Top and lateral seal was expected to be provided by the lacustrine Kipper Shale of the Emperor Sub-Group. The secondary objective was to test a possible NW extension to the Kipper gas accumulation in the upper part of the Golden Beach Sub-Group.

All major seismic mapping horizons below the Base Gippsland Limestone were intersected high to prognosis, mainly attributed to higher than modelled velocities used pre-drill in the Lakes Entrance Fm affecting the depth conversion. The top Emperor S/G (Kipper Shale)

was intersected some 260m high to prediction and is much thicker than predicted in the downthrown Judith fault block.

Strong gas shows while drilling and low hydrocarbon saturations interpreted from logs are taken to indicate that Judith tested a valid trap with tight reservoir (low effective porosity of 6-12% and permeabilities measured by RFT of <1md) in the lower part of the Emperor Sub-Group (Admiral Fm) and sands within the Kipper Shale section. The secondary objective to test the top of the Golden Beach below the Campanian volcanics showed that the Kipper Field is bound by the Kipper fault and laterally sealed by the juxtaposition of the Kipper Shale. The sands intersected at the top of the Golden Beach are interpreted to be locally distributed on the downthrown side of the Judith Fault.

## 3.2 REGIONAL STRUCTURE AND GEOLOGY

Vic/P47 is located offshore on the northern margin of the Gippsland Basin, straddling the Northern Platform and Northern Terrace, approximately 350 km east of Port Melbourne. The southern or 'neck' portion of the permit that incorporates the Moby-1 prospect lies to the south of the Lake Wellington Fault System that separates the platform from the terrace. The Generalised Stratigraphic Column reflecting the Early Cretaceous to Recent gross lithostratigraphic units of the Gippsland Basin (Figure 4) summarises much of the following discussion.

### 3.2.1 Geological Evolution

The east-west trending Gippsland Basin was formed as a consequence of Gondwana break-up (Rahmanian et al 1990; Willcox et al 1992; Willcox et al 2001; Norvik & Smith 2001; Norvik et al 2001) and the basin evolution is recorded by several depositional sequences that range from Early Cretaceous to Recent in age (Thomas et al 2003).

The profound tectonic control on sedimentary systems in the basin is exemplified by several basin-wide angular unconformities that are easily recognised on seismic sections. Other time-breaks are only recognised using biostratigraphic age determinations delineating missing sections. This is of particular relevance in the context of the upper Latrobe Group, where extensive channel incision and subsequent infill processes resulted in complex sedimentary sequences that developed at slightly different time intervals, the extent of which cannot be resolved by seismic mapping alone.

### 3.2.2 Tectonic History

The Gippsland Basin is an asymmetric graben formed by the incipient break-up of Australia and Antarctica (Otway Rift) during the earliest Cretaceous (130-96 Ma). As part of this Early Cretaceous rift system, the Gippsland Basin architecture initially featured a classic extensional geometry consisting of a depocentre (the Central Deep) flanked by platforms and terraces. These are defined by the Rosedale and Lake Wellington Fault systems on the northern basin margin and by the Darriman and Foster Fault systems on the southern margin. The Central Deep hosts most of the oil and gas fields and, to the east, is characterised by rapidly increasing water depths which exceed 3000m in the Bass Canyon (Hill et al 1998). The eastern boundary of the basin is defined by the Cape Everard Fault System, a prominent NNE-striking basement high clearly evident from the aeromagnetic data (Moore & Wong 2002). The western onshore extent of the basin is traditionally placed

at the Mornington High, but for the units described in this report it is essentially represented by out-crops of Early Cretaceous Strzelecki Group sediments (Hocking 1988). A tectonic elements and basin setting map is included herein as Figure 3 (modified after Wong D., Bernecker T. & Moore D., 2001.).

Crystalline basement is formed by the low grade metamorphic and igneous rocks of the Palaeozoic Tasman Fold Belt that have a general north-south tectonic grain and are cross-cut by NE-SW trending basement-involved fault zones formed during the Cretaceous rift phase.

Australia commenced its separation from Antarctica during the Cenomanian. The plate suture did not extend into the Gippsland Basin, but instead continued down the western side of Tasmania. The break-up created an unconformity at the end of the Early Cretaceous, not only in those basins where new oceanic crust formed but also further east in the Bass and Gippsland Basins.

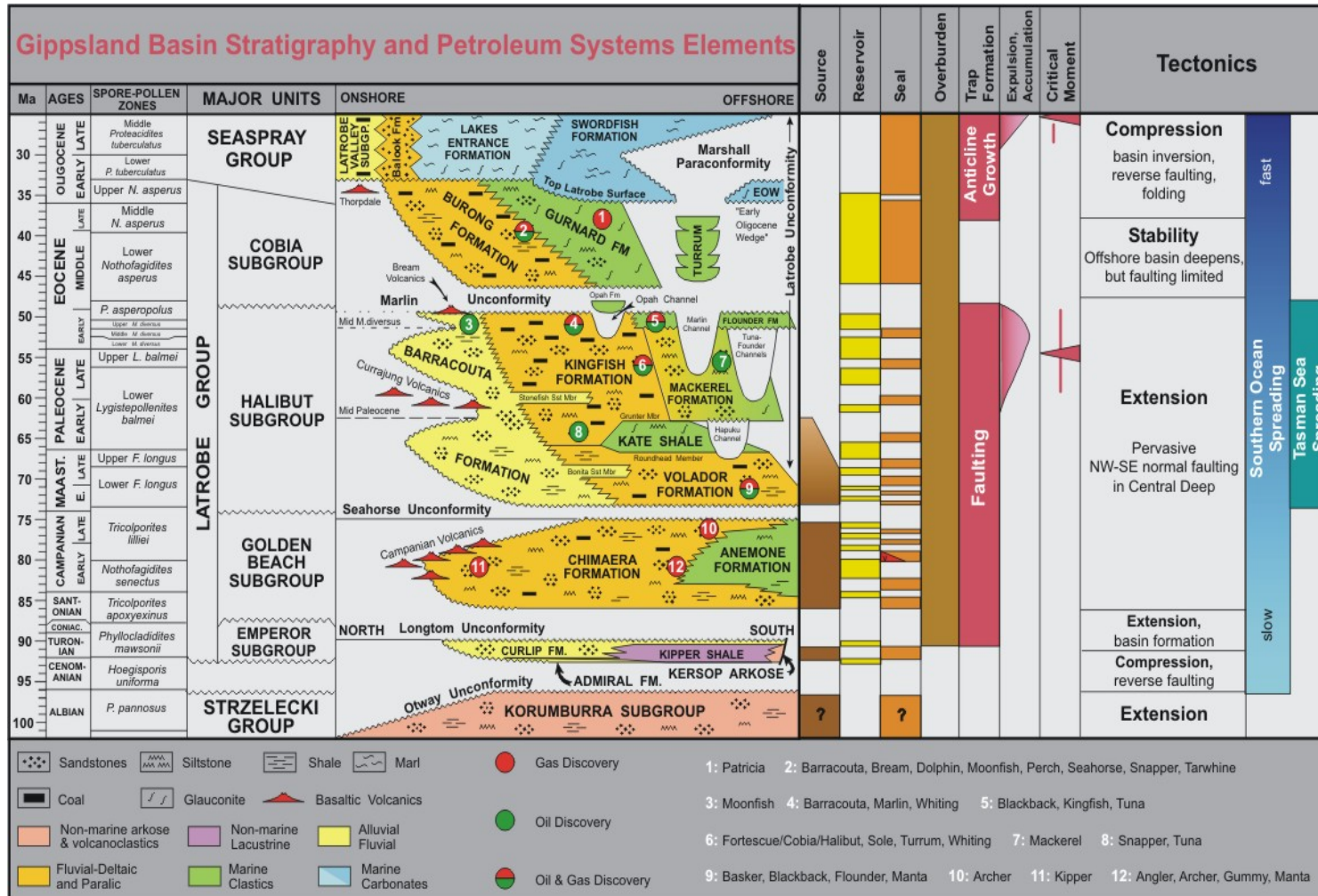
Initial rifting in the Early Cretaceous resulted in 30% crustal extension (Power et al 2001) and created a complex system of grabens and half-grabens. A compressional phase accompanied by uplift occurred between 100 and 95 Ma which has been linked to the separation of Australia from Antarctica (Duddy & Green, 1992). This produced a new basin configuration and provided the accommodation space for large volumes of basement derived sediments. A second phase of crustal extension, produced by rifting between Australia and the Lord Howe Rise (Tasman Rift), began at the end of the Early Cretaceous and produced northwest-southeast oriented basement-involved normal faults and established the Central Deep as the main depocentre. The first marine incursion is recorded by Late Santonian sediments in the eastern part of the basin (Partridge, 1999). Many of the earlier generated faults were reactivated during this tectonic phase.

Rifting was followed by the development of a margin-sag basin characterised by rapid subsidence. Extensional tectonism prevailed until the Early Eocene and produced pervasive NW-SE trending normal faults. By the Middle Eocene, sea-floor spreading had ceased in the Tasman Sea and a period of compressional tectonism began to affect the Gippsland Basin, initiating a series of NE to ENE trending anticlines (Smith, 1988). Compression and structural growth peaked in the Middle Miocene and resulted in basin inversion. All the major fold structures at the top of the Latrobe Group which became the hosts for the large oil and gas accumulations such as Barracouta, Tuna, Kingfish, Snapper and Halibut are all related to this tectonic episode.

A second regional event at this stage was a widespread mid-Eocene marine transgression that is recognised in the Gippsland, Taranaki and southern Australian margins (Norvik et al, 2001). Plate reorganisation occurred at this time leading to the onset of fast spreading south of Australia, obduction in New Caledonia and other movements in New Zealand. The Lakes Entrance Formation became a widespread depositional unit at this time and was succeeded by prograding carbonate wedge deposits of the Gippsland Limestone that continue to be deposited today.

Tectonism has continued to overprint the basin as documented by localised uplift during the Late Pliocene to Pleistocene. This is also reflected in the uplift of Pliocene sediments on the Barracouta, Snapper and Marlin anticlines as well as around the township of Lakes Entrance on the Victorian coastline. Ongoing tectonic activity is episodically recorded by seismic events around the major basin bounding faults.

The superposition of different age structures in the Gippsland Basin has produced a structural style characterised by multi-directional fault, fold and erosional patterns, allowing a range of trapping mechanisms, from large anticlines to complex, fault-controlled rotated blocks and truncation plays. The timing of the structuring, specifically the large compressional anticlines initiated in the Late Eocene, is particularly critical to the entrapment of most of the hydrocarbons in the basin, as the key geometry of the traps was in place prior to the generation of most of the oil and gas.



After Bernecker et. al., 2003

FIGURE 4 GENERALISED STRATIGRAPHIC COLUMN OF THE GIPPSLAND BASIN (AFTER BERNECKER, T., THOMAS, H. & DRISCOLL, J., 2003).

### 3.3 STRATIGRAPHY

Moby-1 penetrated a sedimentary section ranging in age from Early Cretaceous to Recent. The lithologies described herein follow the convention that the dominant lithology is mentioned first. Depths are measured depths (MD) in metres below the Drill Floor (DF) which was 21.5m above Mean Sea Level (MSL) and 74.5m above the seafloor, unless otherwise stated.

No ditch cuttings samples were collected over the 914mm (36”) and 445mm (17 ½”) hole sections drilled between the seabed (74.5mMD RT) and 325mMD RT in Moby-1. Following installation of the marine riser, the well was drilled from 325mMD RT to 660mMD RT (Total Depth) with full returns.

The wellsite lithological descriptions of the cuttings samples are contained in Appendix 1 of the Moby-1 Well Completion Report (Basic Data). A composite log of the lithology is provided in Enclosure 1, this volume. The lithology described hereunder is a synthesis of the lithological descriptions of cuttings, sidewall cores and petrophysical and petrological data. Table 1 below summarises the formations intersected and the relevant depths to the top of the formation.

Formation/Age	Depth	Depth	True Thickness	Seismic Time TWT
(Drill Floor = 21.5m)	(mMD RTRT)	(mTVDSS) *	(m)	(msec)
<b>Miocene</b> – <b>Pliocene/Recent</b> Gippsland Limestone (Seafloor)	74.5	53.0	435.9	70.7
<b>Oligocene-Early</b> <b>Miocene</b> Lakes Entrance Fm	510.4	488.9	45.1	513.5
<b>Oligocene</b> 'Early Oligocene Wedge'	553.0	532.5	2.5	557.0
<b>Middle Eocene-Early</b> <b>Oligocene</b> Gurnard Fm	555.5	534.0	31.5	559.0
<b>Paleocene to Early</b> <b>Eocene</b> Kingfish Fm	587.0	565.5	2.5	590.0
<b>Early Cretaceous (Late</b> <b>Albian)</b> Strzelecki Group	589.5	568.0	70.5+	592.6
<b>TOTAL DEPTH</b>	660.0	638.5		651.7

TABLE 1: MOBY-1 STRATIGRAPHIC TABLE.

**\*Subsea depths in metres below Mean Sea Level (MSL) and corrected for hole deviation where appropriate.**

The stratigraphy encountered was essentially as predicted with most of the formation tops slightly high to prognosis. The primary objective Gurnard Formation was encountered below base seal and 15.5m high to prognosis. Furthermore, the well reached total depth in the Early Cretaceous (Mid-Late Albian) Strzelecki Group. The sub-division of the sedimentary section of Moby-1 by formation boundaries and chronostratigraphic units as shown on the composite log (Enclosure 1) were determined primarily using a combination of wireline logs, lithological descriptions, drilling parameters and biostratigraphic data. A basic biostratigraphic report is included as Appendix 12 of the Moby-1 Well Completion Report – Basic Data and an interpretive biostratigraphic report is included herein as Appendix 3. Log correlation with nearby offset wells was also used to define formation tops.

### 3.3.1 Gippsland Limestone/Recent Seafloor – 510.4mMD RT (53-488.9mTVDSS)

True Vertical Thickness	435.9m
Age:	Miocene-Pliocene/Recent
Palynozone:	Not defined
Depositional Environment:	Marine
Seismic Time:	0.0707 Sec TWT

No ditch cuttings were collected over the upper portion of the Gippsland Limestone above 325mMD RT and no open hole wireline logs were recorded above 325mMD RT. A cased hole wireline gamma ray was recorded from 321.76mMD RT to seafloor at 74.5mMD RT, while a cased hole sonic (MAC) was also recorded to seafloor. Lithology above 325mMD RT is interpreted from surrounding offset well data and ROP.

The Gippsland Limestone is interpreted to consist of calcarenite with interbedded and intergradational calcisiltite and calcilutite above 325mMD RT. The lower part of the unit below 325mMD RT consists predominantly of argillaceous calcilutite and calcisiltite with minor calcarenite.

The Gippsland Limestone unconformably overlies the Lakes Entrance Formation at 510.4mMD RT (-488.9mTVDSS), at a seismic time of approximately 513.5msec TWT. This interpretation is based on the first appearance of marl in the section and correlation with offset wells, although it is still not a definitive boundary.

The unconformable nature of the contact at 510.4mMD RT is based on regional evidence only and is not able to be documented directly in Moby-1.

No direct biostratigraphic age dating was attempted in Moby-1 through the Gippsland Limestone, however based on regional evidence the sequence is defined as being Miocene to Pliocene in age with a probable veneer of Recent age sediments.

#### Lithology

**74.5 – 325mMD RT (250.5m)** *Calcarenite, Calcisiltite and Calcilutite*  
**ROP range (average): 8-330 (71) m/hr**

No Samples – Returns to Seafloor

**325 – 510.4mMD RT (185.4m)** *Argillaceous Calcilutite and Argillaceous Calcisiltite with minor Calcarenite*  
**ROP range (average): 15-318 (75) m/hr**

**Calcilutite (30-100%):** argillaceous, off white-light grey, very soft, amorphous, micritic with trace fine shell fragments, forams and trace very fine sand-silt.

**Calcisiltite:** light-medium dark grey, firm, argillaceous with trace very fine sand, silt, grading to *Calcilutite* and *Calcarenite*

**Calcarenite:** pale yellowish brown, light grey, hard, partly recrystallised, clasts shell fragments, forams with trace clay matrix

**3.3.2 Lakes Entrance Formation 510.4 – 553.0mMD RT (488.9 – 531.5mTVDSS)**

True Vertical Thickness	42.6m
Age:	Late Oligocene-Early Miocene
Palynozone:	P. tuberculatus / Operculodinium
Depositional Environment:	Open Marine
Seismic Time:	0.5135 Sec. TWT

The Lakes Entrance Formation consists of marl grading to argillaceous calcilutite and calcilutite with abundant interbedded calcareous claystone.

The Lakes Entrance Formation overlies a thin interval interpreted as the 'Early Oligocene Wedge' (EOW) at 553mMD RT (-531.5mTVDSS), at a seismic time of 557msec TWT. The contact is defined by an increase in gamma ray response from 65 API units above 553mMD RT to 80-85 API units below, while the DLL log (R<sub>D</sub> curve) exhibits a slight increase from 2 ohm-m above 553mMD RT to 3 ohm-m below.

The unconformable nature of the contact at 553mMD RT is not able to be documented directly in Moby-1 and is based on regional evidence only and by correlation with offset wells.

Palynological age dating of two sidewall core samples over the gross interval 538-547mMD RT within the lower part of the Lakes Entrance Formation places this unit within the *Proteacidites tuberculatus* Spore Pollen Zone and *Operculodinium* Microplankton Superzone of Late Oligocene to Early Miocene age.

**Lithology**

**510.4 - 553m (42.6m)**

*Marl (grading to Argillaceous Calcilutite and Calcilutite) with abundant interbedded Calcareous Claystone*

**ROP range (average): 13-155 (37) m/hr**

**Marl** (Trace-30%): very light to light medium grey, very soft - soft, dispersive in part, amorphous, clay matrix (35-44%) grading to *Argillaceous Calcilutite* in part, trace-5% calcisilt, trace very fine dark green disseminated glauconite, trace fossil fragments and forams.

**Calcilutite:** argillaceous, soft to slightly firm, massive, very light to medium grey and greenish grey, trace dark grey, argillaceous matrix (0-30%), grading to *Calcilutite* and *Argillaceous Calcisiltite* in part, trace fossil fragments including coral debris, bryozoan, spicules, shell fragments and forams, trace fine dark green disseminated glauconite and trace-5% medium to coarse nodular glauconite, trace fine pyrite, trace coarse nodular pyrite.

**Claystone:** calcareous, light grey to brownish grey, trace light greenish grey, soft, amorphous to blocky, 15-25% calcareous matrix, trace – 5% calcisilt, trace light brownish yellow fossil fragments, trace fine dark green disseminated glauconite and nodular glauconite, trace fine pyrite, trace coarse nodular pyrite.

### 3.3.3 'Early Oligocene Wedge' (EOW) 553 – 555.5mMD RT (531.5- 534mTVDSS)

True Vertical Thickness	2.5m
Age:	Early Oligocene
Palynozone:	Upper <i>N. asperus</i>
Depositional Environment:	marine
Seismic Time:	0.557 Sec. TWT

The 'Early Oligocene Wedge' (EOW) is interpreted to consist of calcareous claystone based on documentation of calcareous claystone slightly higher in the section and with a common gamma ray response.

The 'Early Oligocene Wedge' (EOW) unconformably overlies the Gurnard Formation at 555.5mMD RT (-534mTVDSS), at a seismic time of approximately 0.559 seconds TWT. The contact is defined by correlation with offset wells and a marked change in wireline log response. The gamma ray exhibits an increase from 80 API units above 555.5mMD RT to 100-120 API units below and the DLL log ( $R_D$  curve) exhibits an increase from 3 ohm-m above 555.5mMD RT to 4-17 ohm-m below. The resistivity increase within the Gurnard Formation occurs partly in response to gas within objective reservoir sequence. There is also a spike in the density at the formation boundary from 2.2-2.25g/cc above 555.5mMD RT to 2.5g/cc below. These wireline log changes occur in response to a marked lithological change from calcareous claystone above 555.5mMD RT to mainly siltstone and silty/glaucouitic sandstone below.

The unconformable nature of the contact at 555.5mMD RT is based on regional evidence only and is not able to be documented directly in Moby-1.

Recognition of this condensed interval as the 'Early Oligocene Wedge' (EOW) is based upon the assignment of drilled ditch cuttings from the interval 553-556mMD RT to the Upper *N. asperus* palynozone of Early Oligocene age.

#### Lithology

**553 – 555.5m (2.5m)** *Calcareous Claystone*  
**ROP range (average): 15-23 (20) m/hr**

**Claystone:** calcareous, light grey to brownish grey, trace light greenish grey, soft, amorphous to blocky, 15-25% calcareous matrix, trace – 5% calcisilt, trace light brownish yellow fossil fragments, trace fine dark green disseminated glauconite and nodular glauconite, trace fine pyrite, trace coarse nodular pyrite.

### 3.3.4 Gurnard Formation 555.5 – 587mMD RT (534 – 565.5mTVDSS)

True Vertical Thickness	31.5m
Age:	Middle-Late Eocene
Palynozone:	Lower to Middle <i>N. asperus</i>
Depositional Environment:	Shallow marine
Seismic Time:	0.559 Sec. TWT

The Gurnard Formation, which was the primary reservoir objective in Moby-1, consists of a complex lithological mix of intergradational siltstone and silty/glaucouitic sandstone which are defined petrographically as lithic arkose containing 8-12% feldspar, 5-10% lithic grains and 10-15% glauconite and mica. The sands also contain an abundant mix of detrital

clay (5-10%) and authigenic clay (10-15%) matrix. The sequence also includes rare greensand and claystone interbeds.

The sequence consists of a number of depositional cycles characterised by slightly fining-upward and coarsening-upward trends as defined by subtle bell-shaped and funnel-shaped gamma ray motifs respectively, generally in the range of 90-130 API units. The most distinctive feature of the Gurnard Formation is a 4m thick radioactive interval of feldspathic sandstone at the base of the unit characterised by a gamma ray response >400 API units. The radioactivity occurs in response to accessory zircon, tourmaline and titanium oxide identified petrographically within the sandstone. The sandstone also contains some 25% of chloritic clay matrix.

The Gurnard Formation unconformably overlies the Kingfish Formation at 587mMD RT (-565.5mTVDSS), at a seismic time of approximately 0.590 seconds TWT. The contact is well defined by the gamma ray curve which exhibits a decrease from 400API units above 587mMD RT to 40-80 API units below, while the sonic log displays a reduction in interval transit time from 135  $\mu$ sec/ft above 587mMD RT to 120  $\mu$ sec/ft below.

The unconformable nature of the contact at 587mMD RT is indirectly based upon palynological evidence in Moby-1 and regional evidence by correlation with offset wells and is referred to herein as the Early Eocene Unconformity. This unconformity is documented directly in Moby-1, whereby marine rocks assigned to the Lower *N. asperus* palynozone of Middle Eocene age, directly overlie non-marine rocks arguably assigned to a mixed assemblage of Eocene, reworked Early Cretaceous and possibly reworked Triassic palynomorphs, but older than Lower *N. asperus*. The most likely correlation is with the Early Eocene *Proteacidites asperopolus* Zone which has been recorded from similar sandstones immediately beneath the Gurnard Formation in the offset Flathead-1 and Patricia-1 wells.

Palynological age dating of sidewall core samples and drilled ditch cuttings over the gross interval 558.5-586mMD RT throughout the Gurnard Formation, places this unit within the Lower and Middle *N. asperus* palynozone of Middle and Late Eocene age.

## Lithology

**555.5 – 583m (27.5m)**

*Siltstone with abundant interbedded  
Glaucinitic/Silty/Argillaceous Sandstone, minor  
Greensand and rare Claystone*

**ROP range (average): 6-35 (20) m/hr**

**Siltstone** (20 – 70%): medium to dark yellowish brown, dark brown grey to brown black, quartz silt to very fine quartz, soft to firm, occasionally hard, non-calcareous, 10-20% detrital clay matrix, grading to *Argillaceous Siltstone*, locally arenaceous with 10-20% very fine quartz, grading to *Arenaceous Siltstone*, trace-15% fine to coarse glauconite, locally in patches, trace-1% white mica, soft, nil to very poor visible porosity

**Sandstone**: argillaceous, medium yellowish brown, firm, friable to soft, loose in part, very fine to fine, (dom vL-vfU, max fU), sub-angular-sub-rounded, poor to moderately sorted, 10-15% quartz silt, 5-10% detrital clay matrix, trace – 5% fine glauconite and glauconite nodules, trace mica (biotite and muscovite), trace large forams (*Amphistegina?*), corals, bryozoan fragments, with poor – good inferred porosity and;

**Sandstone:** arkosic/silty, pale to dark yellowish brown and grey orange, quartz silt to fine quartz, dominantly very fine, sub-angular, low to medium sphericity, moderate to well sorted, common to abundant cementation(?), 20% quartz silt matrix, 5-10% detrital clay matrix, 10-15% authigenic clay (mainly chlorite) matrix, 5-15% coarse patchy and pelletal glauconite, trace-10% fine mica, 5-10% feldspar, trace-5% lithic fragments, firm to hard, nil to occasionally fair visible inter-granular porosity.

**Greensand:** dark yellowish green to dusky green, soft – firm, loose grains in part, very fine to coarse grained, trace nodular glauconite, trace – 20% quartz sand, trace shell fragments.

**Claystone:** “pisolitic”/glauconitic, pale yellowish brown to moderate brown, light grey, soft, diffusely laminated, slightly calcareous, 20% well-rounded, medium to coarse dark brown, well-rounded fine-grained weathered glauconite pellets, generally firm, some soft, common reddish-brown areas which may be oxidized.

**583-587m (4m)**

*Sandstone*

**ROP range (average): 14-42 (27) m/hr**

**Sandstone (100%):** litharenitic, medium dark grey, soft to firm, very fine-fine (dom vfU, max vcL), occasional medium to very coarse sub-rounded quartz grains, sub-angular to sub-rounded, low to medium sphericity, poor to moderately well sorted, very slightly calcareous with 5-8% siderite cement, trace-10% pyrite cement, 10-30% quartz silt matrix, trace-5% detrital clay matrix, 20-30% authigenic clay (mainly chlorite) matrix, 10% zircon/tourmaline, 5-8% very fine black-dark grey, dark brown, orange lithic fragments (volcanic & sedimentary), 5% feldspar, trace fine carbonaceous fragments, 1-3% glauconite, 3-5% fine white mica, poor visible inter-granular porosity

**3.3.5 Kingfish Formation**

**587 – 589.5mMD RT (565.5 - 568mTVDSS)**

True Vertical Thickness	2.5m
Age:	Early Eocene?
Palynozone:	P. asperopolus?
Depositional Environment:	Non-marine to shallow coastal marine
Seismic Time:	0.5900 Sec. TWT

The Kingfish Formation which formed a secondary reservoir objective in Moby-1 (compare Barracouta Formation) consists of a thin interval of argillaceous sandstone, defined petrographically as a feldspathic litharenite with a semi-serrate-type gamma ray response of 40-80 API units. The sandstone consists of only 10% quartz with 20% rock fragments, 15% feldspar and several other minor components which make up the rock framework. The remainder of the rock consists predominantly of authigenic and detrital clay matrix.

The Kingfish Formation unconformably overlies the Strzelecki Group at 589.5mMD RT (-568mTVDSS), at a seismic time of approximately 0.5926 seconds TWT. The contact is well defined on wireline logs, with the gamma ray exhibiting a decrease from 40 API units above 589.5mMD RT, to a uniform 80-100 API units below, while DLL log (R<sub>D</sub>) curve exhibits a decrease from 5-10 ohm-m above 589.5mMD RT to 3-4 ohm-m below.

The unconformable nature of the contact at 589.5mMD RT is indirectly based upon palynological evidence in Moby-1 and regional evidence by correlation with offset wells and represents the most significant unconformity identified in Moby-1 where some >50

million years of section is missing. The section immediately above 589.5 m MDRT is palynologically assigned to the *P. asperopolus* palynozone of Early Eocene age, directly overlying rocks assigned to the Upper *C. paradoxa* palynozone of Early Cretaceous (late Albian) age. The entire Late Cretaceous, Palaeocene and most of the Early Eocene section equivalent to the Emperor and Golden Beach Sub-Groups and most of the Halibut Sub-Group are absent through a combination of erosion and non-deposition.

Palynological analysis of a sidewall core sample from 588 mMD contained a limited assemblage but was dominated by a bisaccate gymnosperm pollen called *Podocarpidites*, while the remainder of the assemblage comprised a mixture of Early Cretaceous and Eocene species. Although diagnostic Eocene species favour an age assignment no older than the *P. asperopolus* Zone, any age assignment is best left as indeterminate. However, given the limited assemblage recorded, it is consistent with the *P. asperopolus* Zone ages obtained from similar sandstones immediately below the Gurnard Formation in offset wells (Patricia-1 and Flathead-1).

### Lithology

**587 – 589.5 (2.5m)**

*Sandstone*

**ROP range (average): 15-28 (20) m/hr**

**Sandstone** (100%): feldspathic, litharenitic, medium light grey, soft, friable, fine (dom fL, max mL) sub-rounded to well rounded, moderately sorted, non-calcareous, trace siderite and pyrite cement, trace detrital clay matrix, 10-15% authigenic clay (chlorite) matrix, 30-40% lithic fragments (volcanic, sedimentary and chert), 15% feldspar, poor visible intergranular porosity.

### 3.3.6 Strzelecki Group

**589.5 – 660mMDRT (568 – 638.5mTVDSS)**

True Vertical Thickness

70.5m

Age:

Early Cretaceous (Late Albian)

Palynozone:

Upper *C. paradoxa*

Depositional Environment:

Non-marine

Seismic Time:

0.5926 Sec. TWT

The Strzelecki Group consists of a thick sequence of fine to medium grained litharenite that consists mainly of volcanic and sedimentary lithic fragments and feldspar set within a matrix of authigenic clay (mainly chlorite) and minor detrital clay. The sequence is characterised by a relatively uniform gamma ray response between 80 and 100 API units, at least to the base of the gamma ray response at 622mMD RT, while the resistivity ( $R_D$  curve) response is also relatively uniform between 2.2 and 4.0 ohm-m.

Palynological age dating of drilled ditch cuttings over the gross interval 613-630mMD RT throughout the in the central part of the Strzelecki Group, places this unit within the Upper *C. paradoxa* palynozone of Middle to Late Albian (Early Cretaceous) age. A shallower sidewall core sample from 605 mMD and drilled ditch cuttings between 589 and 604 mMD were effectively barren of palynomorphs and therefore the age was indeterminate.

Moby-1 reached a total depth within the Strzelecki Group at a depth of 660mMD RT (-638.5mTVD SS). This is 35m below the original programmed total depth of the well.

## Lithology

**589.5 – 660m (70.5m)**

*Sandstone*

**ROP range (average): 8-119 (43) m/hr**

**Sandstone (100%):** litharenitic, medium light grey, soft, friable, fine to medium (dom fL, max mL) sub-rounded to sub-angular, locally well rounded, moderately sorted, non-calcareous, trace siderite and pyrite cement, trace detrital clay matrix, 10-15% authigenic clay (chlorite) matrix, 30-40% lithic fragments (20% volcanic, 14% sedimentary and 9% chert), 10-15% feldspar, poor visible inter-granular porosity.

### 3.4 STRUCTURE AND SEAL

The Moby-1 well was designed to test the Moby Prospect, primarily to target the seismic amplitude anomaly identified on the Baleen 3D survey, interpreted to represent gas within reservoirs of the Gurnard Formation (outside of the area of a small four-way dip closure to the west). Although the Moby Prospect is present on a significant anticline with over 70km<sup>2</sup> areal closure, it was drilled in a crestal location by Flathead-1 and Whale-1 which both failed to encounter suitable reservoirs within the Gurnard Formation. Better reservoir development was interpreted from well and seismic data to exist downdip at the Moby-1 location.

The most significant observation on the Baleen 3D dataset is that the top Gurnard Formation reservoir sequence is nearly always marked by a decrease in acoustic impedance contrast relative to its overburden. When the Gurnard reservoir is gas bearing, as in the Patricia and Baleen Fields, the event experiences a sharp drop in acoustic impedance compared to water filled sands. This significantly increases the confidence in its interpretation and identifies areas most likely to be gas filled.

Moby-1 was designed to test the hydrocarbon saturation and nature of the amplitude anomaly to confirm that it was not 'fizz gas'. It was also designed to determine reservoir quality in the Gurnard Formation, the underlying Latrobe Group Kingfish Formation and the upper part of the Strzelecki Group. It was designed to determine if potential seals exist between the Gurnard Formation, Kingfish Formation and Strzelecki Group reservoirs and whether any gas pay in the Gurnard was in communication with the Kingfish Formation.

Top seal was likely to be provided by shales of the Lakes Entrance Formation. A seismic flat spot downdip of Moby shows no suggestion of intra-formational sealing within the Gurnard Formation. However, a seal was thought to separate the Gurnard and Kingfish formations and any hydrocarbon fill (as was the case in Patricia-1). The Kingfish Formation in Flathead-1, up-dip of Moby probably contains either live or residual oil. It is probable that this thin interval is not in communication with the sequence downdip. However, Moby-1 may encounter an oil zone in communication with the Flathead-1 oil. The upper part of the Strzelecki Group may have better reservoir characteristics, although usually these sandstones are tight.

Small scale faulting is evident within the Gippsland Limestone at the well location, especially at 352msec TWT (Figure 6). This equates to a depth of approximately 310-340m sub-sea.

Examination of the velocity depth trends for the wells in the region show a linear trend of velocity increasing with depth down to the top of the Latrobe group. The velocity depth trend was determined from Judith-1 as  $V = 1660 + 1.2 Z$  (Z is depth in metres from mean sea level).

This velocity function was used to depth convert the top Gurnard Formation reservoir level and resulted in depth conversion values accurate to less than 2% at the wells. The residual error was gridded and corrected to produce a depth map conformable with the well data.

The stratigraphic section encountered in Moby-1 was essentially as predicted pre-drill, with all of the formation tops encountered slightly high to prognosis. Consequently, the seismic interpretation and depth modeling established pre-drill requires no substantial changes post-drill. Furthermore, the VSP survey confirmed the velocity profile established pre-drill and also identified the gas/fluid contact 'flat spot' which was not apparent at the well location on the Moby 3D survey acquired in 2005.

A post-drill structural interpretation of the Moby-1 fault block is included as Figure 5 and a post-drill interpretation of the 3D seismic Inline601 through the Moby-1 well is included as Figure 6.

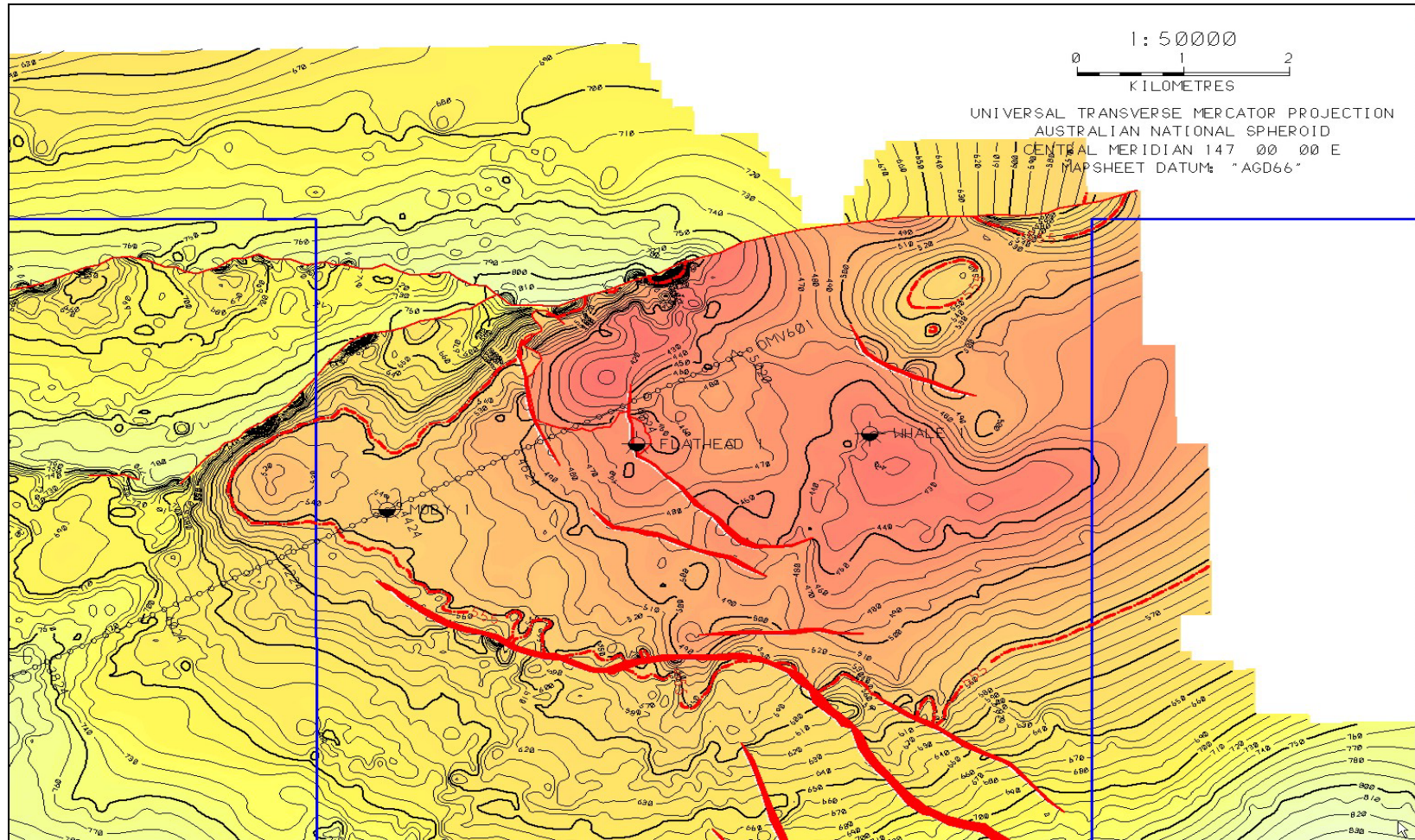


FIGURE 5 POST-DRILL STRUCTURAL INTERPRETATION OF MOBY FAULT BLOCK

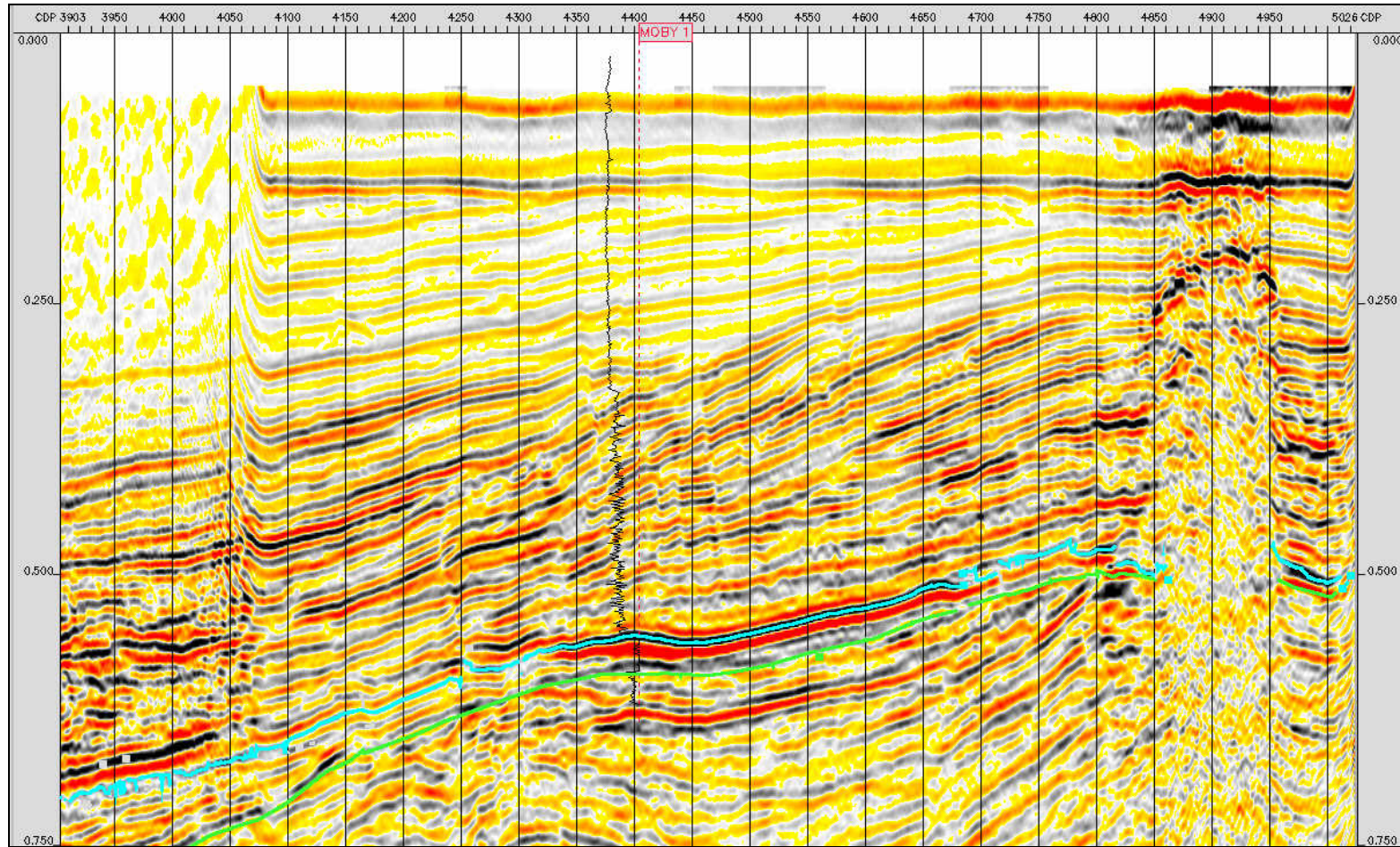


FIGURE 6 SEISMIC INLINE 601 DISPLAYING POST-DRILL INTERPRETATION

### 3.5 SOURCE AND MIGRATION

Moby-1 encountered anomalous gas readings while drilling through the Gurnard Formation, while drilled ditch cuttings of siltstone and silty/glaucconitic sandstone over the gross interval 562–574mMD RT, also within the Gurnard Formation, exhibited 5-20% dull to moderately bright yellow fluorescence, with a slow to moderately fast blue-white cut and solid blue-white ring residue. At 568–571mMD RT, fluorescence increased to 60% dull to moderately bright yellow fluorescence, with an instantaneous blue-white cut and a solid blue-white residue. Nil to trace fluorescence only occurred below 574mMD RT (-552.5 m TVDSS), approximately coincident with an interpreted free water level at 555 m TVDSS. Furthermore, a number of sidewall core samples acquired over the gross interval 555.9-586mMD throughout the entire Gurnard Formation also exhibited variable direct fluorescence and cut fluorescence. Two gas samples were recovered on wireline test from a depth of 568.8 m MDRT (-547.3 m TVDSS) within the Gurnard Formation, while a water sample with a trace oil scum was recovered from a depth of 588.5 m MDRT (-567 m TVDSS) in the Kingfish Formation.

Geochemical biomarker analysis of hydrocarbon extracts taken from five (5) sidewall cores acquired within the Gurnard Formation indicate the hydrocarbons are characterised as biodegraded and mature in nature and thought to be sourced from strongly terrestrial organic matter, possibly with some resin input. Furthermore, geochemical analysis of the oil scum recovered on the water sample from the Kingfish Formation contains a low abundance of biodegraded hydrocarbon, but appears to have been severely contaminated with an alkene-based product, the origin of which is unclear.

Moby-1 is located on the flanks of a structural closure on which two earlier wells, namely Flathead-1 and Whale-1 were drilled on the crest of the same structure, and which also recorded anomalous hydrocarbon occurrences. This data supports Moby-1 being located on a migration pathway from a proven hydrocarbon kitchen to the south and southeast within the deeper parts of the Central Deep of the Gippsland Basin.

### 3.6 RELEVANCE TO THE OCCURRENCE OF HYDROCARBONS

#### 3.6.1 Gas Readings

During the drilling of Moby-1, a continuous record of ditch gas was made using an automatic FID total gas and chromatograph detector. Ditch gas readings are summarised in Table 3 below. No cuttings gas analyses or headspace gas analyses were undertaken.

Total gas, chromatographic breakdown of the ditch gas and trip gas was recorded from 325m to 660mMD RT throughout the 311mm (12 ¼”) hole section and 216mm (8 ½”) hole section below 325mMD RT. Trace to minor amounts of total gas consisting entirely of methane (C<sub>1</sub>) was recorded upon commencement of first drilling returns in the 311mm (12 ¼”) hole and which continued in the 216mm (8 ½”) hole section. Trace amounts of ethane (C<sub>2</sub>), pentane (C<sub>3</sub>), isobutene (iC<sub>4</sub>) and n-butane (nC<sub>4</sub>) was recorded below approximately 468mMD RT. Background gas levels increased slightly below 515mMD RT, increasing further to low to moderate levels of methane (C<sub>1</sub>) and ethane (C<sub>2</sub>) and with continuing trace C<sub>3</sub> to C<sub>5</sub> below 556mMD RT. The maximum total gas recorded was 1.64% at 570mMD RT, consisting of 18,184ppm C<sub>1</sub>, 178ppm C<sub>2</sub>, 23ppm C<sub>3</sub>, 6ppm iC<sub>4</sub>, 4ppm nC<sub>4</sub> and 5ppm iC<sub>5</sub> and 3ppm nC<sub>5</sub>. Background levels remained moderately uniform to 587mMD RT, decreasing progressively below this depth to TD. No H<sub>2</sub>S was detected while drilling. Two isotube gas samples were collected during the period of slightly elevated gas readings between 556m and 587mMD RT, however these have not been analysed.

Depth Range (mMD RT)	Total Gas (%)	Methane (C1) ppm	Ethane (C2) ppm	Propane (C3) ppm	Iso- Butane (i- C4) ppm	Normal- Butane (n-C4) ppm	Iso- Pentane (i-C5) ppm	Normal Pentane (n-C5) ppm
325-490	0.09	1026	6	3	1	1	0	0
490-555	0.31	3278	24	4	1	1	1	2
555-583	0.85	8741	74	8	1	1	1	1
583-600	0.32	3588	26	4	1	0	0	0
600-660	0.11	1460	8	3	1	0	1	1

**TABLE 2. SUMMARY OF GAS READINGS RECORDED FOR ALL LITHOLOGY INTERVALS**

### 3.6.2 Hydrocarbon Shows Recorded in Ditch Cuttings

All ditch cuttings were examined for direct, cut and crush cut fluorescence and residues while drilling Moby-1. Cuttings of sandstone over the gross interval 562–574mMD RT within the Gurnard Formation exhibited 5-20% dull to moderately bright yellow fluorescence, with a slow to moderately fast blue-white cut and solid blue-white ring residue. At 568–571mMD RT, fluorescence increased to 60% dull to moderately bright yellow fluorescence, with an instantaneous blue-white cut and a solid blue-white residue. Nil to trace fluorescence only occurred below 574mMD RT.

### 3.6.3 Hydrocarbon Shows recorded in Sidewall Core Samples

A number of sidewall core samples over the gross interval 555.9 - 586mMD throughout the entire Gurnard Formation exhibited fluorescence. A total of eleven (11) of the sixteen (16) sidewall cores collected within the Gurnard Formation exhibited fluorescence attributable to hydrocarbons. These are listed below in Table 4.

SWC NO.	DEPTH (mRT)	Actual Lithology	Hydrocarbon Show
1	651.50	sandstone	nil
2	621.00	sandstone	nil
3	605.00	sandstone	nil
4	597.50	sandstone	nil
5	590.00	sandstone	nil
6	588.00	sandstone	nil
7	586.00	sandstone	Fair, even yellowish-white fluorescence, fast bluish-white blooming cut. Solid yellowish-white residual ring
8	585.00	sandstone	nil
9	584.00	sandstone	Fair, patch pale gold fluorescence, rapid yellowish- white streaming cut Solid bluish-white residual ring
10	580.00	siltstone	nil
11	575.70	sandstone	nil
12	574.00	siltstone	nil
13	572.00	sandstone	Patchy pale yellow fluorescence, rapid bluish-white blooming cut, faint, patchy yellowish-white residual ring
14	571.00	siltstone	Even, fair pale yellow fluorescence, Slow, poor bluish-white cut, faint, patchy yellowish-white residual ring
15	569.00	sandstone	Patchy, bright pale yellow fluorescence, Slow, bluish-white blooming cut, faint, patchy yellowish-white residual ring

SWC NO.	DEPTH (mRT)	Actual Lithology	Hydrocarbon Show
16	568.50	sandstone	Patchy, pale yellow sample fluorescence, slow, bluish-white streaming cut, bright, solid yellowish-white residual ring.
17	567.30	sandstone	Patchy pale yellow fluorescence, slow, bluish-white blooming cut, faint, solid yellowish-white residual ring.
18	566.00	sandstone	Dull to fair, even, pale yellow fluorescence, slow, bluish-white streaming cut, fair, patchy yellowish-white residual ring
19	563.00	sandstone	Dull, even pale yellow fluorescence, rapid bluish-white streaming cut, poor, pale yellow residual ring.
20	561.30	siltstone	nil
21	560.00	sandstone	Faint, patchy pale yellow fluorescence, slow, very poor bluish-white fluorescence, poor, pale yellow residual ring.
22	558.50	sandstone	nil
23	555.90	claystone	5-10% patchy dull pale yellow direct fluorescence. Solvent fluorescence not checked
24	547.00	calcilutite	nil
25	538.00	calcilutite	nil

**TABLE 3: HYDROCARBON SHOWS RECORDED IN SIDEWALL CORE SAMPLES**

### 3.7 FORMATION EVALUATION

#### 3.7.1 Borehole Temperature Data

There were no temperature surveys run in Moby-1. Three maximum recording thermometers were used on all wireline logging runs to record the borehole temperature. The following temperatures were recorded on three of the four open hole logging runs conducted at final TD (660mMD RT):

Run No.	Wireline Log	Max. Recorded Temperature (°C)	Depth (mTVDSS) (corrected to top of tool string)	Hours Since Last Circulation	t/(Tx+t)
1	DLL-MLL-MAC-ZDL-CN-GR-TTRM	42.7°C	584.8m	8.5 hrs	0.8647
2	RCI-GR (Pressure & Samples)	44.4°C	573.9m	23.25 hrs	0.9459
3	SLR-GR	45°C	633.2m	40.90 hrs	0.9685
4	SWC-GR	N/A	N/A	47.35 hrs	N/A

Note: t = Time Since Circulation Stopped; Tx=Last Circulation

**Table 2: Wireline Recorded Temperature Data**

There is a growing database of evidence to suggest that the standard Horner calculated derivation for a static bottom hole temperature (SBHT) underestimates the SBHT in many Australian offshore basins. Consequently, the Horner derived SBHT is herein modified by a factor of 1.09 which was established by Doug Waples (pers. comm.), so something of the order of 10% above Horner has been a conventional rule of thumb commonly used. This is herein referred to as the Modified Horner Technique.

Another method of calculating SBHT is the Shell Technique. This technique utilises a simple relationship that involves the proportional addition of 15<sup>o</sup>C, 30<sup>o</sup>C or 35<sup>o</sup>C to the BHT recorded on the first logging run only when measured as 50<sup>o</sup>C, 100<sup>o</sup>C or 150<sup>o</sup>C. This technique approximately coincides with a modified Horner technique (ie 1.09 x Horner) calculated temperature, however data suggests that use of this technique may slightly over-estimate the SBHT.

In Moby-1, the Horner derived SBHT is calculated as 45.6<sup>o</sup>C (Figure 7), the Modified Horner SBHT is 49.7<sup>o</sup>C and the Shell Technique derived SBHT is 55.5<sup>o</sup>C. Assuming a seabed measured temperature of 15<sup>o</sup>C, the present day geothermal gradient using the Horner SBHT is 5.75<sup>o</sup>C/100m, using the Modified Horner SBHT is 6.52<sup>o</sup>C/100m and using the Shell derived SBHT is 7.62<sup>o</sup>C/100m.

MOBY-1 - WIRELINE HORNER PLOT

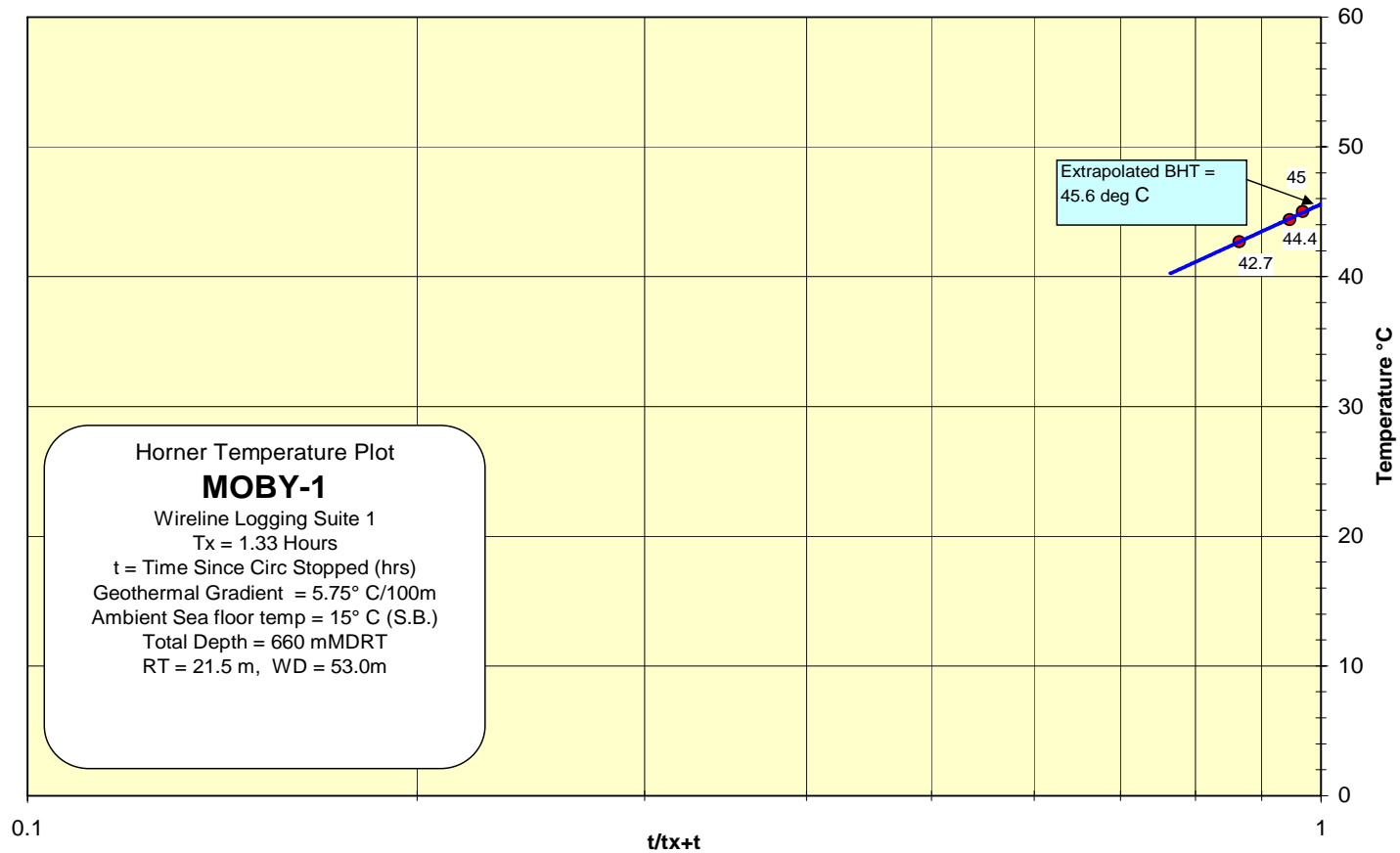


FIGURE 7 HORNER EXTRAPOLATED BHT

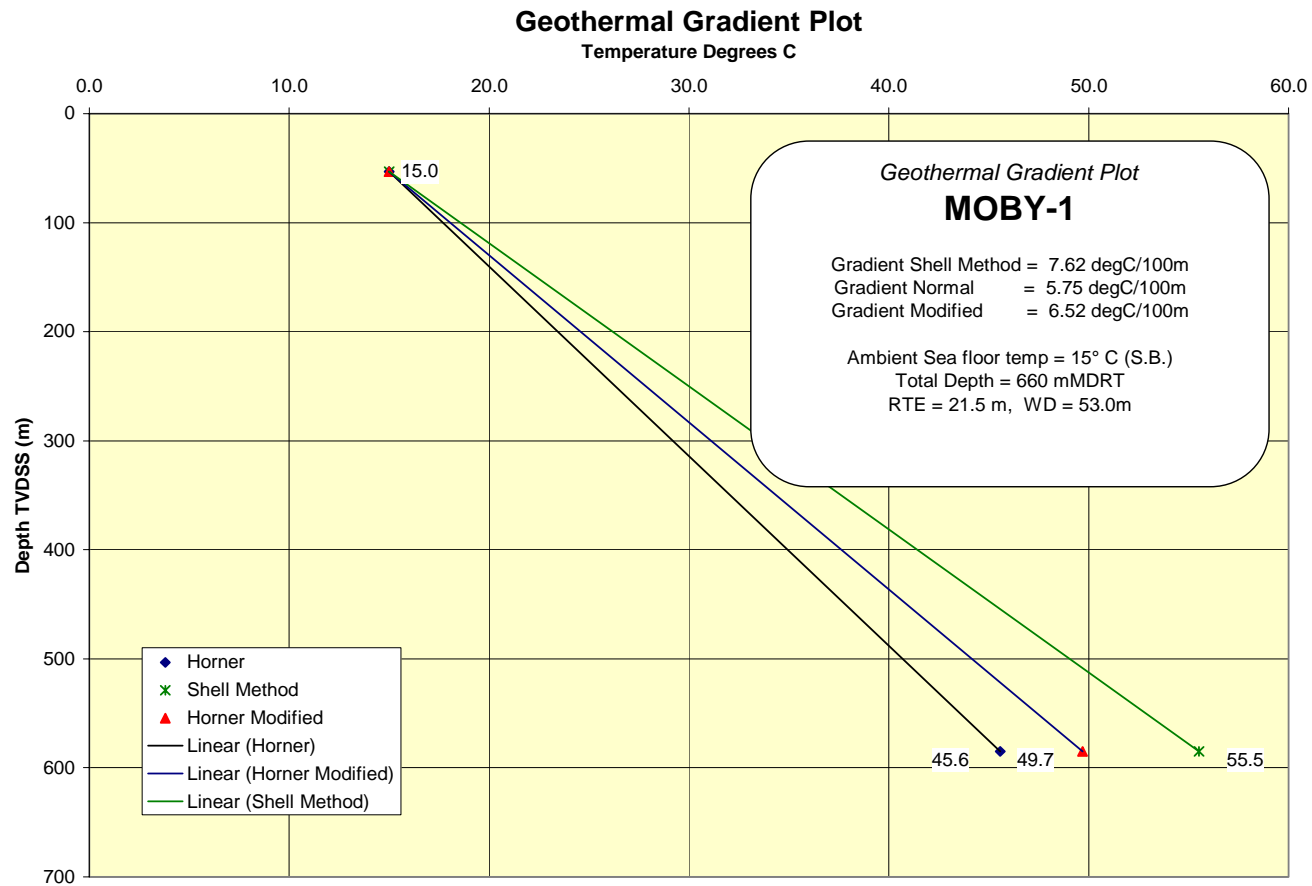


FIGURE 8 GEOTHERMAL GRADIENT PLOT

### 3.7.2 Wireline Testing

One run was made with the BakerAtlas Reservoir Characterization Instrument (RCI) in Moby-1, the results of which are presented in Section 2.2.8 of the Moby-1 Well Completion Report - Basic Data issued under separate cover. Pressure data was acquired over the gross interval 558.5-613 m MDRT across potential reservoir zones. A total of 40 pressure drawdown pre-tests were attempted, the results of which are illustrated in Figure 9 below. The cross plot clearly displays a high degree of scatter observed in the pre-test data and that no fluid gradients can be interpreted directly from these data. Mostly, the pre-test data indicates that the Gurnard Formation appears tight or having low permeability, but with no supercharging effect apparent.

In addition to collecting reservoir pressure data, two gas samples were taken at 568.8 m MDRT and a water sample was taken at 588.5 m MDRT. By applying a typical gas and water gradient through each of these respective pressure levels, it is possible to estimate a free water level at approximately 576.5 m MDRT (-555 m TVDSS) as shown in Figure 9. This depth is also consistent with the down-dip limit on seismic of the amplitude anomaly interpreted to represent gas.

For further detailed discussion and analysis of the RCI data, refer to the Petrophysical Evaluation included herein as Appendix 2 and the BakerAtlas RCI Pressure, Mobility and Gradient Report included herein as Appendix 5.

### 3.7.3 DST Testing

No drill stem test was performed on Moby-1.

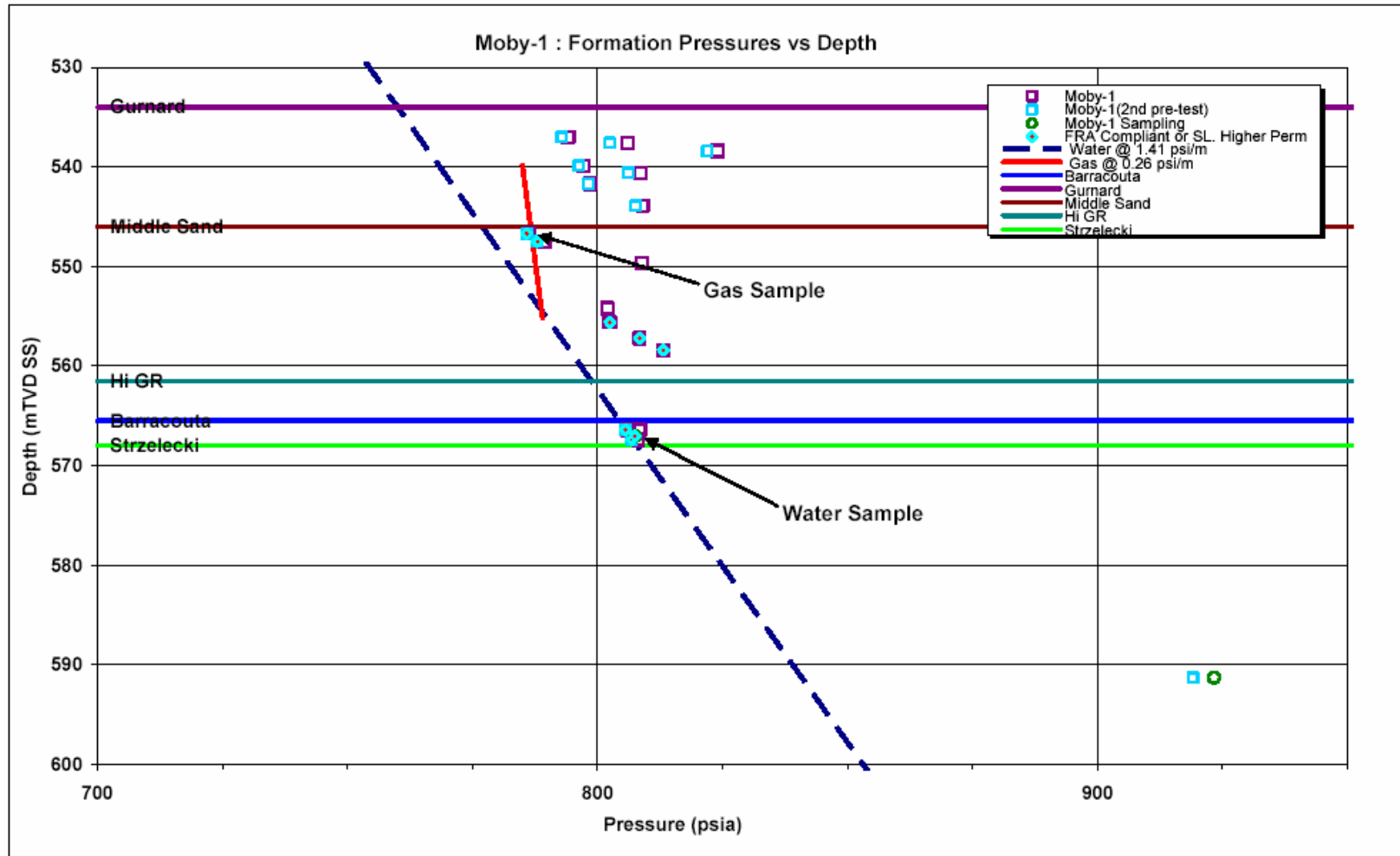


FIGURE 9: RCI PLOT OF PRESSURE DATA IN MOBY-1

### 3.7.4 Porosity, Permeability and Formation Fluids

The Gurnard Formation (555.5-587 m MDRT) which was the primary reservoir objective in Moby-1 consists of a complex lithological mix of intergradational siltstone and silty/glaucconitic sandstone which are defined petrographically as lithic arkose containing 8-12% feldspar, 5-10% lithic grains and 10-15% glauconite and mica. The sands also contain an abundant mix of detrital clay (5-10%) and authigenic clay (10-15%) matrix. The sequence also includes rare greensand and claystone interbeds. Overall, the reservoir potential improves slightly with increasing depth and coincides with a decrease in detrital clay and increasing grain size. Pore-filling cements consist of chlorite with lesser amounts of kaolinite and smectite. The main authigenic non-clay cements are siderite and pyrite which are more common in the deeper part of the section. Petrographic analysis indicates that reduction in primary porosity is largely a result of increasing amounts of diagenetic smectite-illite and kaolinite blocking pores. The high volume of iron-bearing minerals eg chlorite, siderite and pyrite means that the formation is highly acid sensitive.



FIGURE 10: IMAGE OF VERY FINE GRAINED LITHIC ARKOSE TYPICAL OF GURNARD FORMATION; SWC-11 FROM 575.7MMD

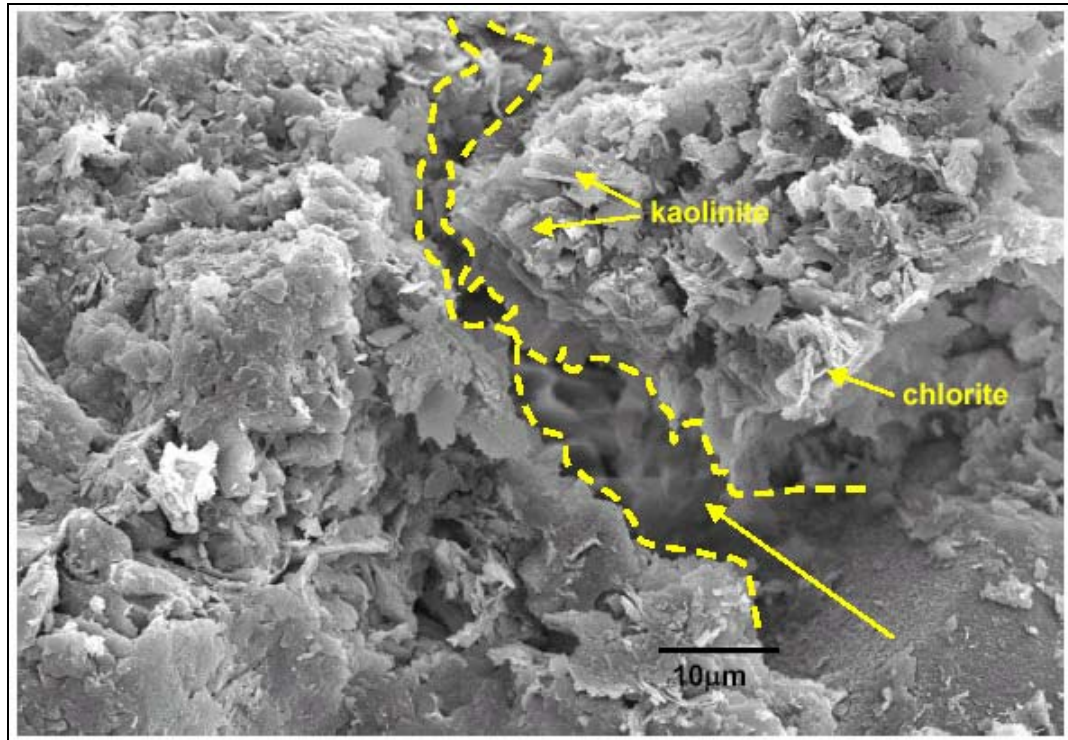


**FIGURE 11: SEM OF SWC-11 SHOWING DETAILS OF FINE GRAIN SIZE OF LITHIC ARKOSE LITHOLOGY IN GURNARD FORMATION AND DEVELOPMENT OF CHLORITE AND SMECTITE BLOCKING PORE THROATS AND REDUCING PERMEABILITY**

Full details of the petrographic analysis of the main lithologies within the Gurnard Formation are included in the petrology report by Core Laboratories Australia, included as Appendix 4.

A total of 15 of 16 percussion sidewall core samples acquired in the Gurnard Formation had basic ambient core analysis performed on them which consisted of He-injection porosity, permeability and grain density. The results of these analyses are included in Table 3 below.

SAMPLE NUMBER	DEPTH (m)	Ambient conditions		POROSITY POINT COUNT (%)	GRAIN DENSITY (g/cc)	COMMENTS
		PERMEABILITY	POROSITY TOTAL (%)			
		Kair (md)				
1	651.50	584	36.7		2.67	
2	621.00	1100	38.6		2.70	
3	605.00	781	31.6	10.6	2.69	
4	597.50	1050	35.8		2.67	
5	590.00	316	36.3		2.64	
6	588.00	446	35.9	1.6	2.65	
7	586.00	822	38.9		2.72	
8	585.00	300	36.1	3.4	2.95	
9	584.00	415	38.1		2.75	
10	580.00	1210	33.3		2.72	
11	575.70	176	34.3	6.4	2.64	
12	574.00	1240	35.9		2.67	
13	572.00	640	37.7		2.86	
14	571.00	232	39.2		2.76	
15	569.00	102	39.2		2.68	
16	568.50	417	38.1	12.0	2.71	
17	567.30					Sample not suitable for analysis
18	566.00	267	38.9		2.73	
19	563.00	140	36.6		2.77	
20	561.30	180	35.5		2.67	
21	560.00	1850	36.4		2.66	
22	558.50	247	34.2	7.6	2.67	
23	555.90					Not analysed
24	547.00					Not analysed
25	538.00					Not analysed
<b>MIN</b>		<b>102.0</b>	<b>31.6</b>	<b>1.6</b>	<b>2.6</b>	
<b>MAX</b>		<b>1850.0</b>	<b>39.2</b>	<b>12.0</b>	<b>3.0</b>	
<b>AVERAGE</b>		<b>596.0</b>	<b>36.5</b>	<b>6.9</b>	<b>2.7</b>	

**Table 3: Summary of Basic Core Analysis Results and Point Count Porosity from Petrology Analysis**

The measured porosities range from 33.3 to 39.2 % (average 36.7 %) and measured permeabilities range from 102 to 1850 md (average 549 md). These figures must be treated with care as the cores were of the percussion type which tends to be destructive in nature (refer Petrophysical Evaluation included herein as Appendix 2 for further discussion). The above mentioned porosity data should be compared to the porosity described from point count analysis in thin section of six cores as also listed in Table 3 above. The latter are generally less than 1/3<sup>rd</sup> the value measured from He-Injection core analysis. The core measured permeability data should also be treated with caution as they do not reconcile with the low mobilities observed from the RCI tool (refer Section 3.6.2 above) and they do not reconcile with the general log response which shows much less density-neutron cross-over than would be expected from gas-filled sands of this permeability and porosity (refer Petrophysical Evaluation).

Assuming cut-offs of  $V_{clay} \leq 40\%$ ,  $PHIE \geq 10\%$  and  $S_{wt} \leq 60\%$ , log analysis of the Gurnard Formation indicates there is 16.8 m of net reservoir sand with a net:gross of 53.41%, PHIE of 22.45% and  $V_{clay}$  of 28.07%. Net gas pay is calculated to be 12.5 m resulting in a net:gross of 39.67% with an  $S_{wt}$  of 46.74%. Owing to the high and variable clay content in the reservoir, means that resistivity responses will be subdued and the large amount of micro-porosity means that irreducible water volumes may be high.

The Kingfish Formation (587-589.5 m MDRT) which formed a secondary reservoir objective in Moby-1 (cf Barracouta Formation) consists of a thin interval of argillaceous

sandstone, defined petrographically as a feldspathic litharenite. A single percussion sidewall core sample from 588 m MDRT was measured with a core porosity of 35.9% and permeability of 446 md. The measured porosity compares with a point count porosity of 1.6% determined petrographically. This rock type contains abundant volcanic ash which has subsequently been altered to smectite and kaolin. Assuming the same cut-offs as those applied to the Gurnard Formation, log analysis indicates there is 2.5 m of net reservoir sand (100% net:gross) with a PHIE of 24.17% and Vclay of 7.31%. Net gas pay is nil and the interval is interpreted to be 100% water saturated. This is confirmed by interpolated RCI pressure data with a gradient of 1.41 psi/m based upon the recovery of formation water from 588.5 m MDRT.

The Strzelecki Group (589.5-660 mMDRT) consists of a thick sequence of fine to medium grained litharenite that consists mainly of volcanic and sedimentary lithic fragments and feldspar set within a matrix of authigenic clay (mainly chlorite) and minor detrital clay. Five sidewall core samples submitted for core analysis had measured porosities in the range of 31.6 to 38.6% (average 35.8%) and permeabilities in the range of 316 to 1100 md (average 766 md). The measured porosity of 31.6% at 605 m MDRT compares with a point count porosity of 10.6% determined petrographically. Assuming the same cut-offs as those applied to the Gurnard Formation and Kingfish Formation, log analysis indicates there is 1.2 m of net reservoir sand (1.7% net:gross) with a PHIE of 16.58% and Vclay of 37.14%. Net gas pay is nil and the interval is interpreted to be 100% water saturated.

A Petrophysical Evaluation of Moby-1 is included herein as Appendix 2 and a Petrophysical Summary Plot is included as Enclosure 2.

### 3.7.5 Geochemical Analysis

Geochemical analyses were performed by Geotechnical Services Pty Ltd (GeoTech), the details of which are included as Appendix 6. The analyses included:

1. one oil sample collected as a scum on top of a formation water sample during an RCI wireline test from a depth of 588.5mMD RT from the Kingfish Formation.
2. six (6) sidewall core samples collected over the gross interval 560-588mMD RT within the Gurnard Formation and Kingfish Formation. The purpose of these analyses was to characterise the hydrocarbons extracted from the sediments in terms of source, maturity and depositional environment and then correlate these findings with the oil sample recovered in Moby-1 as noted above.
3. one mud or drilling fluid sample collected while drilling at a depth of 550mMD RT. This sample was extracted and GC-MS analysis performed in an attempt to characterise the sample.

Analysis of the oil sample indicates that it is severely contaminated with an alkene-based product similar to some drilling fluids. However, the origin of the contamination is uncertain given that the mud does not contain any alkene components as itemized in the mud reports. Nor were there any alkene-based components identified during analysis of the mud sample itself.

Analysis of the six sidewall core extracts (560mMD, 568mMD, 572mMD, 584mMD, 586mMD and 588mMD) indicates that they are all biodegraded with no evidence to the

presence of any n-alkanes being visible on the saturate chromatograms. Five of the six extracts analysed are very similar to each other based upon GC-MS analysis, while the sixth sample from 588mMD is different. Based upon biomarker data from the 560mMD and 586mMD sample extracts, the hydrocarbons are characterised as mature and are thought to be sourced from strongly terrestrial organic matter and possibly with some resin input.

Although the oil sample does contain a low abundance of biodegraded hydrocarbons, it is unclear if these hydrocarbons are naturally occurring or whether they are associated with the alkene component. The biodegraded nature of both the oil sample and the Moby-1 sediment extracts indicates that the hydrocarbons may be natural, while other geochemical data suggest that the oil is different to the extracts and hence more likely due to contamination.

### 3.8 CONCLUSIONS AND CONTRIBUTIONS TO GEOLOGICAL KNOWLEDGE

- ❖ The stratigraphic section encountered in Moby-1 was essentially as predicted with all of the formation tops slightly high to prognosis.
- ❖ The primary objective Middle to Late Eocene Gurnard Formation was intersected at 555.5mMD RT (534mTVVDSS), 16m high to prediction and consists of argillaceous and silty sandstone, siltstone with minor greensand and claystone. All lithologies are generally rich in glauconite.
- ❖ Log evaluation, analysis of the RCI pressure and sampling data and core analysis confirms the likely presence of a 21m gross column of gas within the Gurnard Formation, with an estimated free water level at approximately 555mTVDSS.
- ❖ Core measured porosities through the Gurnard Formation average 36.8% (31.6-39.2%), while measured permeabilities are in the range of 102-1850md (average 543 md). These latter figures are some 30% higher than those recorded from petrographic analyses and do not reconcile with the low mobilities observed with the RCI tool and with the general log response expected from gas-filled sands of such high permeability and porosity.
- ❖ Geochemical analysis of sidewall core extracts from the Gurnard Formation and Kingfish Formation indicates that they are all biodegraded with no evidence to the presence of any n-alkanes. Based upon biomarker data, the hydrocarbons are characterised as mature and are thought to be sourced from strongly terrestrial organic matter and possibly with some resin input.
- ❖ The well reached TD within the early Cretaceous Strzelecki Group at 660mMD RT (-638.5mTVVDSS), 35 metres below the originally programmed total depth of the well. The well was subsequently plugged and abandoned as a new field gas discovery in the Gurnard Formation.

## 4. REFERENCES

**Megallaa, M., Bernecker, T. And Frankel, E., 1998.** Hydrocarbon prospectivity of the Northern Terrace, offshore Gippsland Basin, for the 1998 Acreage Release. Victorian Initiative for Minerals and Petroleum Report 56. Department of Natural Resources and Environment.

**Norvick, M. & Smith, M.A., 2001.** Mapping the plate tectonic reconstructions of southern and southeastern Australia and implications for petroleum systems. *The Australian Petroleum Production and Exploration Association Journal*, **41 (1)**, pp. 15-35.

**Norvick, M.S., Smith, M.A. & Power, M.R., 2001.** The plate tectonic evolution of eastern Australasia guided by the stratigraphy of the Gippsland Basin. In Hill, K.C. & Bernecker, T. (Eds) *Eastern Australasian Basins Symposium, A Refocused Energy Perspective for the Future*, Petroleum Exploration Society of Australia, Special Publication, pp. 15-23.

**Rahmanian, V.D., Moore, P.S., Mudge, W.J. & Spring, D.E., 1990.** Sequence stratigraphy and the habitat of hydrocarbons, Gippsland Basin. In: Brook S, J. (ed.), *Classic Petroleum Provinces*, Geological Society Special Publication No. 50, pp. 525-541.

**Thomas, H., Bernecker, T. & Driscoll, J., 2003.** Hydrocarbon Prospectivity of Areas V03-3, V03-4 - Offshore Gippsland Basin, Victoria, Australia. 2003 Acreage Release. *Victorian Initiative for Minerals and Petroleum Report 80*. Department of Primary Industries.

**Willcox, J.B., Colwell, J.B., & Constantine, A.E., 1992.** New ideas on Gippsland Basin regional tectonics. In Barton C.M., Hill, K., Abele, C. Foster, J. & Kempton, N. (Eds) *Energy, Economics and*

*Environment – Gippsland Basin Symposium*, Australasian Institute of Mining and Metallurgy, pp. 93-110.

**Willcox, J.B., Sayers, J., Stagg, H.M.J. & Van De Beuque, S., 2001.** Geological framework of the Lord Howe Rise and adjacent ocean basins. In Hill, K.C. & Bernecker, T. (Eds) *Eastern Australasian Basins Symposium, A Refocused Energy Perspective for the Future*, Petroleum Exploration Society of Australia, Special Publication, pp. 211-225.

**Wong D., Bernecker T. & Moore D., 2001.** Otway Basin. In: Woollands, M.A. & Wong, D., (eds.), *Petroleum Atlas of Victoria, Australia*. Department of Natural Resources and Environment

# **APPENDIX 1**

---

## **Well Card**

---



## Well Card: Moby-1

<b>Location</b>	Latitude	38° 01' 44.25" S		<b>Participating Interests</b>		
	Longitude	148° 30' 27.40" E		Bass Strait Oil Company Ltd (Operator)	40%	
	UTM Co-ordinates	632,316.41m E 5,789,884.86m N		Eagle Bay Resources NL	25%	
	Datum	AGD 66		Moby Oil & Gas Limited	35%	
	Elevation	+21.5m				
	Water Depth	53m (MSL)				
<b>Permit</b>	VIC/P47			Primary Objective	Gurnard Fm	
<b>Rig on Contract</b>	02:45 Hrs 5 <sup>th</sup> October 2004			Secondary Objective	Barracouta	
<b>Spudded</b>	16:45 Hrs 7 <sup>th</sup> October 2004					
<b>Reached T.D.</b>	20:30 Hrs 11 <sup>th</sup> October 2004			<b>Completion Details/Plugs</b>		
<b>Rig Released</b>	13:00 Hrs 17 <sup>th</sup> October 2004			Plug # 1	660 – 505m	42.8 bbls of 15.8 ppg Class G
<b>Structure Type</b>		Faulted 4-way dip anticline		Plug # 2	370 – 270m	43 bbls of 15.8 ppg Class G
<b>Rig</b>	DOGC Semi-Submersible	"Ocean Patriot"		Plug # 3	160 - 100	30 bbls of 15.8 ppg Class G
<b>Status</b>	P & A	Gas Discovery		<b>Casing Details</b>		
<b>Hole Size (mm)</b>	660 x 914	445	311	Size (mm)	Wt (ppf)	Depth (m)
<b>Depth (m)</b>	101	325	328	508 x 762	133 x 330	97.5
<b>Hole Size (mm)</b>	216			340	68	321.76
<b>Depth (m)</b>	660					
<b>Total Depth</b>	660mMD	638.5mTVDSS				

<b>Formation</b>	<b>Depth (mMD RT)</b>	<b>Depth (mTVD SS)</b>	<b>Thickness (m)</b>	<b>TWT (ms)</b>	<b>Remarks</b>
Gippsland Limestone (Seafloor)	74.5	53.0	435.9	70.7	
Lakes Entrance Fm	510.4	488.9	45.1	513.5	
Early Oligocene Wedge	553.0	531.5	2.5	557.0	
Gurnard Fm	555.5	534.0	31.5	559.0	
Kingfish Fm	587.0	565.5	2.5	590.1	
Strzelecki Group	589.5	568.0	70.5+	592.6	
<b>TOTAL DEPTH</b>	660.0	638.5		651.7	Approx. TWT

### WIRELINE LOGGING SUMMARY

<b>RUN</b>	<b>TOOL STRING</b>	<b>INTERVAL (M)</b>	<b>BHT (C)/TIME SINCE CIRC.</b>	<b>PLAYBACK SCALES</b>
1	DLL-MLL-MAC-ZDL-CNL-DSL-TTRM	659 – 321.5m (GR-MAC to 75m)	42.7 @ 584.8m/8.5 Hrs	1:200 1:500
2	RCI-GR	613 – 558.5m; 22 P/T with 13 repeat draw-downs; 1 x LS; 17 good; 4 x curtailed; take 2 x 840cc gas samples at 568.8m and 1 x 4l water sample at 588.5m	44.4 @ 573.9m/23.25 Hrs	1:200 1:500
3	SLR (VSP)	650 – 90m	45 @ 633.2m/40.9 Hrs	
4	SWC-GR	651.5 – 538m (Shot 25; Rec 25)	NR	



## CORE SUMMARY

Core	Interval	Cut	Recovered	%
NO CONVENTIONAL CORES WERE CUT				

## SIDEWALL CORES

SWC No.	DEPTH (mRT)	REC (cm)	Actual Lithology	SWC No.	DEPTH (mRT)	REC (cm)	Actual Lithology
1	651.50	4.2	sandstone	14	571.00	4.2	siltstone
2	621.00	3.5	sandstone	15	569.00	3.8	sandstone
3	605.00	3.5	sandstone	16	568.50	3.6	sandstone
4	597.50	3.5	sandstone	17	567.30	3.0	sandstone
5	590.00	3.5	sandstone	18	566.00	5.0	sandstone
6	588.00	5.0	sandstone	19	563.00	3.5	sandstone
7	586.00	4.3	sandstone	20	561.30	4.1	siltstone
8	585.00	4.4	sandstone	21	560.00	5.0	sandstone
9	584.00	3.2	sandstone	22	558.50	5.0	sandstone
10	580.00	3.5	siltstone	23	555.90	4.5	claystone
11	575.70	4.8	sandstone	24	547.00	4.2	calclutite
12	574.00	3.5	siltstone	25	538.00	5.0	calclutite
13	572.00	4.0	sandstone				

## WELL TESTING SUMMARY

DRILL STEM TESTS (DSTs) No DSTs were conducted								
Test No.	Formation	Perforation Interval (m)	Flow Min	Shut Min	Ship Psig	Fthp Psig	Chokes	Remarks

## DRILLING SUMMARY

<p>The Diamond Offshore General Company MODU "Ocean Patriot" was mobilized from the Tap Oil Tawatawa-1 location off the east coast of New Zealand and towed across the Tasman Sea by two AHSV's ("Far Grip" &amp; "Pacific Wrangler"). Moby-1 operations commenced at 02:45 Hrs 5<sup>th</sup> October 2004, when the first anchor was dropped at the Moby-1 location. Anchor handling operations were delayed by bad weather, while additional delays were caused by having to re-run a number of anchors. Positioning the rig on location was completed by 05:30 Hrs 7<sup>th</sup> October 2004 at which time the rig was ballasted down to drilling draft. The final location for Moby-1 was confirmed as being 2.4m from the proposed location on a bearing of 270.28<sup>o</sup> True. The final fix for Moby-1 was:</p> <p style="margin-left: 40px;">Latitude: 38<sup>o</sup> 01' 44.25" S  Longitude: 148<sup>o</sup> 30' 27.40" E  Easting: 632, 316.41m  Northing: 5, 789, 884.86m  DATUM: AGD 66.</p> <p>The TGB was run and landed at 74.5mMD RT. Made up 914mm (36") BHA and ran in hole with ROV assisting through TGB and tagged seafloor at 74.5m corrected to Mean Sea Level (MSL). The water depth at Mean Sea Level was recorded as 53.0m, with a drill floor elevation of 21.5m. The well was spudded at 16:45 Hrs 7<sup>th</sup> October 2004 with a 914mm (36") hole drilled from seafloor (74.5mMD RT) to a depth of 101mMD RT, pumping 50 bbl gel sweeps every 9m. Ran 762mm (30") casing and cemented with 758.8 sacks (160.8 bbl), cement slurry at 15.8 ppg.</p> <p>Made up 445mm (17 1/2") BHA and installed guide ropes to BHA and guide lines. Ran in hole and tagged cement at 96.7mMD RT. Drilled cement and casing shoe from 96.7mMD to 98mMD RT and continued drilling to 325mMD RT, pumping 40 bbl guar gum sweeps every 15m and 50 bbl gel sweeps before every connection. Pumped 100</p>
--

bbl hi-vis sweep at 1100gpm and conducted wiper trip to 762mm (30") casing shoe. Took weight at 315mMD RT and reamed back to 325mMD RT. Circulated bottoms up at 1100 gpm and displaced hole to 350 bbl hi-vis mud. Dropped single shot survey tool and pulled out of hole to 203mMD RT. Recovered survey tool and continued pulling out of hole, jetting 762mm (30") housing on the way out of hole.

Ran 340mm (13 3/8") casing to 321.8mMD RT and cemented with 140 bbls (295 sacks) of 12.5 ppg Class G Lead cement followed by 71 bbls (335 sacks) of 15.8 ppg Class G Tail cement. Displaced cement with 116 bbls of seawater. Bumped plugs and pressure tested casing to 2000 psi. Observed returns to seabed throughout cementing. Ran BOP's while testing choke and kill lines to 300 psi for 5 minutes and 3000 psi for 10 minutes and marine riser. Landed BOP's and pressure tested wellhead connection to 300 psi for 5 minutes and 3000 psi for 10 minutes.

Made up 311mm (12 1/4") bit and ran in hole. Washed down from 286mMD RT and tagged top of cement at 295.5mMD RT. Drilled plugs, cement and shoe track and cleaned rat hole to 325mMD RT. Drilled ahead in 311mm (12 1/4") hole from 325m to 328mMD RT. Displaced well to 10 ppg KCL/Polymer mud system, displacing choke and kill lines. Pressure tested lines to 1000 psi and performed FIT to 1.7 SG (14.16 ppg), OK. Pulled out of hole laying down 311mm (12 1/4") BHA.

Made up 216mm (8 1/2") BHA and ran in hole to 328mMD RT and drilled ahead to 660mMD RT (TD), taking Anderdrift survey every connection. Circulated hole clean, dropped multi-shot and pulled out of hole from 660m to 248mMD RT, working tight spots between 612m and 560mMD RT. Finished pulling out of hole and retrieved EMS tool.

Rigged up Baker Atlas for running wireline logs and ran the following logs; RUN#1: DLL-MLL-MAC-ZDL-CNL-DSL-TTRM over the interval 659-321.5mMD RT with GR-MAC through casing to 75mMD RT; RUN#2: RCI-GR over the interval 558.3-612.8mMD RT for pressures and samples; RUN#3: SLR-GR (VSP survey) over the interval 659-80mMD RT and RUN#4: SWC-GR over the interval 651.5-538mMD RT; shot 25 cores, recovered 25 cores; rigged down Baker Atlas.

Commenced plug and abandonment operations at 22:30 Hrs 13th October 2004. Picked up and ran in hole with 73mm (2 7/8") tubing cement stinger on 127mm (5") drill pipe to 650mMD RT and pumped 42.8 bbls of 15.8 ppg Class G cement slurry setting Plug#1 from 660mMD to 505mMD RT. Pulled out of hole to 370mMD RT and pumped 43 bbls of 15.8 ppg Class G cement slurry setting Plug#2 from 370mMD to 270mMD RT. Ran in hole with 127mm (5") open ended drill pipe and tagged top of cement Plug#2 at 259mMD RT. Pressure tested casing against lower annular to 500 psi, OK. Picked up 340mm (13 3/8") cement retainer and ran in hole to 160mMD RT and set same. Pumped 30 bbls of 15.8 ppg Class G cement slurry, setting cement Plug#3 from 160m to 100mMD.

Picked up wellhead jetting tool and wear bushing retrieval tool and ran in hole to 74mMD RT while jetting stack and wellhead. Landed out wear bushing retrieval tool and pulled out of hole. Pulled riser and BOP's and secured same. Picked up 508mm x 762mm (20" x 30") spear and cutting assembly and ran in hole stabbing into 18 3/4" wellhead and cut 508mm (20") casing at 77.39mMD RT and pulled out of hole with casing cut-off stub and housing. Re-dressed spear and RIH, stabbing into 762mm (30") housing, cutting 762mm (30") casing at 76.84mMD RT.

Commenced anchor handling operations at 18:00 Hrs 16<sup>th</sup> October 2004. Last anchor racked at 13:00 Hrs 17<sup>th</sup> October 2004 and the rig released to Santos. Total time on Moby-1 location was 12.427 days.

## GEOLOGICAL SUMMARY

Moby-1 was spudded at 16:45 Hrs 7<sup>th</sup> October 2004 and penetrated a sedimentary section ranging in age from Tertiary to Late Cretaceous. The stratigraphic section encountered was essentially as predicted with all of the formation tops slightly high to prognosis. A comparison of the Actual and Predicted section drilled in Moby-1, including a brief summary of drilling and formation evaluation data is included in Enclosure 2. The geological formations and data encountered for each hole section are discussed below.

The Miocene to Pliocene Gippsland Limestone was encountered at seafloor (covered by a veneer of Recent sediments) at 74.5mMD RT (-53mTVDSS), the upper part of which down to a depth of 325mMD RT was drilled riserless in the 914mm (36") and 445mm (17 1/2") hole sections. Intermediate 340mm (13 3/8") casing was subsequently run to 321.8mMD RT and the BOP's and marine riser nipped up, below which 311mm (12 1/4") hole was drilled to 328mMD RT and 216mm (8 1/2") hole was drilled to total depth at 660mMD RT (-638.5mTVDSS). The main hole sections to total depth were wireline logged after reaching TD and provide the depth control for the stratigraphic sub-divisions included herein, together with the assistance of biostratigraphic control.

The lower part of the Gippsland Limestone below 325mMD RT consists of argillaceous calcilutite with minor calcarenite and argillaceous calcisiltite. The base Gippsland Limestone/Top Lakes Entrance Formation is identified at 510.4mMD RT (-488.9mTVDSS). It was encountered 63.9 metres low to prognosis, based upon the appearance of marl in the section. The Oligocene to early Miocene Lakes Entrance Formation consists of marl grading to and interbedded with argillaceous calcilutite, calcilutite and calcareous claystone. The basal part of the Lakes Entrance Formation is differentiated at 553mMD RT (-531.5mTVDSS) and defined herein as the Early Oligocene Wedge.

The primary objective Middle Eocene Gurnard Formation was intersected at 555.5mMD RT (534mTVDSS), 16m high to prediction and consists of argillaceous and silty sandstone, siltstone with minor greensand and claystone. All lithologies are generally rich in glauconite. The Early Eocene Kingfish Formation was intersected at 587mMD RT (565.5mTVDSS), 9.5m high to prognosis. The interval which is only 2.5m thick and consists of feldspathic lithic sandstone, rests unconformably on the Early Cretaceous (Late Albian) Strzelecki Group at 589.5mMD RT (-568.0mTVDSS), 17m high to prognosis. The Strzelecki Group consists predominantly of argillaceous lithic sandstone.

The well reached TD within the Strzelecki Group at 660mMD RT (-638.5mTVDSS), which was reached at 20:34 Hrs 11<sup>th</sup> October 2004. Baker Atlas wireline logs were run at this depth. The primary wireline log recorded was the DLL-MLL-MAC-DSL-ZDL-CN-TTRM-4401 which was logged from 659m to 321.5mMD RT, after which the GR-MAC were logged up through casing to the seafloor, although the acoustic signal deteriorated towards the seafloor. This log represents the primary depth control for Moby-1. TD was shallow to driller's TD by 1m owing to possible fill on bottom and the 340mm (13 3/8") casing shoe was found 0.25m shallower than driller's depth. The second logging run was with the RCI-GR tool for formation pressures and samples, which was logged from 613m to 558.5mMD RT after being tied into the first logging run for depth control. A total of 40 pre-test levels were attempted which included 13 repeat tests and 4 tests were tight; collected 2 x gas samples at 568.8mMD RT within the Gurnard Formation and 1 x formation water sample at 588.5mMD RT from the Barracouta Formation.

The third run in the hole was for a VSP/checkshot survey with the SLR tool across the interval 650-90mMD RT and the fourth run was to acquire percussion sidewall cores (SWC-GR). Twenty five (25) shots attempted and 25 cores were successfully recovered (100%).

Trace to minor amounts of total gas consisting entirely of methane (C<sub>1</sub>) were recorded upon commencement of first drilling returns in the 311mm (12 1/4") hole section below 325mMD RT and which continued in the 216mm (8 1/2") hole section. Trace amounts of ethane (C<sub>2</sub>), pentane (C<sub>3</sub>), iso-butane (iC<sub>4</sub>) and n-butane (nC<sub>4</sub>) were recorded below approximately 468mMD RT. Background gas levels increased slightly below 515mMD, increasing further to low to moderate levels of methane (C<sub>1</sub>) and ethane (C<sub>2</sub>) and continuing trace C<sub>3</sub> to C<sub>5</sub> below 556mMD. The maximum total gas recorded was 1.64% at 570mMD, consisting of 18,184ppm C<sub>1</sub>, 178ppm C<sub>2</sub>, 23ppm C<sub>3</sub>, 6ppm iC<sub>4</sub>, 4ppm nC<sub>4</sub> and 5ppm iC<sub>5</sub> and 3ppm nC<sub>5</sub>. Background levels remained moderately uniform to 587mMD, decreasing progressively below this depth to TD.

Sandstone cuttings over the gross interval 562-574mMD RT exhibited 5-20% dull - moderately bright yellow fluorescence, with a slow to moderately fast blue-white cut and solid blue-white ring residue. At 568-571mMD RT, fluorescence increased to 60% dull to moderately bright yellow fluorescence, with an instantaneous blue-white cut and a solid blue-white residue. Nil to trace fluorescence only occurred below 574mMD RT. Weak to moderate fluorescence was exhibited in eleven sidewall core samples over the gross interval 555.9-586mMD RT, entirely within the Gurnard Formation.

Final total depth was 660mMD RT (-638.5mTVDSS). This is 35 metres below the originally programmed total depth of the well.

Log evaluation, analysis of the RCI pressure and sampling data and core analysis confirms the likely presence of a 21m gross column of gas within the Gurnard Formation, with an estimated free water level at approximately 555mTVDSS. Core measured porosities through the Gurnard Formation average 36.8% (31.6-39.2%), while measured permeabilities are in the range of 102-1850md (average 543 md). These latter figures are some 30% higher than those recorded from petrographic analyses and do not reconcile with the low mobilities observed with the RCI tool or with the general log response expected from gas-filled sands of such high permeability and porosity. Moby-1 was plugged and abandoned as a new field gas discovery and the rig released at 13:00 hrs 17<sup>th</sup> October 2004. A composite well log of the lithology intersected in Moby-1 is included as Enclosure 1.

## **APPENDIX 2**

---

# **Petrophysical Report**

---

**By The Saros Group Pty Ltd**

# Petrophysical Evaluation Moby-1

Prepared for:  
**Bass Strait Oil Company Ltd**

**CONFIDENTIAL**

The Saros Group Pty Ltd

Petroleum Services

P.O. Box 2079

MILTON QLD 4064



**the saros group**  
Our experts. Your results.

All interpretations are opinions based on inferences from electrical, core, fluid or other measurements and we cannot and do not guarantee the accuracy or correctness of any interpretations, and we shall not except in the case of gross or willful negligence on our part be liable or responsible for any loss costs, damages or expenses incurred or sustained by anyone resulting from any interpretation made by the authors of this report.

**DOCUMENT ISSUE APPROVAL**

Project and Document No:	BSO01
Document Version	Version 1 Draft
Date	20/01/2005
Title	Petrophysical Evaluation Moby-1
Client	Ian Reid – Bass Strait Oil Company
Document Name	BSO1 Petrophysical Evaluation Moby-1.doc

	Name	Position	Signature	Date
Prepared by:	Paul Theologou	Petrophysicist		15 <sup>th</sup> January, 2005
Reviewed by:	Tony Zoitsas	Director		16 <sup>th</sup> January, 2005

**DISTRIBUTION**

Organisation	Attention	Copy Nos.	Comment	Actioned
BSOC	Ian Reid	1	Draft via email	16/1/05
LPM	Bob Fisher	1	Draft via email	16/1/05
BSOC	Ian Reid	2	Final Copy	19/1/05

## TABLE OF CONTENTS

<b>INTRODUCTION .....</b>	<b>1</b>
<b>DATA AVAILABILITY AND QUALITY .....</b>	<b>1</b>
Mudlog & Drilling Data .....	1
Wireline Log Data .....	1
Formation Test Data .....	1
Formation Pressure Data .....	1
Percussion Sidewall Cores .....	2
Geochemistry .....	2
Petrology .....	3
Core Analysis .....	3
<b>BOREHOLE DATA .....</b>	<b>4</b>
Hole Conditions .....	4
Mud Properties .....	4
<b>SHOWS .....</b>	<b>4</b>
<b>LOG ANALYSIS METHODOLOGY .....</b>	<b>6</b>
Preparation .....	6
Log QC and Environmental Corrections .....	6
Interpretation Technique .....	6
Lithology .....	6
Fluid parameters .....	7
Formation Brine .....	7
Porosity Determination .....	7
From MULTIMIN Analysis .....	7
Saturation Evaluation .....	7
Dual-Water Equation .....	8
Saturation equation parameters .....	8
Permeability Evaluation .....	9
<b>CUTOFFS .....</b>	<b>9</b>
<b>RESULTS .....</b>	<b>9</b>
<b>RECOMMENDATIONS .....</b>	<b>10</b>
<b>APPENDIX 1: FORMATION PRESSURE DATA SUMMARY .....</b>	<b>11</b>
<b>APPENDIX 2: MULTIMIN REPORTS .....</b>	<b>13</b>
<b>ENCLOSURE 1: EVALUATION SUMMARY DEPTH PLOT (1:200) .....</b>	<b>19</b>

### Tables

Table 1. Summary of wireline log suites

Figure 1. RCI Plot for Moby-1.

Figure 2. Porosity permeability data from analysis of percussion sidewall cores. The permeability data is interpreted to be erroneously high due to the effects of sample disruption during coring.

Table 2. Summary of basic core analysis results and point count porosity from percussion sidewall cores in Moby-1.

Table 3. Summary of oil and gas shows as recorded by the wellsite geologist.

Figure 3. Mudlog from Moby-1 over the Gurnard Formation.

Table 4. Summary of cutoffs applied in this analysis

Table 5. Reservoir and pay lumping summary.

## INTRODUCTION

Moby-1 is located in VIC/P47 approximately 350km east of Port Melbourne and 5 km east of the Patricia-Baleen subsea completion. Moby-1 was drilled as a gas exploration well in the VIC/P47 Block of the Gippsland Basin offshore Victoria.

The Moby-1 well was designed to test the Moby Prospect, primarily to target the seismic amplitude anomaly identified on the Baleen 3D survey, interpreted to represent gas within reservoirs of the Gurnard Formation. Although the Moby Prospect is present on a significant anticline with over 70km<sup>2</sup> areal closure, it was drilled in a crestal location by Flathead-1 and Whale-1 which were both interpreted to have failed to encounter suitable reservoirs within the Gurnard Formation. Better reservoir development is interpreted from well and seismic data to exist downdip at the Moby-1 location. The key geological issues relating to the economic success of Moby-1 pre-drill were reservoir quality and gas composition. Gas was considered likely, although oil may also occur.

## DATA AVAILABILITY AND QUALITY

### Mudlog & Drilling Data

Moby-1 was spudded on the 7<sup>th</sup> October 2004 and was drilled with the 17 ½" hole section was drilled to 325m after which the 13 3/8" casing was set. The 12 ¼" hole was then drilled to 328m as part of a casing cleaning trip. The TD section of the hole was then drilled with an 8 ½" bit to a depth of 660mRT.

### Wireline Log Data

Wireline logging of Moby-1 was performed by Baker Atlas. Table 1 summarises the logs acquired.

Suite/Run	Tool String	Interval (mMDRT)	BHT (degC)
1 / 1	DLL-MLL-MAC-ZDL-CNL-DSL-TTRM	659 - 321.5m (GR to 75m)	42.7
1 / 2	RCI-GR	613 - 558.5m Take 21 P/T levels, 13 repeat; 4 tight; took 2 x samples at 568.8m and 1 x sample at 588.5m	44.4
1 / 3	MLR (VSP)	650 - 90m	45.0
1 / 4	SWC - GR	651.5 - 538m; Shot 25; Rec 25	N/A

**Table 1. Summary of wireline log suites**

### Formation Test Data

#### Formation Pressure Data

A RCI-GR tool was run over the potential reservoir intervals in Moby-1 and 40 drawdown pre-tests were attempted. Baker Atlas conducted a Formation Rate Analysis (FRA) on the pre-test data and concluded only 3 of the pre-tests were FRA compliant. In the majority of the other cases cylindrical flow was not observed and therefore formation pressures were not considered to be reliable. In some of the non-FRA compliant cases, a higher mobility was observed and the pressures in these 5 cases were considered acceptable to use (Appendix 1). Figure 1 is a plot of formation fluid pressure data from Moby-1. This plot clearly shows the high degree of scatter observed in the pre-test data, and that no fluid gradients can be interpreted directly from this data. Two gas samples were taken at 568.8 mRT, and a water sample was taken at 588.5 mRT. These sample points also correspond with build-up analysis indicating either FRA compliant or close to FRA compliant data. In order to try and define the free water level, typical values for water and gas gradients have been applied to the

pressure data at the sample points, which results in an estimated free water level at approximately 555 mTVDSS. This is consistent with the downdip limit on seismic of the amplitude anomaly, interpreted to represent gas (Ian Reid, personal communication).

Figure 1 also shows that there is a definite trend of over estimation of formation pressure in the non-FRA compliant tests. Baker-Atlas have indicated that this is the result of low formation permeability but not super-charging.

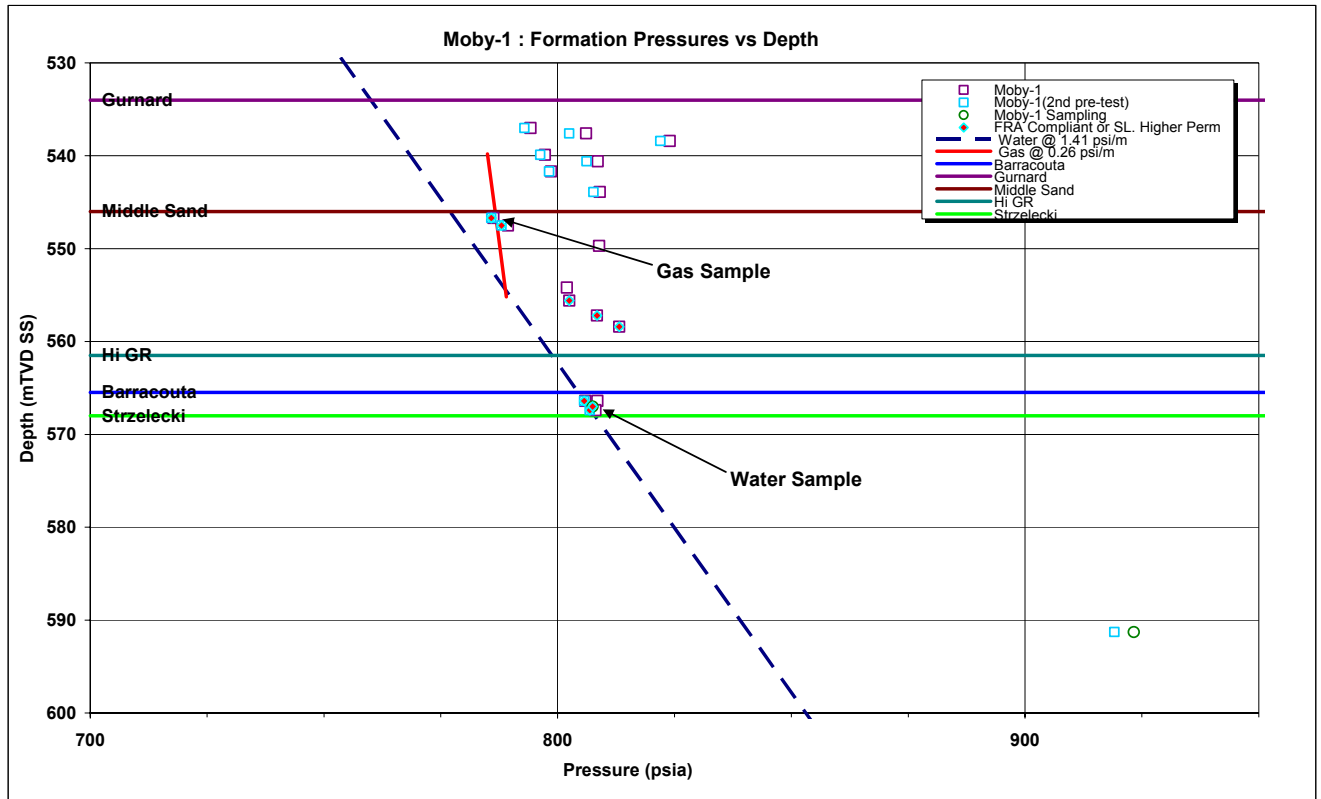


Figure 1. RCI Plot for Moby-1.

**Percussion Sidewall Cores**

A total of 25 percussion sidewall cores were recovered from 25 attempts. A comprehensive SWC evaluation program was undertaken to attempt to characterise the formation. The evaluation program consisted of the following components - Palynology (8 samples) – for stratigraphic correlation; geochemistry (5 samples) – to characterise hydrocarbons; petrology (6 samples) – to identify mineral species, diagenetic history and porosity, permeability and grain density (22 samples) – to characterize reservoir potential/properties. Additional palynological samples are being evaluated but are not expected to affect this petrophysical evaluation.

*Geochemistry*

Five samples which showed fluorescence were extracted to try and identify the properties of any liquid hydrocarbons present, and the relationship to the gas phase within the reservoir. At the time of this report, the geochemical analysis was in progress however initial results indicate that the liquid phase is a biodegraded extract.

### Petrology

Six samples were sent for petrological analysis which included thin section description, XRD and SEM (core Laboratories, 2005). These samples are texturally and compositionally dissimilar, but can be separated into two groups. The shallowest samples are well sorted; the deeper samples are poorly to moderately sorted. Petrographically, these samples vary from being lithic arkoses (rich in potassium feldspars) to litharenites (rich in volcanic rock fragments), some of which are feldspathic. Detrital clay tends to decrease with depth. Grain size generally increases towards the bottom, varying from upper very fine grained (0.090 mm) to lower medium grained (0.320 mm). Samples within the Gurnard formation also contain up to 13% glauconite, and heavy minerals such as zircon and rutile were found to be up to 10% in volume. The presence of these radioactive heavy minerals explains the high gamma ray recorded between 583 and 587 mRT.

Pore-filling cements consist of common to abundant chlorite, with smaller amounts of kaolinite and smectite. The main authigenic non-clay cements are siderite and pyrite; these minerals are more common in the deepest samples. Petrographic analysis indicated that the reduction of primary porosity was largely the result of increasing amounts of diagenetic smectite-illite and kaolinite blocking pores. The high volume of iron bearing minerals eg chlorite, siderite and pyrite means that the formation is highly acid sensitive and care should be taken in planning stimulation programmes.

### Core Analysis

Twenty two samples had basic ambient core analysis performed on them which consisted of He-injection porosity, permeability and grain density. Figure 2 is a plot of porosity – permeability data from the percussion sidewall core data. The measured porosities range from 31.6 to 39.2 %, and the measured permeability ranges from 102 to 1850 md. The nature of the coring method tends to be quite destructive and core analysis results should be treated with due care, in particular permeability measurements. It is considered unlikely that these permeabilities are representative of the true formation permeability as they do not reconcile with the low mobilities observed from the RCI tool, and they do not reconcile with the general log response which shows much less D-N gas cross-over than would be expected from gas filled sands of this permeability and porosity.

Table 2 is a summary of the basic core data and also shows a comparison between the measured core porosity and that described from point counting in thin sections. There is a large difference between the two values with the point count porosity being generally less than 1/3 the value measured from He Injection core analysis. This difference is interpreted to be the result of the high degree of micro-porosity being present within the samples. The micro-porosity will not tend to be recorded by the petrologist – instead this will be associated with the clay volumes counted, however micro-porosity will be included as part of the He injection porosity measurement. The high degree of micro-porosity compared with visible porosity supports the low formation mobility indicated by the RCI pre-tests, and is at odds with the high permeability measured in the laboratory.

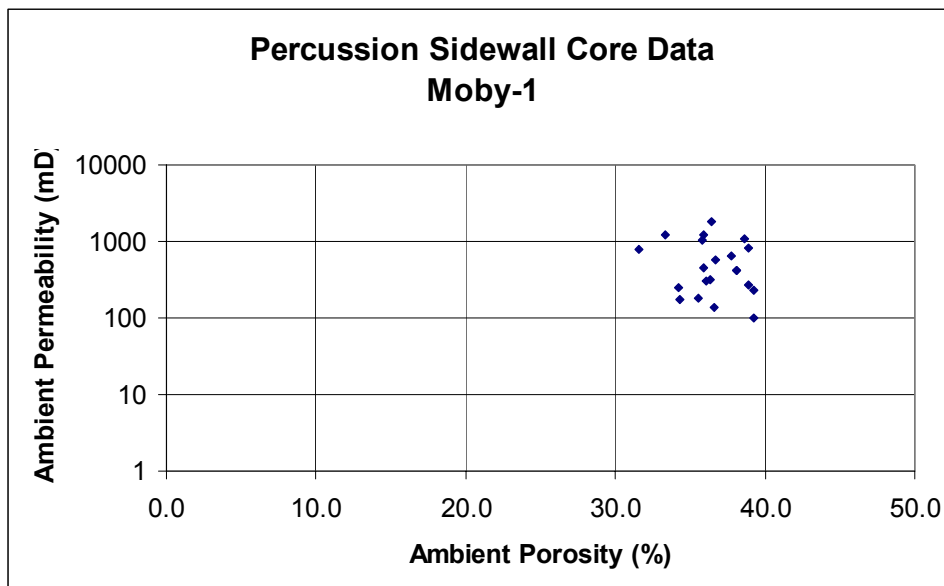


**Figure 2. Porosity permeability data from analysis of percussion sidewall cores. The permeability data is interpreted to be erroneously high due to the effects of sample disruption during coring.**

SAMPLE NUMBER	DEPTH (m)	Ambient conditions		POROSITY POINT COUNT (%)	GRAIN DENSITY (g/cc)	COMMENTS
		PERMEABILITY	POROSITY TOTAL (%)			
		Kair (md)				
1	651.50	584	36.7		2.67	
2	621.00	1100	38.6		2.70	
3	605.00	781	31.6	10.6	2.69	
4	597.50	1050	35.8		2.67	
5	590.00	316	36.3		2.64	
6	588.00	446	35.9	1.6	2.65	
7	586.00	822	38.9		2.72	
8	585.00	300	36.1	3.4	2.95	
9	584.00	415	38.1		2.75	
10	580.00	1210	33.3		2.72	
11	575.70	176	34.3	6.4	2.64	
12	574.00	1240	35.9		2.67	
13	572.00	640	37.7		2.86	
14	571.00	232	39.2		2.76	
15	569.00	102	39.2		2.68	
16	568.50	417	38.1	12.0	2.71	
17	567.30					Sample not suitable for analysis
18	566.00	267	38.9		2.73	
19	563.00	140	36.6		2.77	
20	561.30	180	35.5		2.67	
21	560.00	1850	36.4		2.66	
22	558.50	247	34.2	7.6	2.67	
23	555.90					Not analysed
24	547.00					Not analysed
25	538.00					Not analysed
<b>MIN</b>		<b>102.0</b>	<b>31.6</b>	<b>1.6</b>	<b>2.6</b>	
<b>MAX</b>		<b>1850.0</b>	<b>39.2</b>	<b>12.0</b>	<b>3.0</b>	
<b>AVERAGE</b>		<b>596.0</b>	<b>36.5</b>	<b>6.9</b>	<b>2.7</b>	

**Table 2. Summary of basic core analysis results and point count porosity from percussion sidewall cores in Moby-1.**

## BOREHOLE DATA

### Hole Conditions

In general the borehole was in good condition over the reservoir section. The good borehole conditions have allowed acquisition of a good quality wireline dataset throughout most of the interval.

### Mud Properties

The well was drilled using a KCL-PHPA mud through the target formations (KCl of 6 wt%). The mud weight through the 8 ½" section was approximately 10 lb/gal.

## SHOWS

Relatively poor shows were observed. Table 3 is a summary of the oil and gas shows observed by the wellsite geologist on Moby-1. Maximum shows were observed over the interval 562 – 574 mRT by both a gas peak over background and up to 60% direct fluorescence. Figure 3 is a graphical display of the mudlog over the main target interval.

Gas Data									
Depth (mRT)	Type	% TG	C1 ppm	C2	C3	iC4	nC4	iC5	NC5
328 – 490m	BG	0.09	1008	6	3	1	1	1	2
490 - 555	BG	0.31	3278	24	4	1	1	1	2
555 – 574	BG	0.98	9968	85	10	1	1	1	1
574 – 583	BG	0.57	6158	52	5	1	1	1	1
583 - 600	BG	0.32	3588	26	4	1	0	0	1
600 - 660	BG	0.11	1460	8	3	1	1	1	1

Type: TG-Total Recorded Gas (%), BG-Back Ground (%), P-Peak, C-Connection, T-Trip, W-Wipertrip, FC-Flow Check, P-Pumps off

Oil Show								
Depth (mRT)	Oil stain	Fluor% / Color	Fluor Type	Cut Fluor	Cut Type	Res Ring	Gas Peak	BG
562-568	nil	10 – 20% dull-mod bright yellow	Direct	Slow, to moderately fast, blue-white cut	Isopropyl alcohol	Solid, bluish-white	1.37	0.3
568 - 571	nil	60% dull – moderately bright yellow	Direct	Instantaneous blue-white cut	Isopropyl alcohol	Solid, bluish-white	1.78	1.0
571 - 574	nil	5% dull-moderately bright yellow	Direct	Instantaneous blue-white cut	Isopropyl alcohol	Solid, bluish-white	1.76	0.8
574 - 580	nil	Trace dull yellow	Direct	Slow blue-white	Isopropyl alcohol	Patchy bluish-white	0.69	0.6

Table 3. Summary of oil and gas shows as recorded by the wellsite geologist.

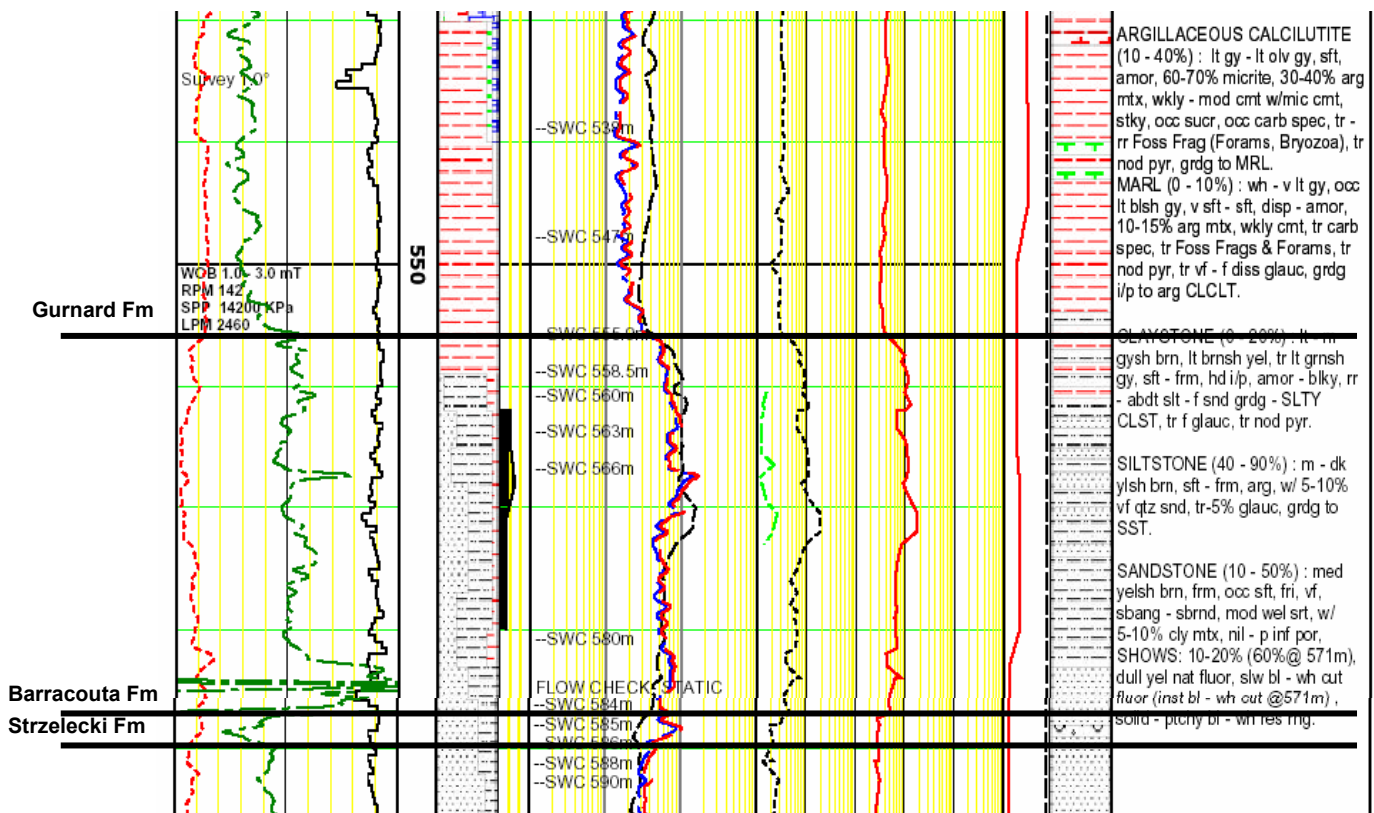


Figure 3. Mudlog from Moby-1 over the Gurnard Formation.

## LOG ANALYSIS METHODOLOGY

### Preparation

Wireline data were loaded from DLIS files into Geolog6 software. The logs were checked for depth-matching and general acquisition quality.

### Log QC and Environmental Corrections

Environmental corrections were applied as required using the *Geolog* software. The GR log was corrected for holesize and mud weight. The neutron log (CN) was environmentally corrected for borehole size and salinity, temperature and pressure, mud cake and mud weight using *Geolog6*. The density log (ZDEN) was corrected for borehole size and mud fluid, while the resistivity logs were borehole and invasion corrected. In addition, the environmentally corrected gamma logs were further corrected for KCl % using the BPB correction charts as Baker Atlas do not provide working algorithms for that correction.

The reprocessing of the MAC sonic data resulted in a significant shift in DT to a slower time through the better quality portions of the Gurnard Formation. In fact the DT value through this sequence is close to 190 us/ft which is the travel time of the mud filtrate. These very slow transit velocities make it extremely difficult to effectively utilise the sonic measurement as part of a petrophysical evaluation through poorly consolidated sequences such as these. For this reason the uncertainty associated with the DT was made very high, effectively removing it from the analysis. However the slow transit time is an indicator of poor consolidation (and high porosity) as well as a potential gas indicator.

### Interpretation Technique

Standard resolution data from Moby-1 was interpreted using MULTIMIN software, which is an optimising petrophysical module within GEOLOG6. Optimising petrophysics relies on obtaining the best match between a model, the measured data and the predicted results. For each logging tool, response equations are used to define the influence of each of the mineral and fluid volumes. The mineral and fluid parameters and the response equations are then used to reconstruct the actual wireline measurements and predict the volumes of minerals and fluids present within the reservoir. For example we can define the response of the density tool to the formation if we know the response (or endpoint parameters) of each of the components that make up the formation e.g. the following would be the density response of a formation containing oil and water in the pore space, and having a matrix of quartz and albite.

$$\hat{\rho}_b = \rho_{oil}v_{oil} + \rho_{fw}v_{fw} + \rho_{qtz}v_{qtz} + \rho_{alb}v_{alb}$$

Such equations can be written for each of the wireline measurements. These equations are then solved simultaneously to define the best combination of various volumes, such that the original log measurements are as closely matched as possible.

### Lithology

MULTIMIN relies on the knowledge of the logging response of the various known minerals and fluids that may occur within the formation under investigation. These responses are generally constant from basin to basin (with some exceptions) and are fairly well identified through the publication of research into the topic.

A petrological investigation was undertaken by Core Laboratories on 6 sidewall core samples selected from the Gurnard and Strzelecki Formation. There was insufficient petrological data to identify statistical relationships between various mineralogical components, however the petrology was very useful in identifying the main mineral species present, and importantly the main clay types present. Based on this petrological information, the following is a list of the volume components that were integrated into the models used in this study (details supplied in Appendix 2).

### Gurnard/Barracouta Formations

#### Framework:

Quartz  
Zircon  
K-Feldspar  
Siderite

#### Clays:

Glauconite  
Smectite  
Chlorite

#### Fluids:

Formation Brine  
Gas

### Strzelecki Formation

#### Framework:

Quartz  
Zircon  
K-Feldspar

#### Clays:

Illite  
Chlorite  
Smectite

#### Fluids:

Formation Brine

It is important to note that Multimin estimates the volume of mineral components (clays and framework grains) which means that a  $V_{sh}$  is not actually calculated as defined by typical deterministic analyses. If you look at typical shales across the world, they contain on average around 40% quartz, and 60% clay minerals, which surprises many people.

### Fluid parameters

#### Formation Brine

Collection of formation water sample was attempted in Moby-1 using the RCI tool, and sodium thiocyanate tracer used in the mud, helped to determine that the sample consisted of 10% mud filtrate. Correction of the sample for mud filtrate contamination indicated that the formation water had a total dissolved salts content of approximately 5.5 kppm. This equates to a formation water salinity of 1.0 ohmm @ 25degC which is the value used for this analysis. In the adjacent Patricia-Baleen field a formation water resistivity of approximately 0.7 ohmm @ 25degC was used which equates to a water salinity of 8kppm

### Porosity Determination

#### From MULTIMIN Analysis

Total porosity is calculated from the MULTIMIN analysis from a combination of the individual fluid components, which in the unflushed zone corresponds to:

$$\phi_t = V_{freewat} + V_{hc} + V_{bndwat}$$

Where;

$V_{freewat}$  = volume of free water

$V_{bndwat}$  = volume of bound water

$V_{hc}$  = volume of hydrocarbons.

### Saturation Evaluation

The interpretation presented in this report has utilised MULTIMIN for all results, including water saturations. The following is a description of the conductivity model used in MULTIMIN for the estimation of water saturation.

### Dual-Water Equation

Water saturation in this study has been determined within the MULTIMIN package using the Dual Water equation. The Dual water model uses the concept of cation exchange capacity to explain shaly sand conductivity. This model assumes that the waters in a formation can be considered to be of two kinds – a free water of normal salinity and clay bound water of altered salinity and increased conductivity. The dual-water equation is as follows:

$$C_t = \phi_t^{m_0} S_{wt}^{n_0} \left[ C_{fw} + \frac{\alpha v_q^h Q_v}{S_w^t} (C_{bw} - C_{fw}) \right]$$

Where;

- $C_t$  = total conductivity (mho/m)
- $C_{bw}$  = clay bound water conductivity (mho/m)
- $C_{fw}$  = free water conductivity (mho/m)
- $m_0$  = dual-water cementation exponent
- $n_0$  = dual-water saturation exponent
- $Q_v$  = concentration of cations (meq/cm<sup>3</sup>)
- $V_q^h$  = volume of clay bound water (cm<sup>3</sup>/meq)
- $S_{wt}$  = water saturation of total porosity (v/v)
- $\alpha$  = expansion factor for diffuse layer
- $\phi_t$  = total porosity (v/v)

Parameters for the dual-water equation have been calculated using the following relationships;

$$\alpha = \sqrt{\frac{0.35}{\langle n \rangle}}$$

$$C_{wb} = \frac{\beta}{\alpha v_q^H}$$

$$\beta = 2.05 \frac{(T + 8.5)}{(22 + 8.5)}$$

$$v_q^H = 0.3 \frac{96}{(T + 25)}$$

Where;

- $T$  = temperature (°C)
- $\beta$  = equivalent conductivity of Na counter ions @ 22°C (S/m)
- $\langle n \rangle$  = brine salt concentration (mol/dm<sup>3</sup>)

### Saturation equation parameters

Electrical properties special core analysis data was not available at the time of this analysis, therefore a cementation exponent ( $m$ ) of 2.2 was used together with a saturation exponent ( $n$ ) of 2. These values were considered to be reasonable estimates given the type of lithology present within the formation.

## Permeability Evaluation

In the absence of representative core data an intrinsic permeability logs was derived using the Coates free fluid index (FFI) was used as the model for permeability prediction. The basic equation takes on the following form;

$$K_{FFI} = C \left[ \phi_e^2 \frac{(\phi_t - BV_{irr})}{BV_{irr}} \right]^X$$

Where;

$\phi_e$  = log analysis effective porosity

$\phi_t$  = log analysis total porosity

$BV_{irr}$  = bulk volume irreducible water

C = constant multiplier

X = exponent

The default values for C and X of 100 and 2 respectively were used in this analysis. The estimated permeability values should be used with extreme caution as they are not calibrated to good quality core data. They may give a good indication of relative values of intrinsic permeability between formations, however are unlikely to be a reliable estimate of the true value at any one depth.

## CUTOFFS

The following cutoffs were used to define net sand, net reservoir and net HIP in Moby-1.

Vclay	≤ 40%
Effective Porosity	≥ 10%
Sw <sub>t</sub>	≤ 60%

**Table 4. Summary of cutoffs applied in this analysis**

## RESULTS

Table 5 is a summary of the net reservoir and pay calculated as part of this analysis. The results indicate the possible presence of net gas pay down to just above the base of the Gurnard Formation. The presence of complex lithologies, which include lithic rich sands, four clay types, potassium feldspar and heavy minerals makes formation evaluation of this sequence quite difficult. A high degree of uncertainty remains in the analysis results, particularly with the prediction of permeability and water saturation.

The log analysis predicts that the Barracouta Formation is wet, which reconciles with the water/filtrate sample taken in that formation. However the presence of gas below 577 mRT does not reconcile with formation pressure data interpretation, which predicts this to be the depth of the free water level based on limited formation pressure data. With the available data from this well, it is unlikely that this can be reconciled.

It is difficult to make comment on the likely producibility of the reservoir sequence. Core data from the adjacent Patricia-Baleen field would indicate good permeabilities in the 100's of millidarcies for this range of porosities. Percussion core samples from Moby-1 showed high permeability however they are likely to be affected by the percussive coring process. RCI mobility data indicates that the mobility of the reservoir is quite low, with many tight tests and most pressures being over-pressured due to poor quality test results. The predicted permeability has a very high uncertainty associated with it, and in the authors opinion is likely to be optimistic.

WELL	TOP (M)	BASE (M)	INTERVAL	GROSS (M)	NET (M)	NTG (M/M)	PHIT (%)	PHIE (%)	VCL (%)	PERM (MD)
MOBY-1	555.5	587	GURNARD FM	31.5	16.8	53.41	35.91	22.45	28.07	548.76
MOBY-1	587	589.5	BARRACOUTA FM	2.5	2.5	98.14	28.23	24.17	7.31	4771.19
MOBY-1	589.5	660	STRZELECKI FM	70.5	1.2	1.73	30.67	16.58	37.14	42.4

WELL	TOP (M)	BASE (M)	INTERVAL	GROSS (M)	NET (M)	NTG (M/M)	PHIT (%)	PHIE (%)	SWT (%)	VCL (%)	PERM (MD)	HVOLH (V/V.H)
MOBY-1	555.5	587	GURNARD FM	31.5	12.5	39.67	36.2	21.39	46.74	31.12	65.83	2.409
MOBY-1	587	589.5	BARRACOUTA FM	2.5	0	0	-	-	-	-	-	0
MOBY-1	589.5	660	STRZELECKI FM	70.5	0	0	-	-	-	-	-	0

**Table 5. Reservoir and pay lumping summary. Note that permeability values are un-calibrated and should be used with caution.**

## RECOMMENDATIONS

The complex nature of the formation makes formation evaluation difficult for the Gurnard and Strzelecki Formations. The high and variable clay content means that resistivity responses will be subdued, and the large amount of micro-porosity means that irreducible water volumes may be quite high. Further hard data is required in order to calibrate the saturation equations so that uncertainty in the analysis can be reduced.

For future drilling programs the following steps are recommended in order to reduce the uncertainty in the formation evaluation results:

- Consider modifying the wireline logging suite to incorporate a NMR log (capable of full gas polarisation). This will provide a resistivity independent estimate of the volume of water within the formation (through hydrocarbon zones), as well as providing an effective porosity through the reservoir. It may be possible to build a log suite that sacrifices some other logs if cost is an issue. The minimum suite required would be NMR-RHOB-Resistivity-GR. This suite should allow full evaluation of the formation for the key reservoir parameters.
- Acquire whole core through the Gurnard Formation – as part of any appraisal drilling it is considered imperative that a whole core is acquired as soon as practical in the program. This is required to confirm the presence of reservoir quality formation, provide core calibration points for porosity and permeability, and provide core samples to undergo special core analysis for properties such as electrical parameters and capillary pressure measurements.
- Should only sidewall coring be undertaken on future wells, it is recommended that mechanical sidewall cores be taken in preference to percussion sidewall cores, so that reservoir properties can be better evaluated. However, given the cost in rig time whole core may be more cost effective.

## **APPENDIX 1: FORMATION PRESSURE DATA SUMMARY**

No.	DEPTH	DEPTH	DEPTH	IHP (PSIA)	FFP			FHP		VOL (CC)	D. MOB (mD/cp)	Comments
	(mMDRT)	(mTVDRRT)	(mTVDSS)		(PSIA)	(PSIA)	(PSIA)	(PSIA)	(psi)			
					1st Press	2nd Press	Okay Data	FHP-IHP				
3	558.5	558.50	537.00	986.7	794.2			988.2	1.5	9.9	12.3	Not FRA Compliant not see spherical flow
3	558.5	558.50	537.00	986.7		792.9		988.2	1.5	10	10.2	Not FRA Compliant not see spherical flow
4	559.1	559.10	537.60	990.5	806.1			991.3	0.8	10.1	7.2	Not FRA Compliant not see spherical flow
4	559.1	559.10	537.60	990.5		802.5		991.3	0.8	10.1	8.7	Not FRA Compliant not see spherical flow
6	559.9	559.90	538.40	992.4	824			991.8	-0.6	10	8.1	Not FRA Compliant not see spherical flow
6	559.9	559.90	538.40	992.4		822		991.8	-0.6	10	19.6	Not FRA Compliant not see spherical flow
7	561.4	561.40	539.90	994.8	797.3			995.2	0.4	9.8	12.3	Not FRA Compliant not see spherical flow
7	561.4	561.40	539.90	994.8		796.3		995.2	0.4	11	21.3	Not FRA Compliant not see spherical flow
8	562.1	562.10	540.60	996	808.6			995.4	-0.6	10	13.7	Not FRA Compliant not see spherical flow
8	562.1	562.10	540.60	996		806.2		995.4	-0.6	10.2	13.4	Not FRA Compliant not see spherical flow
9	563.2	563.20	541.70	997.3	798.6			997.1	-0.2	10.1	13.7	Not FRA Compliant not see spherical flow
9	563.2	563.20	541.70	997.3		798.2		997.1	-0.2	10.1	13.6	Not FRA Compliant not see spherical flow
10	565.7	565.70	544.20	1004.3	0			1004.4	0.1	0	0	
11	565.4	565.40	543.90	1005.5	809			1002.3	-3.2	9.8	11.8	Not FRA Compliant not see spherical flow
11	565.4	565.40	543.90	1005.5		807.7		1002.3	-3.2	10.1	13.8	Not FRA Compliant not see spherical flow
12	568.2	568.20	546.70	1008.2	786.3			1006.3	-1.9	9.3	12.9	Not FRA Compliant not see spherical flow higher perm
12	568.2	568.20	546.70	1008.2		785.8	785.8	1006.3	-1.9	9.8	22	Not FRA Compliant not see spherical flow higher perm
13	569	569.00	547.50	1012.2	789.4			1010.7	-1.5	9.7	19.1	Not FRA Compliant not see spherical flow higher perm
13	569	569.00	547.50	1012.2		788	788	1010.7	-1.5	9.7	15	Not FRA Compliant not see spherical flow higher perm
14	571.2	571.20	549.70	1016.3	808.9			1011.9	-4.4	9.8	8.4	Not FRA Compliant not see spherical flow
15	575.7	575.70	554.20	1021.2	802			1020.1	-1.1	9.9	7.5	Not FRA Compliant not see spherical flow
16	577.1	577.10	555.60	1024.7	802.5		802.5	1022.7	-2.0	9.9	7.4	Not FRA Compliant not see spherical flow
17	578.7	578.70	557.20	1027.6	808.4		808.4	1025.7	-1.9	10	6.8	Not FRA Compliant not see spherical flow pressure derivative comir
18	579.9	579.90	558.40	1028.2	813.2		813.2	1027.7	-0.5	9.9	7.1	Not FRA Compliant not see spherical flow pressure derivative comir
19	587.9	587.90	566.40	1045	808.5			1042	-3.0	9.6	53.5	FRA Compliance see spherical flow pressure is going up
19	587.9	587.90	566.40	1045	805.9			1042	-3.0	9.6	67	FRA Compliance see spherical flow pressure is going up
19	587.9	587.90	566.40	1045		805.7	805.7	1042	-3.0	9.5	64	FRA Compliance see spherical flow
20	588.9	588.90	567.40	1046.6	808.1			1043.6	-3.0	9.9	58.3	FRA Compliance see spherical flow pressure is going up
20	588.9	588.90	567.40	1046.6		806.9	806.9	1043.6	-3.0	10.2	148.3	FRA Compliance see spherical flow
21	591.1	591.10	569.60	1050.3				1047.3	-3.0	0		
22	593.2	593.20	571.70	1053.1				1051.2	-1.9	0		
23	596.9	596.90	575.40	1059				1057.5	-1.5	0		
25	608.1	608.10	586.60	1079.5				1079.6	0.1	0		
26	612.8	612.80	591.30	1087.8	923.3			1086.2	-1.6	10.3	8.4	
26	612.8	612.80	591.30	1087.8		919.1		1086.2	-1.6	10.1	7.8	
28	568.2	568.20	546.70	1005.9				1007.9	2.0	0		FLOW
29	568.5	568.50	547.00	1010.7				1007.9	-2.8	0		FLOW
30	568.2	568.20	546.70	1008.5				1007.5	-1.0	0		FLOW
34	561.4	561.40	539.90	999.2				999	-0.2	0		FLOW
35	561.7	561.70	540.20	1000.3				1000.1	-0.2	0		FLOW
36	561.7	561.70	540.20	1001.5				1001.3	-0.2	0		
37	558.5	558.50	537.00	993.3				988.7	-4.6	0		FLOW
38	558.4	558.40	536.90	991.4				991.1	-0.3	0		FLOW
39	588.9	588.90	567.40	1047.6				1046	-1.6	0		
40	588.5	588.50	567.00	1046.8	807.5		807.5	1046.5	-0.3	8.7	175	
41	572	572.00	550.50	1016.5				1015.9	-0.6	0		FLOW
42	572.1	572.10	550.60	1016.5				1015	-1.5	0		FLOW
43	572.2	572.20	550.70	1013.4				1015.4	2.0	0		FLOW
44	571	571.00	549.50	1014.7				1013.1	-1.6	0		FLOW
45	571.9	571.90	550.40	1017.8				1014.9	-2.9	0		FLOW
46	573	573.00	551.50	1019.6				1017.5	-2.1	0		FLOW

## **APPENDIX 2: MULTIMIN REPORTS**

1

```

*****
*
*           MULTIMIN REPORT
*
*   Project : BS001
*   User id  : pault
*   Date    : 16-Jan-2005 17:50:52
*
*****
    
```

1

MULTIMIN REPORT for well MOBY-1 interval GURNARD FM (555.51 - 586.98 metres) Project BS001  
 Reported by pault on 16-Jan-2005 at 17:50  
 Analysed by pault on 16-Jan-2005 at 16:51

Page 1

MODELS:

Type	Name	Cond#	Cutoff	Expression
Primary	GURNARD_FINAL	6.570	10.0	

FORMATION FLUID PARAMETERS:

Fluid properties option = DEPTH  
 Oil Gravity Degrees API = 50.00 dapi Gas specific gravity = 0.745  
 Rws = 1.0000 @ 25.00 degC Cwbs = - @ - degF Rmfs = 0.0860 @ 21.70 degC

BOREHOLE PARAMETERS:

Mud base = WATER Mud density = 10.000 lb/g KCl concentration of mud = 6.00 %  
 SHT = - BHT = - degC  
 Rms = 0.1044 @ 21.68 degC Rmcs = 0.149 @ 21.81 degC Total depth = - metres

Average temperature of 41.47 degC by SONDE method.  
 Average pressure of 973.80 psi by MUD\_DENS method.

1

MULTIMIN REPORT for well MOBY-1 interval GURNARD FM (555.51 - 586.98 metres) Project BS001  
 PRIMARY MODEL GURNARD\_FINAL:  
 Cementation factor m = 2.100 Saturation exponent n = 2.100 Linear dual-water w = 2.00  
 Expansion of clay bound water is enabled.

Page 2

Component	QUARTZ	ORTHOCL	SIDER	GLAUCON	CHLOR	SMECT	SPCMIN2	XGAS	XBNDWAT	XFREWAT	UGAS
Error of prediction	0.1057	0.0158	0.0763	0.1102	0.3043	0.2842	0.0019	0.0616	0.2171	0.1819	0.2999

EQUATION RESPONSES:

Log	Method	Uncertainty	QUARTZ	ORTHOCL	SIDER	GLAUCON	CHLOR	SMECT	SPCMIN2	XGAS	XBNDWAT	XFREWAT	UGAS
Formation density [G/C3]		0.0264	2.650	2.570	3.960	2.850	3.420	2.630	4.500	-0.102	1.062	1.062	0.000
RHO_COR	Linear												
Neutron [V/V]		0.0140	-0.050	-0.006	0.184	0.510	0.500	0.218	0.000	0.145	0.960	0.960	0.000
TNPH_COR	Non-linear												
Sonic transit time [US/F]		10.0000	55.0	53.5	43.8	49.4	85.3	85.3	90.0	250.0	189.0	189.0	0.0
DT	Linear												
Photoelectric absorption [B/C3]		0.3200	5.04	8.71	72.20	19.10	27.17	7.61	307.00	0.01	0.80	0.80	0.00
U	Linear												
Total gamma [GAPI]		12.0000	1.0	260.0	6.0	150.0	56.0	168.0	20000.0	0.0	0.0	28.8	0.0
GR_COR	Linear												
Spectral potassium [%]		0.4000	0.0000	10.2100	0.0000	5.9400	0.4200	0.5800	0.0000	0.0000	0.0000	3.1440	0.0000
POTA_COR	Linear												
Unflushed conductivity [MH/M]		0.0100	0.00	0.00	0.00	0.00	0.00	0.00	0.00	0.00	0.00	0.00	0.00
CT	Dual-water nonlinear												
Flushed conductivity [MH/M]		0.0100	0.00	0.00	0.00	0.00	0.00	0.00	0.00	0.00	11.91	16.98	0.00
CXO	Dual-water nonlinear												

CONSTRAINTS:

Value	Type	Uncertainty	QUARTZ	ORTHOCL	SIDER	GLAUCON	CHLOR	SMECT	SPCMIN2	XGAS	XBNDWAT	XFREWAT	UGAS
<PROG UNITY>	1.000 Tool	0.0100	1.000	1.000	1.000	1.000	1.000	1.000	1.000	0.000	0.000	0.000	1.000
<PROG POROSITY>	0.000 Tool	0.0100	0.000	0.000	0.000	0.000	0.000	0.000	0.000	1.000	1.000	1.000	-1.000
<PROG X BNDWAT>	0.000 Tool	0.0100	0.000	0.000	0.000	0.470	0.117	0.697	0.000	0.000	-1.000	0.000	0.000
<PROG U BNDWAT>	0.000 Tool	0.0100	0.000	0.000	0.000	0.700	0.174	1.036	0.000	0.000	0.000	0.000	0.000
<PROG WATER MUD>	0.000 <=	-	0.000	0.000	0.000	0.000	0.000	0.000	0.000	0.000	1.000	1.000	0.000
<USER CONSTR1>	0.000 Tool	0.0100	0.000	0.000	0.000	0.000	0.000	0.000	0.000	0.000	0.000	0.000	0.000
<USER CONSTR2>	0.000 Tool	0.0100	-1.000	6.692	0.000	0.000	0.000	0.000	0.000	0.000	0.000	0.000	0.000

PROPERTIES AND BOUNDS:

Mineral grain density	2.650	2.570	3.960	2.960	2.940	2.630	4.500	0.000	0.000	0.000	0.000	0.000
Mineral cation exchange capacity	0.000	0.000	0.000	0.600	0.150	1.000	0.000	0.000	0.000	0.000	0.000	0.000
Lower Bound	0.000	0.000	0.000	0.000	0.000	0.000	0.000	0.000	0.000	0.000	0.000	0.000
Upper Bound	1.000	1.000	1.000	1.000	1.000	1.000	1.000	0.500	0.500	0.500	0.500	0.500

1

MULTIMIN REPORT for well MOBY-1 interval GURNARD FM (555.51 - 586.98 metres) Project BS001

Page 3

PRIMARY MODEL GURNARD\_FINAL (continued):

Component	UBNDWAT	UFREWAT
Error of prediction	0.3698	0.6954

EQUATION RESPONSES:

Log	Method	Uncertainty		
Formation density [G/C3]		0.0264	0.000	0.000
RHO_COR	Linear			
Neutron [V/V]		0.0140	0.000	0.000
TNPH_COR	Non-linear			
Sonic transit time [US/F]		10.0000	0.0	0.0
DT	Linear			
Photoelectric absorption [B/C3]		0.3200	0.00	0.00
U	Linear			
Total gamma [GAPI]		12.0000	0.0	0.0
GR_COR	Linear			
Spectral potassium [%]		0.4000	0.0000	0.0000
POTA_COR	Linear			
Unflushed conductivity [MH/M]		0.0100	6.85	1.94
CT	Dual-water nonlinear			
Flushed conductivity [MH/M]		0.0100	0.00	0.00
CXO	Dual-water nonlinear			

CONSTRAINTS:

Value	Type	Uncertainty		
<PROG UNITY>	1.000 Tool	0.0100	1.000	1.000
<PROG POROSITY>	0.000 Tool	0.0100	-1.000	-1.000
<PROG X BNDWAT>	0.000 Tool	0.0100	0.000	0.000
<PROG U BNDWAT>	0.000 Tool	0.0100	-1.000	0.000
<PROG WATER MUD>	0.000 <=	-	-1.000	-1.000
<USER CONSTR1>	0.000 Tool	0.0100	0.000	0.000
<USER CONSTR2>	0.000 Tool	0.0100	0.000	0.000

PROPERTIES AND BOUNDS:

Mineral grain density	0.000	0.000
Mineral cation exchange capacity	0.000	0.000
Lower Bound	0.000	0.000
Upper Bound	0.500	0.500

MULTIMIN REPORT for well MOBY-1 interval BARRACOUTA FM (587.05 - 589.49 metres)  
 Reported by pault on 16-Jan-2005 at 17:50  
 Analysed by pault on 16-Jan-2005 at 16:51

Project BS001

MODELS:

Type	Name	Cond#	Cutoff	Expression
Primary	GURNARD_FINAL	6.572	10.0	

FORMATION FLUID PARAMETERS:

Fluid properties option = DEPTH  
 Oil Gravity Degrees API = 50.00 dapi Gas specific gravity = 0.745  
 Rws = 1.0000 @ 25.00 degC Cwbs = - @ - degF Rmfs = 0.0860 @ 21.70 degC

BOREHOLE PARAMETERS:

Mud base = WATER Mud density = 10.000 lb/g KCl concentration of mud = 6.00 %  
 SHT = - BHT = - degC  
 Rms = 0.1044 @ 21.68 degC Rmcs = 0.149 @ 21.81 degC Total depth = - metres  
 Average temperature of 41.52 degC by SONDE method.  
 Average pressure of 1002.76 psi by MUD\_DENS method.

1

MULTIMIN REPORT for well MOBY-1 interval BARRACOUTA FM (587.05 - 589.49 metres)

Project BS001

PRIMARY MODEL GURNARD\_FINAL:

Cementation factor m = 2.100 Saturation exponent n = 2.100 Linear dual-water w = 2.00  
 Expansion of clay bound water is enabled.

Component	QUARTZ	ORTHOCL	SIDER	GLAUCON	CHLOR	SMECT	SPCMIN2	XGAS	XBNDWAT	XFREWAT	UGAS
Error of prediction	0.1062	0.0159	0.0763	0.1104	0.3042	0.2846	0.0019	0.0618	0.2175	0.1822	0.3003

EQUATION RESPONSES:

Log	Method	Uncertainty	QUARTZ	ORTHOCL	SIDER	GLAUCON	CHLOR	SMECT	SPCMIN2	XGAS	XBNDWAT	XFREWAT	UGAS
Formation density [G/C3]	Linear	0.0264	2.650	2.570	3.960	2.850	3.420	2.630	4.500	-0.099	1.062	1.062	0.000
RHO_COR	Linear												
Neutron [V/V]	Linear	0.0140	-0.050	-0.006	0.184	0.510	0.500	0.218	0.000	0.151	0.960	0.960	0.000
TNPH_COR	Non-linear												
Sonic transit time [US/F]	Linear	10.0000	55.0	53.5	43.8	49.4	85.3	85.3	90.0	250.0	189.0	189.0	0.0
DT	Linear												
Photoelectric absorption [B/C3]	Linear	0.3200	5.04	8.71	72.20	19.10	27.17	7.61	307.00	0.01	0.80	0.80	0.00
U	Linear												
Total gamma [GAPI]	Linear	12.0000	1.0	260.0	6.0	150.0	56.0	168.0	20000.0	0.0	0.0	28.8	0.0
GR_COR	Linear												
Spectral potassium [%]	Linear	0.4000	0.0000	10.2100	0.0000	5.9400	0.4200	0.5800	0.0000	0.0000	0.0000	3.1440	0.0000
POTA_COR	Linear												
Unflushed conductivity [MH/M]	Dual-water nonlinear	0.0100	0.00	0.00	0.00	0.00	0.00	0.00	0.00	0.00	0.00	0.00	0.00
CT	Dual-water nonlinear												
Flushed conductivity [MH/M]	Dual-water nonlinear	0.0100	0.00	0.00	0.00	0.00	0.00	0.00	0.00	0.00	11.89	16.97	0.00
CXO	Dual-water nonlinear												

CONSTRAINTS:

Value	Type	Uncertainty	QUARTZ	ORTHOCL	SIDER	GLAUCON	CHLOR	SMECT	SPCMIN2	XGAS	XBNDWAT	XFREWAT	UGAS
<PROG UNITY>	1.000 Tool	0.0100	1.000	1.000	1.000	1.000	1.000	1.000	1.000	0.000	0.000	0.000	1.000
<PROG POROSITY>	0.000 Tool	0.0100	0.000	0.000	0.000	0.000	0.000	0.000	0.000	1.000	1.000	1.000	-1.000
<PROG X BNDWAT>	0.000 Tool	0.0100	0.000	0.000	0.000	0.470	0.117	0.697	0.000	0.000	-1.000	0.000	0.000
<PROG U BNDWAT>	0.000 Tool	0.0100	0.000	0.000	0.000	0.700	0.174	1.036	0.000	0.000	0.000	0.000	0.000
<PROG WATER MUD>	0.000 <=	-	0.000	0.000	0.000	0.000	0.000	0.000	0.000	0.000	1.000	1.000	0.000
<USER CONSTR1>	0.000 Tool	0.0100	0.000	0.000	0.000	0.000	0.000	0.000	0.000	0.000	0.000	0.000	0.000
<USER CONSTR2>	0.000 Tool	0.0100	-1.000	6.692	0.000	0.000	0.000	0.000	0.000	0.000	0.000	0.000	0.000

PROPERTIES AND BOUNDS:

Mineral grain density	ORTHOCL	SIDER	GLAUCON	CHLOR	SMECT	SPCMIN2	XGAS	XBNDWAT	XFREWAT	UGAS
	2.570	3.960	2.960	2.940	2.630	4.500	0.000	0.000	0.000	0.000
Mineral cation exchange capacity	0.000	0.000	0.000	0.600	0.150	1.000	0.000	0.000	0.000	0.000
Lower Bound	0.000	0.000	0.000	0.000	0.000	0.000	0.000	0.000	0.000	0.000
Upper Bound	1.000	1.000	1.000	1.000	1.000	1.000	0.500	0.500	0.500	0.500

1

MULTIMIN REPORT for well MOBY-1 interval BARRACOUTA FM (587.05 - 589.49 metres)

Project BS001

PRIMARY MODEL GURNARD\_FINAL (continued):

Component	UBNDWAT	UFREWAT
Error of prediction	0.3704	0.6965

EQUATION RESPONSES:

Log	Method	Uncertainty

Formation density [G/C3]	0.0264	0.000	0.000
RHO_COR Linear			
Neutron [V/V]	0.0140	0.000	0.000
TNPH_COR Non-linear			
Sonic transit time [US/F]	10.0000	0.0	0.0
DT Linear			
Photoelectric absorption [B/C3]	0.3200	0.00	0.00
U Linear			
Total gamma [GAPI]	12.0000	0.0	0.0
GR_COR Linear			
Spectral potassium [%]	0.4000	0.0000	0.0000
POTA_COR Linear			
Unflushed conductivity [MH/M]	0.0100	6.85	1.94
CT Dual-water nonlinear			
Flushed conductivity [MH/M]	0.0100	0.00	0.00
CXO Dual-water nonlinear			

CONSTRAINTS: Value Type Uncertainty

<PROG UNITY>	1.000	Tool	0.0100	1.000	1.000
<PROG POROSITY>	0.000	Tool	0.0100	-1.000	-1.000
<PROG X BNDWAT>	0.000	Tool	0.0100	0.000	0.000
<PROG U BNDWAT>	0.000	Tool	0.0100	-1.000	0.000
<PROG WATER MUD>	0.000	<=	-	-1.000	-1.000
<USER CONSTR1>	0.000	Tool	0.0100	0.000	0.000
<USER CONSTR2>	0.000	Tool	0.0100	0.000	0.000

PROPERTIES AND BOUNDS:

Mineral grain density	0.000	0.000
Mineral cation exchange capacity	0.000	0.000
Lower Bound	0.000	0.000
Upper Bound	0.500	0.500

MULTIMIN REPORT for well MOBY-1 interval STRZELECKI FM (589.57 - 659.28 metres)  
 Reported by pault on 16-Jan-2005 at 17:50  
 Analysed by pault on 16-Jan-2005 at 16:51

Project BS001

MODELS:

Type	Name	Cond#	Cutoff	Expression
Primary	STRZ	-	10.0	

FORMATION FLUID PARAMETERS:

Fluid properties option = DEPTH  
 Oil Gravity Degrees API = 50.00 dapi Gas specific gravity = 0.745  
 Rws = 1.0000 @ 25.00 degC Cwbs = - @ - degF Rmfs = 0.0860 @ 21.70 degC

BOREHOLE PARAMETERS:

Mud base = WATER Mud density = 10.000 lb/g KCl concentration of mud = 6.00 %  
 SHT = - BHT = - degC  
 Rms = 0.1044 @ 21.68 degC Rmcs = 0.149 @ 21.81 degC Total depth = - metres  
 Average temperature of 42.33 degC by SONDE method.  
 Average pressure of 1028.86 psi by MUD\_DENS method.

1

MULTIMIN REPORT for well MOBY-1 interval STRZELECKI FM (589.57 - 659.28 metres)

Project BS001

PRIMARY MODEL STRZ:

Cementation factor m = 2.100 Saturation exponent n = 2.100 Linear dual-water w = 2.00  
 Expansion of clay bound water is enabled.

Component	QUARTZ	ORTHOCL	ILLITE	CHLOR	SMECT	SPCMIN2	XBNDWAT	XFREWAT	UBNDWAT	UFREWAT
Error of prediction	0.0271	0.0057	0.0148	0.0128	0.0354	0.0006	0.0248	0.0282	0.0337	0.0398

EQUATION RESPONSES:

Log	Method	Uncertainty	QUARTZ	ORTHOCL	ILLITE	CHLOR	SMECT	SPCMIN2	XBNDWAT	XFREWAT	UBNDWAT	UFREWAT
Formation density [G/C3]	Linear	0.0264	2.650	2.570	2.780	3.420	2.630	4.500	1.049	1.049	0.000	0.000
RHO_COR	Linear											
Neutron [V/V]	Linear	0.0140	-0.050	-0.006	0.247	0.500	0.218	0.000	0.953	0.953	0.000	0.000
TNPH_COR	Non-linear											
Sonic transit time [US/F]	Linear	10.0000	55.0	53.5	100.0	85.3	85.3	90.0	189.0	189.0	0.0	0.0
DT	Linear											
Photoelectric absorption [B/C3]	Linear	0.3200	5.04	8.71	11.12	27.17	7.61	307.00	0.78	0.78	0.00	0.00
U	Linear											
Total gamma [GAPI]	Linear	12.0000	1.0	260.0	160.0	56.0	168.0	20000.0	0.0	9.6	0.0	0.0
GR_COR	Linear											
Spectral potassium [%]	Linear	0.4000	0.0000	10.2100	7.0000	0.4200	0.5800	0.0000	0.0000	1.0480	0.0000	0.0000
POTA_COR	Linear											
Unflushed conductivity [MH/M]	Dual-water nonlinear	0.0500	0.00	0.00	0.00	0.00	0.00	0.00	0.00	0.00	12.44	4.30
CT	Dual-water nonlinear											
Flushed conductivity [MH/M]	Dual-water nonlinear	0.0500	0.00	0.00	0.00	0.00	0.00	0.00	18.51	22.52	0.00	0.00
CXO	Dual-water nonlinear											

CONSTRAINTS:

Value	Type	Uncertainty	QUARTZ	ORTHOCL	ILLITE	CHLOR	SMECT	SPCMIN2	XBNDWAT	XFREWAT	UBNDWAT	UFREWAT
<PROG UNITY>	1.000 Tool	0.0100	1.000	1.000	1.000	1.000	1.000	1.000	0.000	0.000	1.000	1.000
<PROG POROSITY>	0.000 Tool	0.0100	0.000	0.000	0.000	0.000	0.000	0.000	1.000	1.000	-1.000	-1.000
<PROG X BNDWAT>	0.000 Tool	0.0100	0.000	0.000	0.184	0.117	0.697	0.000	-1.000	0.000	0.000	0.000
<PROG U BNDWAT>	0.000 Tool	0.0100	0.000	0.000	0.274	0.174	1.036	0.000	0.000	0.000	-1.000	0.000
<USER CONSTR1>	0.000 Tool	0.0100	0.000	0.000	-1.000	1.000	0.000	0.000	0.000	0.000	0.000	0.000
<USER CONSTR2>	0.000 Tool	0.0100	1.000	-5.000	0.000	0.000	0.000	0.000	0.000	0.000	0.000	0.000

PROPERTIES AND BOUNDS:

Mineral grain density	2.650	2.570	2.780	2.940	2.630	4.500	0.000	0.000	0.000	0.000
Mineral cation exchange capacity	0.000	0.000	0.250	0.150	1.000	0.000	0.000	0.000	0.000	0.000
Lower Bound	0.000	0.000	0.000	0.000	0.000	0.000	0.000	0.000	0.000	0.000
Upper Bound	1.000	1.000	1.000	1.000	1.000	1.000	0.500	0.500	0.500	0.500

1

```

*****
*                                     *
*           MULTIMIN REPORT           *
*                                     *
*       *** End of Report ***         *
*                                     *
*   Project : BS001                   *
*   User id  : pault                   *
*   Date    : 16-Jan-2005 17:50:52    *
*   Pages   : 8                       *
*                                     *
*****
    
```

**ENCLOSURE 1: EVALUATION SUMMARY DEPTH PLOT (1:200)**

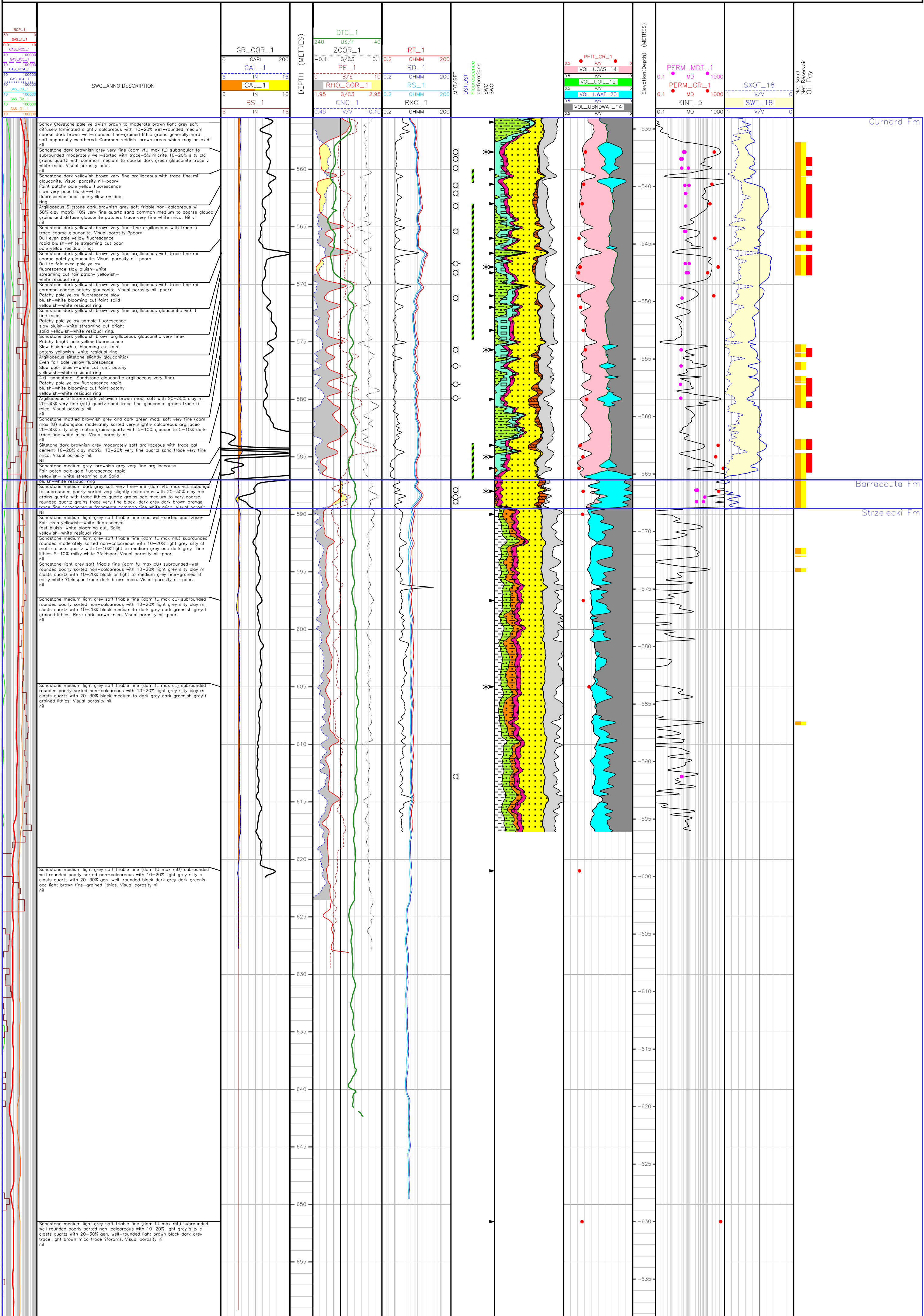
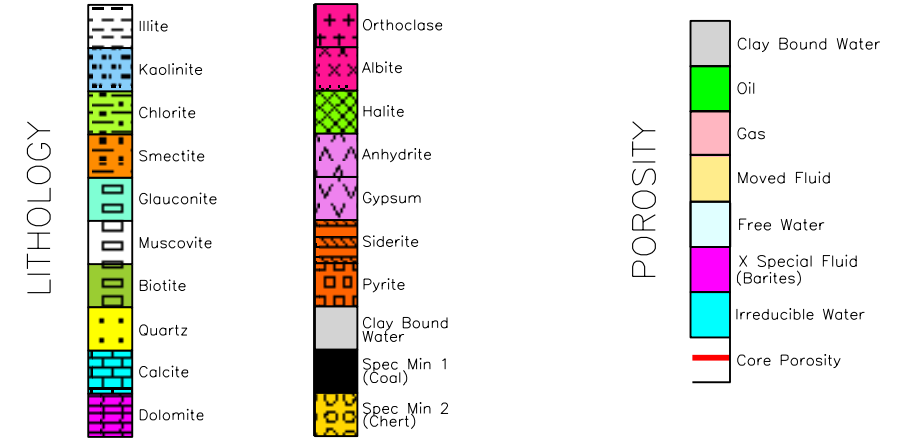
# Petrophysical Analysis of: MOBY-1

COMPANY: BASS STRAIT OIL COMPANY LTD  
 LOCATION: VIC/P47  
 LATITUDE: 38° 01' 44" S  
 LONGITUDE: 148° 30' 27" E  
 X COORDINATE: 632316.41  
 Y COORDINATE: 5789884.86  
 HORIZONTAL UNITS: METRES  
 DATE PLOTTED: 19-Jan-2005

DATUM FOR ELEVATION: MSL  
 WATER DEPTH: 53.00  
 MEASUREMENT REF.: RT  
 ELEVATION MEAS. REF.: 21.50  
 DRILLED DEPTH: 660.00  
 VERTICAL UNITS: METRES  
 DATE LOGGED: 12-OCT-2004  
 VERTICAL SCALE: 1:200

Bit Size: 8.5 in  
 Mud Type: KCL/PHPA  
 DFD: 10.0003  
 BHT: 42.7 C

Rm 0.104 @ 21.680C  
 Rrf: 0.086 @ 21.700C  
 Rrc: 0.149 @ 21.810C  
 KCl: 6%



## **APPENDIX 3**

---

# **Palynology Report**

---

**By Dr Alan Partridge**

**Palynological analysis of interval  
from 538 to 630 metres in Moby-1,  
offshore Gippsland Basin.**

by

**Alan D. Partridge**

**Biostrata Pty Ltd**

A.B.N. 39 053 800 945

**Biostrata Report 2005/01A**

**16<sup>th</sup> March 2005**

**Palynological analysis of interval from 538 to 630 metres  
in Moby-1, offshore Gippsland Basin.**

by Alan D. Partridge

## Table of Contents

### INTERPRETATIVE DATA

Summary .....	page 3
Table 1. Stratigraphic and Palynological Summary of Moby-1 .....	page 3
Introduction .....	page 3
Sample Processing and Basic Analyses .....	page 4
Geological Discussion .....	page 4
<i>Seaspray Group</i> .....	page 4
<i>Latrobe Group</i> .....	page 5
<i>Gurnard Formation</i> .....	page 5
<i>Kingfish Formation</i> .....	page 5
<i>Strzelecki Group</i> .....	page 6
Biostratigraphy .....	page 6
<i>Proteacidites tuberculatus</i> Zone & <i>Operculodinium</i> Superzone .....	page 6
Upper <i>Nothofagidites asperus</i> Zone or younger .....	page 7
Middle <i>Nothofagidites asperus</i> Zone .....	page 7
Lower <i>Nothofagidites asperus</i> Zone .....	page 8
Undifferentiated Eocene .....	page 8
Upper <i>Coptospora paradoxa</i> Zone .....	page 9
References .....	page 9
Table 2. Interpretative data for Moby-1 .....	page 11
Description of Range Chart .....	page 12

### BASIC DATA

Table 3. Basic sample data for Moby-1 .....	page 13
Table 4. Basic assemblage data for Moby-1 .....	page 14

**Palynological analysis of interval from 538 to 630 metres  
in Moby-1, offshore Gippsland Basin.  
by Alan D. Partridge**

**INTERPRETATIVE DATA**

**Summary**

Palynological analyses have been performed on thirteen sidewall core and eight cuttings samples between 538 and 630m in Moby-1. The section investigated consists of the basal 20 metres of the Seaspray Group, overlying a thin 33 metre section of the Latrobe Group. The latter is entirely of Eocene age, and consists of a basal sandstone 2.5 metre thick, overlain by marine sediments of the Gurnard Formation which are 31.5 metre thick. These Tertiary units in turn unconformably overlie the Strzelecki Group. The ~70 metres of the latter group penetrated before TD was reached is Mid to Late Albian in age. Results of the analyses are summarised in Tables 1 and 2 below:

**Table 1. Stratigraphic and Palynological Summary of Moby-1**

AGE	STRATIGRAPHY	PALYNOLOGY	DEPTHS (mKB)
Recent to Late Oligocene	<b>SEASPRAY GROUP</b> Undifferentiated Seafloor to 553m	<i>P. tuberculatus</i> SP Zone and <i>Operculodinium</i> MP Superzone	538 to 547m
Early Oligocene	“Early Oligocene Wedge” 553 to 555.5m	Upper <i>N. asperus</i> SP Zone or younger and <i>Fromea leos</i> MP Zone	556m (slightly displaced)
Late to Middle Eocene	<b>LATROBE GROUP</b> <b>Cobia Subgroup</b>	Middle <i>N. asperus</i> SP Zone <i>Gippslandica extensa</i> MP Zone Lower <i>N. asperus</i> SP Zone <i>Deflandrea. heterophlycta</i> MP Zone	558.5 to 561.3m 558.5m 568.5 to 586m 575.7 to 580m
	Gurnard Formation 555.5 to 587m		
Undifferentiated Eocene	<b>Halibut Subgroup</b> Kingfish Formation 587 to 589.5m	SP Zone Indeterminate but no older than Eocene	588m
Mid to Late Albian	<b>STRZELECKI GROUP</b> Wonthaggi Formation 589.5 to 660mTD	Upper <i>Coptospora paradoxa</i> SP Zone	613 to 630m

SP = Spore-Pollen; MP = Microplankton

**Introduction**

The Moby-1 well is located in permit VIC/P47 on the north-eastern margin of the offshore basin, and was drilled by the Bass Strait Oil Company Ltd in October 2004. Palynological analyses were conducted on 21 sample comprising 13 sidewall cores, seven individual cuttings samples and one composite cuttings sample. All samples have been processed in the palynological laboratory facilities of Core Laboratories Australia Pty Ltd in Perth. Palynological slides from an initial suite of nine samples were received on 13<sup>th</sup> December 2004, and the results of microscope analysis of these samples were provided in Provisional Report No. 1 issued on 14<sup>th</sup> December 2004. Based on

these initial results additional sidewall core and cuttings samples were submitted for laboratory processing in January 2005. The prepared palynological slides from these extra samples were all received by 30<sup>th</sup> January and the results of microscope analysis of them were provided in Provisional Report No. 2 issued on 11<sup>th</sup> February 2005.

### Sample Processing and Basic Analyses

In the laboratory processing it was requested that all samples be oxidised prior to the application of zinc bromide density separation used to remove the undissolved mineral matter. This modified procedure was considered necessary to remove finely disseminated pyrite within the samples and impregnating the palynomorphs. The revised methodology is believed to have improved both the amount of organic residue recovered and the concentration of the palynomorphs on the slides.

Basic sample data such as lithologies (were recorded), weights of sample processed, and measured organic yields (were recorded) are provided in Table 3. The basic data on the estimated visual yields, palynomorph concentrations and preservation, and number of species of spore-pollen (SP) and microplankton (MP) recorded from individual samples are provided in Table 4. The visual yield from the samples varies from very low to high, with the concentration of palynomorph on the slides also highly variable from very low to high, while palynomorph preservation is mostly poor. The recorded spore-pollen diversity varies from very low to high and has an average of >35 species per sample, whereas the recorded microplankton diversity is typically low to moderate with a much lower average of ~7 species per sample.

The final zones and ages assigned to the samples, zone confidence ratings, and zone identification criteria for each of the samples are summarised on Table 2. The distribution of the palynomorphs identified in the samples are displayed on the accompanying StrataBugs™ range chart. Author citations for most of the recorded spore-pollen species can be sourced from papers by Dettmann (1963), Helby *et al.* (1987), Macphail (1999), Stover & Partridge (1973, 1982) and the catalogue of megaspores by Batten & Kovach (1990), while the author citations for the microplankton species can be sourced from the indexes for dinocysts and other organic-walled microplankton prepared by Fensome *et al.* (1990) and Williams *et al.* (1998). Manuscript species names and combinations are indicated by “sp. nov.” or “comb. nov.” on the range chart, and “ms” after their binomials names in the text and tables.

### Geological Discussion.

In the following section the results of the palynological analyses are integrated with the lithological descriptions and electric logs to subdivide the section penetrated in Moby-1 into the stratigraphic units shown on Table 1. The nomenclature used primarily follows the revisions of Partridge (1999), which has been published in outline by Bernecker & Partridge (2001; Appendix). The interval discussed consists of the basal 20 metres of the Seaspray Group, the 34 metre thick section of the Latrobe Group and the uppermost 70.5 metres of the Strzelecki Group.

**Seaspray Group:** The shallowest two sidewall cores analysed at 538m and 547m are dominated by marine dinocysts characteristic of the *Operculodinium* Superzone. Although this marine superzone, and the associated terrestrial spore-pollen zone cannot be further subdivided the extremely high abundances of dinocysts in the samples (average >85%) is most similar to latest Oligocene to Early Miocene assemblages in other wells. Consequently, the Early to middle Oligocene time interval is either highly condensed through the basal eight metres of the Seaspray Group, or largely missing. The marked change to a spore-pollen dominated assemblage, and the identification of the important *Fromea leos* microplankton Zone, in the cuttings collected over the interval 553-556m indicates that at least part of this basal eight metres belongs to the enigmatic “Early Oligocene Wedge” (see

Appendix *in* Bernecker & Partridge, 2001). The preferred top of this EOW is placed at 553m based on the gamma ray log and cuttings descriptions, but it is possible on the available palynology that it could lie slightly higher at 548m.

**Latrobe Group:** The thin section of Latrobe Group encountered in Moby-1 is interpreted to consist of the Gurnard Formation of the Cobia Subgroup and an extremely thin section of the Kingfish Formation of the Halibut Subgroup. The older Late Cretaceous Golden Beach and Emperor subgroups are missing in the well.

**Gurnard Formation:** This 31.5 metre thick formation is identified between 555.5m and 587m based on the elevated readings on the gamma ray log and the associated glauconitic lithologies. The palynological analyses confirms that the formation is a marine unit with low microplankton (mostly dinocysts) abundances and species diversity. In the sidewall cores the microplankton abundances range from <1% to 12% and species diversity from 3 to 10 species. Higher values in the cuttings are due to the counting of caved microplankton. Both the spore-pollen and dinocysts also confirm an age range of late Middle to Late Eocene. The bottom 4 metres of the formation is characterised by a very high gamma ray spike. The three sidewall cores recovered from this interval are fine-grained sandstone, which are quartzose rather than glauconitic. The sidewall core analysed from the middle of this spike unfortunately gave a poor assemblage which could only be assigned to the broad *N. asperus* Zone, although it clearly belongs to the Lower *N. asperus* subzone and has a Middle Eocene age based on superposition. Comparison with the nearby Patricia-1 well suggests that this basal interval may be equivalent to the *Enneadocysta partridgei* dinocyst Zone and therefore be early Middle Eocene in age.

**Kingfish Formation:** The thin 2.5 metre thick quartz sandstone lying below the gamma ray spike is interpreted to be equivalent to the youngest part of the Kingfish Formation of the Halibut Subgroup. The non-marine spore-pollen assemblage recovered from the sidewall core at 588m from the middle of this unit consists of a mixture of Eocene, reworked Early Cretaceous, and possibly reworked Triassic species. Although only a limited number of palynomorphs were recovered the lack of any significant *Nothofagidites* pollen abundance strongly suggests the assemblage is older than the immediately overlying Lower *N. asperus* Zone. The most likely correlation is with the Early Eocene *Proteacidites asperopolus* Zone which has been recorded from similar sandstones immediately beneath the Gurnard Formation in the both Flathead-1 and Patricia-1.

Assigning this very thin section of Latrobe "coarse clastics" in Moby-1 to the Kingfish Formation may not be entirely appropriate, but currently it is the best available name. The typical Kingfish Formation is composed of the thick and coal-rich, lower coastal successions of Paleocene to Early Eocene age underlying the middle portion of the Central Deep, as exemplified by the type section in Veilfin-1. In contrast, the Moby-1 well is located on the Northern Platform at the feather-edge of deposition of the "Kingfish time-package" where there was insufficient accommodation during the time interval to allow either the accumulation of significant sedimentary section, or the preservation of coals.

Other possible stratigraphic assignments for this interval would be to the Barracouta or Mackerel formations as both are coal-poor. The application of the Barracouta Formation should however be restricted to the coal-poor alluvial to fluvial plain facies which lie **landward** of the coal-rich coastal plain facies of the Kingfish Formation. The Barracouta Formation is distributed across the western half of the Gippsland Basin and during deposition was a considerable distance (>50 km) landward of the Paleocene to Early Eocene palaeoshorelines. Similarly, the Mackerel Formation should be restricted to the progradational marine sandstones that lie **seaward** of the coastal plain facies of the Kingfish Formation. The Mackerel Formation can be characterised by lacking coal, and by most

palynological samples containing marine dinocysts. Although the sandstone interval under discussion in Moby-1 lies close to the mapped Coal Line<sup>1</sup> of *P. asperopolus* Zone age, the lack of any marine dinocysts from this interval favours a non-marine deposition environment landward of the palaeoshoreline, and hence assignment of the interval to the coastal plain facies of the Kingfish Formation, rather than to the wholly marine facies of the Mackerel Formation. Ultimately, the best nomenclature solution would be to recognise these thin “coarse clastic” sandstones in the Patricia-Moby-Flathead area as a separate local member of the Kingfish Formation. This local member would largely be restricted to the Northern Platform where there was insufficient accommodation to allow for the preservation of coal, which typifies the Kingfish Formation elsewhere. It would be inappropriate however to give the unit the higher rank of a formation as it clearly has a very restricted geographic distribution in the basin.

**Strzelecki Group:** Moby-1 penetrates only 70.5 metres into the Strzelecki Group below the longest duration unconformity in the well where >50 million years of section is missing. As is typical of the volcanoclastic lithologies throughout this group only some of the palynological samples gave meaningful results. The *Coptospora paradoxa* Zone assignment and Albian age, derived from the deepest cuttings analysed, is considered to apply to the whole interval. This age assignment is also consistent with the *C. striatus*, *C. paradoxa* and *P. pannosus* zone assignments given to samples analysed from the Strzelecki Group in adjacent wells. In general, index species for the younger two zones are relatively rare and are never present in all samples. In their absence assemblages inevitably default to the older *C. striatus* Zone. The occurrence of the youngest *P. pannosus* Zone reported by Dettmann (1987) from Patricia-1 is also problematic as it represents the only known occurrence of this zone in the basin and for that reason alone must be considered doubtful.

The portion of the Strzelecki Group penetrated in Moby-1 is assigned to the Wonthaggi Formation following the recent adoption of this name by Constantine *et al.* (1998) as the preferred formation designation for the bulk of the volcanoclastic succession. The name is a contraction of the Wonthaggi Coal Measures originally proposed by Medwell (1954).

## Biostratigraphy.

The samples analysed in Moby-1 are classified according to the spore-pollen zonation scheme originally proposed by Stover & Evans (1974) and Stover & Partridge (1973, 1982), and more recently updated and refined by Partridge (1999). Those samples which contain diagnostic marine dinocyst assemblages are also classified according to the parallel microplankton scheme originally proposed by Partridge (1975, 1976), and subsequently substantially refined and modified by Partridge (1999). A recent published summary of both these zonation schemes can also be found in the latest edition of the *Geology of Victoria* (Partridge & Dettmann, 2003).

### ***Proteacidites tuberculatus* spore-pollen Zone and *Operculodinium* microplankton Superzone**

**Interval: 538 to 547 metres**

**Age: Late Oligocene to Early Miocene**

The assemblages from the two shallowest sidewall analysed are overwhelmingly dominated by marine microplankton (mainly dinocysts), which average 85% of the combined spore-pollen and microplankton counts. Based on the high abundance of *Spiniferites* spp. (average 74%), and common occurrence of *Operculodinium centrocarpum* (average 10%) within the microplankton counts both samples can be assigned to the *Operculodinium* Superzone. Other dinocysts recorded,

---

<sup>1</sup> Refer to Bernecker & Partridge (2005) for definition and discussion of the term Coal Lines, and maps of their distribution through time in the Gippsland Basin.

which are considered typical of the superzone, include *Dapsilidinium pseudocolligerum*, *Protoellipsodinium simplex* ms and *Pyxidinosia pontus* ms. The associated spore-pollen assemblages are dominated by *Nothofagidites* pollen (average 32%), and can be assigned to the *P. tuberculatus* Zone based on presence of eponymous species at 538m, and *Proteacidites rectomarginis* at 547m, in otherwise relatively low diversity assemblages.

Although too few palynomorphs were recovered from the next deepest cuttings sample at 550m, for a confident zone assignment, the limited assemblage recorded is nevertheless consistent with those from the shallower two sidewall cores.

### **Upper *Nothofagidites asperus* spore-pollen Zone or younger, and *Fromea leos* microplankton Zone**

**Cuttings sample at: 556 metres**

**Age: Early Oligocene**

Relative to the assemblages recovered from the overlying sidewall cores, the palynological assemblage from the cuttings at 555m (representative of interval 553 to 556m) displays a marked decline in abundance of microplankton (to ~17%), and an increase in the diversity of the spore-pollen species. There is also a slight increase in abundance of gymnosperm pollen (to 38% of spore-pollen count), with *Araucariacites australis* (18%) and *Dilwynites granulatus* (5%) prominent, and *Phyllocladidites mawsonii* frequent at 3%. Yet there is no evidence of any Eocene index species, which were not found until the underlying sidewall core at 558.5m. Based on these criteria the best assignment for the cuttings sample is considered to be the Upper *N. asperus* Zone. A younger basal *P. tuberculatus* Zone age cannot however be completely excluded because on the presence of rare specimens of the spores *Cyatheacidites annulatus*, *Cyathidites subtilis* and *Foveotriletes lacunosus*, even though these species are most likely caved along with many of the dinocysts.

Supporting the spore-pollen zone assignment is the rare presence of the acritarch *Fromea leos* ms which has a restricted range extending from the upper part of the Upper *N. asperus* Zone into the very base of the *P. tuberculatus* Zone.

### **Middle *Nothofagidites asperus* spore-pollen Zone**

**Interval: 558.5 to 561.3 metres, possibly extending to 566 metres**

**Age: Late Eocene**

The top of the Middle *N. asperus* Zone, and top of the Eocene, can be confidently placed at the sidewall core at 558.5m based on the presence of *Triorites magnificus*, the key index species for the zone, associated with a number of secondary index species including *Proteacidites adenanthoides*, *P. crassus*, *P. rugulatus* and *Santalumidites cainozoicus* which also have their LADs (Last Appearance Datums) at the top of this zone (see definition in Stover & Partridge, 1982). The zone extends at least to 561.3m based on the occurrence of *Foveotriletes palaequetrus* which is known to have a FAD (First Appearance Datum) in the upper half of the Middle *N. asperus* Zone, and may extend as deep as 565m based on the FAD of *Proteacidites reticulatus* (which is a weak secondary index species for the zone), and the local absence of *Proteacidites pachypolus*. However, in the absence of more definitive index species it is preferable to treat the samples at 565m and 566m as transitional between the Middle and Lower *N. asperus* zones.

Supporting the interpretation of a transition interval is the overall assemblage composition. The samples at 558.5m and 561.3m are dominated by *Nothofagidites* pollen (average 50%), and contain only minor *Haloragacidites harrisii* pollen (average <3%), whereas in the deeper samples at 565m and 566m the amount of *Nothofagidites* pollen declines (to an average of <30%) while *H. harrisii* pollen increases (to an average of 12%). The latter change give the deeper two samples a greater

similarity with the underlying Lower *N. asperus* Zone where *Nothofagidites* pollen averages 27% and *H. harrisii* averages 18%.

Microplankton abundance is low ranging from <1% in sidewall cores to 6% in the cuttings, the latter reflecting some contamination from down-hole cavings from the Seaspray Group. Consequent on this low abundance microplankton diversity is low and zone index species are very rare. Only the sidewall core at 558.5m, at the top of the interval, can be assigned to a zone as it contains multiple poorly preserved specimens of *Gippslandica extensa* which is diagnostic of the *G. extensa* range Zone. In the Gippsland Basin *G. extensa* has an near identical range to *Corrudinium incompositum* diagnostic of the *C. incompositum* Zone. Both zones are lateral equivalents with the *G. extensa* Zone being characteristic of coal measures successions and more nearshore portions of the Gurnard Formation, whereas the *C. incompositum* Zone is most characteristic of more abundant and diverse microplankton assemblages from distal offshore portions of the Gurnard Formation.

### **Lower *Nothofagidites asperus* spore-pollen Zone**

**Interval: 568.5 to 586 metres**

**Age: Middle Eocene**

The six sidewall cores and two cuttings over this interval all belong to the Lower *N. asperus* Zone based on a combination of common *Nothofagidites* pollen (average 27%), and consistent presence of the species *Nothofagidites falcatus* (in 7 of 8 samples) and *Proteacidites pachypolus* (also in 7 of 8 samples). The former species is the key individual index species for the base of the broader *N. asperus* Zone, whereas the latter species is generally rare and inconsistent in the younger Middle *N. asperus* Zone in the Gippsland Basin, even though the species tends to remain more prominent and consistent in this younger subzone in the Bass and Otway basins. Other index species that are prominent and occur no older than this zone are *Tricolpites simatus* and *Tricolporites leuros*, while *Proteacidites recavus* is more consistent and prominent in this subzone relative to its occurrence in the younger Middle subzone. The only species recorded with a range known to be restricted to the Lower subzone is *Plicodiporites crescentis* ms found at 580m. This species is now considered to have a restricted range near the middle of the Lower *N. asperus* Zone.

Microplankton abundances in the productive sidewall cores are low (3 to 12%, average 6%) as is diversity (average 7.5 species), so it is not surprising that the key zone index species are rare. The sidewall core at 575.7m is assigned to the *Deflandrea heterophlycta* Zone on the presence of a single poorly preserved specimen of the eponymous species, while the sidewall core at 580m is assigned to same zone based on a questionable specimen of the acritarch *Paucilobimorpha* (al. *Tritonites*) *inaequalis*. The latter species is considered to be restricted to this zone by Marshall & Partridge (1988). Other species recorded are of limited zone value, but it is worth noting that the index species *Enneadocysta partridgei* diagnostic of the underlying *E. partridgei* Zone was not found, even though it has previously been recorded from cuttings at 460-63m in Flathead-1 and from the *E. partridgei* Zone identified over the basal six metres of the Gurnard Formation in Patricia-1.

### **Undifferentiated Eocene**

**Sidewall core at 588 metres.**

A low organic yield, sufficient to prepare just a single palynological slide, was extracted from the small amount of sandstone (4.5 grams) available for analysis from the sidewall core at 588m. The assemblage contained less than 100 palynomorphs and was dominated (~40%) by bisaccate gymnosperm pollen referred to *Podocarpidites*. Although most specimens are similar to long-ranging Cretaceous to Tertiary bisaccates, there is a significant proportion that are reminiscent of Triassic bisaccates referred to *Falcisporites australis*, and therefore some reworking of these older

forms is considered likely. The remainder of the assemblage comprises a mixture of Early Cretaceous and Eocene species. Diagnostic of the former and clearly reworked are *Ceratosporites equalis*, *Leptolepidites verrucatus* and *Annulispora folliculosa*. Diagnostic of the latter are *Proteacidites reticulosabratus*, *Santalumidites cainozoicus* and *Nothofagidites deminutus* which favour an age assignment no older than the *Proteacidites asperopolus* Zone. Supporting this possible assignment is the low abundance of *Nothofagidites* pollen (3%) compared to the overlying assemblages. But, contradicting such a zone assignment is the lack of a concomitant increase in abundance of *Haloragacidites harrisii* pollen (which is only 2%) as would normally be expected in the *P. asperopolus* Zone. Unfortunately, due to the low yield it also cannot be excluded that some of the Tertiary species may have been introduced by down-hole cavings.

In summary, the sample is probably Eocene but any zone assignment is best left as indeterminate. The limited assemblage recorded is however consistent with the *P. asperopolus* Zone ages obtained from the similar sandstones immediately below the Gurnard Formation in Patricia-1 and Flathead-1.

### **Upper *Coptospora paradoxa* spore-pollen Zone**

**Interval: 613 to 630 metres**

**Age: Mid to Late Albian**

On lithology and electric log character the top of the Strzelecki Group is picked at 589.5m, but definitive Early Cretaceous assemblages are not recorded until the deeper cuttings at 613m and 630m. The shallower sidewall core at 605m and composite cuttings between 589 and 604m unfortunately failed to yield enough palynomorphs for age determination.

The best sample is the deepest cuttings at 630m which yielded an abundant and highly diverse assemblage with surprisingly little contamination from down-hole cavings. The assemblage is assigned to the Upper *C. paradoxa* Zone based on the presence of the key index species *Coptospora paradoxa* and *Pilosisporites grandis*. Other diagnostic species include the megaspores *Arcellites hexapartitus*, *Balmeisporites holodictyus* and *Minerisporites marginatus* and the miospores *Crybelosporites striatus*, *Foraminisporis asymmetricus* and *Ruffordiaspora* (al. *Cicatricosisporites australiensis*). Overall the assemblage is about equally dominated by spores and gymnosperm pollen with the most abundant components being *Podocarpidites* spp. (30%), and spores of *Cyathidites* spp. (19%) and *Baculatisporites/Osmundacidites* (22.5%).

The shallower cuttings at 613m is unfortunately badly contaminated by caved palynomorphs, mainly marine dinocysts from the Seaspray Group, which constitute >65% of the assemblage count. Although key Cretaceous index species are rare, the sample is considered to be no younger than the *C. paradoxa* Zone based on a combination of superposition and the presence of *Crybelosporites striatus*.

## **References**

- BATTEN, D.J. & KOVACH, W.L., 1990. Catalogue of Mesozoic and Tertiary Megaspores. *American Association of Stratigraphic Palynologists, Contributions Series Number 24*, p.1-227.
- BERNECKER, T., & PARTRIDGE, A.D., 2001. Emperor and Golden Beach Subgroups: The onset of Late Cretaceous sedimentation in the Gippsland Basin, SE Australia. **In** *Eastern Australian Basins Symposium. A Refocused Energy Perspective for the Future*, K.C. Hill & T. Bernecker, editors, *Petroleum Exploration of Australia, Special Publication*, p.391-402.
- BERNECKER, T., & PARTRIDGE, A.D., 2005. Approaches to palaeogeographic reconstructions of the Latrobe Group, Gippsland Basin, Southeastern Australia. *APPEA Journal*, vol.45, pt.1 [in press].

- CONSTANTINE, A.E., CHINSAMY, A., VICKERS-RICH, P. & RICH, T.H., 1998. Periglacial environments and polar dinosaurs. *South African Journal of Science*, vol.94, p.137-141.
- DETTMANN, M.E., 1963. Upper Mesozoic microfloras from southeastern Australia. *Proceedings Royal Society Victoria*, vol.77, pt.1, p.1-148.
- DETTMANN, M.E., 1987. Palynology report Patricia No.1, 672m — 880m, Gippsland Basin. *Report for Lasmo Energy Australia Ltd*, 18p. (7 October)
- FENSOME, R.A., WILLIAMS, G.L., BARSS, M.S., FREEMAN, J.M. & HILL, J.M., 1990. Acritarchs and fossil Prasinophytes: An index to genera, species and infraspecific taxa. *AASP Contribution Series No. 25*, p.1-771.
- HELBY, R., MORGAN, R. & PARTRIDGE, A.D., 1987. A palynological zonation of the Australian Mesozoic. **In** *Studies in Australian Mesozoic Palynology*, P.A. Jell, editor, *Memoir Association Australasian Palaeontologists 4*, p.1-94.
- MACPHAIL, M.K., 1999. Palynostratigraphy of the Murray Basin, inland Southeastern Australia. *Palynology* vol.23, p.197-240.
- MARSHALL, N.G. & PARTRIDGE, A.D., 1988. The Eocene acritarch *Tritonites* gen. nov. and the age of the Marlin Channel, Gippsland Basin, southeastern Australia. *Memoir Association of Australasian Palaeontologists 5*, p.239–257.
- MEDWELL, L.M., 1954. A review and revision of the flora of the Victorian Lower Jurassic. *Proceedings Royal Society of Victoria*, vol.65, p.63–111.
- PARTRIDGE, A.D., 1975. Palynological zonal scheme for the Tertiary of the Bass Strait Basin (Introducing Paleogene Dinoflagellate Zones and Late Neogene Spore-Pollen Zones). *Geological Society of Australia (Victorian Division) Symposium on the Geology of Bass Strait and Environs, Melbourne, November, 1975. Esso Australia Ltd Palaeontological Report 1975/17* (unpubl.).
- PARTRIDGE, A.D., 1976. The geological expression of eustasy in the early Tertiary of the Gippsland Basin. *The APEA Journal*, vol.16, pt.1, p.73–79.
- PARTRIDGE, A.D., 1999. Late Cretaceous to Tertiary geological evolution of the Gippsland Basin, Victoria. PhD thesis, La Trobe University, Bundoora, Victoria, p.i-xxix, p.1-439, 165 figs, 9 pls (unpubl.).
- PARTRIDGE, A.D. & DETTMANN, M.E., 2003. Chapter 22.4.2 Plant microfossils. **In** *Geology of Victoria*, W.D. Birch, editor, *Geological Society of Australia Special Publication 23*, p.639-652.
- STOVER, L.E. & EVANS, P.R., 1974 [imprint 1973]. Upper Cretaceous–Eocene spore-pollen zonation, offshore Gippsland Basin, Australia. **In** *Mesozoic and Cainozoic palynology: Essays in honour of Isabel Cookson*. J.E. Glover & G. Playford, editors, *Geological Society of Australia Special Publication 4*, p.55-72, pls 1-4.
- STOVER, L.E. & PARTRIDGE, A.D., 1973. Tertiary and late Cretaceous spores and pollen from the Gippsland Basin, southeastern Australia. *Proceedings Royal Society of Victoria*, vol.85, pt.2, p.237-286.
- STOVER, L.E. & PARTRIDGE, A.D., 1982. Eocene spore-pollen from the Werillup Formation, Western Australia. *Palynology* 6, p.69–95.
- WILLIAMS, G.L., LENTIN, J.K. & FENSOME, R.A., 1998. The Lentin and Williams index of fossil dinoflagellates 1998 edition. *American Association of Stratigraphic Palynologists, Contributions Series, no. 34*, p.1-817.

**Table 2: Interpretative data for Moby-1, offshore Gippsland Basin.**

Sample Type	Depth metres	Spore-Pollen Zones (Microplankton Zones)	CR*	Comments and Key Species Present
SWC 25	538	<i>P. tuberculatus</i> Zone ( <i>Operculodinium</i> Superzone)	B3 B3	FAD of zone index <i>Proteacidites tuberculatus</i> MP abundance >90%; with <i>Spiniferites</i> species ~ 84%
SWC 24	547	<i>P. tuberculatus</i> Zone ( <i>Operculodinium</i> Superzone)	B4 B2	FAD in SWCs of <i>Protoellipsodinium simplex</i> ms MP abundance 78%; with <i>Spiniferites</i> species ~68%
Cuttings	550	Indeterminate		Very low yield with ~30 palynomorphs recovered.
Cuttings	556	Upper <i>N. asperus</i> or younger ( <i>Fromea leos</i> Zone)	D4 D3	FADs of <i>Cyatheacidites annulatus</i> , <i>Proteacidites rectomarginis</i> and <i>Fromea leos</i> ms in assemblage with MP >15%, & <i>Araucariacites</i> + <i>Dilwynites</i> 23%.
SWC 22	558.5	Middle <i>N. asperus</i> Zone ( <i>Gippslandica extensa</i> )	B1 B3	FADs & LADs of index species <i>Triorites magnificus</i> and <i>Gippslandica extensa</i> . MP abundance <3%.
SWC 20	561.3	Middle <i>N. asperus</i> Zone	B3	FAD of secondary species <i>Foveotriletes palaequetrus</i> . MP rare <1%. <i>Nothofagidites</i> 53% > <i>H. harrisii</i> ~3%
Cuttings	565	Lower to Middle <i>N. asperus</i> Zones	D4	LAD of <i>Proteacidites recavus</i> . MP abundance ~6%. <i>Nothofagidites</i> 15% approx equal to <i>H. harrisii</i> ~13%
SWC 18	566	Lower to Middle <i>N. asperus</i> Zones	B4	FAD of <i>Proteacidites reticulatus</i> . MP abundance ~4%. <i>Nothofagidites</i> 44% > <i>H. harrisii</i> ~10%
SWC 16	568.5	Lower <i>N. asperus</i> Zone	B1	LAD of consistent <i>Proteacidites pachypolus</i> . MP ~4%. <i>Nothofagidites</i> 32% > <i>H. harrisii</i> ~22%
SWC 14	571	Lower <i>N. asperus</i> Zone	B4	LAD of <i>Enneadocysta</i> sp. cf. <i>E. pectiniformis</i> MP ~8%. <i>Nothofagidites</i> 37% > <i>H. harrisii</i> ~24%
SWC 12	574	<i>N. asperus</i> Zone undiff.	B4	Poor assemblage without subzone index species. MP <3%. <i>H. harrisii</i> 26% > <i>Nothofagidites</i> 20%.
SWC 11	575.7	Lower <i>N. asperus</i> Zone ( <i>Deflandrea heterophlycta</i> Zone)	B2 B3	FAD & LAD of index form <i>Deflandrea heterophlycta</i> MP ~12%. <i>Nothofagidites</i> 33% > <i>H. harrisii</i> ~22%
Cuttings	577	Lower <i>N. asperus</i> Zone	D2	MP ~25%, but mostly caved from Seaspray Group. <i>H. harrisii</i> 27% > <i>Nothofagidites</i> 20%.
SWC 10	580	Lower <i>N. asperus</i> Zone ( <i>Deflandrea heterophlycta</i> Zone)	B1 B5	FADs of <i>Plicodiporites crescentis</i> ms & questionable specimen of acritarch <i>Paucilobimorpha inaequalis</i> . MP <5%. <i>Nothofagidites</i> 29% > <i>H. harrisii</i> 6%.
SWC 8	585	<i>N. asperus</i> Zone undiff.	B5	Low yield with <100 palynomorphs. Assigned to zone on abundance of <i>Nothofagidites</i> ~25% of count.
Cuttings	586	Lower <i>N. asperus</i> Zone	D1	MP ~17%, but mostly caved from Seaspray Group. <i>H. harrisii</i> 20% approx equal to <i>Nothofagidites</i> 23%.
SWC 6	588	Mixed Eocene and reworked spore-pollen but zone indet.		Low yield assemblage dominated by bisaccate gymnosperm pollen >40% of count.
*Cuttings	589 to 604	Indeterminate and essentially BARREN		Very low yield with less than 20 palynomorph grains recovered.
SWC 3	605	Indeterminate		Very low yield with <25 palynomorph recovered.
Cuttings	613	<i>C. paradoxa</i> Zone by superposition	D4	LAD of <i>Crybelosporites striatus</i> in cuttings dominated (>60%) by cavings from Seaspray Group.
Cuttings	630	<i>Coptospora paradoxa</i> Zone	D1	FAD of <i>Coptospora paradoxa</i> in diverse Albian assemblage.

\*Composite cuttings

FAD & LAD = First and Last Appearance Datums.  
MP = Abbreviation for Microplankton.

**\*Confidence Ratings used in STRATDAT database and applied to Table 2.**

<b>Alpha codes:</b> Linked to sample		<b>Numeric codes:</b> Linked to fossil assemblage		
<b>A</b>	Core	<b>1</b>	<b>Excellent confidence:</b>	High diversity assemblage recorded with key zone species.
<b>B</b>	Sidewall core	<b>2</b>	<b>Good confidence:</b>	Moderately diverse assemblage with key zone species.
<b>C</b>	Coal cuttings	<b>3</b>	<b>Fair confidence:</b>	Low diversity assemblage recorded with key zone species.
<b>D</b>	Ditch cuttings	<b>4</b>	<b>Poor confidence:</b>	Moderate to high diversity assemblage without key zone species.
<b>E</b>	Junk basket	<b>5</b>	<b>Very low confidence:</b>	Low diversity assemblage without key zone species.

**Description of Range Chart.**

The distribution of the palynomorphs identified in the samples are presented on the accompanying StrataBugs™ range chart which displays the recorded palynomorph species in the samples proportional to their depth in the well and in terms of their relative abundance (as a percentage). The palynomorphs recorded are split between different categories. The terrestrial spore-pollen are divided between spores, gymnosperm pollen and angiosperm pollen, which are plotted in separate panels with their abundances expressed in terms of the total spore-pollen count. This is followed by a panel showing the total count of marine and non-marine microplankton as a percentage relative to the combined spore-pollen and microplankton count. Next the percentage abundance of individual species in the microplankton count is displayed in panel labelled Microplankton. Then plotted are Other palynomorphs, with abundances expressed as a percentage of sum of the total Spore-Pollen plus Other palynomorphs counted. Finally, Permian and Triassic species in the assemblages are plotted as Reworked in panel labelled RW. Within each of the panels the species are plotted according to either their highest/youngest occurrence or in alphabetical order.

The following codes or abbreviations apply to the individual species occurrences and abundances on the range chart:

Numbers	=	Absolute abundance or number of specimens counted
+	=	Species outside of count
C	=	Caved species
R	=	Reworked species
?	=	Questionable identification of species.

## BASIC DATA

**Table 3. Basic sample data for Moby-1, offshore Gippsland Basin.**

Sample Type	Depth metres	Lithology	Wt gms	VOM	Org. Yield
SWC 25	538	Calcilutite	9.7		
SWC 24	547	Calcilutite	7.1		
Cuttings	550	(not recorded)	12.0		
Cuttings	556	Light to medium grey calcareous claystone to marl? (powder to 5 mm clumps)	17.6	0.2	0.011
SWC 22	558.5	Glaucinitic Sandstone: dark brownish grey	7.5	0.5	0.066
SWC 20	561.3	Argillaceous Glaucinitic Siltstone: dark brownish grey	8.9	0.6	0.067
Cuttings	565	Medium to light grey siltstone? (powder to 10 mm clumps)	17.5	0.2	0.011
SWC 18	566	Sandstone: dark yellowish brown, trace glauconite	8	0.5	0.062
SWC 16	568.5	Sandstone: dark yellowish brown, argillaceous, glauconitic	10.2	0.4	0.039
SWC 14	571	Argillaceous Siltstone: slightly glauconitic	9.6	0.5	0.052
SWC 12	574	Argillaceous Siltstone: dark yellowish brown, trace of glauconite	4.5		
SWC 11	575.7	Glaucinitic Sandstone: mottled brownish grey to dark green	6.6	0.7	0.106
Cuttings	577	Dark grey sandstone (powder to 10 mm clumps)	19.2	0.4	0.020
SWC 10	580	Siltstone: dark brownish grey	5.3		
SWC 8	585	Sandstone: medium dark grey	7.6		
Cuttings	586	Medium brown green-grey sandstone (powder to 10 mm clumps)	19.5	0.4	0.020
SWC 6	588	Sandstone: medium light grey	4.5		
Cuttings	589 to 604	(not recorded)	18.5		
SWC 3	605	Sandstone: medium light grey (Strzelecki ?)	6.6		
Cuttings	613	Medium green-grey greywacke (powder to 10 mm clumps)	19.3	0.2	0.010
Cuttings	630	Medium grey greywacke (powder to 8 mm clumps)	18.7	0.5	0.026

Wt = Weight of sample processed in grams.

VOM = Volume of wet organic residues in cubic centimetres.

Org. Yield = Organic Yield — VOM divided by Wt.

## BASIC DATA

**Table 4. Basic assemblage data for Moby-1, offshore Gippsland Basin.**

Sample Type	Depth metres	Visual Yield	Palynomorph Concentration	Preservation	No. SP Species	No. MP Species	MP%
SWC 25	538	Moderate	High	Poor-fair	30+	12+	>90%
SWC 24	547	Low	High	Poor	25+	13+	78%
Cuttings	550	Moderate	Very low	Poor	3+	6+	
Cuttings	556	Moderate	High	Poor-fair	44+	11+	15%
SWC 22	558.5	High	High	Very poor	47+	10+	<3%
SWC 20	561.3	Moderate	Very low	Very poor-fair	29+	3+	<1%
Cuttings	565	Low	Moderate	Poor-fair	36+	5+	6%
SWC 18	566	High	Moderate-high	Poor	47+	4+	4%
SWC 16	568.5	High	High	Poor-fair	55+	10+	4%
SWC 14	571	High	High	Very poor	51+	9+	8%
SWC 12	574	Low	Low-moderate	Very poor	27+	2+	<3%
SWC 11	575.7	High	Moderate	Very poor	37+	9+	12%
Cuttings	577	High	High	Poor	57+	17+	25% †
SWC 10	580	Low	High	Poor	72+	12+	5%
SWC 8	585	Very low	Low	Poor	22+	4+	
Cuttings	586	High	High	Fair-good	63+	13+	17% †
SWC 6	588	Very low	Very low	Very poor	23		
Cuttings*	589 to 604	Very low	Very low	Very poor	8+	1+	
SWC 3	605	Very low	Very low	Very poor	6+		
Cuttings	613	Low	Low	Poor-fair	18+ (10+)	1+ (4+)	
Cuttings	630	High	High	Fair-good	34+	4+	

\*Composite Cuttings

**Averages:      35+      7+**

MP = Microplankton

SP = Spore-Pollen

Numbers in brackets in two right-hand columns refer to caved species.

† = Microplankton abundance inflated by down-hole cavings from Seaspray Group.



## **APPENDIX 4**

---

# **Petrographic Analysis of Six Samples Selected from Well Moby-1**

---

**By Core laboratories Australia Pty Ltd**



**CORE LABORATORIES  
AUSTRALIA PTY LTD**

447-449 Belmont Ave, Kewdale, Perth WA 6105  
Tel : (61 8) 9353 3944 Fax : (61 8) 9353 1369  
Email : corelab@corelab.com.au

**PETROGRAPHIC ANALYSIS  
OF SIX SAMPLES SELECTED FROM  
WELL MOBY 1**

**Prepared for  
BASS STRAIT OIL COMPANY LTD.**

**CONFIDENTIAL**

**CORE LABORATORIES CANADA LTD**  
CL Job # 52135-04-3656

December, 2004

These analyses, opinions or interpretations are based on observations and materials supplied by the client to whom, and for whose exclusive and confidential use, this report is made. The interpretations or opinions expressed represent the best judgment of Core Laboratories, (all errors and omissions excepted); but Core Laboratories and its officers and employees, assume no responsibility and make no warranty or representations, as to the productivity, proper operations, or profitability of any oil gas or other mineral well or sand in connection with which such report is used or relied upon.

## TABLE OF CONTENTS

<b>SUMMARY</b>	<b>1</b>
<b>INTRODUCTION</b>	<b>2</b>
<b>PROCEDURES AND DATA BASE</b>	<b>2</b>
<b>PETROGRAPHIC ANALYSIS</b>	<b>3</b>
Rock Type And Framework Constituents	3
Detrital Clay Matrix	3
Diagenetic Products	3
Porosity And Reservoir Quality	4
Potential For Formation Damage	4
<b>REFERENCES</b>	<b>4</b>
<b>TABLES, FIGURES AND PLATES</b>	
Table 1. Listing of Samples Selected for Petrographic Analysis	
Table 2. Petrographic Summary	
Table 3. X-Ray Diffraction Analysis	
Figure 1. Ternary Diagram - Sandstone Composition	
Plates 1-6. Thin Section and SEM Photomicrographs and Photographs, and Descriptions	

## SUMMARY

- **Six** sidewall core samples have been selected from **Well Moby 1** for petrographic analysis. The shallowest three samples are glauconite- and biotite-bearing sandstones. The rest are sandstones rich in volcanic material.
- These samples are texturally and compositionally dissimilar, but can be separated into **two groups**. Grain size generally increases towards the bottom, varying from upper very fine grained (0.090 mm) to lower medium grained (0.320 mm). The shallowest samples are well sorted; the deeper samples are poorly to moderately sorted. Petrographically, these samples vary from being **lithic arkoses** (rich in potassium feldspars) to **litharenites** (rich in volcanic rock fragments), some of which are feldspathic. Detrital clay content decreases with depth, from 9.2% to 1.2%.
- Pore-filling cements consist of common to abundant **chlorite**, with smaller amounts of kaolinite and smectite. The main authigenic non-clay cements are **siderite** and **pyrite**; these minerals are more common in the deepest samples.
- The **pore system** is of dominantly **intergranular** type, with a secondary **solutional** component. Point count porosity varies from 1.6% to 12%. Primary intergranular pores are poorly interconnected. Secondary pores, created by the dissolution of feldspars and volcanic fragments, are of minor to fair abundance. Common ineffective **micropores** are associated with detrital clays, glauconite, and authigenic chlorite and kaolinite.
- **Reservoir quality** appears to be **fair to good** for the three shallowest samples, and poor to fair for the three deepest samples.

## INTRODUCTION

This report presents the results of thin section petrography of six sidewall core samples from the **Moby 1** well. These samples have been selected from the depth interval 558.5 - 605.00 m (Table 1). The purpose of this study is to determine the:

- a) **Rock type** and framework constituents.
- b) **Diagenetic** products.
- c) **Pore system** type.
- d) **Reservoir quality** and potential for **formation damage** in the sampled zone.

## PROCEDURES AND DATA BASE

Six thin sections were prepared by impregnating the samples with blue-dyed epoxy to identify porosity, and to prevent delicate mineral constituents (e.g. authigenic clays) from being destroyed during grinding. These samples were half stained with sodium cobaltinitrate to identify alkali feldspars, and also Alizarin Red-S and potassium ferricyanide to distinguish calcite from dolomite and identify ferroan carbonates.

Point count modal analyses (250 points) were conducted to provide the relative proportions of framework grains, detrital clay matrix, pore-filling constituents and pore volume. Relevant data are provided in Table 2, and plotted on a ternary diagram (Figure 1). An overview and high magnification photomicrographs were taken for each sample. Thin section photomicrographs are shown on Plates 1 through 6.

Scanning electron microscope (SEM) analyses were conducted on freshly broken surfaces of all samples, in order to illustrate pore system properties and the types and modes of occurrence of pore-filling constituents, especially mineral precipitates at pore throats. Smectite on photographs indicate illite-smectite mixed-layer clay.

X-ray diffraction (XRD) analysis was used to obtain semi-quantitative mineralogical data for all samples (Table 3). Rock samples were ground to 12 microns, to ensure homogeneity, and analysed, using standard XRD procedures. Less than 4 micron-size fractions of these samples were analysed to determine the type and relative proportions of commonly diagenetic clay mineral species.

## PETROGRAPHIC ANALYSIS

### **ROCK TYPE AND FRAMEWORK CONSTITUENTS**

The three shallowest samples are texturally and mineralogically comparable, all being upper very fine grained, well to very well sorted sandstones, with minor to moderate amounts of detrital clay matrix. Grains are generally loosely packed, and exhibit mostly tangential and fairly wide surface contacts. These sandstones are rich in glauconite and biotite. They are massive with some poorly distinct laminations, defined by the orientation of glauconite and biotite grains. These samples are **lithic arkoses** (Table 1).

By contrast, the three deepest samples are rich in volcanic rock fragments. Average grain size varies from lower fine grained (0.165 mm) to lower medium grained (0.320 mm). In these sandstones, monocrystalline quartz content decreases in amount from 20% to 10%, with depth. Chert and sedimentary rock fragments are minor in abundance, with the exception of sample SWC-3 where these particles are present in appreciable amounts. Volcanic rock fragments are present in all three samples, varying from being a minor constituent (in the shallowest samples) to 20% (in the deepest sample). Plagioclases and potassium feldspars are moderate to common; the latter are relatively more abundant. Accessory components include glauconite, micas (biotite is more common than muscovite) and heavy minerals. Glauconite and biotite, occurring mostly in the shallowest samples, are coarser grained than the other components. Titanium oxides (probably rutile) form 8.4% of sample SWC-16; zircon forms 10% of sample SWC-8. Based on the relative proportions of framework components, these samples are classified as **litharenites**, with the shallower two samples being **feldspathic** (Table 1).

### **DETRITAL CLAY MATRIX**

Detrital clay matrix content generally decreases with depth.

### **DIAGENETIC PRODUCTS**

The main authigenic mineral is **chlorite** derived by the alteration of biotite and glauconite grains (in the shallowest samples); it also occurs as pore fill (in the deepest samples). Sample SWC-8 contains the greatest quantity (25%) of pore-filling chlorite, occurring as cement. Isopachous chlorite in the litharenite sample SWC-3 coats most of the framework grains. Vermicular **kaolinite** (Table 2), fairly common in the deepest samples, has precipitated alongside flaky **smectite**. Blocky **siderite** was also found as patchy pore-filling cement in sample SWC-8. In this sample, **pyrite** occurs as individual grains, possibly suggesting a detrital source.

Authigenic pyrite postdates all other authigenic minerals, occurring as pore fill, and as replacement.

### ***POROSITY AND RESERVOIR QUALITY***

Pores are primarily **intergranular**, with minor volumes of dissolution pores (after feldspars and volcanic lithoclasts). Also, micropores are very common, being associated with detrital and authigenic clays and glauconite grains. Thin section porosity ranges between 1.6% (in sample SWC-6) and 12% (in sample SWC-16). Higher porosity is due to smaller amounts of chlorite; chlorite, however, typically blocks pore throats, resulting in reduced permeability. Lower porosity is due to common amounts of smectite and kaolinite, replacing volcanic ash; and completely occluding primary pores.

Reservoir potential appears to be fair to good within the three shallowest samples and poor to fair within the deepest samples.

### ***POTENTIAL FOR FORMATION DAMAGE***

Several iron-bearing minerals were detected as cements, and as replacement. These minerals are: chlorite (max=25%), siderite (max=8.4%), and pyrite (max=10%), all percentages of rock volume. This sampled interval is highly **acid sensitive**, due to iron-bearing minerals that can react with hydrochloric acid (HCl), creating iron hydroxide gels. Therefore, hydrofluoric acid (HF), or mud acids (HCl/HF mixture), should not be used to stimulate the sampled interval, and presumably formation rocks above and below it. If HCl acid stimulation is planned to clean perforations, the acid should contain an iron-sequestering agent, which should be recovered before being spent, in order to minimize the potential for adverse iron-rich mineral reactions.

**Illite-smectite** mixed-layer clays form a maximum of 10% of the total rock volume, indicating problematic swelling of clays in the presence of fresh water, causing reduction in permeability. Kaolinite (4% from the total rock volume), may cause a relatively low fines migration problem.

## **REFERENCES**

Folk, R.L. (1980) *Petrology of Sedimentary Rocks*. Hemphill Publishing Company, Austin, Texas, 184p.

**Table 1. Listing of the Selected Samples for Petrographic Analysis**

<b>Depth (m)</b>	<b>Sample ID</b>	<b>Point Count Porosity (%)</b>	<b>Classification (Folk, 1980)</b>	<b>Reservoir Quality (estimated)</b>
558.5	SWC-22	7.6	Lithic arkose	Fair
568.5	SWC-16	12.0	Lithic arkose	Fair to good
575.7	SWC-11	6.4	Lithic arkose	Fair
585.0	SWC-8	3.4	Feldspathic litharenite	Poor
588.0	SWC-6	1.6	Feldspathic litharenite	Poor
605.0	SWC-3	10.6	Litharenite	Fair

**Table 2. Petrographic Summary**

Company: Bass Strait Oil Company Ltd.  
Well: Moby 1

C.L. File No. 52135-04-3656  
Date: December, 2004  
Petrologist: Simona Vari

Well ID	BSOC MOBY 1					
Sample ID	SWC-22	SWC-16	SWC-11	SWC-8	SWC-6	SWC-3
Depth (m)	558.5	568.5	575.7	585.0	588.0	605.0
ROCK TYPE (Folk et al., 1980) Classification	Sandstone Lithic arkose	Sandstone Lithic arkose	Sandstone Lithic arkose	Sandstone Felds. lith.	Sandstone Felds. lith.	Sandstone Litharenite

**FRAMEWORK GRAINS**

<b>Quartz</b>	Monocrystalline	22.8	23.6	21.6	11.8	10.6	10.8
<b>Rock</b>	Chert	2.4	3.4	2.8	3.2	6.0	8.6
<b>Fragments</b>	Sedimentary	2.4	2.6	5.6	1.6	3.2	14.0
	Volcanic	2.8	0.8	0.4	5.2	10.8	20.4
<b>Feldspars</b>	Potassium feldspar	10.0	6.8	9.2	4.8	10.6	7.6
	Plagioclase feldspar	2.0	1.2	2.8	1.2	3.2	6.0
<b>Accessory Grains</b>	Phosphate grains	-	-	-	-	-	-
	Glauconite	9.2	7.6	13.6	2.8	1.2	0.4
	Micas	10.8	6.8	10.8	3.6	0.4	1.2
	Zircon>Tourmaline	1.2	0.8	0.8	10.0	0.8	-
	Titanium oxides	-	8.4	-	2.4	-	-

**MATRIX**

<b>Matrix</b>	Detrital clays	9.2	6.0	4.0	2.4	2.4	1.2
---------------	----------------	-----	-----	-----	-----	-----	-----

**AUTHIGENIC MINERALS**

<b>Clays</b>	Chlorite	12.4	11.6	9.6	25.6	14.2	14.8
	Kaolinite	< 1.0	2.8	3.6	2.8	9.0	2.4
	Illite & Smectite	1.2	0.8	3.6	0.8	19.8	0.4
<b>Non-Clay Cements</b>	Calcite	-	-	-	-	-	-
	Dolomite	-	-	-	-	-	-
	Siderite	-	-	-	8.4	2.8	0.4
	Hematite	-	-	-	-	-	-
	Pyrite	6.0	4.8	5.2	10.0	3.4	1.2

**POROSITY**

<b>Primary:</b>	Intergranular	6.8	10.8	5.6	3.0	0.4	9.0
<b>Secondary:</b>	Dissolution	0.8	1.2	0.8	0.4	1.2	1.6
	Microporosity	Common	Common	Common	Common	Common	Common

**TEXTURE**

<b>Grain Size (mm)</b>	0.105 (vfU)	0.100 (vfU)	0.090 (vfU)	0.165 (fL)	0.270 (mL)	0.320 (mL)
<b>Sorting</b>	Very well	Very well	Well	Poor	Moderate	Moderately well
<b>Roundness</b>	Sa-Sr	Sa-Sr	Sa-Sr	Sa-Sr	Sa-Sr	Sa-Sr
<b>Grain Contacts</b>	Loose to point	Loose to point	Loose to point	Loose	Point to long	Point to long



A = Angular; Sa = subangular; Sr = subrounded; R = Rounded

**Table 3. X-Ray Diffraction Analysis (Combined Whole Rock and Clay)**

Company: Bass Strait Oil Company Ltd  
 Well: Moby 1  
 File No: 52135-04-3656



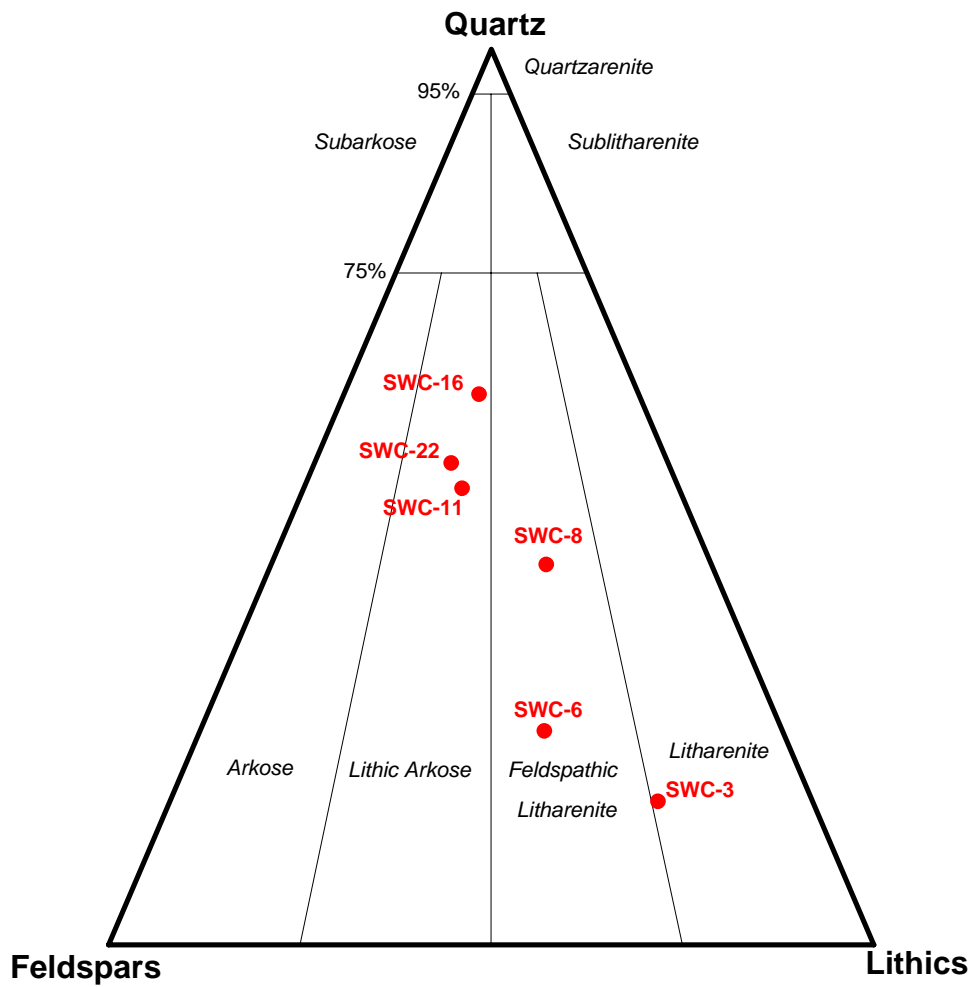
Sample ID	SWC-22	SWC-16	SWC-11	SWC-8	SWC-6	SWC-3
Depth (m)	558.5	568.5	575.7	585.0	588.0	605.0
<b>Whole Rock Weight %</b>						
Quartz	76	67	67	44	56	49
K-Feldspar	4	2	4	4	11	6
Plagioclase	1	3	1	1	3	15
Anhydrite	0	0	0	0	0	0
Calcite	0	0	0	0	0	0
Ferroan Dolomite	0	0	0	0	0	0
Dolomite	0	0	0	0	0	0
Gypsum	0	0	0	0	0	0
Halite	0	0	0	0	0	0
Siderite	0	7	0	25	1	1
Pyrite	2	1	2	1	1	1
Rutile	0	5	0	2	0	0
Total Clay	17	15	26	23	28	28
<b>Relative Clay %</b>						
Smectite	0	0	0	0	0	0
Illite / Smectite *	11	17	17	8	15	38
Illite & Mica	35	46	37	19	8	20
Kaolinite	19	12	12	19	19	10
Chlorite	35	25	34	54	58	32

**\* Illite / Smectite Mixed-Layer Clay**

The percentage of smectite layers in illite / smectite clay

60%-80%    60%-80%    60%-80%    60%-80%    60%-80%    60%-80%

**Figure 1**  
**Ternary Diagram - Sandstone Classification (Folk, 1980)**  
**Bass Strait Oil Company Ltd.**  
**MOBY 1 Well**





# THIN SECTION PETROGRAPHY

Company: Bass Strait Oil Company Ltd.  
Well: Moby 1

Depth (m) 558.5  
Sample ID SWC-22  
Point Count Porosity (%) 7.6

Plate 1B



## Depositional texture

Rock type	Sandstone
Classification (Folk)	Lithic arkose
Average grain size (mm)	0.105 (vfU)
Sorting	Very well
Grain contacts	Loose to point
Features	Massive

## Framework Grains

Monocrystalline quartz	22.8
Chert	2.4
Sedimentary	2.4
Volcanic	2.8
Potassium feldspar	10.0
Plagioclase feldspar	2.0

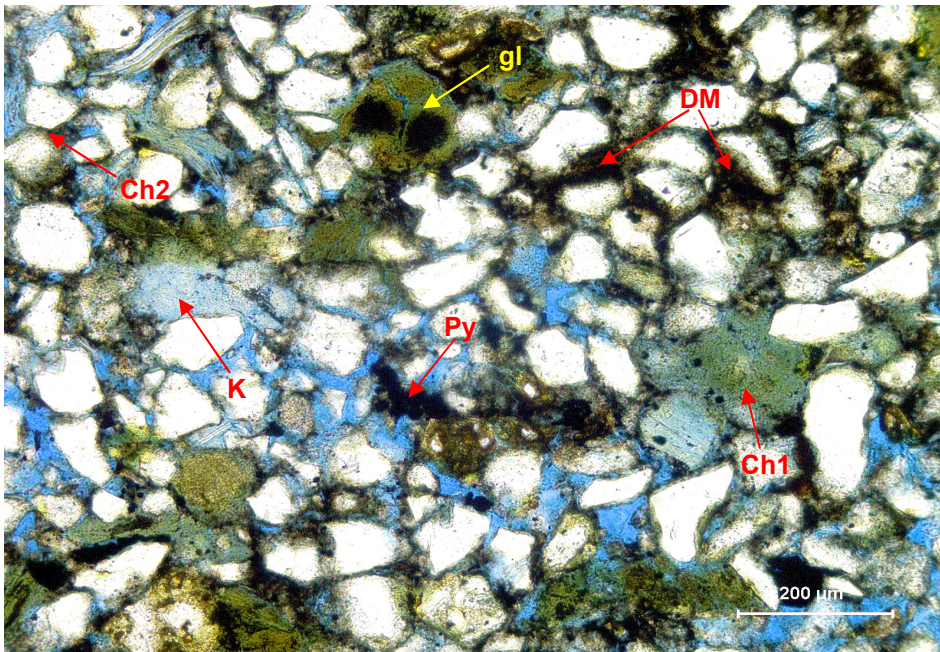
## Accessory Minerals

Phosphate grains	-
Glauconite	9.2
Micas	10.8
Zircon>Tourmaline	1.2
Titanium oxides	-

## Matrix

Detrital Clays	9.2
----------------	-----

Plate 1C



## Authigenic minerals

Chlorite	12.4
Kaolinite	< 1.0
Illite & smectite	1.2
Calcite	-
Dolomite	-
Siderite	-
Hematite	-
Pyrite	6.0

## Porosity

Intergranular	6.8
Dissolution	0.8
Microporosity	Common

## Petrographic description

This upper very fine grained, very well sorted sandstone contains "pockets" of detrital clays (DM, yellow circle). Glauconite (gl) and biotite are commonly present as dispersed grains. Chlorite occurs as the main grain-replacement (Ch1) and grain-coating (Ch2) mineral. Kaolinite (K) and framboids of pyrite (Py) reduce some pores. Primary pores are moderately preserved and low interconnected due to the chlorite coating.



Trace (<1%)  
Minor (1-5%)  
Moderate (5-10%)  
Common (10-20%)  
Abundant (>20%)

C.L. File No. 52135-04-3656

**Company: Bass Strait Oil Company Ltd.**  
**Well: MOBY 1**  
**Depth (m): 558.5**



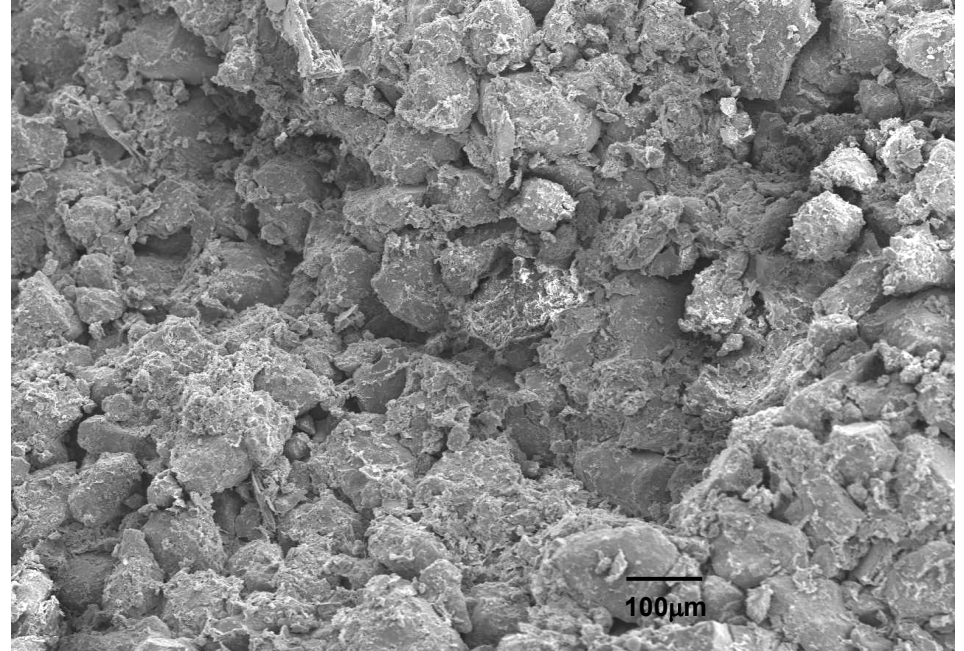
**Sample SWC-22 - LITHIC ARKOSE**

Plate 1D (x100): This detrital-rich sandstone has abundant chlorite cement that occurs mostly as replacement of detrital clays, glauconite and biotite grains.

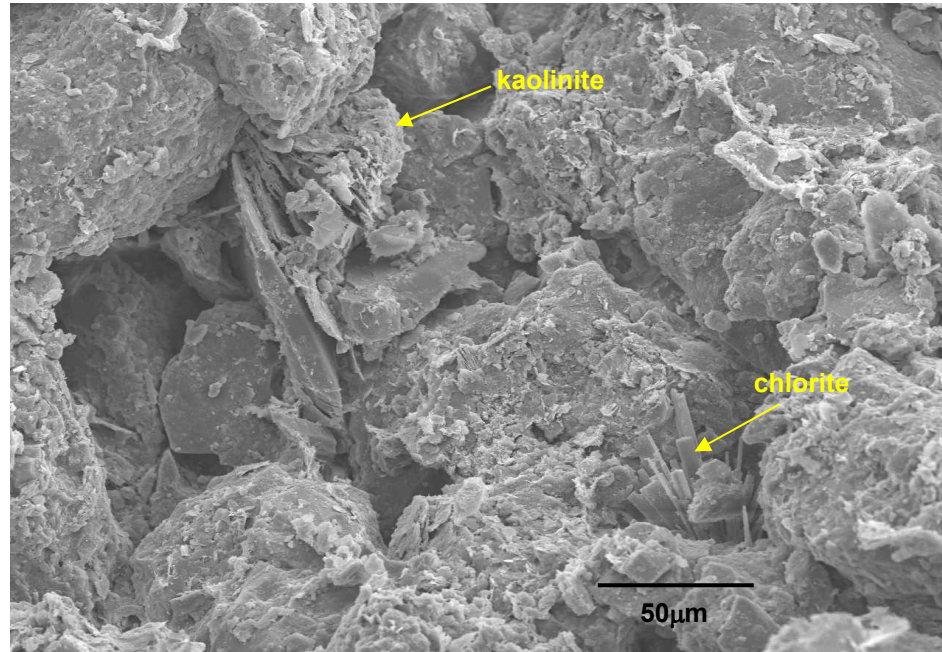
Plate 1E (x450): Authigenic kaolinite bucklets line pores and acicular chlorite replaces biotite.

Plate 1F (x1500): Authigenic chlorite flakes form a coat on framework grains and "bridges" between the grains, blocking the pore throats.

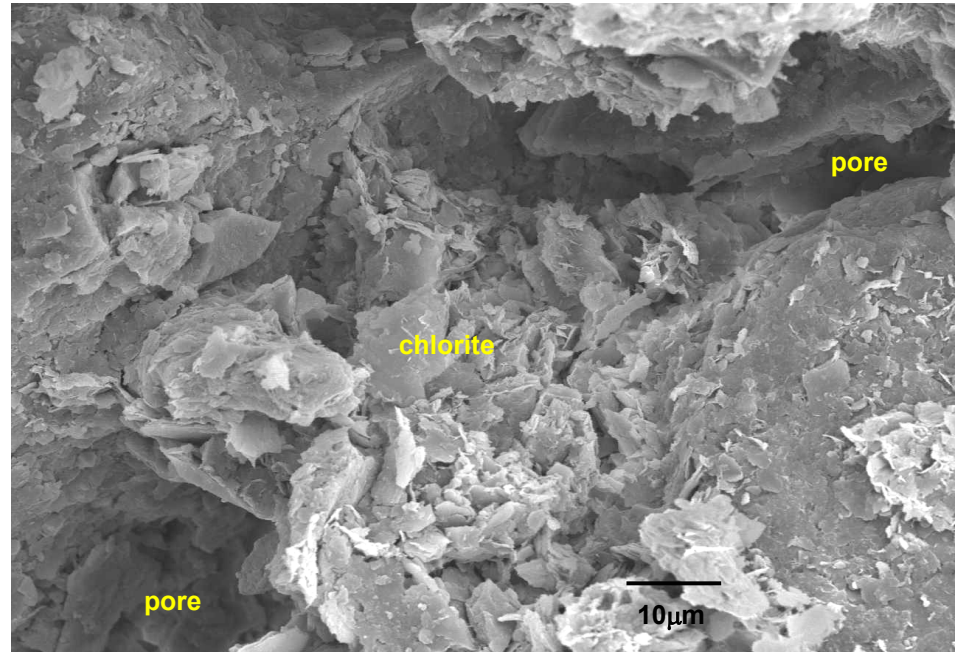
**Plate 1D**



**Plate 1E**



**Plate 1F**





**Sample:** SWC-16  
**Depth (m):** 568.5  
**Porosity (%):** 38.1  
**Permeability (md):** 417

**4mm**

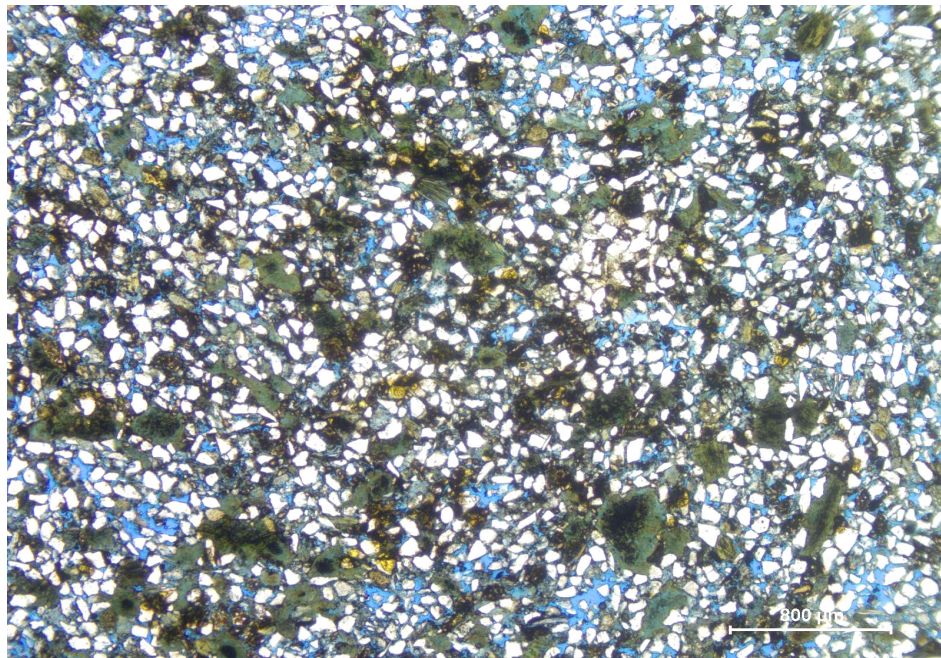


# THIN SECTION PETROGRAPHY

Company: Bass Strait Oil Company Ltd.  
Well: Moby 1

Depth (m) 568.5  
Sample ID SWC-16  
Point Count Porosity (%) 12.0

Plate 2B



## Depositional texture

Rock type	Sandstone
Classification (Folk)	Lithic arkose
Average grain size (mm)	0.100 (vfU)
Sorting	Very well
Grain contacts	Loose to point
Features	Massive

## Framework Grains

Monocrystalline quartz	23.6
Chert	3.4
Sedimentary	2.6
Volcanic	0.8
Potassium feldspar	6.8
Plagioclase feldspar	1.2

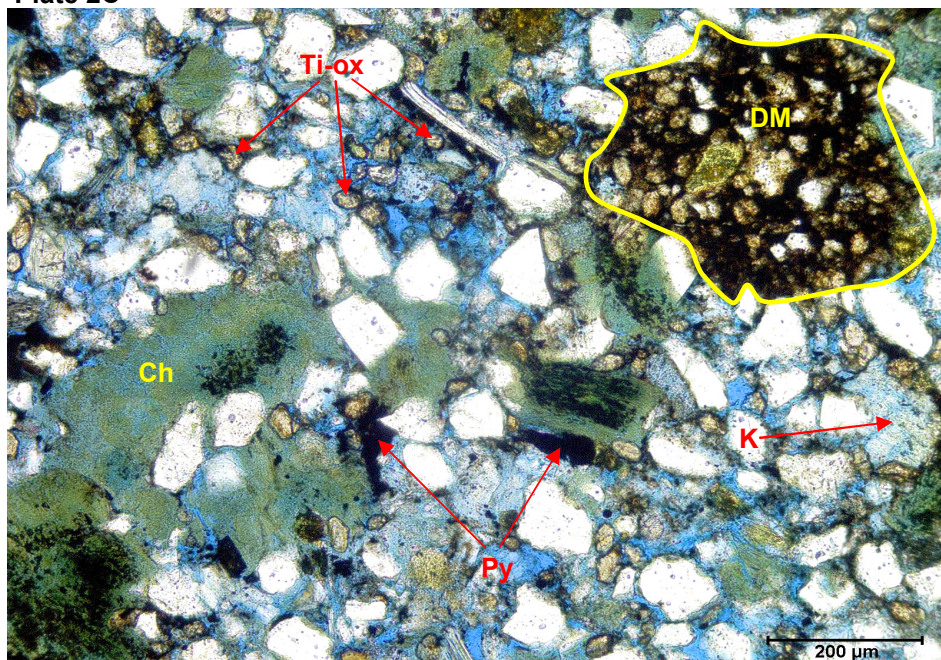
## Accessory Minerals

Phosphate grains	-
Glaucanite	7.6
Micas	6.8
Zircon>Tourmaline	0.8
Titanium oxides	8.4

## Matrix

Detrital Clays	6.0
----------------	-----

Plate 2C



## Authigenic minerals

Chlorite	11.6
Kaolinite	2.8
Illite & smectite	0.8
Calcite	-
Dolomite	-
Siderite	-
Pyrite	4.8

## Porosity

Intergranular	10.8
Dissolution	1.2
Microporosity	Common

## Petrographic description

Moderate amounts of detrital clay matrix (DM) occur as isolated patches in this upper very fine grained, very well sorted sandstone. Heavy minerals such as titanium oxides (Ti-ox) are present in moderate amounts. Chlorite (Ch), pyrite (Py) and kaolinite (K) are the main authigenic cements. They occur mostly as grain-replacement and to a lesser extent as pore-filling. Common micropores are associated with chlorite and glauconite. Intergranular pores are commonly preserved.



Trace (<1%)  
Minor (1-5%)  
Moderate (5-10%)  
Common (10-20%)  
Abundant (>20%)

C.L. File No. 52135-04-3656

**Company: Bass Strait Oil Company Ltd.**  
**Well: MOBY 1**  
**Depth (m): 568.5**



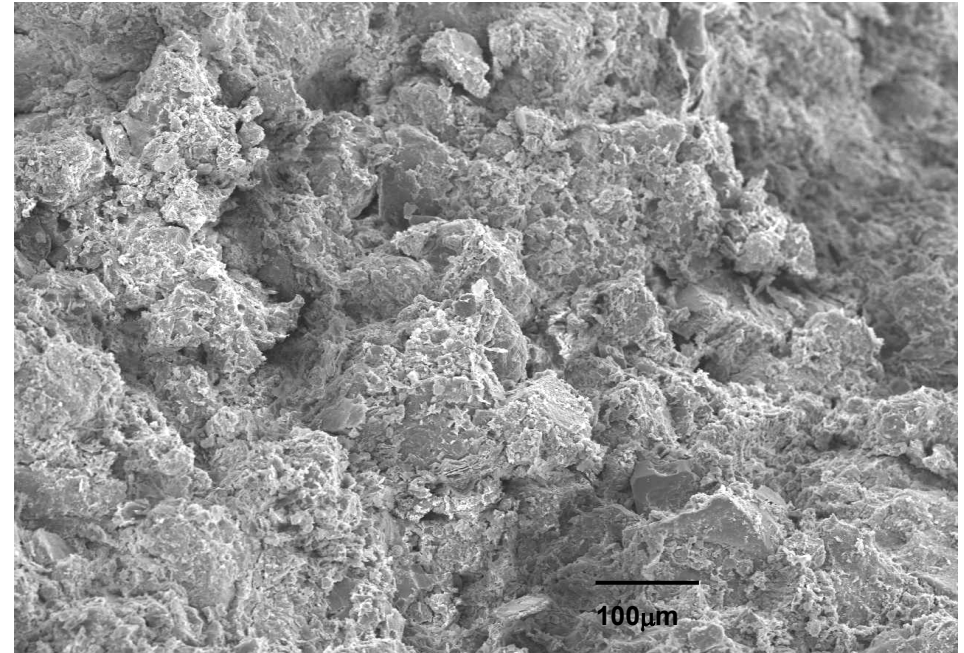
**Sample SWC-16 - LITHIC ARKOSE**

Plate 2D (x150): Moderate to common amounts of detrital and authigenic clays coat and surround the framework grains, blocking the intergranular pore spaces.

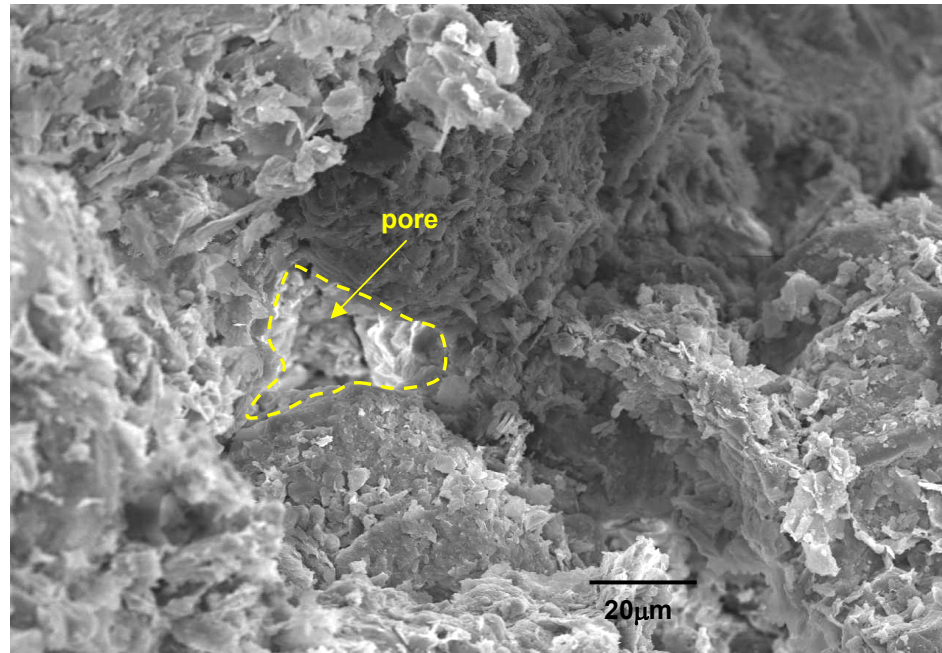
Plate 2E (x800): A closer view displays the flakes of smectite mixed with chlorite, which are the main pore-reducing minerals.

Plate 2F (x1000): Small amounts of vermicular kaolinite are also observed as pore-filling cement.

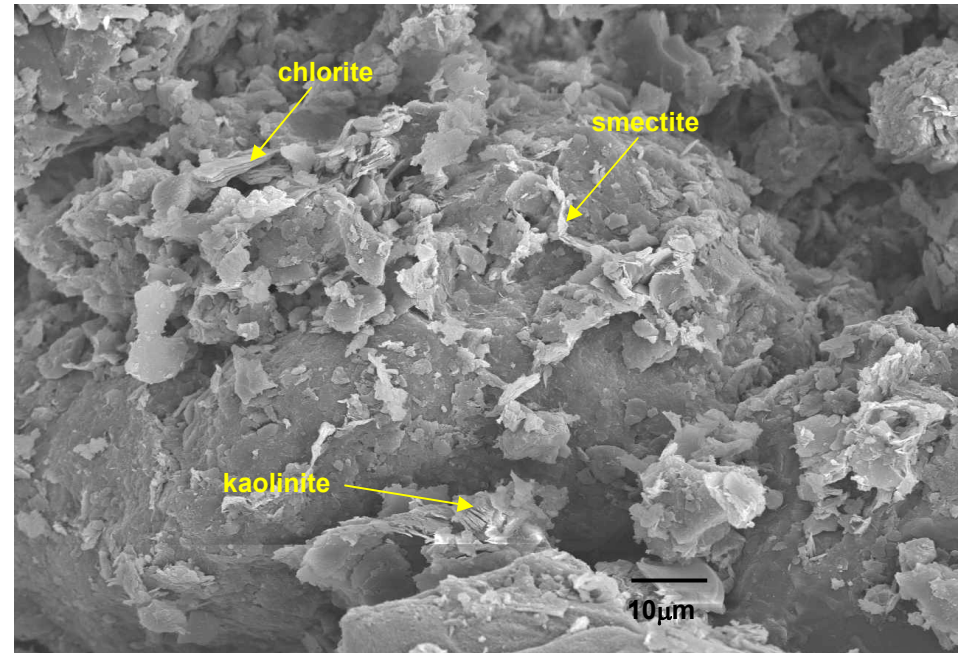
**Plate 2D**



**Plate 2E**



**Plate 2F**





**Sample:** SWC-11  
**Depth (m):** 575.7  
**Porosity (%):** 34.3  
**Permeability (md):** 176

4mm

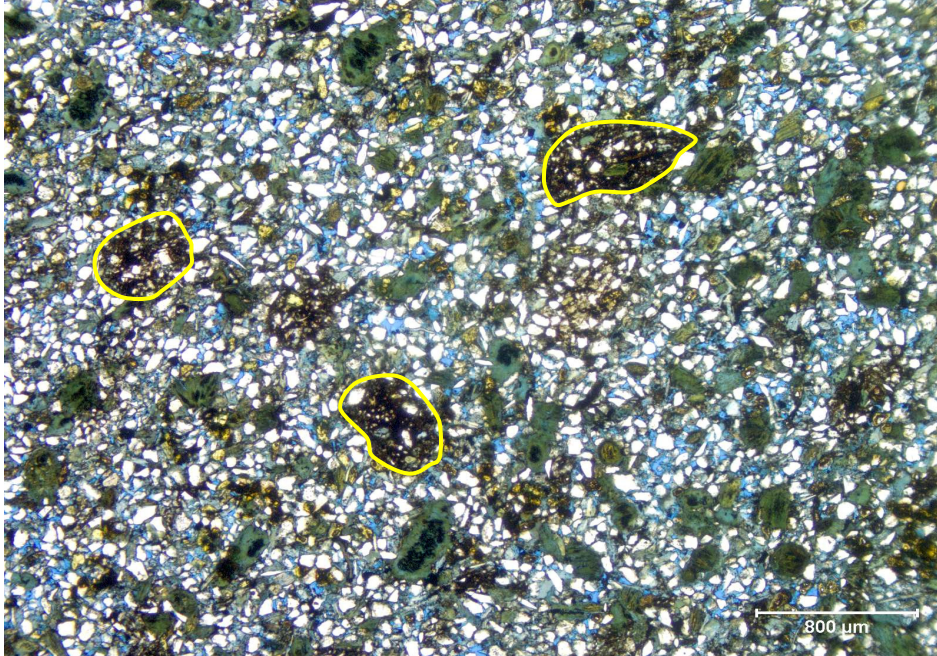


# THIN SECTION PETROGRAPHY

Company: Bass Strait Oil Company Ltd.  
Well: Moby 1

Depth (m) 575.7  
Sample ID SWC-11  
Point Count Porosity (%) 6.4

Plate 3B



### Depositional texture

Rock type Sandstone  
Classification (Folk) Lithic arkose  
Average grain size (mm) 0.090 (vfU)  
Sorting Well  
Grain contacts Loose to point  
Features Massive

### Framework Grains

Monocrystalline quartz 21.6  
Chert 2.8  
Sedimentary 5.6  
Volcanic 0.4  
Potassium feldspar 9.2  
Plagioclase feldspar 2.8

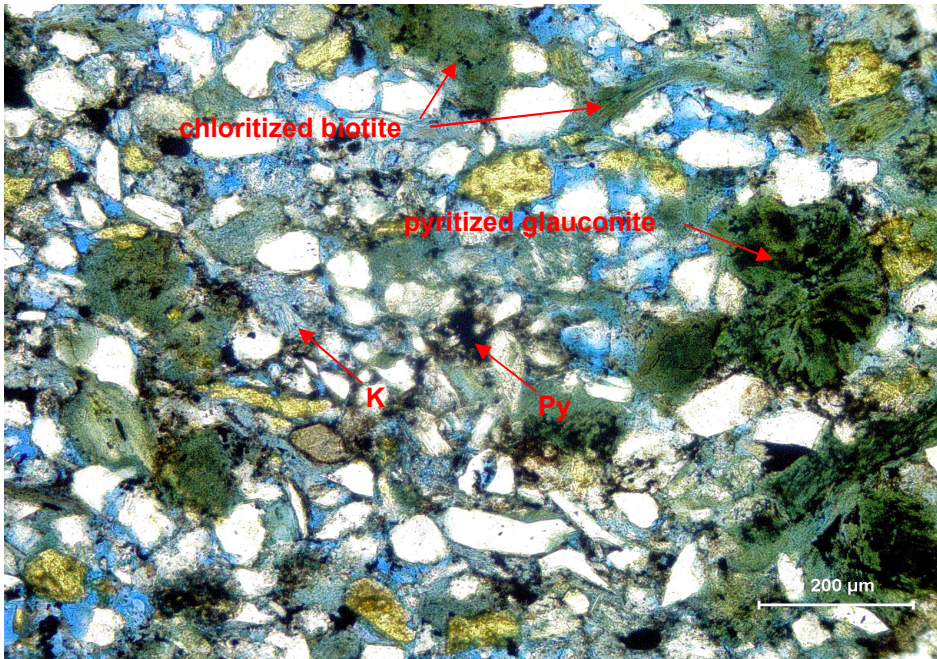
### Accessory Minerals

Phosphate grains -  
Glauconite 13.6  
Micas 10.8  
Zircon>Tourmaline 0.8  
Titanium oxides -

### Matrix

Detrital Clays 4.0

Plate 3C



### Authigenic minerals

Chlorite 9.6  
Kaolinite 3.6  
Illite & smectite 3.6  
Calcite -  
Dolomite -  
Siderite -  
Hematite -  
Pyrite 5.2

### Porosity

Intergranular 5.6  
Dissolution 0.8  
Microporosity Common

### Petrographic description

Minor amounts of detrital clay matrix are concentrated in small "pockets" (yellow circles) in this upper very fine grained, well sorted sandstone. Commonly pyritized and chloritized glauconite and biotite are coarser grained, compared to the other components. Minor to moderate amounts of kaolinite (K) and pyrite (Py) have reduced some primary pores. The visible pores are mostly intergranular and a few secondary pores.



Trace (<1%)  
Minor (1-5%)  
Moderate (5-10%)  
Common (10-20%)  
Abundant (>20%)

C.L. File No. 52135-04-3656

**Company: Bass Strait Oil Company Ltd.**  
**Well: MOBY 1**  
**Depth (m): 575.7**



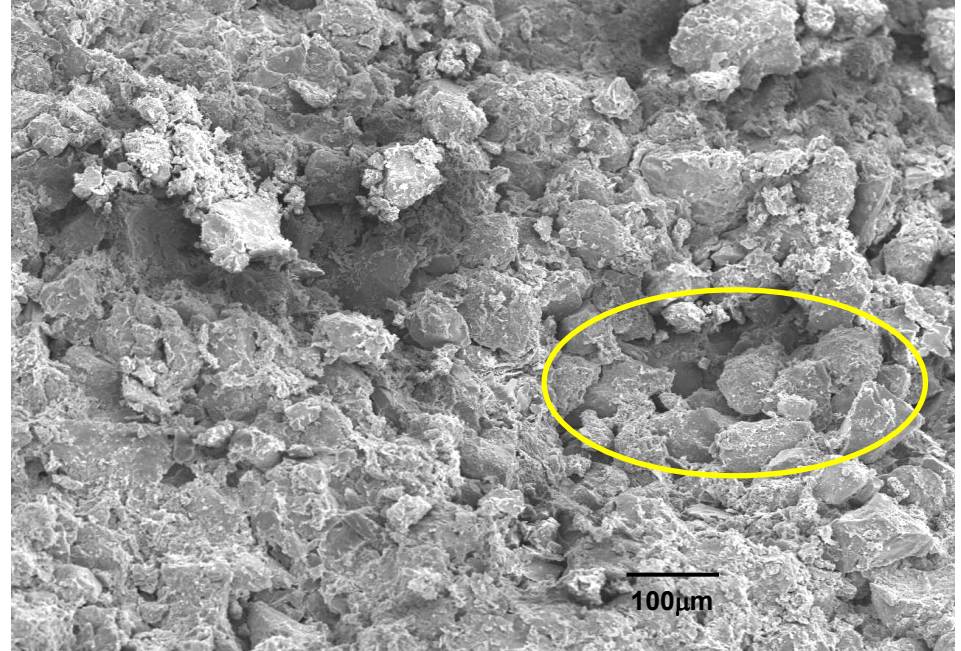
**Sample SWC-11 - LITHIC ARKOSE**

Plate 3D (x100): This upper very fine grained sandstone has patches of detrital clays and authigenic clays. Locally, "cleaner areas" (yellow circle) preserved well connected intergranular pores.

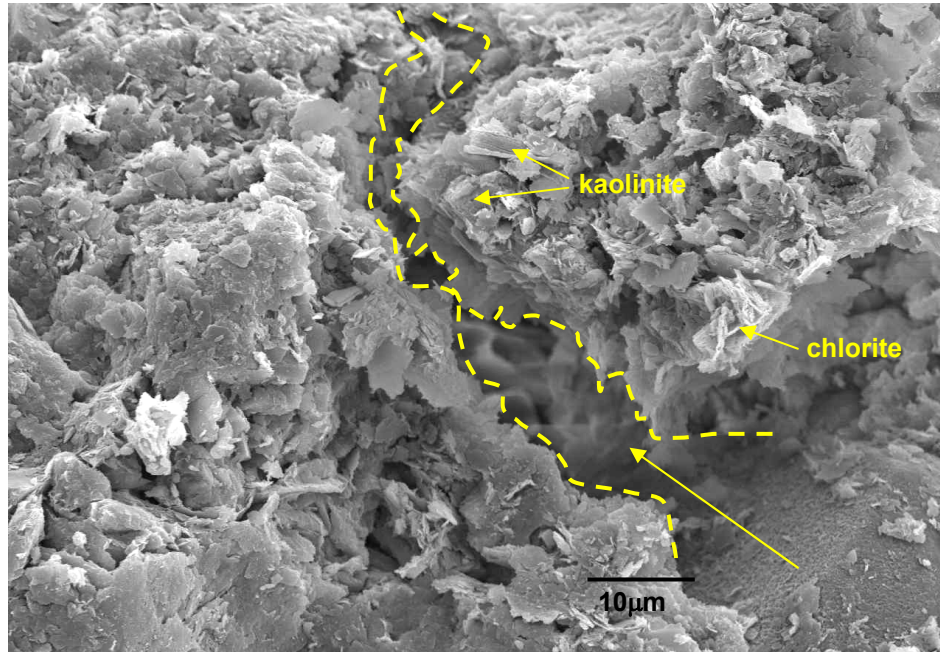
Plate 3E (x1500): Permeability is expected to be low, due to chlorite and smectite cements that partially or completely blocked the pore throats (yellow arrow).

Plate 3F (x1500): Note the chlorite flakes that probably replaced the large clasts of biotite.

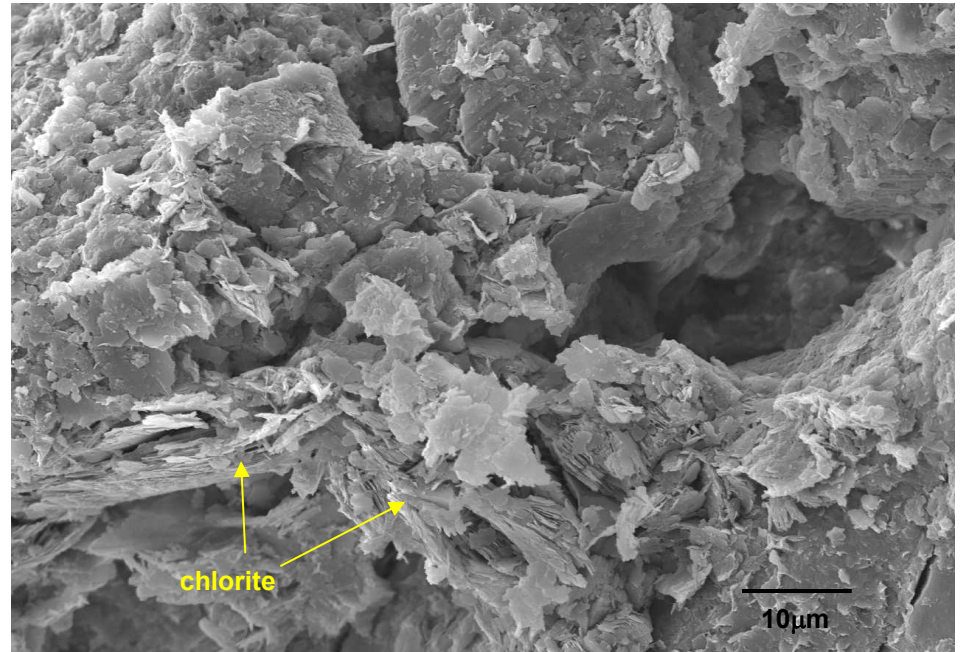
**Plate 3D**



**Plate 3E**



**Plate 3F**

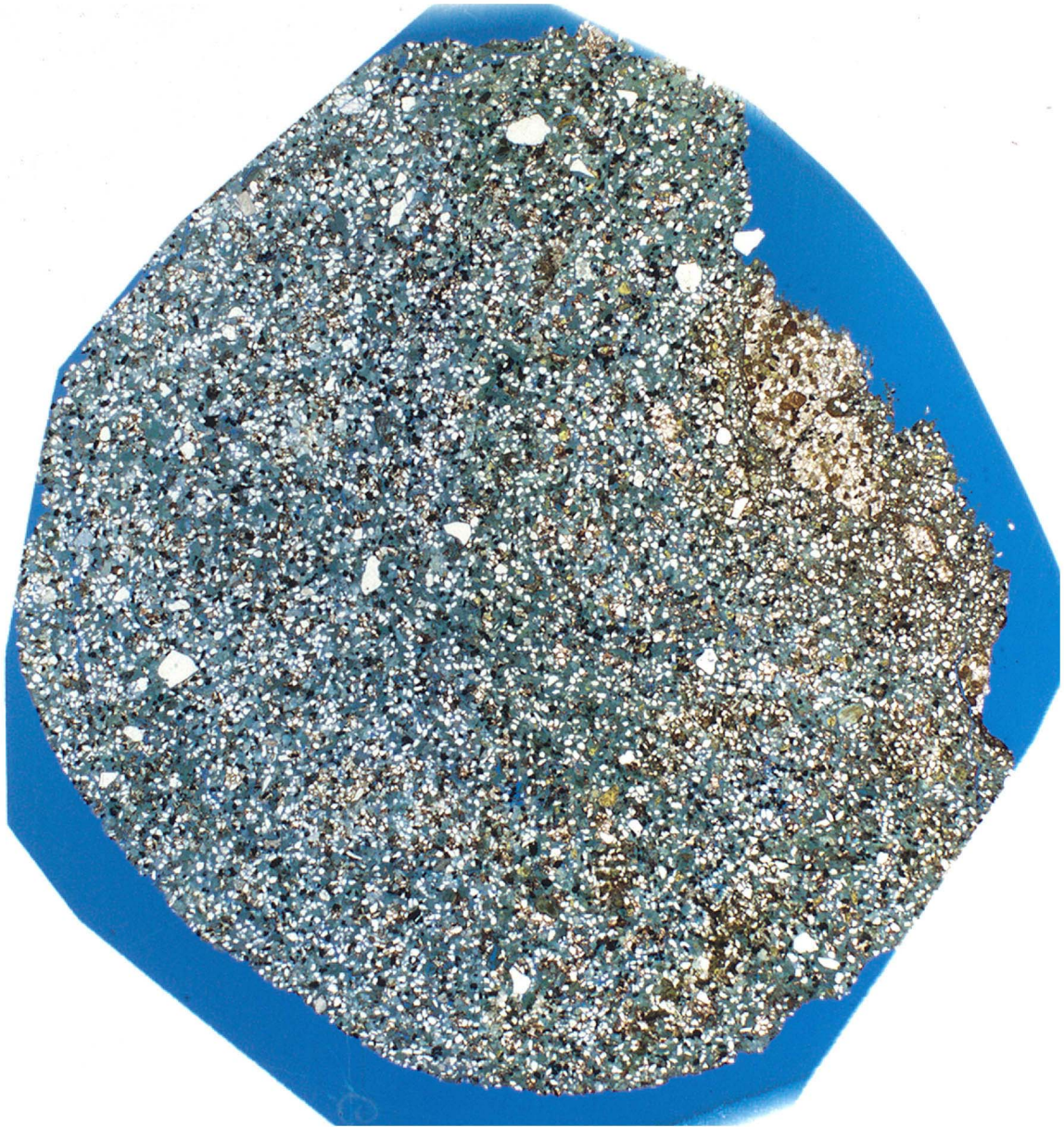


**Company:** Bass Strait Oil Company Ltd.

52135-04-3656

**Well:** Moby 1

**Plate:** 4A



<b>Sample:</b>	SWC-8
<b>Depth (m):</b>	585.0
<b>Porosity (%):</b>	36.1
<b>Permeability (md):</b>	300

4mm

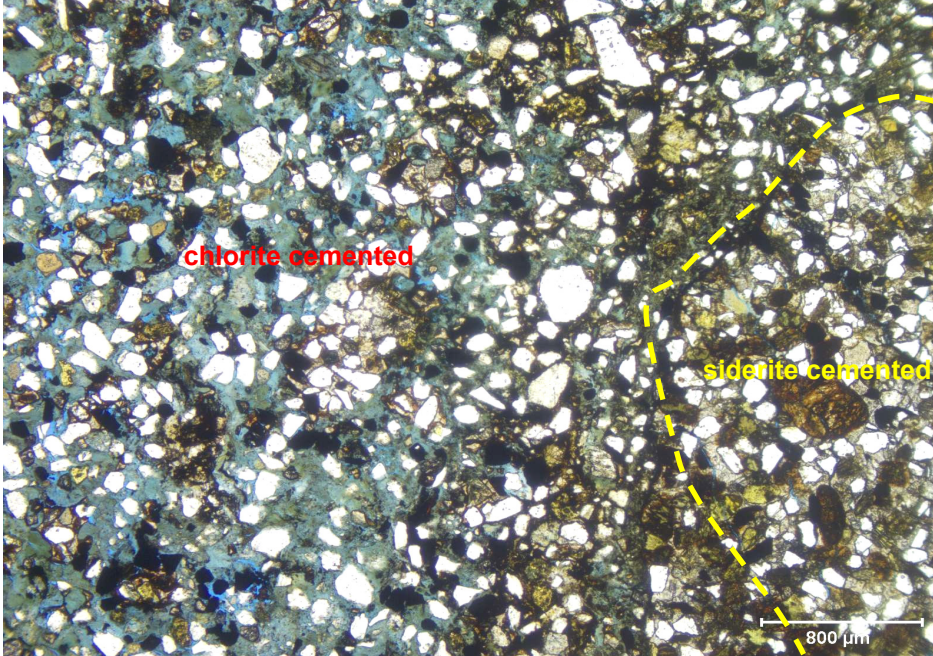


# THIN SECTION PETROGRAPHY

Company: Bass Strait Oil Company Ltd.  
Well: Moby 1

Depth (m) 585.0  
Sample ID SWC-8  
Point Count Porosity (%) 3.4

Plate 4B



### Depositional texture

Rock type	Sandstone
Classification (Folk)	Felds. lith.
Average grain size (mm)	0.165 (fL)
Sorting	Poor
Grain contacts	Loose
Features	Massive

### Framework Grains

Monocrystalline quartz	11.8
Chert	3.2
Sedimentary	1.6
Volcanic	5.2
Potassium feldspar	4.8
Plagioclase feldspar	1.2

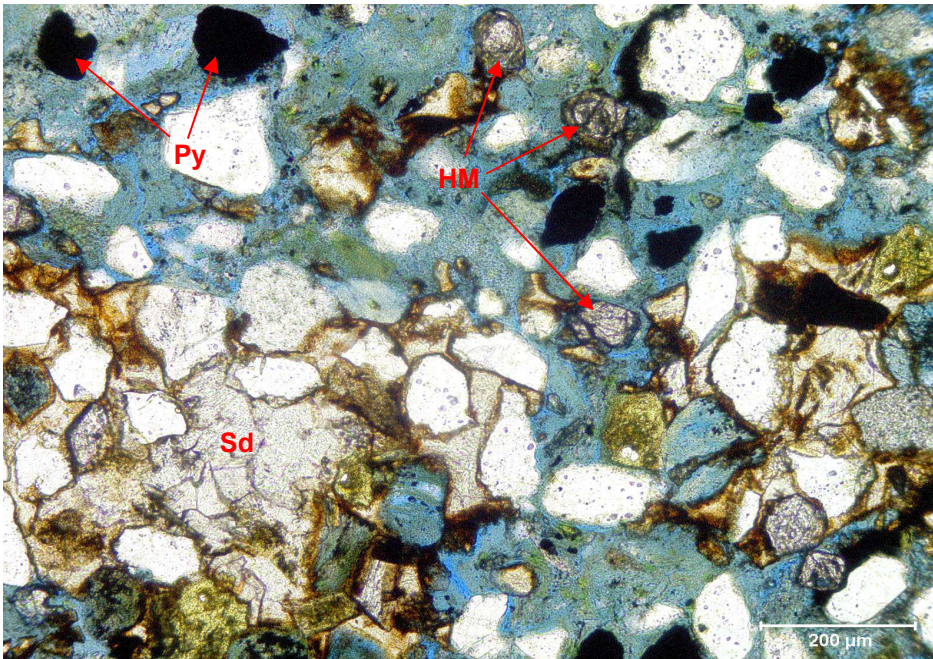
### Accessory Minerals

Phosphate grains	-
Glauconite	2.8
Micas	3.6
Zircon>Tourmaline	10.0
Titanium oxides	2.4

### Matrix

Detrital Clays	2.4
----------------	-----

Plate 4C



### Authigenic minerals

Chlorite	25.6
Kaolinite	2.8
Illite & smectite	0.8
Calcite	-
Dolomite	-
Siderite	8.4
Hematite	-
Pyrite	10.0

### Porosity

Intergranular	3.0
Dissolution	0.4
Microporosity	Common

### Petrographic description

This lower fine grained, poorly sorted sandstone has low visible porosity. Due to abundant microcrystalline chlorite (greenish areas) and patches of blocky siderite cement (Sd), intergranular pores were drastically closed. Heavy minerals (HM) such as titanium oxides, zirconium and pyrite (Py) occur in common amounts as individual grains.



Trace (<1%)  
Minor (1-5%)  
Moderate (5-10%)  
Common (10-20%)  
Abundant (>20%)

C.L. File No. 52135-04-3656

**Company: Bass Strait Oil Company Ltd.**  
**Well: MOBY 1**  
**Depth (m): 585.0**



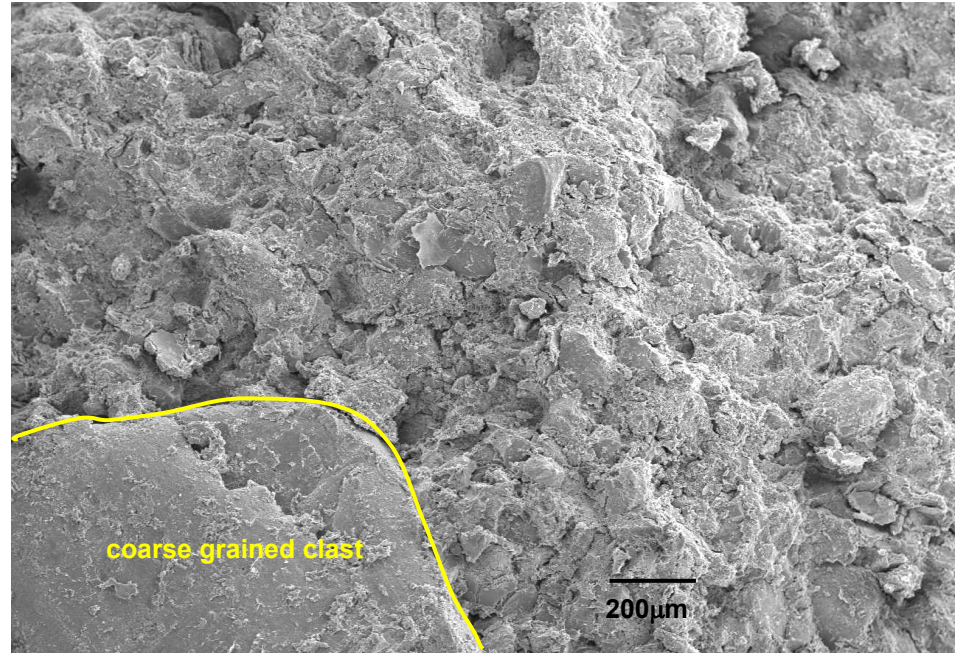
**Sample SWC-8 - FELDSPATHIC LITHARENITE**

Plate 4D (x60): The fine sand grains of this poorly sorted sandstone are not visible in this SEM image; due to abundant chlorite that coated the grains.

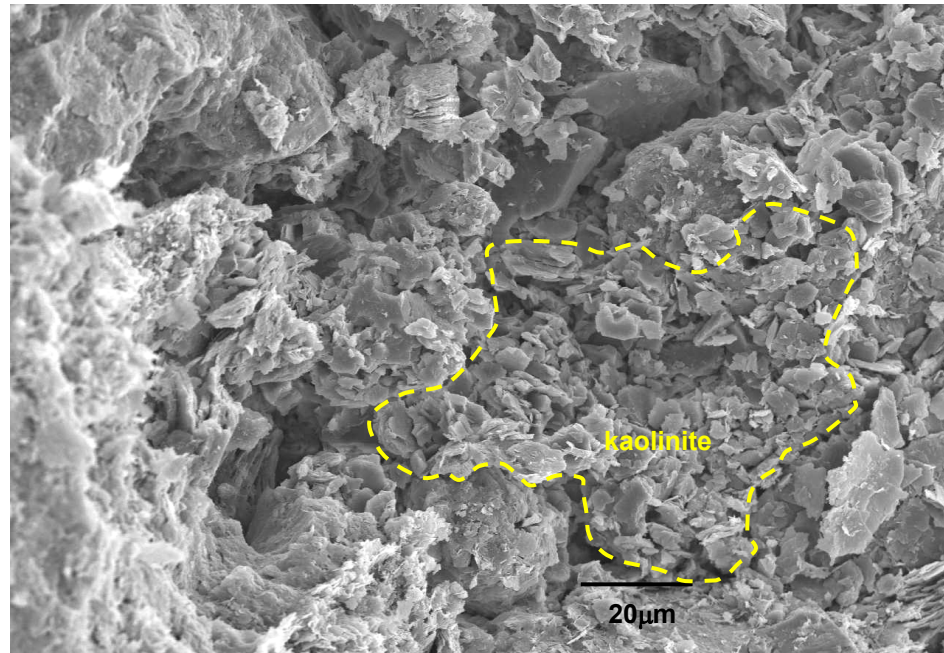
Plate 4E (x800): Chaotic precipitations of kaolinite bucklets are observed as complete fillings of the pores.

Plate 4F (x850): Stacks of kaolinite crystals (yellow arrows) are observed lining the pores.

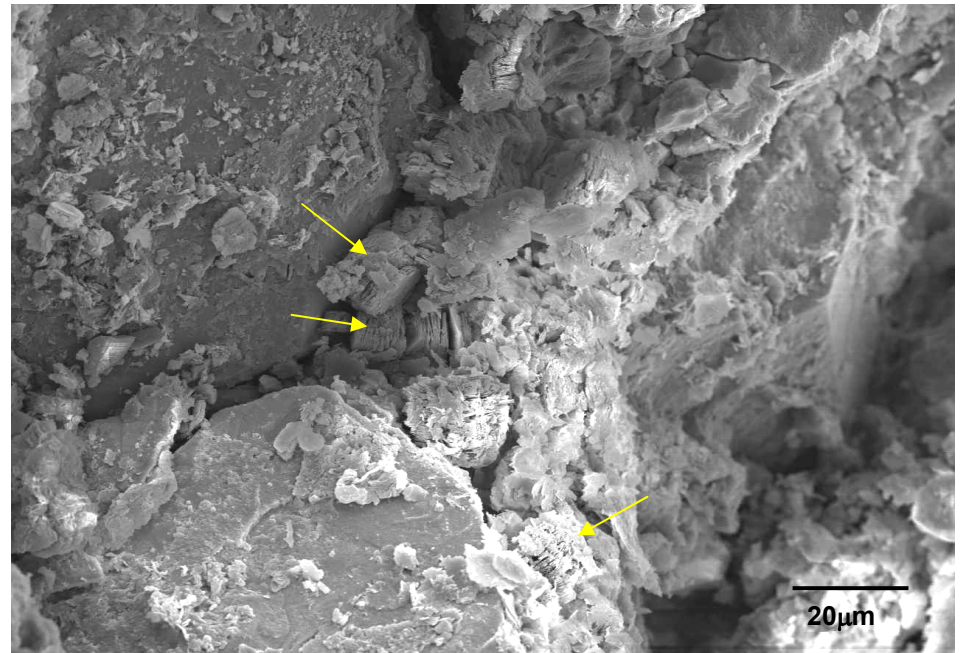
**Plate 4D**



**Plate 4E**



**Plate 4F**

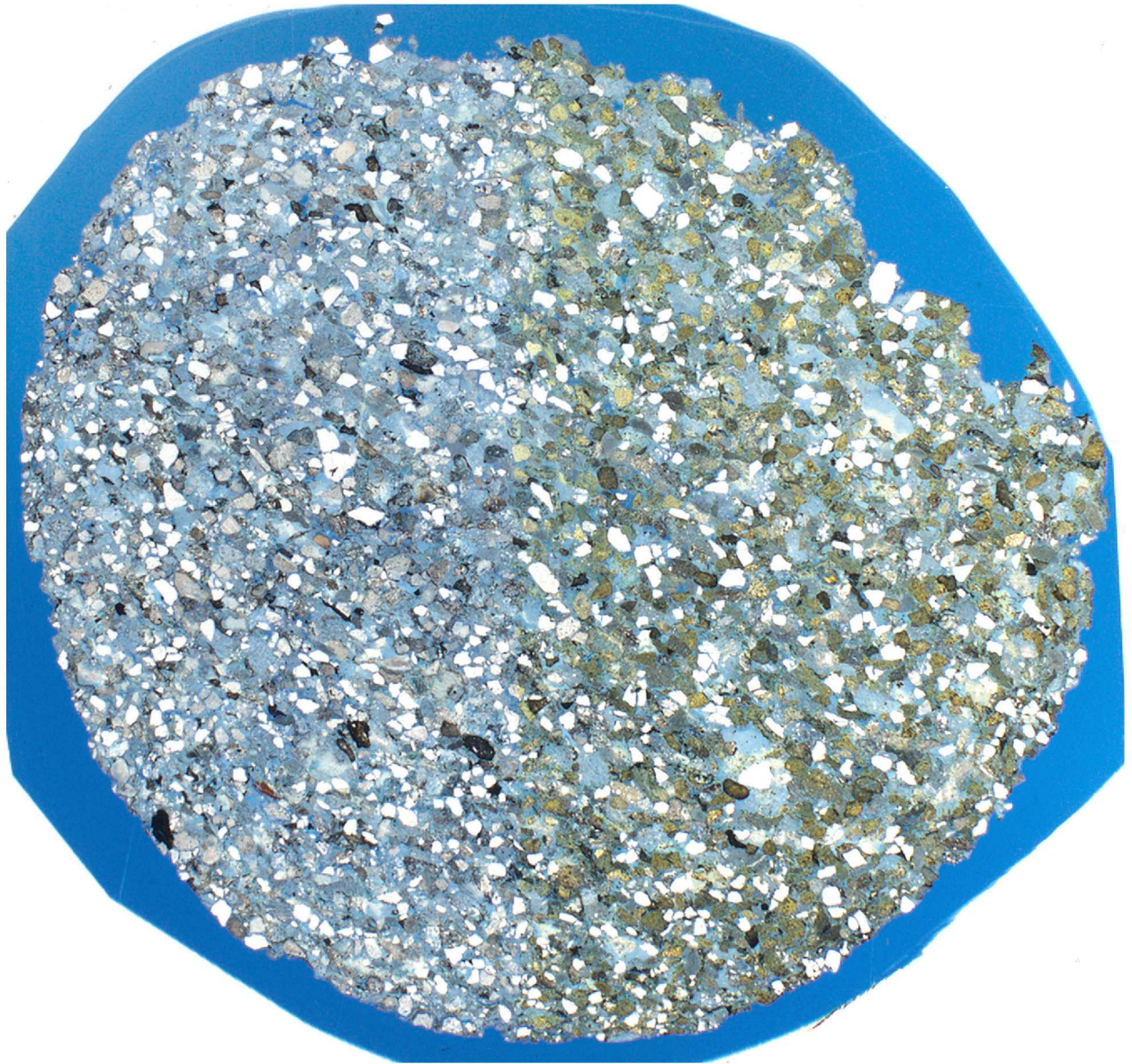


**Company:** Bass Strait Oil Company Ltd.

52135-04-3656

**Well:** Moby 1

**Plate:** 5A



<b>Sample:</b>	SWC-6
<b>Depth (m):</b>	588.0
<b>Porosity (%):</b>	35.9
<b>Permeability (md):</b>	446

4mm

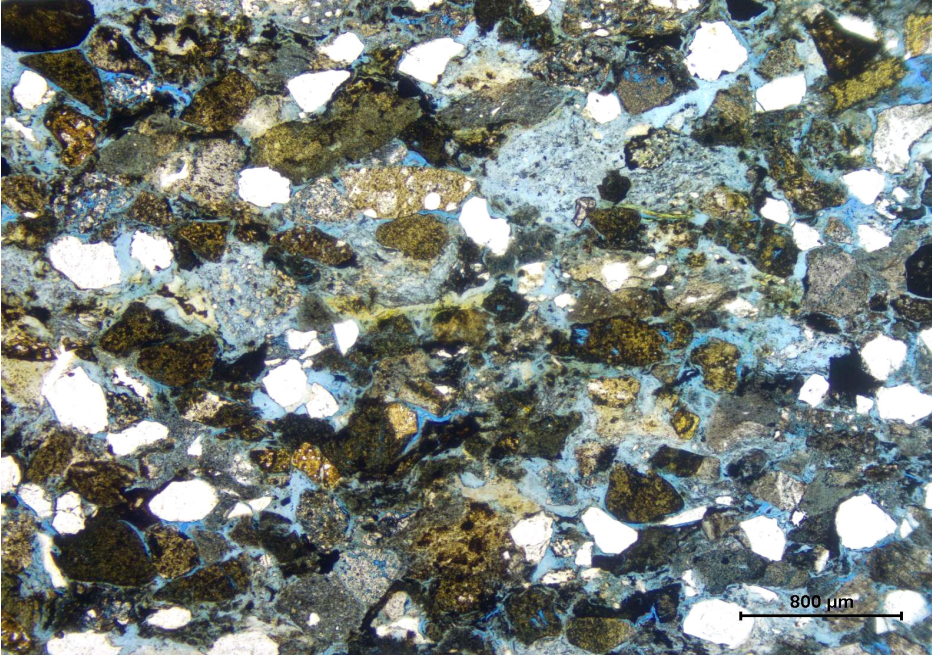


# THIN SECTION PETROGRAPHY

Company: Bass Strait Oil Company Ltd.  
Well: Moby 1

Depth (m) 588.0  
Sample ID SWC-6  
Point Count Porosity (%) 1.6

Plate 5B



### Depositional texture

Rock type Sandstone  
Classification (Folk) Felds. lith.  
Average grain size (mm) 0.270 (mL)  
Sorting Moderate  
Grain contacts Point to long  
Features Massive

### Framework Grains

Monocrystalline quartz 10.6  
Chert 6.0  
Sedimentary 3.2  
Volcanic 10.8  
Potassium feldspar 10.6  
Plagioclase feldspar 3.2

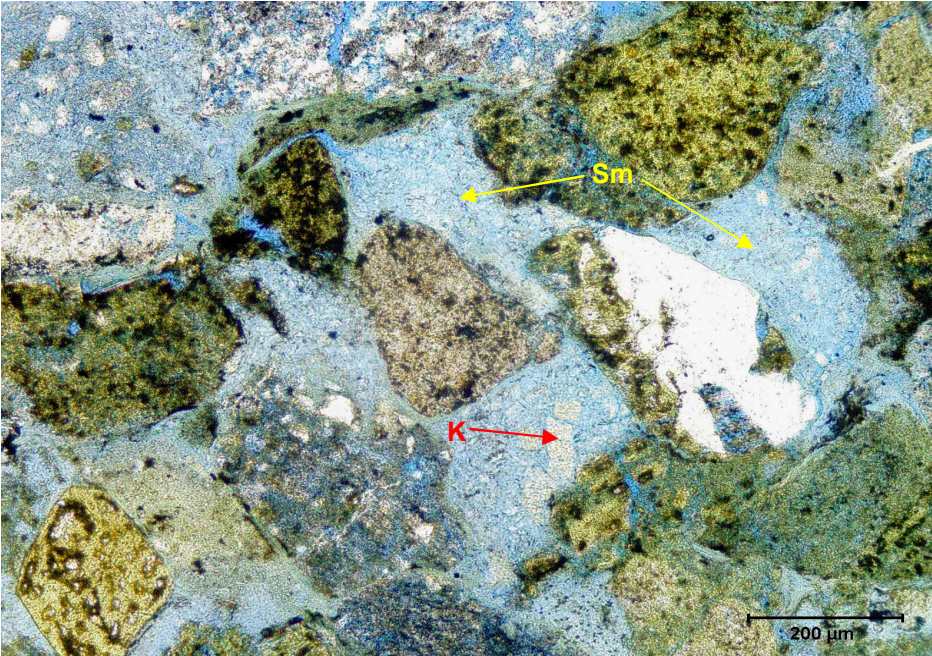
### Accessory Minerals

Phosphate grains -  
Glauconite 1.2  
Micas 0.4  
Zircon>Tourmaline 0.8  
Titanium oxides -

### Matrix

Detrital Clays 2.4

Plate 5C



### Authigenic minerals

Chlorite 14.2  
Kaolinite 9.0  
Illite & smectite 19.8  
Calcite -  
Dolomite -  
Siderite 2.8  
Hematite -  
Pyrite 3.4

### Porosity

Intergranular 0.4  
Dissolution 1.2  
Microporosity Common

### Petrographic description

Volcanic rock fragments and feldspars are the main components of this moderately sorted, lower medium grained sandstone. The binding material is very fine volcanic ash that was completely altered into smectite (Sm) and kaolinite (K). Visible porosity is very low, with only traces of primary pores and minor dissolution pores.



Trace (<1%)  
Minor (1-5%)  
Moderate (5-10%)  
Common (10-20%)  
Abundant (>20%)

C.L. File No. 52135-04-3656

**Company: Bass Strait Oil Company Ltd.**  
**Well: MOBY 1**  
**Depth (m): 588.0**



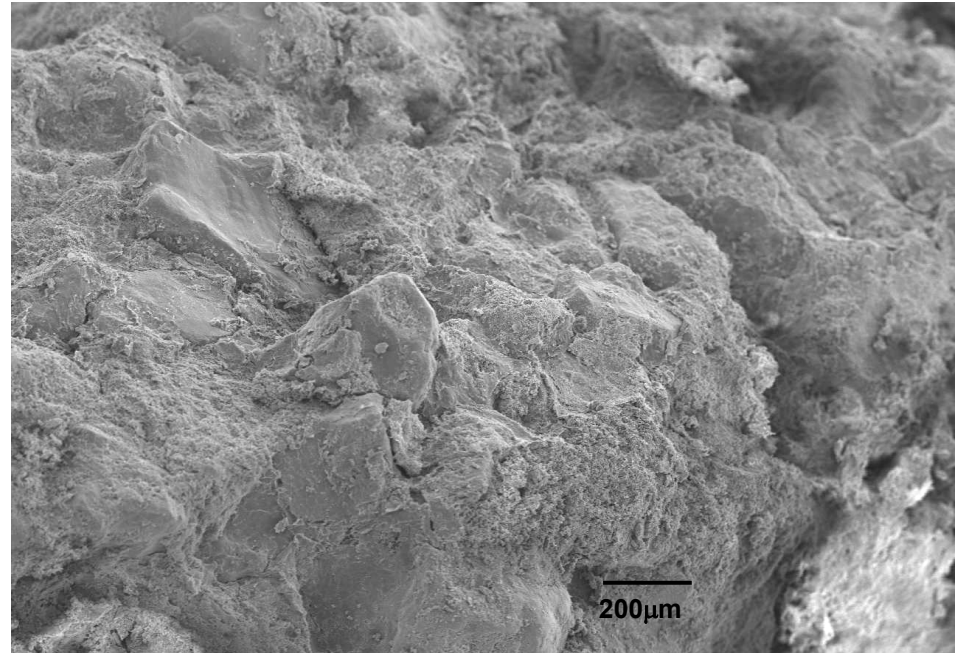
**Sample SWC-6 - FELDSPATHIC LITHARENITE**

Plate 5D (x60): This lower medium grained sandstone has no visible porosity due to abundant volcanic ash that was completely replaced by smectite and kaolinite.

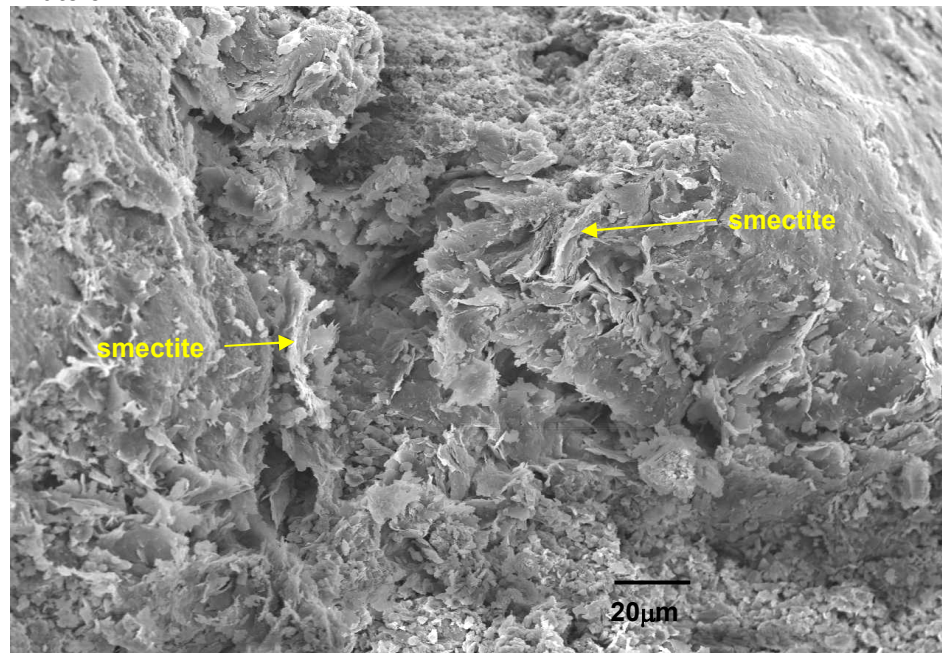
Plate 5E (x600): A closer view shows the slightly crenulated to flaky smectite clay coating a detrital grains.

Plate 5F (x800): Authigenic kaolinite is loosely attached to the framework grains and completely occludes the pore spaces.

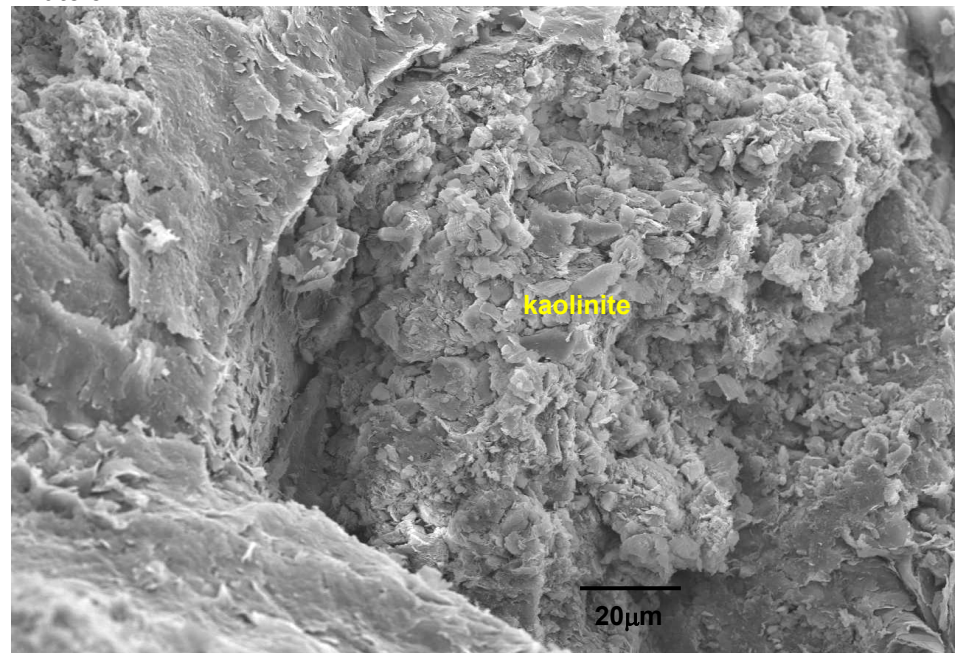
**Plate 5D**



**Plate 5E**



**Plate 5F**



**Well:** Moby 1

**Plate:** 6A



<b>Sample:</b>	SWC-3
<b>Depth (m):</b>	605.0
<b>Porosity (%):</b>	31.6
<b>Permeability (md):</b>	781

4mm

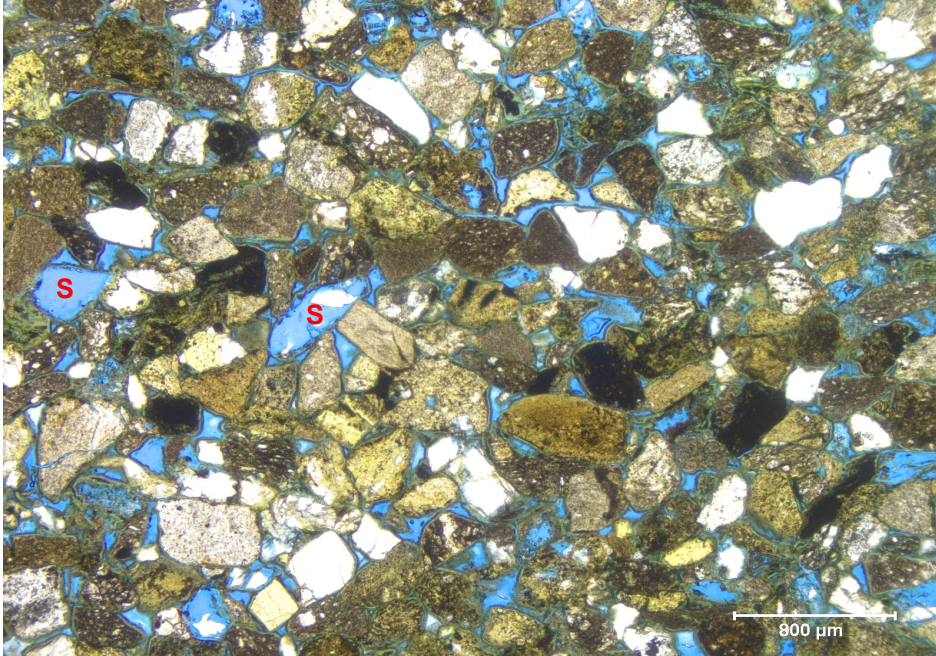


# THIN SECTION PETROGRAPHY

Company: Bass Strait Oil Company Ltd.  
Well: Moby 1

Depth (m) 605.0  
Sample ID SWC-3  
Point Count Porosity (%) 10.6

Plate 6B



## Depositional texture

Rock type	Sandstone
Classification (Folk)	Litharenite
Average grain size (mm)	0.320 (mL)
Sorting	Moderately well
Grain contacts	Point to long
Features	Massive

## Framework Grains

Monocrystalline quartz	10.8
Chert	8.6
Sedimentary	14.0
Volcanic	20.4
Potassium feldspar	7.6
Plagioclase feldspar	6.0

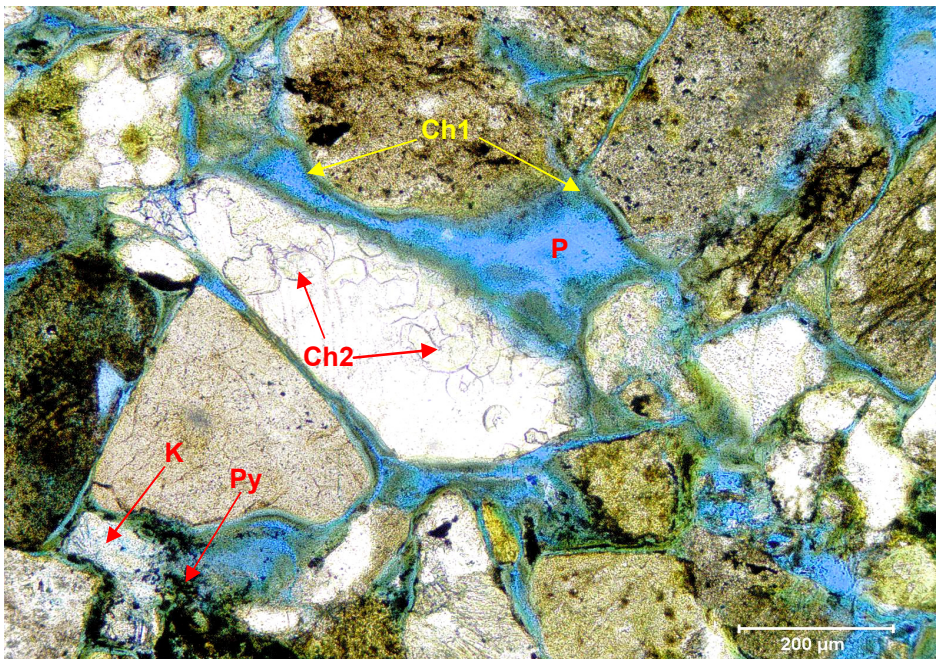
## Accessory Minerals

Phosphate grains	-
Glauconite	0.4
Micas	1.2
Zircon>Tourmaline	-
Titanium oxides	-

## Matrix

Detrital Clays	1.2
----------------	-----

Plate 6C



## Authigenic minerals

Chlorite	14.8
Kaolinite	2.4
Illite & smectite	0.4
Calcite	-
Dolomite	-
Siderite	0.4
Hematite	-
Pyrite	1.2

## Porosity

Intergranular	9.0
Dissolution	1.6
Microporosity	Common

## Petrographic description

Most of the porosity is intergranular pores (P), with minor secondary pores (S) formed by complete dissolution of volcanic fragments. The main formation damage potential within this sample is the isopachous-fringe chlorite cement (Ch1) that rims most of the grains. Vermicular chlorite (Ch2) altered some rock fragments. Minor amounts of kaolinite and pyrite fill pores.



Trace (<1%)  
Minor (1-5%)  
Moderate (5-10%)  
Common (10-20%)  
Abundant (>20%)

C.L. File No. 52135-04-3656

**Company: Bass Strait Oil Company Ltd.**  
**Well: MOBY 1**  
**Depth (m): 605.0**



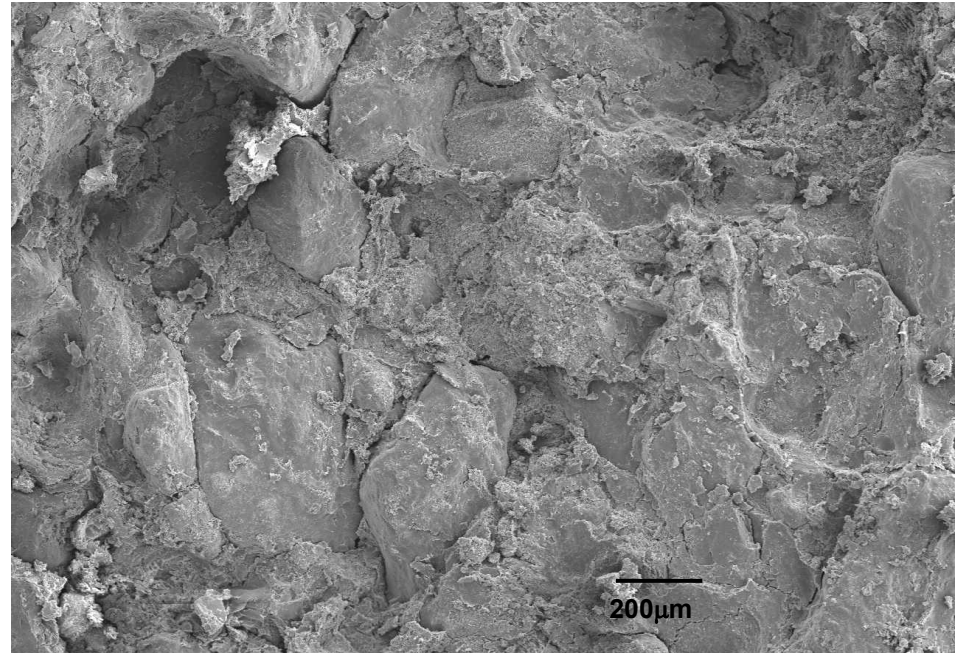
**Sample SWC-3 - LITHARENITE**

Plate 6D (x60): Porosity is completely closed by authigenic clays in this lower medium grained, moderately sorted sandstone.

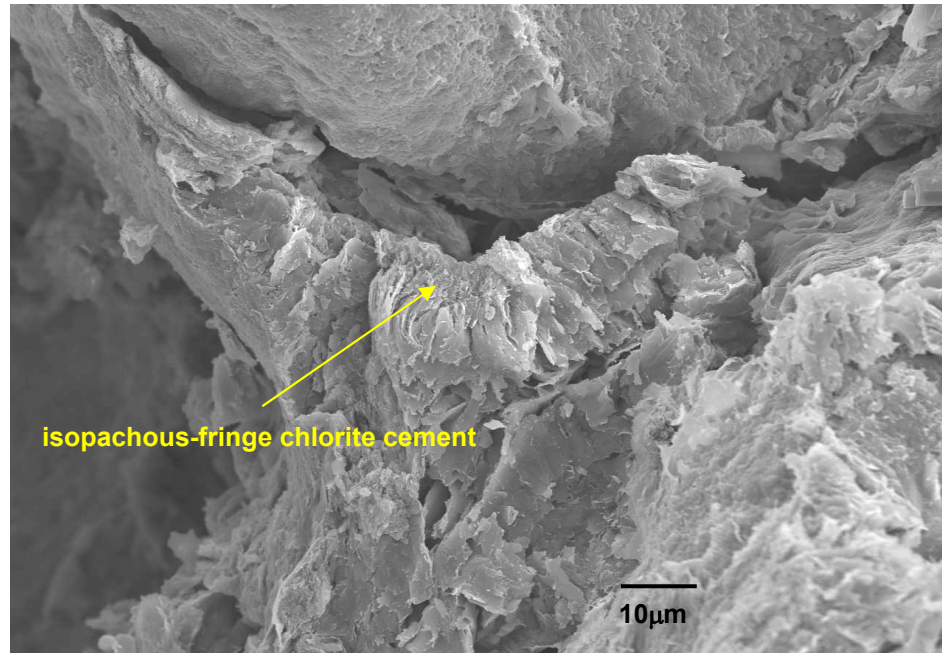
Plate 6E (x1500): Grain-coating chlorite is very common in this sample, rimming most of the grains and creating the fragile "bridges" between the grains.

Plate 6F (x1500): Pore throats were drastically reduced by chlorite pore-lining.

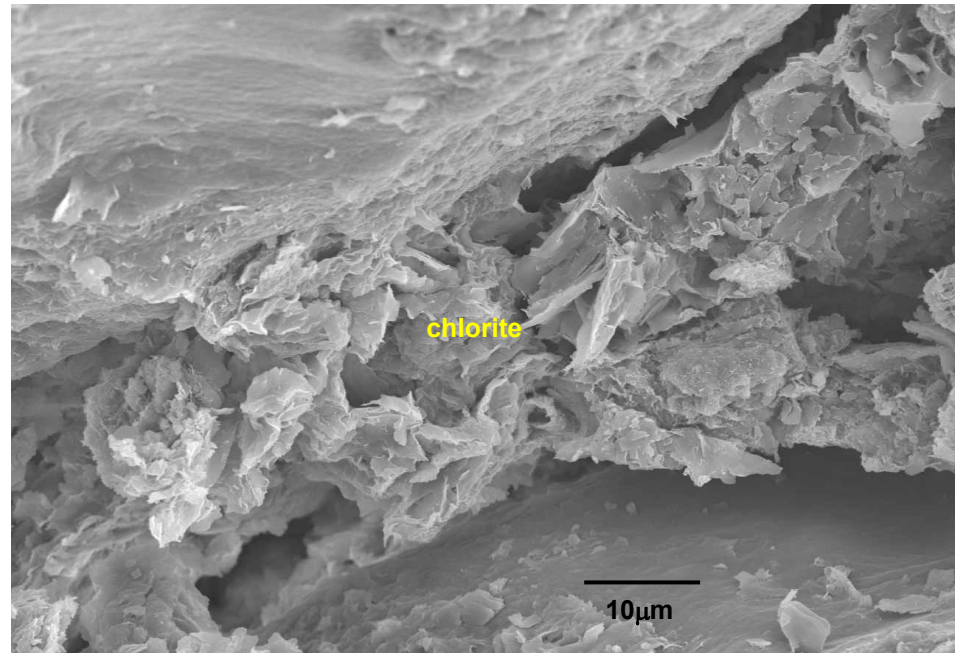
**Plate 6D**



**Plate 6E**



**Plate 6F**



## **APPENDIX 5**

---

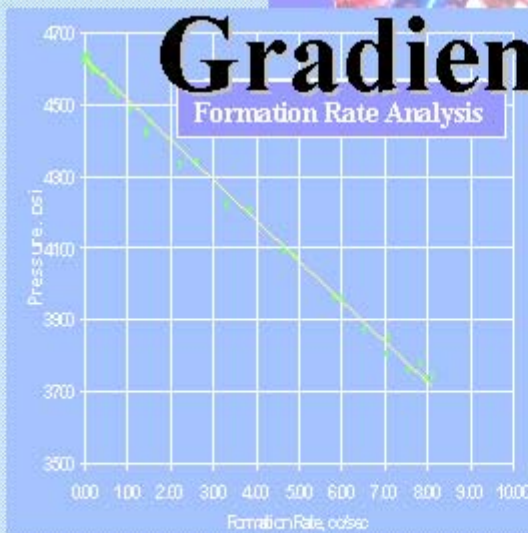
# **RCI ANALYSIS: Pressure, Mobility and Gradient Report for Well Moby-1**

---

**By BakerAtlas GeoScience**

**CONFIDENTIAL**

**Pressure, Mobility, and  
Gradient Report**



**RCI Formation Pressure Test Validation and Analysis**  
**for Well MOBY-1**  
**BASS STRAIT OIL COMPANY LIMITED.**

---

**Table of Contents**

1. Introduction .....	3
2. Executive Summary .....	4
3. Formation Pressure vs. Depth .....	10
4. Recommendations for future tests .....	17
5. Input Data for PTA Analysis .....	17
6. List of Tables .....	17
7. List of Figures .....	17
8. Summary of Results .....	19
9. Analysis Methods .....	86
Pressure Transient Analysis (PTA) .....	86
What is Pressure Transient? .....	86
Is it similar to Well Test Analysis? .....	86
What information do we obtain from Pressure Transient Analysis (PTA)? .....	87
How to analyse pressure transient data obtained from wireline formation testers? .....	87
10. Theory and Equations - Formation Rate Analysis (FRA) and Drawdown Mobility calculated from Field .....	91
11. Example of FRA plot indicating some problem .....	94

## 1. Introduction

This report presents the results from the RCI Formation Pressure Test Validation and Analysis. This report is a combined result of Flow Rate Analysis (FRA) and Pressure Transient Analysis (PTA) for the exploration well MOBY-1. The pressure transient data was obtained from this well using the Reservoir Characterization Instrument (RCI) on 12<sup>th</sup> October 2004. A total of 40 pressure tests were performed in this well between 558.5m and 612.8m MD.

This study was conducted in order to QC the final build-up pressure obtained from the RCI tool. A total of 40 tests, including the sample points, were examined closely for this particular well. The RCI pressure points reported from the field did not provide any clear fluid gradients and hence the need for this study which aims to validate final build-up pressure and then use these valid pressure points to plot fluid gradients. This study applies the Flow Rate Analysis (FRA) and Pressure Transient Analysis (PTA) techniques as powerful tools to examine the quality of final build-up pressure and to validate formation pressure at each test depth. This study also aims to evaluate the reason for scattering of final build-up pressure.

The results are shown in section 8 (Summary of Results). For each test depth, the FRA plot was prepared with Wireline Formation Test Analyzer (WFTA<sup>SM</sup>) software. The plot of pressure versus formation rate was analysed. If the FRA plot indicates a good straight line then this test can be verified as FRA compliant. This means that the tool communicates with the formation and the measured final build-up pressure represents formation pressure. In other words, the flow in porous media follows Darcy's Law. However, for this MOBY-1 well, it was found that most tests were low permeability to tight formation. There are only three pressure tests that are FRA compliant. Those pressure tests are i800a19, i800a20, and i800a40. After the FRA technique was used to verify the final build-up pressure, then the Pressure Transient Analysis (PTA) was used to examine the pressure response and pressure derivative in detail. The use of the PTA technique helps to obtain more accurate estimates of spherical permeability and also obtains more reservoir parameters, i.e. formation pressure, tool compressibility, skin factor, tool storage and radius of an investigation.

Pressure Transient Analysis (PTA) uses an extension to advanced well testing techniques in order to match the pressure data from wireline formation testers. The PTA software, Interpret 2003, was used to analyse the pressure transient tests. The powerful Flow Rate Analysis (FRA) technique was added in this software in order to initially estimate reservoir parameters. The detailed explanation of both PTA and FRA theories are stated in sections 9 and 10.

This report consists of 11 sections. Section 2 shows a summary of the results. Section 3 shows a fluid gradient obtained from RCI field plot (i.e. the field measurement). Section 4 provides recommendations for future work. Section 5 indicates an input parameter that was used in the PTA analysis. Sections 6 and 7 show the lists of tables and figures and all analysis results are shown in Section 8. Sections 9 and 10 explain the principle and theory for both PTA and FRA analysis techniques. Section 11 shows the examples of FRA plots indicating problems in RCI tests.

## 2. Executive Summary

Table 1 shows the validation from FRA analysis obtained from WFTA software. The theory and equations used in the FRA technique are shown in Section 10. If a straight-line is obtained from the plot of formation rate vs. pressure, the particular test will be identified as “FRA Compliant”. In this particular well, most tests were identified as “NOT FRA Compliant” because non-straight lines are observed in those FRA plots. The reason for this is that most pressure points were tested in low permeability to tight zones. The FRA plots show the distinct “hook shape” indicating low permeability to tight reservoir. Tests with NOT FRA Compliant mean that the piston rate is higher than the formation rate. Even though the slowest rate was used to conduct these tests, the piston rate still cannot match with the formation rate due to the very slow movement of fluid from the formation.

The pressure points were examined in detail and the results show that there is no supercharged effect for this particular well. This is because pressure points in all tests shows an agreement in final build-up pressure (to within a few psi) between pre-test and repeated tests. Even though the repeated test has slightly lower final build-up pressure compared to the pre-test (within few psi), this is due to the fact that in a low permeability reservoir, it takes longer for the pressure to stabilize. If there was a supercharging effect, the difference in final build-up pressure of the pre-test and repeated test should be greater than a few psi (as shown in Figure 1). Figure 2 shows an example of the FRA plot in the case of supercharging effect. The FRA shows a distinct straight line with a steep slope at zero formation rate. In this well, none of the pressure tests indicate the same shape of FRA plot (as shown in the FRA plot in section 8) and therefore it is concluded that there is no supercharging effect.

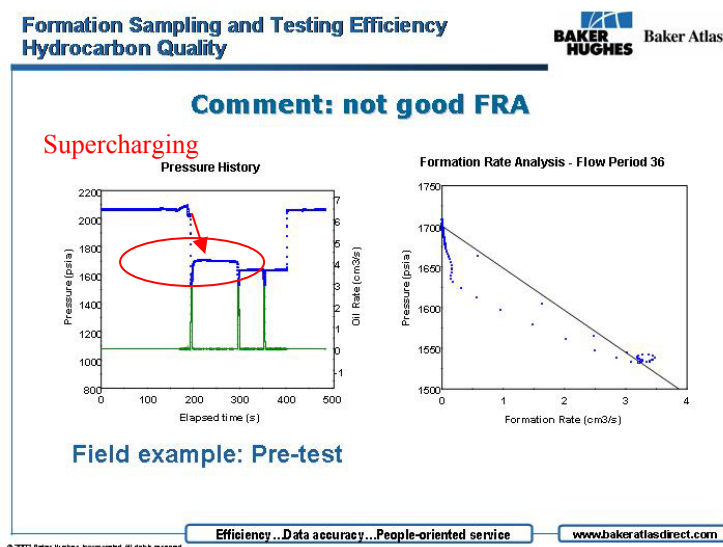


Figure 1 shows the pressure history plot in the left hand side. The final build-up pressure of the pre-test is significantly higher than the repeated test

Formation Sampling and Testing Efficiency  
Hydrocarbon Quality

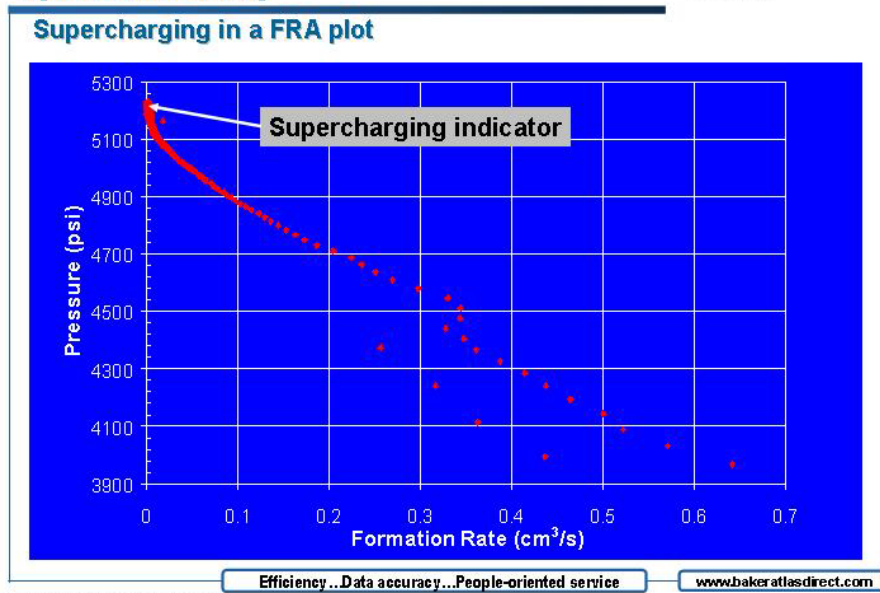


Figure 2 show the FRA plot of a test with supercharging effect. The supercharging can be identified by the changing in slope at zero formation rate. The slope gets steeper at the left hand side of this plot.

In the pre-test, pressure drops from hydrostatic to the flowing pressure. For the repeated test, pressure drops from the last build-up pressure to second flowing pressure, as shown in Figure 3. Even though the field engineer tried to decrease the piston rate in the repeated test, as shown by the green points, the flowing pressure in the repeated test is still lower than that of the pre-test (as shown by the blue points). Therefore, the repeated test takes longer to reach the formation pressure. In all pressure tests, the final build-up pressure of the pretest was found to be higher than the repeated test. The final build-up pressure of the repeated test has not stabilized or reached the formation pressure.

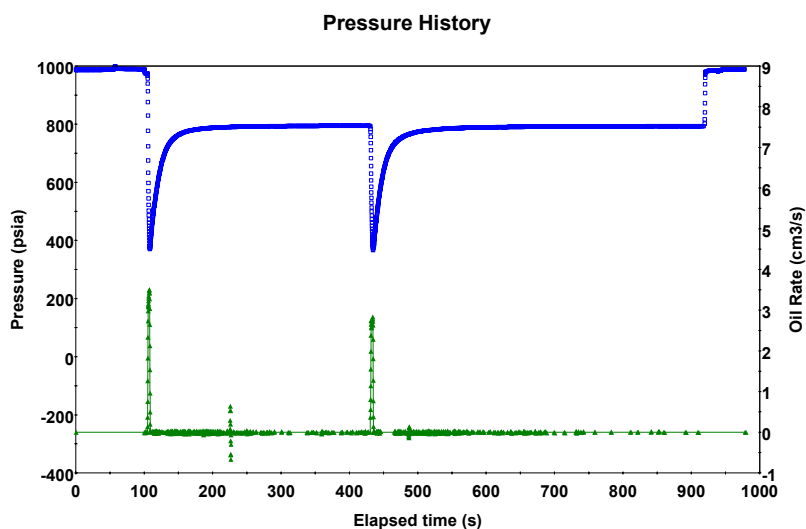


Figure 3 The pressure history of file no i800a03 (@558.5 m-TVD). The flowing bottom hole pressure of the repeat is lower than the pre-test and therefore pressure takes longer to reach the formation pressure.

The FRA plot was used to validate pressure points and the results show that only three pressure points were validated as FRA compliant, i.e. i800a19, i800a20, and i800a40. This means that the flow communicates with the formation and the flow in porous media follows Darcy's Law.

After the FRA method was used to validate pressure points, the final build-up pressure was examined in detail. In other words, the final build-up pressure was zoomed in order to see the quality of the pressure data. The Pressure Transient Analysis (PTA) software, Interpret 2003, was used for this purpose. Another main objective of using the pressure transient analysis technique is to estimate the spherical permeability using the same principle as advanced well test analysis techniques. A spherical flow regime is identified when a negative half slope is identified from pressure derivatives. Such tests are highlighted in yellow (when the flow is fully developed) and the estimated spherical permeability represents the true formation spherical permeability. Three tests indicating this spherical flow are i800a19, i800a20, and i800a40.

However, when the spherical flow does not fully develop, the estimated spherical permeability is just that i.e., an estimation. In this particular well, since the tests zones are low permeability to tight formation, the spherical flow cannot be seen in pressure derivatives. The diagnosis negative half slope was placed at the location closed to the late time pressure derivative data. As a result, the estimated spherical flow means the minimum of spherical permeability. Most tests in this well were fall into this category. The pressure transient analysis results are shown in Table 2.

Please note that for this analysis, since the mud viscosity was not known, a viscosity of 1 cp was assumed for the PTA analysis, as shown in Section 4. If the actual mud is known, it can be input in the analysis for more accurate estimation of spherical permeability.

In addition, another objective of using the PTA technique is to obtain more reservoir parameters, i.e. system compressibility, probe skin, tool storage and radius of investigation. The summary of the results is shown in Table 2.

Using the pressure transient analysis technique, pressure response and pressure derivative plots were examined in detail. The results show that even though only three pressure test indicates spherical flow regime, there are another two pressure tests indicating slightly higher permeability (not tight formation). These tests are in file nos. i800a12, i800a13. These pressure points were included when the fluid gradient was evaluated (the detailed discussion of pressure gradient plot are shown in the next section). Table 1 also shows the validation in terms of fluid gradient and the mobility calculation.

Table 1 Results from FRA validation

File No	Measure d Depth (m)	TVD Depth (m)	TVDSS Depth (m)	Final Build-up (psi)	FRA Compliant	Equivalent Mud Weight (g/cc)	Validation for fluid gradient plot	Validation for mobility calculation
03_0	558.5	558.5	537	794.2	Not FRA Compliant	1.000	No	Yes
03_1	558.5	558.5	537	792.9	Not FRA Compliant	0.998	No	Yes
04_0	559.1	559.1	537.6	806.1	Not FRA Compliant	1.014	No	Yes
04_1	559.1	559.1	537.6	802.5	Not FRA Compliant	1.009	No	Yes
06_0	559.9	559.9	538.4	824	Not FRA Compliant	1.035	No	Yes
06_1	559.9	559.9	538.4	822	Not FRA Compliant	1.032	No	Yes
07_0	561.4	561.4	539.9	797.3	Not FRA Compliant	0.999	No	Yes
07_1	561.4	561.4	539.9	796.3	Not FRA Compliant	0.997	No	Yes
08_0	562.1	562.1	540.6	808.6	Not FRA Compliant	1.011	No	Yes
08_1	562.1	562.1	540.6	806.2	Not FRA Compliant	1.008	No	Yes
09_0	563.2	563.2	541.7	798.6	Not FRA Compliant	0.997	No	Yes
09_1	563.2	563.2	541.7	798.2	Not FRA Compliant	0.996	No	Yes
10_0	565.7	565.7	544.2	0	No Seal	0.000	No	No
11_0	565.4	565.4	543.9	809	Not FRA Compliant	1.006	No	Yes
11_1	565.4	565.4	543.9	807.7	Not FRA Compliant	1.004	No	Yes
12_0	568.2	568.2	546.7	786.3	Not FRA Compliant	0.973	Yes	Yes
12_1	568.2	568.2	546.7	785.8	Not FRA Compliant	0.972	No	Yes
13_0	569	569	547.5	789.4	Not FRA Compliant	0.975	Yes	Yes
13_1	569	569	547.5	788	Not FRA Compliant	0.974	No	Yes
14_0	571.2	571.2	549.7	808.9	Not FRA Compliant	0.996	No	Yes
15_0	575.7	575.7	554.2	802	Not FRA Compliant	0.979	No	Yes
16_0	577.1	577.1	555.6	802.5	Not FRA Compliant	0.978	No	Yes
17_0	578.7	578.7	557.2	808.4	Not FRA Compliant	0.982	No	Yes
18_0	579.9	579.9	558.4	813.2	Not FRA Compliant	0.986	No	Yes
19_0	587.9	587.9	566.4	808.5	FRA Compliant	0.967	Yes	Yes
19_1	587.9	587.9	566.4	805.9	FRA Compliant	0.964	Yes	Yes

**Table 1 Results from FRA validation**

File No	Measure d Depth (m)	TVD Depth (m)	TVDSS Depth (m)	Final Build-up (psi)	FRA Compliant	Equivalent Mud Weight (g/cc)	Validation for fluid gradient plot	Validation for mobility calculation
20	588.9	588.9	567.4	808.1	FRA Compliant	0.965	Yes	Yes
20	588.9	588.9	567.4	806.9	FRA Compliant	0.963	Yes	Yes
21	591.1	591.1	569.6	0	Not FRA Compliant	0.000	No	No
22	593.2	593.2	571.7	0	Not FRA Compliant	0.000	No	No
23	596.9	596.9	575.4	0	Not FRA Compliant	0.000	No	No
25	608.1	608.1	586.6	0	Not FRA Compliant	0.000	No	Yes
26	612.8	612.8	591.3	923.3	Not FRA Compliant	1.059	No	Yes
26	612.8	612.8	591.3	919.1	Not FRA Compliant	1.054	No	Yes
28	568.2	568.2	546.7	0	Not FRA Compliant	0.000	No	No
29	568.5	568.5	547	0	Not FRA Compliant	0.000	No	No
30	568.2	568.2	546.7	0	Not FRA Compliant	0.000	No	No
34	561.4	561.4	539.9	0	Not FRA Compliant	0.000	No	No
35	561.7	561.7	540.2	0	Not FRA Compliant	0.000	No	No
36	561.7	561.7	540.2	0	Not FRA Compliant	0.000	No	No
37	558.5	558.5	537	0	Not FRA Compliant	0.000	No	No
38	558.4	558.4	536.9	0	Not FRA Compliant	0.000	No	No
39	588.9	588.9	567.4	0	No seal	0.000	No	No
40	588.5	588.5	567	807.5	FRA Compliant	0.965	Yes	No
41	572	572	550.5	0	Not FRA Compliant	0.000	No	No
42	572.1	572.1	550.6	0	Not FRA Compliant	0.000	No	No
43	572.2	572.2	550.7	0	Not FRA Compliant	0.000	No	No
44	571	571	549.5	0	Not FRA Compliant	0.000	No	No
45	571.9	571.9	550.4	0	Not FRA Compliant	0.000	No	No
46	573	573	551.5	0	Not FRA Compliant	0.000	No	No

Table 2 Summary of results obtained from PTA analysis

File No	Depth m-MD	Depth m-TVD	Depth m-TVDSS	Analysis model	Formation Pressure (psia)	Spherical Permeability (mD)	Compressibility (system) (1/psi)	Probe Skin	Tool Storage (bbl/psi)	Radius of Investigation (m)	Comments
03	558.5	558.5	537	Spherical flow	795.7	0.219	5.74E-05	-0.83	1.26E-07	0.61	Unable to identify spherical flow
04	559.1	559.1	537.6	Spherical flow	810.5	0.116	5.44E-05	-0.44	1.20E-07	0.91	Unable to identify spherical flow
06	559.9	559.9	538.4	Spherical flow	826.2	0.098	3.53E-05	-0.69	7.76E-08	0.61	Unable to identify spherical flow
07	561.4	561.4	539.9	Spherical flow	799.1	0.138	6.46E-05	-0.82	1.42E-07	0.91	Unable to identify spherical flow
08	562.1	562.1	540.6	Spherical flow	813.5	0.047	6.60E-05	-0.86	1.45E-07	0.61	Unable to identify spherical flow
09	563.2	563.2	541.7	Spherical flow	800.3	0.123	6.98E-05	-0.83	1.54E-07	0.91	Unable to identify spherical flow
11	565.4	565.4	543.9	Spherical flow	809.8	0.320	6.05E-05	-0.83	1.33E-07	0.61	Unable to identify spherical flow
12	568.2	568.2	546.7	Spherical flow	786.7	0.676	8.15E-05	-0.89	1.79E-07	0.91	Can see spherical flow-higher permeability
13	569	569	547.5	Spherical flow	789.7	0.683	6.61E-05	-0.84	1.46E-07	1.22	Can see spherical flow-higher permeability
14	571.2	571.2	549.7	Spherical flow	810.3	0.394	6.51E-05	-0.29	1.43E-07	0.91	Unable to identify spherical flow
15	575.7	575.7	554.2	Spherical flow	806.1	0.349	6.28E-05	0.02	1.38E-07	0.91	Unable to identify spherical flow
16	577.1	577.1	555.6	Spherical flow	802.7	0.697	5.94E-05	0.37	1.31E-07	0.91	Unable to identify spherical flow
17	578.7	578.7	557.2	Spherical flow	810.3	0.986	5.95E-05	2.85	1.31E-07	2.13	Unable to identify spherical flow
18	579.9	579.9	558.4	Spherical flow	813.8	0.598	5.98E-05	0.38	1.32E-07	1.22	Unable to identify spherical flow
19	587.9	587.9	566.4	Spherical flow	805.5	12.680	8.29E-06	-0.41	1.83E-08	2.44	Can see spherical flow
20	588.9	588.9	567.4	Spherical flow	806.9	18.980	5.84E-06	-0.43	1.29E-08	3.35	Can see spherical flow
25	608.1	608.1	586.6	Spherical flow	1201.4	0.047	3.29E-05	-0.57	7.24E-08	0.30	Unable to identify spherical flow
26	612.8	612.8	591.3	Spherical flow	930.0	0.218	4.79E-05	-0.64	1.05E-07	0.91	Unable to identify spherical flow
40	588.5	588.5	567	Spherical flow	807.2	13.82	1.08E-04	-0.63	2.38E-07	3.66	Can see spherical flow

### 3. Formation Pressure vs. Depth

Fluid gradient for well MOBY-1 was obtained from RCI field measurement. The results for the entire interval (537 to 591.3 m-TVDSS) before pressure points are validated, are shown in Figure 1. From this figure, it shows that pressure points are very scattered. A reasonable fluid gradient cannot be obtained from this figure.

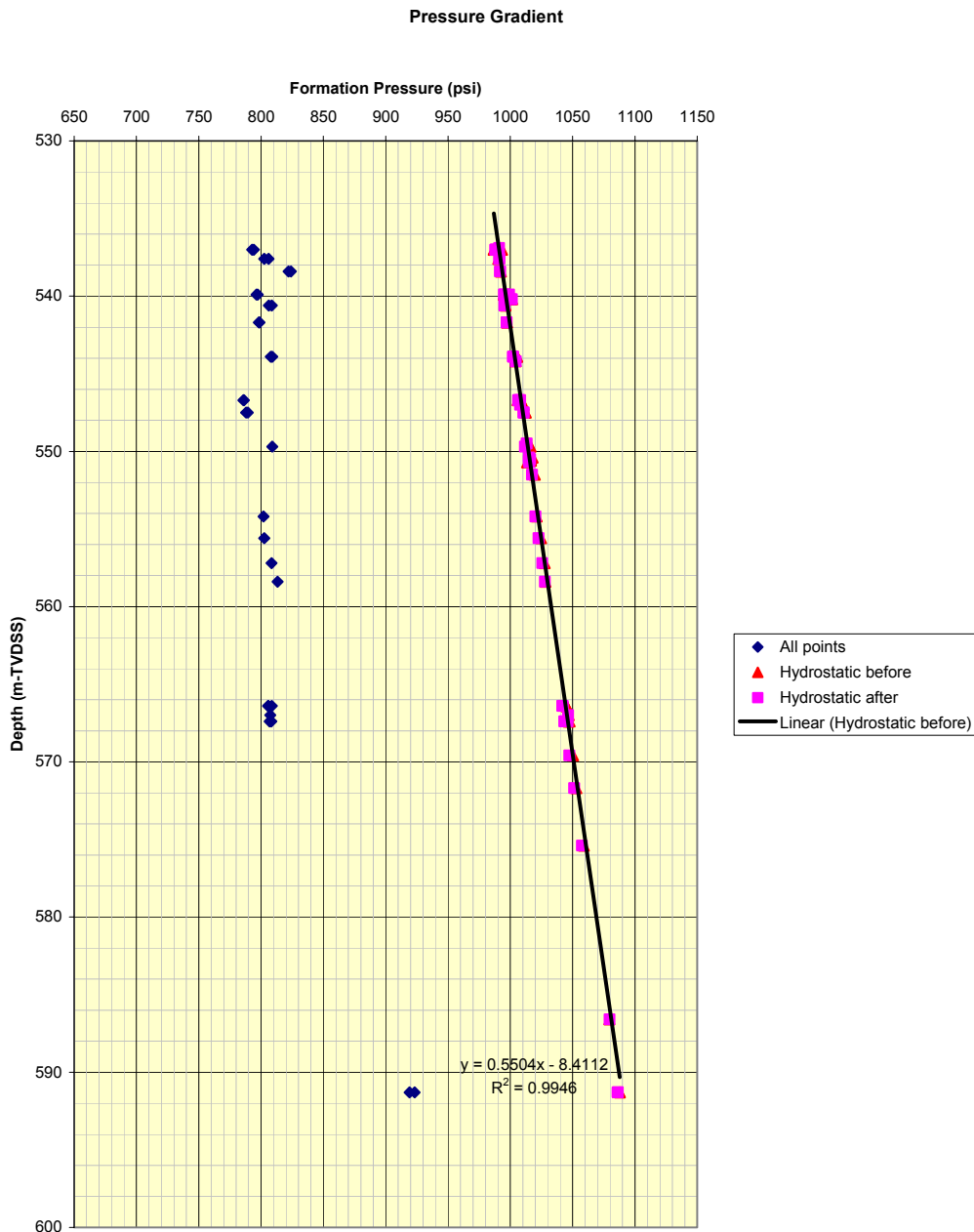
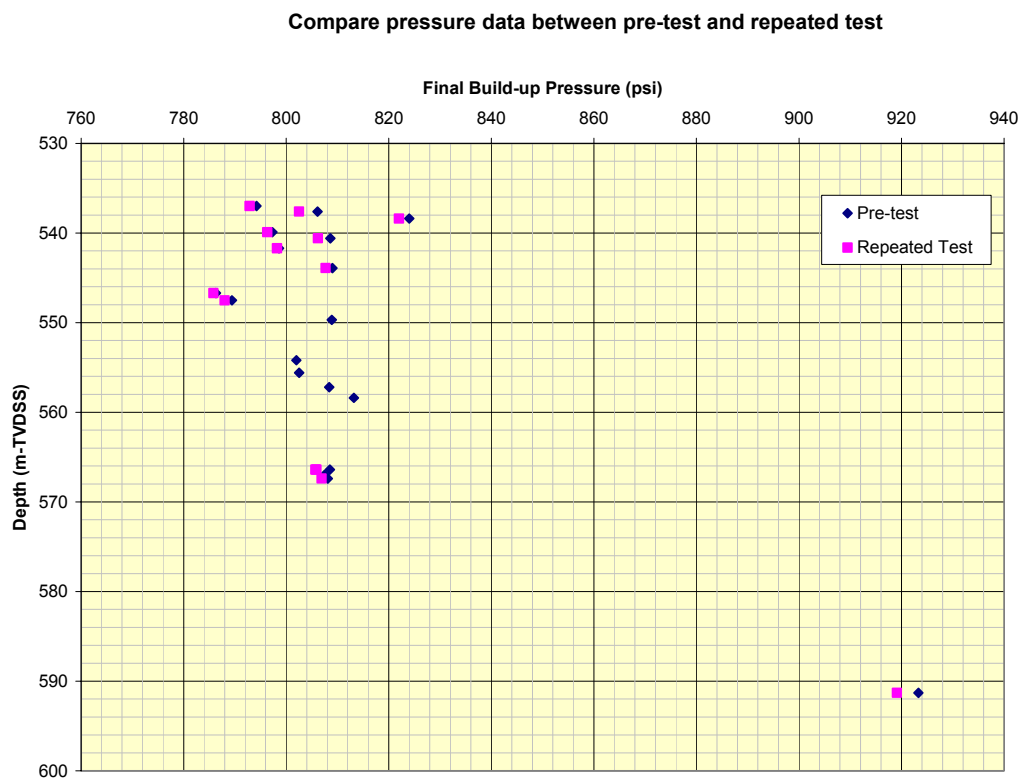


Figure 4 The pressure gradient obtained from RCI for the entire test interval before validated pressure points

It is clear from section 2 that the final build-up pressure of the pre-test is higher than the final build-up pressure of the repeated test (as shown in Figure 5). This is because the reservoir has low permeability and therefore the test with greater pressure drop takes longer for the pressure to stabilize. It is also clear in the last section that there is no supercharging effect in this particular well. In most tests, the final build-up pressure of the pre-test were selected to plot the fluid gradient except file no i800a19 and i800a20. The repeat test of these two files indicated a trend of stabilizing of the final build-up pressure compared to the pre-test. Figure 5 shows that the trend of the fluid gradient is not much different when using the pre-tests or the repeat tests (i.e. pressure data still scattered).



**Figure 5 shows comparison between final build-up pressure of pre-test and the repeat test at the same depth.**

Figure 6 shows hydrostatic pressure before and after pressure tests. The hydrostatic pressure shows an agreement between recorded pressure at most tested points (within 1 psi). At some points, the pressure difference is between 2-3 psi. Only one pressure point has a larger pressure difference (4.5 psi). This is within the acceptable range concerning all uncertainties. There are few operational comments regarding the hydrostatic pressure:

- Normally, the engineer would try to wait until hydrostatic before and after are within 1-2 psi of each other. However, this is not always possible. Part of the reason for this is that the fluid inside the tool (between transducer and packer) changes as the test progresses. At the beginning, mud fills the fluid lines. At the end of the test, a mix between filtrate, mud, and formation fluids fill the same fluid lines. Since the density of those fluids cannot be estimated, we cannot compensate for any differences due to this effect.

- Secondly, most tests were tight to very low permeability. With drawdowns performed under these conditions, there is a chance that some formation solids (and/or mud cake) come into the probe section. When/if this happens, a restriction might form in the probe that may affect the reading of the “hydrostatic after” pressure. This is not to be confused with the tool being plugged.
- Finally, due to operational circumstances, it is not advisable to remain stationary at the pressure point for too long, especially after the pre-test and/or sample attempt has been completed. In an ideal world, it would certainly be preferable to wait until both before and after pressures are stable, but it is not recommended to wait too much just for the hydrostatic pressure at the end of a test.

Compare Hydrostatic Pressure Before and After Pressure Test

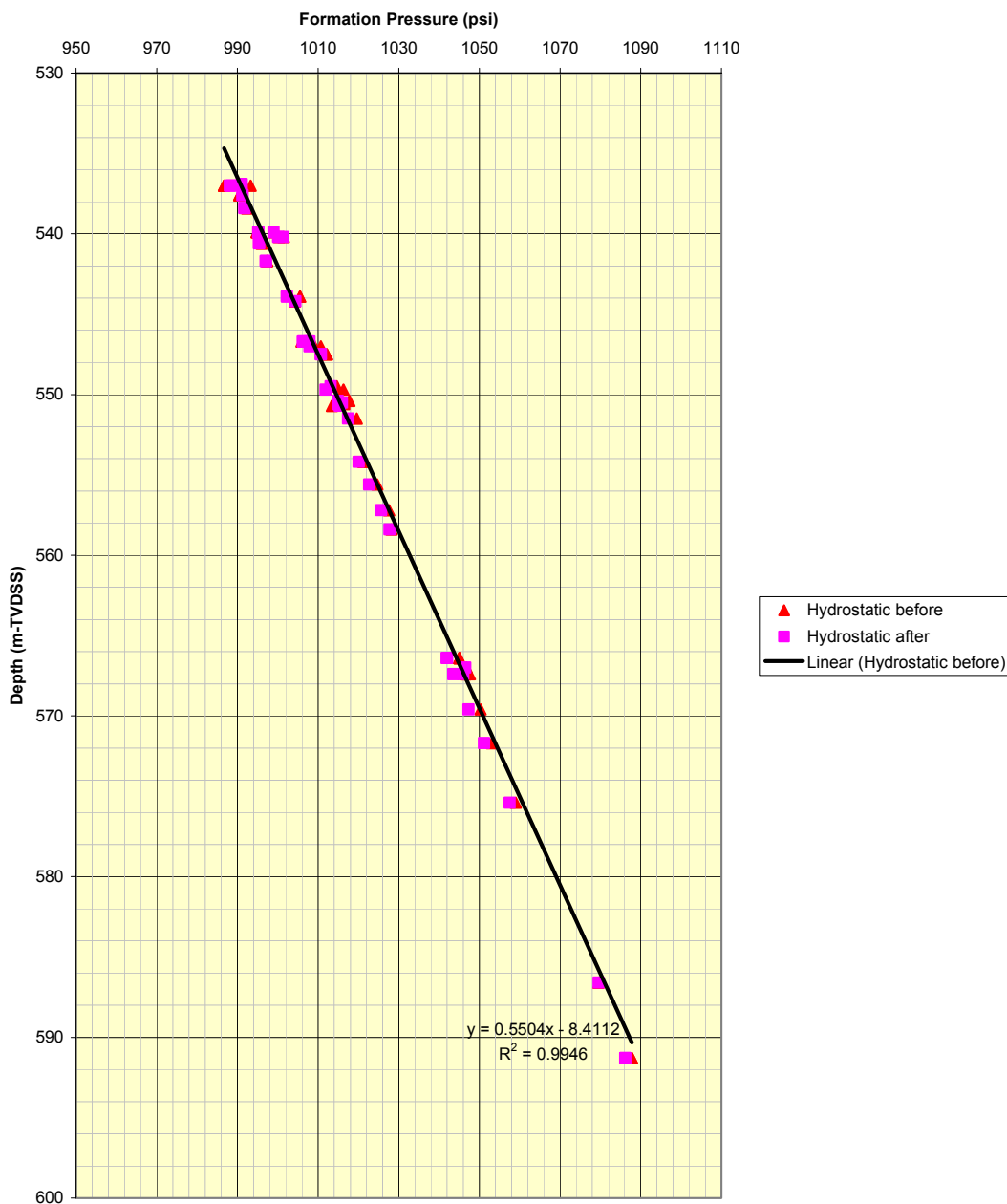
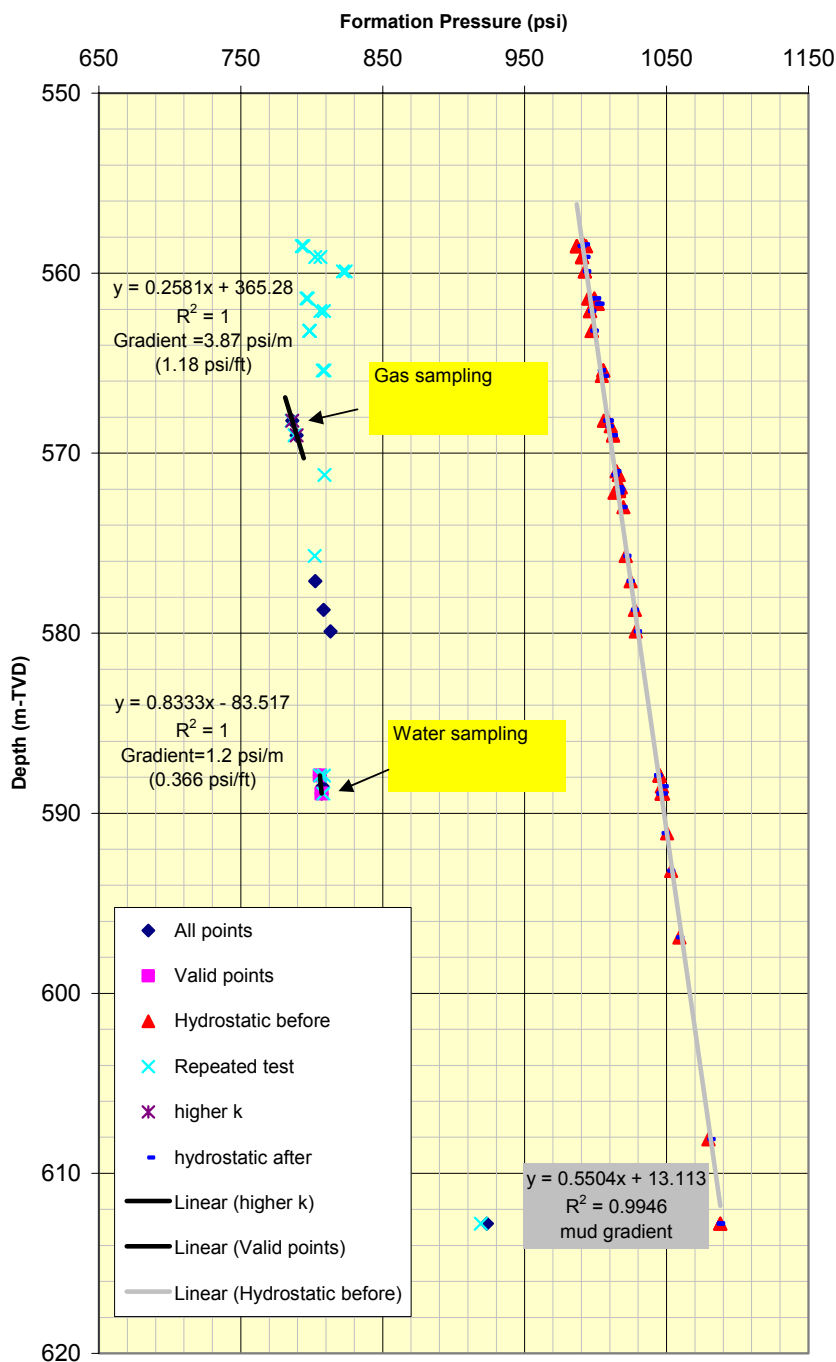


Figure 6 shows hydrostatic pressure before and after the pressure tests

After the final build-up pressures were screened using FRA and PTA techniques, three pressure points with FRA compliance are identified at depths of 566.4m-TVDSS (i800a19), 567.4m-TVDSS (i800a20) and 567.0 m-TVDSS (i800a40). The valid pressure points are shown as pink points in Figure 7.

**Pressure Gradient for MOBY-1**



**Figure 7 Pressure gradient obtained from valid pressure points**

In the top zone, two pressure points, file no i800a12 (@ 546.7 m-TVDSS) and i800a13 (@ 547.5 m-TVDSS) are not FRA compliant. However, this top zone has slightly higher permeability (as seen when spherical flow develops in log-log plot, as shown in figures 35 and 38). When the pressure gradient was plotted, a gradient of 26.68 kPa/m (3.87 psi/m or 1.18 psi/ft) was calculated from these two pressure points (as shown in Figure 7). This gradient does not represent any reservoir fluid. However, in this top zone, gas sampling was attempted (at a depth of 547.3 m-TVDSS, file no i800a31). If the typical gas gradient of 2.034 kPa/m (0.295 psi/m or 0.09 psi/ft) was used to plot fluid gradient, the gas gradient line is shown in Figure 8.

At depths between 566.4 and 567.4 m-TVDSS, there are three valid pressure points. These pressure points are FRA compliant. Pressure derivatives in the log-log plot of these points also indicate spherical flow (as shown in Figures 52, 56 and 72). However, two pressure points (i800a19 and 20) were taken when the tool was descending and another pressure point (i800a40) was taken when the tool was ascending. Thus, only two pressure points can be used to plot the fluid gradient due to temperature effects. Figure 7 shows that a fluid gradient of 8.273 kPa/m (1.2 psi/ft or 0.366 psi/ft) can be estimated from these two pressure point. Again this pressure gradient does not fall into the typical reservoir fluid, e.g. gas, oil or water. However, this gradient is close to the standard water gradient of 9.72 kPa/m (1.41 psi/m or 0.43 psi/ft). If the standard water gradient was used to plot water gradient, as shown in Figure 8, the estimated GWC is approximately at 554 m-TVDSS.

**Pressure Gradient for MOBY-1**

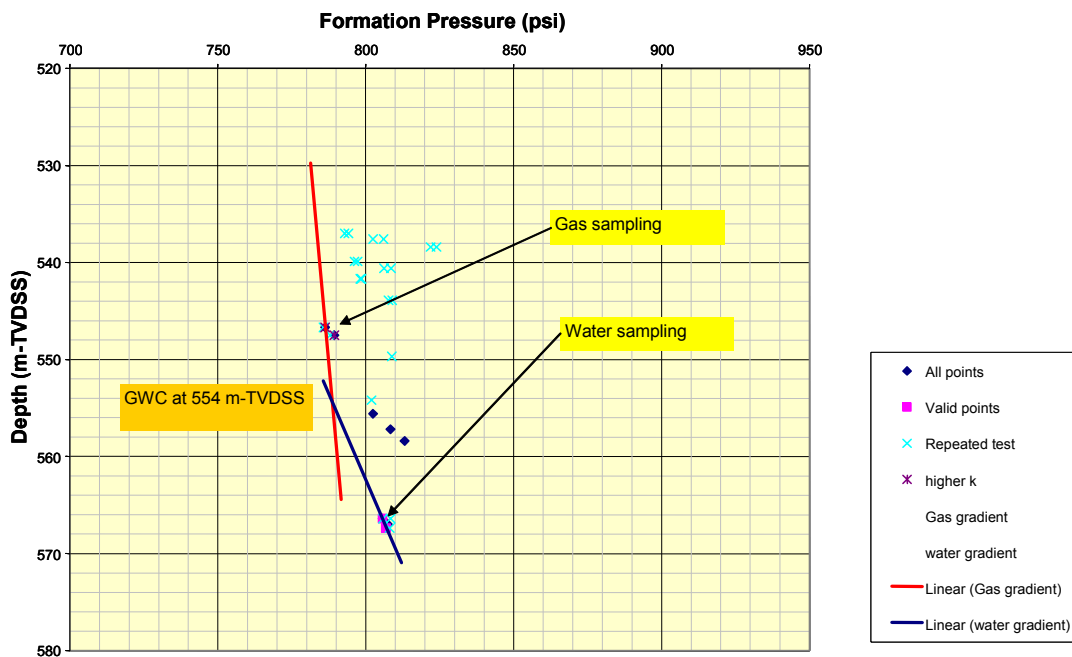


**Figure 8 GWC estimated using the typical gas and water gradient.**

The Baker Atlas standard procedure is that FRA Compliance is the minimum requirement for the fluid gradient plot. In other words, tests with FRA compliance can be used to plot fluid gradients. However, in the case of file i800a19 and i800a20, the final build-up pressure does not seem to stabilize due to low permeability, as show in Figure 9. Also, Figure 10 clearly shows that that pressure derivative of pre-test and repeated tests deviates from spherical flow. This confirms the abnormal final build-up pressure. Therefore the final build-up pressures of these two pressure points do not provide an accurate water gradient.

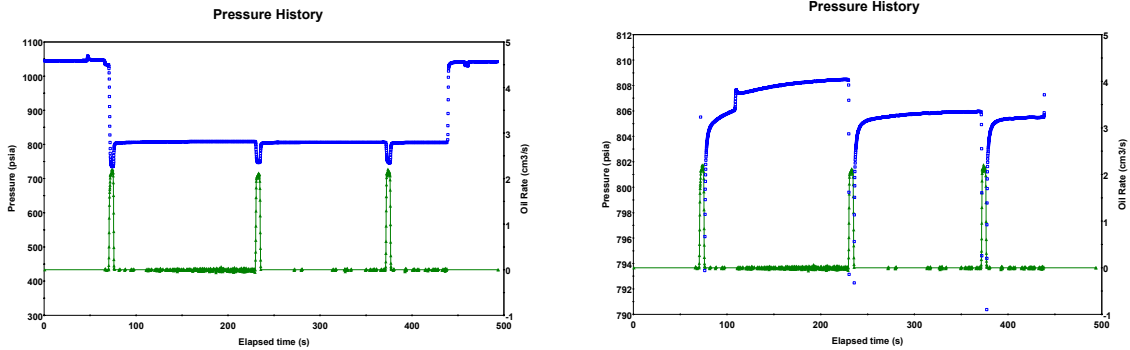


Figure 9 shows pressure history of file no i800a19 (@566.40 m-TVDSS). The plot on the left hand-side shows the full scale whereas the plot on the left hand side shows the zoomed in plot of this file. It is clear that final build-up of the pre-test does not stabilize.

Log-Log Diagnostic - Flow Period 144

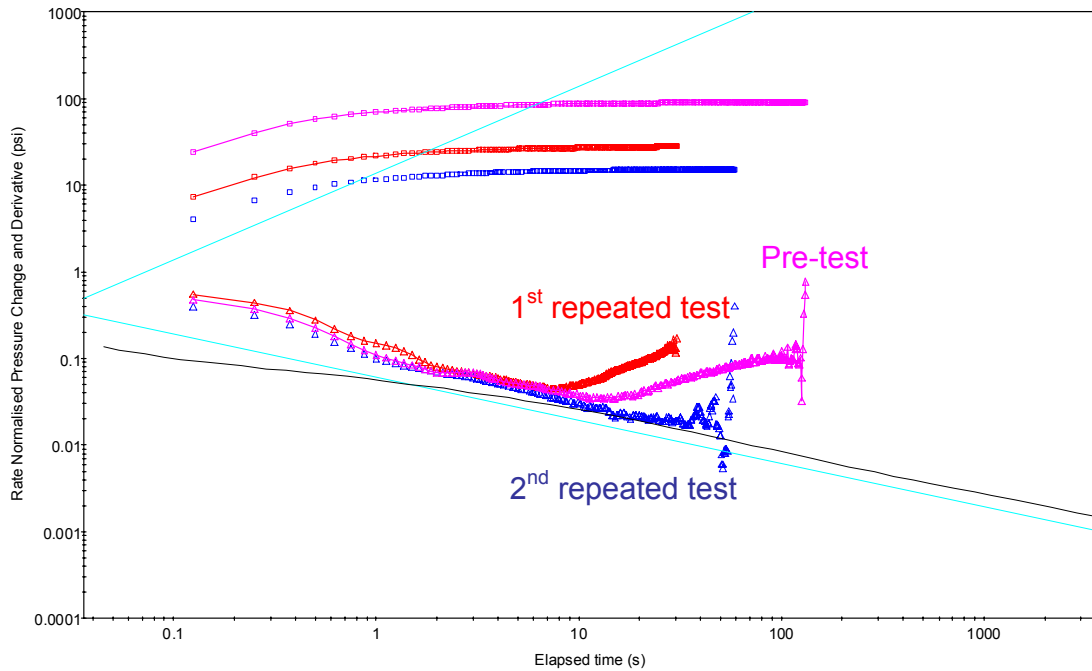
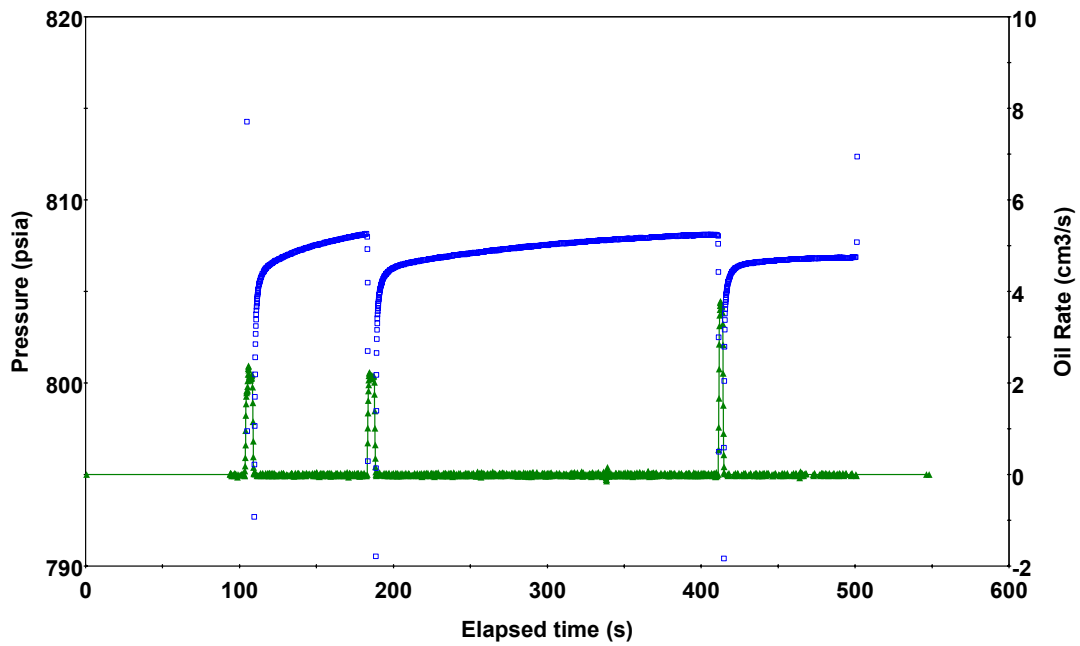
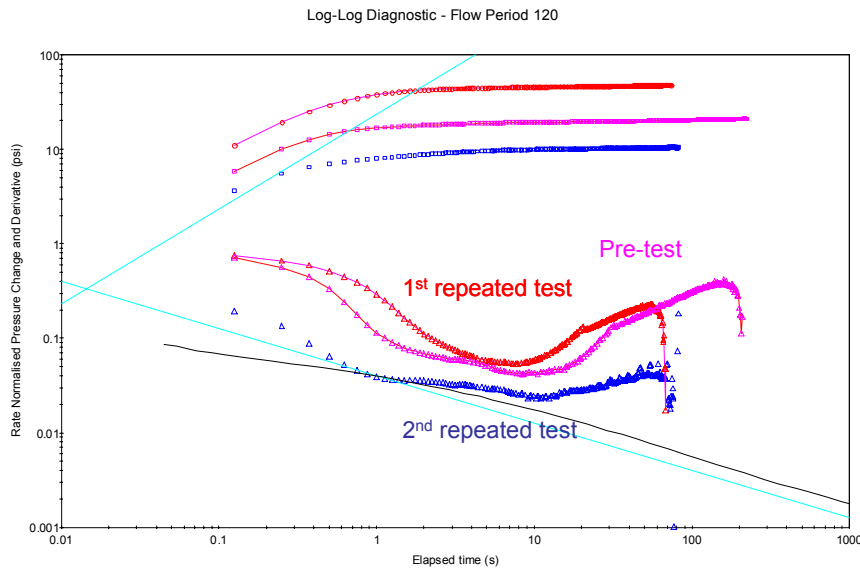


Figure 10 shows the log-log plot of test in file i800a19 (@566.4 m-TVDSS). The pressure derivative of the pre-test and the first repeated test goes upward. This implies that the final build-up pressure does not stabilize at the formation pressure.

**Pressure History**



**Figure 11** The zoomed in plot of pressure history of file no i800a20. It clearly shows that the final build-up pressure of the pre-test and the first repeated test do not stabilize.



**Figure 12** The log-log plot of test in file no i800a20. Pressure derivatives deviate from spherical flow showing the abnormal pressure build-up. This confirms that the final build-up pressure of all testd do not stabilize at the formation pressure.

#### 4. Recommendations for future tests

- When the reservoir is identified as a low permeability zone, the lowest piston rate should be applied in order to match the piston rate with the formation rate.
- Multiple drawdowns are recommended when the measured pressures show inconsistent trend. The repeated test will help to confirm the valid formation pressure.
- Use of real-time FRA is recommended to optimize and validate pressure tests
- Post job FRA and PTA is recommended to evaluate and validate all pressure tests
- The SampleView should be examined closely during the RCI job to detect any changing fluid phase during pumping and sampling

#### 5. Input Data for PTA Analysis

In order to match the pressure transient test, some well, reservoir and probe parameters are listed below:

Input Parameters	Units	Values
Matrix Porosity		0.30-0.39
Probe Diameter	inch	0.72
Tool Internal Volume	cm <sup>3</sup>	350
Geometric Factor		4.67
Fluid Viscosity	cp	1
Total Compressibility	1/psi	1E-5

#### 6. List of Tables

Table 1 Results from FRA validation .....	7
Table 2 Summary of results obtained from PTA analysis.....	9

#### 7. List of Figures

Figure 1 shows the pressure history plot in the left hand side. The final build-up pressure of the pre-test is significantly higher than the repeated test.....	4
Figure 2 show the FRA plot of the test with supercharging effect. The supercharging can be identifies by the changing in slope at zero formation rate. The slope gets steeper at the left hand side of this plot.....	5
Figure 3 The pressure history of file no i800a03 (@558.5 m-TVD). The flowing bottomhole pressure of the repeated is lower than the pre-test, and therefore pressure takes longer to reach the formation pressure.....	5
Figure 4 The pressure gradient obtained from RCI for the entire test interval before validated pressure points.....	10
Figure 5 show comparison between final build-up pressure of pre-test and the repeated test in the same depth.....	11
Figure 6 shows hydrostatic pressure before and after the pressure tests.....	12
Figure 7 Pressure gradient obtained from valid pressure points .....	14
Figure 8 GWC estimated using the typical gas and water gradient.....	14
Figure 9 shows pressure history of file no i800a19 (@566.40 m-TVDSS). The plot on the left hand-side shows the full scale whereas the plot on the left hand side shows the zoomed in plot of this file. It is clear that final build-up of the pre-test does not stabilize.....	15
Figure 10 shows the log-log plot of test in file i800a19 (@566.4 m-TVDSS). Pressure derivative of the pre-test and the first repeated go upward indicating not stabilizing final build-up pressure.....	15
Figure 11 The zoomed in plot of pressure history of file no i800a20. It shows clearly that the final build-up pressure of the pre-test and the first repeated test do not stabilize.....	16

Figure 12 The log-log plot of test in file no i800a20. Pressure derivatives deviate from spherical flow showing the abnormal of pressure build-up. This confirms that the final build-up pressure of all test does not stabilize at the formation pressure. .... 16

Figure 13 File no. g800a03\_0: Depth 558.5 m-MD ..... 20

Figure 14 File no. g800a03\_1: Depth 558.5 m-MD ..... 21

Figure 15 File no. g800a03: Depth 558.5 m-MD ..... 22

Figure 16 File no. g800a04\_0: Depth 559.1 m-MD ..... 23

Figure 17 File no. g800a04\_1: Depth 559.1 m-MD ..... 24

Figure 18 File no. g800a04: Depth 559.1 m-MD ..... 25

Figure 19 File no. g800a06\_0: Depth 559.9 m-MD ..... 26

Figure 20 File no. g800a06\_1: Depth 559.9 m-MD ..... 27

Figure 21 File no. g800a06: Depth 559.9 m-MD ..... 28

Figure 22 File no. g800a07\_0: Depth 561.4 m-MD ..... 29

Figure 23 File no. g800a07\_1: Depth 561.4 m-MD ..... 30

Figure 24 File no. g800a07: Depth 561.4 m-MD ..... 31

Figure 25 File no. g800a08\_0: Depth 562.1 m-MD ..... 32

Figure 26 File no. g800a08\_1: Depth 562.1 m-MD ..... 33

Figure 27 File no. g800a08: Depth 562.1 m-MD ..... 34

Figure 28 File no. g800a09: Depth 563.2 m-MD ..... 35

Figure 29 File no. g800a10\_0: Depth 565.7 m-MD ..... 36

Figure 30 File no. g800a11\_0: Depth 565.4 m-MD ..... 37

Figure 31 File no. g800a11\_1: Depth 565.4 m-MD ..... 38

Figure 32 File no. g800a11: Depth 565.4 m-MD ..... 39

Figure 33 File no. g800a12\_0: Depth 568.2 m-MD ..... 40

Figure 34 File no. g800a12\_1: Depth 568.2 m-MD ..... 41

Figure 35 File no. g800a12: Depth 568.2 m-MD ..... 42

Figure 36 File no. g800a13\_0: Depth 569 m-MD ..... 43

Figure 37 File no. g800a13\_1: Depth 569 m-MD ..... 44

Figure 38 File no. g800a13: Depth 569 m-MD ..... 45

Figure 39 File no. g800a14\_0: Depth 571.2 m-MD ..... 46

Figure 40 File no. g800a14: Depth 571.2 m-MD ..... 47

Figure 41 File no. g800a15\_0: Depth 575.7 m-MD ..... 48

Figure 42 File no. g800a15\_0: Depth 575.7 m-MD ..... 49

Figure 43 File no. g800a16\_0: Depth 577.1 m-MD ..... 50

Figure 44 File no. g800a16\_0: Depth 577.1 m-MD ..... 51

Figure 45 File no. g800a17\_0: Depth 578.7 ft-MD ..... 52

Figure 46 File no. g800a17\_0: Depth 578.7 ft-MD ..... 53

Figure 47 File no. g800a18\_0: Depth 579.9 m-MD ..... 54

Figure 48 File no. g800a18\_0: Depth 579.9 m-MD ..... 55

Figure 49 File no. g800a19\_0: Depth 587.9 m-MD ..... 56

Figure 50 File no. g800a19\_1: Depth 587.9 m-MD ..... 57

Figure 51 File no. g800a19\_2: Depth 587.9 m-MD ..... 58

Figure 52 File no. g800a19: Depth 587.9 m-MD ..... 59

Figure 53 File no. g800a20\_0: Depth 588.9 m-MD ..... 60

Figure 54 File no. g800a20\_1: Depth 588.9 m-MD ..... 61

Figure 55 File no. g800a20\_2: Depth 588.9 m-MD ..... 62

Figure 56 File no. g800a20: Depth 588.9 m-MD ..... 63

Figure 57 File no. g800a21\_0: Depth 591.1 m-MD ..... 64

Figure 58 File no. g800a22\_0: Depth 593.2 m-MD ..... 65

Figure 59 File no. g800a23\_0: Depth 596.9 m-MD ..... 66

Figure 60 File no. g800a25\_0: Depth 608.1 m-MD ..... 67

Figure 61 File no. g800a25\_0: Depth 608.1 m-MD ..... 68

Figure 62 File no. g800a26\_0: Depth 612.8 m-MD ..... 69

Figure 63 File no. g800a26\_1: Depth 612.8 m-MD ..... 70

Figure 64 File no. g800a26: Depth 612.8 m-MD ..... 71

Figure 65 File no. g800a28\_0: Depth 568.2 m-MD (Sampling No flow) ..... 72

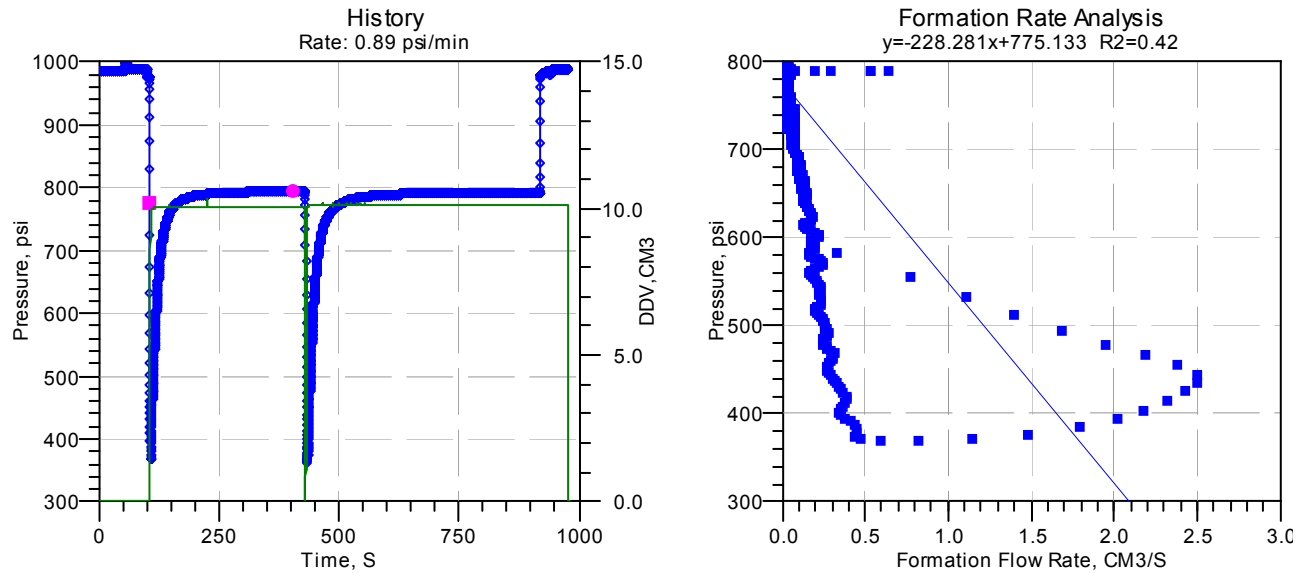
Figure 66 File no. g800a29: Depth 568.5 m-MD (Sampling no flow) .....	73
Figure 67 File no. g800a30: Depth 568.2 m-MD (Sampling No flow).....	74
Figure 68 File no. g800a34: Depth 561.4 ft-MD.....	75
Figure 69 File no. g800a35: Depth 561.7 m-MD(Sampling No flow).....	76
Figure 70 File no. g800a37: Depth 558.5 ft-MD (Sampling-Slow flow) .....	77
Figure 71 File no. g800a39: Depth 588.9 m-MD .....	77
Figure 72 File no. g800a40: Depth 588.5 m-MD (Sampling).....	79
Figure 73 File no. g800a41: Depth 572 m-MD (Sampling No Flow).....	80
Figure 74 File no. g800a42: Depth 572.1 m-MD (Sampling very slow flow) .....	81
Figure 75 File no. g800a43: Depth 572.2 ft-MD (Sampling very slow flow) .....	82
Figure 76 File no. g800a44: Depth 571 m-MD (Sampling very slow flow) .....	82
Figure 77 File no. g800a45: Depth 571.9 m-MD (Sampling very slow flow) .....	84
Figure 78 File no. g800a46: Depth 573 m-MD (Sampling very low rate) .....	85
Figure 79 Typical pressure response of WFT using single probe .....	86
Figure 80 A comparison of pressure response from different scales, i.e. Wireline Formation Test, Drill Stem Test, and Production Well Test (Whittle, 2002).....	87
Figure 81 Log-log plot, field example 9. Spherical flow regime developed in middle time pressure derivatives.....	89
Figure 82 Log-log plot, field example 2. Cylindrical flow regime developed in late time. ....	89
Figure 83 Log-log plot, field example 3. Cylindrical flow regime with extra boundary developed in late time .....	90
Figure 84 Plot of Drawdown Pressure versus Time .....	93

## 8. Summary of Results

**Figure 13 File no. g800a03 0: Depth 558.5 m-MD**

Company: BASS STRAIT OIL COMPANY LTD  
Field: EXPLORATION  
Well: MOBY-1

### Wireline Formation Test Analyzer (WFTA<sup>SM</sup>)



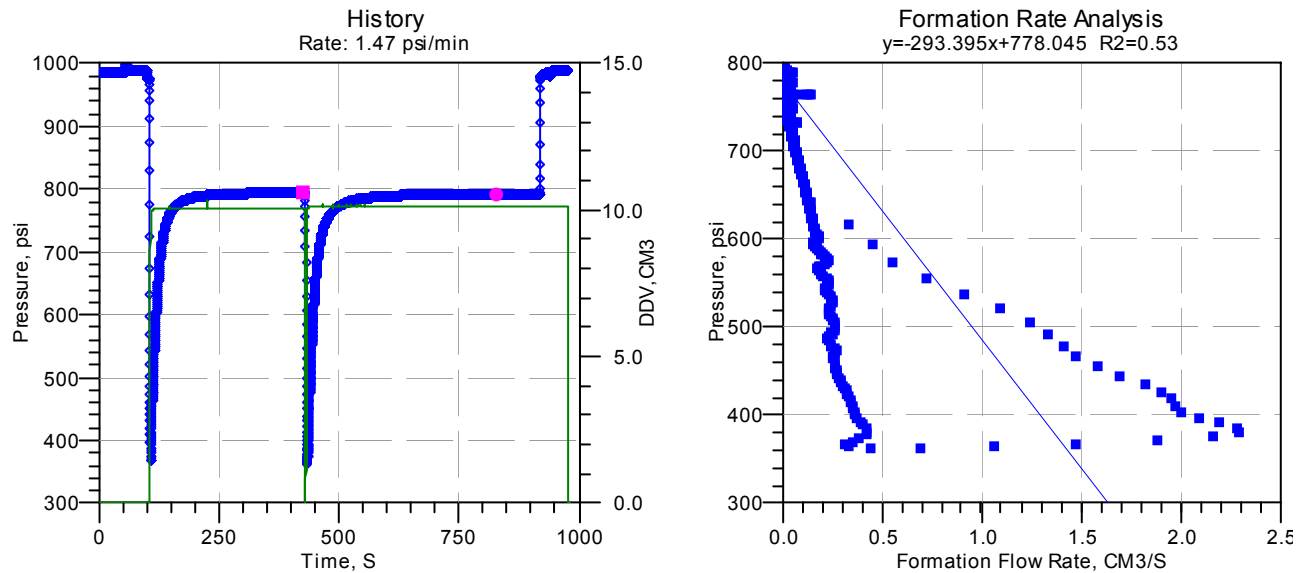
### Pressure Test Results-NOT FRA Compliant

File	Depth		Flow Rate Analysis			Maximum	Final
Number	Measured	TVD	Ct	P*	Mobility	Rate	Buildup
i800a	(ft)	(ft)		(psi)	(mD/cP)	(mD/cP)	(psi)
03	558.5	558.5	$3.7e-5$	775.1	10.9	14.6	794.1

**Figure 14 File no. g800a03 1: Depth 558.5 m-MD**

Company: BASS STRAIT OIL COMPANY LTD  
Field: EXPLORATION  
Well: MOBY-1

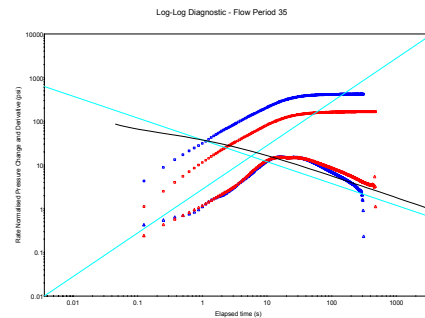
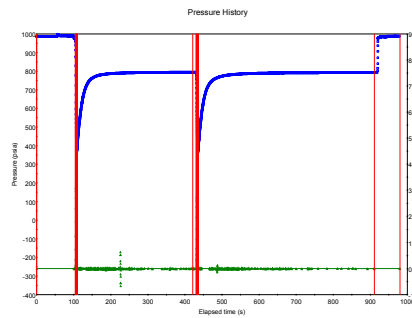
### Wireline Formation Test Analyzer (WFTA<sup>SM</sup>)



### Pressure Test Results-NOT FRA Compliant

File	Depth		Flow Rate Analysis			Maximum	Final
Number	Measured	TVD	Ct	P*	Mobility	Rate	Buildup
i800a	(ft)	(ft)		(psi)	(mD/cP)	(mD/cP)	(psi)
03	558.5	558.5	$3.7 \times 10^{-5}$	778.0	8.4	13.4	792.9

**Figure 15 File no. q800a03: Depth 558.5 m-MD**



**Model**  
Wireline Formation Test (WFT)  
Homogeneous  
Infinite Lateral Extent

**Results**

(pav) <sub>i</sub>	795.697	psia
pwf	375.794	psia
k/u(xyz)	0.2189	mD/cp
k(xyz)	0.2189	mD
c(sys)	5.7447E-005	1/psi
S(p)	-0.83	
C	1.2647E-007	bbbl/psi
ri	2	ft
p*(FRA)	775.244	psia
k/u(FRA)	15.53	mD/cp
c(FRA)	3.3592E-005	1/psi

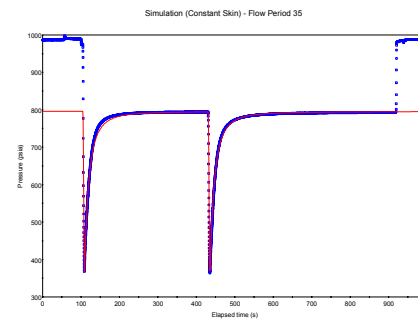
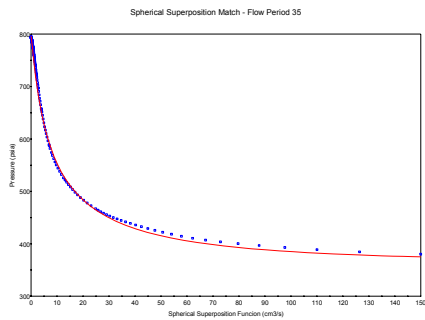
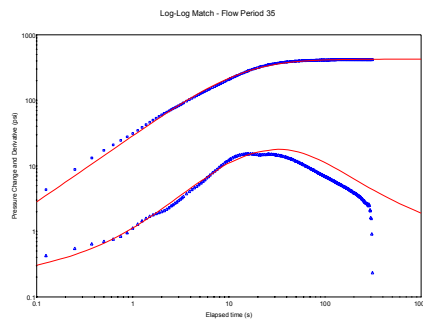
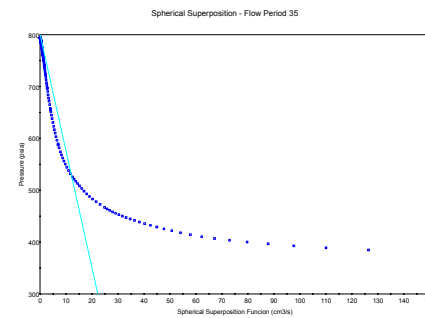
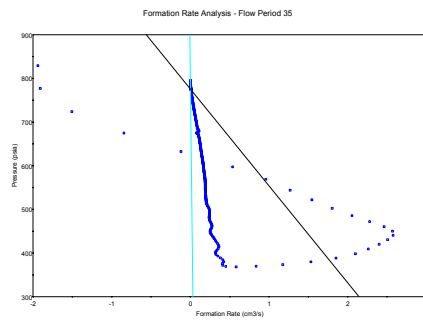
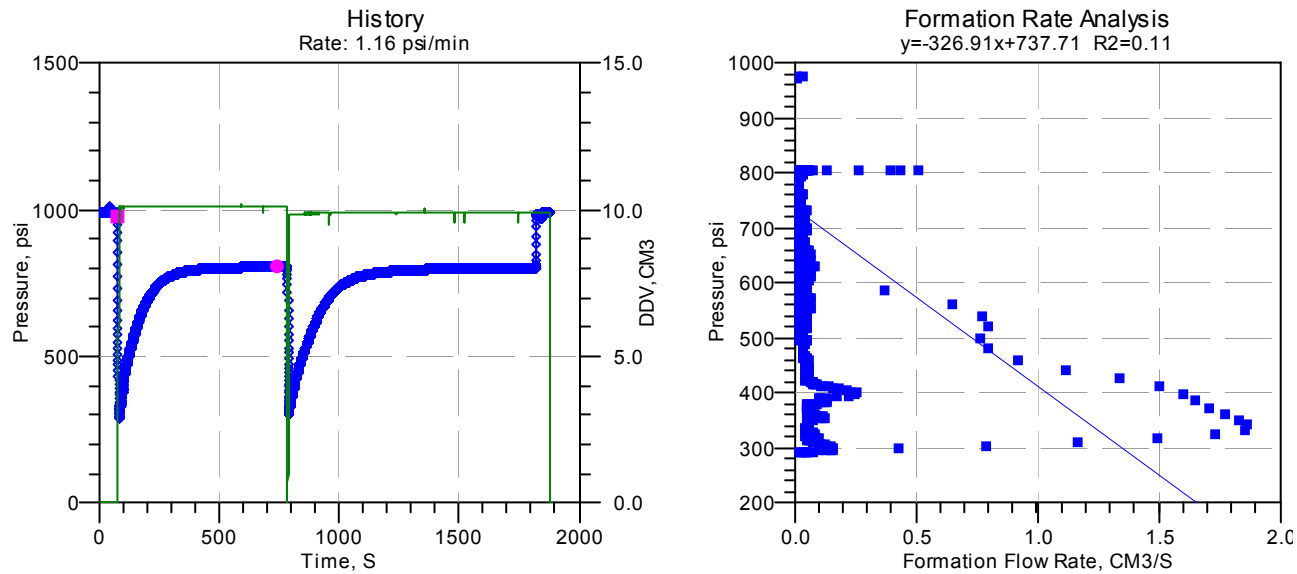


**Figure 16 File no. g800a04 0: Depth 559.1 m-MD**

Company: BASS STRAIT OIL COMPANY LTD  
Field: EXPLORATION  
Well: MOBY-1

### Wireline Formation Test Analyzer (WFTA<sup>SM</sup>)



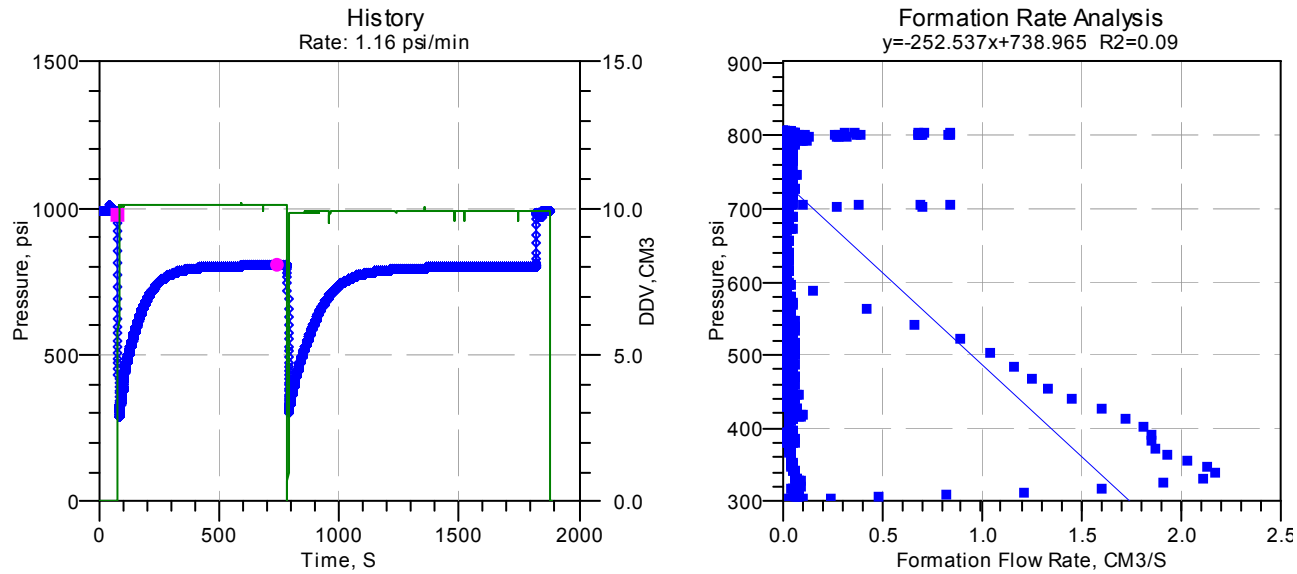
### Pressure Test Results-FRA Compliant

File	Depth		Flow Rate Analysis			Maximum	Final
Number	Measured	TVD	Ct	P*	Mobility	Rate	Buildup
i800a	(ft)	(ft)		(psi)	(mD/cP)	(mD/cP)	(psi)
04	559.1	559.1	3.4e-5	737.7	7.6	9.0	806.0

**Figure 17 File no. g800a04 1: Depth 559.1 m-MD**

Company: BASS STRAIT OIL COMPANY LTD  
Field: EXPLORATION  
Well: MOBY-1

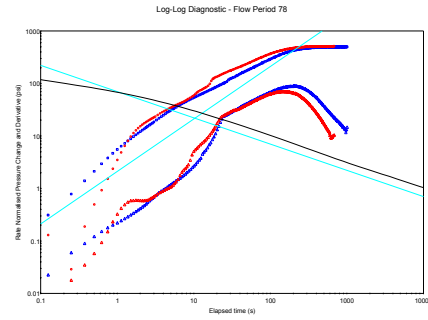
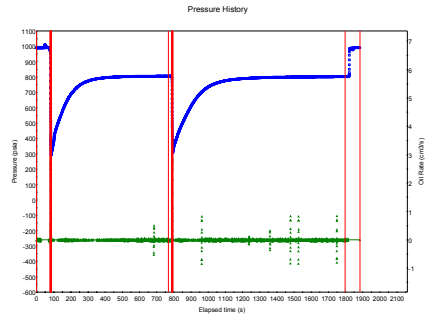
## Wireline Formation Test Analyzer (WFTA<sup>SM</sup>)



### Pressure Test Results-NOT FRA Compliant

File	Depth		Flow Rate Analysis			Maximum	Final
Number	Measured	TVD	Ct	P*	Mobility	Rate	Buildup
i800a	(ft)	(ft)	(ft)	(psi)	(mD/cP)	(mD/cP)	(psi)
04	559.1	559.1	3.4e-5	739.0	9.8	10.6	802.4

**Figure 18 File no. q800a04: Depth 559.1 m-MD**



**Model**  
Wireline Formation Test (WFT)  
Homogeneous  
Infinite Lateral Extent

**Results**

(pav) <sub>i</sub>	810.498	psia
pwf	304.048	psia
k/u(xyz)	0.1158	mD/cp
k(xyz)	0.1158	mD
c(sys)	5.4366E-005	1/psi
S(p)	-0.44	
C	1.1969E-007	bbf/psi
ri	3	ft
p*(FRA)	750.924	psia
k/u(FRA)	8.636	mD/cp
c(FRA)	4.3091E-005	1/psi

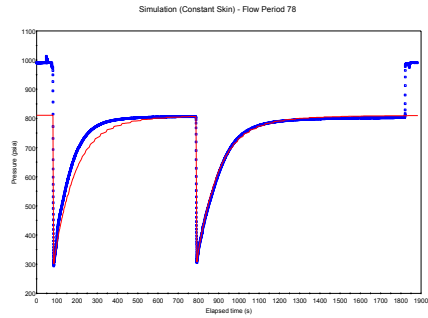
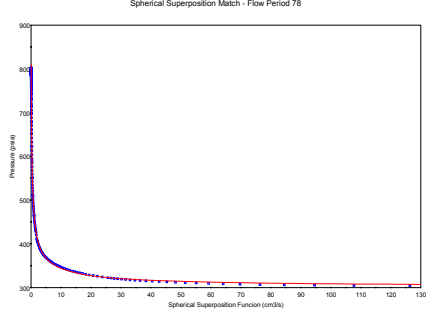
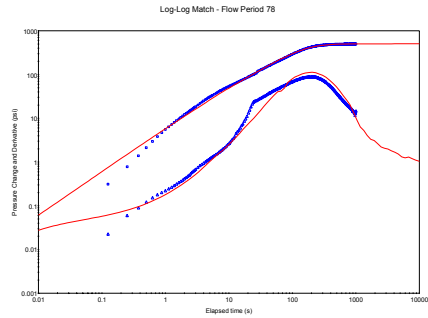
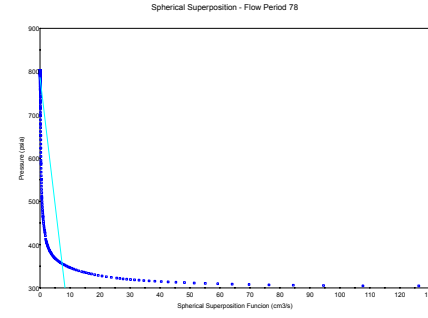
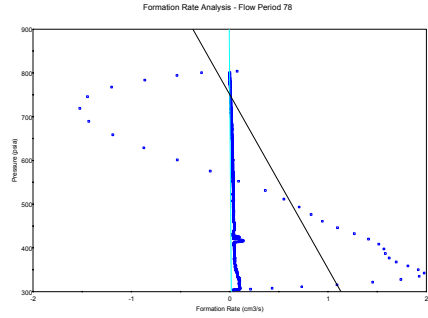
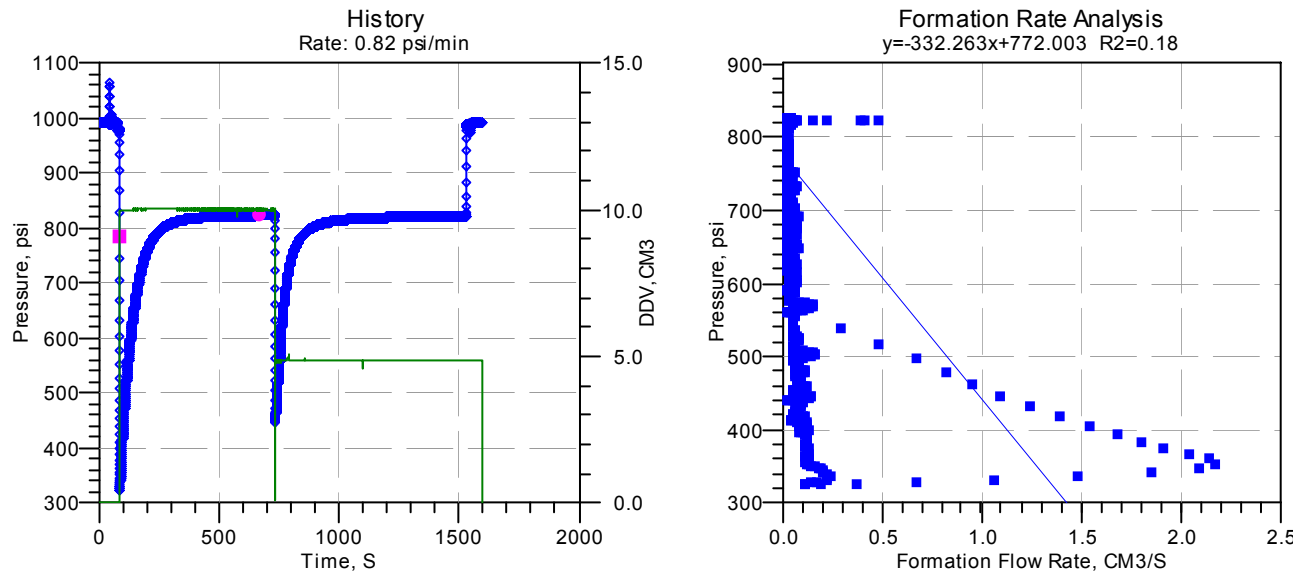


**Figure 19 File no. g800a06 0: Depth 559.9 m-MD**

Company: BASS STRAIT OIL COMPANY LTD  
Field: EXPLORATION  
Well: MOBY-1

## Wireline Formation Test Analyzer (WFTA<sup>SM</sup>)



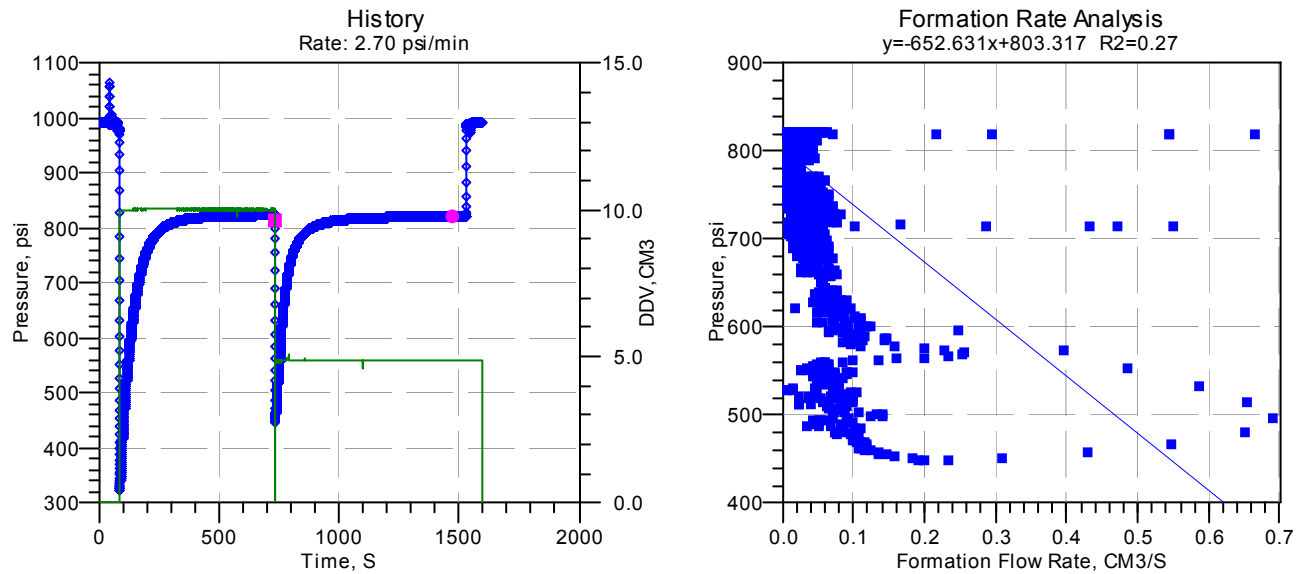
### Pressure Test Results-NOT FRA Compliant

File	Depth		Flow Rate Analysis			Maximum	Final
Number	Measured	TVD	Ct	P*	Mobility	Rate	Buildup
i800a	(ft)	(ft)		(psi)	(mD/cP)	(mD/cP)	(psi)
06	559.9	559.9	3.7e-5	772.0	7.5	10.8	824.0

**Figure 20 File no. q800a06 1: Depth 559.9 m-MD**

Company: BASS STRAIT OIL COMPANY LTD  
Field: EXPLORATION  
Well: MOBY-1

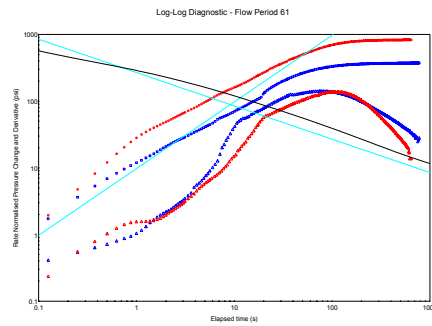
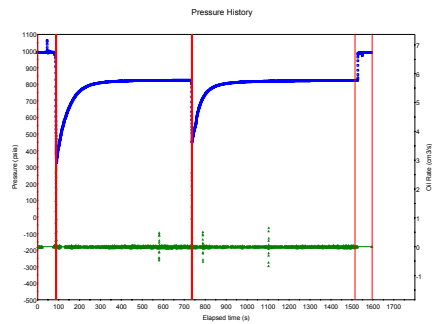
### Wireline Formation Test Analyzer (WFTA<sup>SM</sup>)



### Pressure Test Results-NOT FRA Compliant

File	Depth		Flow Rate Analysis			Maximum	Final	
Number	Measured	TVD	Ct	P*	Mobility	Rate	Buildup	
i800a	(ft)	(ft)		(psi)	(mD/cP)	(mD/cP)	(psi)	
	06	559.9	559.9	3.7e-5	803.3	3.8	3.4	822.0

**Figure 21 File no. q800a06: Depth 559.9 m-MD**



Model	
Wireline Formation Test (WFT)	
Homogeneous	
Infinite Lateral Extent	

Results		
(pav) <sub>i</sub>	826.182	psia
pwf	449.030	psia
k/u(xyz)	0.09833	mD/cp
k(xyz)	0.09833	mD
c(sys)	3.5254E-005	1/psi
S(p)	-0.69	
C	7.7613E-008	bb/psi
ri	2	ft
p*(FRA)	803.651	psia
k/u(FRA)	3.669	mD/cp
c(FRA)	3.37E-005	1/psi

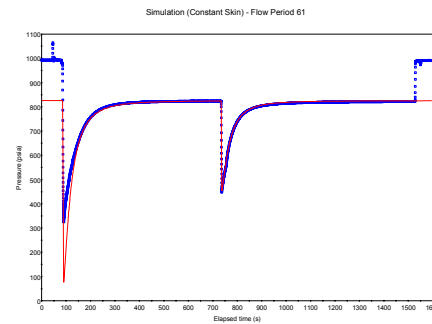
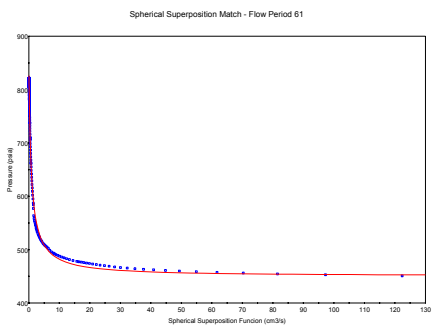
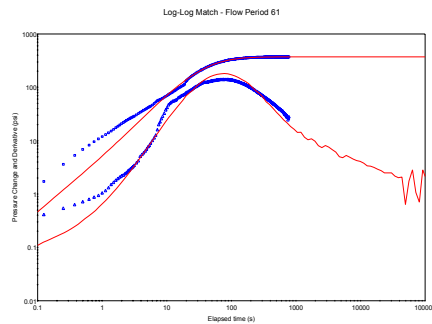
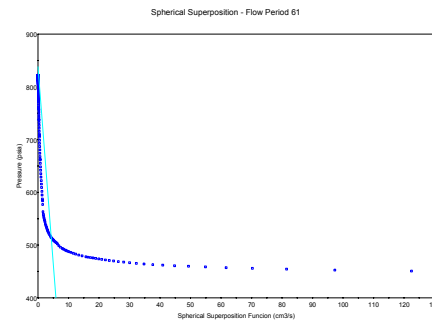
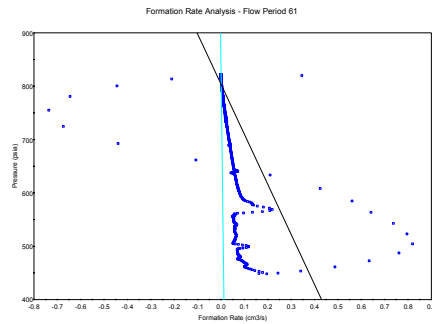
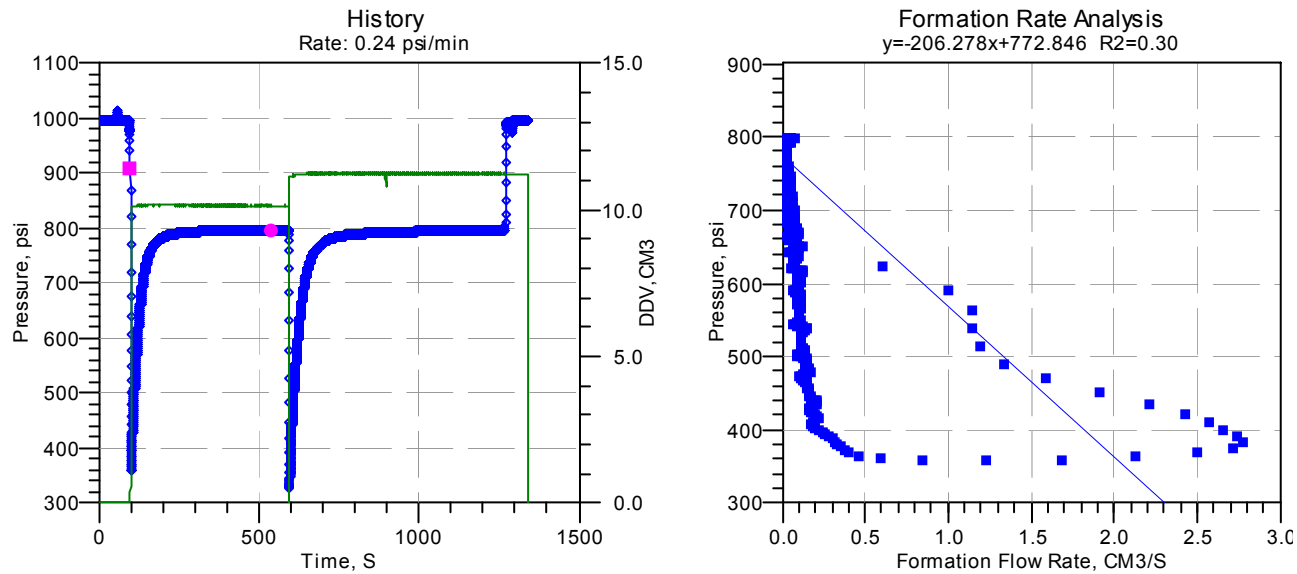


**Figure 22 File no. g800a07 0: Depth 561.4 m-MD**

Company: BASS STRAIT OIL COMPANY LTD  
Field: EXPLORATION  
Well: MOBY-1

### Wireline Formation Test Analyzer (WFTA<sup>SM</sup>)



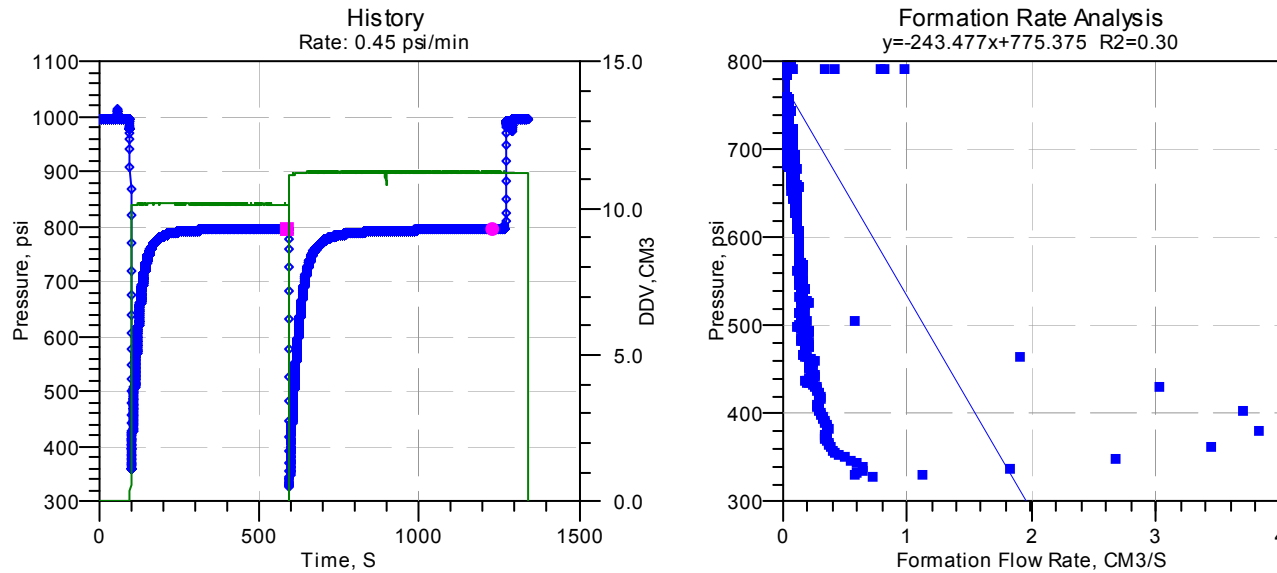
### Pressure Test Results-NOT FRA Compliant

File	Depth		Flow Rate Analysis			Maximum	Final
Number	Measured	TVD	Ct	P*	Mobility	Rate	Buildup
i800a	(ft)	(ft)		(psi)	(mD/cP)	(mD/cP)	(psi)
07	561.4	561.4	$3.3e-5$	772.8	12.0	14.7	797.3

**Figure 23 File no. g800a07 1: Depth 561.4 m-MD**

Company: BASS STRAIT OIL COMPANY LTD  
Field: EXPLORATION  
Well: MOBY-1

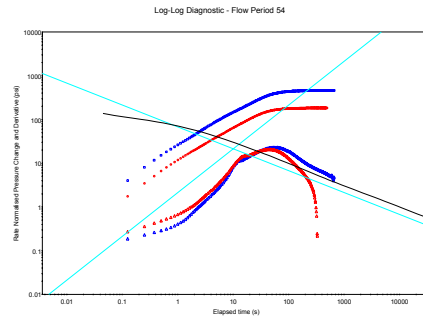
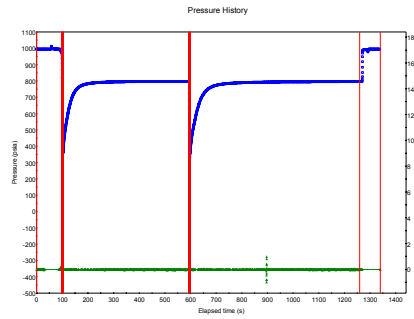
### Wireline Formation Test Analyzer (WFTA<sup>SM</sup>)



### Pressure Test Results-NOT FRA Compliant

File	Depth		Flow Rate Analysis			Maximum	Final	
	Number	Measured	TVD	Ct	P*	Mobility Rate	Buildup	
i800a	(ft)	(ft)		(psi)	(mD/cP)	(mD/cP)	(psi)	
07	561.4	561.4		5.8e-5	775.4	10.2	20.4	796.2

**Figure 24 File no. q800a07: Depth 561.4 m-MD**



**Model**  
Wireline Formation Test (WFT)  
Homogeneous  
Infinite Lateral Extent

**Results**

(pav) <sub>i</sub>	799.063	psia
pwf	334.087	psia
k/u(xyz)	0.1383	mD/cp
k(xyz)	0.1383	mD
c(sys)	6.4552E-005	1/psi
S(p)	-0.82	
C	1.4211E-007	bbbl/psi
ri	3	ft
p*(FRA)	776.395	psia
k/u(FRA)	13.37	mD/cp
c(FRA)	5.7726E-005	1/psi

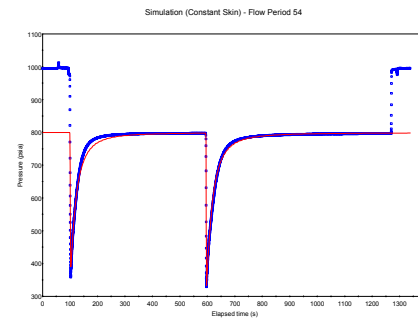
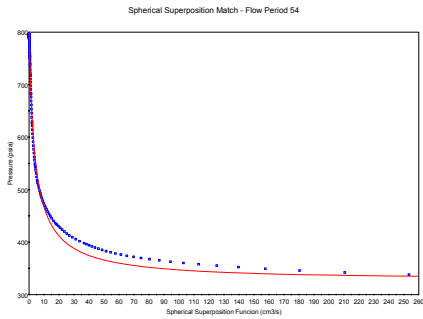
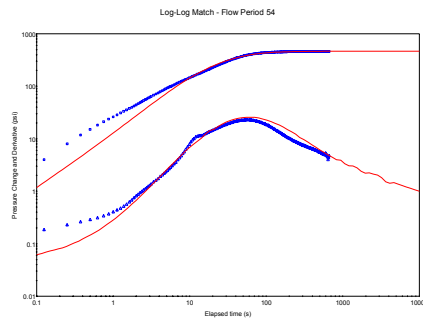
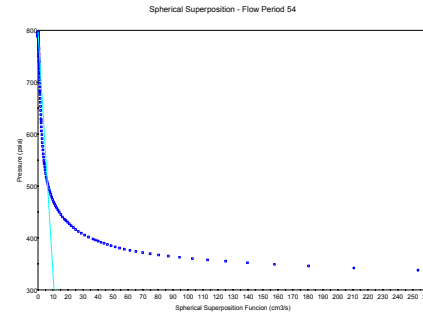
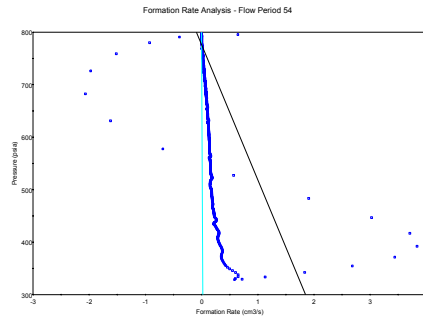
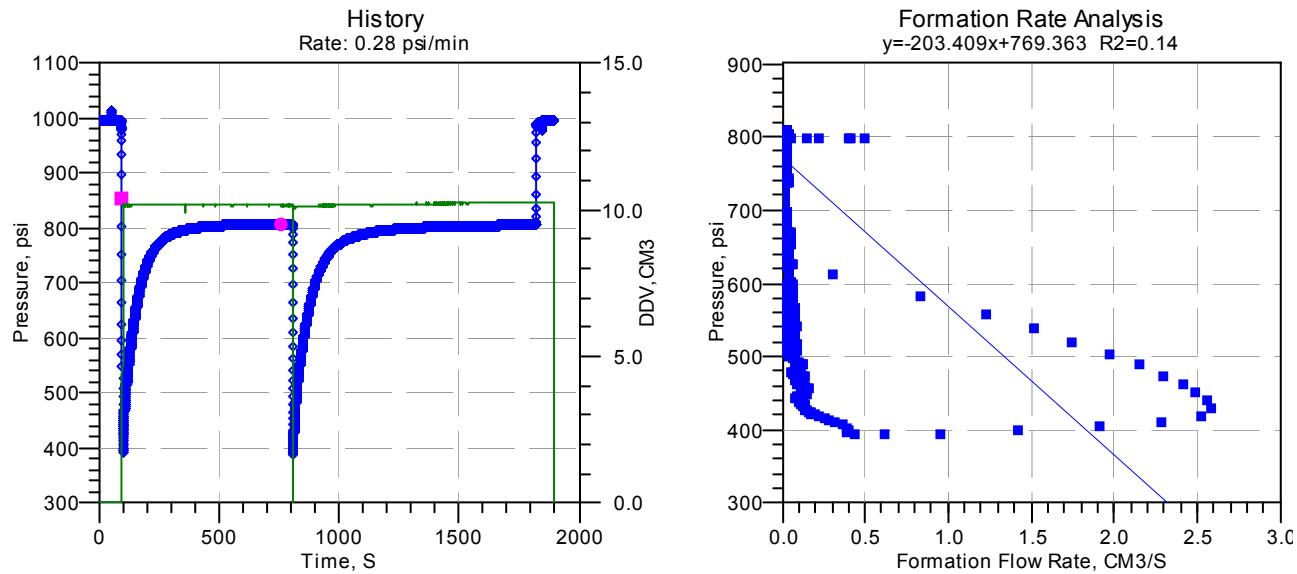


**Figure 25 File no. g800a08 0: Depth 562.1 m-MD**

Company: BASS STRAIT OIL COMPANY LTD  
Field: EXPLORATION  
Well: MOBY-1

### Wireline Formation Test Analyzer (WFTA<sup>SM</sup>)



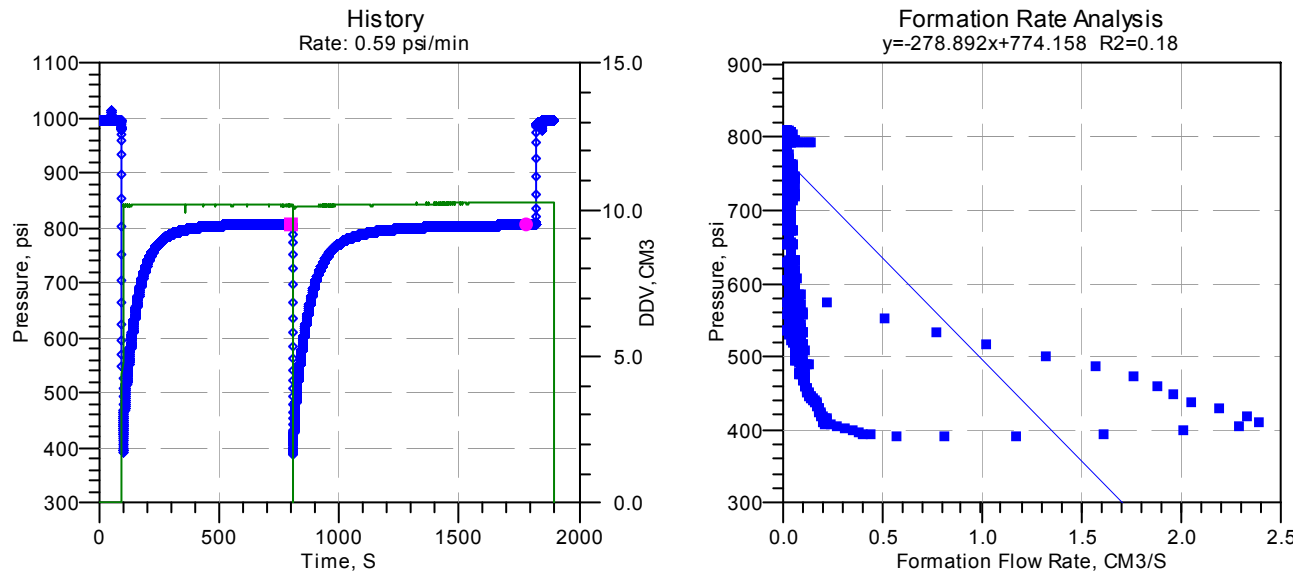
### Pressure Test Results-NOT FRA Compliant

File	Depth		Flow Rate Analysis			Maximum	Final
Number	Measured	TVD	Ct	P*	Mobility	Rate	Buildup
i800a	(ft)	(ft)		(psi)	(mD/cP)	(mD/cP)	(psi)
08	562.1	562.1	3.8e-5	769.4	12.2	15.4	808.5

**Figure 26 File no. g800a08 1: Depth 562.1 m-MD**

Company: BASS STRAIT OIL COMPANY LTD  
Field: EXPLORATION  
Well: MOBY-1

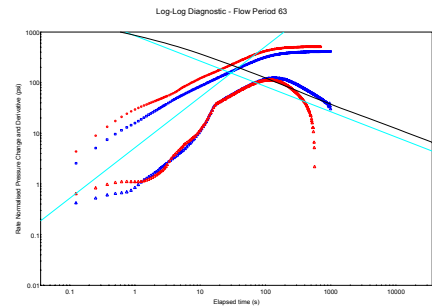
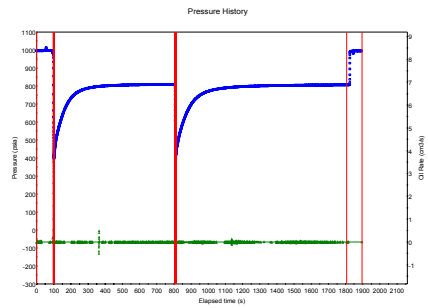
### Wireline Formation Test Analyzer (WFTA<sup>SM</sup>)



### Pressure Test Results-NOT FRA Compliant

File	Depth		Flow Rate Analysis			Maximum	Final
Number	Measured	TVD	Ct	P*	Mobility	Rate	Buildup
i800a	(ft)	(ft)		(psi)	(mD/cP)	(mD/cP)	(psi)
08	562.1	562.1	5.4e-5	774.2	8.9	14.3	806.1

**Figure 27 File no. g800a08: Depth 562.1 m-MD**



Model	
Wireline Formation Test (WFT)	
Homogeneous	
Infinite Lateral Extent	

Results		
(pav) <sub>i</sub>	813.529	psia
pwf	394.166	psia
k/u(xyz)	0.04737	mD/cp
k(xyz)	0.04737	mD
c(sys)	6.5998E-005	1/psi
S(p)	-0.86	
C	1.4529E-007	bbf/psi
ri	2	ft
p*(FRA)	777.167	psia
k/u(FRA)	11.63	mD/cp
c(FRA)	5.3352E-005	1/psi

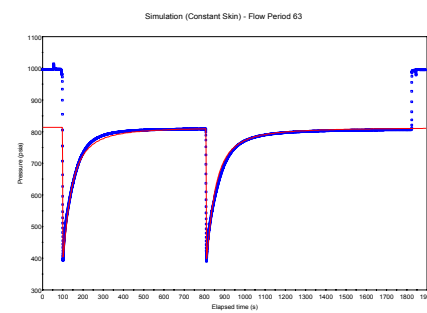
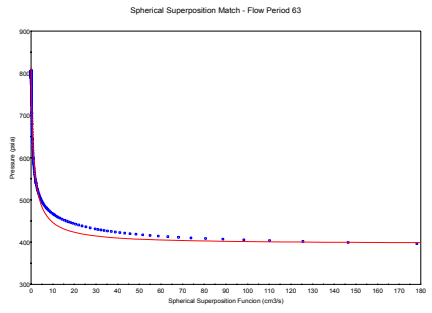
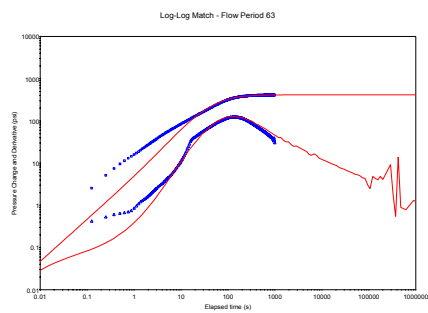
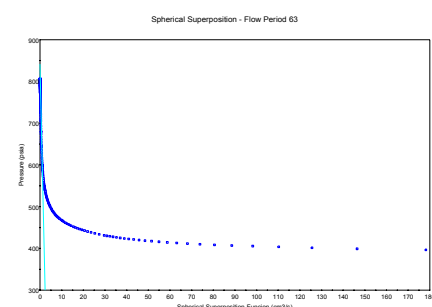
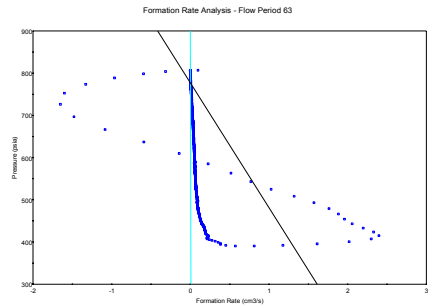
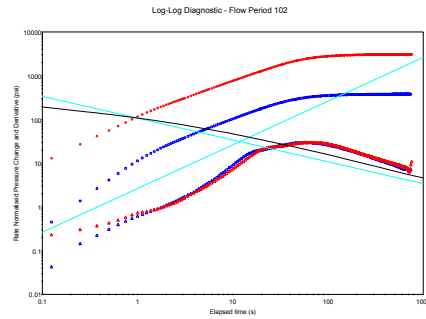
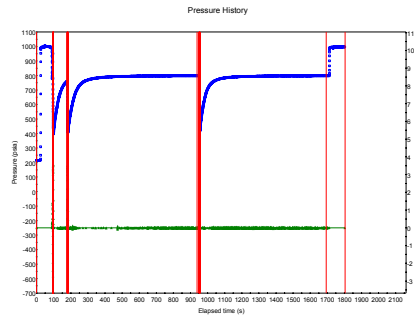


**Figure 28 File no. q800a09: Depth 563.2 m-MD**



**Model**  
Wireline Formation Test (WFT)  
Homogeneous  
Infinite Lateral Extent

**Results**

(pav) <sub>i</sub>	800.315	psia
pwf	417.482	psia
k/u(xyz)	0.1231	mD/cp
k(xyz)	0.1231	mD
c(sys)	6.9754E-005	1/psi
S(p)	-0.83	
C	1.5356E-007	bb/psi
ri	3	ft
p*(FRA)	783.395	psia
k/u(FRA)	7.923	mD/cp
c(FRA)	6.433E-005	1/psi

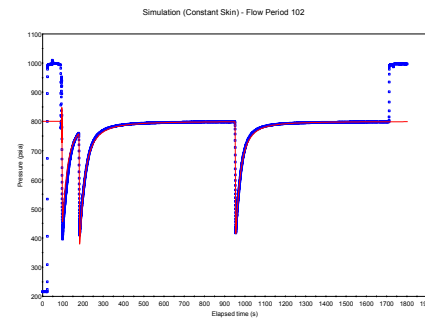
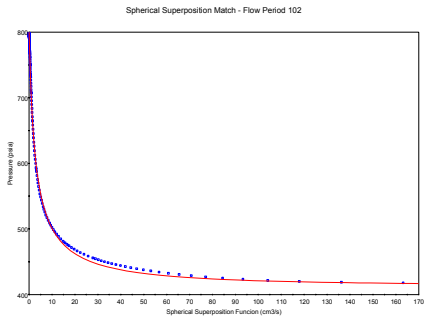
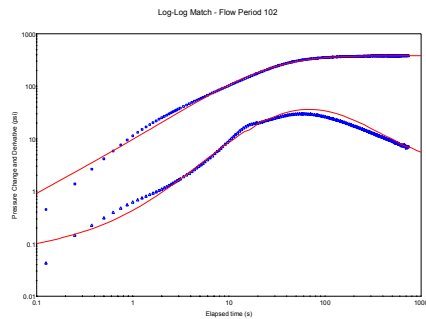
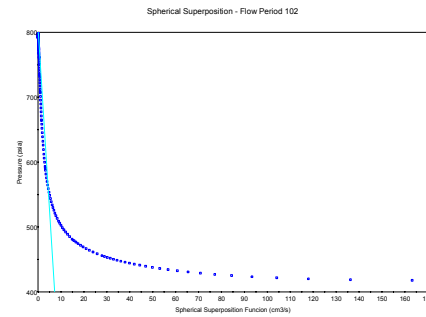
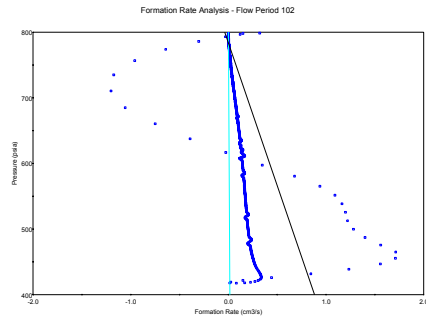
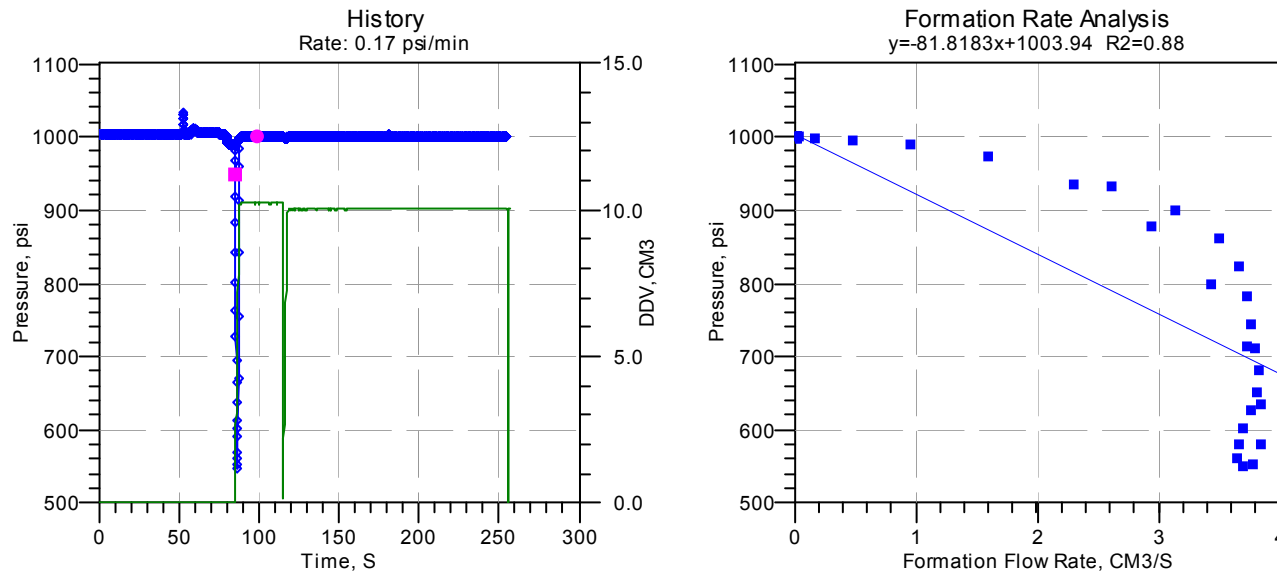


**Figure 29 File no. g800a10 0: Depth 565.7 m-MD**

Company: BASS STRAIT OIL COMPANY LTD  
Field: EXPLORATION  
Well: MOBY-1

### Wireline Formation Test Analyzer (WFTA<sup>SM</sup>)



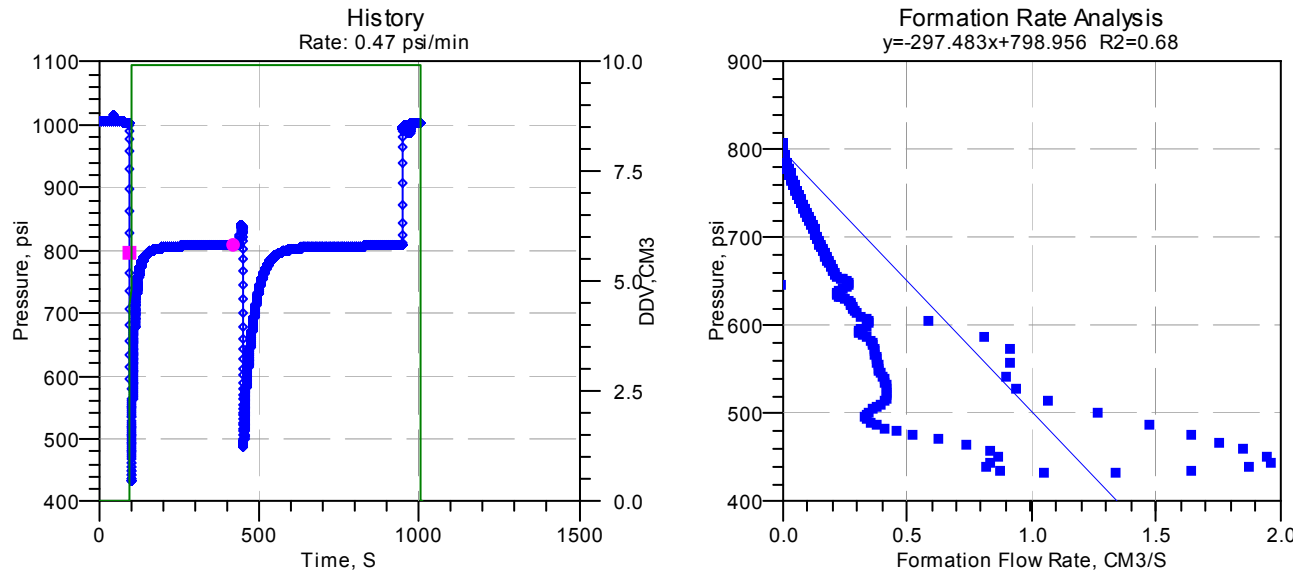
### Pressure Test Results-No Seal

File	Depth		Flow Rate Analysis			Maximum	Final	
Number	Measured	TVD	Ct	P*	Mobility	Rate	Buildup	
i800a	(ft)	(ft)		(psi)	(mD/cP)	(mD/cP)	(psi)	
	10	565.7	565.7	-4.4e-6	1003.9	30.3	21.0	1001.2

**Figure 30 File no. g800a11 0: Depth 565.4 m-MD**

Company: BASS STRAIT OIL COMPANY LTD  
Field: EXPLORATION  
Well: MOBY-1

### Wireline Formation Test Analyzer (WFTA<sup>SM</sup>)



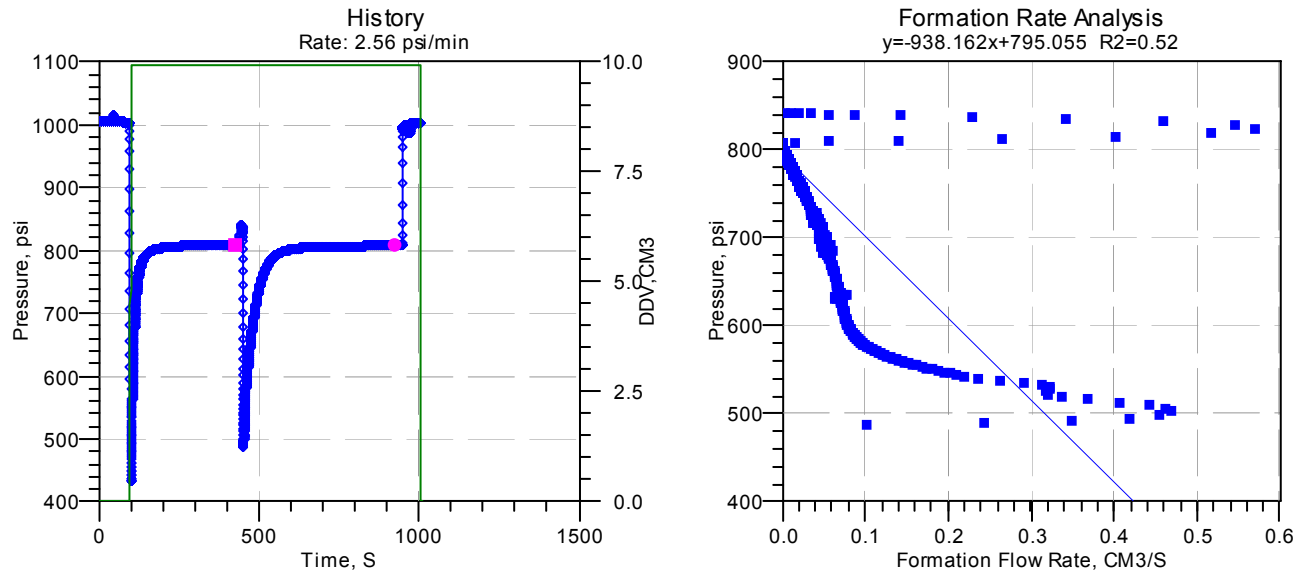
### Pressure Test Results-NOT FRA Compliant

File	Depth		Flow Rate Analysis			Maximum	Final	
	Number	Measured	TVD	Ct	P*	Rate	Buildup	
i800a	(ft)	(ft)		(psi)	(mD/cP)	(mD/cP)	(psi)	
11	565.4	565.4		4.3e-5	799.0	8.3	13.0	808.9

**Figure 31 File no. g800a11 1: Depth 565.4 m-MD**

Company: BASS STRAIT OIL COMPANY LTD  
Field: EXPLORATION  
Well: MOBY-1

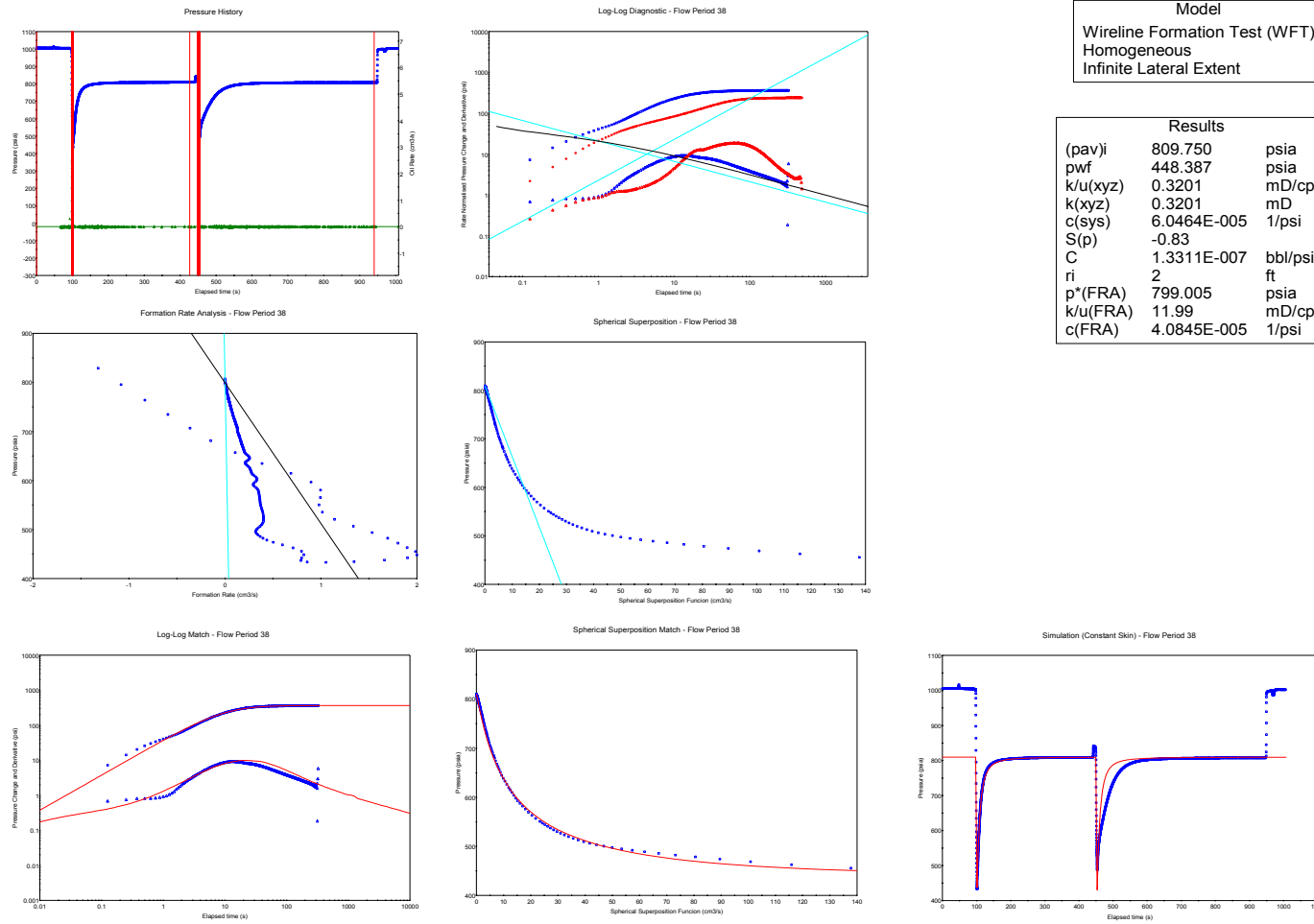
### Wireline Formation Test Analyzer (WFTA<sup>SM</sup>)



### Pressure Test Results-NOT FRA Compliant

File Number	Depth		Flow Rate Analysis			Maximum Rate	Final Buildup	
	Measured (ft)	TVD (ft)	Ct	P* (psi)	Mobility (mD/cP)	(mD/cP)	(psi)	
i800a	11	565.4	565.4	$4.3e-5$	795.1	2.6	3.8	807.7

**Figure 32 File no. q800a11: Depth 565.4 m-MD**



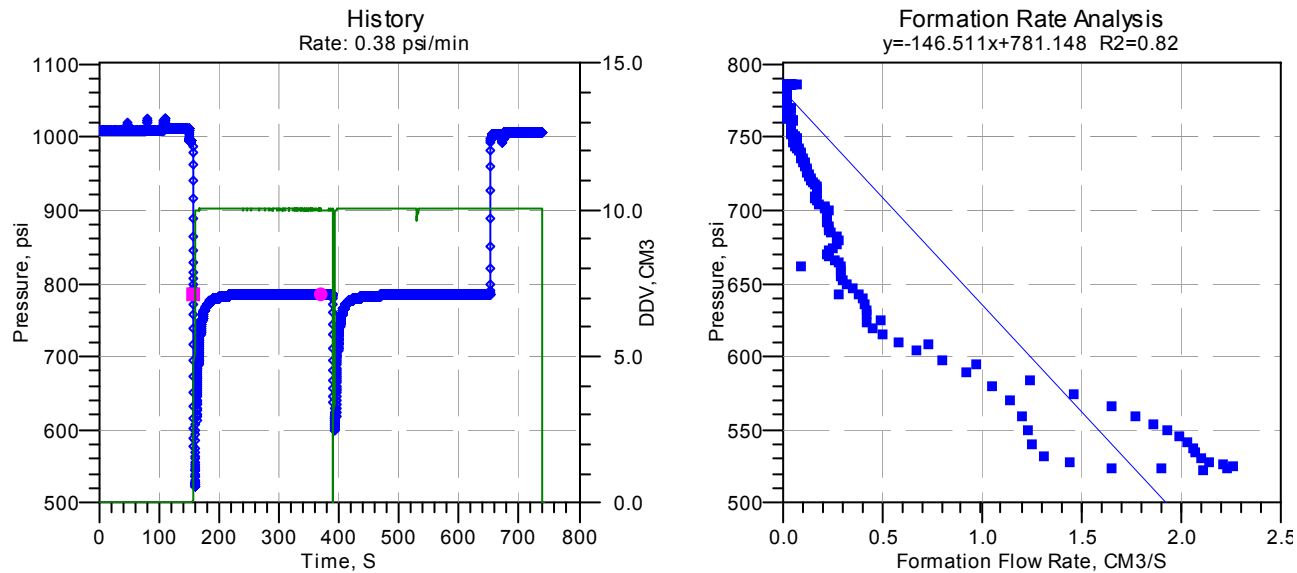
Model	
Wireline Formation Test (WFT)	
Homogeneous	
Infinite Lateral Extent	

Results		
(pav) <sub>i</sub>	809.750	psia
pwf	448.387	psia
k/u(xyz)	0.3201	mD/cp
k(xyz)	0.3201	mD
c(sys)	6.0464E-005	1/psi
S(p)	-0.83	
C	1.3311E-007	bbl/psi
ri	2	ft
p*(FRA)	799.005	psia
k/u(FRA)	11.99	mD/cp
c(FRA)	4.0845E-005	1/psi

**Figure 33 File no. g800a12 0: Depth 568.2 m-MD**

Company: BASS STRAIT OIL COMPANY LTD  
Field: EXPLORATION  
Well: MOBY-1

### Wireline Formation Test Analyzer (WFTA<sup>SM</sup>)



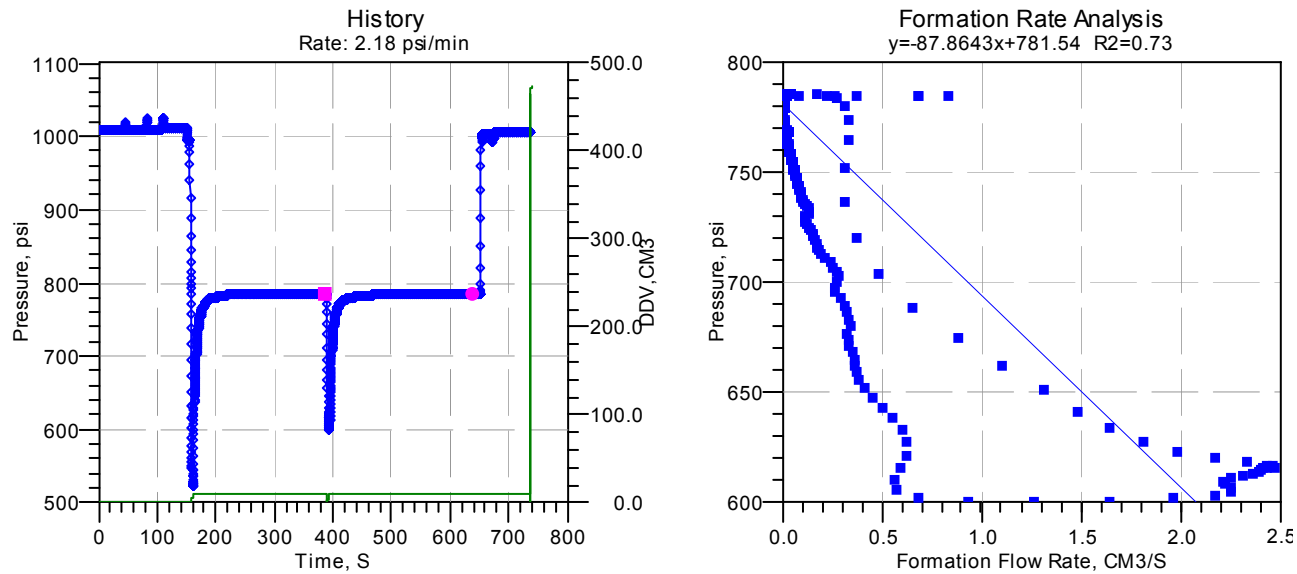
### Pressure Test Results-NOT FRA Compliant

File	Depth		Flow Rate Analysis			Maximum	Final
	Number	Measured	TVD	Ct	P*	Rate	Buildup
i800a	(ft)	(ft)	(ft)		(psi)	(mD/cP)	(psi)
12	568.2	568.2		$3.9 \times 10^{-5}$	781.1	16.9	21.3
							786.3

**Figure 34 File no. g800a12 1: Depth 568.2 m-MD**

Company: BASS STRAIT OIL COMPANY LTD  
Field: EXPLORATION  
Well: MOBY-1

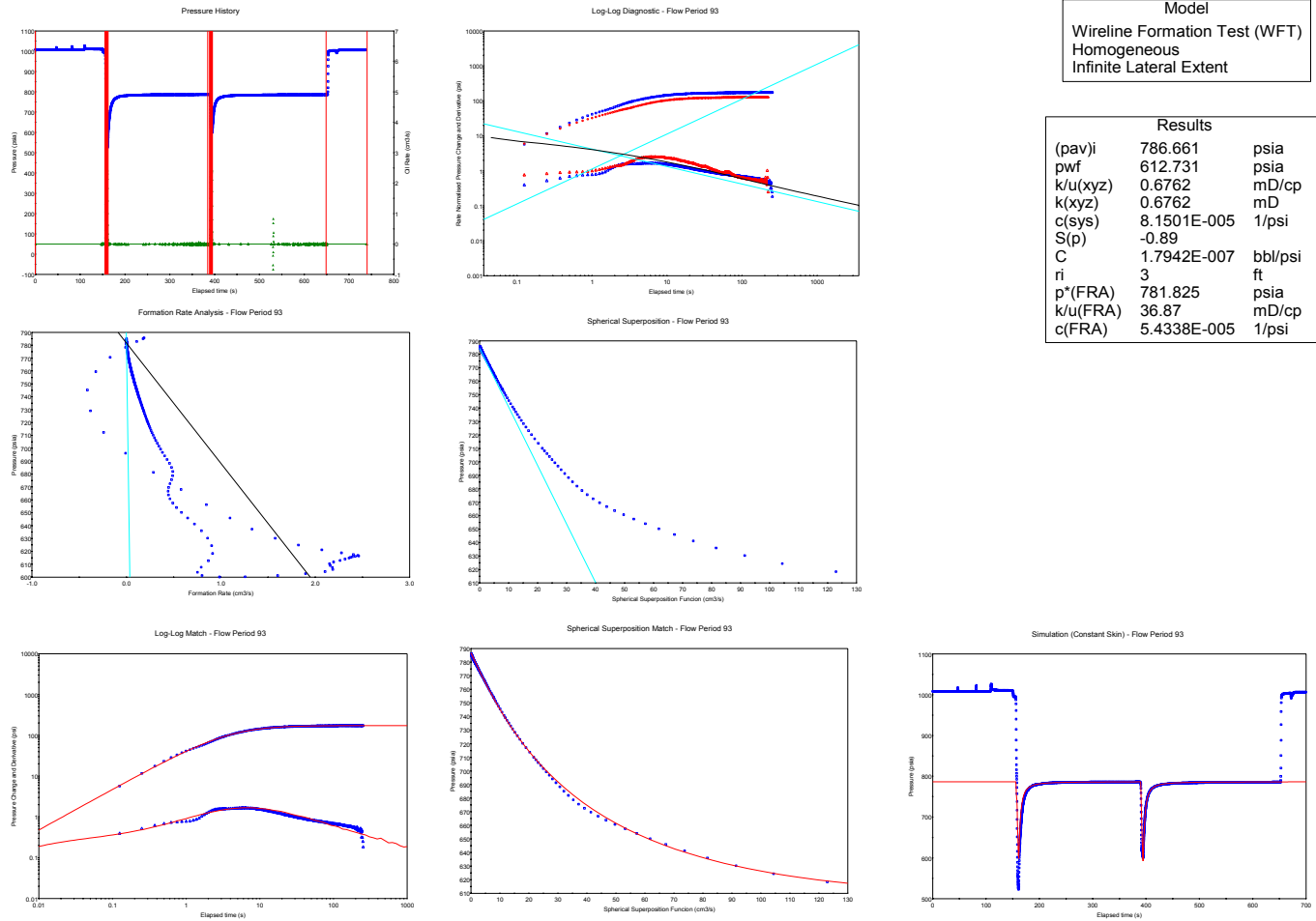
### Wireline Formation Test Analyzer (WFTA<sup>SM</sup>)



### Pressure Test Results-NOT FRA Compliant

File	Depth		Flow Rate Analysis			Maximum	Final	
Number	Measured	TVD	Ct	P*	Mobility	Rate	Buildup	
i800a	(ft)	(ft)		(psi)	(mD/cP)	(mD/cP)	(psi)	
	12	568.2	568.2	3.9e-5	781.5	28.2	23.3	785.8

**Figure 35 File no. q800a12: Depth 568.2 m-MD**



**Model**  
Wireline Formation Test (WFT)  
Homogeneous  
Infinite Lateral Extent

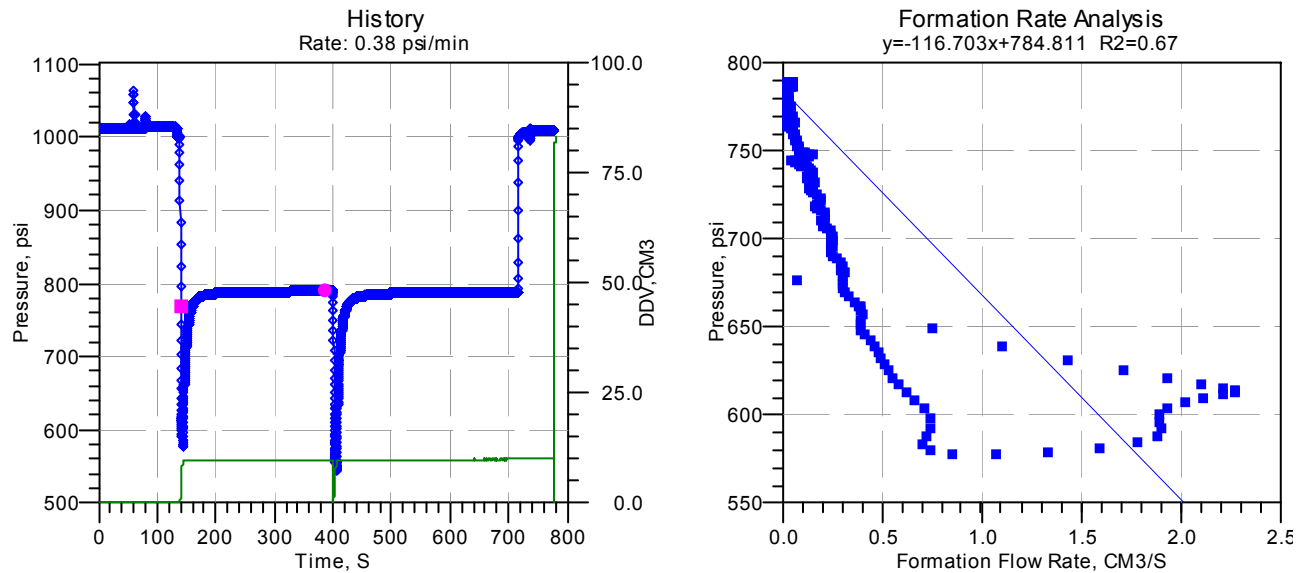
**Results**

(pav)i	786.661	psia
pwf	612.731	psia
k/u(xyz)	0.6762	mD/cp
k(yxz)	0.6762	mD
c(sys)	8.1501E-005	1/psi
S(p)	-0.89	
C	1.7942E-007	bb/psi
ri	3	ft
p*(FRA)	781.825	psia
k/u(FRA)	36.87	mD/cp
c(FRA)	5.4338E-005	1/psi

**Figure 36 File no. g800a13 0: Depth 569 m-MD**

Company: BASS STRAIT OIL COMPANY LTD  
Field: EXPLORATION  
Well: MOBY-1

### Wireline Formation Test Analyzer (WFTA<sup>SM</sup>)



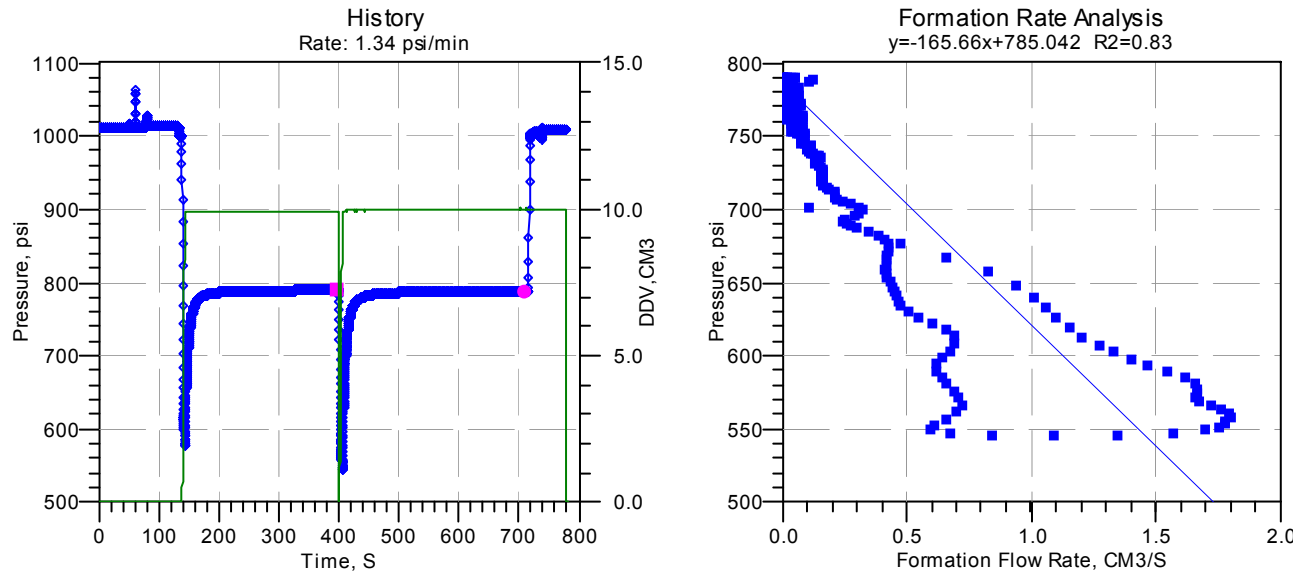
### Pressure Test Results-NOT FRA Compliant

File	Depth		Flow Rate Analysis			Maximum	Final	
Number	Measured	TVD	Ct	P*	Mobility	Rate	Buildup	
i800a	(ft)	(ft)		(psi)	(mD/cP)	(mD/cP)	(psi)	
	13	569	569	5.1e-5	784.8	21.2	26.6	789.4

**Figure 37 File no. g800a13 1: Depth 569 m-MD**

Company: BASS STRAIT OIL COMPANY LTD  
Field: EXPLORATION  
Well: MOBY-1

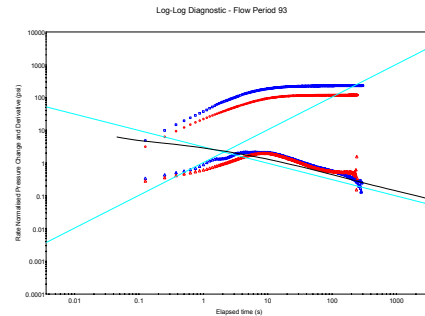
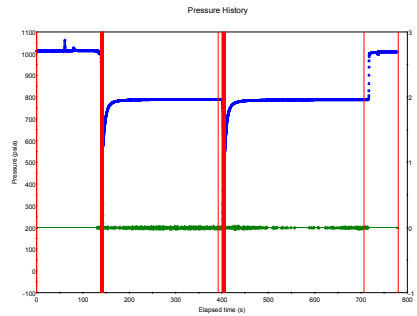
### Wireline Formation Test Analyzer (WFTA<sup>SM</sup>)



### Pressure Test Results-NOT FRA Compliant

File	Depth		Flow Rate Analysis			Maximum	Final
Number	Measured	TVD	Ct	P*	Mobility	Rate	Buildup
i800a	(ft)	(ft)		(psi)	(mD/cP)	(mD/cP)	(psi)
13	569	569	5.1e-5	785.0	15.0	21.2	788.0

**Figure 38 File no. g800a13: Depth 569 m-MD**



**Model**  
Wireline Formation Test (WFT)  
Homogeneous  
Infinite Lateral Extent

**Results**

(pav) <sub>i</sub>	789.717	psia
pwf	559.210	psia
k/u(xyz)	0.6829	mD/cp
k(xyz)	0.6829	mD
c(sys)	6.6114E-005	1/psi
S(p)	-0.84	
C	1.4555E-007	bbbl/psi
ri	4	ft
p*(FRA)	784.523	psia
k/u(FRA)	20.26	mD/cp
c(FRA)	5.9524E-005	1/psi

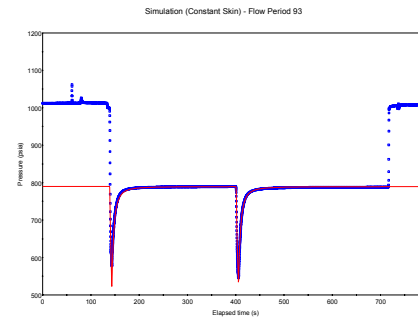
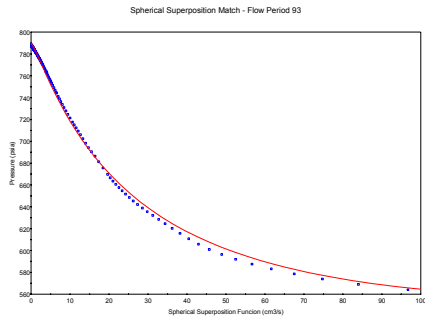
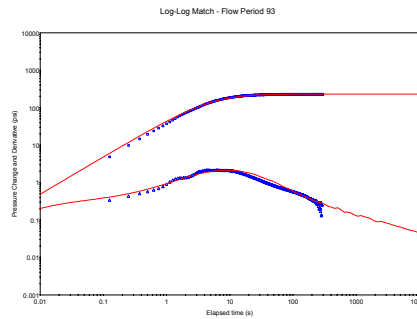
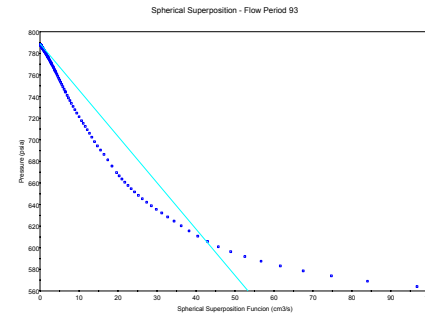
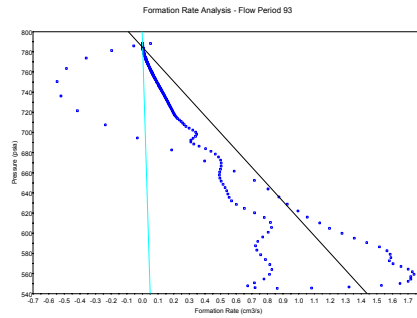
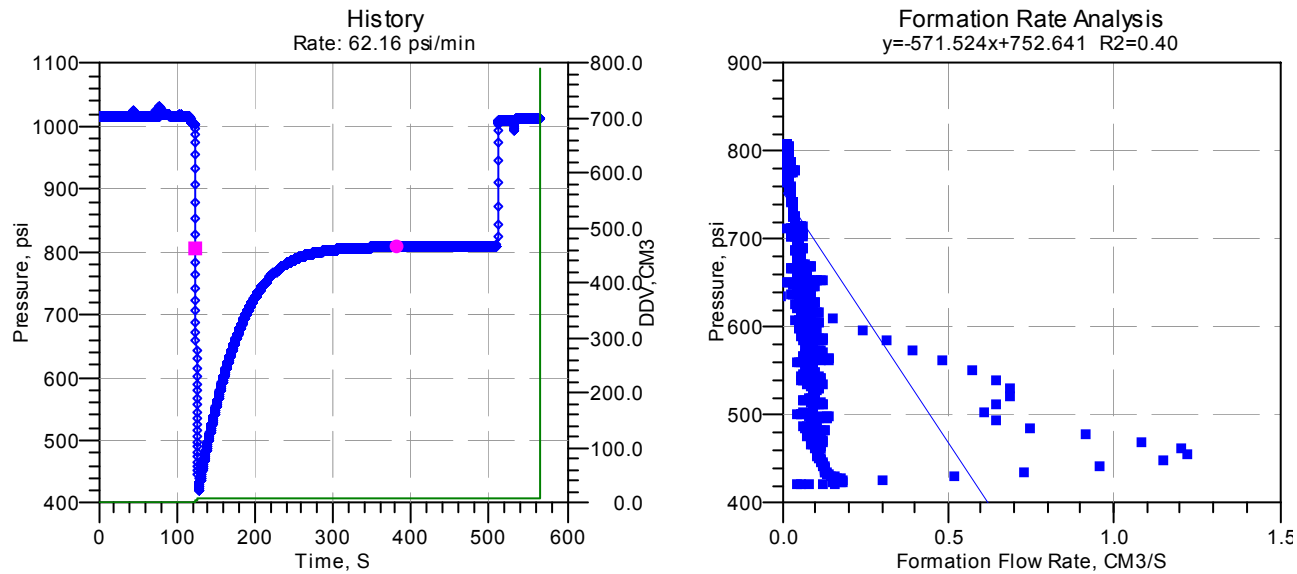


**Figure 39 File no. g800a14 0: Depth 571.2 m-MD**

Company: BASS STRAIT OIL COMPANY LTD  
Field: EXPLORATION  
Well: MOBY-1

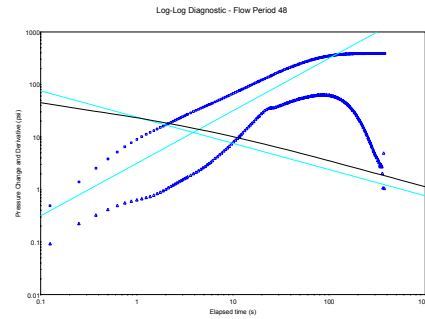
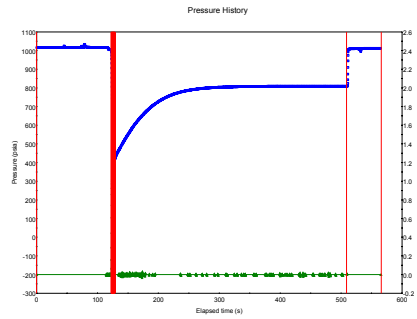
### Wireline Formation Test Analyzer (WFTA<sup>SM</sup>)



### Pressure Test Results-NOT FRA Compliant

File	Depth		Flow Rate Analysis			Maximum	Final
Number	Measured	TVD	Ct	P*	Mobility	Rate	Buildup
i800a	(ft)	(ft)		(psi)	(mD/cP)	(mD/cP)	(psi)
	14	571.2	571.2	5.0e-5	752.6	4.3	7.8 808.9

**Figure 40 File no. q800a14: Depth 571.2 m-MD**



**Model**  
Wireline Formation Test (WFT)  
Homogeneous  
Infinite Lateral Extent

**Results**

(pav) <sub>i</sub>	810.336	psia
pwf	420.397	psia
k/u(xyz)	0.3936	mD/cp
k(xyz)	0.3936	mD
c(sys)	6.5142E-005	1/psi
S(p)	-0.29	
C	1.4341E-007	bb/psi
ri	3	ft
p*(FRA)	771.799	psia
k/u(FRA)	5.768	mD/cp
c(FRA)	4.724E-005	1/psi

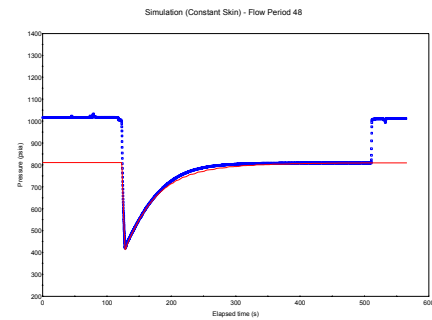
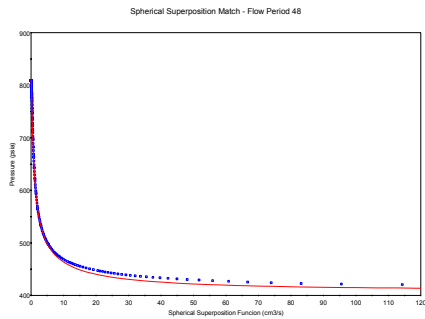
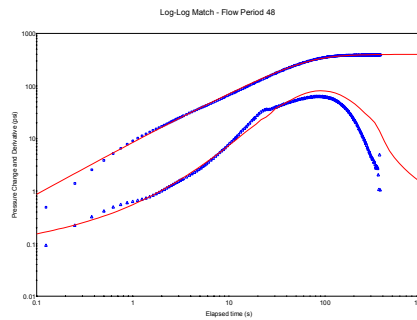
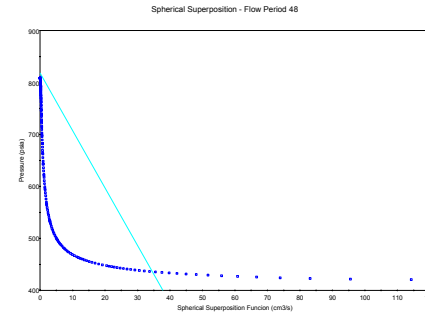
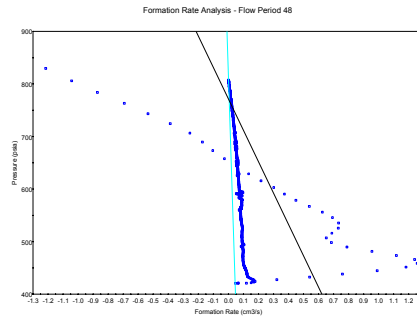
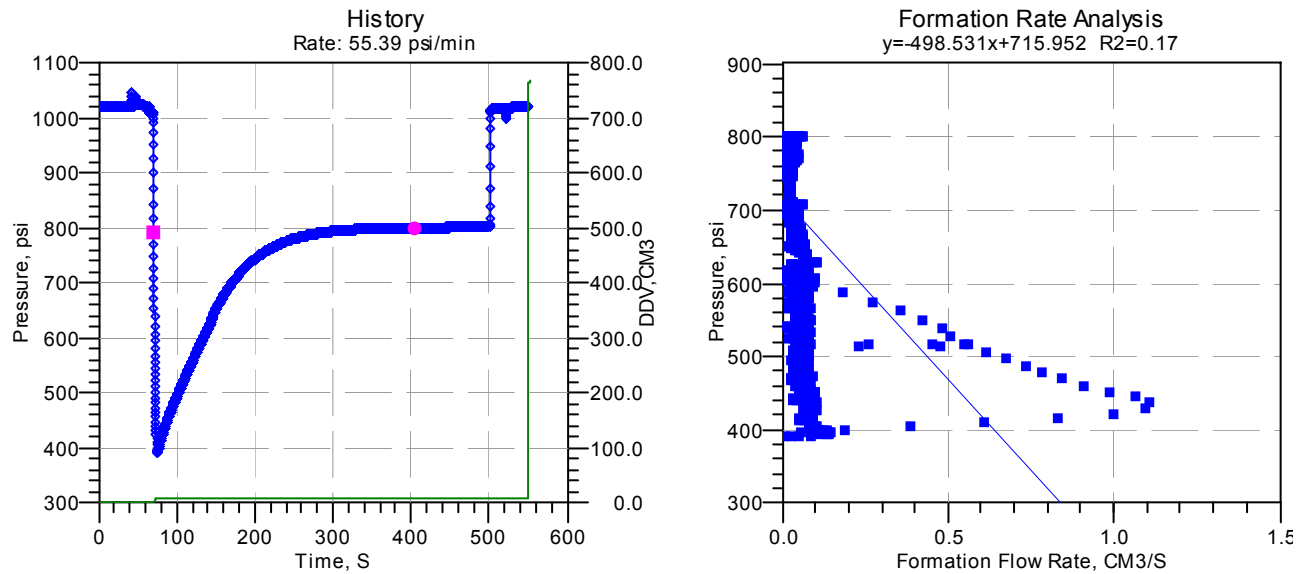


**Figure 41 File no. g800a15 0: Depth 575.7 m-MD**

Company: BASS STRAIT OIL COMPANY LTD  
Field: EXPLORATION  
Well: MOBY-1

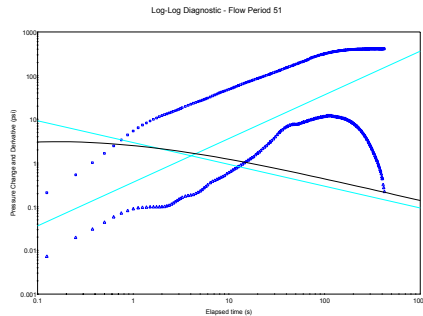
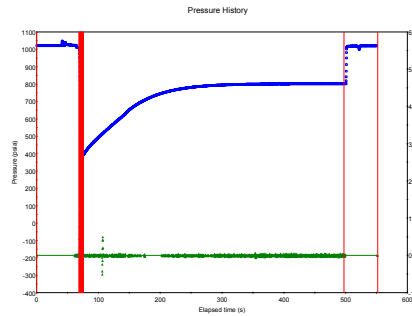
### Wireline Formation Test Analyzer (WFTA<sup>SM</sup>)



### Pressure Test Results-NOT FRA Compliant

File	Depth		Flow Rate Analysis			Maximum	Final
Number	Measured	TVD	Ct	P*	Mobility	Rate	Buildup
i800a	(ft)	(ft)		(psi)	(mD/cP)	(mD/cP)	(psi)
	15	575.7	575.7	5.0e-5	716.0	5.0	6.7 1020.0

**Figure 42 File no. g800a15 0: Depth 575.7 m-MD**



Model  
Wireline Formation Test (WFT)  
Homogeneous  
Infinite Lateral Extent

Results		
(pav) <sub>i</sub>	806.131	psia
pwf	391.852	psia
k/u(xyz)	0.3494	mD/cp
k(xyz)	0.3494	mD
c(sys)	6.2752E-005	1/psi
S(p)	0.02	
C	1.3815E-007	bbbl/psi
ri	3	ft
p*(FRA)	744.435	psia
k/u(FRA)	5.943	mD/cp
c(FRA)	4.6682E-005	1/psi

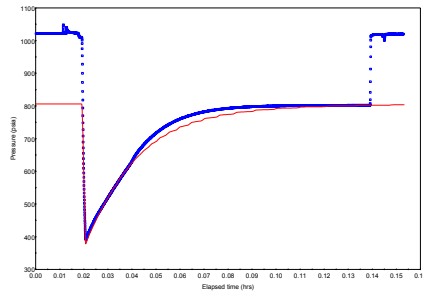
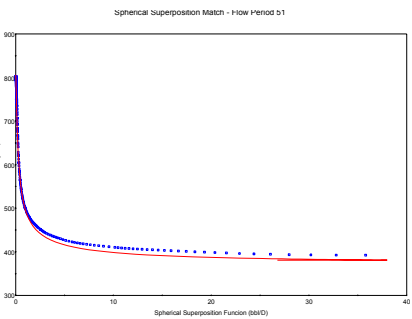
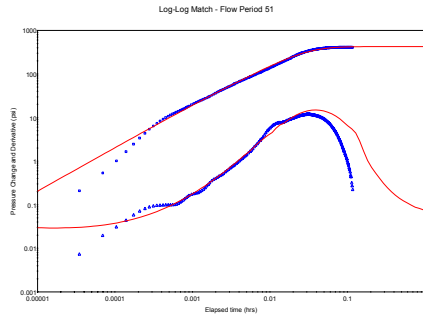
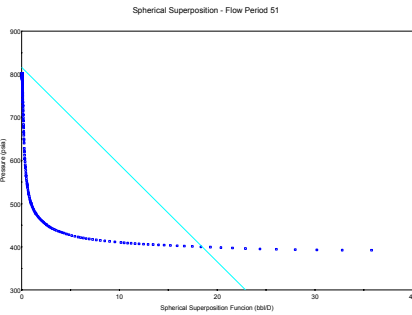
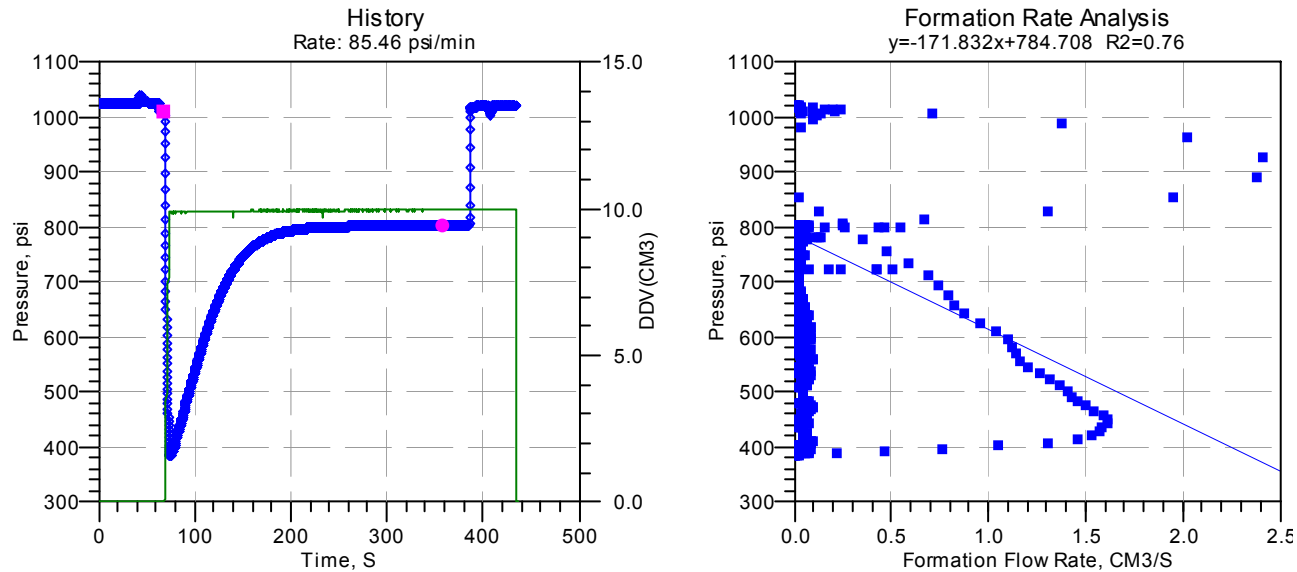


**Figure 43 File no. g800a16 0: Depth 577.1 m-MD**

Company: BASS STRAIT OIL COMPANY LTD  
Field: EXPLORATION  
Well: MOBY-1

### Wireline Formation Test Analyzer (WFTA<sup>SM</sup>)



### Pressure Test Results-NOT FRA Compliant

File	Depth		Flow Rate Analysis			Maximum	Final	
Number	Measured	TVD	Ct	P*	Mobility	Rate	Buildup	
i800a	(ft)	(ft)		(psi)	(mD/cP)	(mD/cP)	(psi)	
	16	577.1	577.1	2.3e-5	784.7	14.4	9.4	1022.5

**Figure 44 File no. g800a16 0: Depth 577.1 m-MD**

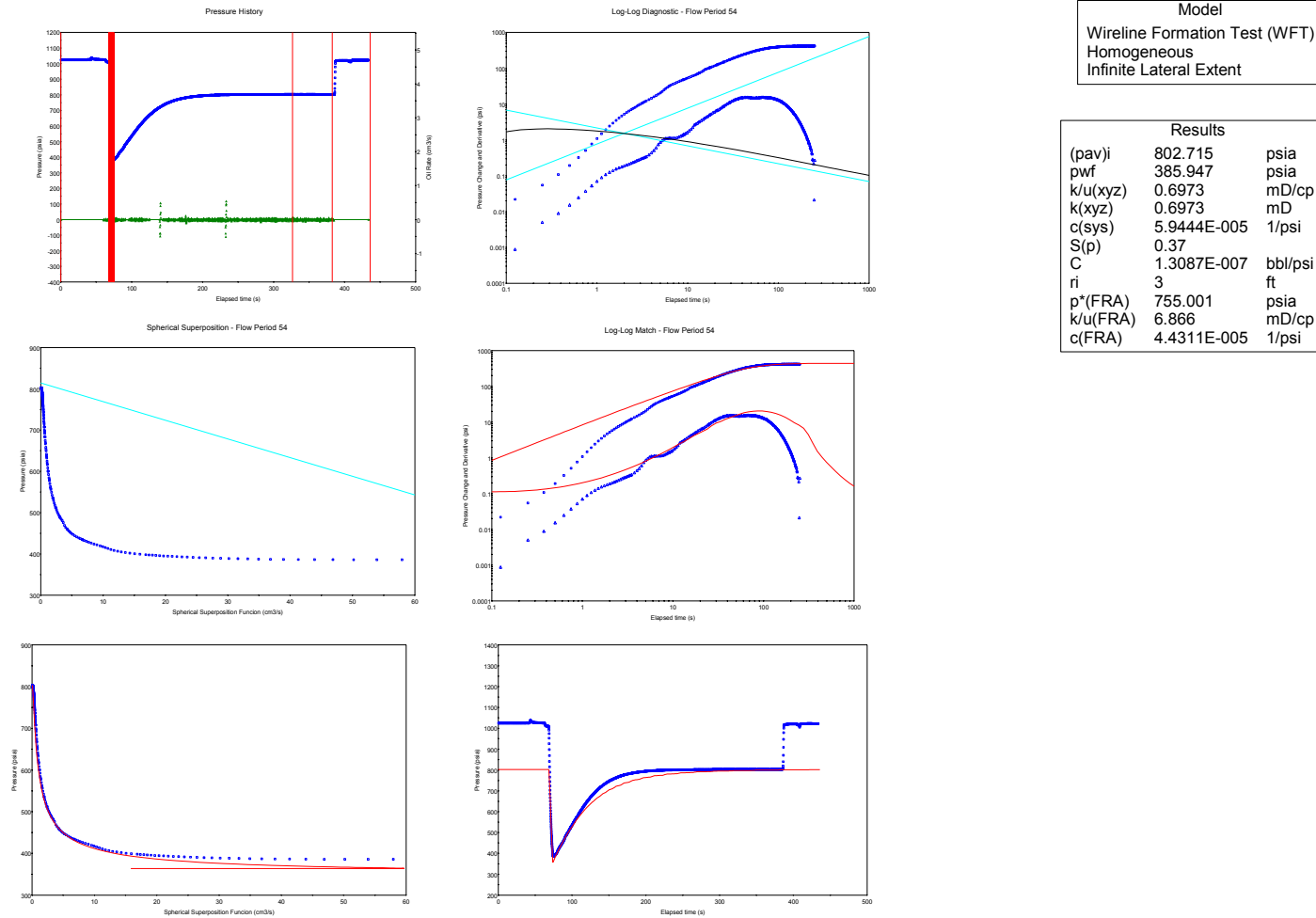
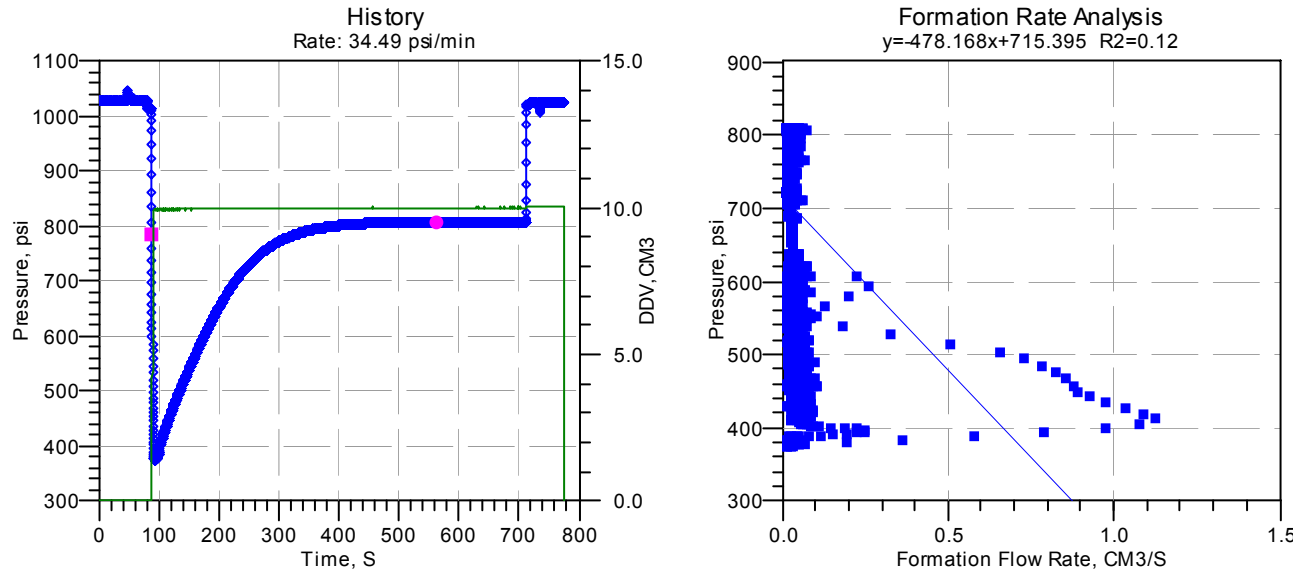


**Figure 45 File no. q800a17 0: Depth 578.7 ft-MD**

Company: BASS STRAIT OIL COMPANY LTD  
Field: EXPLORATION  
Well: MOBY-1

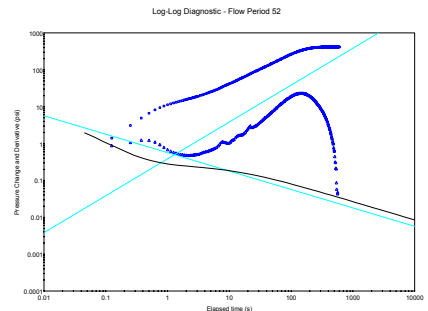
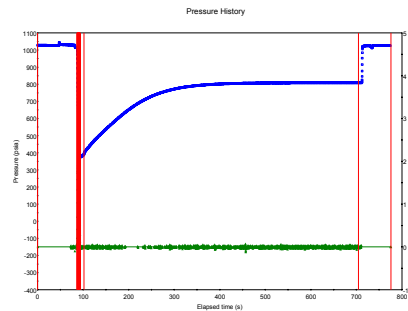
### Wireline Formation Test Analyzer (WFTA<sup>SM</sup>)



### Pressure Test Results-NOT FRA Compliant

File	Depth		Flow Rate Analysis			Maximum	Final
Number	Measured	TVD	Ct	P*	Mobility	Rate	Buildup
i800a	(ft)	(ft)		(psi)	(mD/cP)	(mD/cP)	(psi)
17	578.7	578.7	4.8e-5	715.4	5.2	6.4	1025.7

**Figure 46 File no. q800a17 0: Depth 578.7 ft-MD**



**Model**  
Wireline Formation Test (WFT)  
Homogeneous  
Infinite Lateral Extent

**Results**

(pav) <sub>i</sub>	810.330	psia
pwf	390.887	psia
k/u(xyz)	0.9855	mD/cp
k(xyz)	0.9855	mD
c(sys)	5.9454E-005	1/psi
S(p)	2.85	
C	1.3089E-007	bbl/psi
ri	7	ft
p*(FRA)	747.890	psia
k/u(FRA)	5.631	mD/cp
c(FRA)	4.5443E-005	1/psi

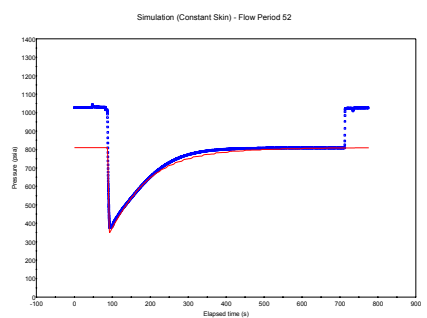
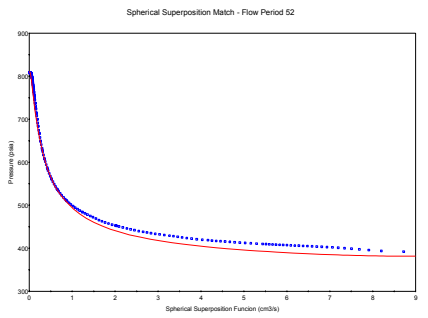
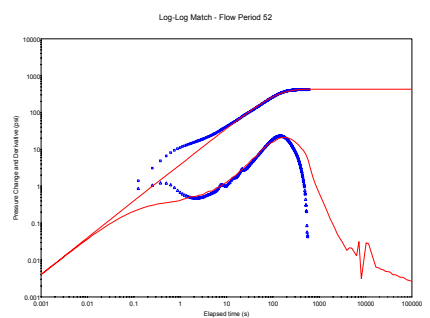
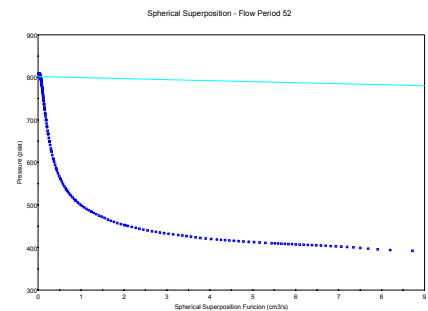
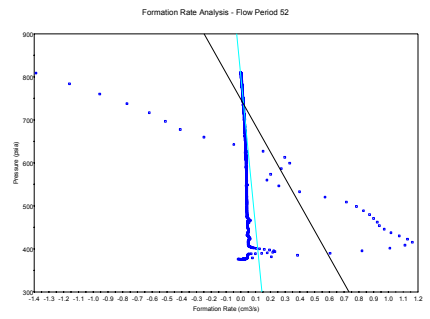
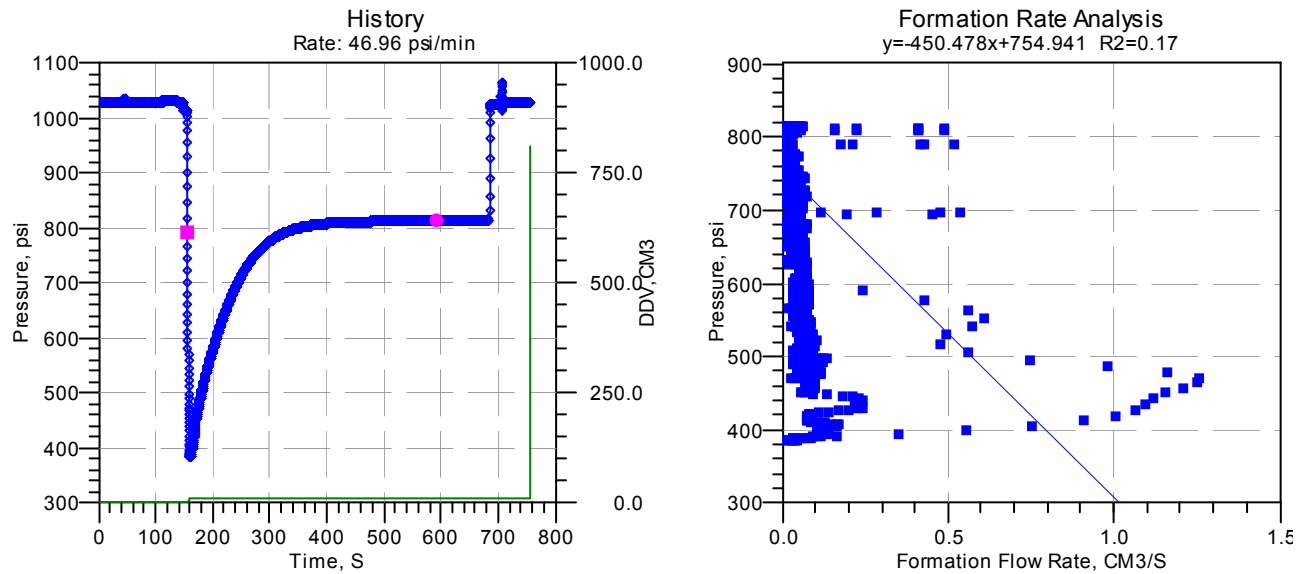


**Figure 47 File no. g800a18 0: Depth 579.9 m-MD**

Company: BASS STRAIT OIL COMPANY LTD  
Field: EXPLORATION  
Well: MOBY-1

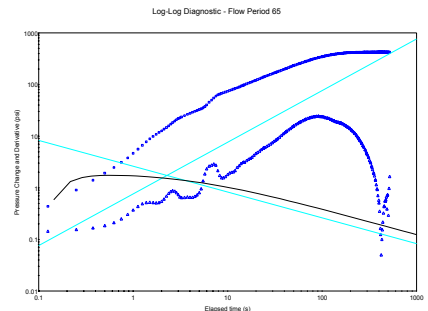
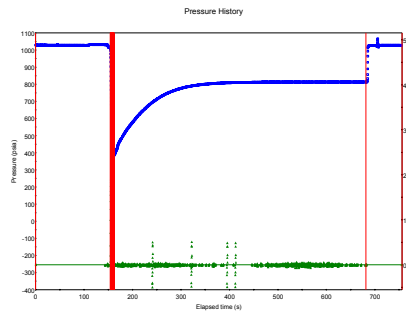
### Wireline Formation Test Analyzer (WFTA<sup>SM</sup>)



### Pressure Test Results-NOT FRA Compliant

File	Depth		Flow Rate Analysis			Maximum	Final
Number	Measured	TVD	Ct	P*	Mobility	Rate	Buildup
i800a	(ft)	(ft)		(psi)	(mD/cP)	(mD/cP)	(psi)
18	579.9	579.9	4.6e-5	754.9	5.5	7.3	1027.6

**Figure 48 File no. g800a18 0: Depth 579.9 m-MD**



**Model**  
Wireline Formation Test (WFT)  
Homogeneous  
Infinite Lateral Extent

**Results**

(pav) <sub>i</sub>	813.830	psia
pwf	387.629	psia
k/u(xyz)	0.5977	mD/cp
k(xyz)	0.5977	mD
c(sys)	5.9846E-005	1/psi
S(p)	0.38	
C	1.3175E-007	bb/psi
ri	4	ft
p*(FRA)	810.763	psia
k/u(FRA)	0.5624	mD/cp
c(FRA)	2.6005E-005	1/psi

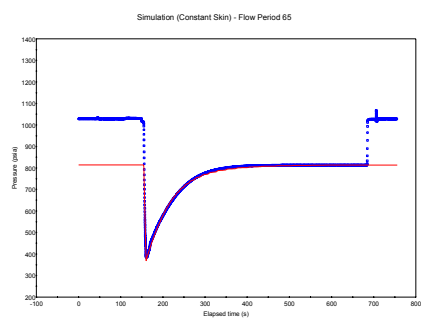
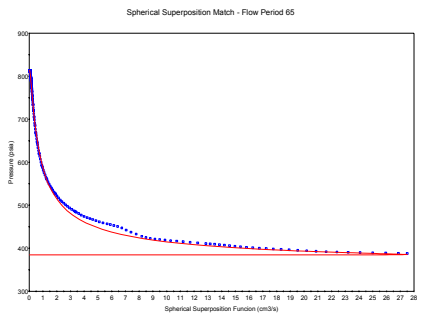
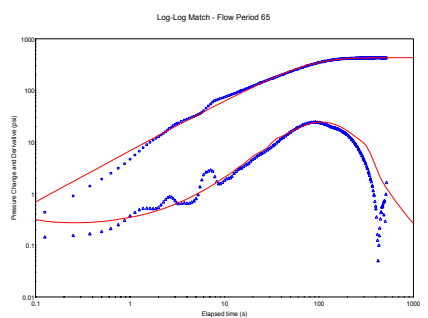
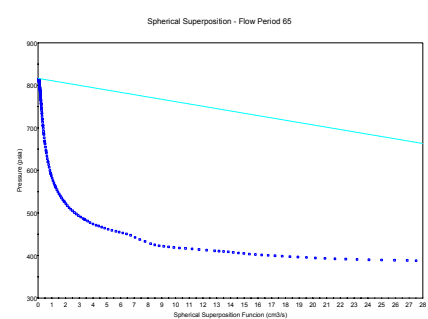
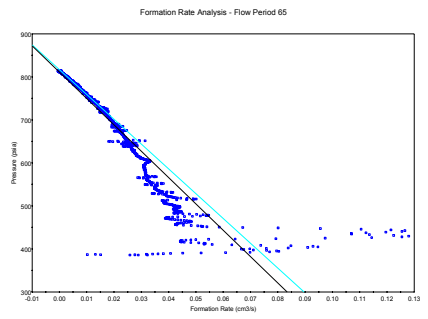
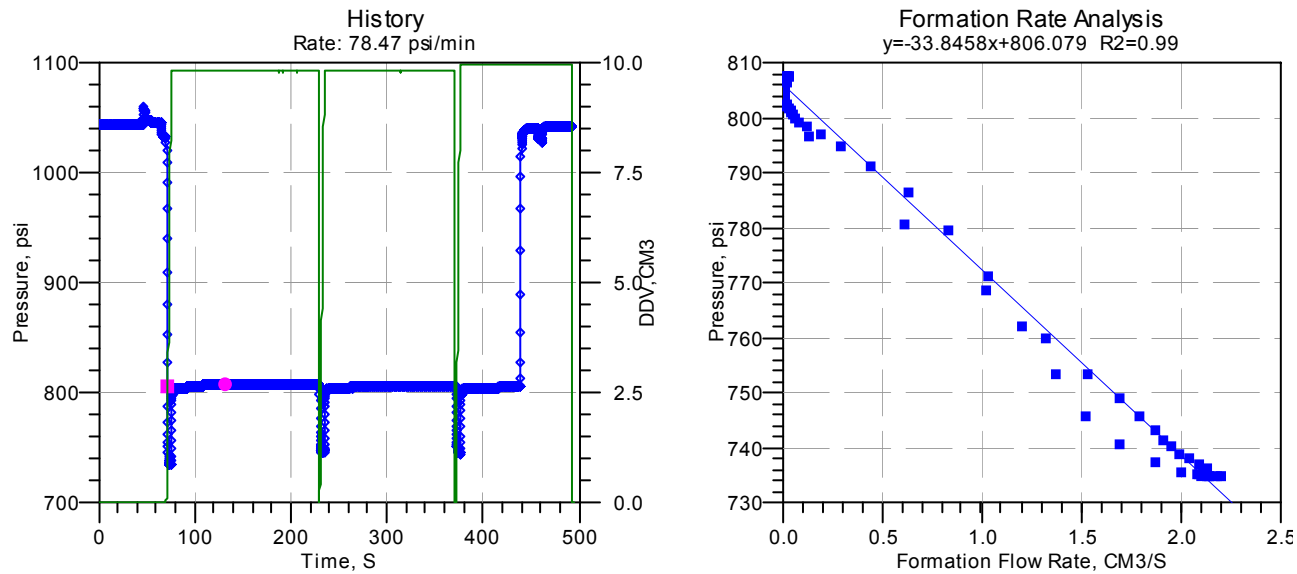


**Figure 49 File no. g800a19 0: Depth 587.9 m-MD**

Company: BASS STRAIT OIL COMPANY LTD  
Field: EXPLORATION  
Well: MOBY-1

## Wireline Formation Test Analyzer (WFTA<sup>SM</sup>)



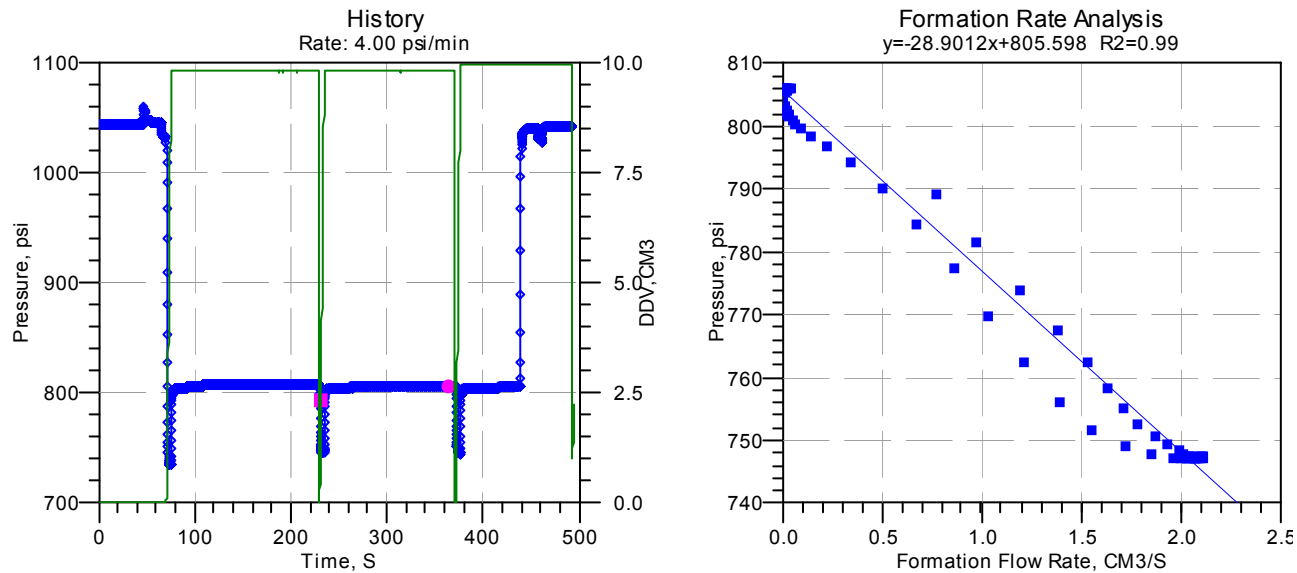
### Pressure Test Results-FRA Compliant

File	Depth		Flow Rate Analysis			Maximum	Final
Number	Measured	TVD	Ct	P*	Mobility	Rate	Buildup
i800a	(ft)	(ft)		(psi)	(mD/cP)	(mD/cP)	(psi)
19	587.9	587.9	3.8e-5	806.1	73.2	75.1	808.5

**Figure 50 File no. g800a19 1: Depth 587.9 m-MD**

Company: BASS STRAIT OIL COMPANY LTD  
Field: EXPLORATION  
Well: MOBY-1

### Wireline Formation Test Analyzer (WFTA<sup>SM</sup>)



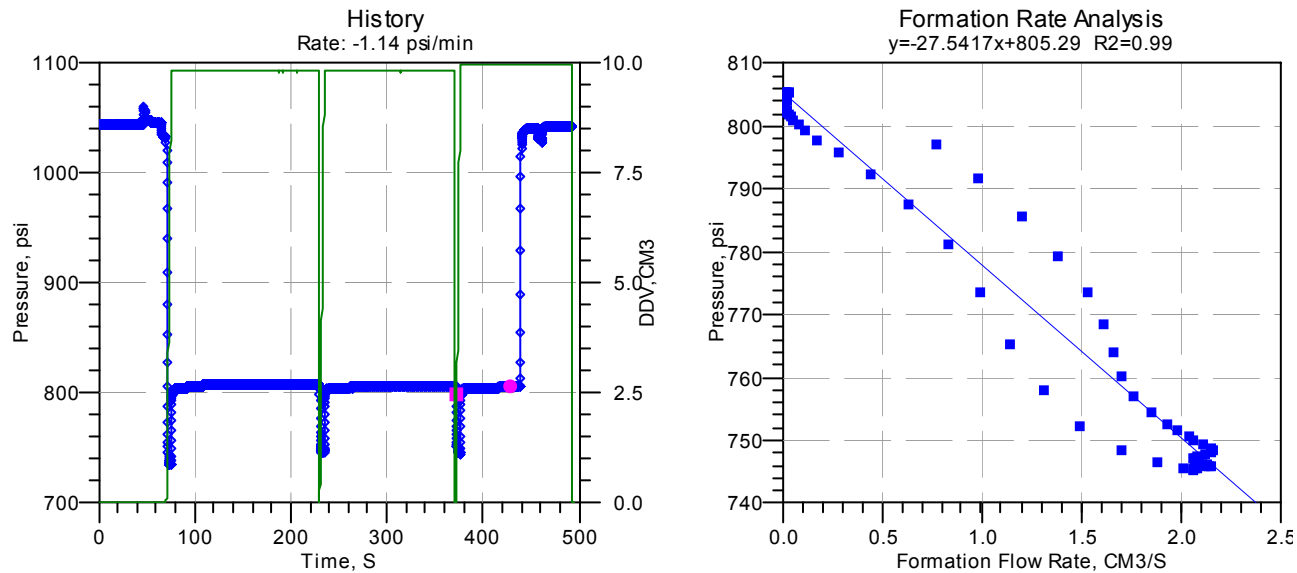
### Pressure Test Results-FRA Compliant

File	Depth		Flow Rate Analysis			Maximum	Final	
Number	Measured	TVD	Ct	P*	Mobility	Rate	Buildup	
i800a	(ft)	(ft)		(psi)	(mD/cP)	(mD/cP)	(psi)	
	19	587.9	587.9	3.8e-5	805.6	85.8	74.0	805.9

**Figure 51 File no. g800a19 2: Depth 587.9 m-MD**

Company: BASS STRAIT OIL COMPANY LTD  
Field: EXPLORATION  
Well: MOBY-1

### Wireline Formation Test Analyzer (WFTA<sup>SM</sup>)



### Pressure Test Results-FRA Compliant

File	Depth		Flow Rate Analysis			Maximum	Final
Number	Measured	TVD	Ct	P*	Mobility	Rate	Buildup
i800a	(ft)	(ft)		(psi)	(mD/cP)	(mD/cP)	(psi)
19	587.9	587.9	3.8e-5	805.3	90.0	76.1	805.5

**Figure 52 File no. q800a19: Depth 587.9 m-MD**

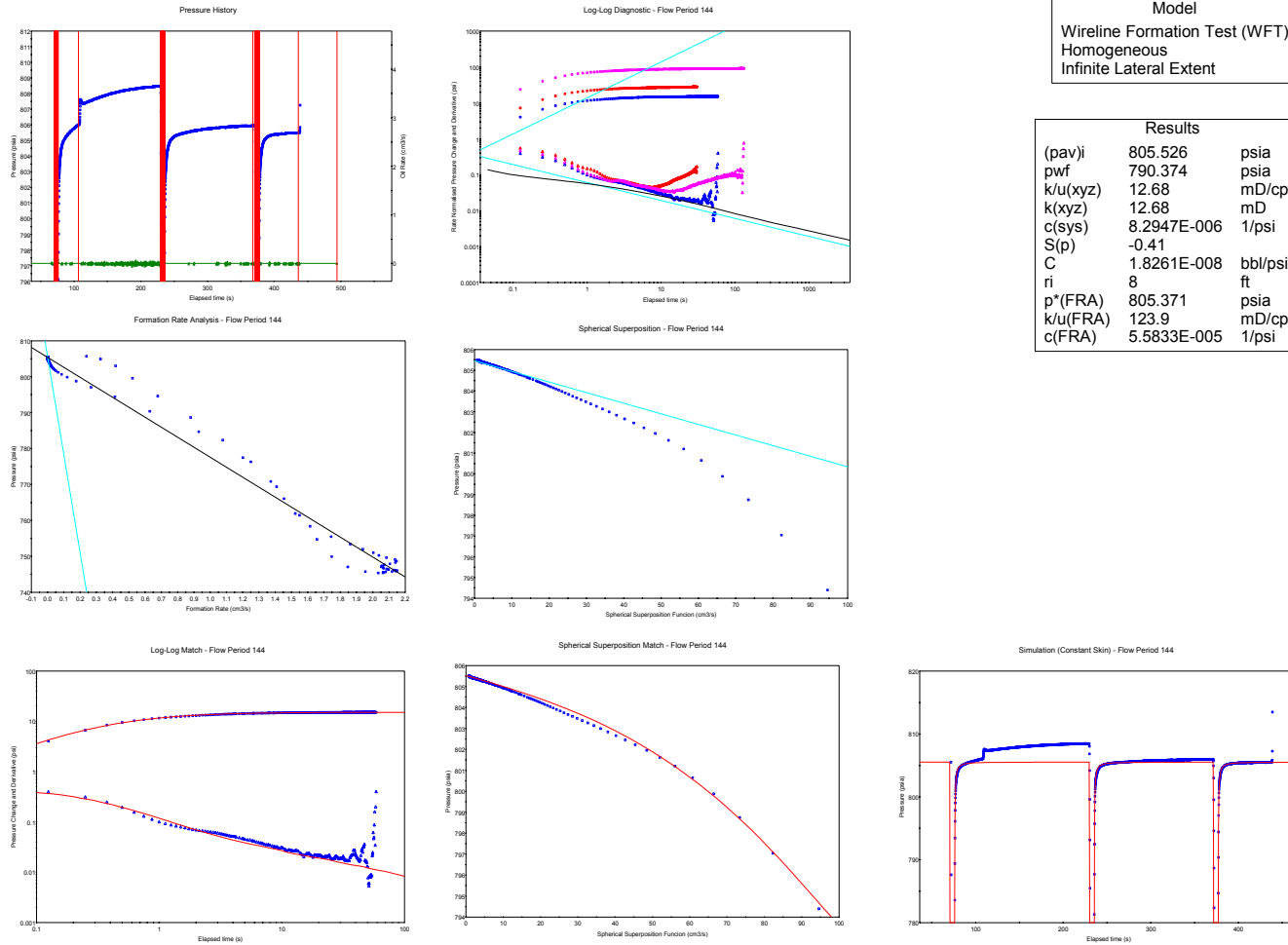
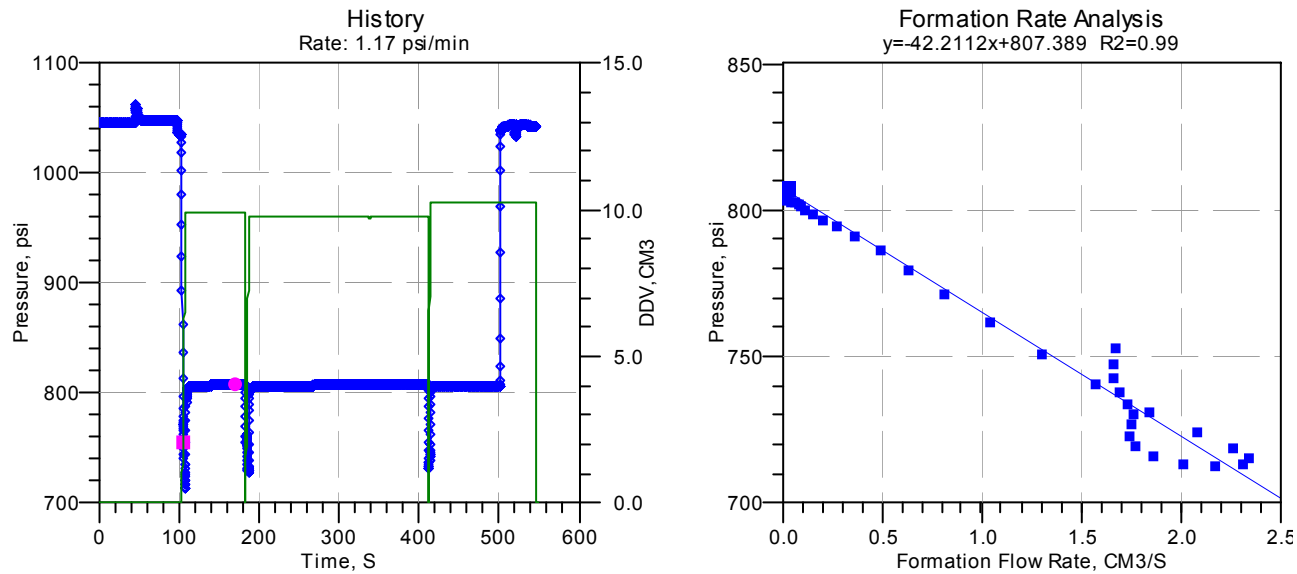


**Figure 53 File no. g800a20 0: Depth 588.9 m-MD**

Company: BASS STRAIT OIL COMPANY LTD  
Field: EXPLORATION  
Well: MOBY-1

### Wireline Formation Test Analyzer (WFTA<sup>SM</sup>)



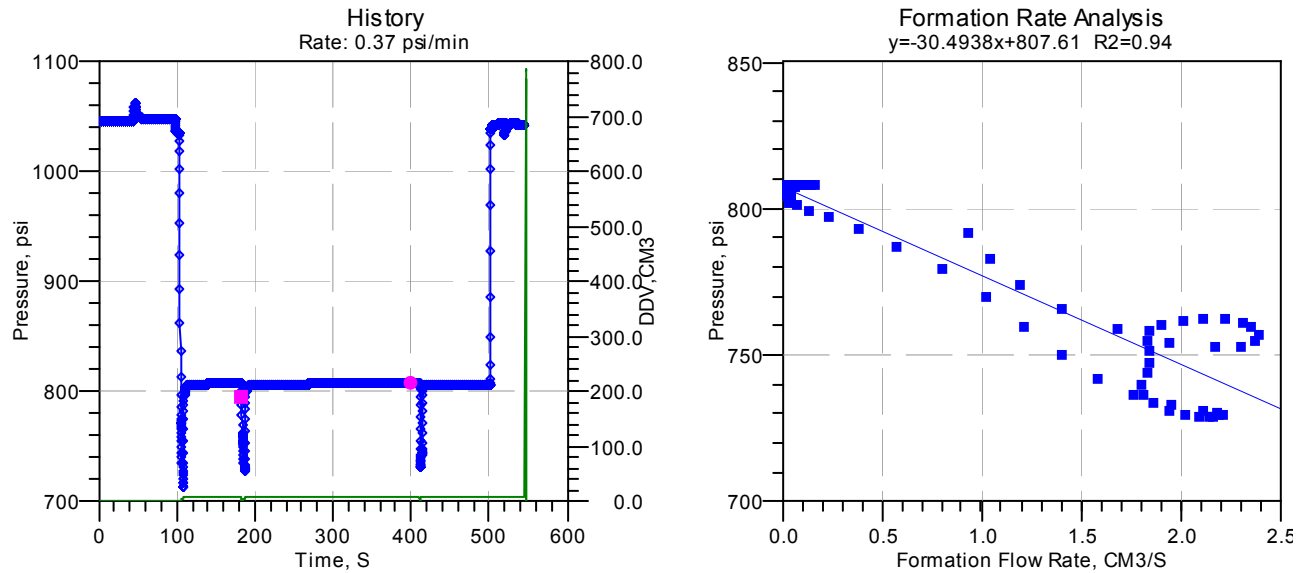
### Pressure Test Results-FRA Compliant

File	Depth		Flow Rate Analysis			Maximum	Final
Number	Measured	TVD	Ct	P*	Mobility	Rate	Buildup
i800a	(ft)	(ft)		(psi)	(mD/cP)	(mD/cP)	(psi)
20	588.9	588.9	3.1e-5	807.4	58.7	61.1	808.1

**Figure 54 File no. g800a20 1: Depth 588.9 m-MD**

Company: BASS STRAIT OIL COMPANY LTD  
Field: EXPLORATION  
Well: MOBY-1

### Wireline Formation Test Analyzer (WFTA<sup>SM</sup>)



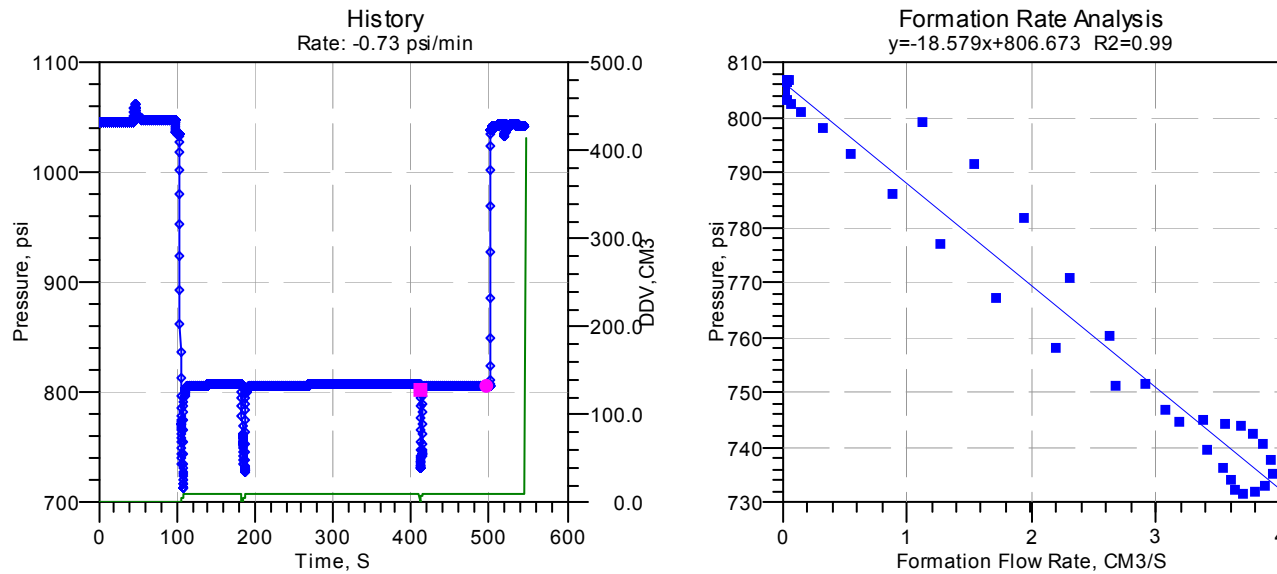
### Pressure Test Results-FRA Compliant

File Number	Depth		Flow Rate Analysis			Maximum	Final	
	Measured (ft)	TVD (ft)	Ct	P* (psi)	Mobility (mD/cP)	Rate (mD/cP)	Buildup (psi)	
i800a	20	588.9	588.9	3.1e-5	807.6	81.3	62.2	808.1

**Figure 55 File no. g800a20 2: Depth 588.9 m-MD**

Company: BASS STRAIT OIL COMPANY LTD  
Field: EXPLORATION  
Well: MOBY-1

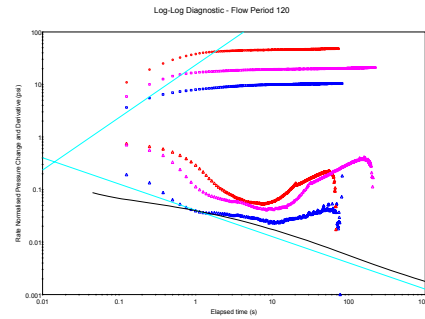
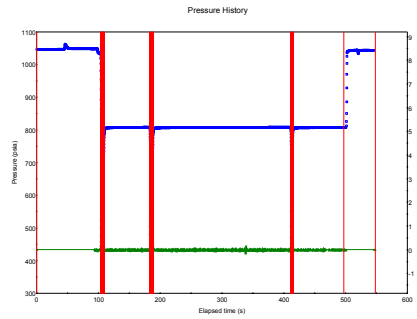
### Wireline Formation Test Analyzer (WFTA<sup>SM</sup>)



### Pressure Test Results-FRA Compliant

File	Depth		Flow Rate Analysis			Maximum	Final	
Number	Measured	TVD	Ct	P*	Mobility	Rate	Buildup	
i800a	(ft)	(ft)		(psi)	(mD/cP)	(mD/cP)	(psi)	
	20	588.9	588.9	3.1e-5	806.7	133.4	103.9	806.8

**Figure 56 File no. q800a20: Depth 588.9 m-MD**



**Model**  
Wireline Formation Test (WFT)  
Homogeneous  
Infinite Lateral Extent

**Results**

(pav) <sub>i</sub>	806.851	psia
pwf	796.458	psia
k/u(xyz)	18.98	mD/cp
k(xyz)	18.98	mD
c(sys)	5.8414E-006	1/psi
S(p)	-0.43	
C	1.286E-008	bb/psi
ri	11	ft
p*(FRA)	806.650	psia
k/u(FRA)	184.8	mD/cp
c(FRA)	4.2811E-005	1/psi

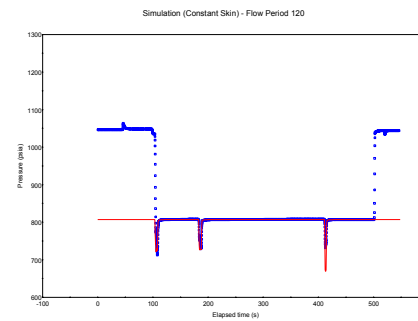
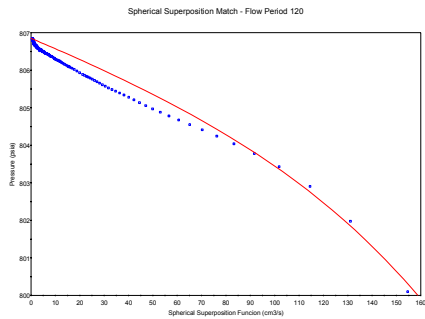
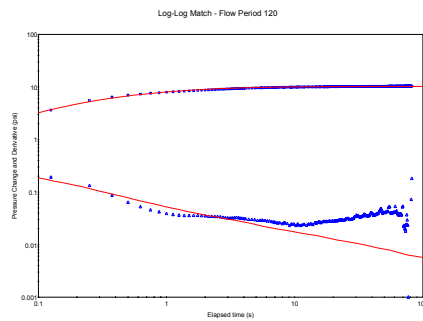
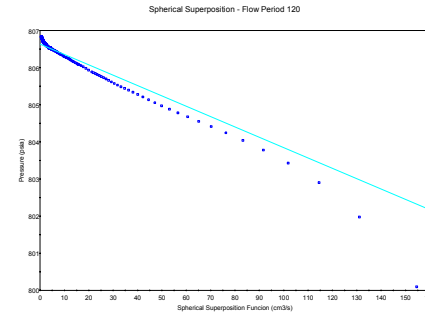
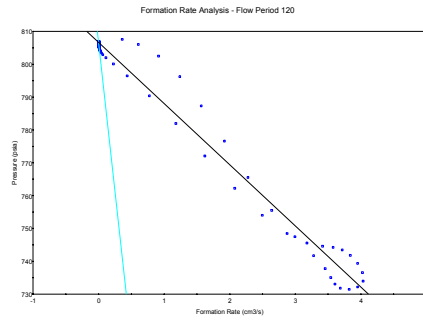
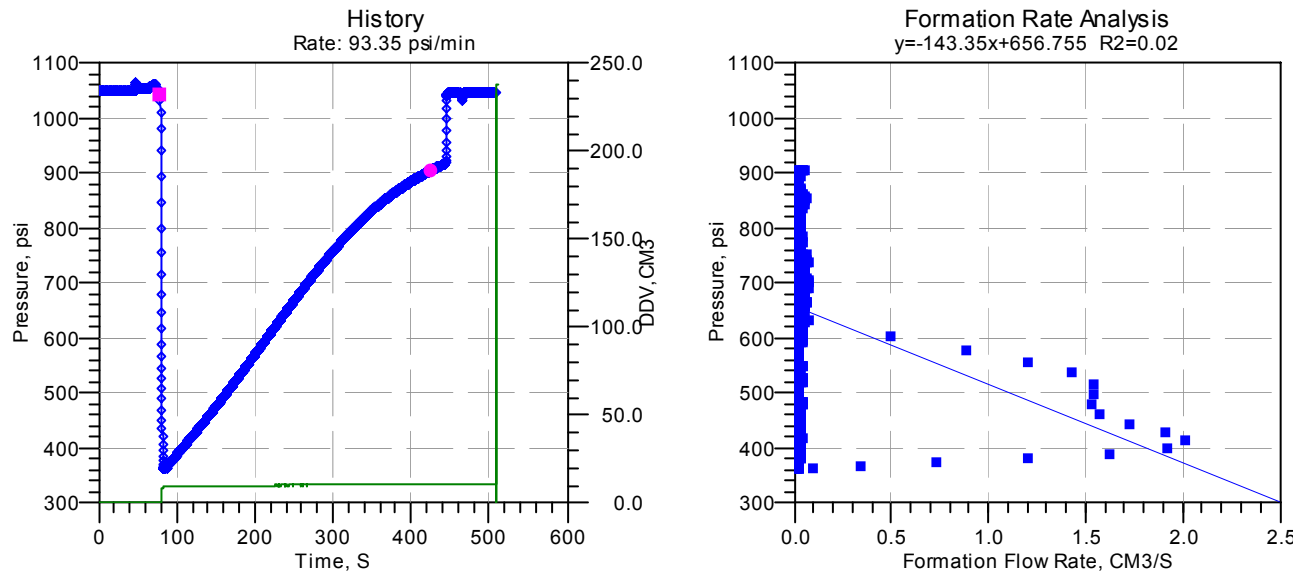


**Figure 57 File no. g800a21 0: Depth 591.1 m-MD**

Company: BASS STRAIT OIL COMPANY LTD  
Field: EXPLORATION  
Well: MOBY-1

### Wireline Formation Test Analyzer (WFTA<sup>SM</sup>)



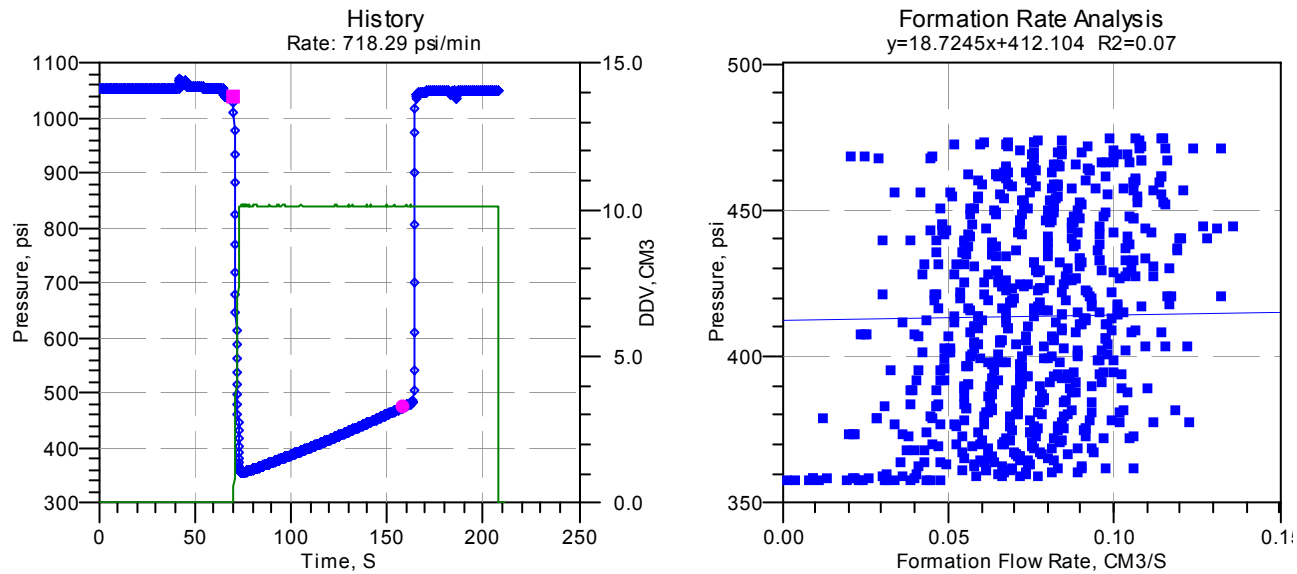
### Pressure Test Results-NOT FRA Compliant (Tight)

File	Depth		Flow Rate Analysis			Maximum	Final	
	Number	Measured	TVD	Ct	P*	Rate	Buildup	
i800a	(ft)	(ft)		(psi)	(mD/cP)	(mD/cP)	(psi)	
	21	591.1	591.1	4.0e-5	656.8	17.3	9.2	1047.2

**Figure 58 File no. g800a22 0: Depth 593.2 m-MD**

Company: BASS STRAIT OIL COMPANY LTD  
Field: EXPLORATION  
Well: MOBY-1

### Wireline Formation Test Analyzer (WFTA<sup>SM</sup>)



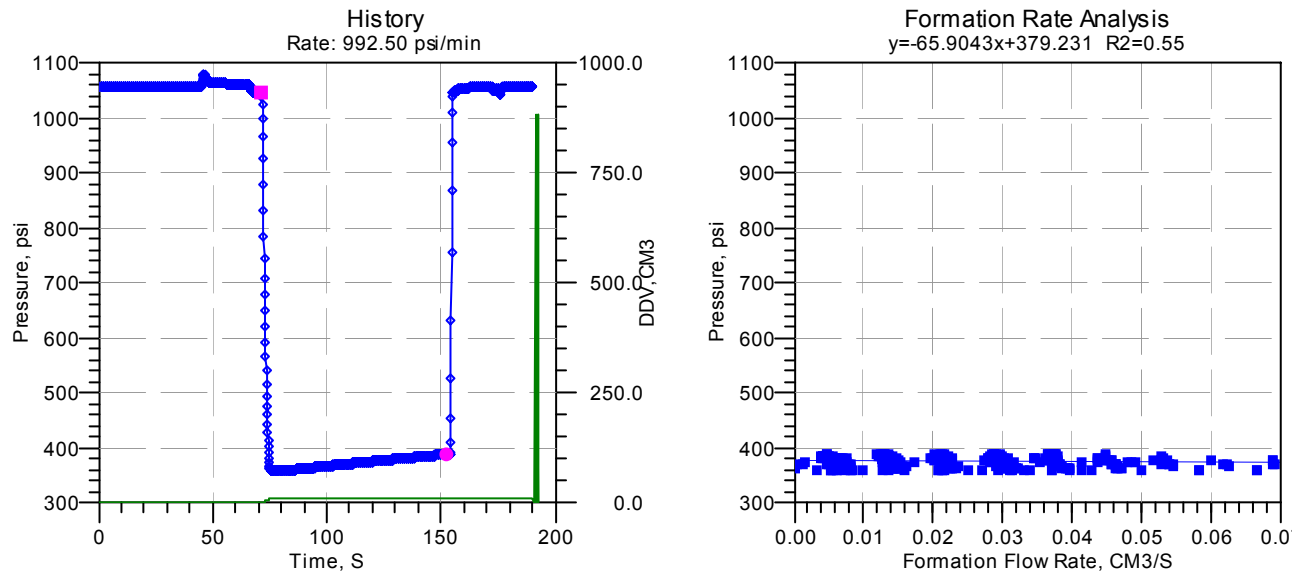
### Pressure Test Results-NOT FRA Compliant (Tight)

File	Depth		Flow Rate Analysis			Maximum	Final
Number	Measured	TVD	Ct	P*	Mobility	Rate	Buildup
i800a	(ft)	(ft)		(psi)	(mD/cP)	(mD/cP)	(psi)
22	593.2	593.2		1.5e-4	412.1	-132.4	2.9 1050.4

**Figure 59 File no. q800a23 0: Depth 596.9 m-MD**

Company: BASS STRAIT OIL COMPANY LTD  
Field: EXPLORATION  
Well: MOBY-1

### Wireline Formation Test Analyzer (WFTA<sup>SM</sup>)



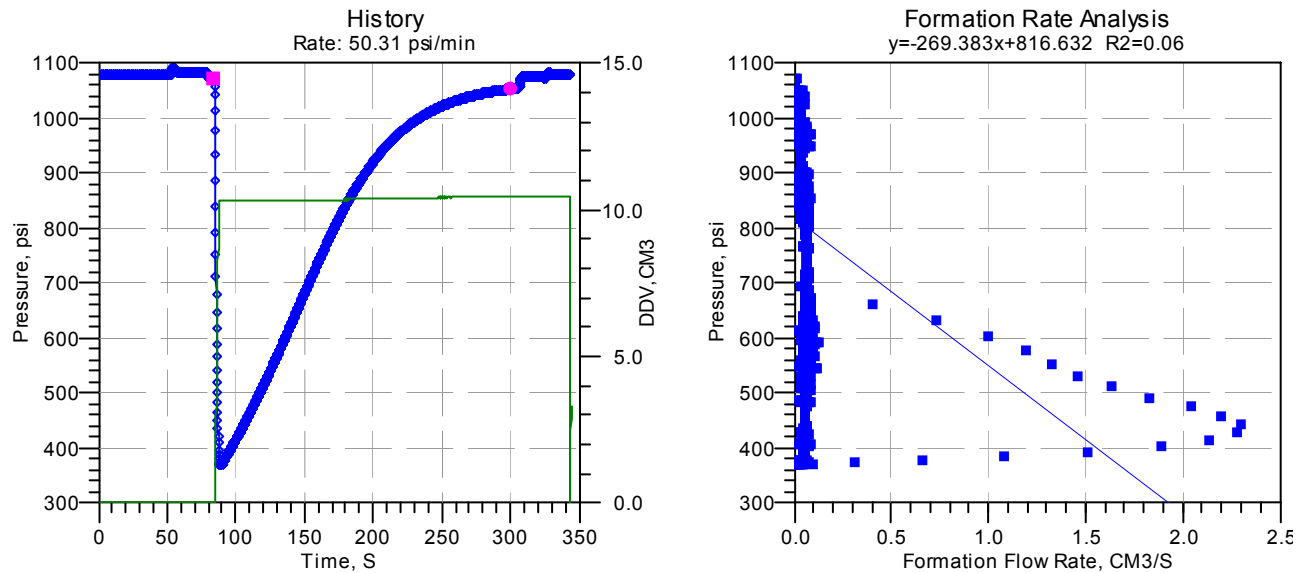
### Pressure Test Results-NOT FRA Compliant (Tight)

File	Depth		Flow Rate Analysis			Maximum	Final	
Number	Measured	TVD	Ct	P*	Mobility	Rate	Buildup	
i800a	(ft)	(ft)		(psi)	(mD/cP)	(mD/cP)	(psi)	
	23	596.9	596.9	9.6e-5	379.2	37.6	6.0	1057.5

**Figure 60 File no. g800a25 0: Depth 608.1 m-MD**

Company: BASS STRAIT OIL COMPANY LTD  
Field: EXPLORATION  
Well: MOBY-1

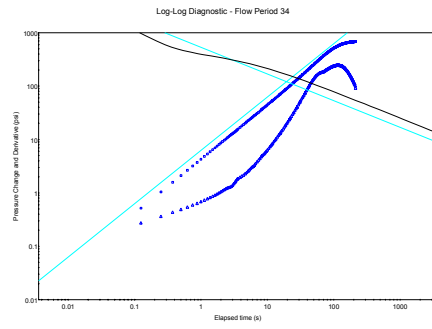
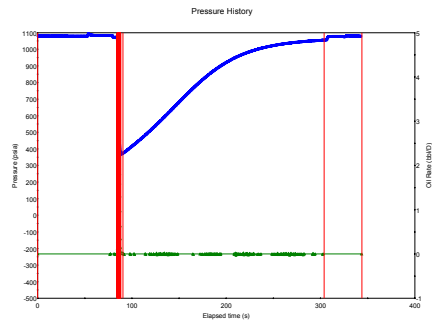
### Wireline Formation Test Analyzer (WFTA<sup>SM</sup>)



### Pressure Test Results-NOT FRA Compliant

File	Depth		Flow Rate Analysis			Maximum	Final	
Number	Measured	TVD	Ct	P*	Mobility	Rate	Buildup	
i800a	(ft)	(ft)		(psi)	(mD/cP)	(mD/cP)	(psi)	
	25	608.1	608.1	3.4e-5	816.6	9.2	8.3	1079.2

**Figure 61 File no. g800a25 0: Depth 608.1 m-MD**



Model	
Wireline Formation Test (WFT)	
Homogeneous	
Infinite Lateral Extent	

Results		
(pav) <sub>i</sub>	1201.373	psia
pwf	373.227	psia
k/u(xyz)	0.04713	mD/cp
k(xyz)	0.04713	mD
c(sys)	3.2872E-005	1/psi
S(p)	-0.57	
C	7.2367E-008	bb/psi
ri	1	ft
p*(FRA)	833.987	psia
k/u(FRA)	11.20	mD/cp
c(FRA)	3.3677E-005	1/psi

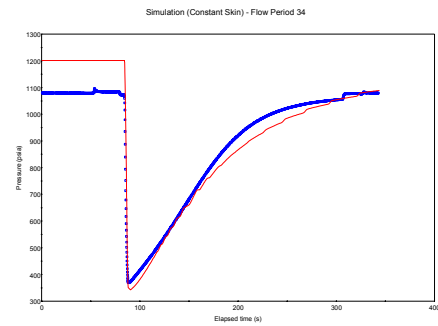
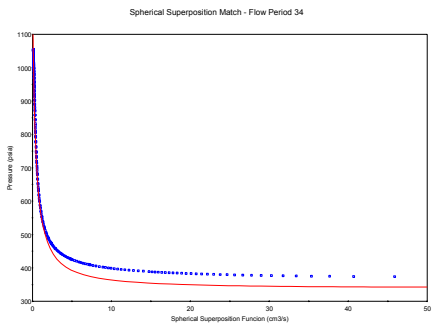
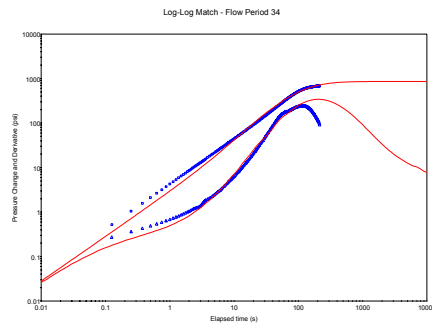
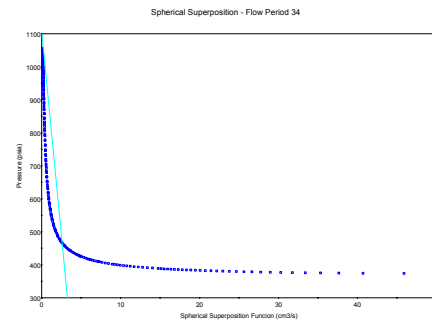
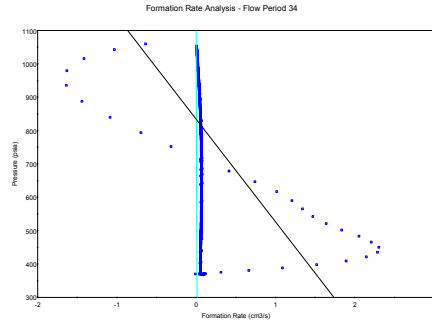
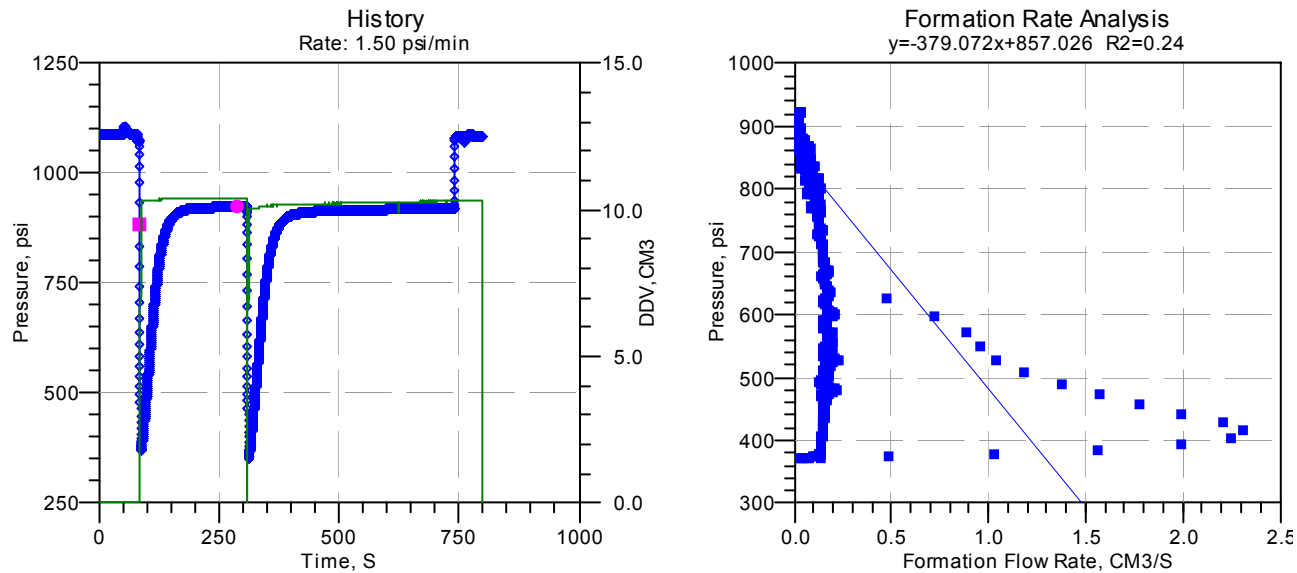


**Figure 62 File no. g800a26 0: Depth 612.8 m-MD**

Company: BASS STRAIT OIL COMPANY LTD  
Field: EXPLORATION  
Well: MOBY-1

## Wireline Formation Test Analyzer (WFTA<sup>SM</sup>)



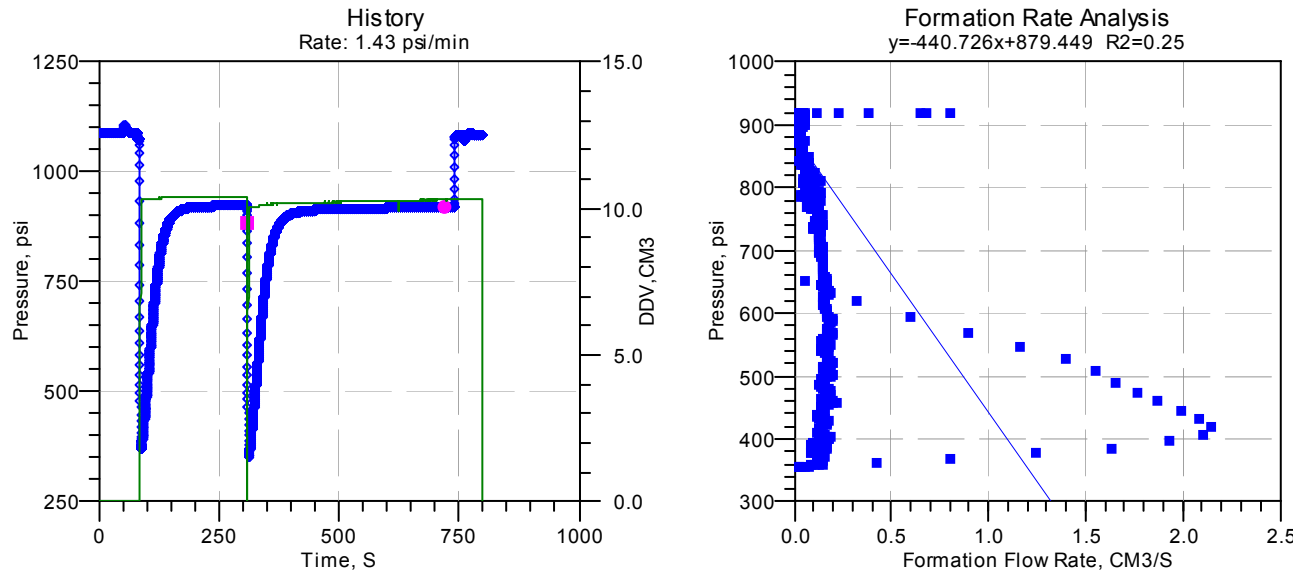
### Pressure Test Results-NOT FRA Compliant

File	Depth		Flow Rate Analysis			Maximum	Final
Number	Measured	TVD	Ct	P*	Mobility	Rate	Buildup
i800a	(ft)	(ft)		(psi)	(mD/cP)	(mD/cP)	(psi)
26	612.8	612.8	3.8e-5	857.0	6.5	10.4	923.3

**Figure 63 File no. g800a26 1: Depth 612.8 m-MD**

Company: BASS STRAIT OIL COMPANY LTD  
Field: EXPLORATION  
Well: MOBY-1

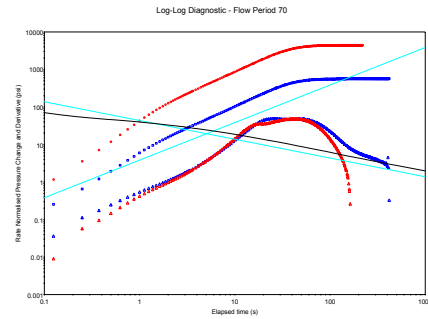
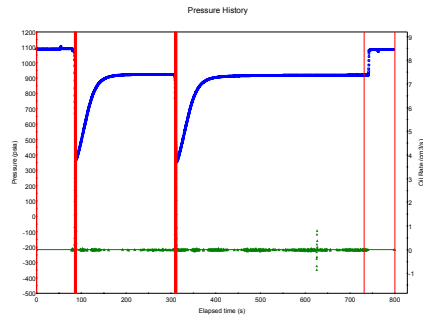
### Wireline Formation Test Analyzer (WFTA<sup>SM</sup>)



### Pressure Test Results – Not FRA Compliant

File	Depth		Flow Rate Analysis			Maximum	Final		
	Number	Measured	TVD	Ct	P*	Rate	Buildup		
i800a	(ft)	612.8	(ft)	612.8	3.8e-5	879.4	5.6	9.7	919.0

**Figure 64 File no. q800a26: Depth 612.8 m-MD**



Model  
Wireline Formation Test (WFT)  
Homogeneous  
Infinite Lateral Extent

Results		
(pav) <sub>i</sub>	929.984	psia
pwf	354.223	psia
k/u(xyz)	0.2175	mD/cp
k(xyz)	0.2175	mD
c(sys)	4.7854E-005	1/psi
S(p)	-0.64	
C	1.0535E-007	bb/psi
ri	3	ft
p*(FRA)	887.522	psia
k/u(FRA)	6.898	mD/cp
c(FRA)	4.1137E-005	1/psi

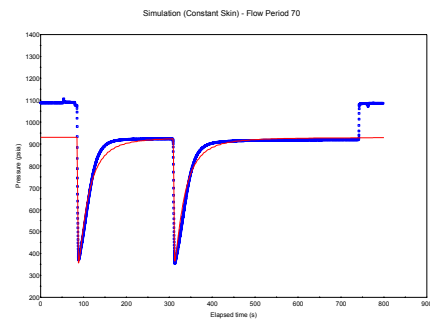
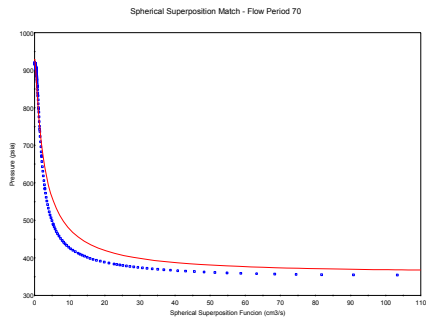
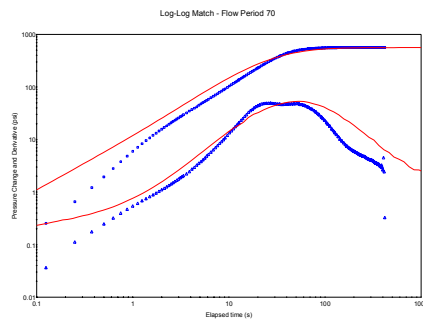
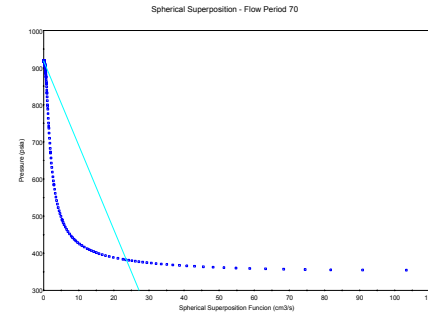
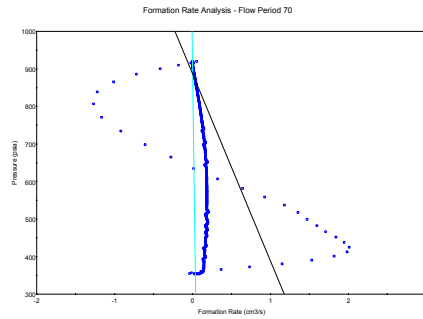
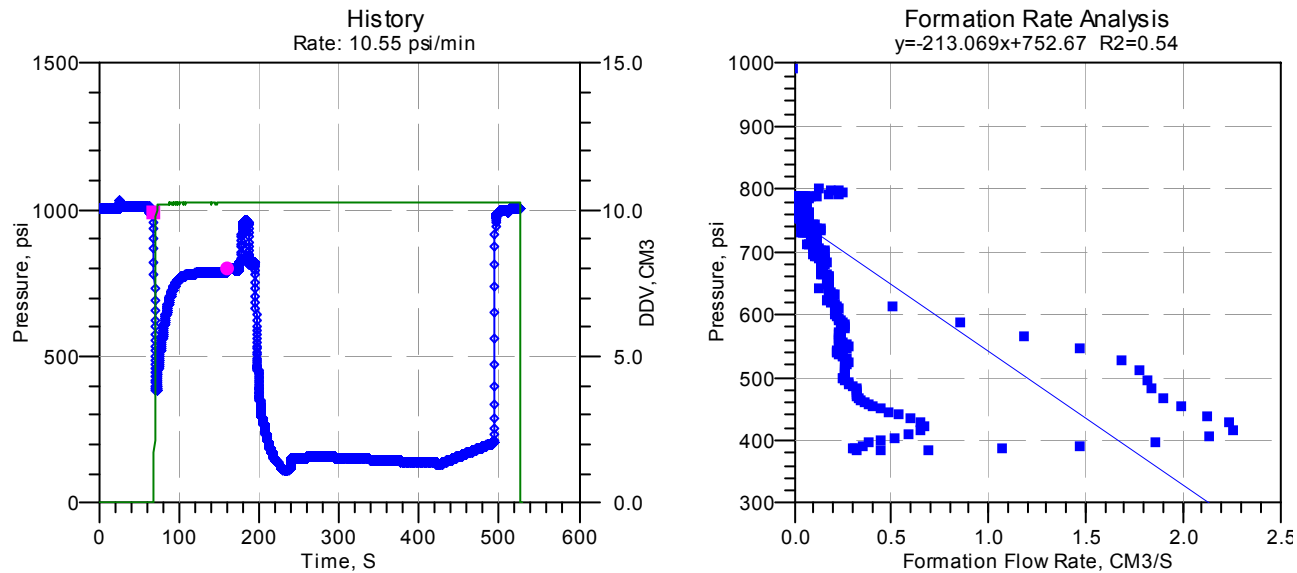


**Figure 65 File no. q800a28 0: Depth 568.2 m-MD (Sampling No flow)**

Company: BASS STRAIT OIL COMPANY LTD  
Field: EXPLORATION  
Well: MOBY-1

### Wireline Formation Test Analyzer (WFTA<sup>SM</sup>)



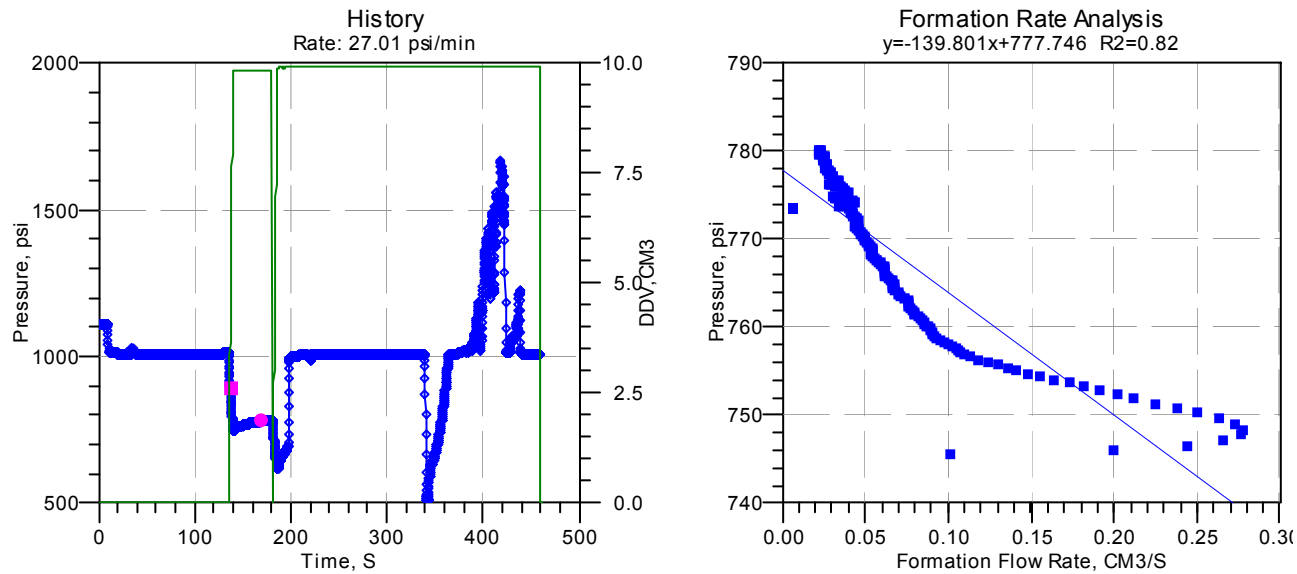
### Pressure Test Results-NOT FRA Compliant

File	Depth		Flow Rate Analysis			Maximum	Final
Number	Measured	TVD	Ct	P*	Mobility	Rate	Buildup
i800a	(ft)	(ft)		(psi)	(mD/cP)	(mD/cP)	(psi)
28	568.2	568.2	3.7e-5	752.7	11.6	13.4	788.1

**Figure 66 File no. g800a29: Depth 568.5 m-MD (Sampling no flow)**

Company: BASS STRAIT OIL COMPANY LTD  
Field: EXPLORATION  
Well: MOBY-1

### Wireline Formation Test Analyzer (WFTA<sup>SM</sup>)



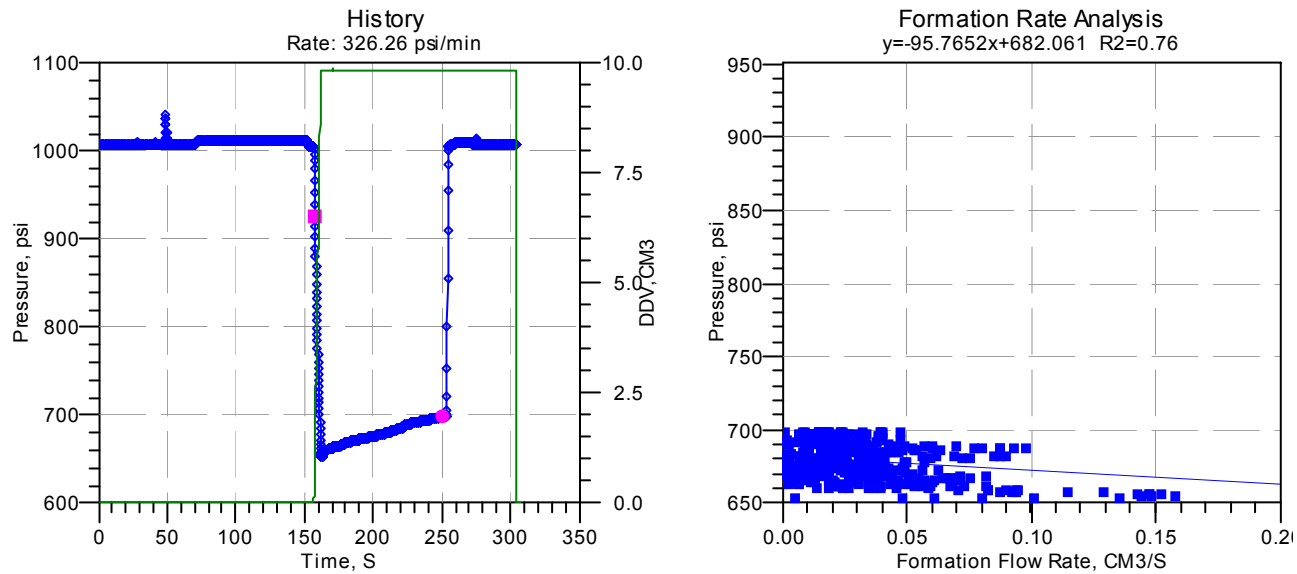
### Pressure Test Results-NOT FRA Compliant

File	Depth		Flow Rate Analysis			Maximum	Final
Number	Measured	TVD	Ct	P*	Mobility	Rate	Buildup
i800a	(ft)	(ft)		(psi)	(mD/cP)	(mD/cP)	(psi)
29	568.5	568.5	1.6e-4	777.7	17.7	4.3	782.3

**Figure 67 File no. g800a30: Depth 568.2 m-MD (Sampling No flow)**

Company: BASS STRAIT OIL COMPANY LTD  
Field: EXPLORATION  
Well: MOBY-1

### Wireline Formation Test Analyzer (WFTA<sup>SM</sup>)



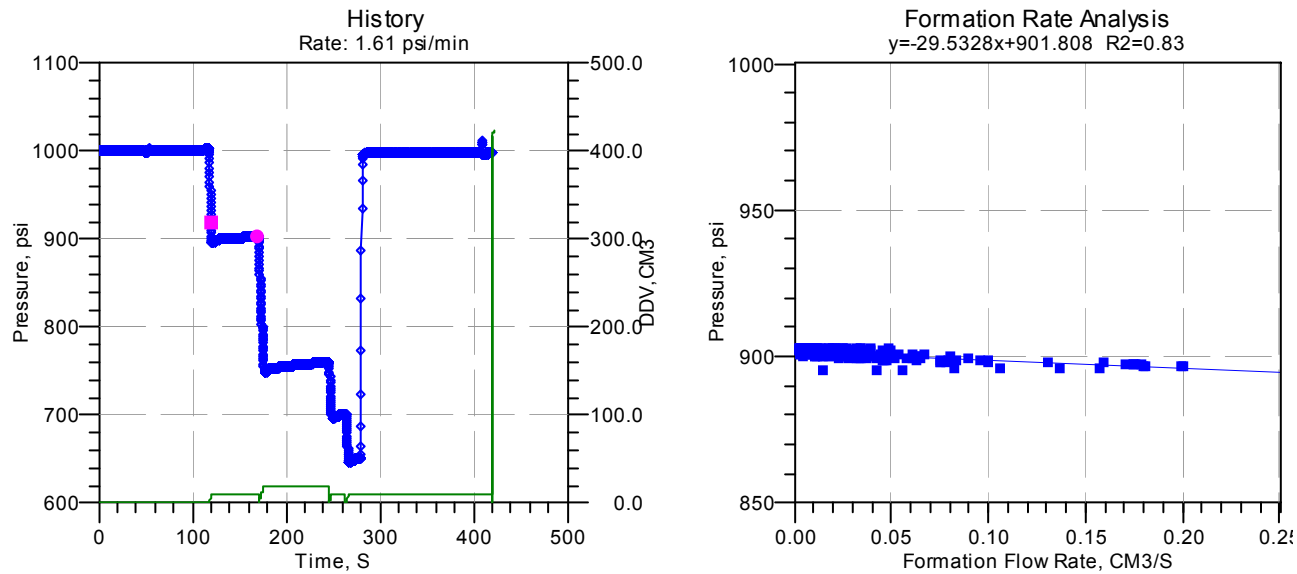
### Pressure Test Results-NOT FRA Compliant

File	Depth	Flow Rate Analysis			Maximum	Final		
Number	Measured	TVD	Ct	P*	Rate	Buildup		
i800a	(ft)	(ft)		(psi)	(mD/cP)	(psi)		
	30	568.2	568.2	1.3e-4	682.1	25.9	8.5	1007.5

**Figure 68 File no. q800a34: Depth 561.4 ft-MD**

Company: BASS STRAIT OIL COMPANY LTD  
Field: EXPLORATION  
Well: MOBY-1

### Wireline Formation Test Analyzer (WFTA<sup>SM</sup>)



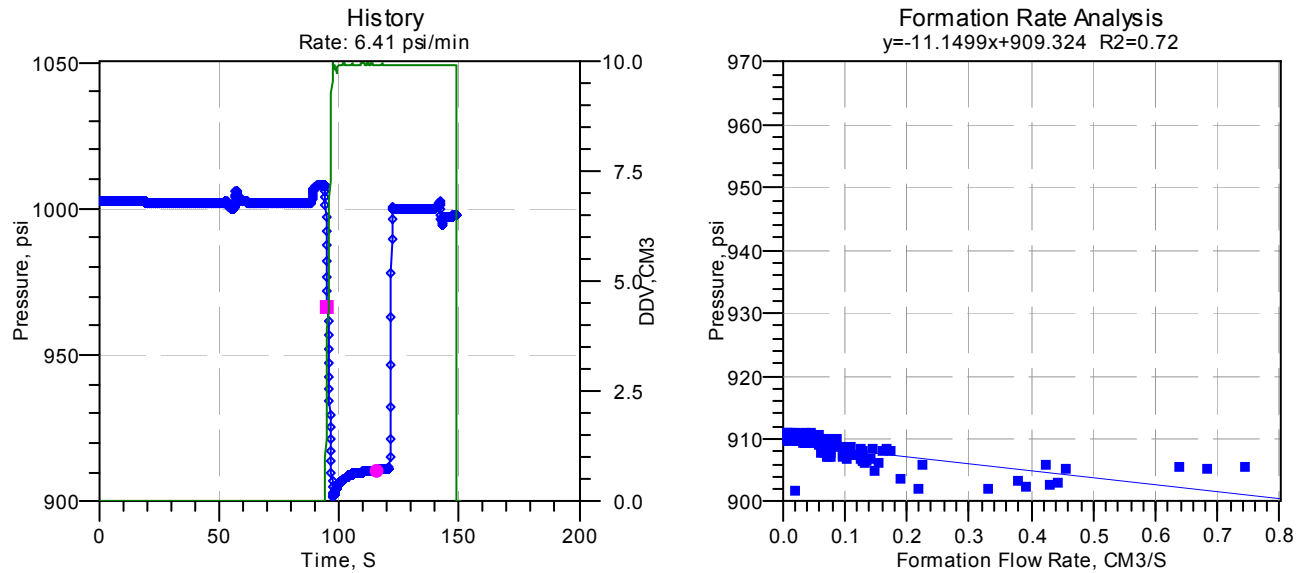
### Pressure Test Results-NOT FRA Compliant

File	Depth		Flow Rate Analysis			Maximum	Final
Number	Measured	TVD	Ct	P*	Mobility	Rate	Buildup
i800a	(ft)	(ft)		(psi)	(mD/cP)	(mD/cP)	(psi)
34	561.4	561.4	3.5e-4	901.8	83.9	2.4	902.6

**Figure 69 File no. g800a35: Depth 561.7 m-MD(Sampling No flow)**

Company: BASS STRAIT OIL COMPANY LTD  
Field: EXPLORATION  
Well: MOBY-1

### Wireline Formation Test Analyzer (WFTA<sup>SM</sup>)



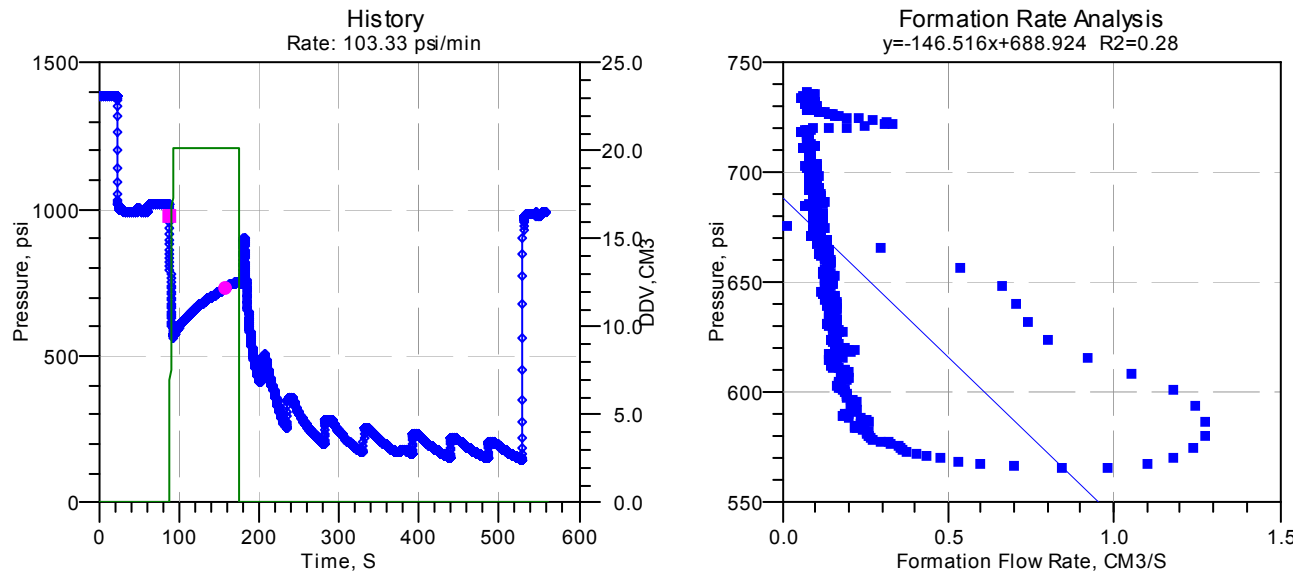
### Pressure Test Results-NOT FRA Compliant

File	Depth	Flow Rate Analysis			Maximum	Final	
Number	Measured	TVD	Ct	P*	Rate	Buildup	
i800a	(ft)	(ft)		(psi)	(mD/cP)	(psi)	
35	561.7	561.7	4.7e-4	909.3	222.3	204.0	911.1

**Figure 70 File no. g800a37: Depth 558.5 ft-MD (Sampling-Slow flow)**

Company: BASS STRAIT OIL COMPANY LTD  
Field: EXPLORATION  
Well: MOBY-1

### Wireline Formation Test Analyzer (WFTA<sup>SM</sup>)



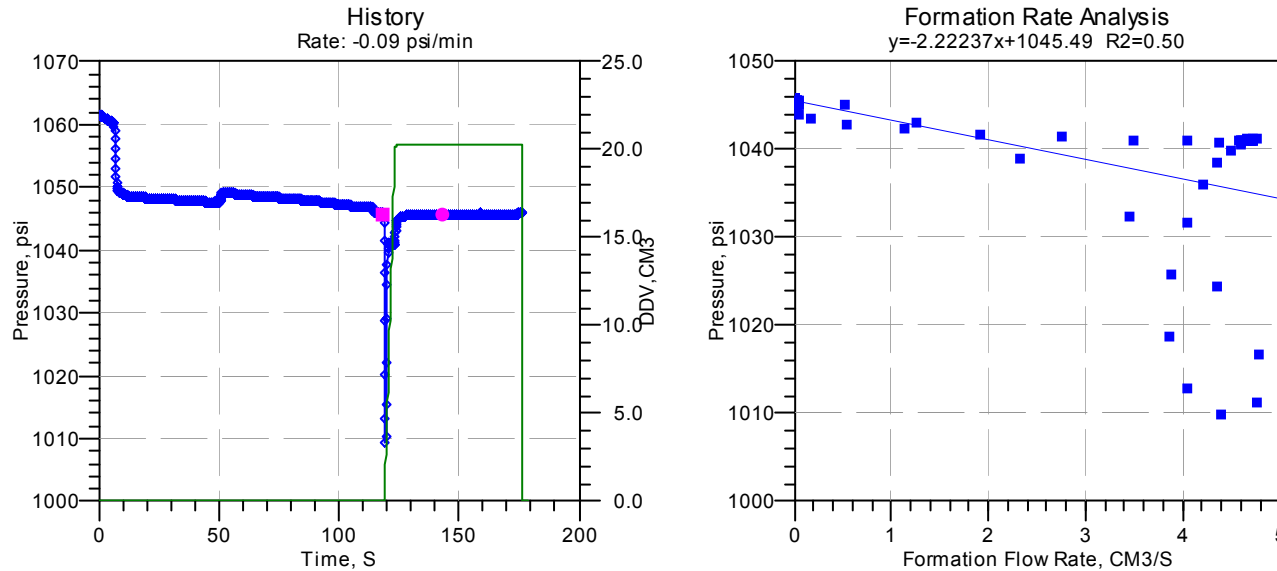
### Pressure Test Results-NOT FRA Compliant

File	Depth		Flow Rate Analysis			Maximum	Final
Number	Measured	TVD	Ct	P*	Mobility	Rate	Buildup
i800a	(ft)	(ft)		(psi)	(mD/cP)	(mD/cP)	(psi)
37	558.5	558.5	1.5e-4	688.9	16.9	18.5	750.3

**Figure 71 File no. g800a39: Depth 588.9 m-MD**

Company: BASS STRAIT OIL COMPANY LTD  
Field: EXPLORATION  
Well: MOBY-1

## Wireline Formation Test Analyzer (WFTA<sup>SM</sup>)



### Pressure Test Results-Not FRA Compliant (no seal)

File	Depth		Flow Rate Analysis			Maximum	Final
	Number	Measured	TVD	Ct	P*	Rate	Buildup
i800a	(ft)	(ft)		(psi)	(mD/cP)	(mD/cP)	(psi)
	39	588.9	588.9	-5.1e-5	1045.5	1115.3	328.4 1046.0

**Figure 72 File no. q800a40: Depth 588.5 m-MD (Sampling)**

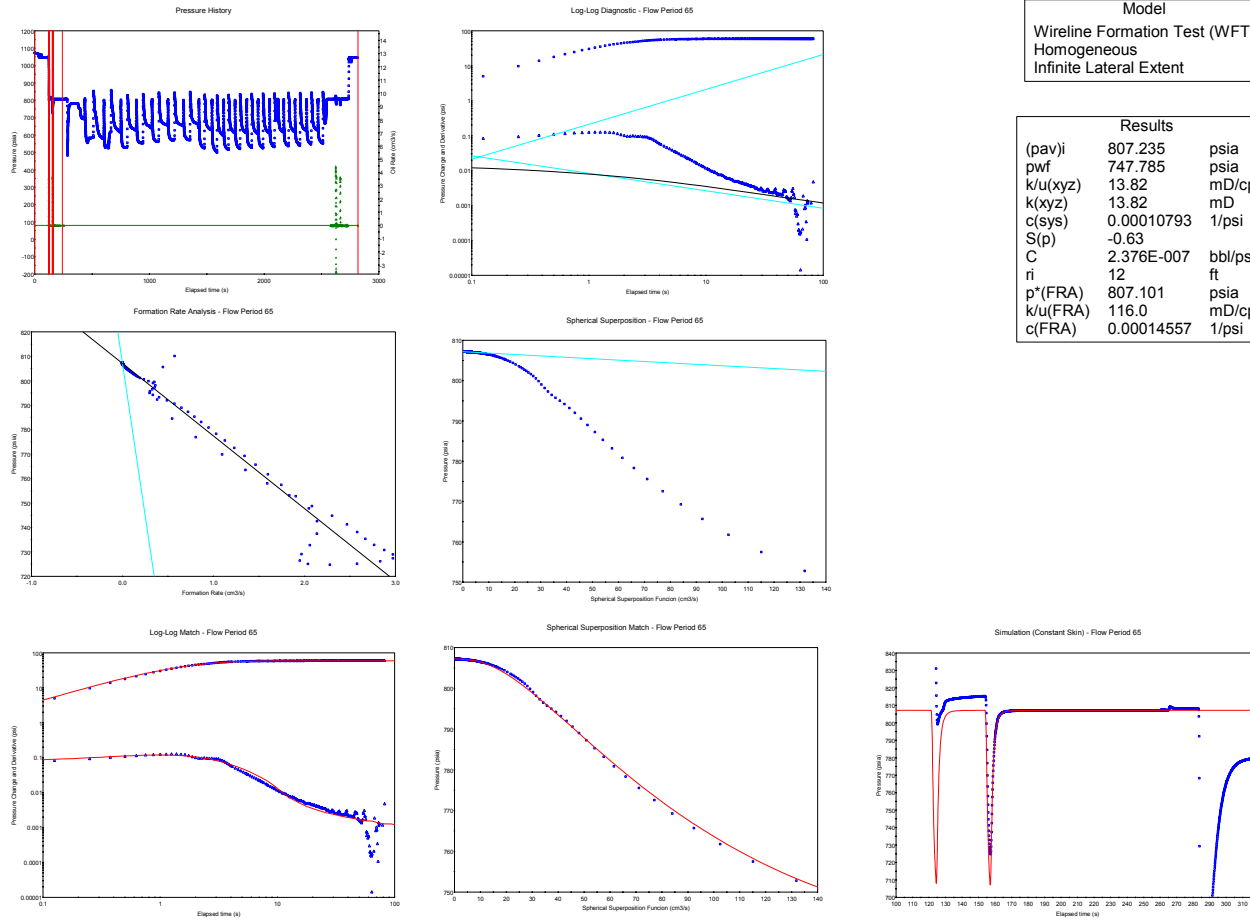
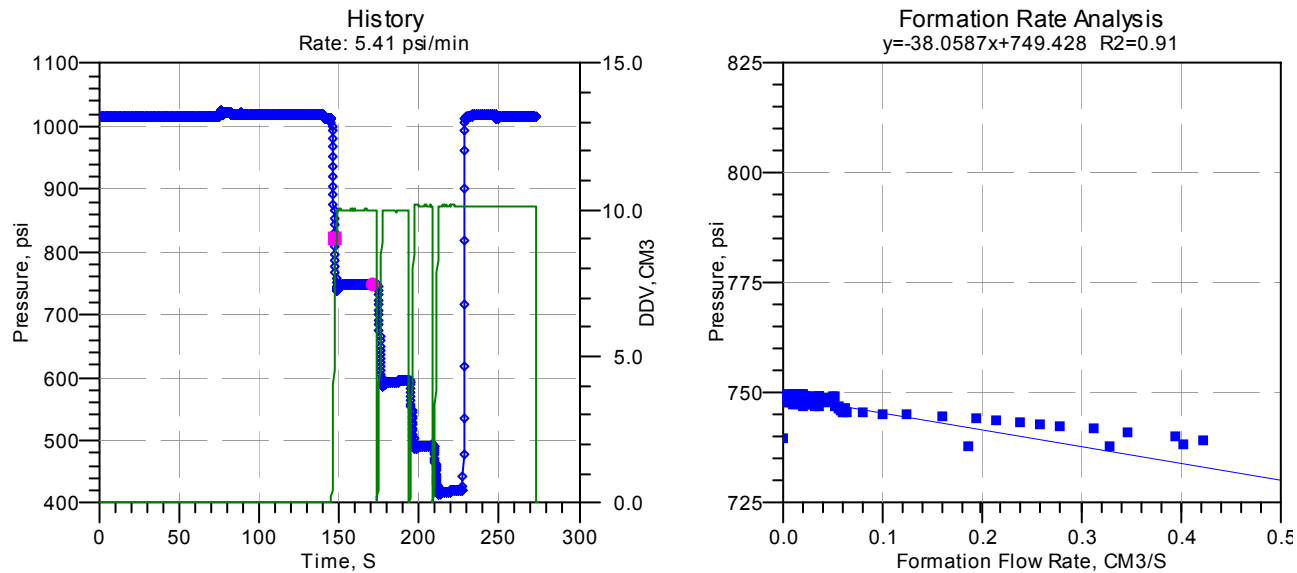


**Figure 73 File no. q800a41: Depth 572 m-MD (Sampling No Flow)**

Company: BASS STRAIT OIL COMPANY LTD  
Field: EXPLORATION  
Well: MOBY-1

### Wireline Formation Test Analyzer (WFTA<sup>SM</sup>)



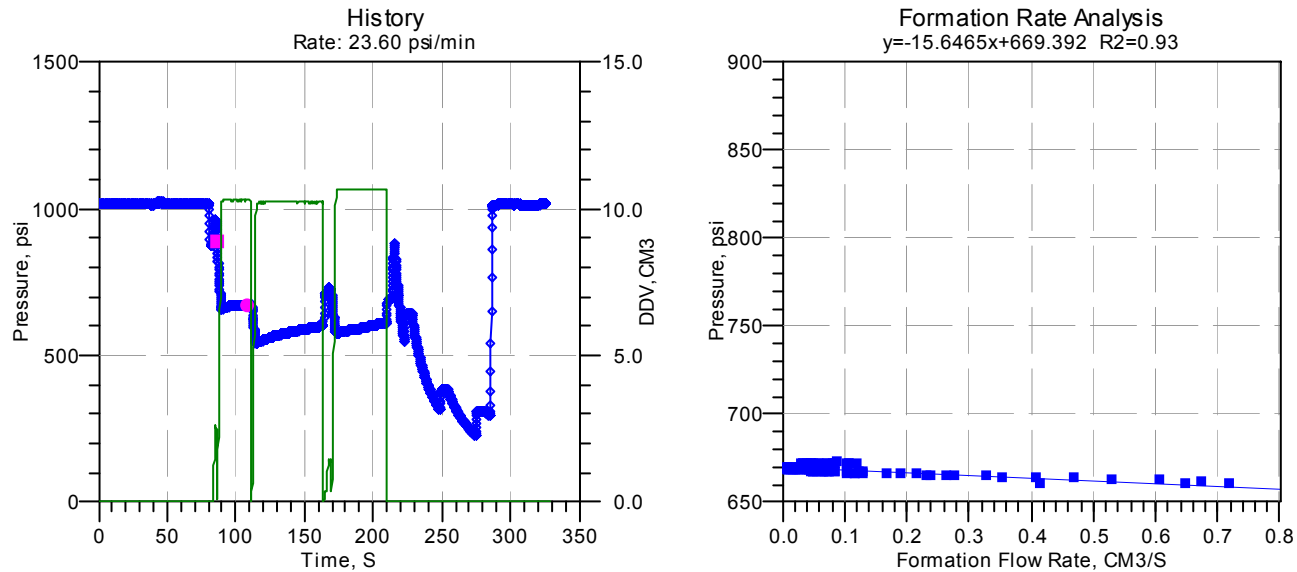
### Pressure Test Results-NOT FRA Compliant

File	Depth		Flow Rate Analysis			Maximum	Final
Number	Measured	TVD	Ct	P*	Mobility	Rate	Buildup
i800a	(ft)	(ft)		(psi)	(mD/cP)	(mD/cP)	(psi)
41	572	572	1.6e-4	749.4	65.1	4.0	749.8

**Figure 74 File no. g800a42: Depth 572.1 m-MD (Sampling very slow flow)**

Company: BASS STRAIT OIL COMPANY LTD  
Field: EXPLORATION  
Well: MOBY-1

### Wireline Formation Test Analyzer (WFTA<sup>SM</sup>)



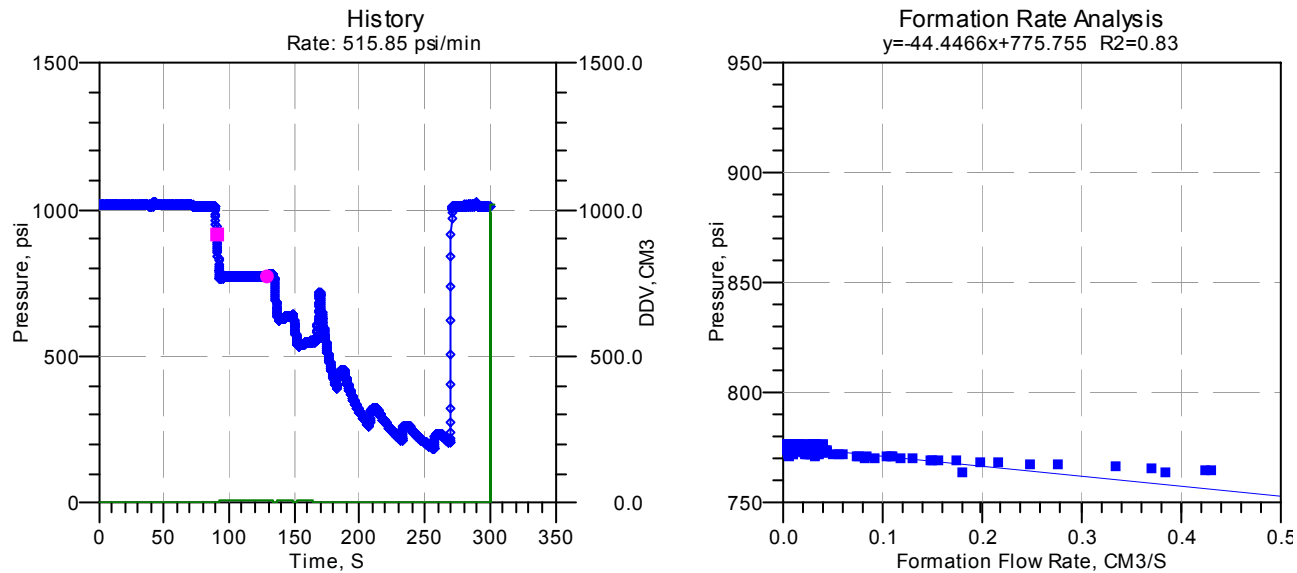
### Pressure Test Results-NOT FRA Compliant

File	Depth		Flow Rate Analysis			Maximum	Final	
Number	Measured	TVD	Ct	P*	Mobility	Rate	Buildup	
i800a	(ft)	(ft)		(psi)	(mD/cP)	(mD/cP)	(psi)	
	42	572.1	572.1	3.6e-4	669.4	158.4	142.8	672.7

**Figure 75 File no. g800a43: Depth 572.2 ft-MD (Sampling very slow flow)**

Company: BASS STRAIT OIL COMPANY LTD  
Field: EXPLORATION  
Well: MOBY-1

### Wireline Formation Test Analyzer (WFTA<sup>SM</sup>)



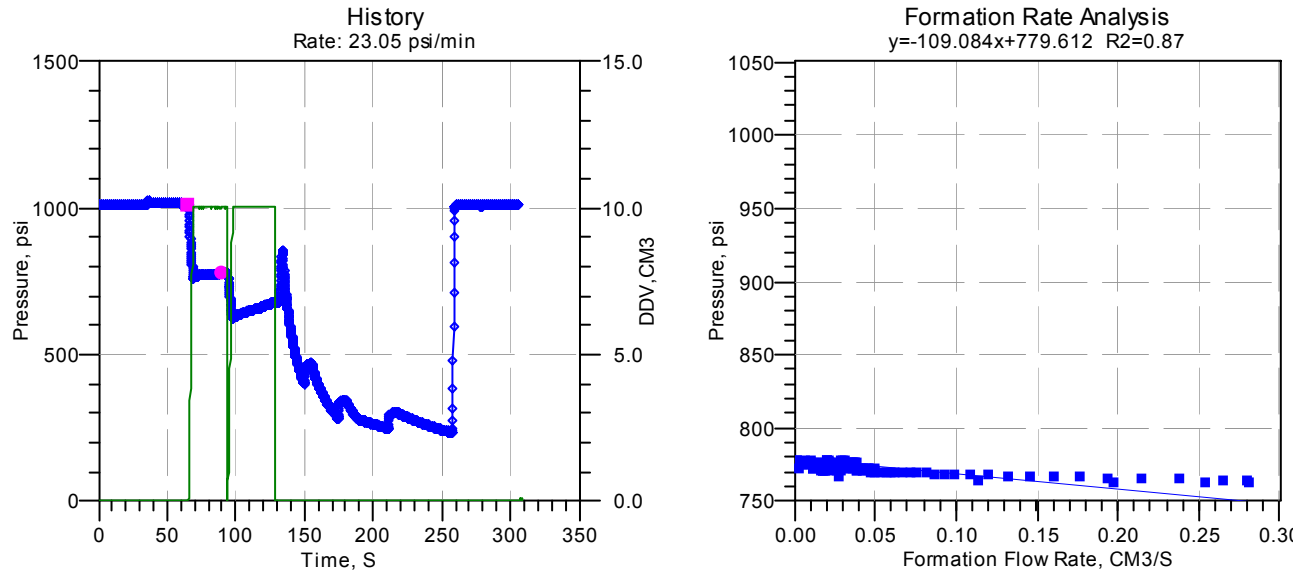
### Pressure Test Results-NOT FRA Compliant

File	Depth		Flow Rate Analysis			Maximum	Final
Number	Measured	TVD	Ct	P*	Mobility	Rate	Buildup
i800a	(ft)	(ft)		(psi)	(mD/cP)	(mD/cP)	(psi)
43	572.2	572.2	2.0e-4	775.8	55.8	79.2	1014.7

**Figure 76 File no. g800a44: Depth 571 m-MD (Sampling very slow flow)**

Company: BASS STRAIT OIL COMPANY LTD  
Field: EXPLORATION  
Well: MOBY-1

## Wireline Formation Test Analyzer (WFTA<sup>SM</sup>)



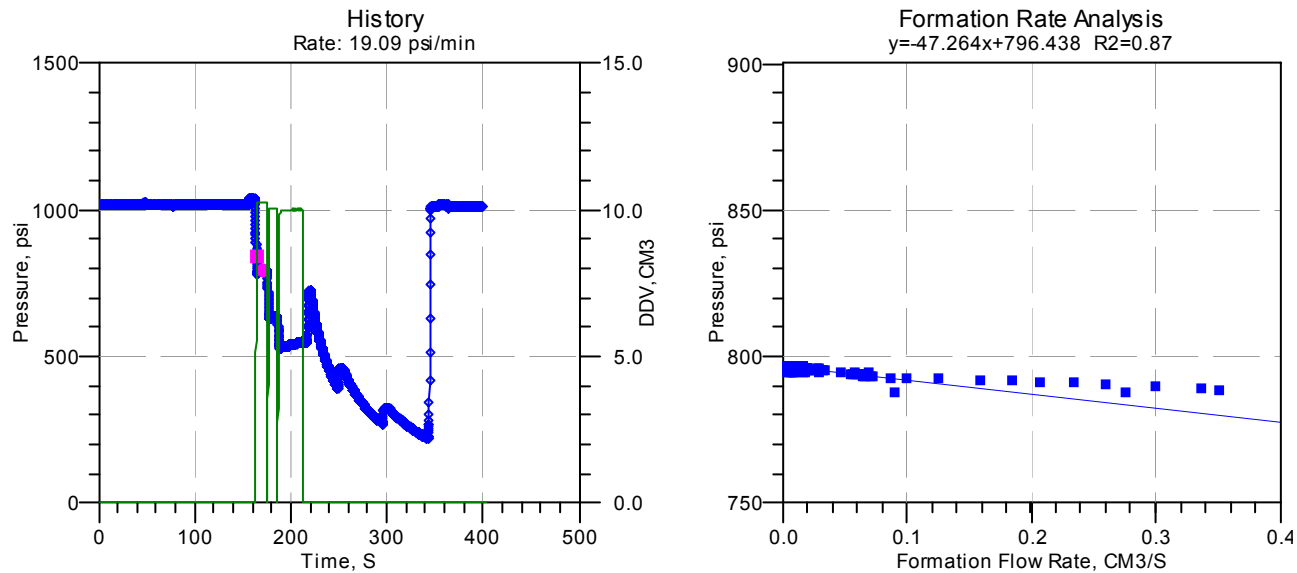
### Pressure Test Results-NOT FRA Compliant

File Number	Depth		Flow Rate Analysis			Maximum	Final	
	Measured (ft)	TVD (ft)	Ct	P* (psi)	Mobility (mD/cP)	Rate (mD/cP)	Buildup (psi)	
i800a	44	571	571	1.5e-4	779.6	22.7	46.7	778.1

**Figure 77 File no. g800a45: Depth 571.9 m-MD (Sampling very slow flow)**

Company: BASS STRAIT OIL COMPANY LTD  
Field: EXPLORATION  
Well: MOBY-1

### Wireline Formation Test Analyzer (WFTA<sup>SM</sup>)



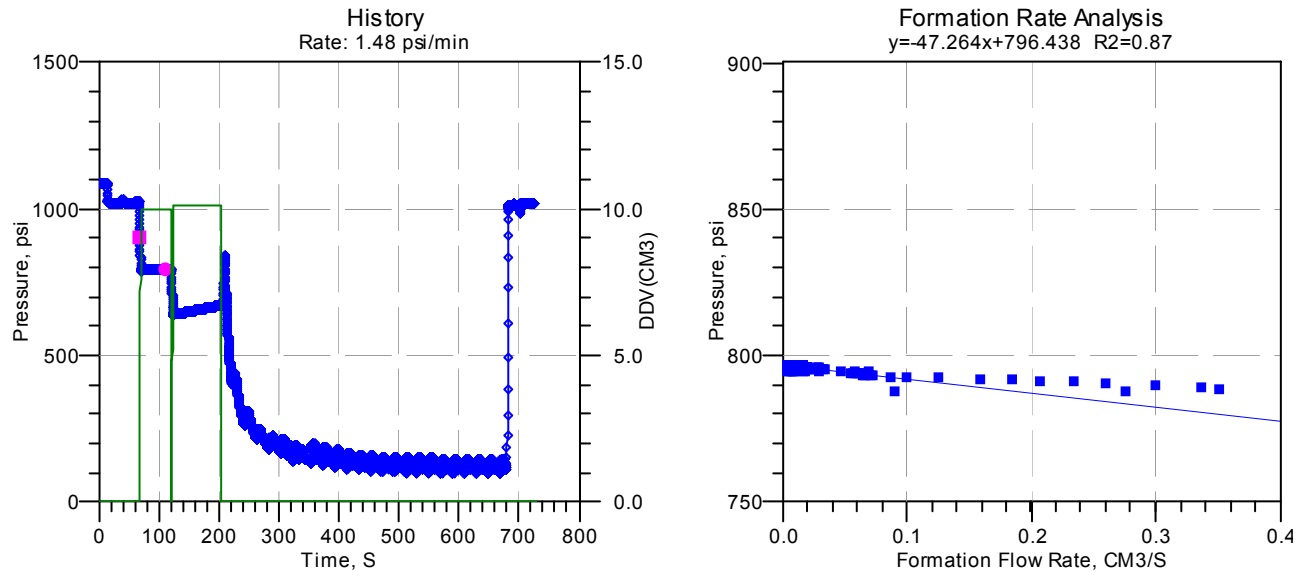
### Pressure Test Results-NOT FRA Compliant

File	Depth		Flow Rate Analysis			Maximum	Final
	Number	Measured	TVD	Ct	P*	Rate	Buildup
i800a	(ft)	(ft)		(psi)	(mD/cP)	(mD/cP)	(psi)
	45	571.9	571.9	1.8e-4	796.4	52.4	5.5 796.8

**Figure 78 File no. q800a46: Depth 573 m-MD (Sampling very low rate)**

Company: BASS STRAIT OIL COMPANY LTD  
Field: EXPLORATION  
Well: MOBY-1

### Wireline Formation Test Analyzer (WFTA<sup>SM</sup>)



### Pressure Test Results-NOT FRA Compliant

File	Depth		Flow Rate Analysis			Maximum	Final	
	Number	Measured	TVD	Ct	P*	Rate	Buildup	
i800a	(ft)	(ft)		(psi)	(mD/cP)	(mD/cP)	(psi)	
	46	573	573	1.8e-4	796.4	52.4	5.5	796.8

## 9. Analysis Methods

### Pressure Transient Analysis (PTA)

#### What is Pressure Transient?

In terms of interpreting and describing WFT pressure response, the initial pressure response measured by a wireline formation test is the hydrostatic pressure, as shown in blue dots in Figure 69. As the tool is set to the formation, the packer begins to compress the mudcake causing a slight pressure rise, but the pressure subsequently drops as the piston within the WFT device moves to withdraw fluid from the formation. Pressure transient data is recorded during pressure tests with gauges located near the probe. If the piston movement can be measured accurately, the "formation rate" can be recorded, illustrated by the green curve in Figure 69. The "superposition method" can then be used to plot pressure drop and pressure derivatives versus time, which can be analysed using the PTA technique.

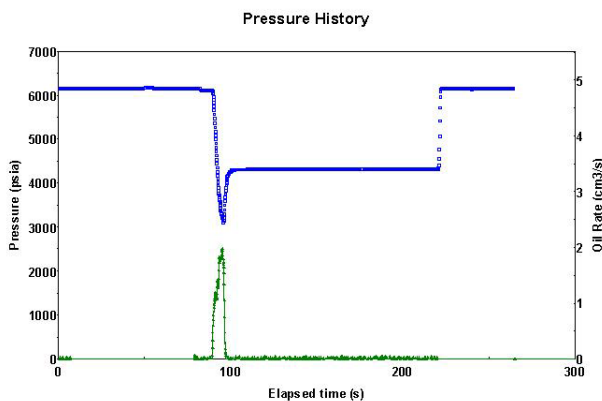


**Figure 79 Typical pressure response of WFT using single probe**

#### Is it similar to Well Test Analysis?

Pressure Transient Analysis uses the same principle to advanced well test analysis techniques. The near-wellbore, reservoir and boundary models are selected from the shape of pressure derivatives to match pressure data in log-log, Horner, and simulation plots.

Compared to a Drill Stem Test (DST), and Production Test (PT), the WFT provides a very small-scale pressure test in terms of both the duration of the test and the volume of fluids produced to the well. Figure 70 illustrates a comparison of pressure derivative curves for WFT versus DST and PT. Even though scales of the radii of investigation of these three test techniques are different, the same advanced well test analysis principle can be used to analyse the pressure response. The pressure response curves can be divided into three periods<sup>20</sup>: i.e. (1) "Early time" which indicates near wellbore behaviour, (2) "middle time" which reflects reservoir behaviour and (3) "late time" which reflects the influence of boundaries within the reservoir. The shape of the pressure derivative curves helps to diagnose which model is influencing a test and during advanced well test interpretation; early, middle and late time models are selected to match the pressure data.

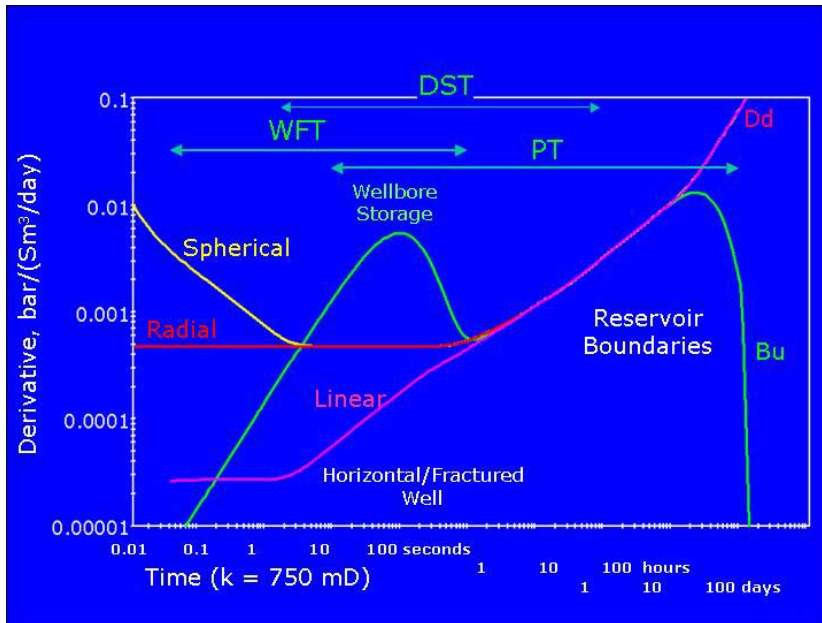


Figure 80 A comparison of pressure response from different scales, i.e. Wireline Formation Test, Drill Stem Test, and Production Well Test (Whittle, 2002)

#### What information do we obtain from Pressure Transient Analysis (PTA)?

Results obtained from pressure transient analysis depend on selected models. Formation pressure and fluid mobility are the typical result from all RCI analysis techniques (i.e. Interpret2001, WFTA, and RCI field plot). Tool storage and skin factor are additional information that could be obtained from pressure transient analysis techniques. Spherical permeability can be obtained if the spherical flow regime is seen in pressure derivatives. Vertical to horizontal permeability ratio, or top and bottom boundary distances can be calculated if the cylindrical flow develops in pressure derivatives and any of this information is known from other sources. Other boundary distances can also be estimated if the flow deviates from the radial flow.

#### How to analyse pressure transient data obtained from wireline formation testers?

A spherical source solution is used to analyse wireline formation pressure data in the pressure transient analysis software, Interpret® 2003. Flow Rate analysis (FRA) technique is applied in one of diagnostic plots. The initial estimation of formation pressure, spherical permeability and tool storage are calculated using the FRA technique. Then the matching curves for log-log, Horner and simulation plots are generated using the initial estimated parameters from the FRA plot. The linear regression technique can be applied to obtain the best match with the pressure transient data.

Probe and reservoir parameters are required for pressure transient analyses. These parameters are:

1. Formation porosity
2. Probe inner diameter
3. Probe tool volume
4. Geometric factor
5. Fluid viscosity
6. Total compressibility

**Wireline Formation Flow Models**

The flow geometry of pressure transient data obtained using a WFT device is much more simplistic compared to data obtained during conventional well testing because of its smaller radius of investigation. In addition, pressure transient analysis of WFT data provides highly localized reservoir information, reflecting reservoir parameters close to the wellbore, which will be masked during conventional well testing. The near wellbore, reservoir and boundary models for WFT data are:

***Tool Storage***

During conventional well testing, pressures in the early time regime are affected by wellbore storage. Similarly, at WFT scale, pressure response in the early time domain is dominated by the tool storage effect, or fluid within the tool. Pressure derivative curves reflecting tool storage effect will show a "hump" in the early time domain, as illustrated in Figure 71.

***Spherical Flow***

The fluid in the formation around wellbore moves into the WFT probe, which has a small radius. The flow-regime geometry from the formation into the WFT probe is spherical and characterized by a straight line pressure derivative curve having a negative half-unit slope in a log-log plot (Figure 71). The spherical flow regime is controlled by the spherical permeability,  $k_{xyz}$  and equations for spherical flow are illustrated in Equations 1 to 3. The spherical flow regime follows the tool storage effect and occurs prior to any reservoir boundary effects which occur in the late time domains.

Dimensionless Pressure Drop

$$p_D h_D = 1 - \frac{1}{\sqrt{\pi \frac{t_D}{r_{sD}^2}}} + S_p \tag{Equation 1}$$

Dimension Pressure Drop

$$\Delta p = \frac{qB\mu}{2a_1 k_{xyz} r_s} \left[ 1 - \sqrt{\frac{\phi\mu c_t r_s^2}{\pi a_2 k_{xyz}}} \frac{1}{\sqrt{\Delta t}} + S_p \right] \tag{Equation 2}$$

The derivative simplifies to:

$$p'_D h_D = \frac{1}{2\sqrt{\pi \frac{t_D}{r_{sD}^2}}} \tag{Equation 3}$$

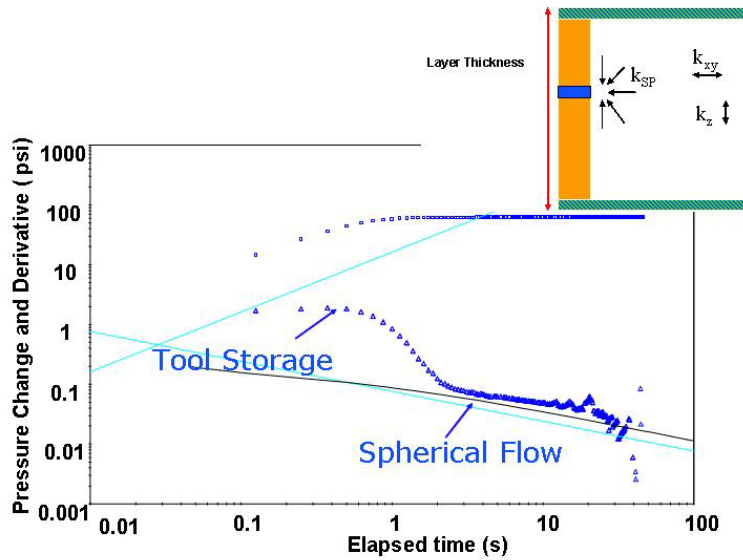


Figure 81 Log-log plot, field example 9. Spherical flow regime developed in middle time pressure derivatives

**Cylindrical Flow (Radial Flow)**

When fluid flows in the formation far from the probe; if the region sampled encounters an upper and lower layer boundary (e.g. a lithological or bed boundary, or a small shale bed or limestone within the sands sampled, which forms boundary for the flow), then the flow geometry changes from a spherical flow to a cylindrical or "radial" flow regime. Radial flow develops if the top and bottom boundaries of the reservoir are no-flow boundaries and these boundaries are close enough for the pressure transients to "reach" and be influenced by them during the test. An example of pressure derivatives indicating stabilization is provided in Figure 72.

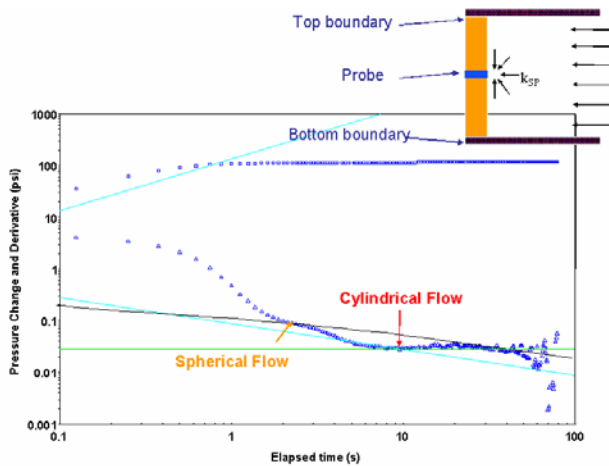


Figure 82 Log-log plot, field example 2. Cylindrical flow regime developed in late time.

The pressure response during radial flow depends only on the horizontal mobility thickness,  $(k_{xy}h/\mu)$ , whilst the time to reach the boundaries depends on the vertical diffusivity  $(k_z/\phi\mu c_i)^{21}$ . Pressure derivatives were expressed in dimensionless term:

$$p_D' = \frac{1}{2} \tag{Equation 4}$$

Pressure derivative was rewritten in dimensional form as<sup>21</sup>:

$$\Delta p' = \frac{qB\mu}{2a_1k_{xy}h} \tag{Equation 5}$$

When a cylindrical flow model is diagnosed in pressure derivative curves, the vertical to horizontal permeability ratio can be calculated if the distances to the upper and lower layer boundary are known from an independent source e.g. a borehole image log or a core. The upper and lower layer boundary distances can be estimated relative to the probe location. In this example, the boundaries are sandstone-mudstone contacts. Using the analytical solution for a cylindrical flow model and boundary distances of 1.6 ft for both top and bottom boundaries, a vertical to horizontal permeability ratio of 0.48 can be calculated. In the same way, if the vertical to horizontal permeability ratio is known, the boundary distances could be estimated.

From observation of various field data, the WFT tests which have repeated tests at the same depth show that the pressure derivative curve of the pre-test usually indicates a negative half slope, whereas the pressure derivative curve of the repeated test shows stabilization in the late time. This is because the flow in the first period is from the area nearby the probe and therefore, the flow geometry is a spherical flow model. On the other hand, the flow in the repeated test is from the area further away. The flow hits top and bottom boundary and therefore, the flow geometry changes from spherical flow to cylindrical flow models.

**Cylindrical Flow with Extra Boundary**

In addition to layer boundaries oriented "perpendicular" to the wellbore axis and probe orientation, and as a result of the small scale of the radius of investigation, extra boundaries (as shown on the top right of Figure 73), i.e. small shale body or fracture, which lie parallel but close to the wellbore, can also induce turbulence which is evident in pressure derivative curves. Figure 73 illustrates a field example for a test in which the pressure derivative deviates from the cylindrical flow stabilization. In this example, the spherical and cylindrical flow can be seen at the time before 1 second. Then the pressure derivative curve trends upward in the late time and then stabilizes at a value twice that of the first stabilization level, indicating the presence of a further no-flow boundary. Subsequently however, after circa 30 seconds, the pressure derivative deviates downward again, stabilizing at a level equivalent to the first stabilisation of cylindrical flow. The re-stabilisation trend in the late time after 30 seconds indicates that the wellbore parallel feature detected does not form a continuous no flow boundary. Fluids at distance in the formation can bypass this boundary to reach the probe in the late time. The results of advanced pressure transient analysis indicate that the wellbore perpendicular boundary is 0.82 ft away from the wellbore, and the radius of investigation<sup>2</sup> of this example pressure test was 10 ft.

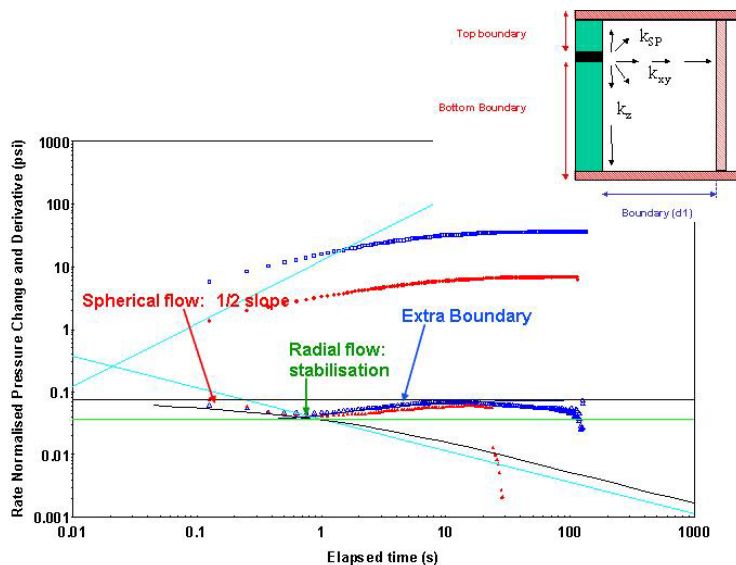


Figure 83 Log-log plot, field example 3. Cylindrical flow regime with extra boundary developed in late time

Fields examples for cylindrical and cylindrical flow with extra boundary show clearly that the use of PTA technique provides more details of reservoir heterogeneities at the sample scale of the wireline formation test tool. The layer boundaries and extra boundary information, e.g. distances from the wellbore, size of the extra boundary, can be input directly into a reservoir simulation model for more accurate simulation results.

## 10. Theory and Equations - Formation Rate Analysis (FRA) and Drawdown Mobility calculated from Field

### Formation Rate Analysis (FRA)

The FRA theory is based on the material balance for the tool's flow-line volume. The key contribution of FRA is to use formation rate in the Darcy Equation instead of piston withdrawal rate. Formation rate is calculated by correcting the piston rate for tool storage effects. Representing the complex flow geometry of probe testing with a geometric factor makes the FRA technique more practical, from which we obtain  $p^*$ , permeability, and fluid compressibility. The Darcy equation is expressed with a geometric factor for isothermal, steady-state flow of a liquid when inertial flow (Forchheimer) resistance is negligible,

$$q_f = \frac{k G_o r_i (p^* - p(t))}{\mu}, \quad \text{Equation 6}$$

where  $q_f$  is the volumetric flow rate into the probe from the formation,  $p^*$  is the formation pressure, and  $p(t)$  is the pressure in the probe.  $G_o$  is a geometric factor that accounts for the complex formation flow geometry and  $r_i$  is the probe radius.

When the variation in fluid density is small, the conservation of mass requires that the accumulation rate,  $q_{ac}$ , should be equal to the difference between formation rate,  $q_f$ , and the drawdown rate,  $q_{dd}$ .  $q_{ac} = q_f - q_{dd}$ . Using the definition of isothermal compressibility, the accumulation rate can be expressed as,

$$q_{ac} = C_t V_t \frac{dp(t)}{dt}, \quad \text{Equation 7}$$

where  $V_t$  is the volume in the tool including probe, flow lines and drawdown chambers and the term  $C_t V_t$  is called the compressive storage of the measuring system. After rearranging the material balance equation, we arrive at the following equation:

$$p(t) = p^* - \frac{\mu C_t V_t}{k G_o r_i} \frac{dp(t)}{dt} - \frac{\mu}{k G_o r_i} q_{dd}. \quad \text{Equation 8}$$

Since  $dp/dt$  and  $q_{dd}$  are the only non-constant variables on the right hand side of equation, the multi-linear regression technique can be used to simultaneously obtain two slopes and an intercept:

$$\frac{\mu C_t V_t}{k G_o r_i}, \quad \frac{\mu}{k G_o r_i}, \quad \text{and} \quad P^* \quad \text{Equation 9}$$

From the slope of  $q_{dd}$ , formation permeability is calculated when the fluid viscosity is known. The slope of the derivative term is to calculate the system compressibility.

The equation can be rearranged to,

$$p(t) = p^* - \left( \frac{\mu}{kG_o r_i} \right) \left( C_t V_t \frac{dp(t)}{dt} + q_{dd} \right) \quad \text{Equation 10}$$

Note that the terms within the last parentheses in the equation correspond to accumulation and drawdown rates, respectively. They act against each other during a drawdown period and together during a buildup period, but the combination, in essence, is the flow rate from the formation

$$q_f = \left( C_t V_t \frac{\partial P(t)}{\partial t} + q_{dd} \right) \quad \text{Equation 11}$$

A plot of  $P(t)$  vs. formation rate should approach a straight line with a negative slope and an intercept  $P^*$  at the  $P(t)$  axis. The absolute value of the slope,  $m$ , is

$$m = \frac{\mu}{kG_o r_i} \quad \text{Equation 12}$$

and permeability is calculated from

$$k = \frac{\mu}{G_o r_i m} \quad \text{Equation 13}$$

In order to apply the FRA method, the drawdown rate,  $q_{dd}$ , should be a function of time not an average piston rate as in the conventional methods. RCI<sup>SM</sup> measures the drawdown volume as a function of time and therefore the drawdown rate at each moment can be calculated. When drawdown rates are not available as in the case of FMT data, only the buildup portion of the test can be considered because the FMT was not designed to measure the drawdown piston rate. In this case a value for compressibility of fluid must be assumed.

Apart from estimating permeability and formation pressure, FRA can be used as a simple graphical quality indicator.<sup>4</sup> Tests with poor graphical correlation (deviation from a straight line) indicate possible problem(s) during the test. Problems include inadequate drawdown rate, insufficient drawdown volume, plugging, tool problem, etc. Tests with poor graphical correlation often are not included in the interpretation if other supporting factors, such as falling in a gradient line, good correlation with nearby well, etc., are not provided.

#### **Drawdown mobility and Final build-up pressure calculated in the RCI field plot**

For a drawdown pressure test, the ECLIPS surface acquisition system produce a real time plot, as shown in a next figure. The system automatically picks the hydrostatic pressure, the flowing pressure and the formation pressure. The system will also pick the start and the end point for the drawdown with corresponding time and the pressures.

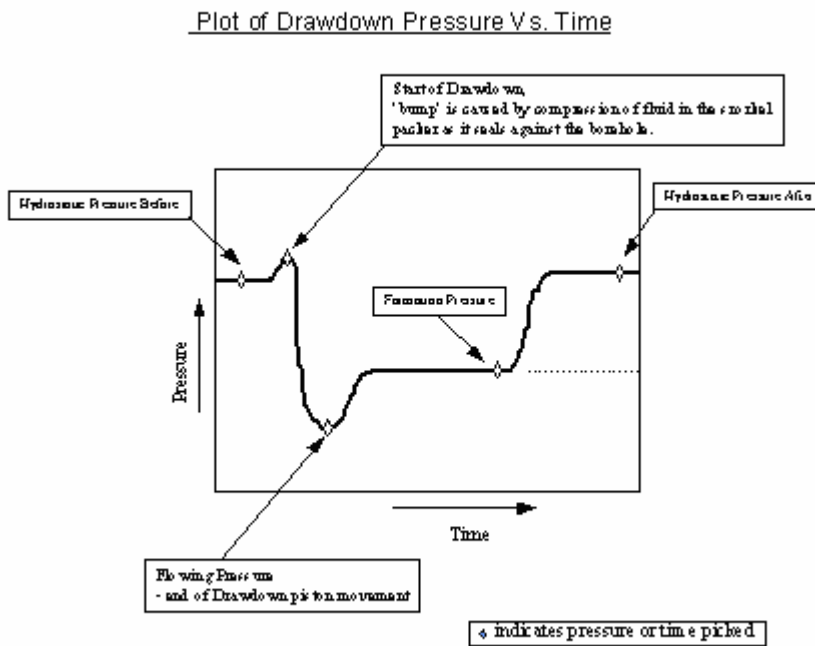


**Figure 84 Plot of Drawdown Pressure versus Time**

It is important to note that the drawdown permeability is derived from the build up portion of pressure curve. The minimum pressure, or flowing pressure is the result of the drawdown taking place.

**Mobility Estimation in the RCI field plot:**

**1) Error in flow rate**

The drawdown rate is the average rate, which is mostly smaller than the maximum formation rate. Because the maximum pressure difference ( $P_{fbu} - P_{flowing}$ ) is used in the calculation, smaller rate means less mobility.

**2) Error in the equation - flow model**

From '*Formation Multi-Tester (FMT) Principles, Theory, and Interpretation*'.

It states

$$\frac{k}{\mu} = 1842 \times C \times \frac{q}{d \Delta p}, \quad \text{Equation 14}$$

where C is the flow shape factor, q is the flow rate in cc/s, d is the probe diameter in inch, and  $\Delta p$  is the pressure drawdown ( $P_{fbu} - P_{flowing}$ ) in psi.

where

$$\text{Flowrate(cc/sec)} = \frac{\text{drawdown chamber volume}}{\text{fill time}} \quad \text{Equation 15}$$

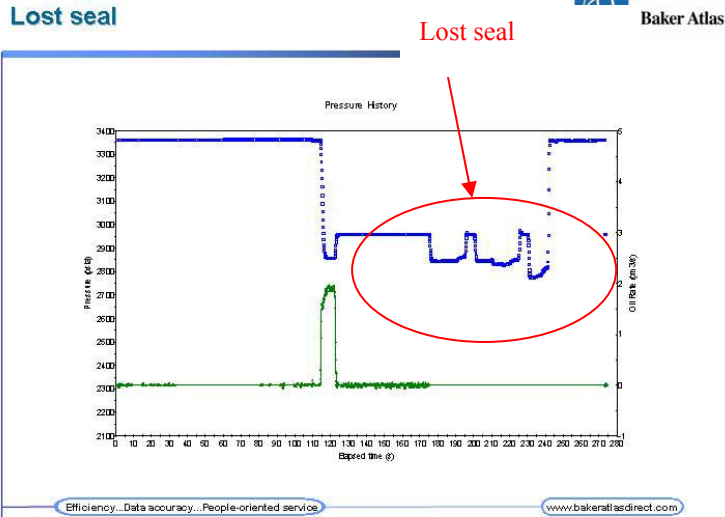
$$\text{Drawdown Pressure}(\Delta p) = \text{Sandface Pressure} - \text{Flowing Pressure}(\text{psi}) \quad \text{Equation 16}$$

## 11. Example of FRA plot indicating some problem

In real time, the pressure history (plot of pressure versus time) and FRA plots can be used to identify lost seal, super-charging effect, tight formation and dry test effects.

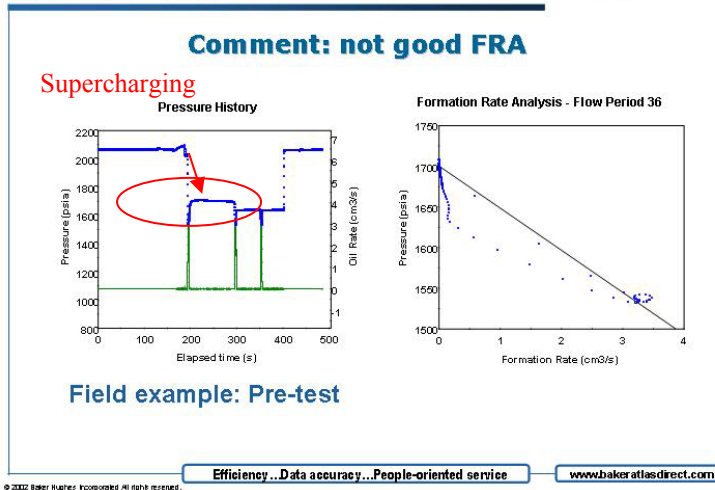
Examples of tests with not FRA compliance:

- Lost seal



- Supercharging

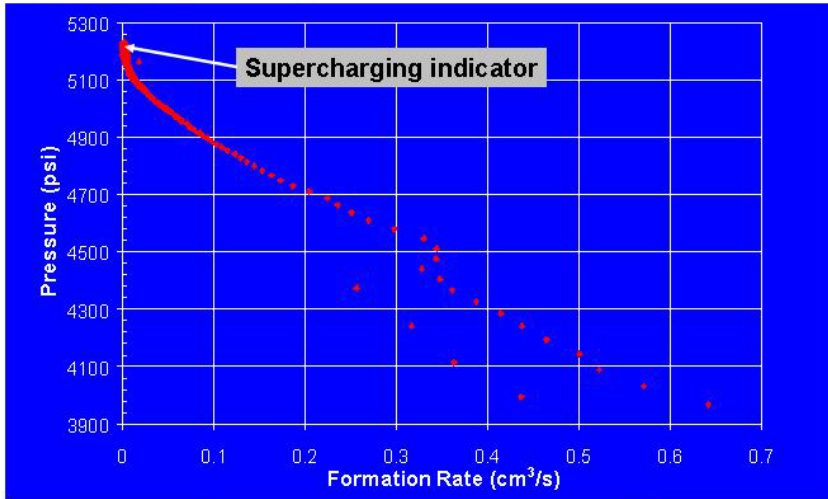
Formation Sampling and Testing Efficiency  
Hydrocarbon Quality



## Formation Sampling and Testing Efficiency Hydrocarbon Quality



### Supercharging in a FRA plot



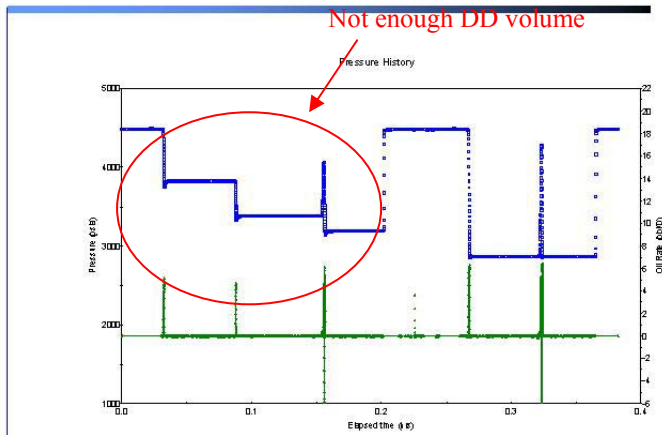
Efficiency...Data accuracy...People-oriented service

[www.bakeratlasdirect.com](http://www.bakeratlasdirect.com)

© 2012 Baker Hughes Incorporated. All rights reserved.

- Not enough drawdown

### Not enough drawdown volume



Efficiency...Data accuracy...People-oriented service

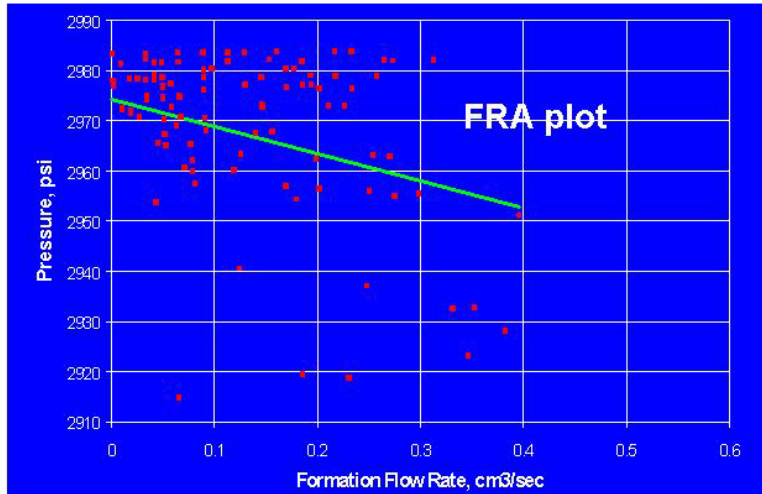
[www.bakeratlasdirect.com](http://www.bakeratlasdirect.com)

© 2012 Baker Hughes Incorporated. All rights reserved.

**Formation Sampling and Testing Efficiency  
Hydrocarbon Quality**



**Drawdown Volume**



Efficiency...Data accuracy...People-oriented service [www.bakeratlasdirect.com](http://www.bakeratlasdirect.com)

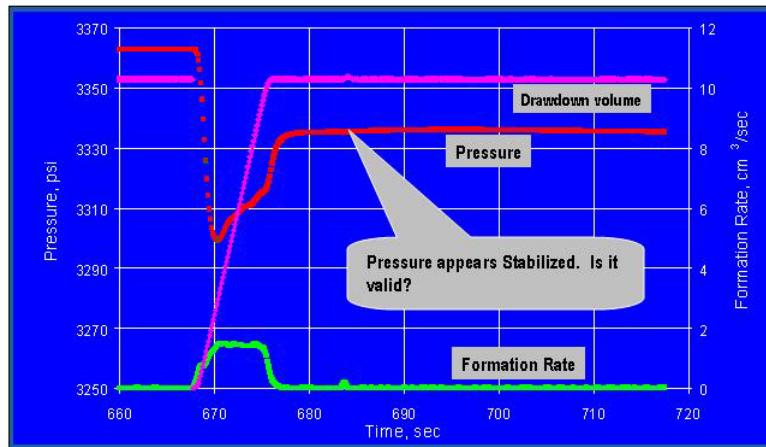
© 2012 Baker Hughes Incorporated. All rights reserved.

- Probe plugging

**Formation Sampling and Testing Efficiency  
Hydrocarbon Quality**



**Probe Plugging**



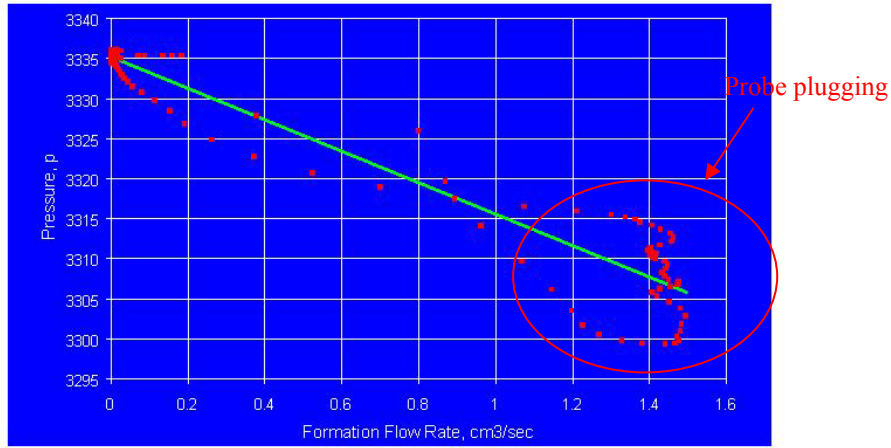
Efficiency...Data accuracy...People-oriented service [www.bakeratlasdirect.com](http://www.bakeratlasdirect.com)

© 2012 Baker Hughes Incorporated. All rights reserved.

**Formation Sampling and Testing Efficiency  
Hydrocarbon Quality**



**Probe Plugging**

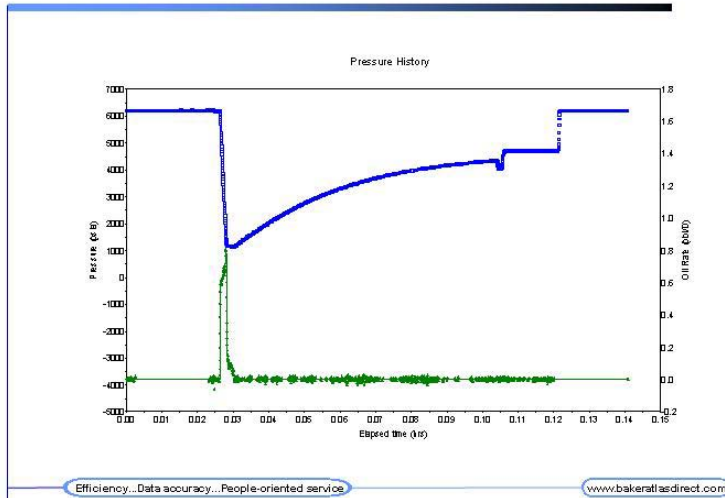


Efficiency...Data accuracy...People-oriented service [www.bakeratlasdirect.com](http://www.bakeratlasdirect.com)

© 2012 Baker Hughes Incorporated. All rights reserved.

- Tight formation

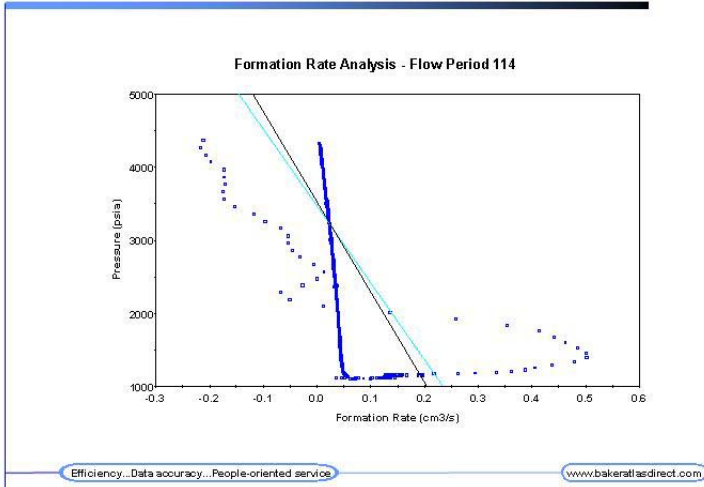
**Tight Formation**



Efficiency...Data accuracy...People-oriented service [www.bakeratlasdirect.com](http://www.bakeratlasdirect.com)

© 2012 Baker Hughes Incorporated. All rights reserved.

## FRA plot for Tight Formation



© 2012 Baker Hughes Incorporated. All rights reserved.

REFERENCES

1. Kasap, E., Georgi, D., Michaels, J., and Shwe, T.: "A New Simplified, Unified Analysis Wireline Formation Tests Data," paper presented at the 1996 SPWLA Annual Logging Symposium, New Orleans, Louisiana, June 16-19, 1998.
2. Kasap, E., Huang, K., Shwe, T. and Georgi, D.: "Formation-Rate-Analysis Technique: Combined Drawdown and Buildup Analysis for Wireline Formation Test Data," *SPEREE*, June 1999, **273**.
3. Ekrem Kasap and Jaedong Lee: "Analysis of Wireline Formation Test Data from Gas and Non-Darcy Flow Conditions," *SPEREE*, April 1999, **116**.
4. Jaedong Lee and John Michaels: "Enhanced Wireline Formations Tests in Low-Permeability Formations: Quality Control Through Formation Rate Analysis," SPE 60293, paper presented at the 2000 SPE Rocky Mountain Regional/Low Permeability Reservoirs Symposium, Denver, CO, 12-15 March 2000.
5. Whittle, T.M., Lee, J., and Gringarten, A. C.: "Will Wireline Formation Tests Replace Well Tests?," *SPE 84086*, presented at the SPE Annual Technical Conference and Exhibition, Denver, Colorado, 5-8 October 2003.
6. Bourdet, D., Whittle, T. M., Douglas, A. A., and Pirard, Y. M.: "A New Set of Type Curves Simplified Well Test Analysis," *World Oil* (May 1983), pp 187-195.
7. Stewart, G., and Wittmann, M.: "Interpretation of the Pressure Response of the Repeat Formation Tester," *SPE 8362*, presented at the 54<sup>th</sup> Annual Fall Technical Conference and Exhibition of the Society of Petroleum Engineers of AIME, Nevada, 23-26 September 1979.
8. Whittle, T.: "Advanced Well Test Analysis Workshop with Interpret 2001," Unpublished Course Notes, 2002.
9. Baker Hughes, "Reservoir Characterization Instrument," *Training Manual* published, 1999.
10. Gringarten, A. C.: "Computer-Aided Well Test Analysis," *SPE 14099*, presented at the SPE 1986 International Meeting on Petroleum Engineering held in Beijing, China, 17-20 March 1986

## **APPENDIX 6**

---

# **HYDROCARBON CHARACTERISATION STUDY – MOBY-1**

---

**By Geotechnical Services Pty Ltd**

**HYDROCARBON  
CHARACTERISATION  
STUDY**

**MOBY-1**

**PROFESSIONAL OPINION**

Prepared by:  
Christine West

Prepared for:  
Bass Strait Oil Company Ltd

May 2005



41- 45 Furnace Road, Welshpool, Western Australia. 6106  
Locked Bag 27, Cannington, Western Australia. 6987  
Email: [geotech@geotechnical-services.com.au](mailto:geotech@geotechnical-services.com.au)

**GEOTECHNICAL  
SERVICES PTY LTD**

Telephone: (08) 9458 8877 (24 Hours)  
Facsimile: (08) 9458 8857  
ACN 050 543 194



**Quality  
Endorsed  
Company**  
ISO 9002 Lic 10551  
Standards Australia  
ABN 58 050 543 194

## **EXECUTIVE SUMMARY**

A sample suite from Moby-1, drilled by Bass Strait Oil Company Ltd, was submitted for geochemical analyses. The sample suite comprised the following samples:

- ❖ one mud sample from 550m
- ❖ one oil sample from 588.5m
- ❖ six sidewall cores in the depth range 560m to 588m taken from a “dirty” reservoir.

The purpose of this report is to characterise the hydrocarbons extracted from the sediments in terms of source, maturity and depositional environment, and to then correlate these with the Moby-1 oil.

### ***Sidewall Core Extracts from Reservoir***

The six sidewall core extracts in the depth range 560m to 588m are all biodegraded to the extent that no n-alkanes are visible in the saturate chromatograms. Based on biomarker data from the 560m and 586m extracts, the hydrocarbons are characterised as mature and are thought to be sourced from strongly terrestrial organic matter, possibly with some resin input.

### ***Oil***

The fluid sample collected from Moby-1 is severely contaminated with alkene-based drilling fluid, the profile of which is similar to Isoteq or LAOs. The origin of this contamination is uncertain given that the mud reports do not list any alkene-containing components. Given that none of the sidewall core extracts show any sign of alkene contamination, it is likely that contamination of the fluid sample has occurred, possibly through the use of a dirty sample container when collecting or transferring the fluid.

The Moby-1 fluid also contains a low abundance of biodegraded hydrocarbons. It is uncertain whether these hydrocarbons are naturally occurring or whether they are associated with the alkene contaminant. The biodegraded nature of both this fluid and the Moby-1 sediment extracts suggests that the hydrocarbons may be natural. However, other geochemical data (eg branched/cyclic and aromatic GC-MS) suggest that the fluid is different to the extracts and hence is more likely due to contamination. Overall, it is believed that the biodegraded hydrocarbons detected in the Moby-1 fluid should not be considered characteristic of Moby-1.

**HYDROCARBON CHARACTERISATION STUDY**

**MOBY-1**

**TABLE OF CONTENTS**

	<b>Page Number</b>
<b>1 INTRODUCTION</b>	<b>4</b>
<b>2 ANALYTICAL PROCEDURES</b>	<b>5</b>
<b>2.1 MUD SAMPLE</b>	<b>5</b>
<b>2.2 OIL SAMPLE</b>	<b>5</b>
<b>2.3 SEDIMENTS</b>	<b>5</b>
<b>3 RESULTS AND INTERPRETATION</b>	<b>6</b>
<b>3.1 MUD SAMPLE</b>	<b>6</b>
<b>3.2 OIL SAMPLE</b>	<b>6</b>
<b>3.3 SEDIMENTS</b>	<b>9</b>
<b>3.4 CORRELATION OF MOBY-1 OIL AND SEDIMENT EXTRACTS</b>	<b>13</b>
<b>4 CONCLUSION</b>	<b>18</b>
<b>5 REFERENCES</b>	<b>20</b>

**APPENDIX A: DATA AND TABLES**

**APPENDIX B: THEORY AND METHODS**

## 1 INTRODUCTION

A sample suite from Moby-1, drilled by Bass Strait Oil Company Ltd, was submitted for geochemical analyses. The sample suite comprised the following samples:

- ❖ one mud sample from 550m
- ❖ one oil sample from 588.5m
- ❖ six sidewall cores in the depth range 560m to 588m taken from a “dirty” reservoir.

The purpose of this report is to characterise the hydrocarbons extracted from the sediments in terms of source, maturity and depositional environment, and to then correlate these with the

One hardcopy and one electronic copy of this report have been sent to Bob Fisher at Bass Strait Oil Company Ltd. Any queries related to it may be directed to Christine West or Dr Birgitta Hartung-Kagi at Geotechnical Services Pty Ltd.

All data and information are proprietary to Bass Strait Oil Company Ltd and regarded as highly confidential by all Geotech personnel.

Geotechnical Services has endeavoured to use techniques and equipment to achieve results and information as accurately as it possibly can. However, such equipment and techniques are not necessarily perfect. Therefore, Geotechnical Services shall not be held responsible or liable for the results of any actions taken on the basis of the information contained in this document. Moreover, this report should not be the sole reference when considering issues that may have commercial implications.

## 2 ANALYTICAL PROCEDURES

### 2.1 MUD SAMPLE

A mud sample from 550m was solvent extracted and the extract analysed by GC-MS. No further work was conducted on the sample.

### 2.2 OIL SAMPLE

An oil sample from 588.5m (labelled Test #37) was initially analysed according to Geotech's whole oil GC-MS protocol. This analysis indicated that the sample was almost entirely alkene-based drilling fluid and hence the analytical programme was put on hold. The oil was subsequently submitted for liquid chromatography, alkene removal and GC-MS of the saturate fraction to determine whether any natural hydrocarbons were present. Aromatic and branched/cyclic GC-MS were also conducted.

### 2.3 SEDIMENTS

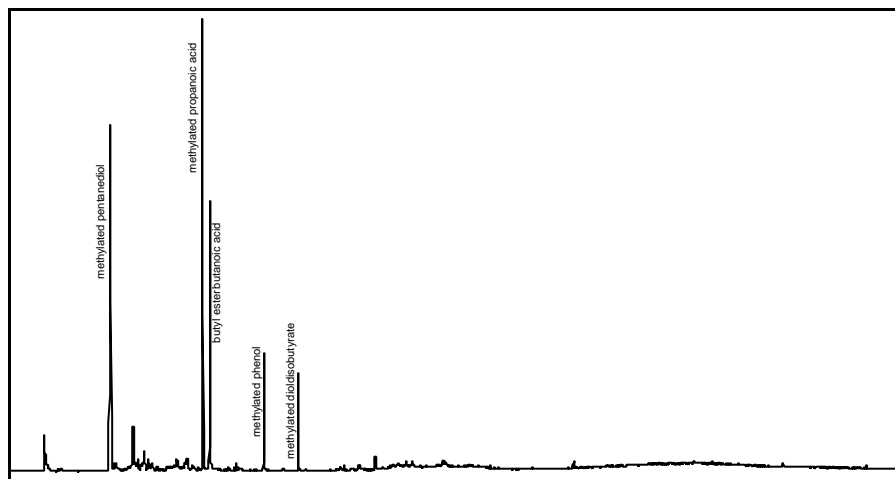
Six sidewall cores in the depth range 560m to 588m were submitted for solvent extraction and characterisation of the sediment extracts. The extracts were initially analysed by GC-MS and then submitted for liquid chromatographic separation. The saturate and aromatic fractions were analysed by GC-MS. The saturate fraction was treated with ZSM5 molecular sieves to isolate the branched/cyclic compounds and these were then analysed by GC-MS.

### 3 RESULTS AND INTERPRETATION

#### 3.1 MUD SAMPLE

Moby-1 was drilled using a KCl/polymer mud system. The mud sample from 550m yielded 5ppm of extract, suggesting that it contains a very low amount of extractable hydrocarbons. This yield is consistent with a KCl/polymer mud system. GC-MS analysis of the extract indicates that the mud comprises mainly organic acids and alcohols (Figure 1).

Figure 1: Chromatogram obtained by GC-MS analysis of the whole extract from the mud sample taken at 550m.



Due to the low hydrocarbon content of the mud and the lack of visible natural hydrocarbons (eg n-alkanes) in the whole extract chromatogram, no further work was conducted on this sample.

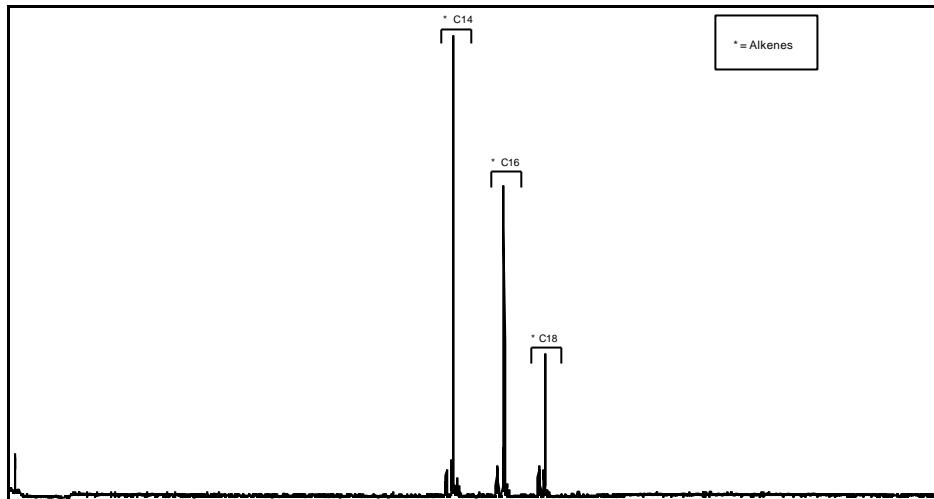
#### 3.2 OIL SAMPLE

The oil sample analysed from Moby-1 was an oil scum collected on top of a formation water sample taken from an RCI sample collected from a depth of 588.5mMD (written communication from client). This oil sample is believed to represent a 3m sand section existing below a “dirty” reservoir (verbal communication with client). Six sidewall cores from this “dirty” reservoir have also been analysed, the data of which are interpreted in Section 3.3.

The sample was initially submitted for whole oil GC-MS and the chromatogram obtained is dominated by alkenes (Figure 2). The lack of visible n-alkanes and other hydrocarbons in the chromatogram suggests that the Moby-1 fluid is heavily contaminated with alkene base fluid. If any natural hydrocarbons are present, their profile is totally masked by the presence of the

alkenes. The origin of the alkenes is uncertain, especially given that the mud at 550m showed no trace of alkenes. Investigation of the mud reports from Moby-1 showed that there is no record of an alkene-containing component being added. The most likely explanation is that a dirty sample container was used to collect the Moby-1 fluid.

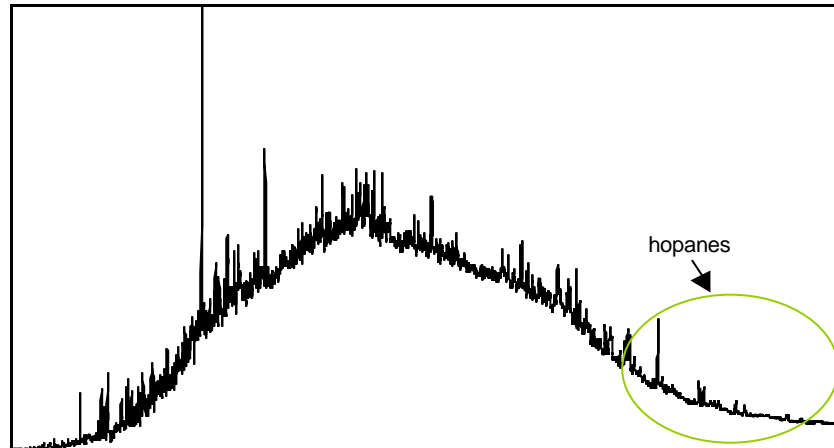
Figure 2: Chromatogram obtained by GC-MS analysis of the whole oil from Moby-1.



The Moby-1 fluid was submitted for liquid chromatographic separation and yielded approximately 63% saturates, 21% aromatics and 16% NSOs (Appendix A Table 1). It is important to note that the saturate component comprises mainly alkenes, but also any other hydrocarbons which may be present. The saturate fraction was then treated to remove the alkene-based compounds. Liquid chromatography data based on the alkene removed data indicate that the oil comprises approximately 44% saturates, 32% aromatics and 24% NSOs (Appendix A Table 3).

The saturate fraction (after alkene removal) was submitted for GC-MS analysis. The chromatogram is dominated by a baseline hump with virtually no n-alkanes present. A series of hopanes is visible in the high molecular weight range (Figure 3). These features are typical of a biodegraded oil. However, it is uncertain whether the hydrocarbons present in the Moby-1 fluid are natural hydrocarbons or whether they are associated with the alkene-based contaminant.

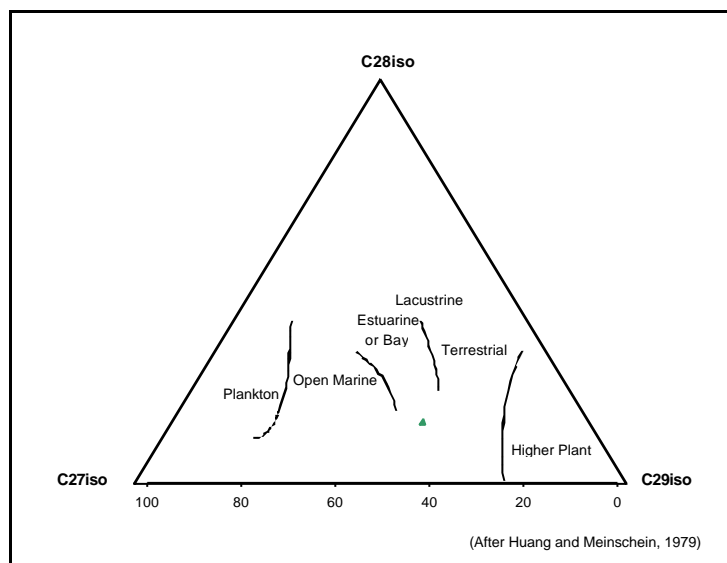
Figure 3: Chromatogram obtained by GC-MS analysis of the saturate fraction of the Moby-1 fluid (alkenes removed).



Assuming that the hydrocarbons present in the Moby-1 fluid were naturally occurring, the aromatic and branched/cyclic fractions from the Moby-1 fluid were submitted for GC-MS analysis in order to characterise the hydrocarbons more fully.

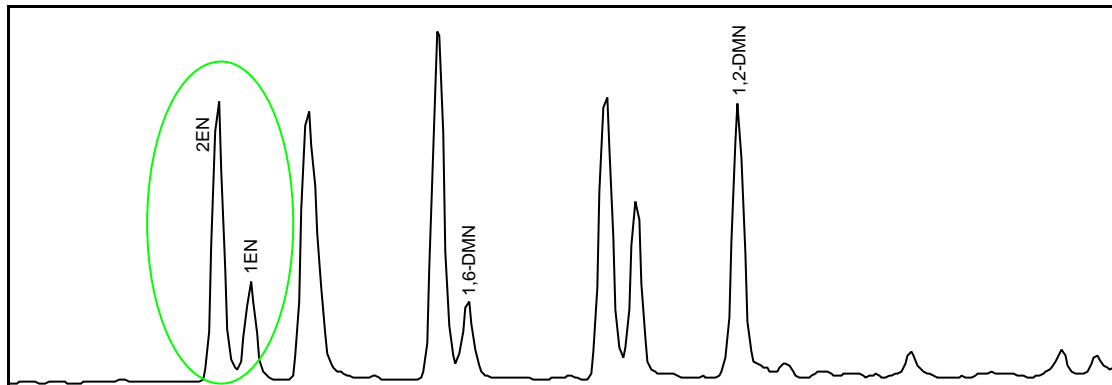
Branched/cyclic GC-MS data characterise the hydrocarbons as fully mature ( $C_{29}S/C_{29}R$  sterane ratio of 1.17). The source is believed to be terrestrial to mixed, as indicated by the  $C_{27}/C_{29}$  diasterane ratio of 0.69 and the corresponding sterane ratio of 1.07. The relative abundance of isosteranes classifies the ecosystem of the source material as an estuary or bay (Figure 4) which is in agreement with the sterane and diasterane assessment. 25-Norhopanes, indicators of severe biodegradation, are present.

Figure 4: Ternary diagram showing the ecosystem of the source material for the Moby-1 fluid.



Aromatic GC-MS data for the Moby-1 fluid has been significantly affected by biodegradation as indicated by the unusual distribution of peaks and the poor peak resolution (Figure 5). Given this, many of the parameters generated by this analysis are believed to be less reliable than the branched/cyclic data. (Note: Branched/cyclic biomarkers are generally more resistant to biodegradation). For example, the MPI of 0.34 (which usually suggests immaturity) is not believed to be accurate.

Figure 5: Fragmentogram (m/z 156) showing the unusual distribution of dimethylnaphthalenes in the Moby-1 fluid.



### 3.3 SEDIMENTS

Six sidewall cores in the depth range 560m to 588m were submitted for solvent extraction and characterisation of the hydrocarbon extracts. The samples were taken from a “dirty” reservoir section (verbal communication with client).

The extract yield varied from 7ppm at 588m to over 20 000ppm at 584m. GC-MS analysis of the extracts showed that all of them are biodegraded to the extent that no n-alkanes are visible in the chromatograms (Figure 6). Of the six extracts analysed, the shallowest five extracts are very similar, whereas the chromatogram for the deepest extract from 588m is different. The compounds observed in the mud extract (refer to Figure 1) were not clearly visible in the sidewall core extracts, suggesting that these had not been contaminated to a significant extent by the mud. No alkenes were apparent in these sediment extracts.

Of the six extracts analysed, five were submitted for liquid chromatography and saturate GC-MS. The remaining extract from 588m yielded insufficient sample material for these analyses. As expected, the saturate chromatograms for the five samples were very similar to the whole extract chromatograms (Figure 7).

Figure 6: Chromatograms obtained by GC-MS analysis of the extracts from Moby-1 SWCs.

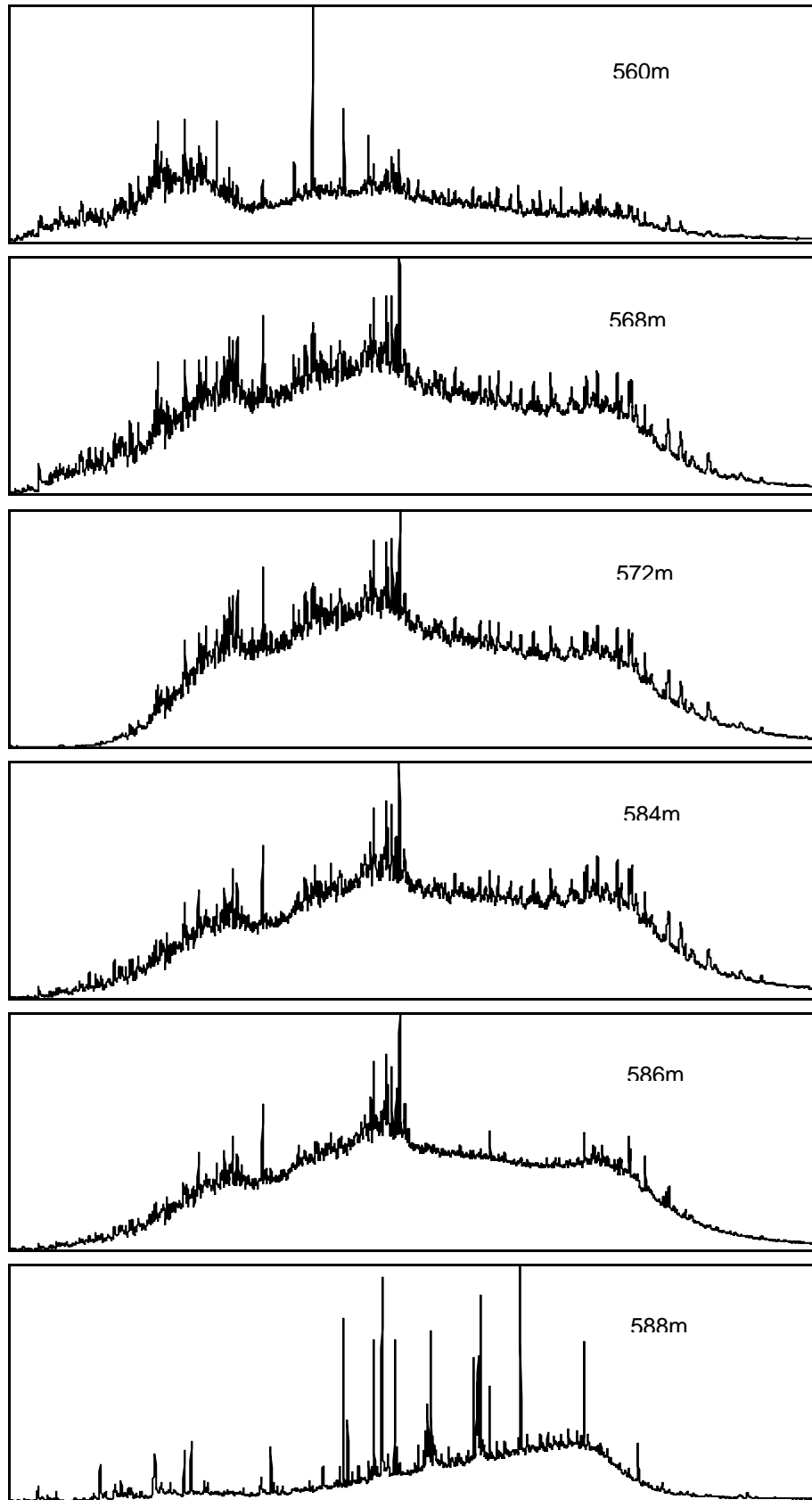
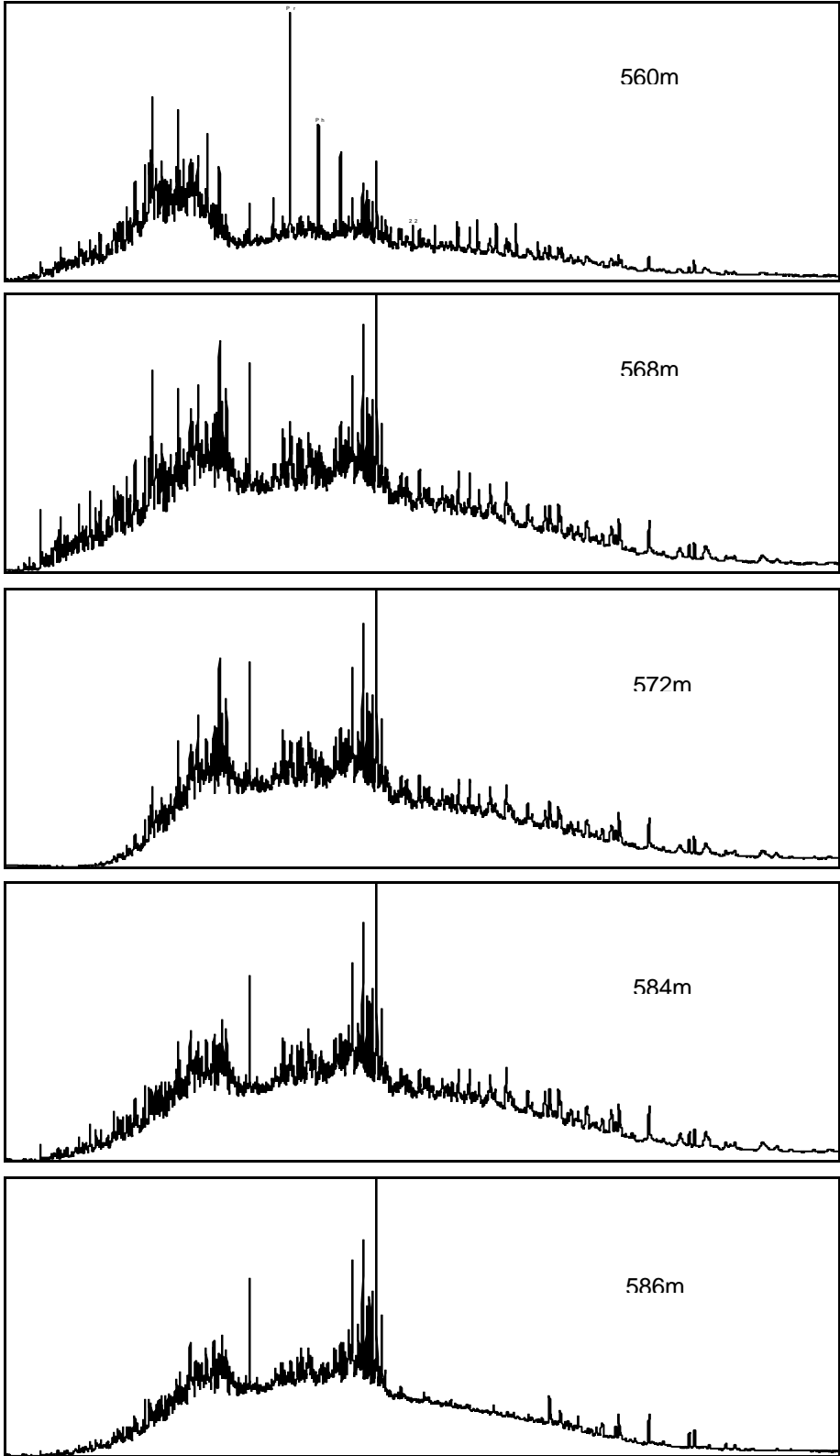


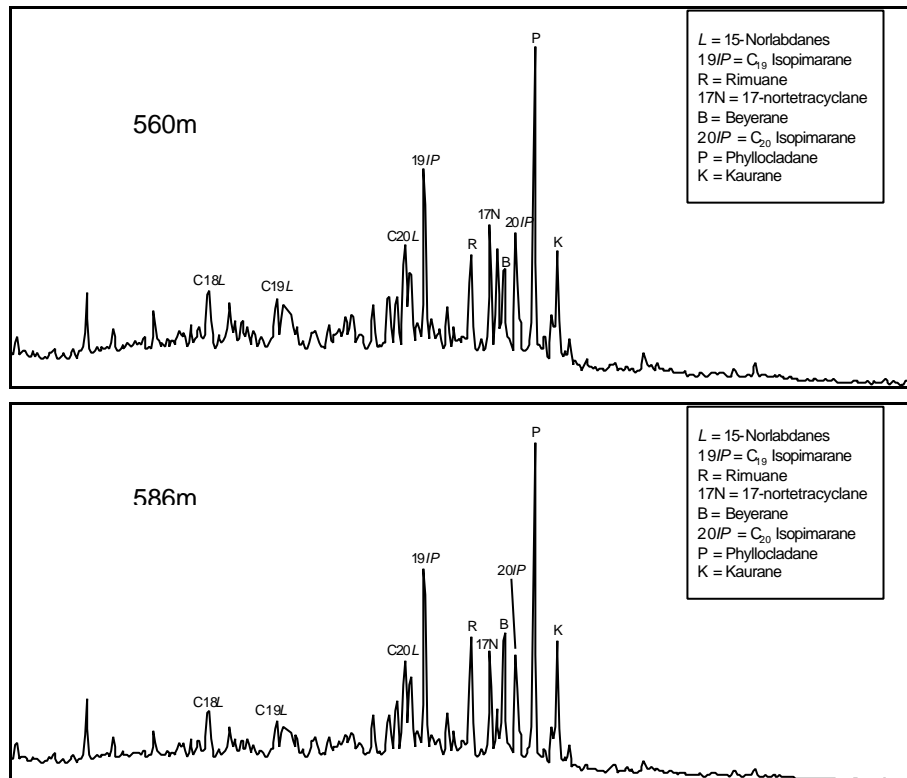
Figure 7: Chromatograms obtained by GC-MS analysis of the saturate fractions from Moby-1 SWCs.



Given the similar nature of the saturate chromatograms, two extracts (560m and 586m) were submitted for aromatic and branched/cyclic biomarker analysis.

The two extracts yielded very similar data, suggesting that the two extracts consist of basically the same hydrocarbons. Both extracts are classified as moderately mature ( $C_{29}S/C_{29}R$  sterane ratios of 0.76 and 0.81, respectively).  $\beta\beta$ -Hopanes, immaturity indicators, have been tentatively identified in these extracts. However, none of the other data suggest immaturity or a mixture of immature and mature hydrocarbons. Both extracts are believed to be sourced from strongly terrestrial organic matter ( $C_{27}/C_{29}$  diasterane ratios of 0.08 and 0.07;  $C_{27}/C_{29}$  sterane ratios of 0.24 and 0.20). A full suite of diterpanes have been identified (eg isopimarane, beyerane, phyllocladane) suggesting higher plant resin input (Figure 8). The ecosystem of the source material is classified as 'higher plant' (Figure 10).

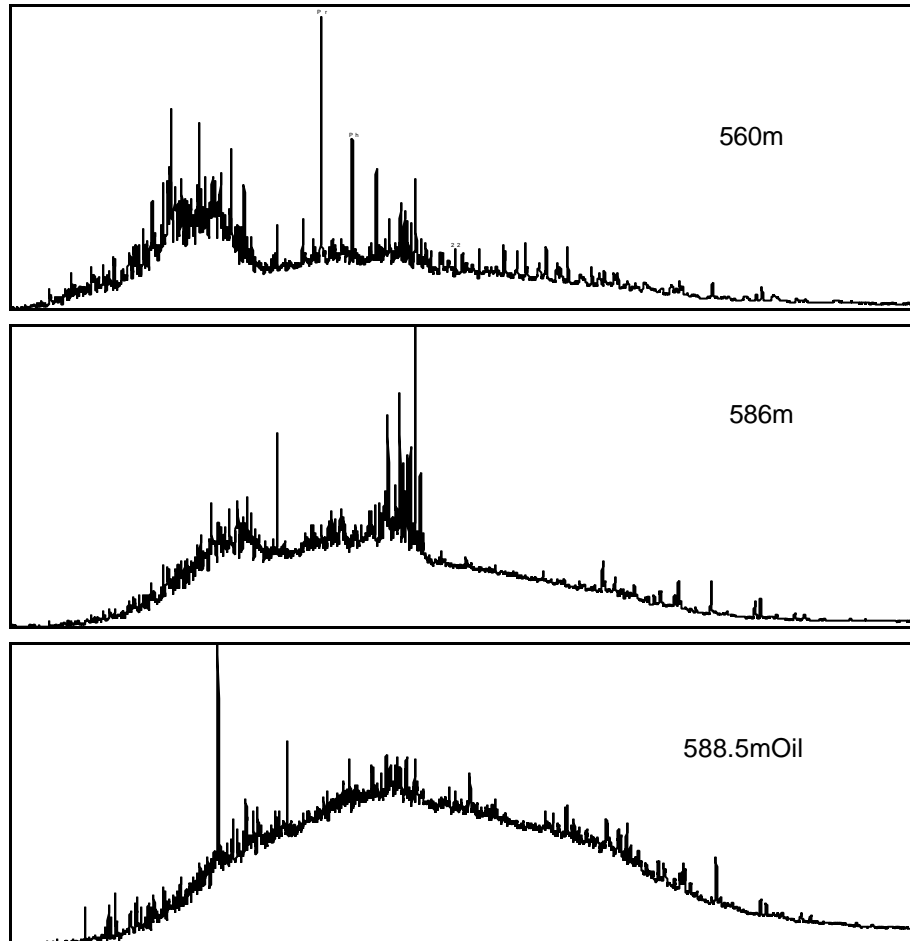
Figure 8: Fragmentogram (m/z 123) showing the presence of diterpanes in the Moby-1 sidewall core extracts.



### 3.4 CORRELATION OF MOBY-1 OIL AND SEDIMENT EXTRACTS

The chromatograms of the Moby-1 sediment extracts and the Moby-1 fluid show some similarities, namely the lack of n-alkanes and the baseline hump (Figure 9). These features are typical of biodegraded hydrocarbons.

Figure 9: Comparison of saturate chromatograms of the Moby-1 oil and sediments.



Although the Moby-1 fluid and the sediment extracts are both biodegraded, there are sufficient differences in the data to suggest that the samples are different. For example, the Moby-1 fluid is believed to be sourced from mixed organic matter whilst the sidewall core extracts are thought to be sourced from strongly terrestrial organic matter. Additionally, the oil is believed to be more mature than the sediment extracts. Given that the oil was sampled so closely in depth to the reservoir samples, it is uncertain as to why there is such a difference between the two groups if the hydrocarbons in the Moby-1 fluid are naturally occurring. It is most likely that the hydrocarbons in the Moby-1 fluid are not characteristic of the well and have been introduced by contamination.

Figure 10: Ternary diagram showing a comparison of the ecosystem of the source material for the Moby-1 samples.

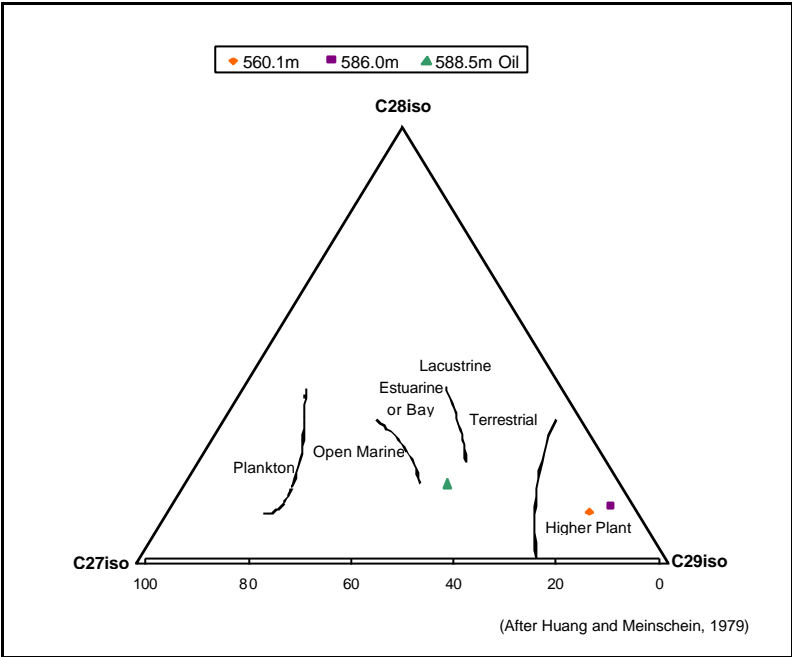


Figure 11: Fragmentogram (m/z 217) showing the sterane distribution in the Moby-1 samples.

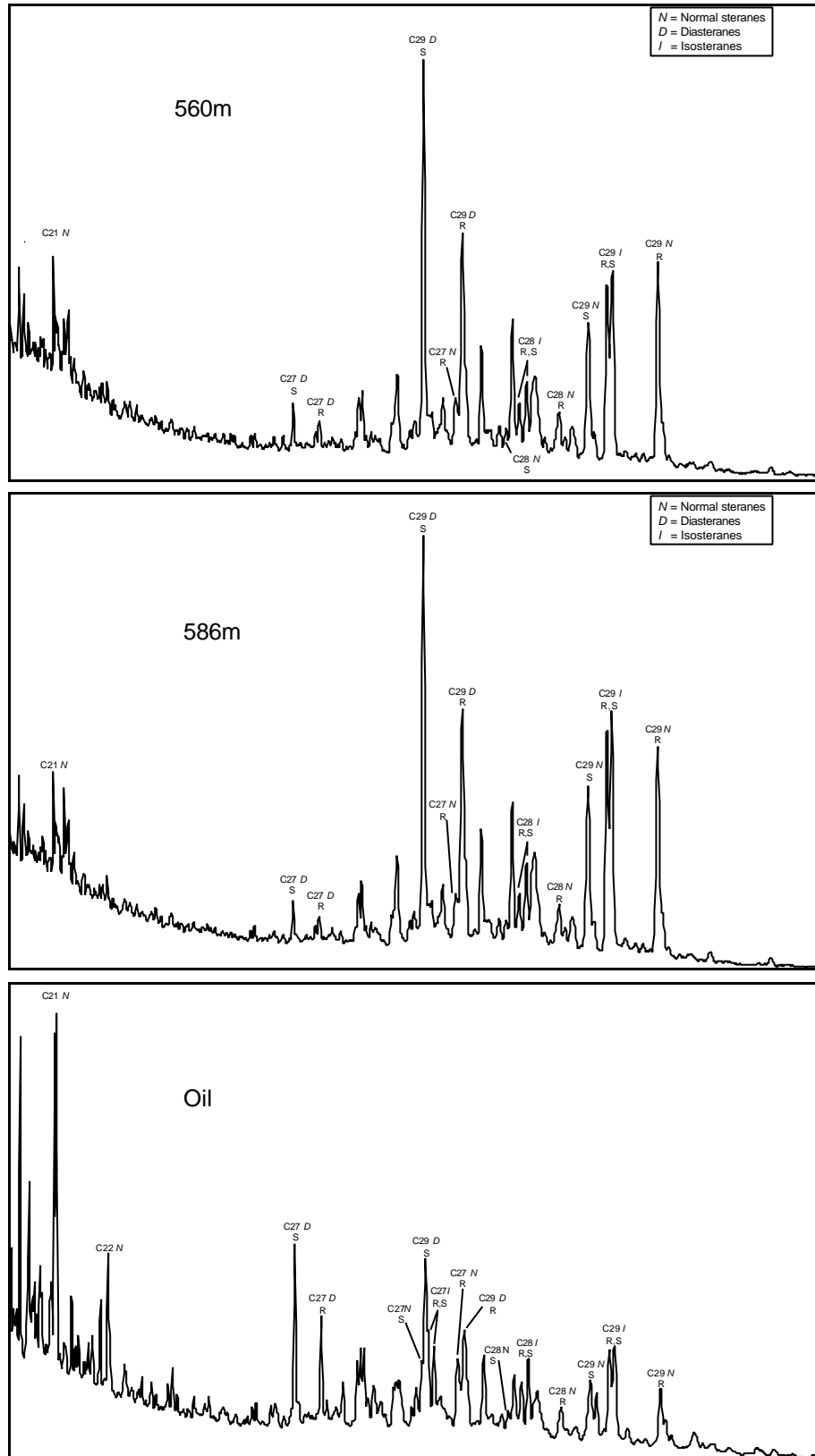


Figure 12: Fragmentogram (m/z 191) showing the hopane distribution in the Moby-1 samples.

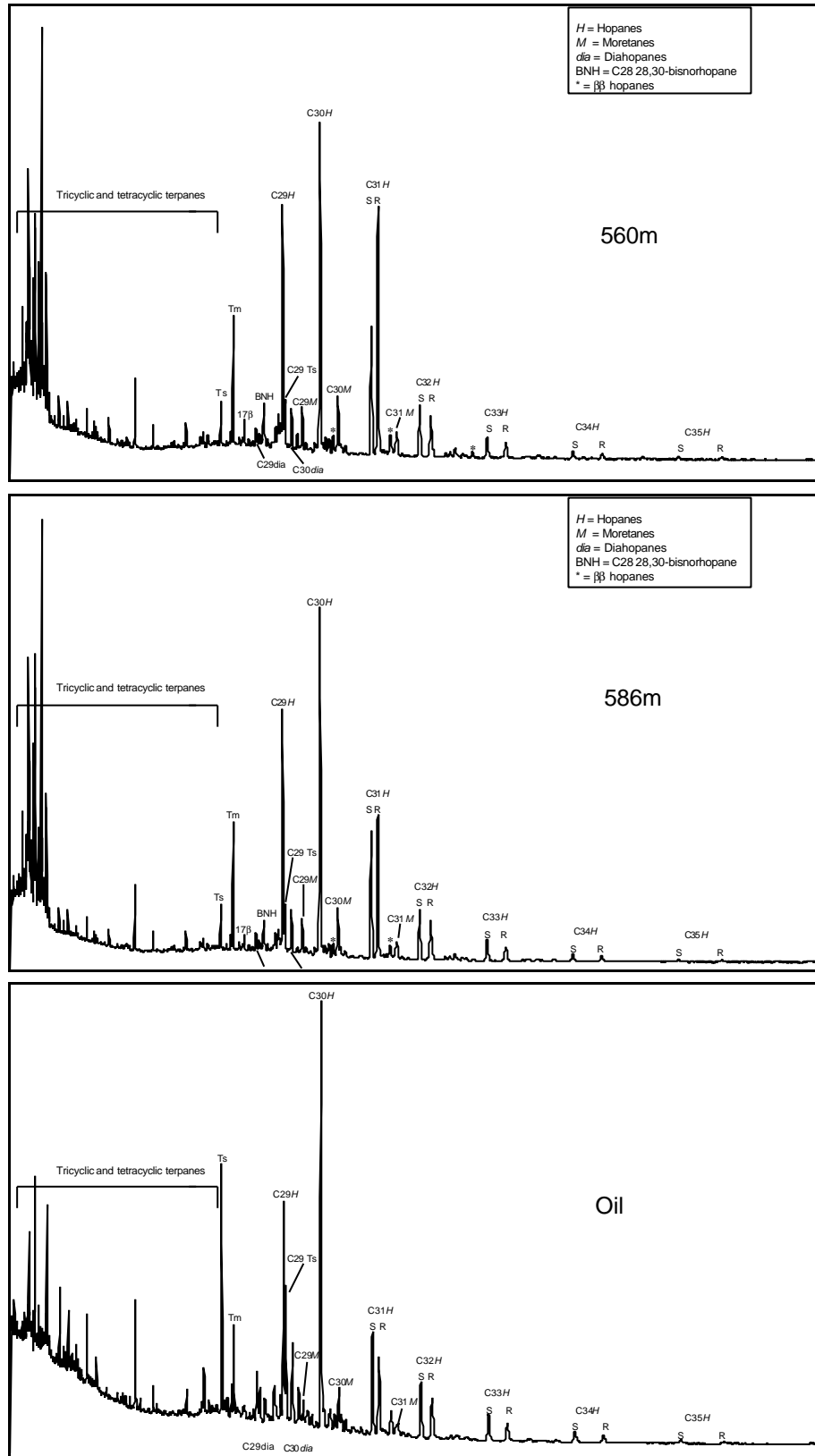
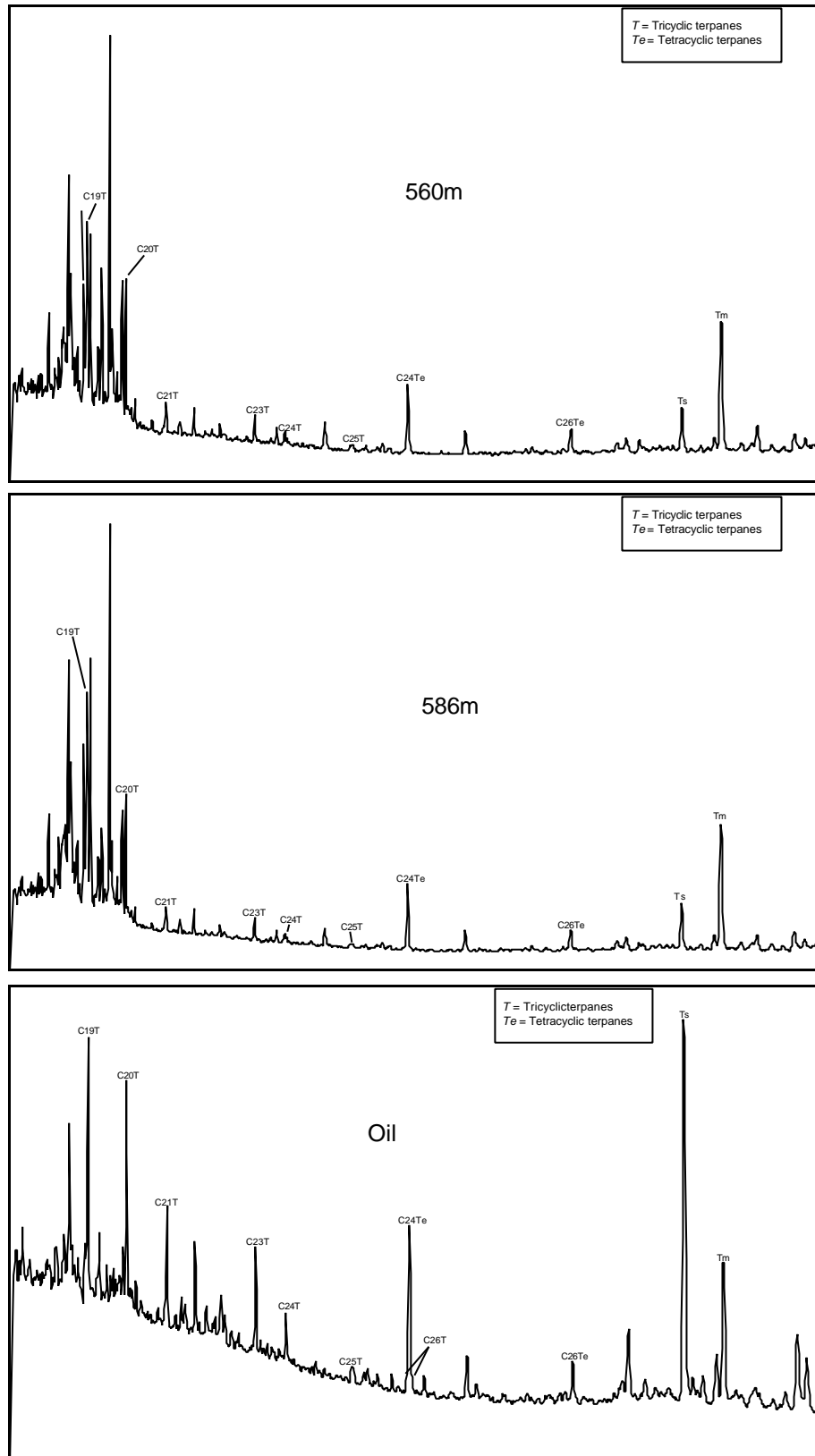


Figure 13: Fragmentogram (m/z 191) showing the tri- and tetracyclic distribution in the Moby-1 samples.



## 4 CONCLUSION

### ***Sidewall Core Extracts from Reservoir***

The six sidewall core extracts in the depth range 560m to 588m are all biodegraded to the extent that no n-alkanes are visible in the saturate chromatograms. Based on biomarker data from the 560m and 586m extracts, the hydrocarbons are characterised as mature and are thought to be sourced from strongly terrestrial organic matter, possibly with some resin input.

### ***Oil***

The fluid sample collected from Moby-1 is severely contaminated with alkene-based drilling fluid, the profile of which is similar to Isoteq or LAOs. The origin of this contamination is uncertain given that the mud reports do not list any alkene-containing components. Given that none of the sidewall core extracts show any sign of alkene contamination, it is likely that contamination of the fluid sample has occurred, possibly through the use of a dirty sample container when collecting or transferring the fluid.

The Moby-1 fluid also contains a low abundance of biodegraded hydrocarbons. It is uncertain whether these hydrocarbons are naturally occurring or whether they are associated with the alkene contaminant. The biodegraded nature of both this fluid and the Moby-1 sediment extracts suggests that the hydrocarbons may be natural. However, other geochemical data (eg branched/cyclic and aromatic GC-MS) suggest that the fluid is different to the extracts and hence is more likely due to contamination. Overall, it is believed that the biodegraded hydrocarbons detected in the Moby-1 fluid should not be considered characteristic of Moby-1.

## 5 REFERENCES

- van Aarssen, B.G.K., Alexander, R. and Kagi, R.I. (2000) Reconstructing the geological history of Australian crude oils using aromatic hydrocarbons. *The APPEA Journal*, 283-292.
- Alexander, R., Kagi, R.I., Rowland, S.J., Sheppard, P.N. and Chirila, T.V. (1985) The effects of thermal maturity on distributions of dimethylnaphthalenes and trimethylnaphthalenes in some Ancient sediments and petroleums. *Geochimica et Cosmochimica Acta* **49**, 385-395.
- Huang, W.-Y. and Meinschein, W.G. (1979) Sterols as ecological indicators. *Geochimica et Cosmochimica Acta* **43**, 739-745.
- Hunt, J.M. (1979) *Petroleum Geochemistry and Geology*. San Francisco: W.H. Freeman.
- Peters, K.E. and Moldowan, J.M., 1993 –The Biomarker Guide - Interpreting molecular fossils in petroleum and ancient sediments. Prentice Hall, Englewood Cliffs, New Jersey 07632.
- Radke, M. and Welte, D.H., 1983 – The methylphenanthrene index (MPI). A maturity parameter based on aromatic hydrocarbons. *Advances in Org. Geochem.*, 1981. J. Wiley and Sons, New York, 504-512.
- Thompson, K.F.M., 1983 – Classification and thermal history of petroleum based on light hydrocarbons. *Geochim. Cosmochim. Acta*. **47**, 303-316.
- Tissot, B.P. and Welte, D.H., 1984 – Petroleum formation and Occurrence. Springer-Verlag, Berlin.
- van Aarssen, B.G.K., Bastow, T.P., Alexander, R and Kagi, R.I., 1999 – Distributions of methylated naphthalenes in crude oils: indicators of maturity, biodegradation and mixing. *Org. Geochem.* **30**, 1213-1227.
- Volkman, J.K., Alexander, R., Kagi, R.I., Rowland, S.J. and Sheppard, P.N., 1984 – Biodegradation of aromatic hydrocarbons in crude oils from the Barrow Sub-basin of Western Australia. *Org. Geochem.* **6**, 619-632.

## **APPENDIX A**

### **DATA AND TABLES**

**DATA AND TABLES**

**MOBY-1**

**TABLE OF CONTENTS**

<b>Analysis</b>	<b>Table</b>	<b>Figure</b>
Whole Oil GC-MS	--	1
Liquid Chromatography (Oil)	1	--
Saturate GC-MS (Oil)	2	2
Liquid Chromatography (Oil, Alkenes Removed)	3	--
Saturate GC-MS (Oil, Alkenes Removed)	4	3
Solvent Extraction	5	4-10
Liquid chromatography (Sediments/Mud)	6	--
Saturate GC-MS (Sediments/Mud)	7	11-15
Aromatic GC-MS	8	16
Branched/cyclic GC-MS	9	17

FIGURE 1

Sample : MOBY-1, 588.5m, Test 37, Oil  
File ID : 345808W



Chromatogram obtained from analysis of the whole oil by GC-MS

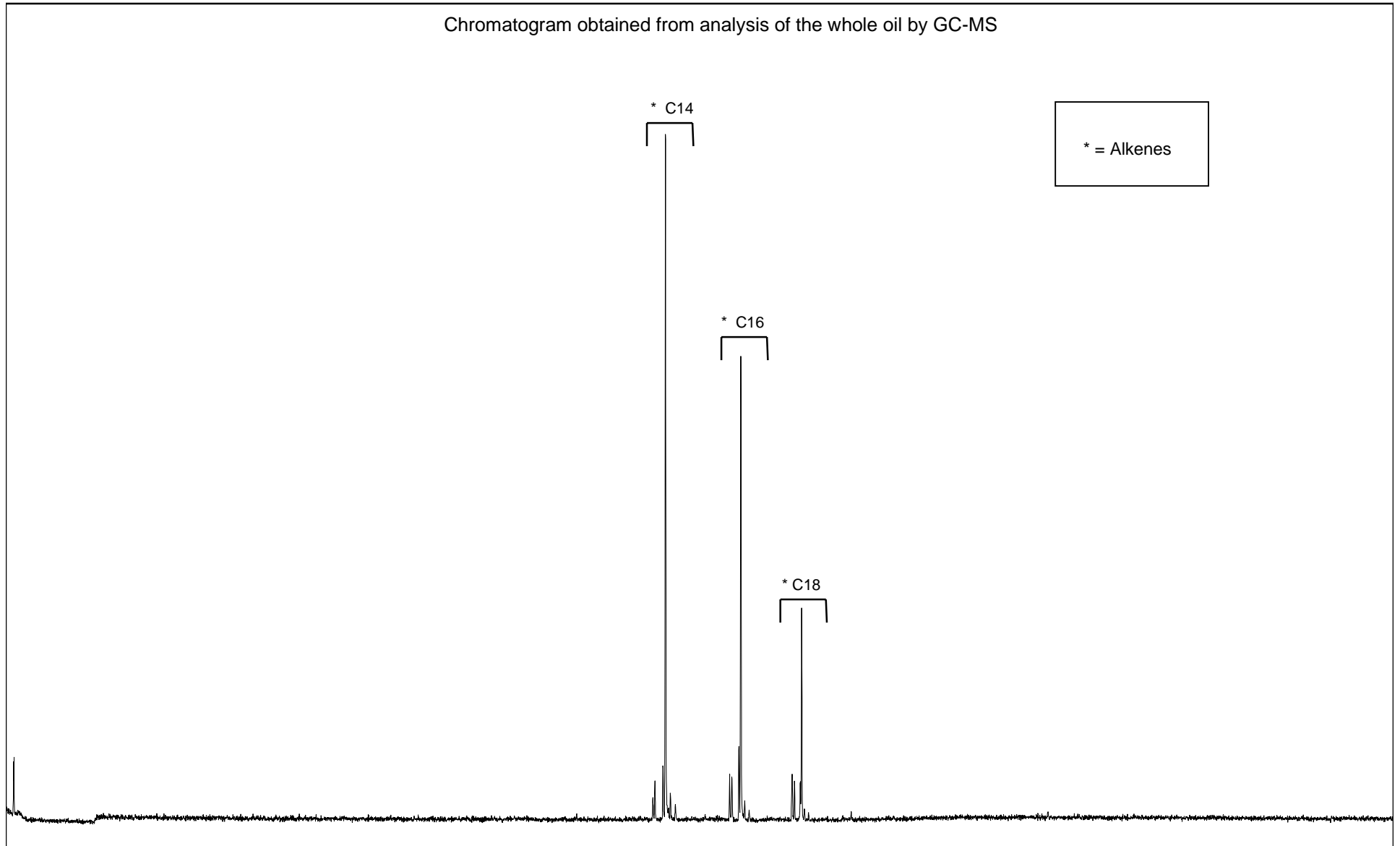


TABLE 1

**LIQUID CHROMATOGRAPHY DATA  
OIL**

**MOBY-1**

Yields (%) and Selected Ratios



DEPTH	Sample Type	-----Hydrocarbons-----			-----Non-hydrocarbons-----			Sats	Asph.	HC
		Sats	Aros	HC's	NSOs	Asph.	Non HC's	Aros	NSO	Non HC
588.5m, Test-37	Oil	63.1	20.9	84.0	16.0	nd	16.0	3.0	nd	5.3

TABLE 2

**ANALYSIS OF SATURATED HYDROCARBONS BY GC-MS**

**OIL**

**MOBY-1**

A. Selected Ratios



DEPTH	Sample Type	Prist./Phyt.	Prist./n-C17	Phyt./n-C18	CPI(1)	CPI(2)	(C21+C22)/(C28+C29)
588.5m, Test-37	Fluid	nd	nd	nd	nd	nd	nd

**MOBY-1**

B. n-Alkane Distributions

DEPTH	nC12	nC13	nC14	nC15	nC16	nC17	Pr	nC18	Ph	nC19	nC20	nC21	nC22	nC23	nC24	nC25	nC26	nC27	nC28	nC29	nC30	nC31
588.5m, Test-37	nd	nd	nd	nd	nd	nd	nd	nd	nd	nd	nd	nd	nd	nd	nd	nd	nd	nd	nd	nd	nd	nd

$$CPI(1) = \frac{(C23+C25+C27+C29)+(C25+C27+C29+C31)}{2 \times (C24+C26+C28+C30)}$$

$$CPI(2) = \frac{(C23+C25+C27)+(C25+C27+C29)}{2 \times (C24+C26+C28)}$$

FIGURE 2

Sample : **MOBY-1, 588.5m, Test-37, Oil**  
File ID : 345808S

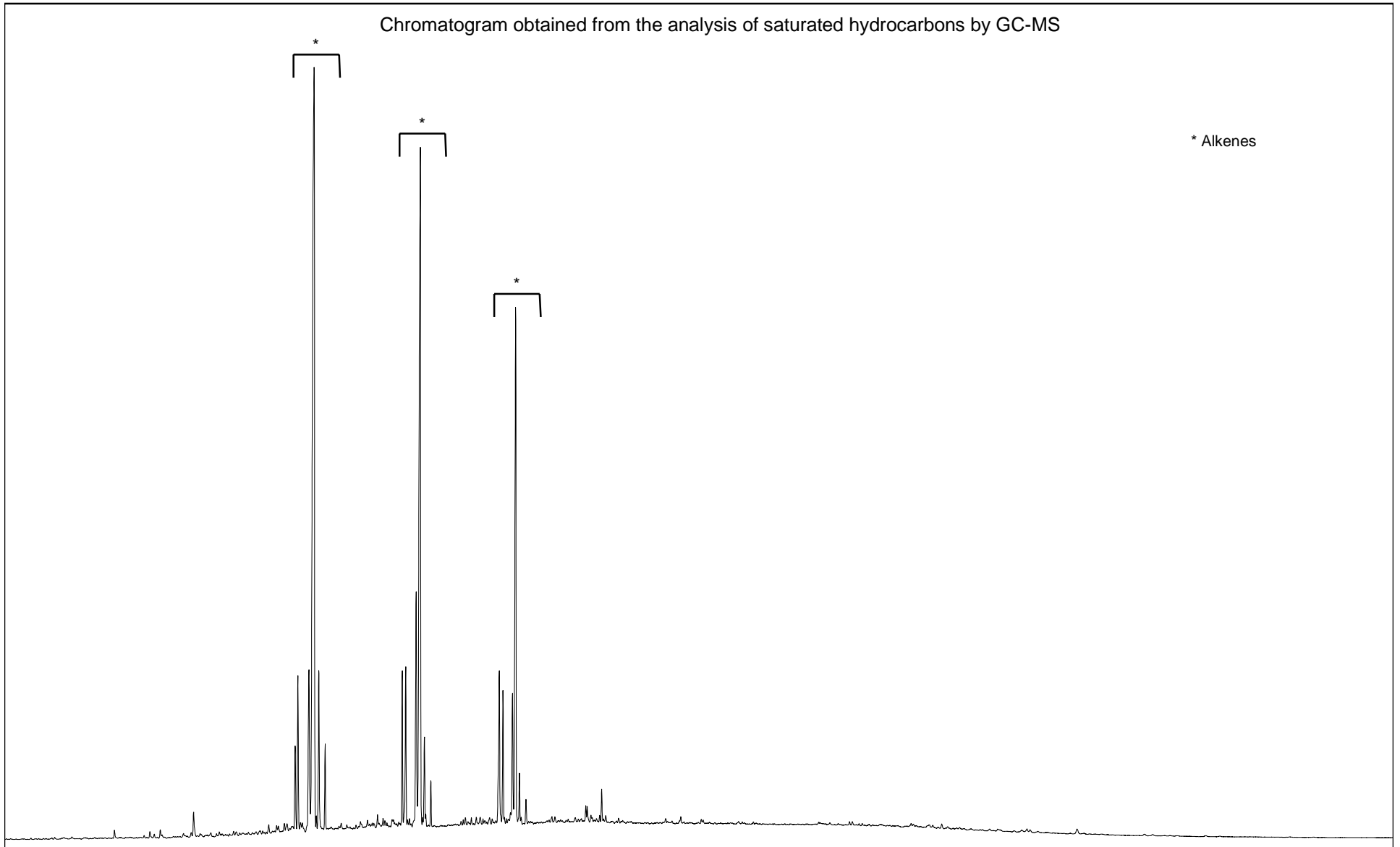


TABLE 3

**LIQUID CHROMATOGRAPHY DATA  
OIL**

**MOBY-1 (Alkenes Removed)**

Yields (%) and Selected Ratios



DEPTH	Sample Type	-----Hydrocarbons-----			-----Non-hydrocarbons-----			Sats	Asph.	HC
		Sats	Aros	HC's	NSOs	Asph.	Non HC's	Aros	NSO	Non HC
588.5m, Test-37	Oil	43.5	32.0	75.5	24.5	nd	24.5	1.4	nd	3.1

TABLE 4

**ANALYSIS OF SATURATED HYDROCARBONS BY GC-MS**

**OIL**

**MOBY-1**

A. Selected Ratios



DEPTH	Sample Type	Prist./Phyt.	Prist./n-C17	Phyt./n-C18	CPI(1)	CPI(2)	(C21+C22)/(C28+C29)
588.5m, Test-37	Oil	nd	nd	nd	nd	nd	nd

**MOBY-1**

B. n-Alkane Distributions

DEPTH	nC12	nC13	nC14	nC15	nC16	nC17	Pr	nC18	Ph	nC19	nC20	nC21	nC22	nC23	nC24	nC25	nC26	nC27	nC28	nC29	nC30	nC31
588.5m, Test-37	nd	nd	nd	nd	nd	nd	nd	nd	nd	nd	nd	nd	nd	nd	nd	nd	nd	nd	nd	nd	nd	nd

$$CPI(1) = \frac{(C23+C25+C27+C29)+(C25+C27+C29+C31)}{2 \times (C24+C26+C28+C30)}$$

$$CPI(2) = \frac{(C23+C25+C27)+(C25+C27+C29)}{2 \times (C24+C26+C28)}$$

FIGURE 3

Sample : **MOBY-1, 588.5m, Test # 37, Oil (Alkenes Removed)**  
File ID : 345808SB



Chromatogram obtained from the analysis of saturated hydrocarbons by GC-MS

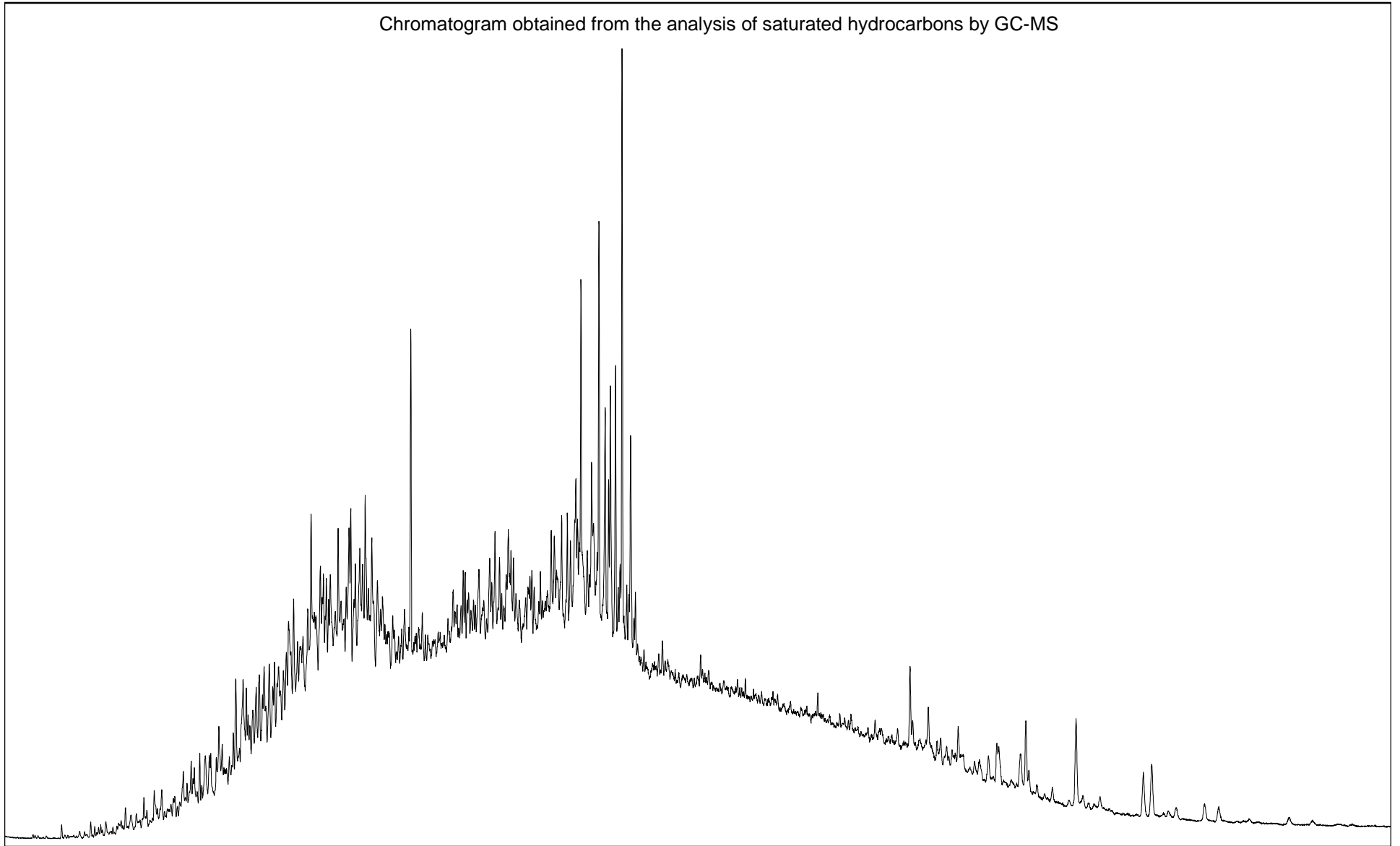


TABLE 5

**SOLVENT EXTRACTION DATA**

**MOBY-1**



DEPTH	Sample Type	Weight of Material Extd. (g)	Total Extract (mg)	Total Extract (ppm)
550.0m	Mud	99.8	0.5	5
560.0m	SWC	21.3	7.8	366
568.0m	SWC	18.5	113.1	6100
572.0m	SWC	21.3	19.8	930
584.0m	SWC	15.4	320.4	20792
586.0m	SWC	21.2	8.7	411
588.0m	SWC	30.1	0.2	7

FIGURE 4

Sample : MOBY-1, 550m, Mud  
File ID : 345807X

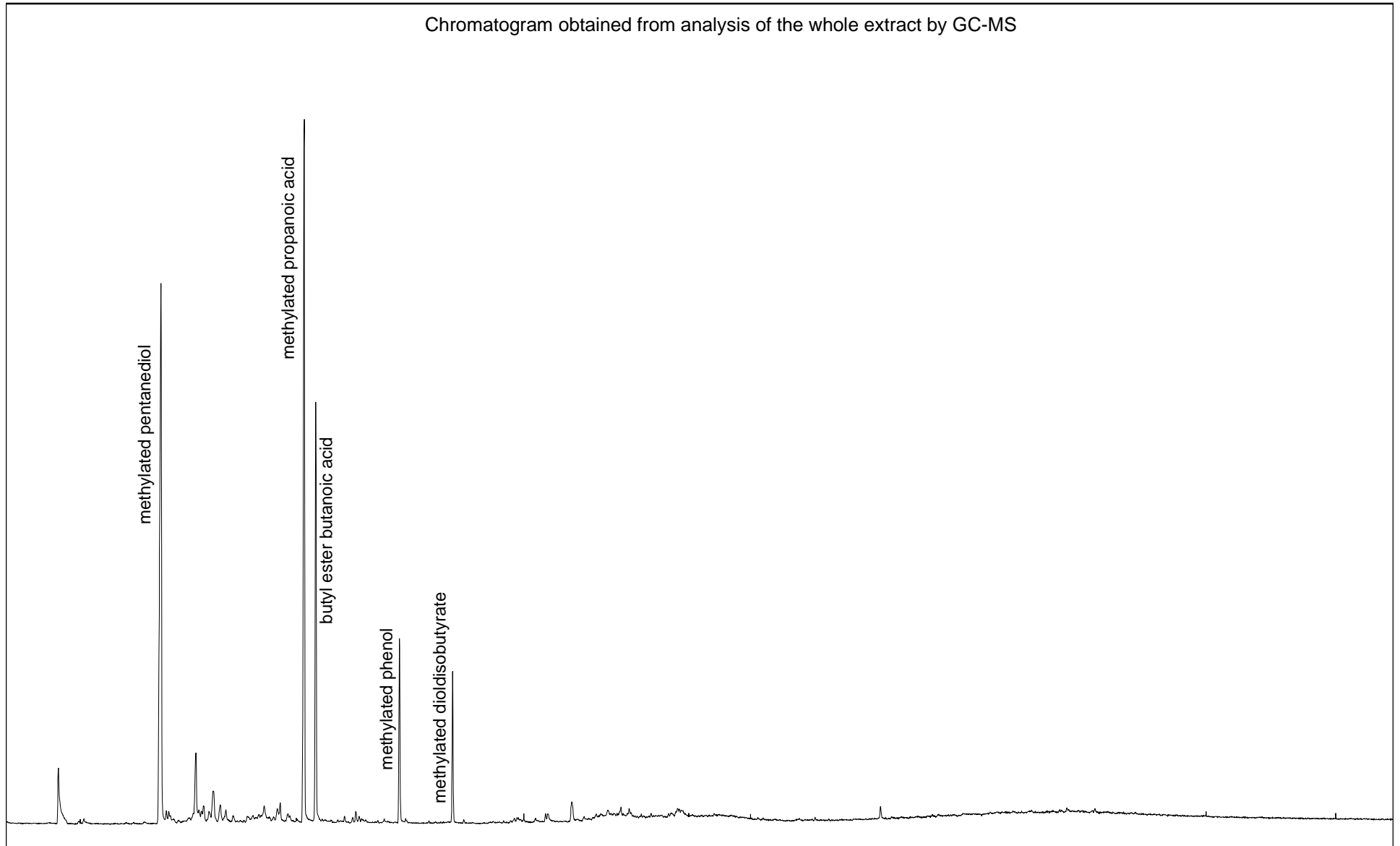


FIGURE 5

Sample : **MOBY-1, 560.0m, SWC # 21**  
File ID : **345801XB**



Chromatogram obtained from analysis of the whole extract by GC-MS

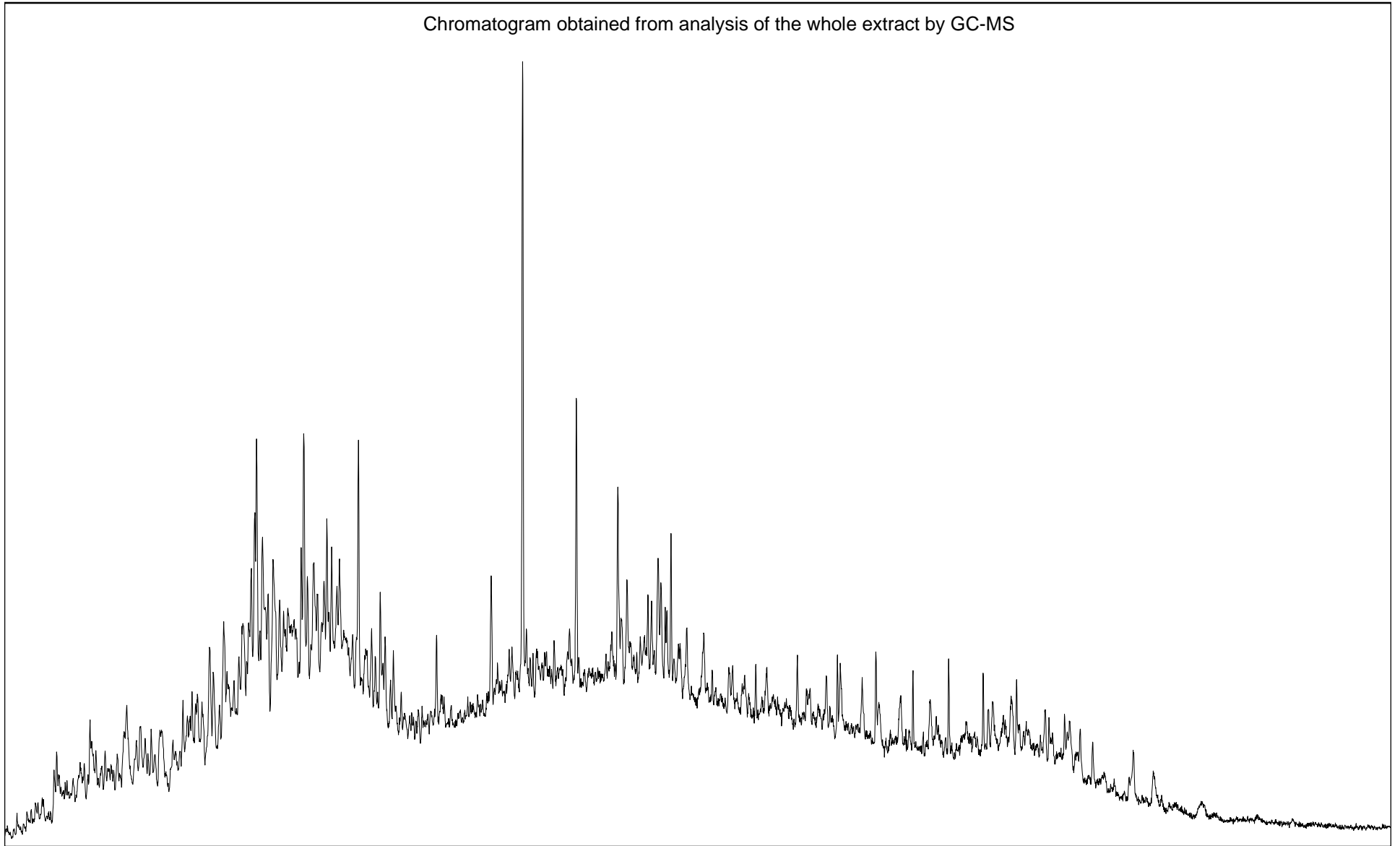


FIGURE 6

Sample : **MOBY-1, 568.0m, SWC # 16**  
File ID : **345802XB**



Chromatogram obtained from analysis of the whole extract by GC-MS

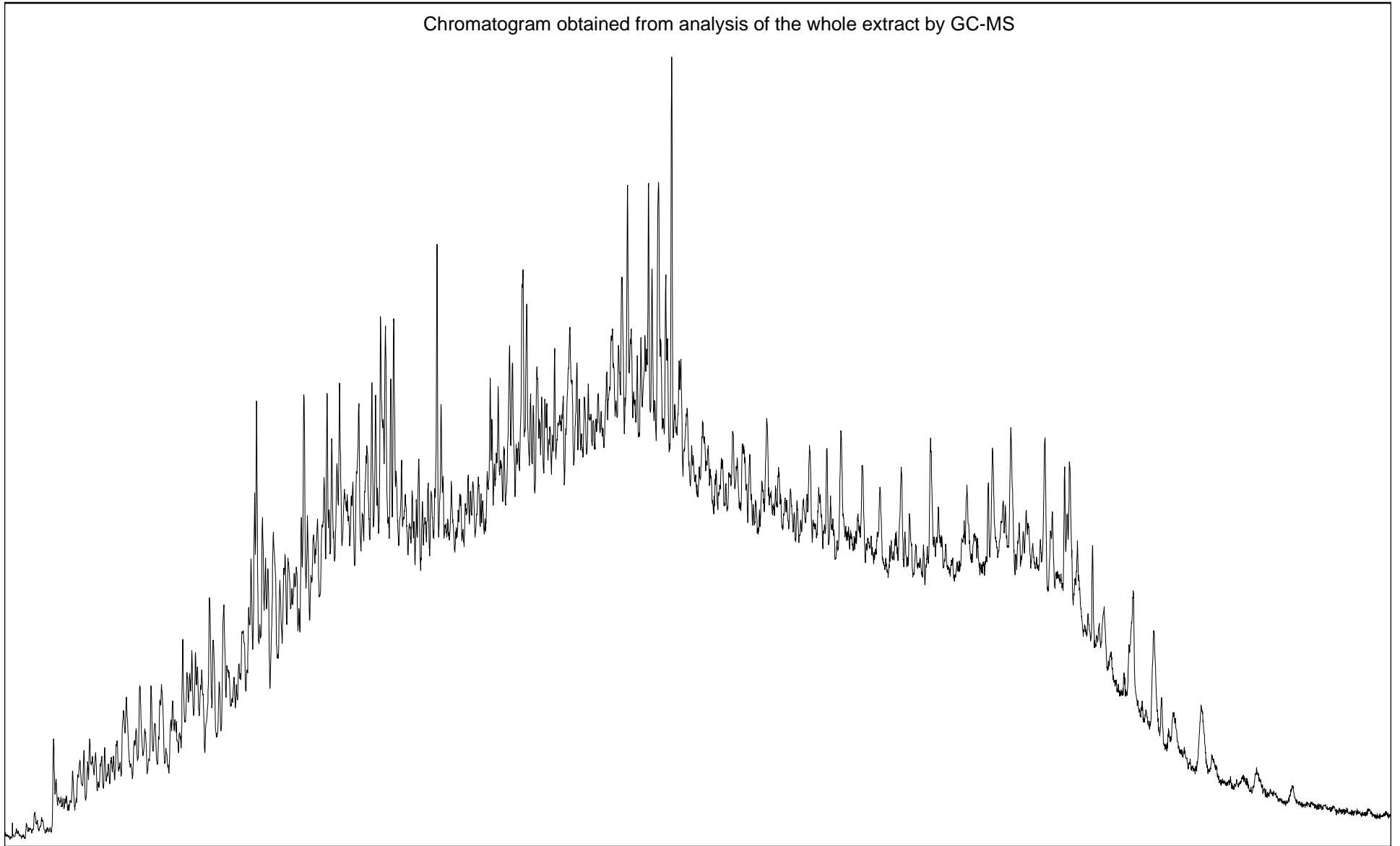


FIGURE 7

Sample : **MOBY-1, 572.0m, SWC # 13**  
File ID : **345803XB**



Chromatogram obtained from analysis of the whole extract by GC-MS

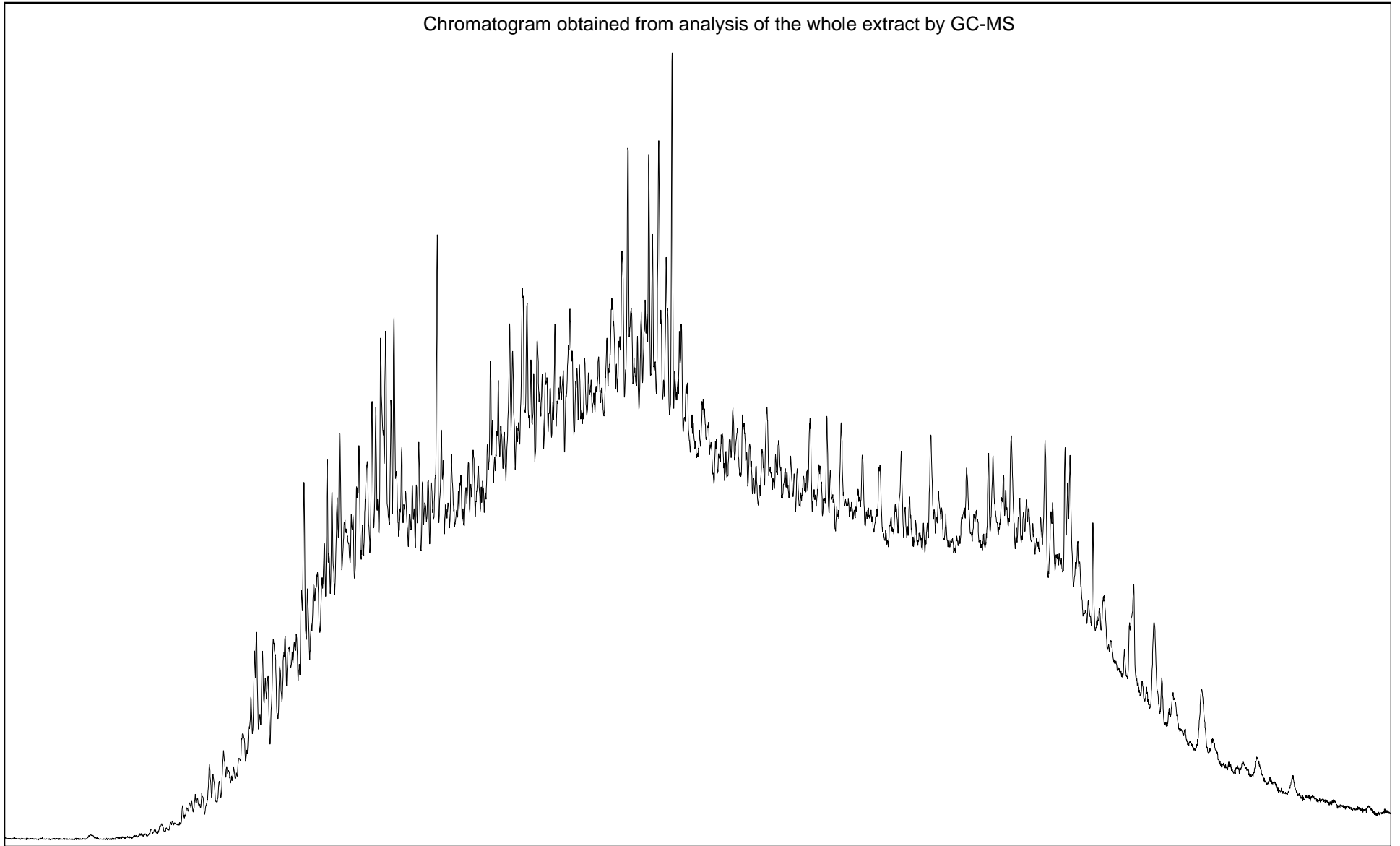


FIGURE 8

Sample : **MOBY-1, 584.0m, SWC # 9**  
File ID : **345804XB**



Chromatogram obtained from analysis of the whole extract by GC-MS

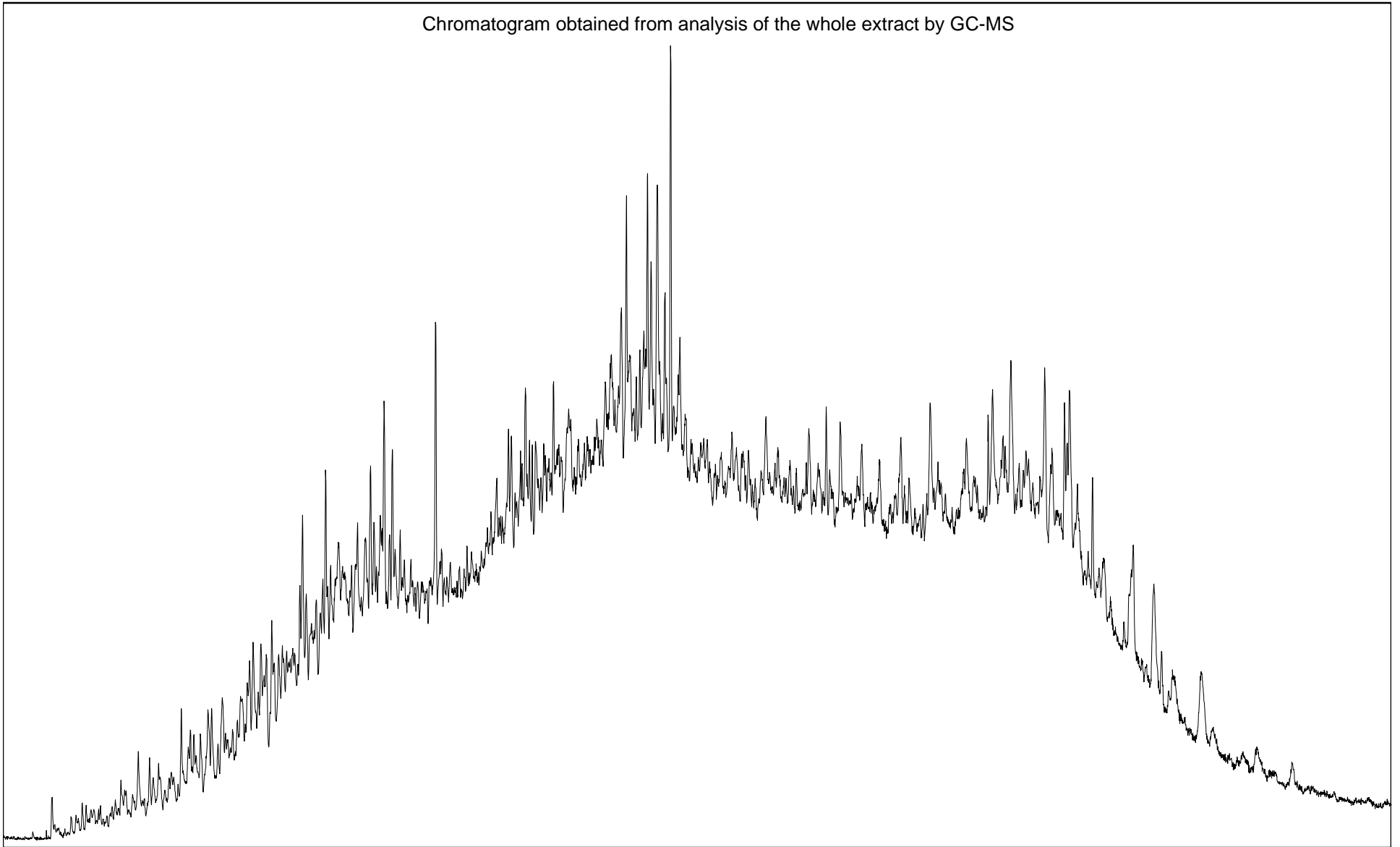


FIGURE 9

Sample : **MOBY-1, 586.0m, SWC # 7**  
File ID : **345805XB**



Chromatogram obtained from analysis of the whole extract by GC-MS

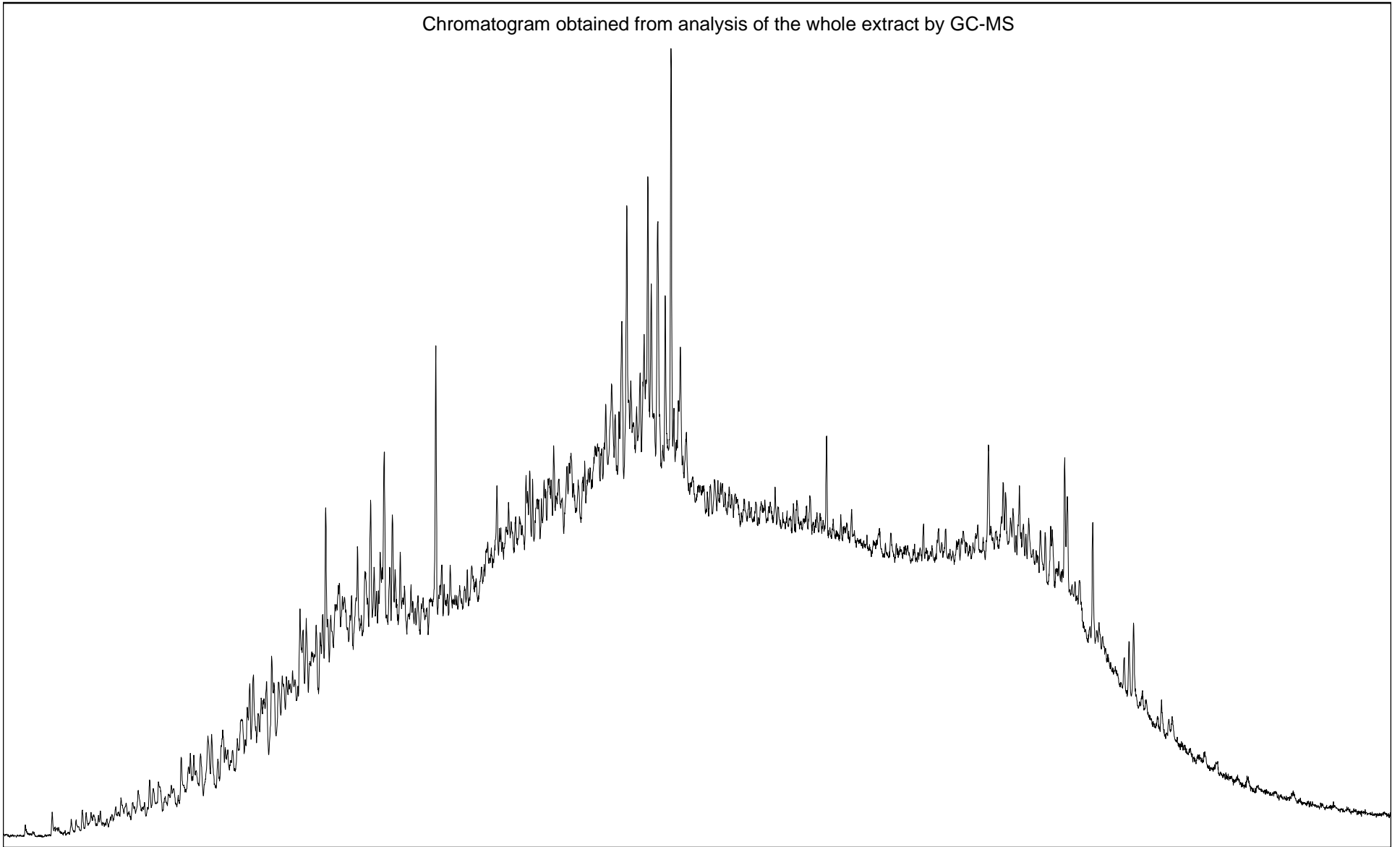


FIGURE 10

Sample : **MOBY-1, 588.0m, SWC # 6**  
File ID : **345806XB**



Chromatogram obtained from analysis of the whole extract by GC-MS

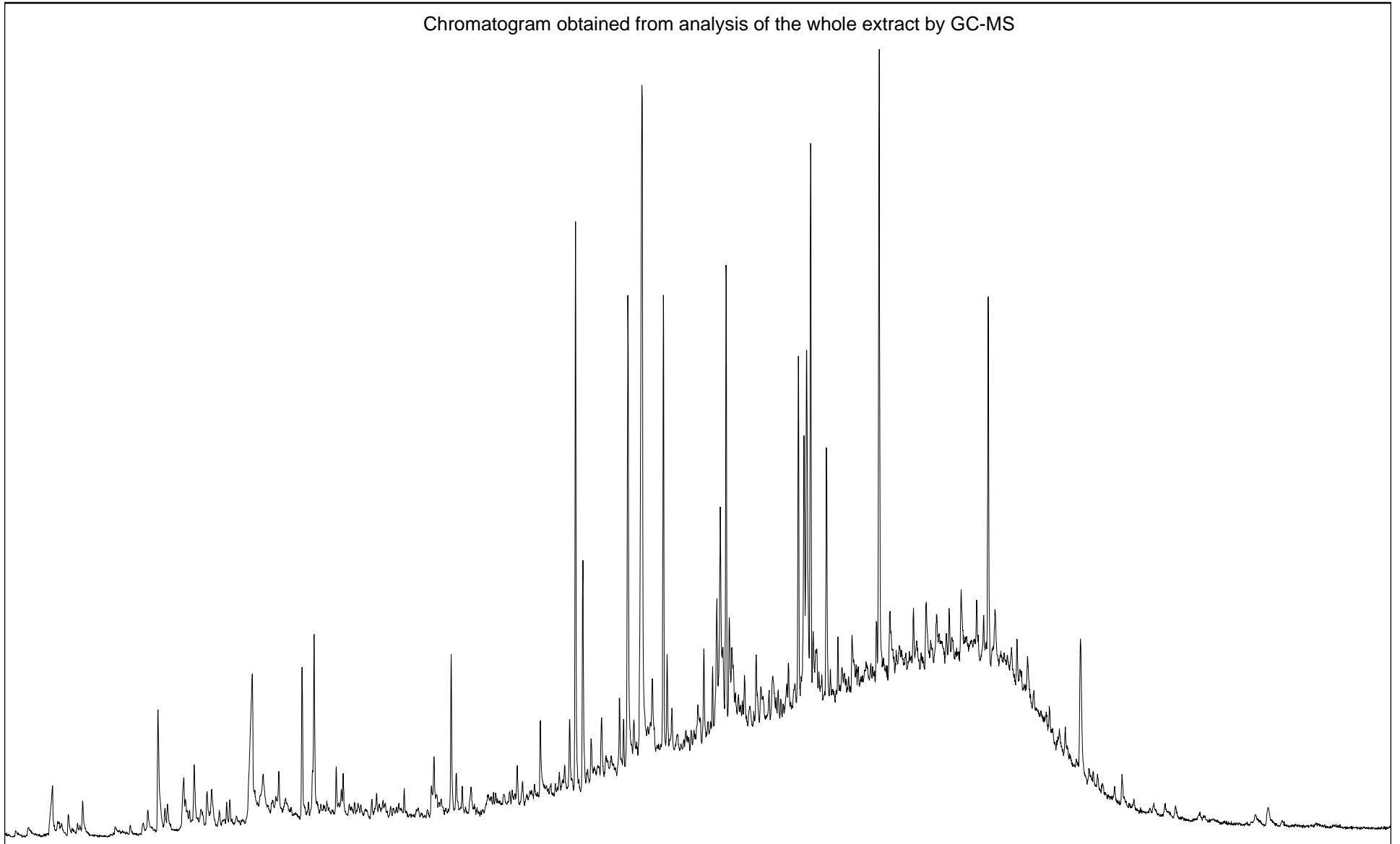


TABLE 6

**LIQUID CHROMATOGRAPHY DATA  
EXTRACT**

**MOBY-1**

## A. Yields (ppm)



DEPTH	Sample Type	-----Hydrocarbons-----			-----Non-hydrocarbons-----			Loss on column
		Sats	Aros	HC's	NSOs	Asph.	Non HC's	
550.0m	Mud	nd	nd	nd	nd	nd	nd	nd
560.0m	SWC	nd	nd	nd	nd	nd	nd	nd
568.0m	SWC	3567	1611	5178	600	nd	600	322
572.0m	SWC	456	254	710	75	nd	75	146
584.0m	SWC	11924	5811	17735	2313	nd	2313	744
586.0m	SWC	nd	nd	nd	nd	nd	nd	nd
588.0m	SWC	nd	nd	nd	nd	nd	nd	nd

**MOBY-1**

## B. Yields (%) and Selected Ratios

DEPTH	Sample Type	-----Hydrocarbons-----			-----Non-hydrocarbons-----			Sats	Asph.	HC
		Sats	Aros	HC's	NSOs	Asph.	Non HC's	Aros	NSO	Non HC
550.0m	Mud	nd	nd	nd	nd	nd	nd	nd	nd	nd
560.0m	SWC	nd	nd	nd	nd	nd	nd	nd	nd	nd
568.0m	SWC	61.7	27.9	90	10.4	nd	10	2.2	nd	8.6
572.0m	SWC	58.1	32.3	90	9.6	nd	10	1.8	nd	9.4
584.0m	SWC	59.5	29.0	88	11.5	nd	12	2.1	nd	7.7
586.0m	SWC	nd	nd	nd	nd	nd	nd	nd	nd	nd
588.0m	SWC	nd	nd	nd	nd	nd	nd	nd	nd	nd

TABLE 7

**ANALYSIS OF SATURATED HYDROCARBONS BY GC-MS  
EXTRACT**

**MOBY-1**

A. Selected Ratios



DEPTH	Sample Type	Prist./Phyt.	Prist./n-C17	Phyt./n-C18	CPI(1)	CPI(2)	(C21+C22)/(C28+C29)
550.0m	Mud	nd	nd	nd	nd	nd	nd
560.0m	SWC	1.82	nd	nd	nd	nd	nd
568.0m	SWC	nd	nd	nd	nd	nd	nd
572.0m	SWC	nd	nd	nd	nd	nd	nd
584.0m	SWC	nd	nd	nd	nd	nd	nd
586.0m	SWC	nd	nd	nd	nd	nd	nd
588.0m	SWC	nd	nd	nd	nd	nd	nd

**MOBY-1**

B. n-Alkane Distributions

DEPTH	nC12	nC13	nC14	nC15	nC16	nC17	Pr	nC18	Ph	nC19	nC20	nC21	nC22	nC23	nC24	nC25	nC26	nC27	nC28	nC29	nC30	nC31
550.0m	nd																					
560.0m	nd	nd	nd	nd	nd	nd	36.8	nd	20.2	15.8	nd	nd	4.3	4.1	4.0	4.7	4.5	5.7	nd	nd	nd	nd
568.0m	nd	41.1	58.9	nd																		
572.0m	nd																					
584.0m	nd																					
586.0m	nd																					
588.0m	nd																					

$$CPI(1) = \frac{(C23+C25+C27+C29)+(C25+C27+C29+C31)}{2 \times (C24+C26+C28+C30)}$$

$$CPI(2) = \frac{(C23+C25+C27)+(C25+C27+C29)}{2 \times (C24+C26+C28)}$$

FIGURE 11

Sample : **MOBY-1, 560.0m, SWC**  
File ID : 345801SB

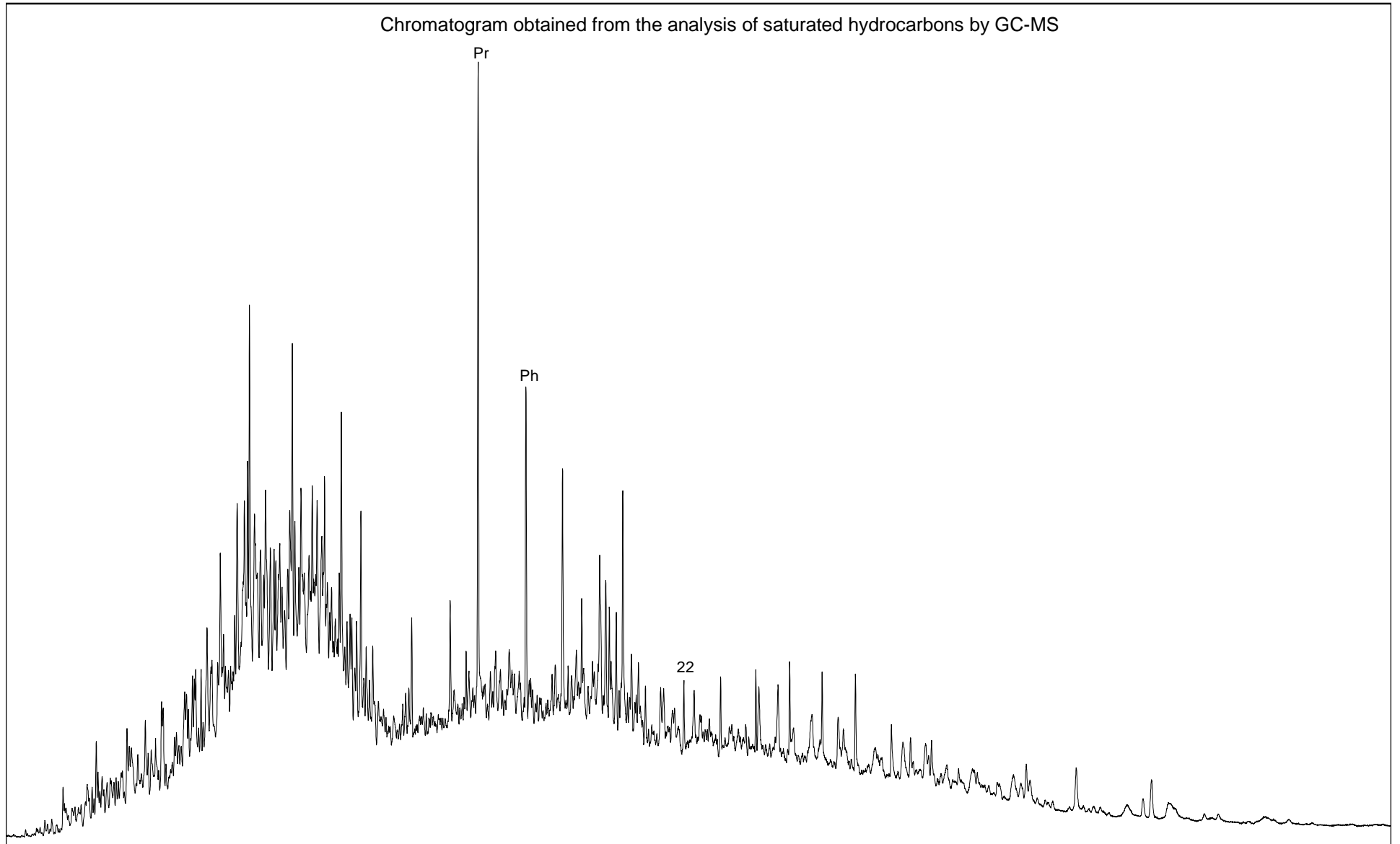


FIGURE 12

Sample : **MOBY-1, 568.0m, SWC**  
File ID : 345802SB



Chromatogram obtained from the analysis of saturated hydrocarbons by GC-MS

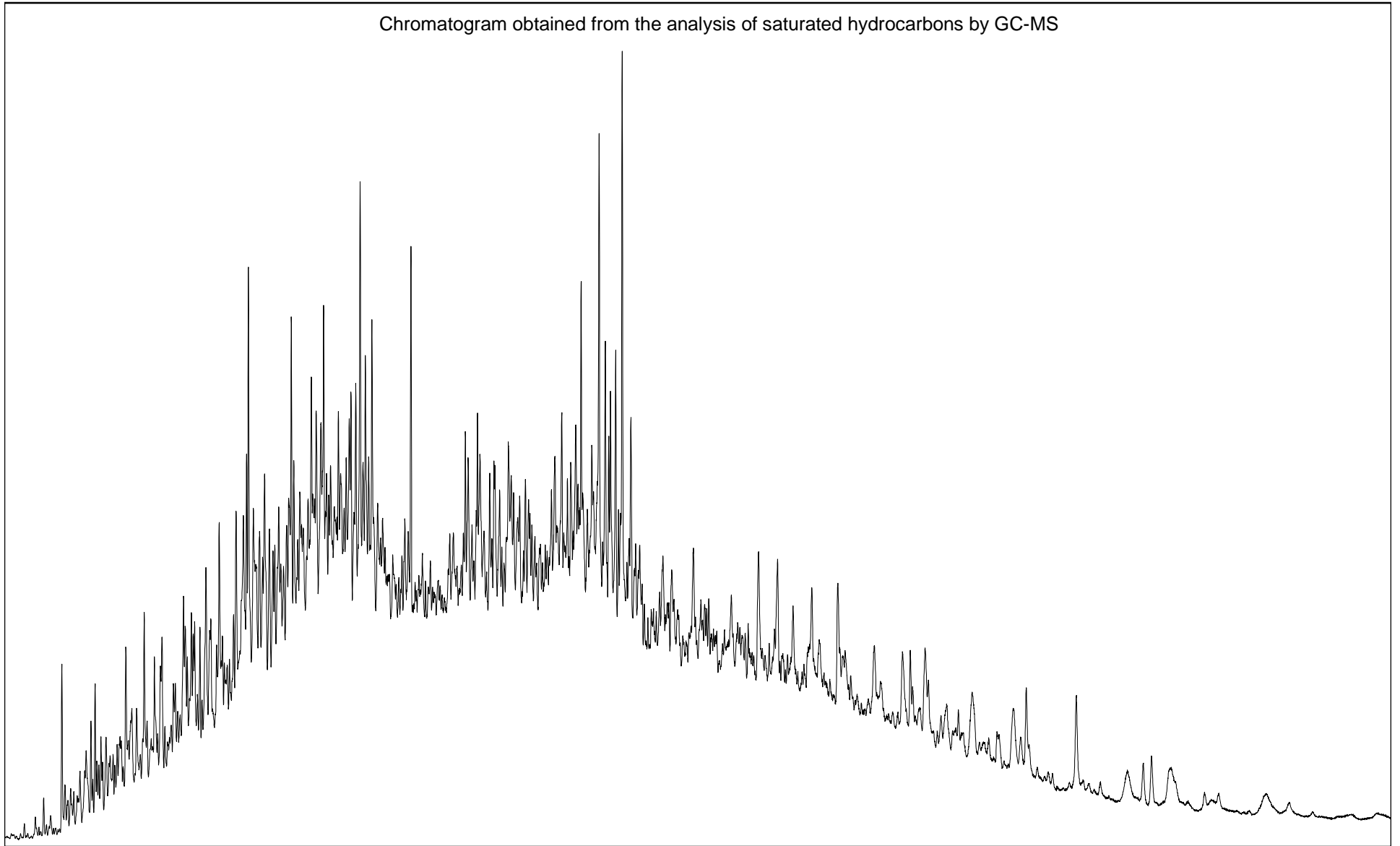


FIGURE 13

Sample : **MOBY-1, 572.0m, SWC**  
File ID : 345803SB



Chromatogram obtained from the analysis of saturated hydrocarbons by GC-MS

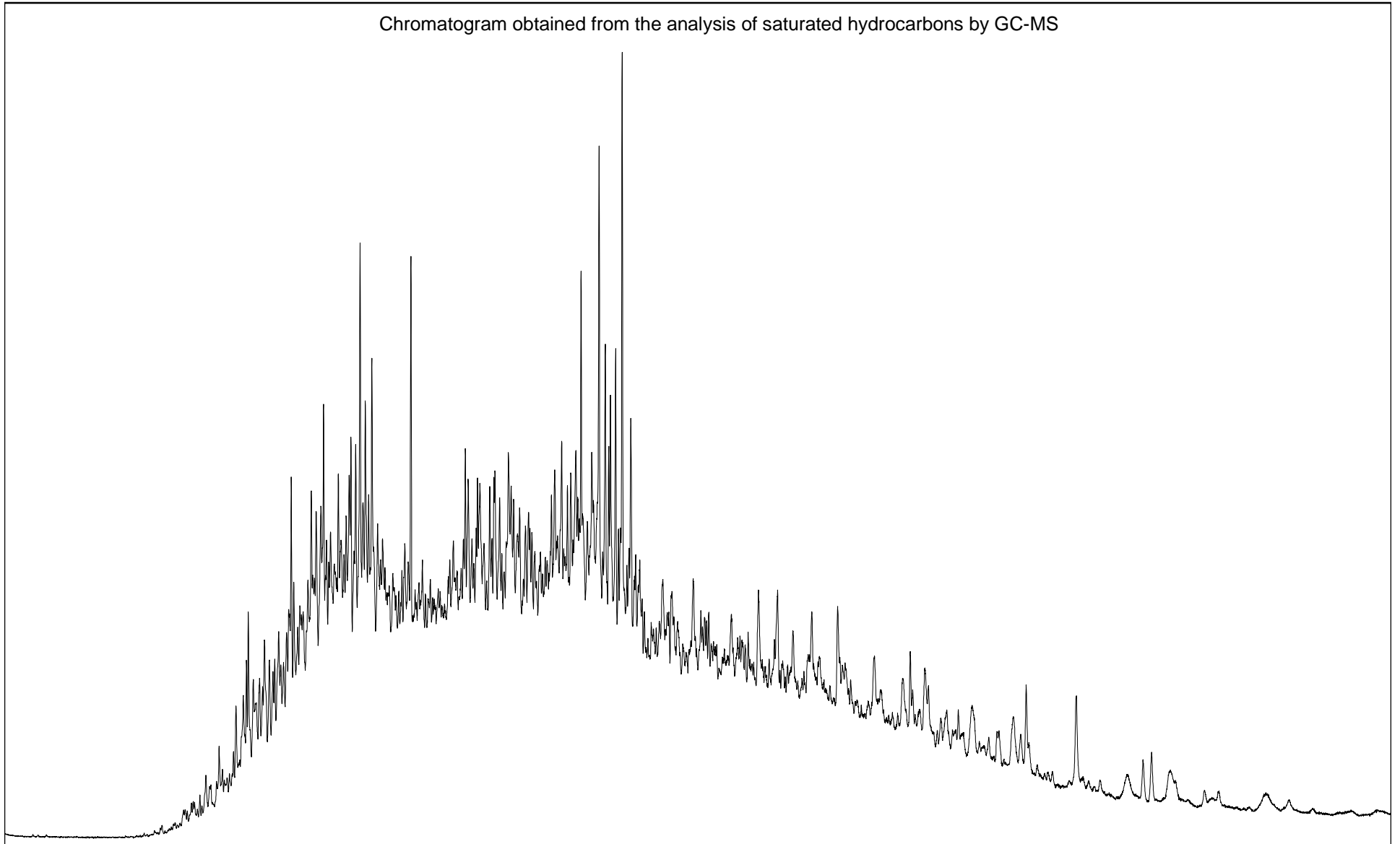


FIGURE 14

Sample : **MOBY-1, 584.0m, SWC**  
File ID : 345804SB



Chromatogram obtained from the analysis of saturated hydrocarbons by GC-MS

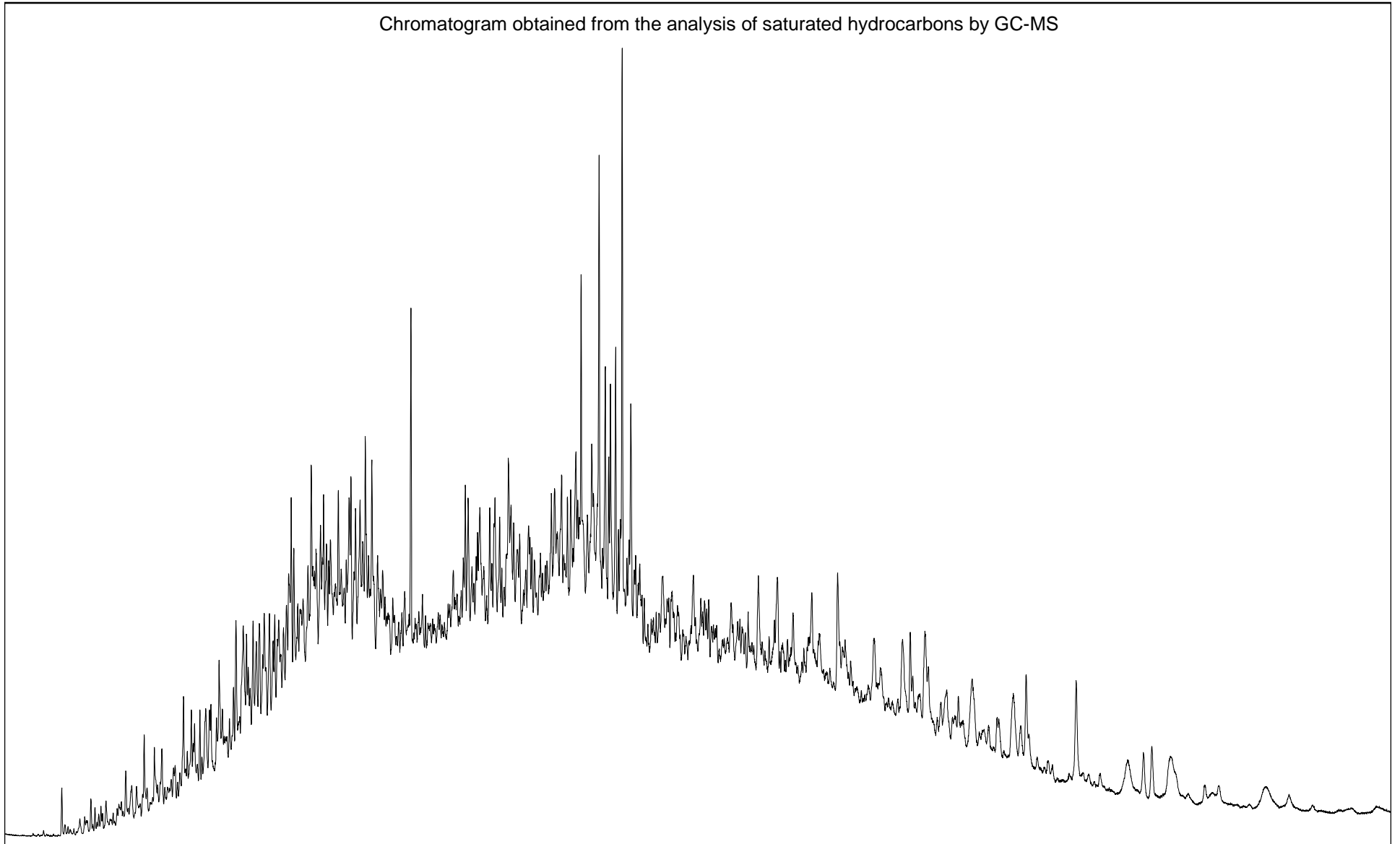


FIGURE 15

Sample : **MOBY-1, 586.0m, SWC**  
File ID : 345805SB



Chromatogram obtained from the analysis of saturated hydrocarbons by GC-MS

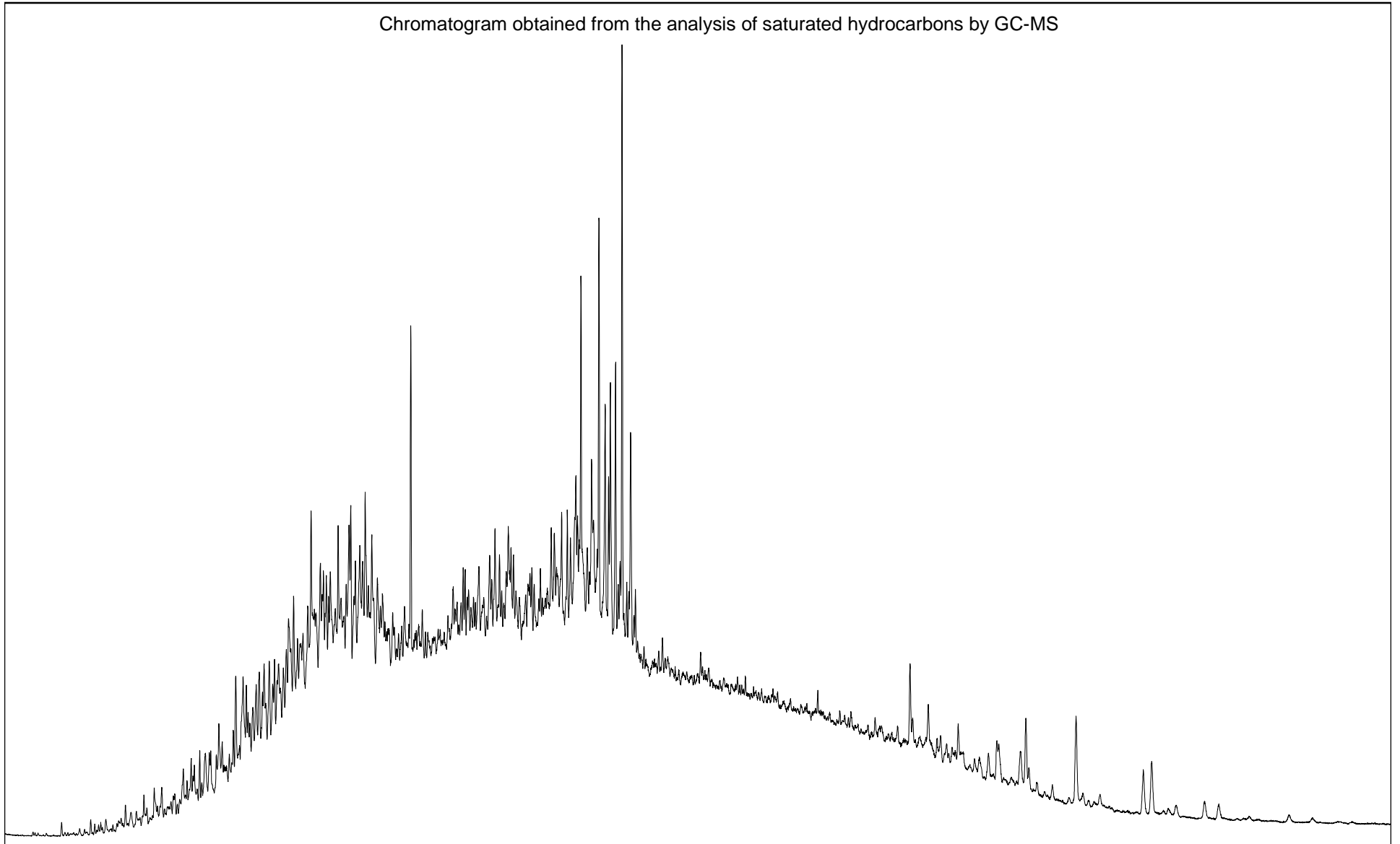


Table 8

## ANALYSIS OF AROMATIC HYDROCARBONS BY GC-MS

## MOBY-1



DEPTH	TYPE	DNR-1	DNR-5	DNR-6	TNR-1	TNR-5	TNR-6	MPR-1	MPI-1	MPI-2	Rc(a)	Rc(b)
560m	SWC 21	2.02	nd	1.14	1.30	3.64	0.85	5.87	0.89	0.85	0.94	1.76
586m	SWC 7	nd										
588.5m, Test #37	Crude Oil	2.26	nd	1.15	0.54	0.75	0.17	1.61	0.34	0.33	0.60	2.10

response factors have not been applied to these ratios

## MOBY-1

DEPTH	TYPE	1,7-DMP/X (m/z 206)	RETENE/9-MP (m/z 219,192)	1MP/9MP	HPI
560m	SWC 21	0.15	nd	0.17	1.10
586m	SWC 7	nd	nd	nd	nd
588.5m, Test #37	Crude Oil	0.33	2.41	0.61	4.25

HPI = Higher Plant Index (i.e (retene + cadalene + iHMN-IV)/1,3,6,7-TeMN )

FIGURE 16A-1

Sample: **MOBY-1, 560.0m, SWC**

File ID: **345801AB**

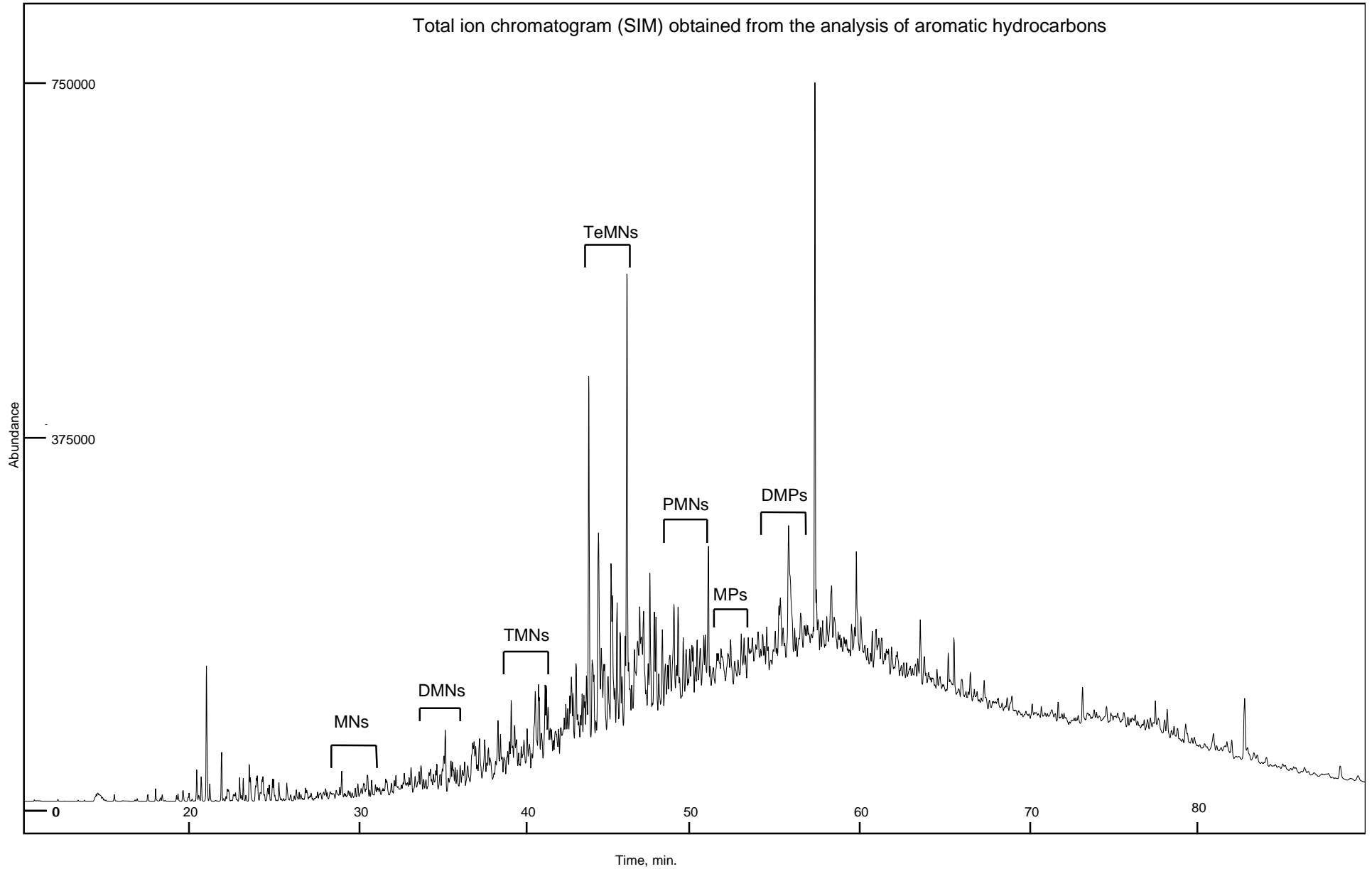


FIGURE 16B-1

Sample: MOBY-1, 560.0m, SWC

File ID: 345801AB

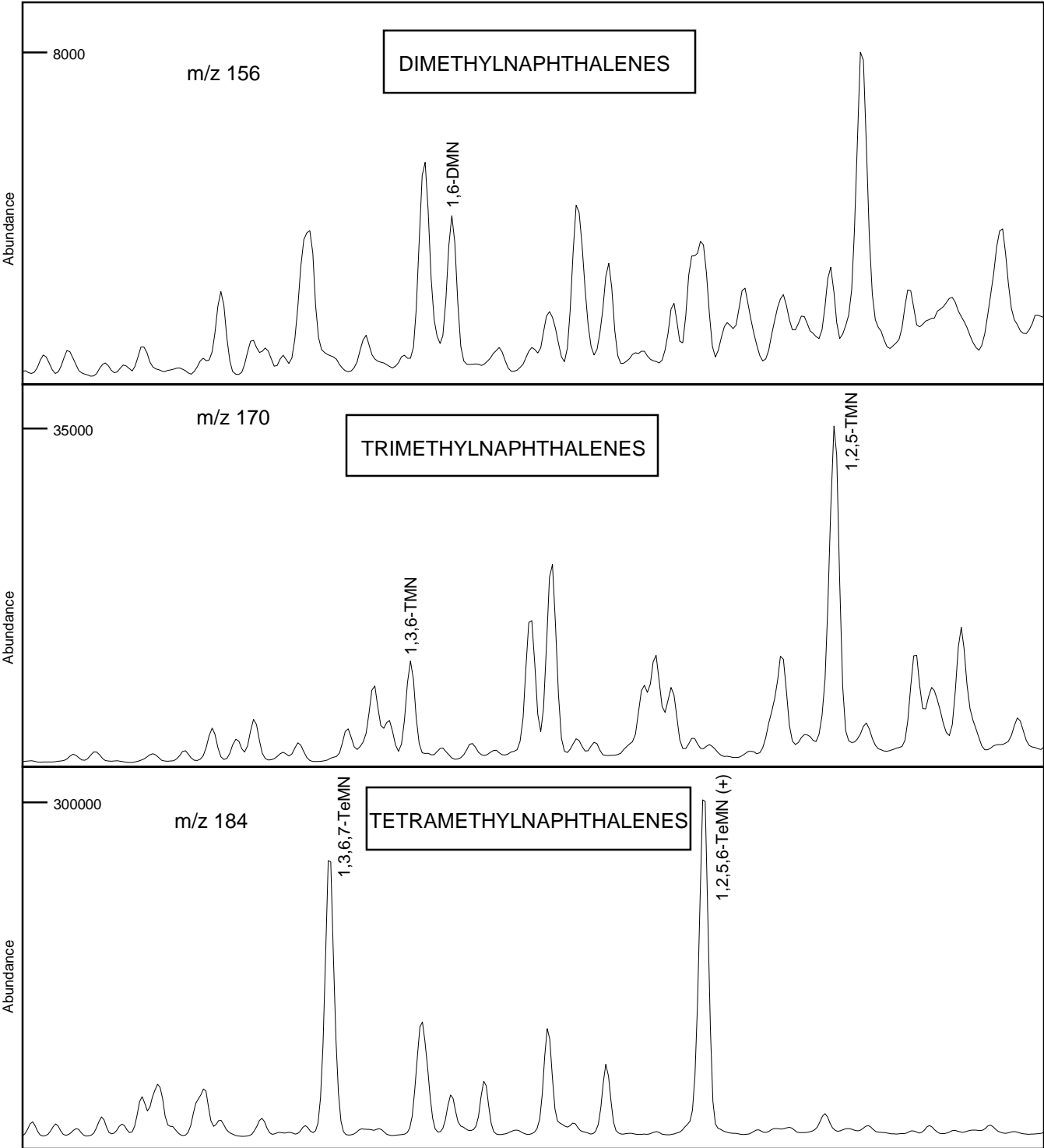


FIGURE 16C-1

Sample: **MOBY-1, 560.0m, SWC**

File ID: **345801AB**

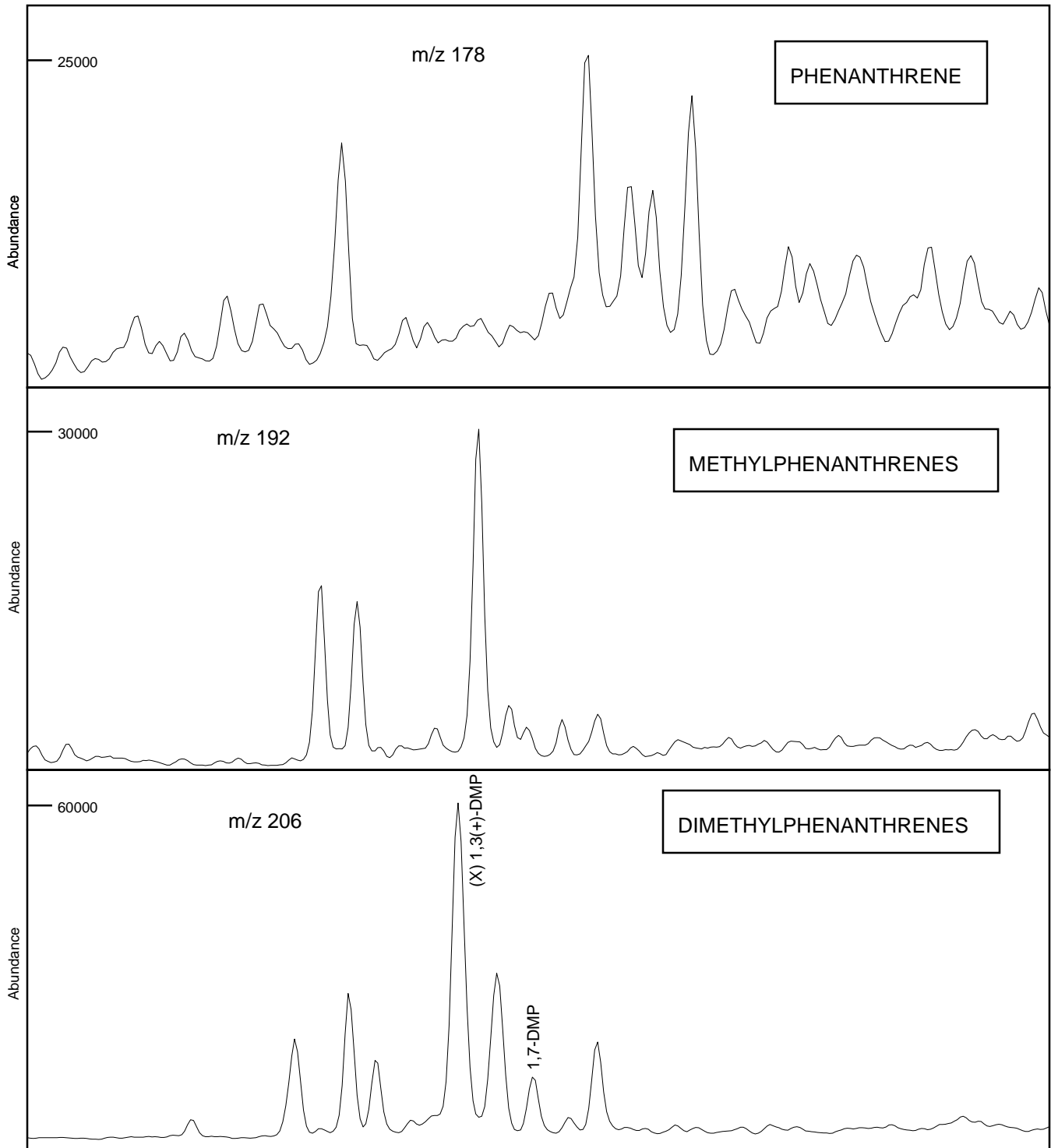


FIGURE 16D-1

Sample: **MOBY-1, 560.0m, SWC**

File ID: **345801AB**

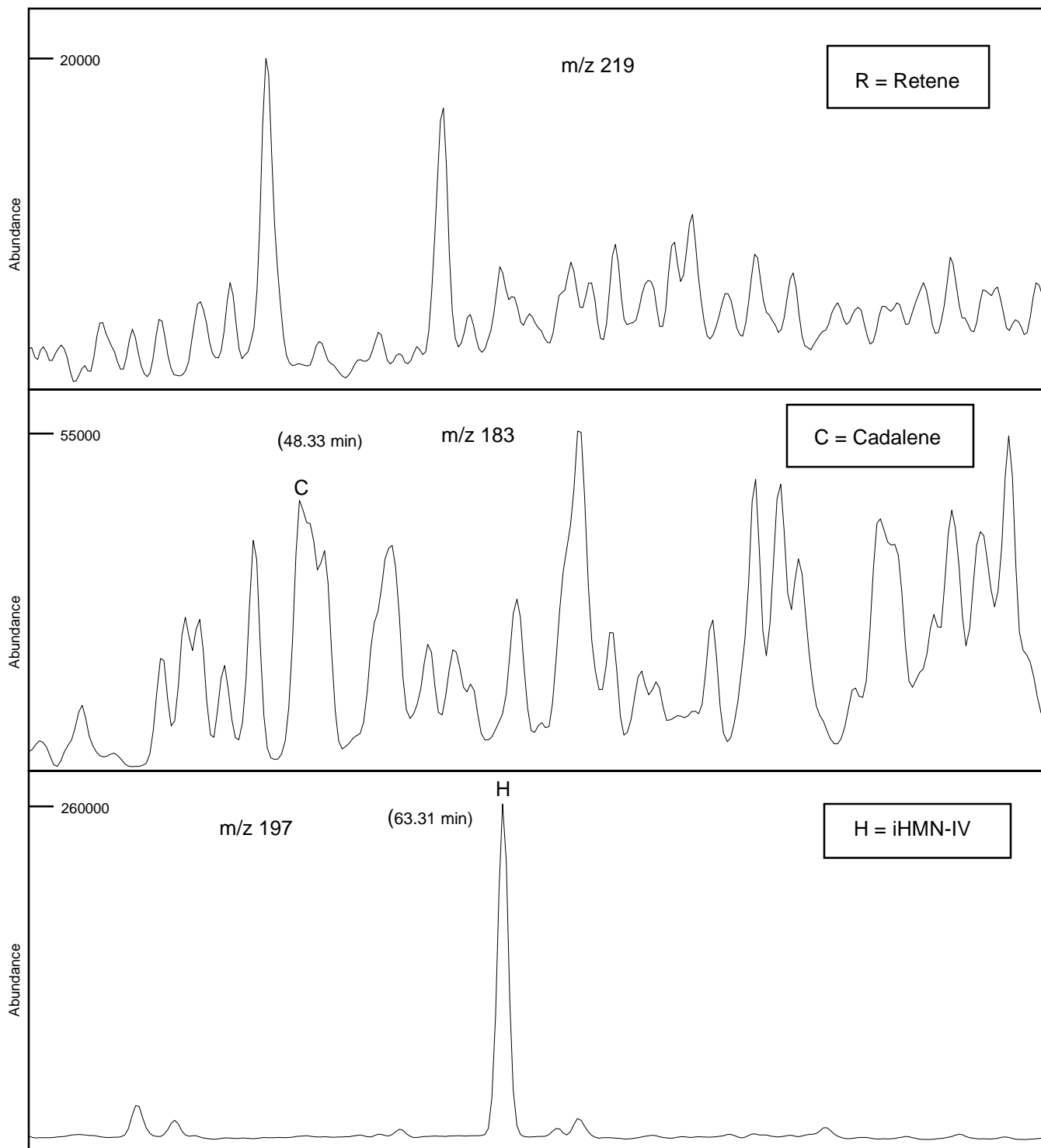


FIGURE 16E-1

Sample: **MOBY-1, 560.0m, SWC**

File ID: **345801AB**

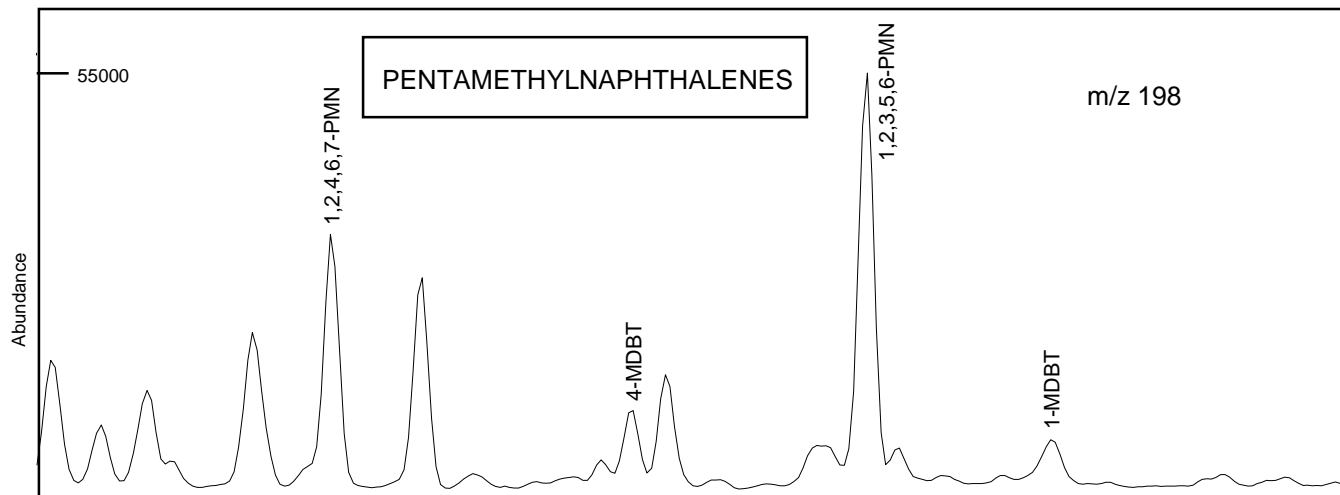


FIGURE 16A-2

Sample: **MOBY-1, 586.0m, SWC**

File ID: **345805AB**

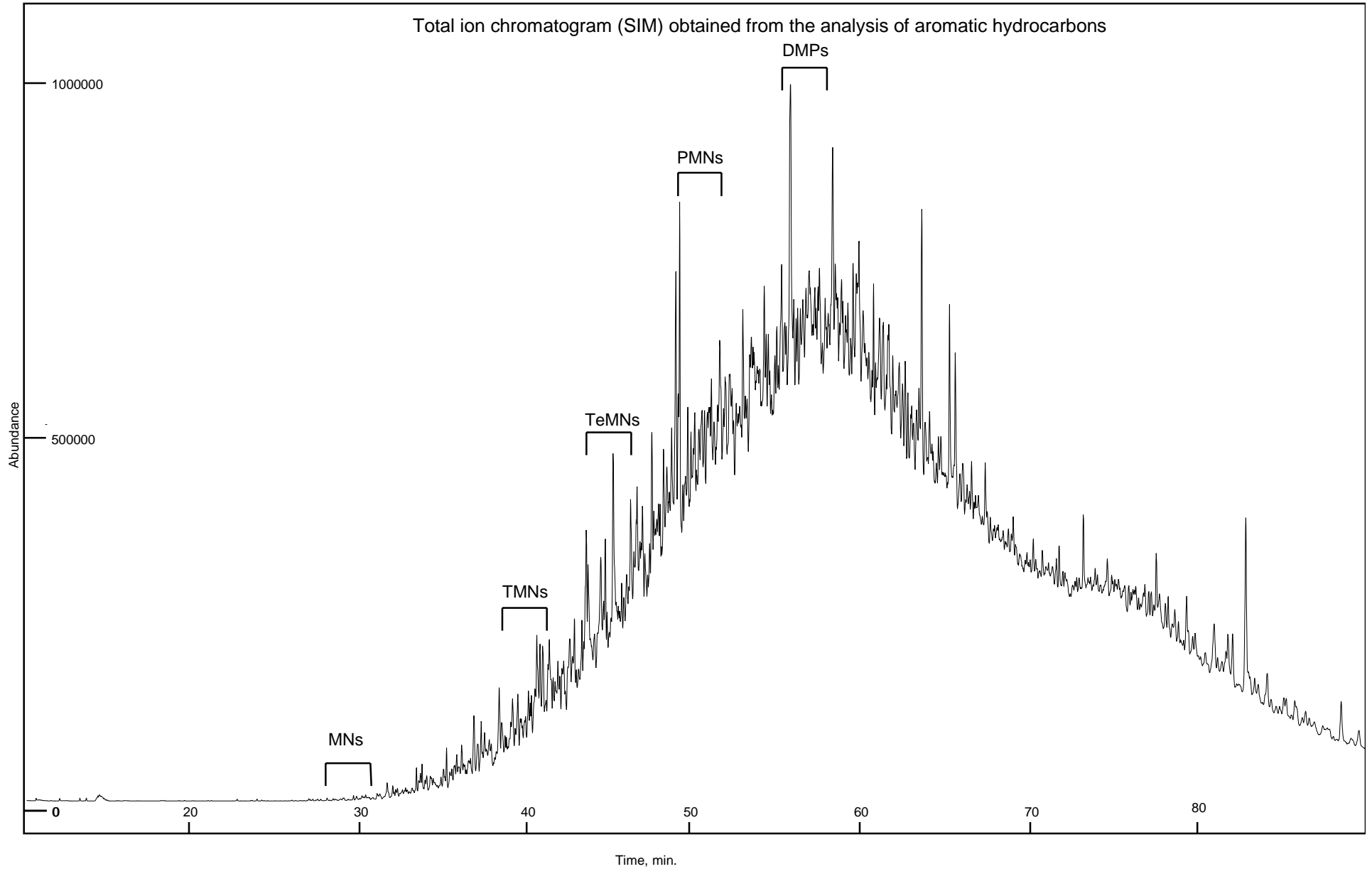


FIGURE 16B-2

Sample: MOBY-1, 586.0m, SWC

File ID: 345805AB

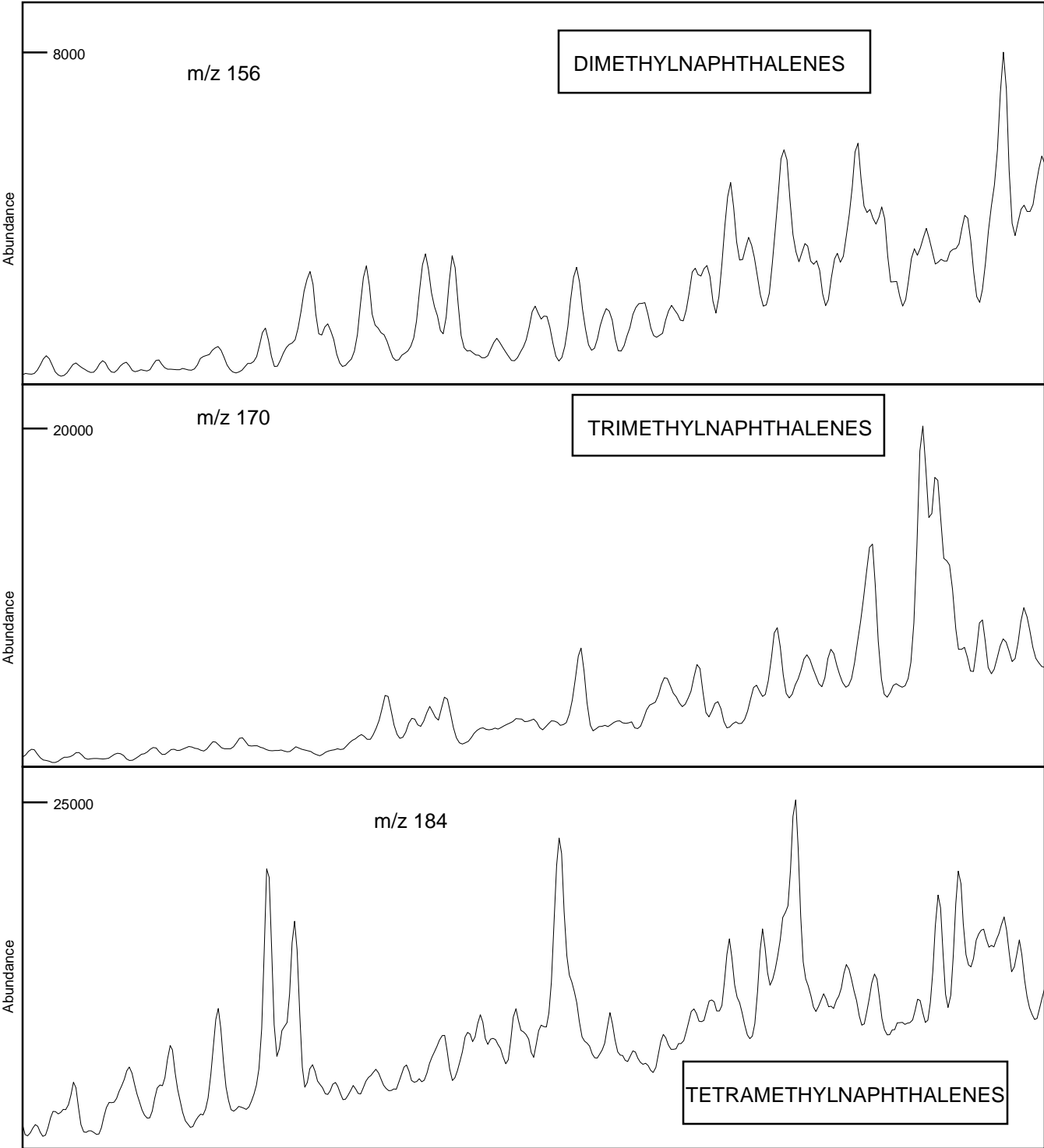


FIGURE 16C-2

Sample: **MOBY-1, 586.0m, SWC**

File ID: **345805AB**

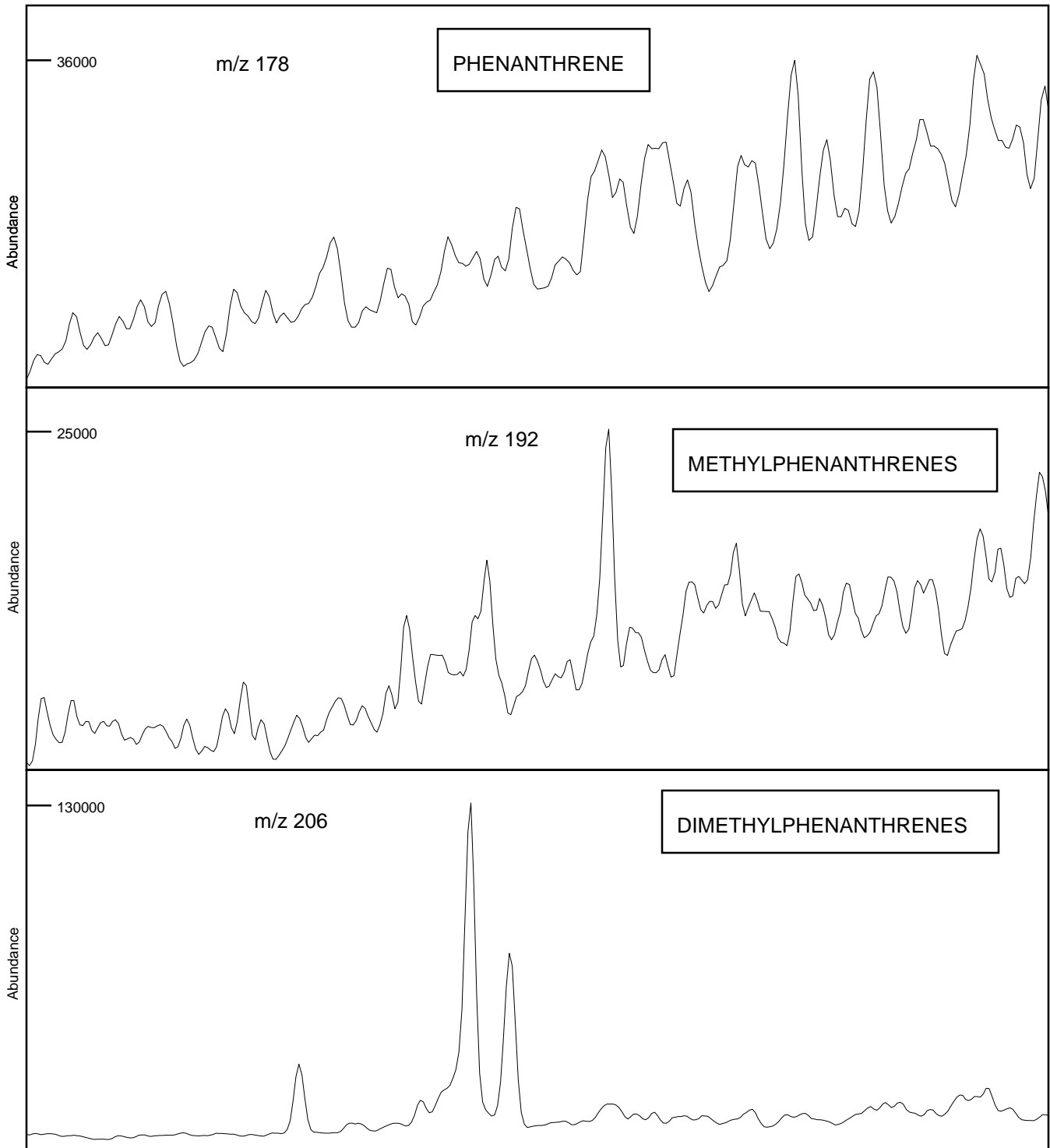


FIGURE 16D-2

Sample: **MOBY-1, 586.0m, SWC**

File ID: **345805AB**

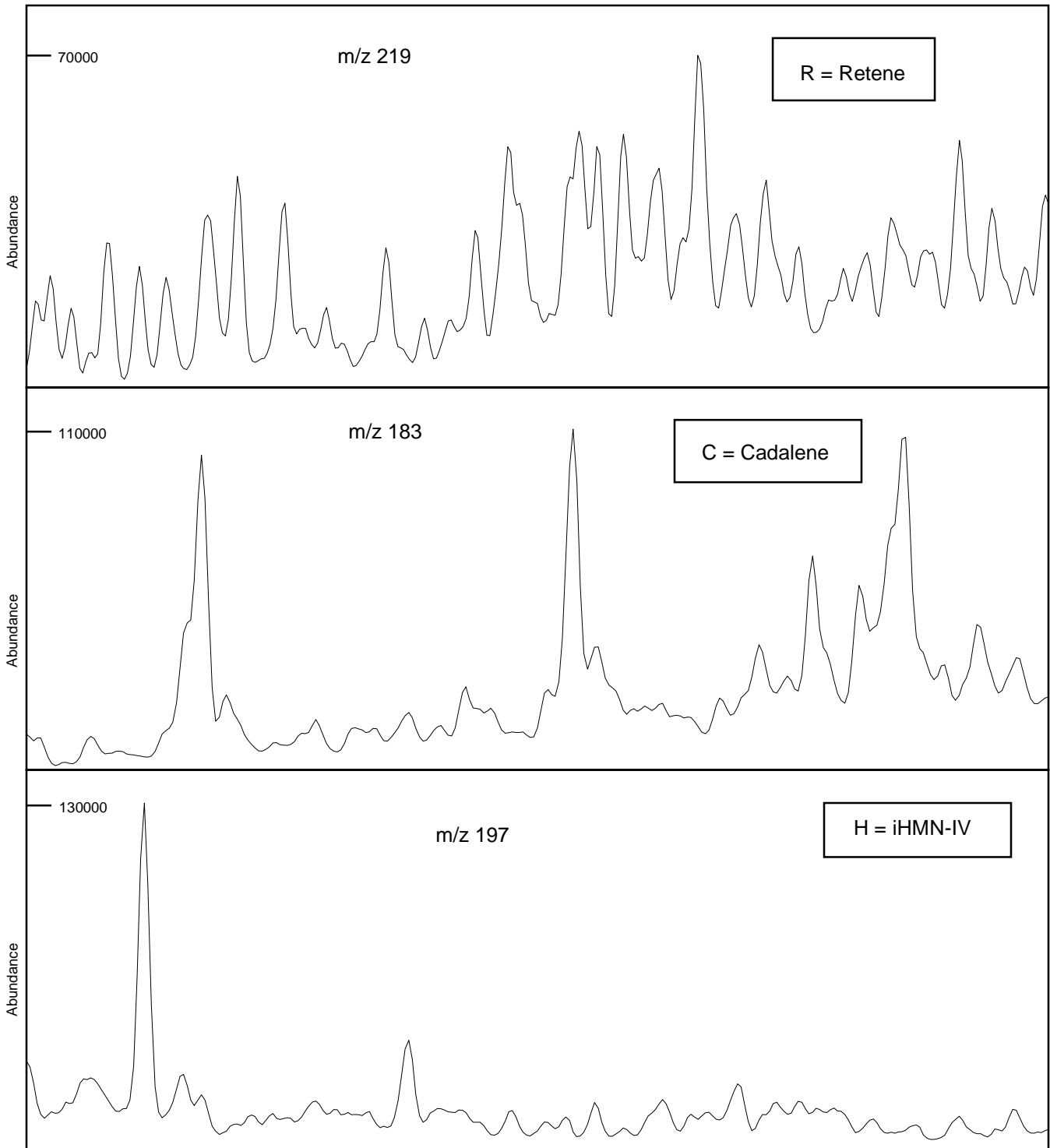


FIGURE 16E-2

Sample: **MOBY-1, 586.0m, SWC**

File ID: **345805AB**

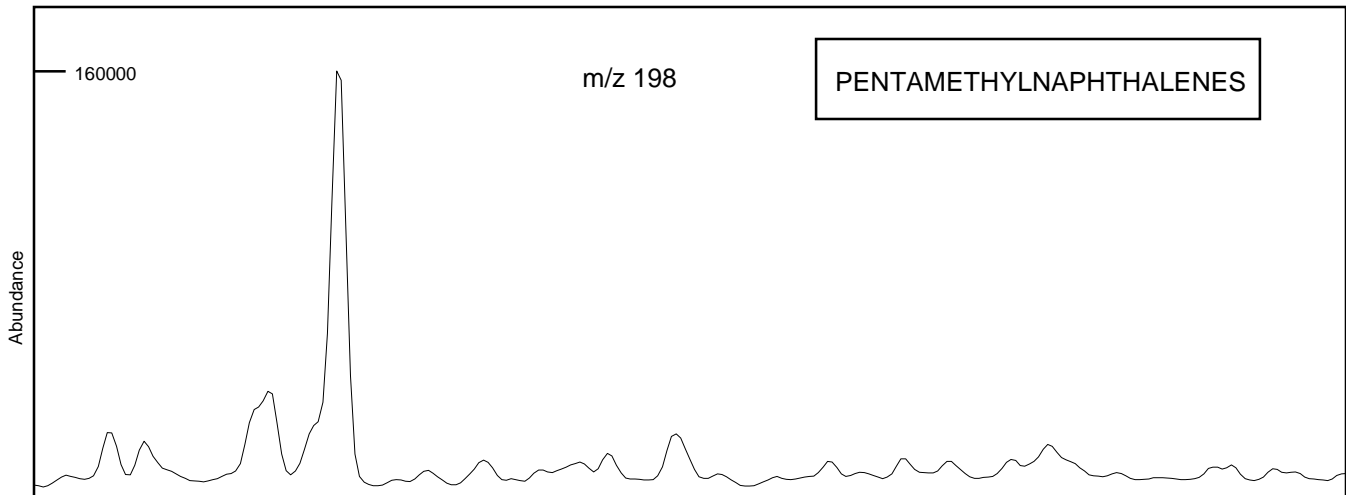


FIGURE 16A-3

Sample: **MOBY-1, 588.5m, Test # 37, Crude Oil**

File ID: **345808AB**

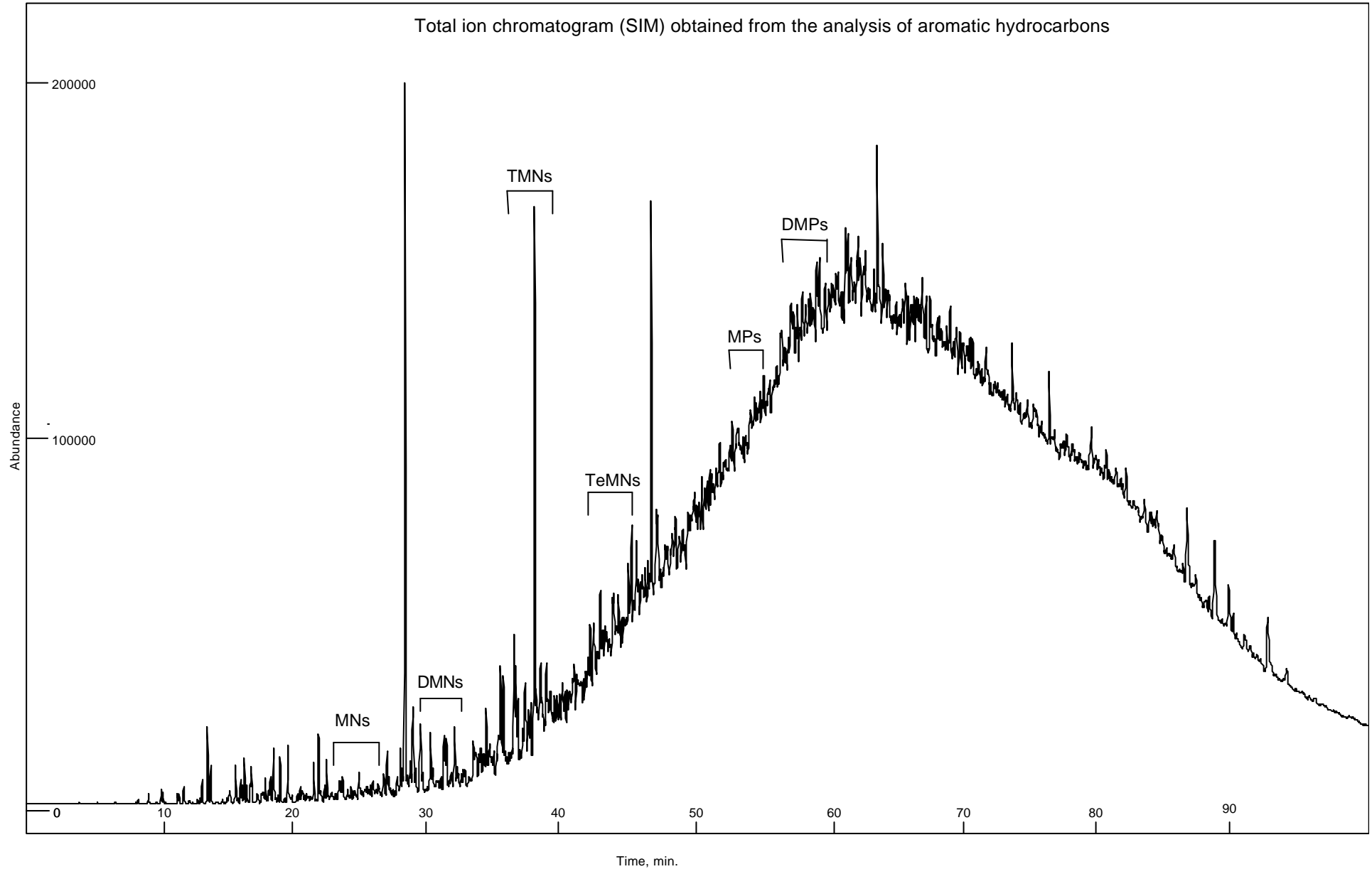


FIGURE 16B-3

Sample: **MOBY-1, 588.5m, Test # 37, Crude Oil**

File ID: **345808AB**

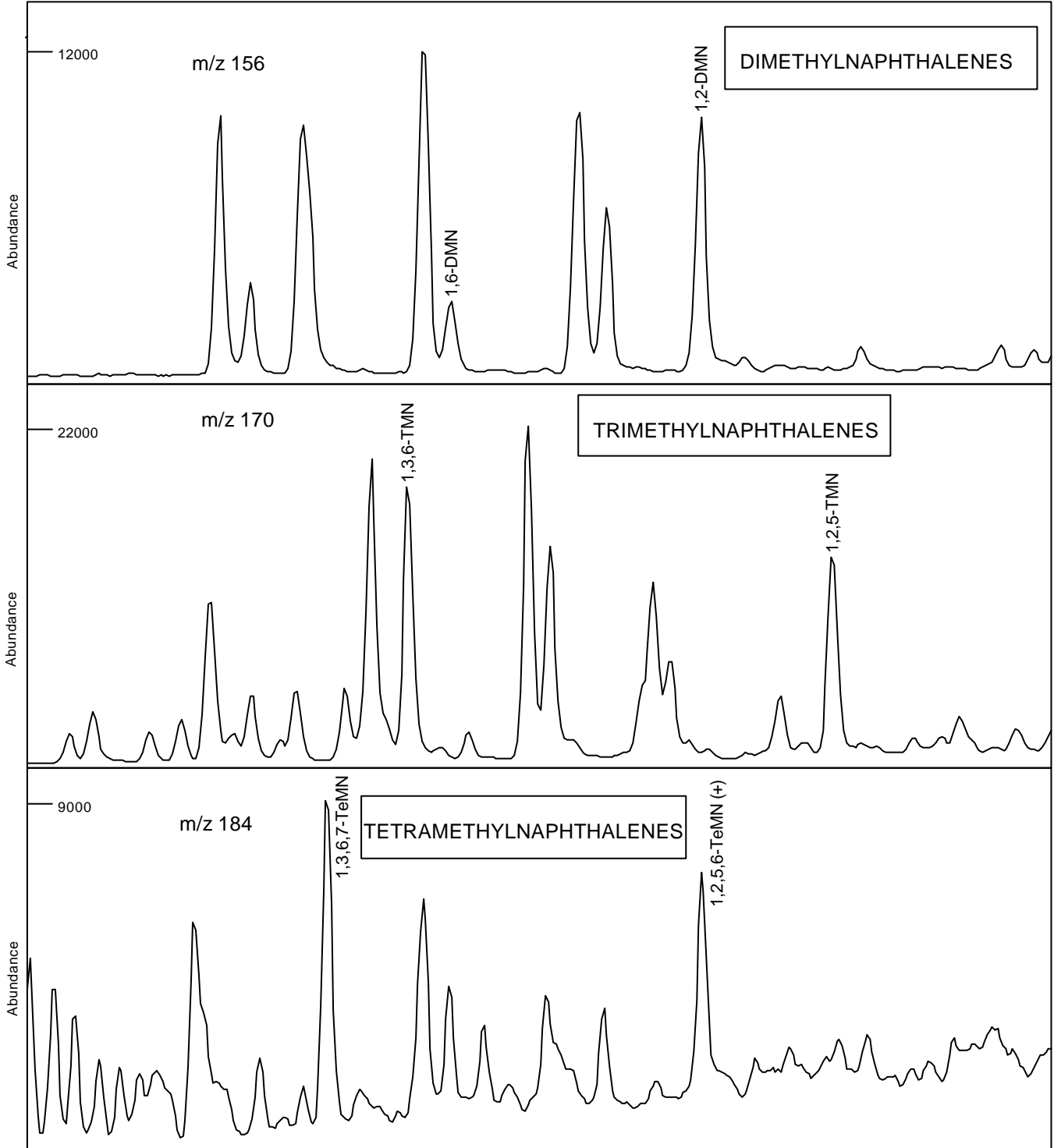


FIGURE 16C-3

Sample: MOBY-1, 588.5m, Test # 37, Crude Oil

File ID: 345808AB

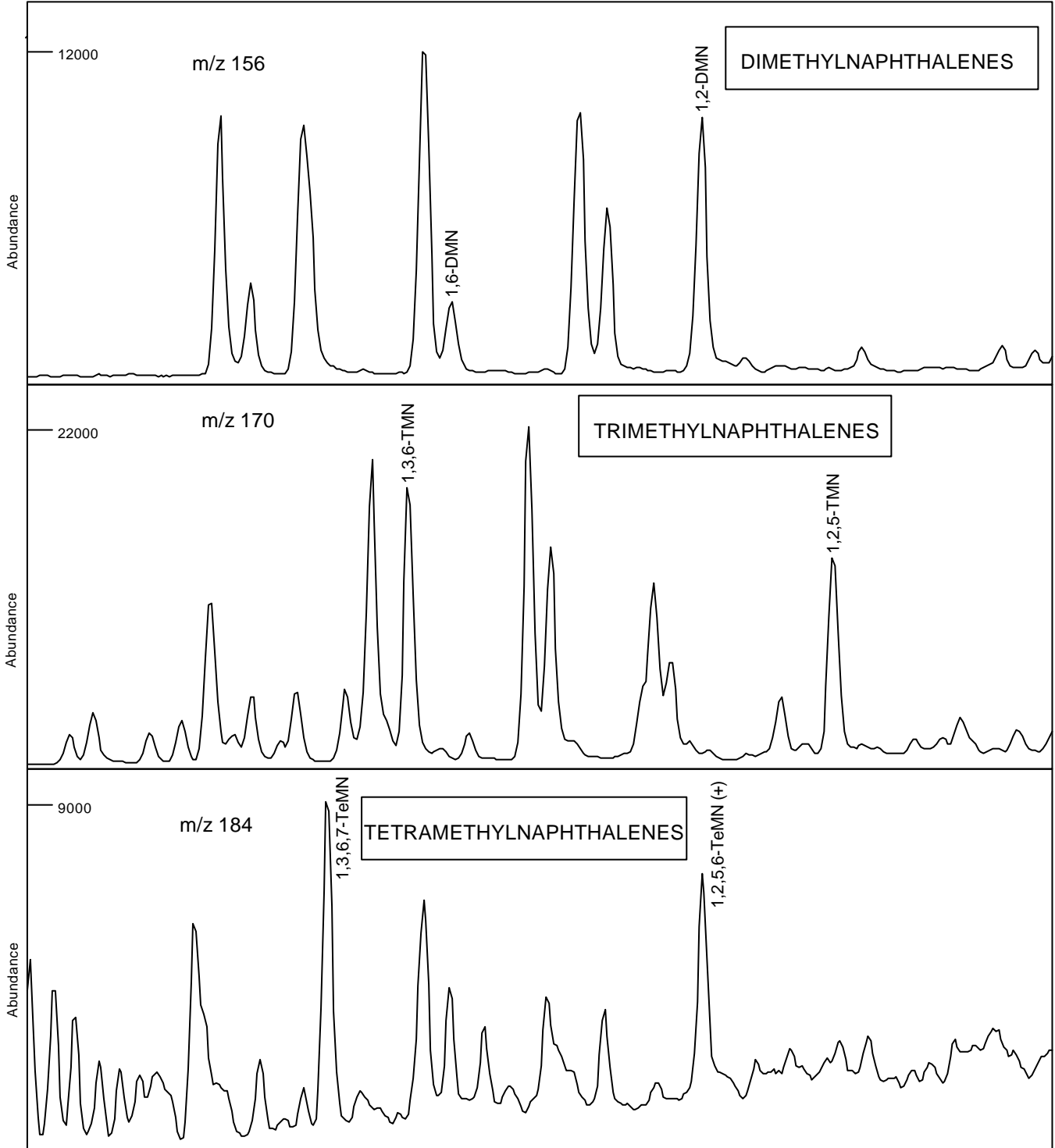


FIGURE 16D-3

Sample: **MOBY-1, 588.5m, Test # 37, Crude Oil**

File ID: **345808AB**

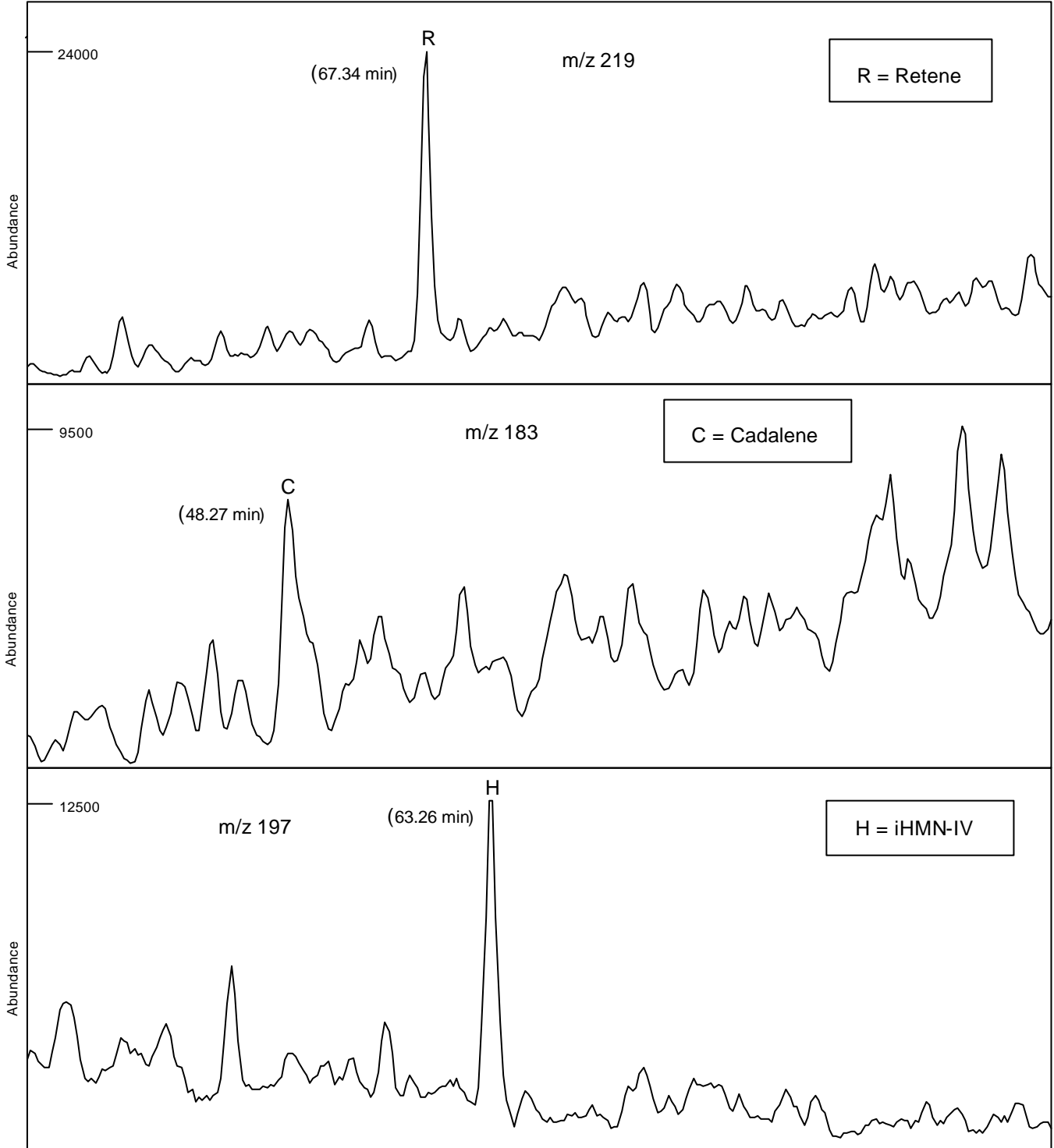


FIGURE 16E-3

Sample: **MOBY-1, 588.5m, Test # 37, Crude Oil**

File ID: **345808AB**

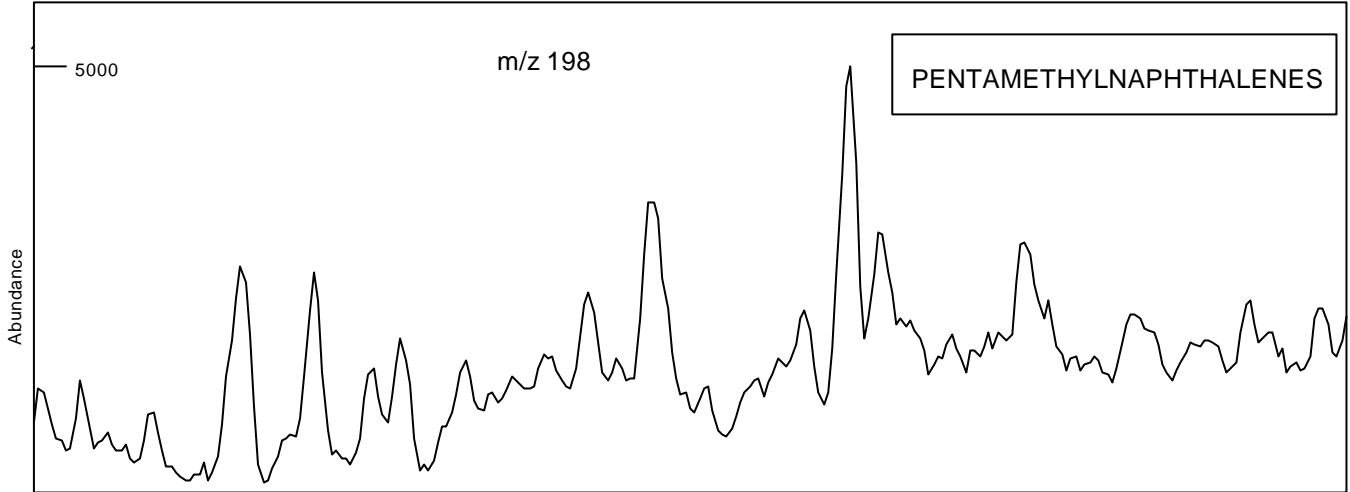


TABLE 9-1

## ANALYSIS OF BRANCHED AND CYCLIC SATURATED HYDROCARBONS BY GC-MS

MOBY-1, 560.0m, SWC



	<i>Selected Parameters</i>	<i>Ion(s)</i>	<i>Value</i>
1.	18 $\alpha$ (H)-hopane/17 $\alpha$ (H)-hopane (Ts/Tm)	191	0.37
2.	C30 hopane/C30 moretane	191	5.85
3.	C31 22S hopane/C31 22R hopane	191	0.53
4.	C32 22S hopane/C32 22R hopane	191	0.97
5.	C29 20S $\alpha\alpha\alpha$ sterane/C29 20R $\alpha\alpha\alpha$ sterane	217	0.76
6.	C29 $\alpha\alpha\alpha$ steranes (20S / 20S+20R)	217	0.43
7.	C29 $\alpha\beta\beta$ steranes	217	0.50
	<hr/> C29 $\alpha\alpha\alpha$ steranes + C29 $\alpha\beta\beta$ steranes		
8.	C27/C29 diasteranes	259	0.08
9.	C27/C29 steranes	217	0.24
10.	18 $\alpha$ (H)-oleanane/C30 hopane	191	nd
11.	<del>C29 diasteranes</del>		
	C29 $\alpha\alpha\alpha$ steranes + C29 $\alpha\beta\beta$ steranes	217	0.76
12.	C30 (hopane + moretane)	191/217	1.18
	C29 (steranes + diasteranes)		
13.	C15 drimane/C16 homodrimane	123	0.54
14.	Rearranged drimanes/normal drimanes	123	0.69

FIGURE 17A-1

Sample : MOBY-1, 560.0m, SWC

File ID : 345801B

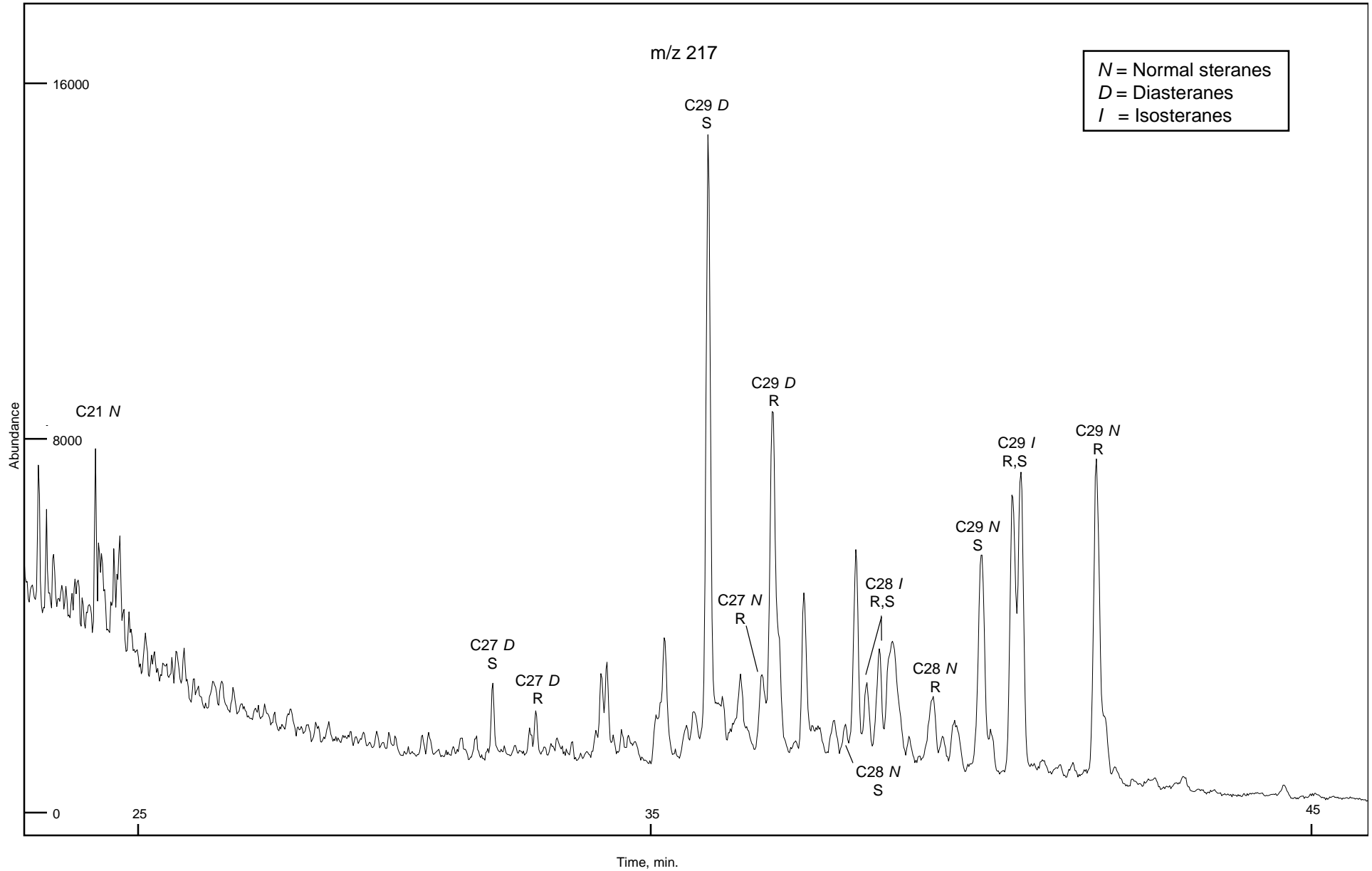


FIGURE 17B-1

Sample : MOBY-1, 560.0m, SWC

File ID : 345801B

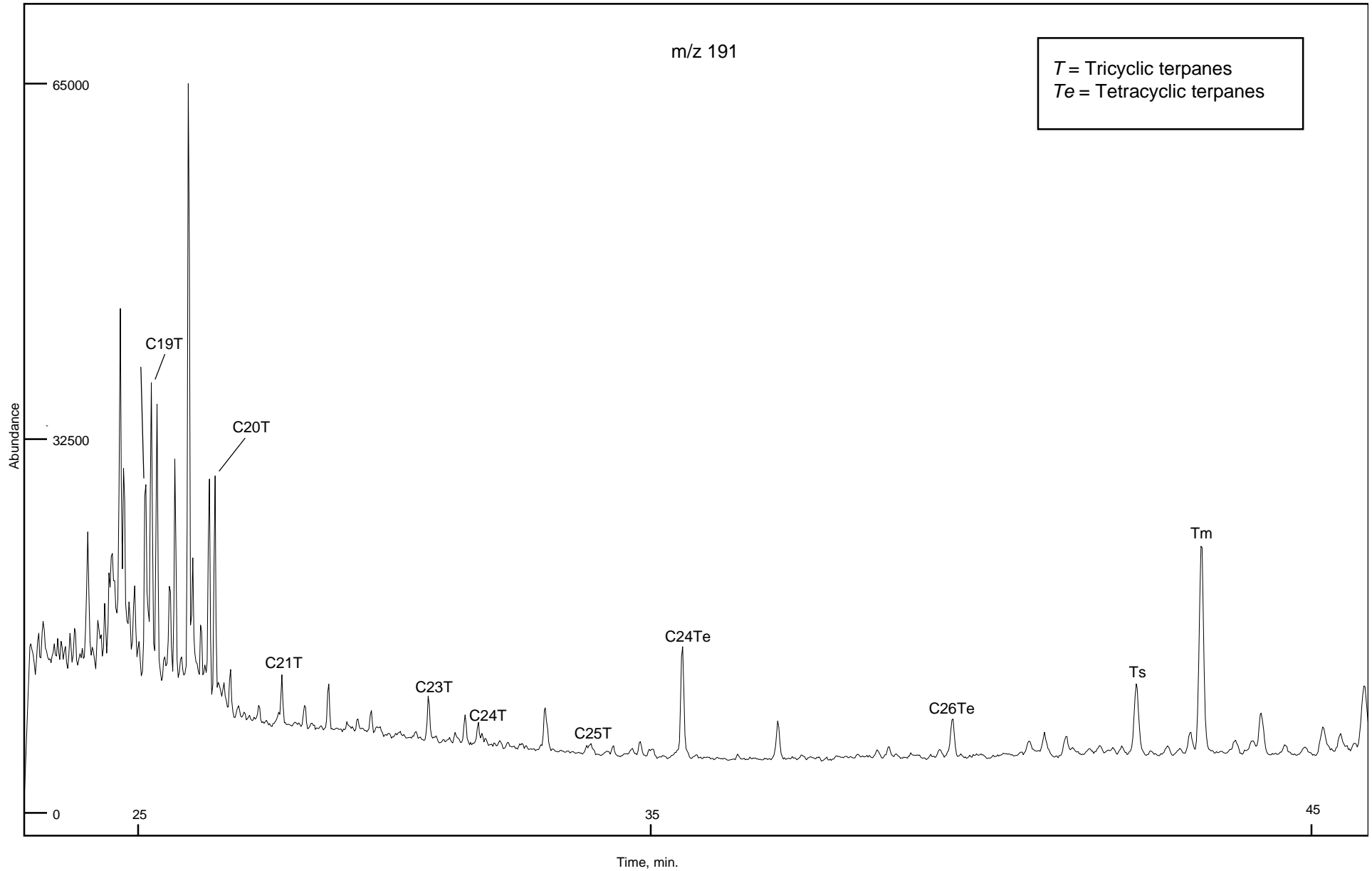


FIGURE 17C-1

Sample : MOBY-1, 560.0m, SWC

File ID : 345801B

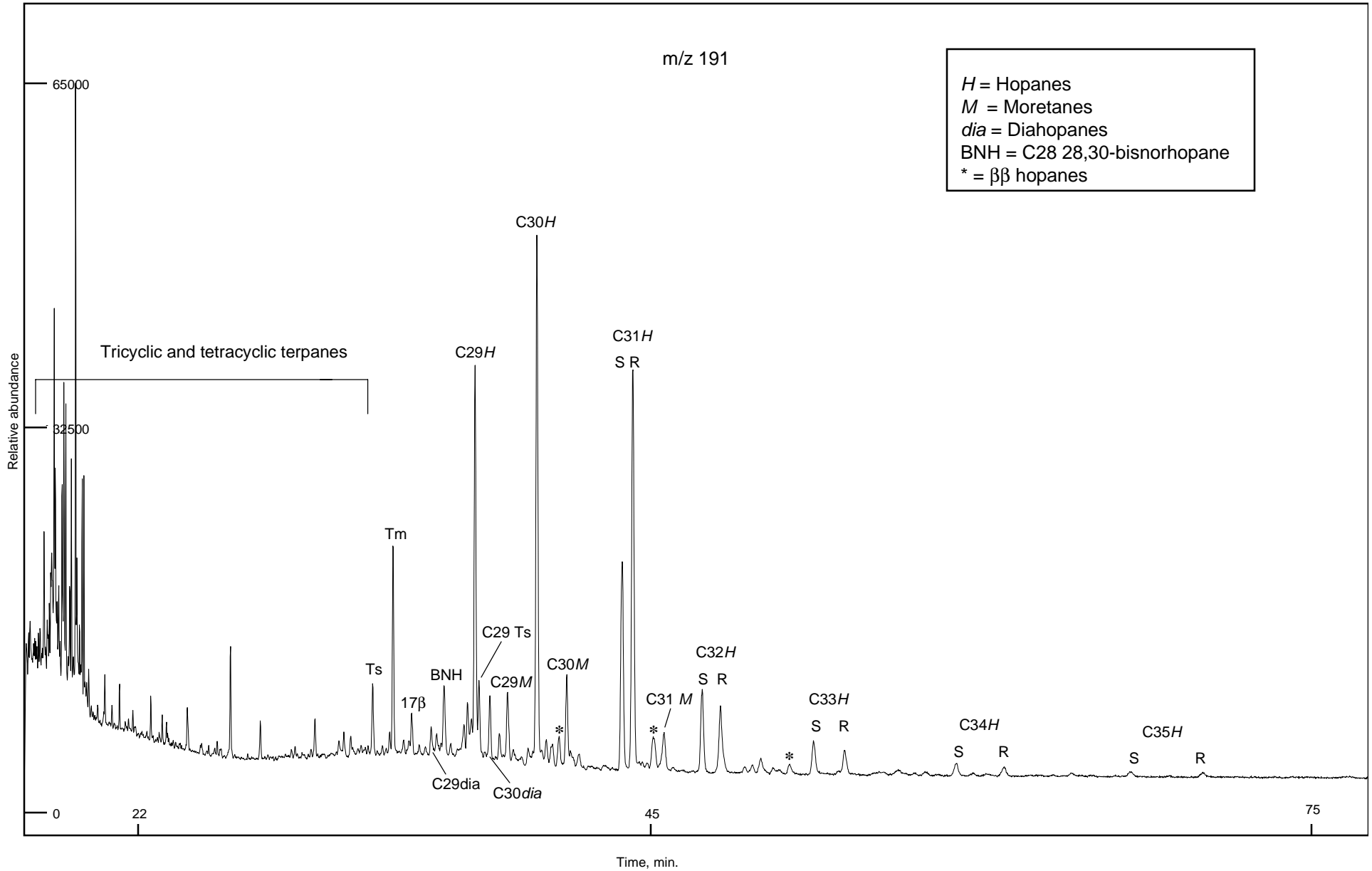


FIGURE 17D-1

Sample : MOBY-1, 560.0m, SWC

File ID : 345801B

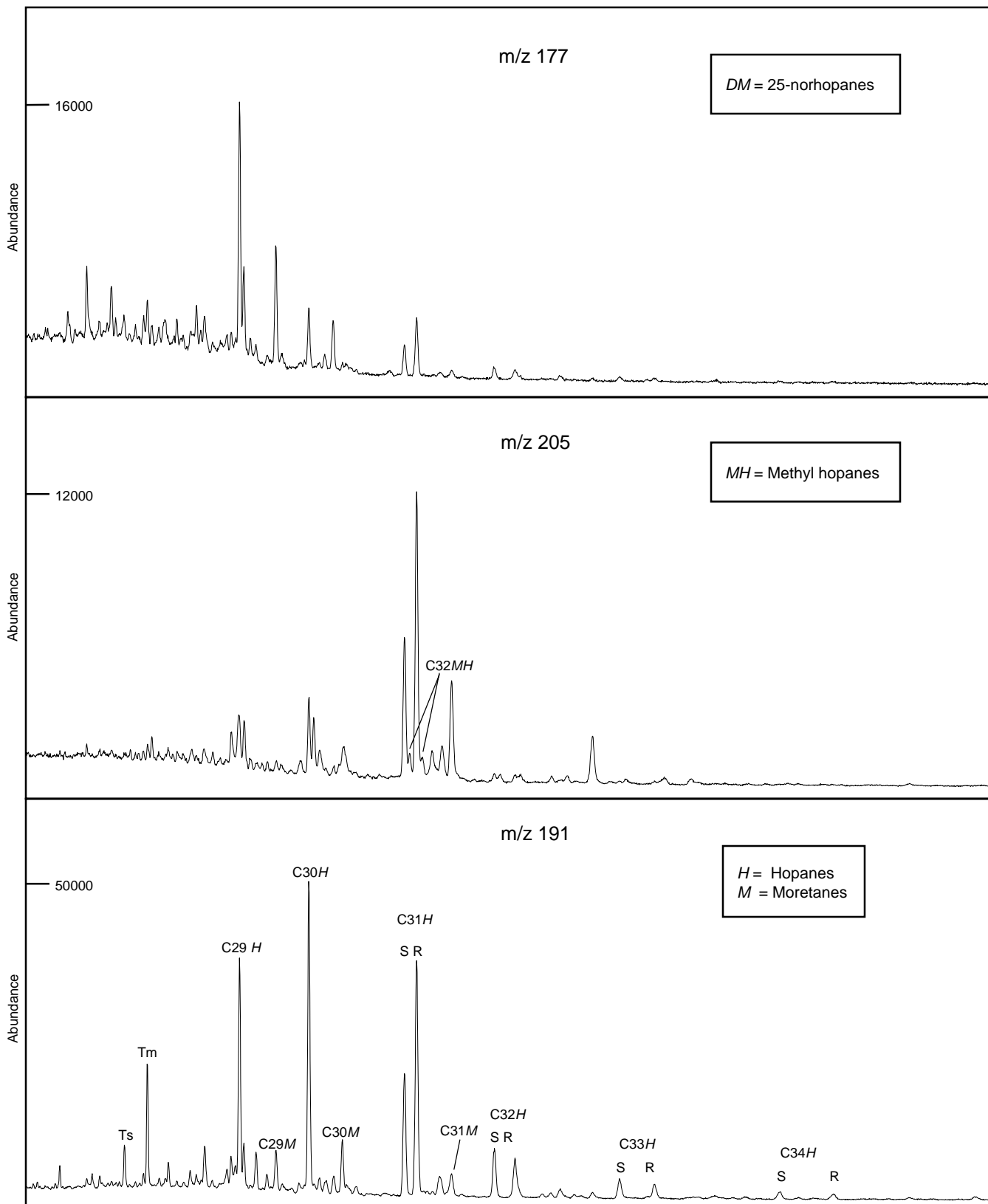


FIGURE 17E-1

Sample : MOBY-1, 560.0m, SWC

File ID : 345801B

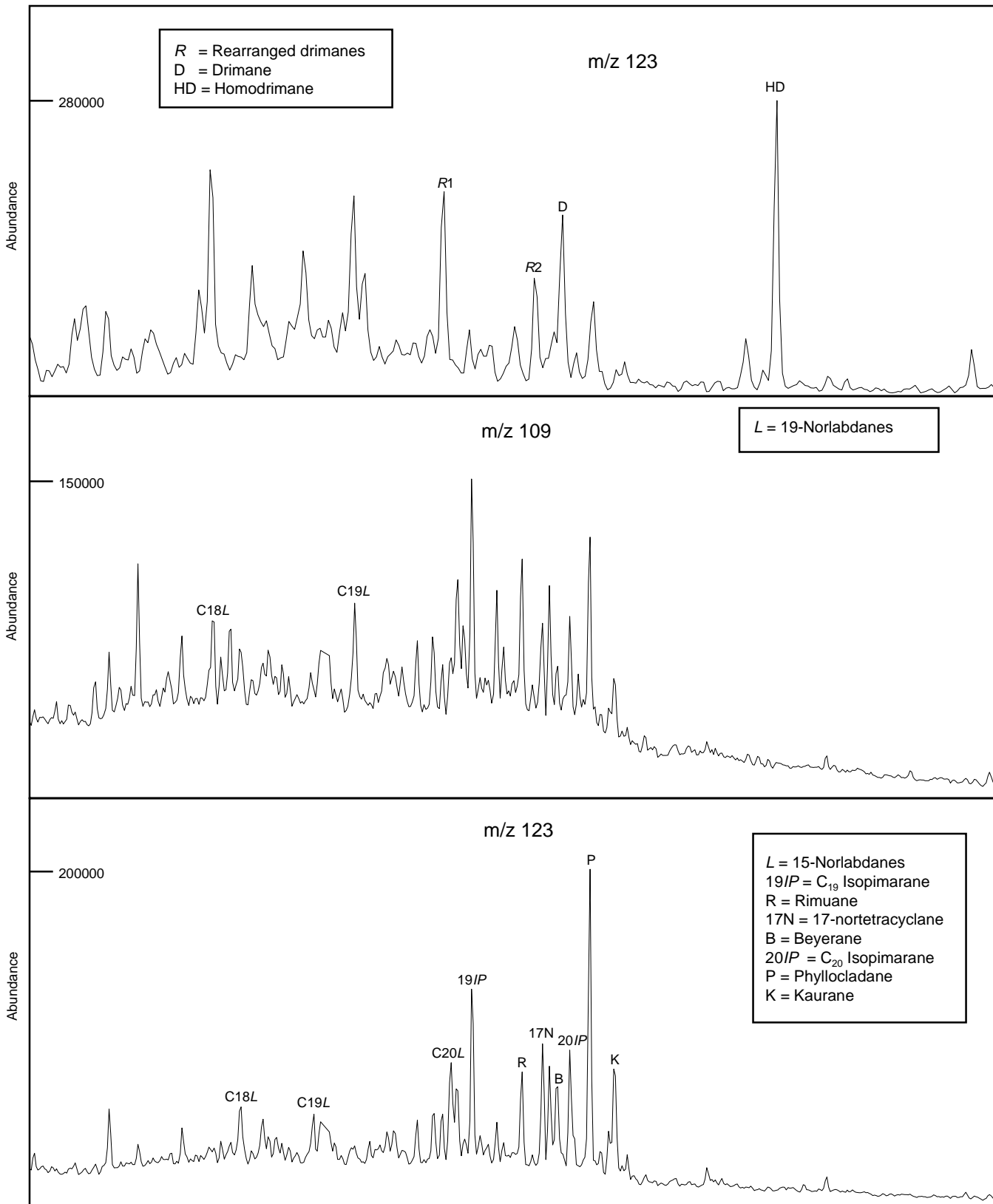


FIGURE 17F-1

Sample : MOBY-1, 560.0m, SWC

File ID : 345801B

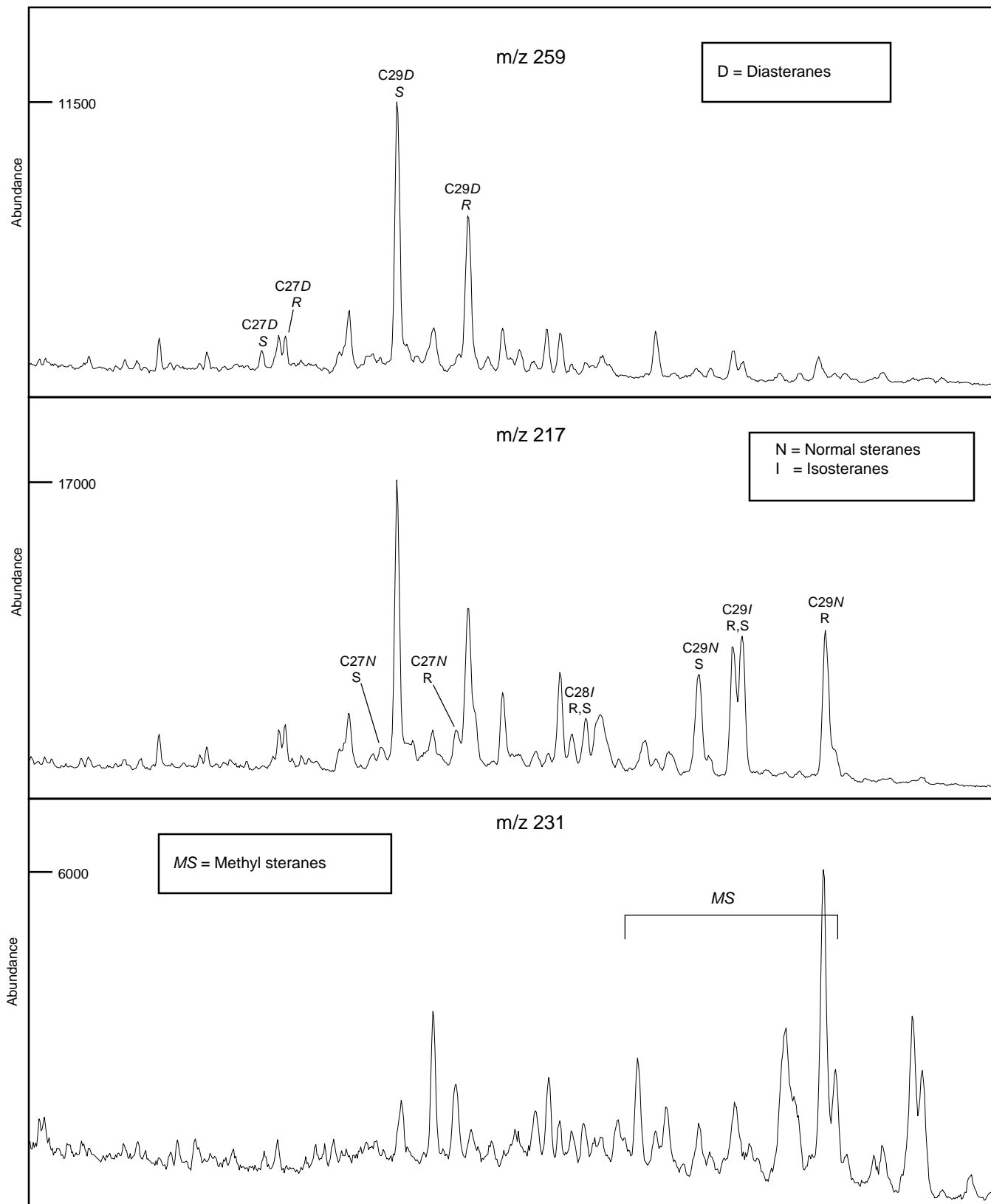


TABLE 9-2

## ANALYSIS OF BRANCHED AND CYCLIC SATURATED HYDROCARBONS BY GC-MS

MOBY-1, 586.0m, SWC



	<i>Selected Parameters</i>	<i>Ion(s)</i>	<i>Value</i>
1.	18 $\alpha$ (H)-hopane/17 $\alpha$ (H)-hopane (Ts/Tm)	191	0.37
2.	C30 hopane/C30 moretane	191	6.55
3.	C31 22S hopane/C31 22R hopane	191	0.87
4.	C32 22S hopane/C32 22R hopane	191	1.13
5.	C29 20S $\alpha\alpha\alpha$ sterane/C29 20R $\alpha\alpha\alpha$ sterane	217	0.81
6.	C29 $\alpha\alpha\alpha$ steranes (20S / 20S+20R)	217	0.45
7.	C29 $\alpha\beta\beta$ steranes	217	0.51
	<hr/> C29 $\alpha\alpha\alpha$ steranes + C29 $\alpha\beta\beta$ steranes		
8.	C27/C29 diasteranes	259	0.07
9.	C27/C29 steranes	217	0.20
10.	18 $\alpha$ (H)-oleanane/C30 hopane	191	nd
11.	<del>C29 diasteranes</del>		
	C29 $\alpha\alpha\alpha$ steranes + C29 $\alpha\beta\beta$ steranes	217	0.70
12.	C30 (hopane + moretane)	191/217	1.18
	C29 (steranes + diasteranes)		
13.	C15 drimane/C16 homodrimane	123	0.41
14.	Rearranged drimanes/normal drimanes	123	nd

FIGURE 17A-2

Sample : MOBY-1, 586.0m, SWC

File ID : 345805B

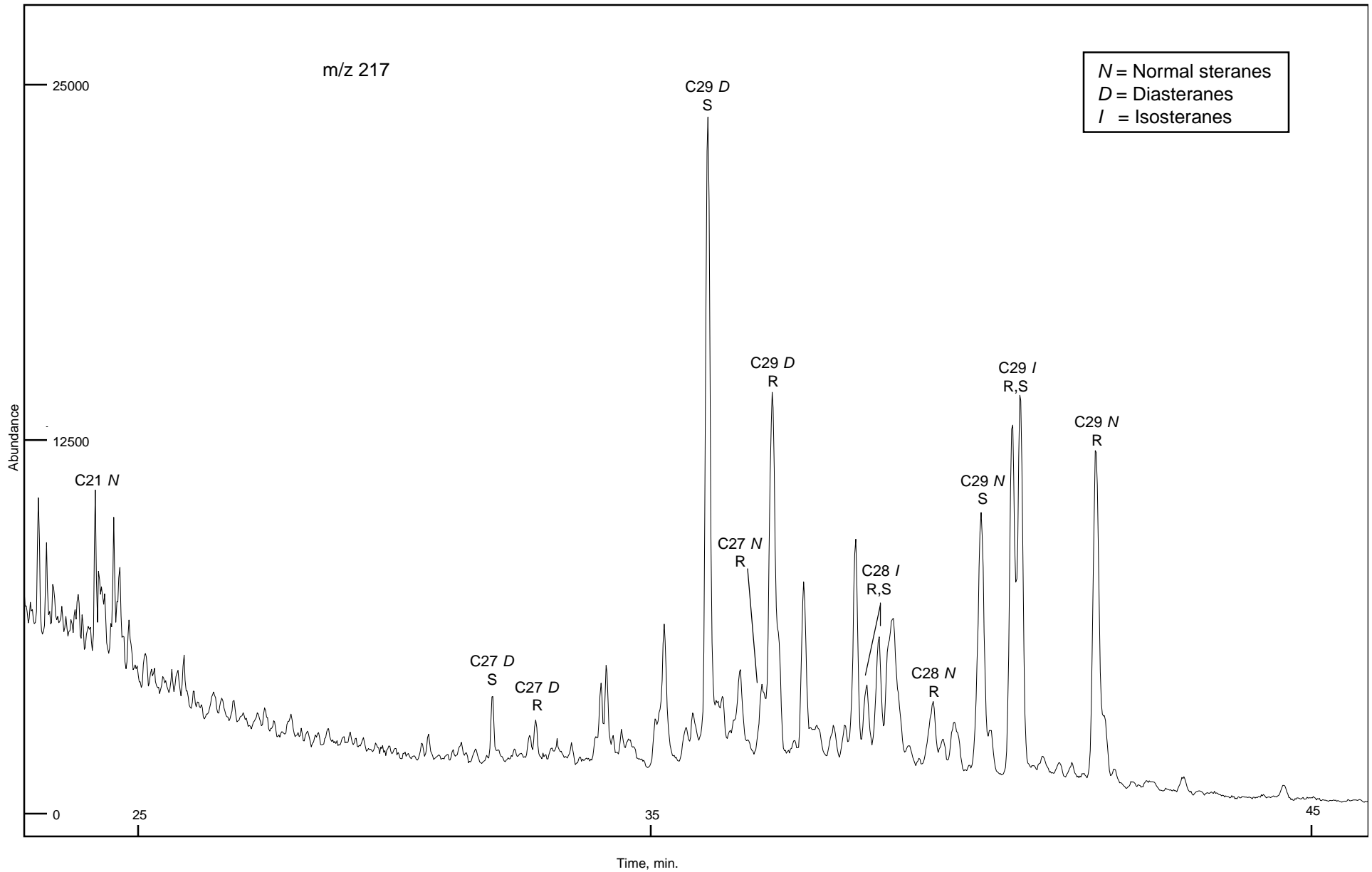


FIGURE 17B-2

Sample : MOBY-1, 586.0m, SWC

File ID : 345805B

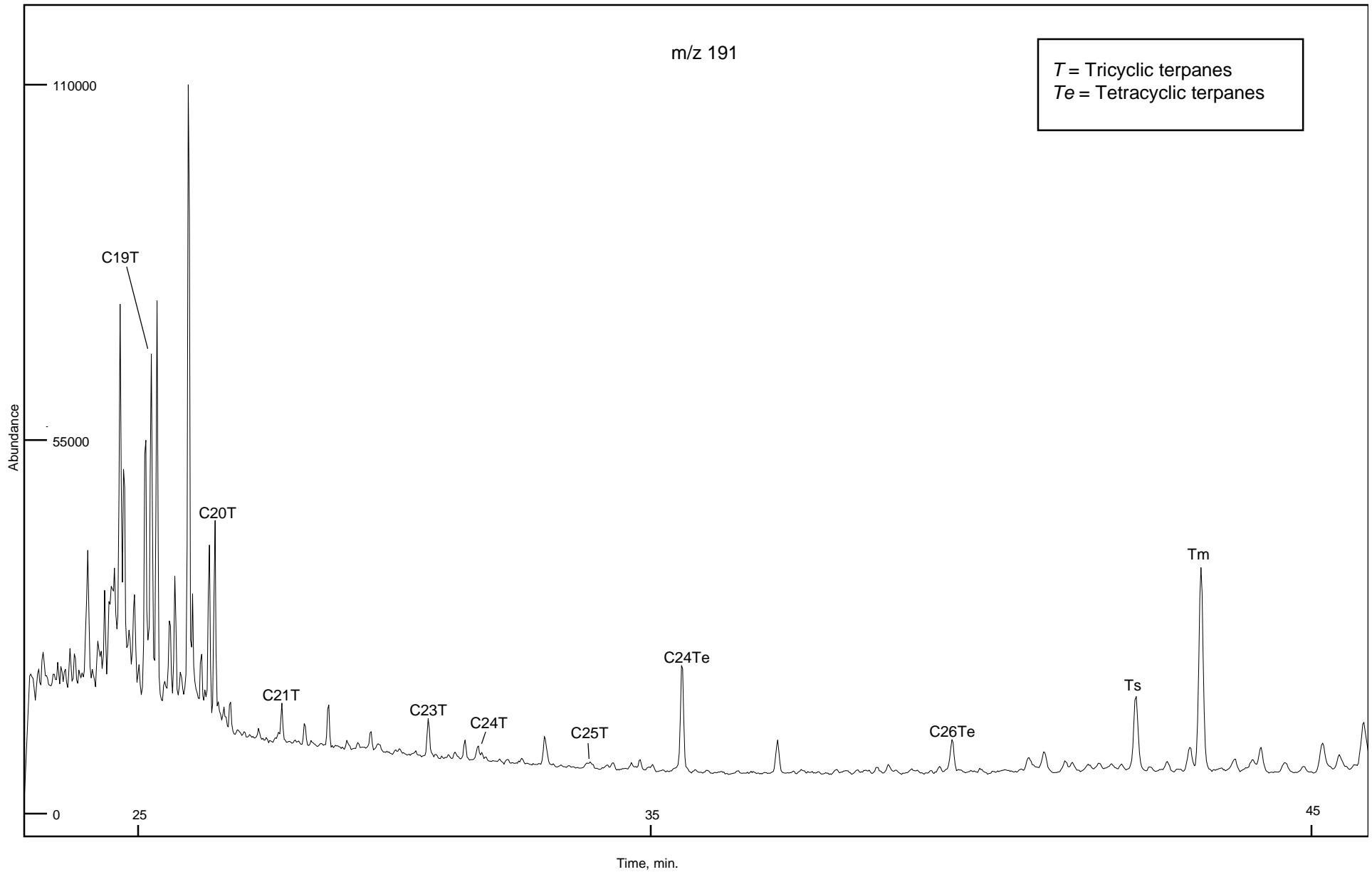


FIGURE 17C-2

Sample : MOBY-1, 586.0m, SWC

File ID : 345805B

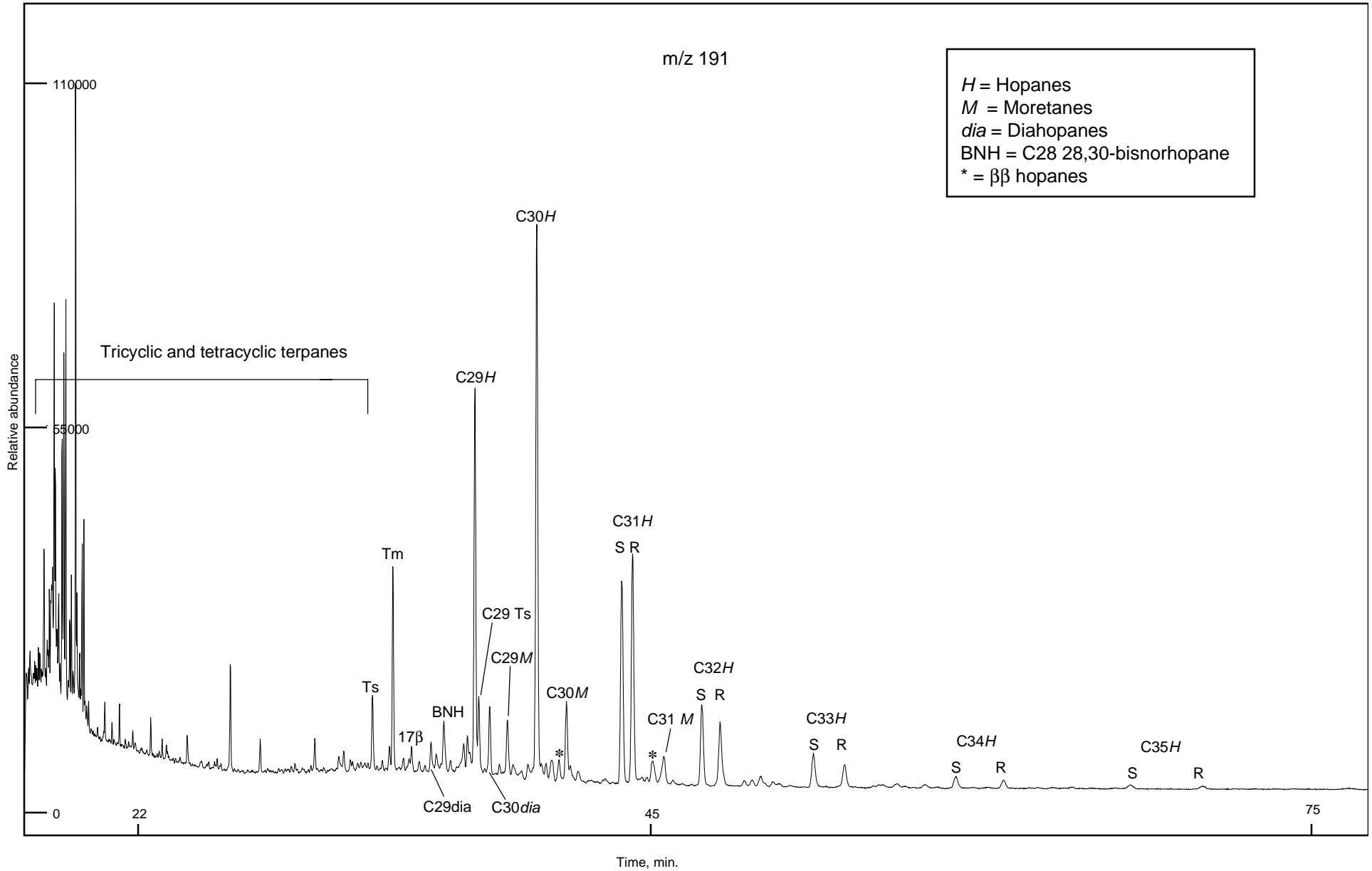


FIGURE 17D-2

Sample : MOBY-1, 586.0m, SWC

File ID : 345805B

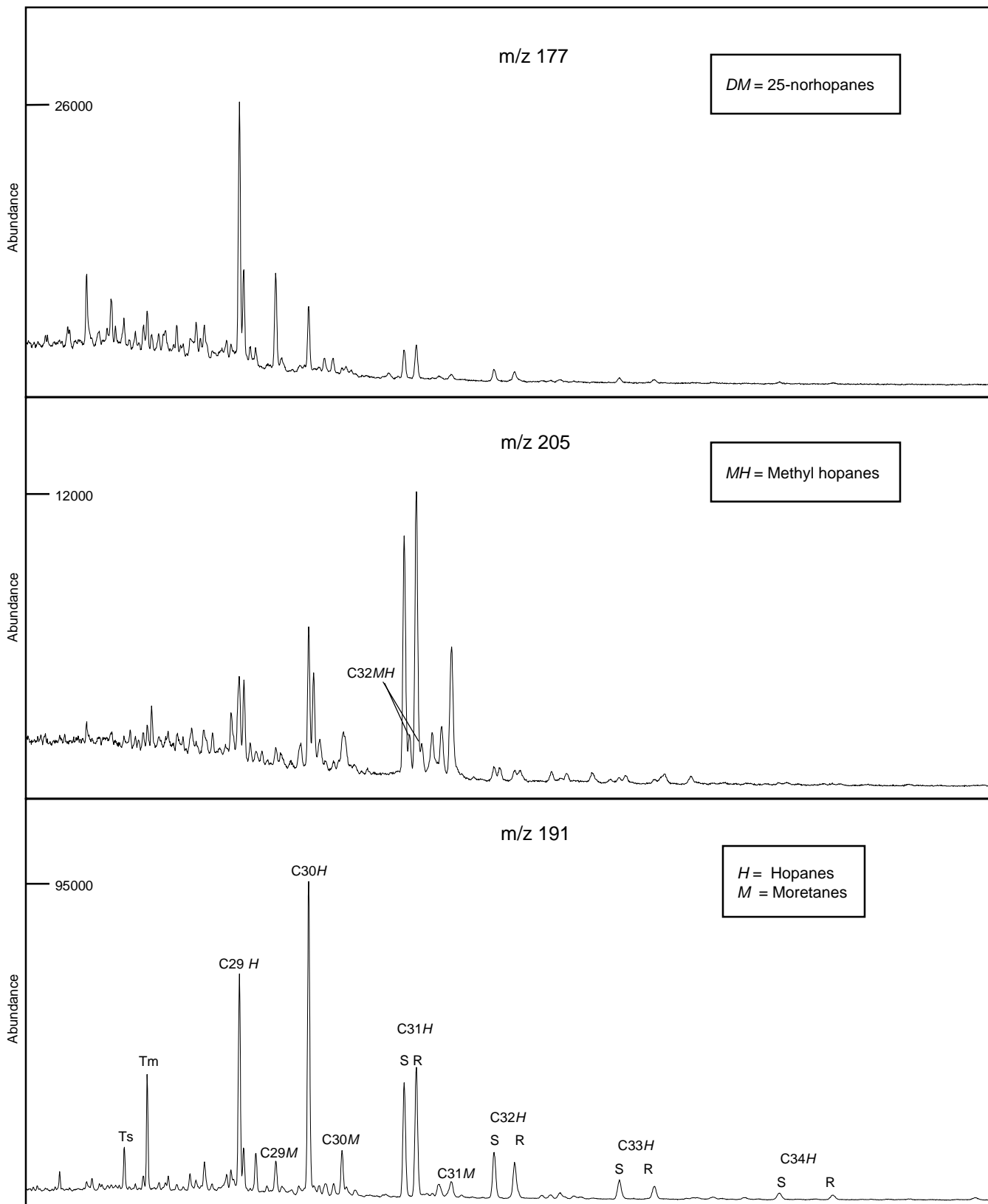


FIGURE 17E-2

Sample : MOBY-1, 586.0m, SWC

File ID : 345805B

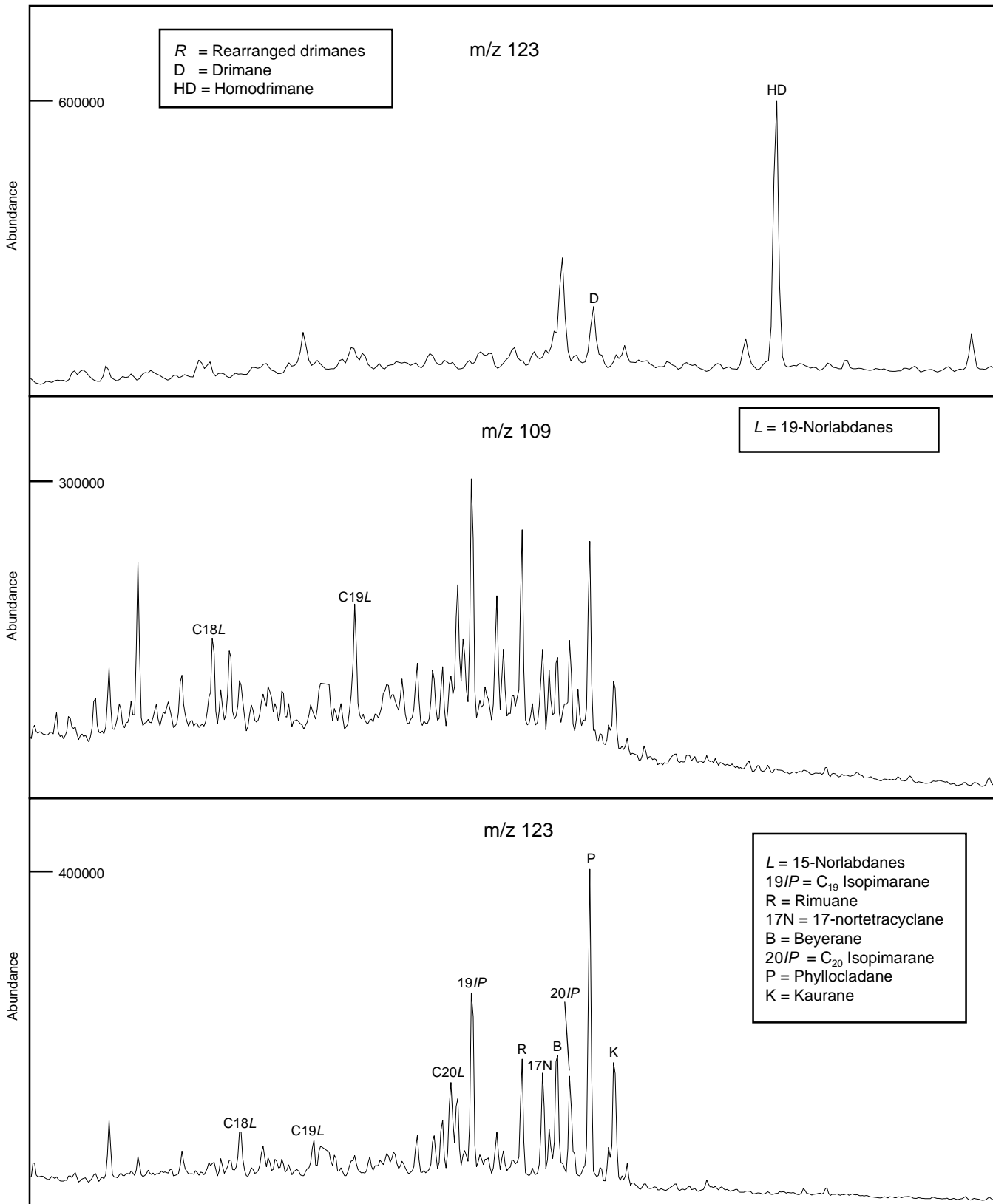


FIGURE 17F-2

Sample : MOBY-1, 586.0m, SWC

File ID : 345805B

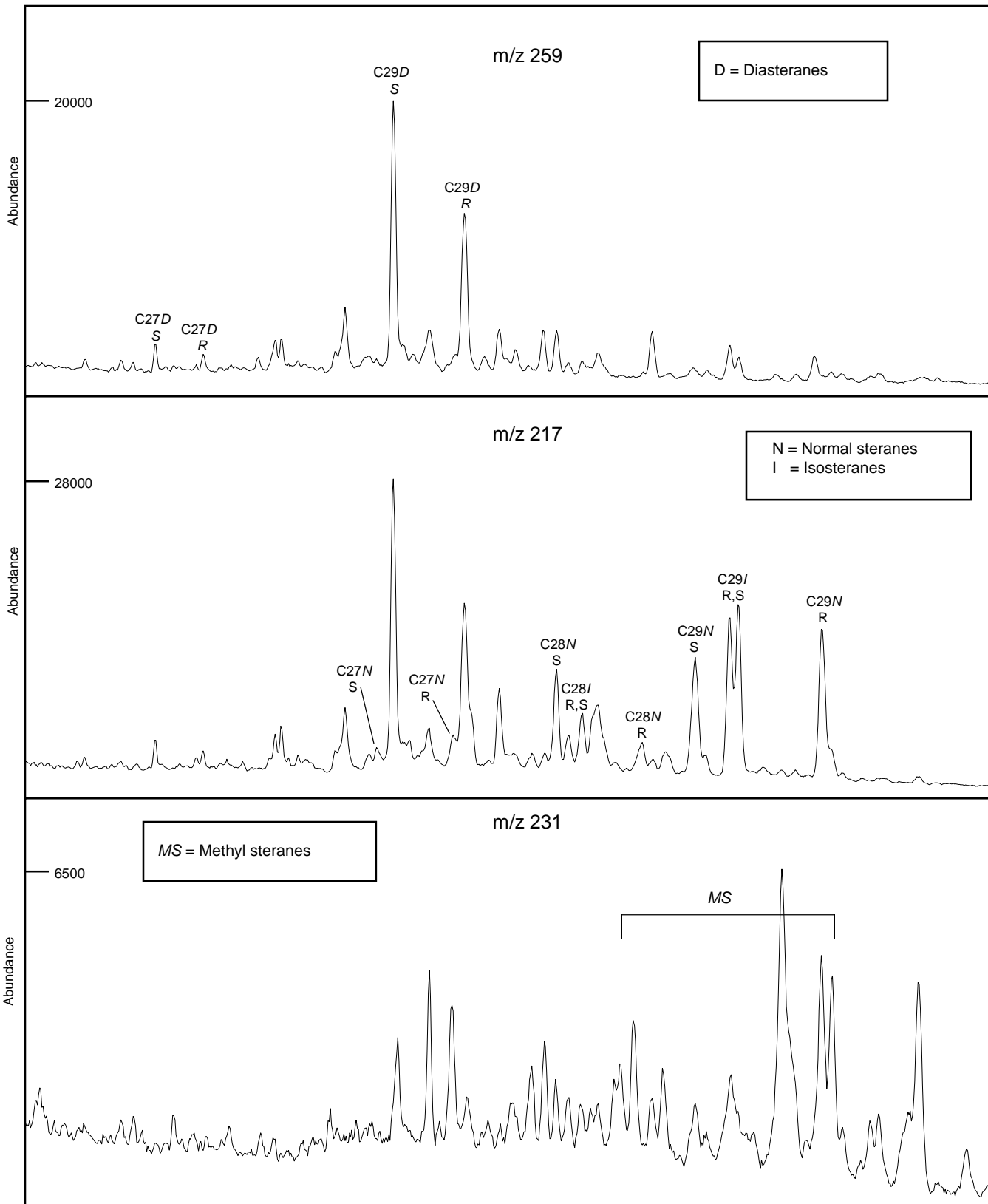


Table 9-3

## ANALYSIS OF BRANCHED AND CYCLIC SATURATED HYDROCARBONS BY GC-MS

MOBY-1, 588.5m, Crude Oil



	<i>Selected Parameters</i>	<i>Ion(s)</i>	<i>Value</i>
1.	18 $\alpha$ (H)-hopane/17 $\alpha$ (H)-hopane (Ts/Tm)	191	2.77
2.	C30 hopane/C30 moretane	191	8.85
3.	C31 22S hopane/C31 22R hopane	191	1.35
4.	C32 22S hopane/C32 22R hopane	191	1.26
5.	C29 20S $\alpha\alpha\alpha$ sterane/C29 20R $\alpha\alpha\alpha$ sterane	217	1.17
6.	C29 $\alpha\alpha\alpha$ steranes (20S / 20S+20R)	217	0.54
7.	<u>C29 <math>\alpha\beta\beta</math> steranes</u> C29 $\alpha\alpha\alpha$ steranes + C29 $\alpha\beta\beta$ steranes	217	0.56
8.	C27/C29 diasteranes	259	0.69
9.	C27/C29 steranes	217	1.07
10.	18 $\alpha$ (H)-oleanane/C30 hopane	191	nd
11.	<u>C29 diasteranes</u> C29 $\alpha\alpha\alpha$ steranes + C29 $\alpha\beta\beta$ steranes	217	0.78
12.	<u>C30 (hopane + moretane)</u> C29 (steranes + diasteranes)	191/217	1.61
13.	C15 drimane/C16 homodrimane	123	0.78
14.	Rearranged drimanes/normal drimanes	123	0.75

FIGURE 17A-3

Sample : **MOBY-1, 588.5m, Test # 37, Crude Oil**

File ID : 345808B

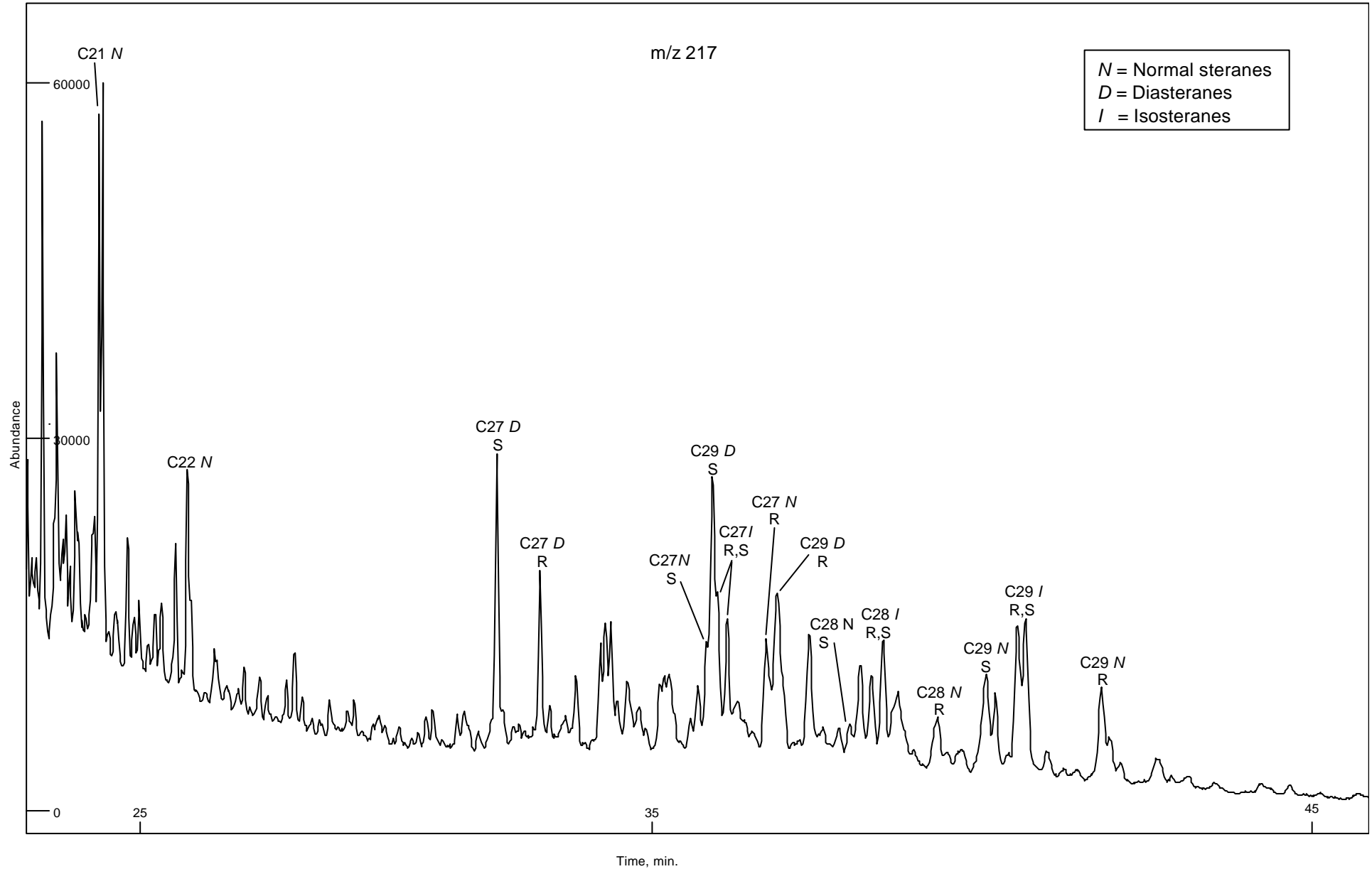


FIGURE 17B-3

Sample : MOBY-1, 588.5m, Test # 37, Crude Oil

File ID : 345808B

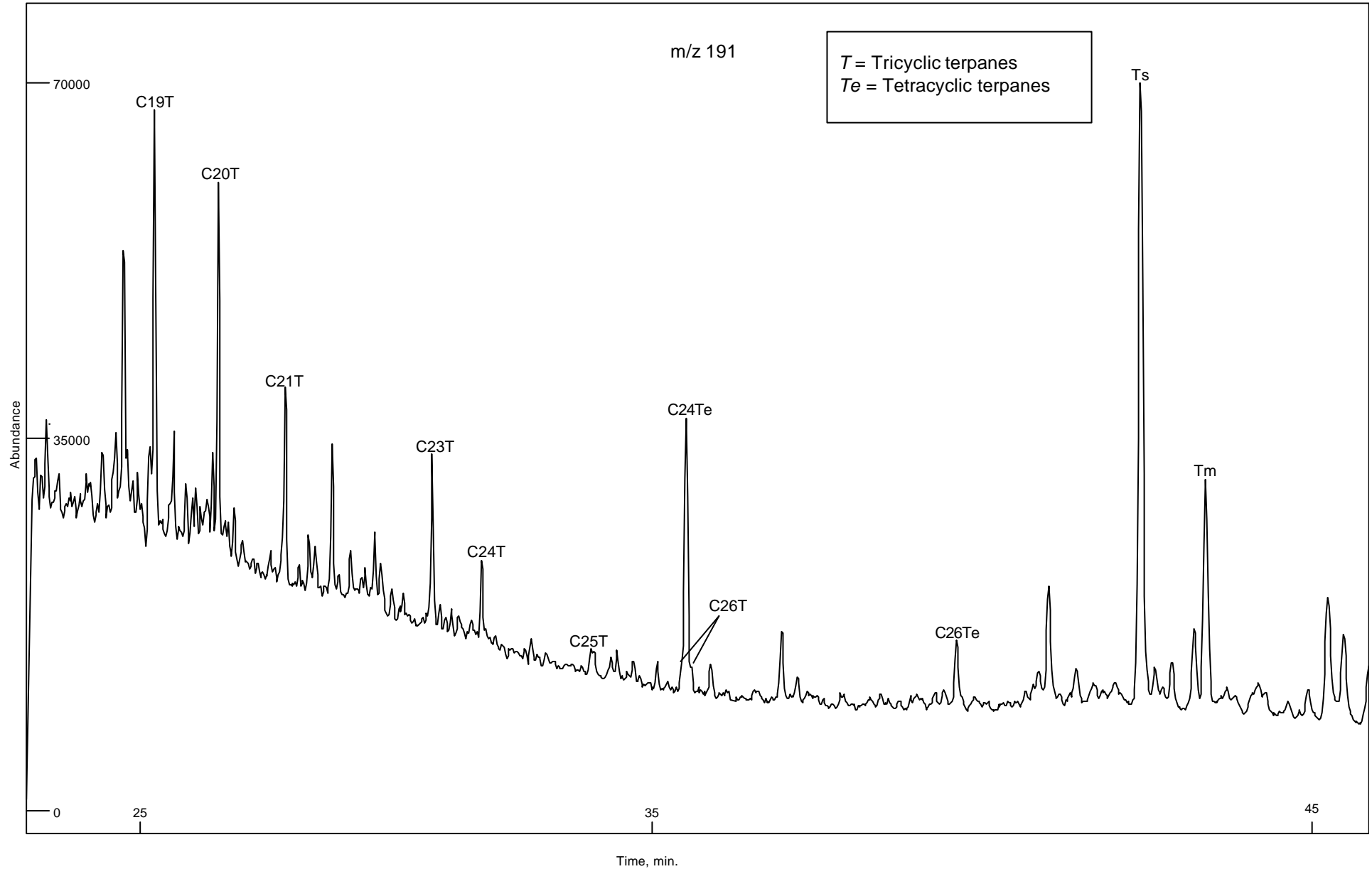


FIGURE 17C-3

Sample : **MOBY-1, 588.5m, Test # 37, Crude Oil**

File ID : 345808B

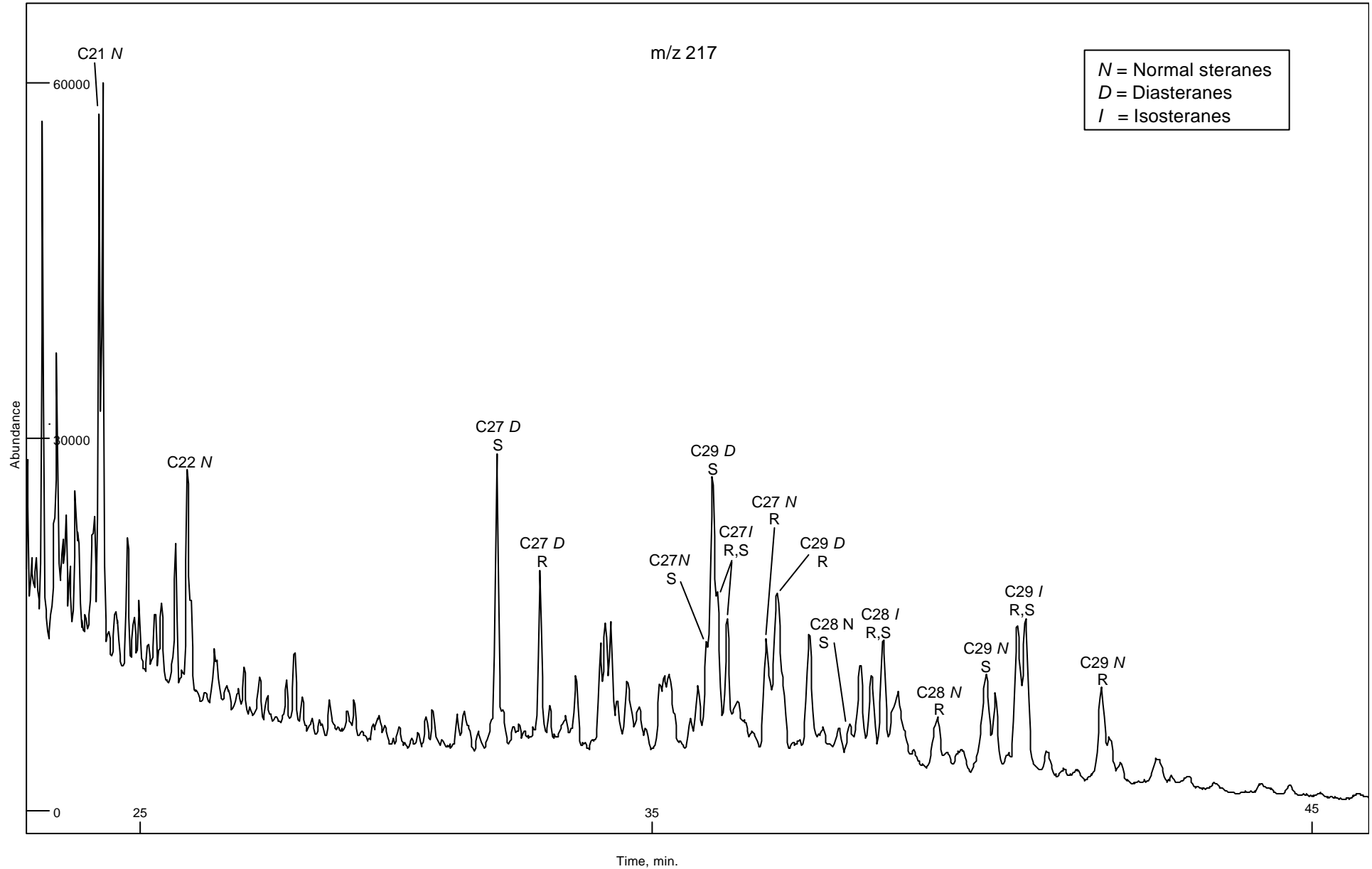


FIGURE 17D-3

Sample : MOBY-1, 588.5m, Test # 37, Crude Oil

File ID : 345808B

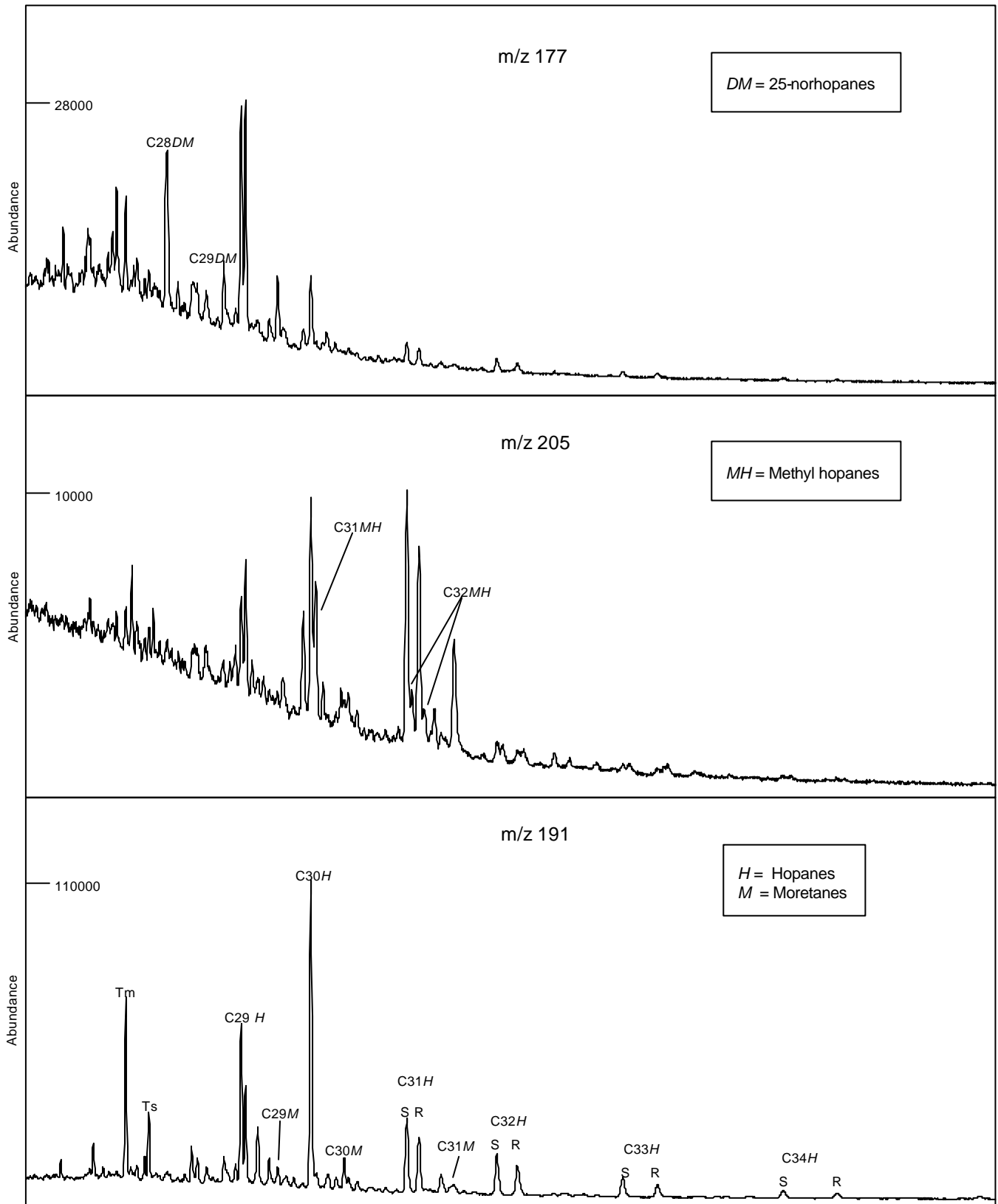


FIGURE 17E-3

Sample : MOBY-1, 588.5m, Test # 37, Crude Oil

File ID : 345808B

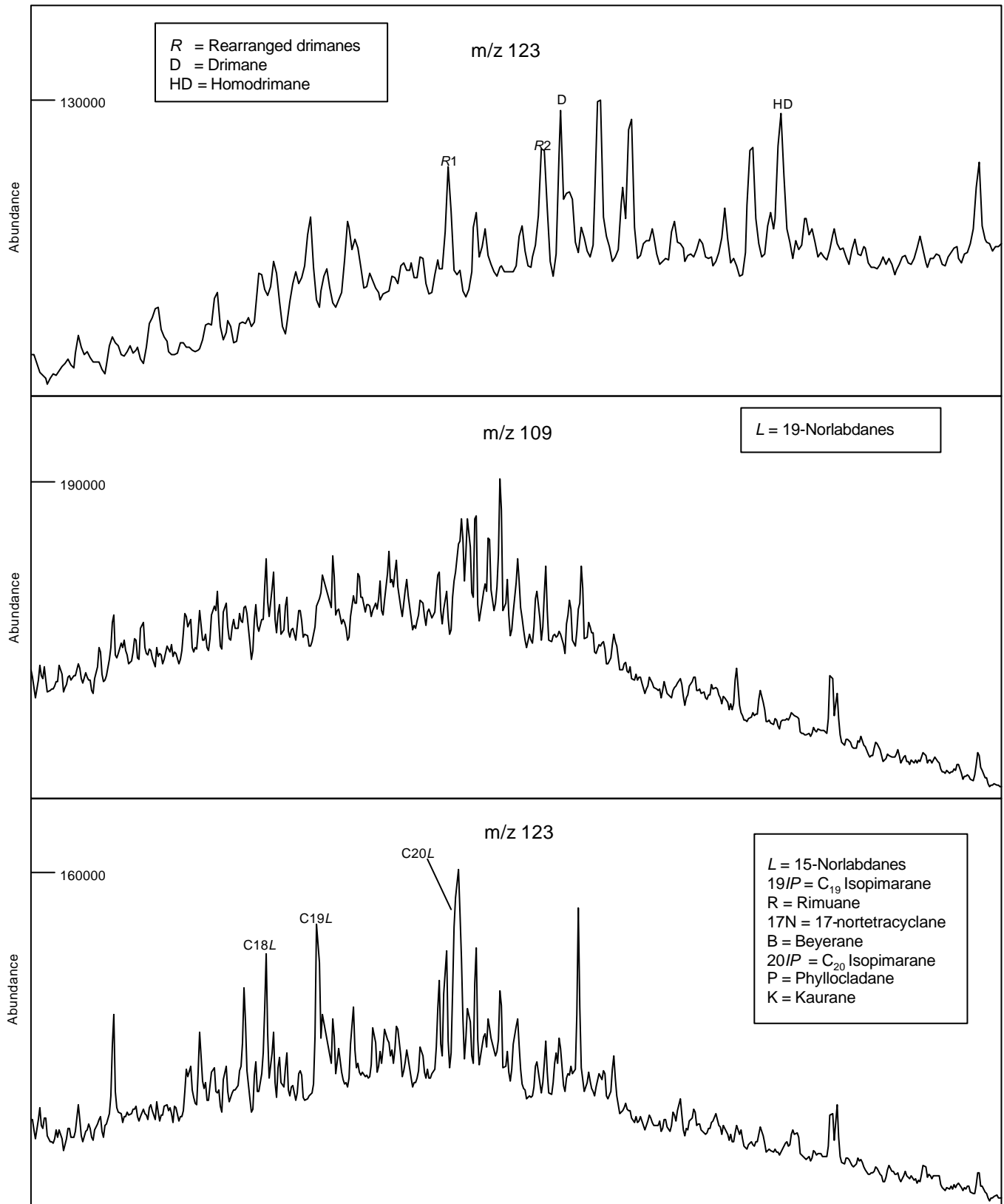
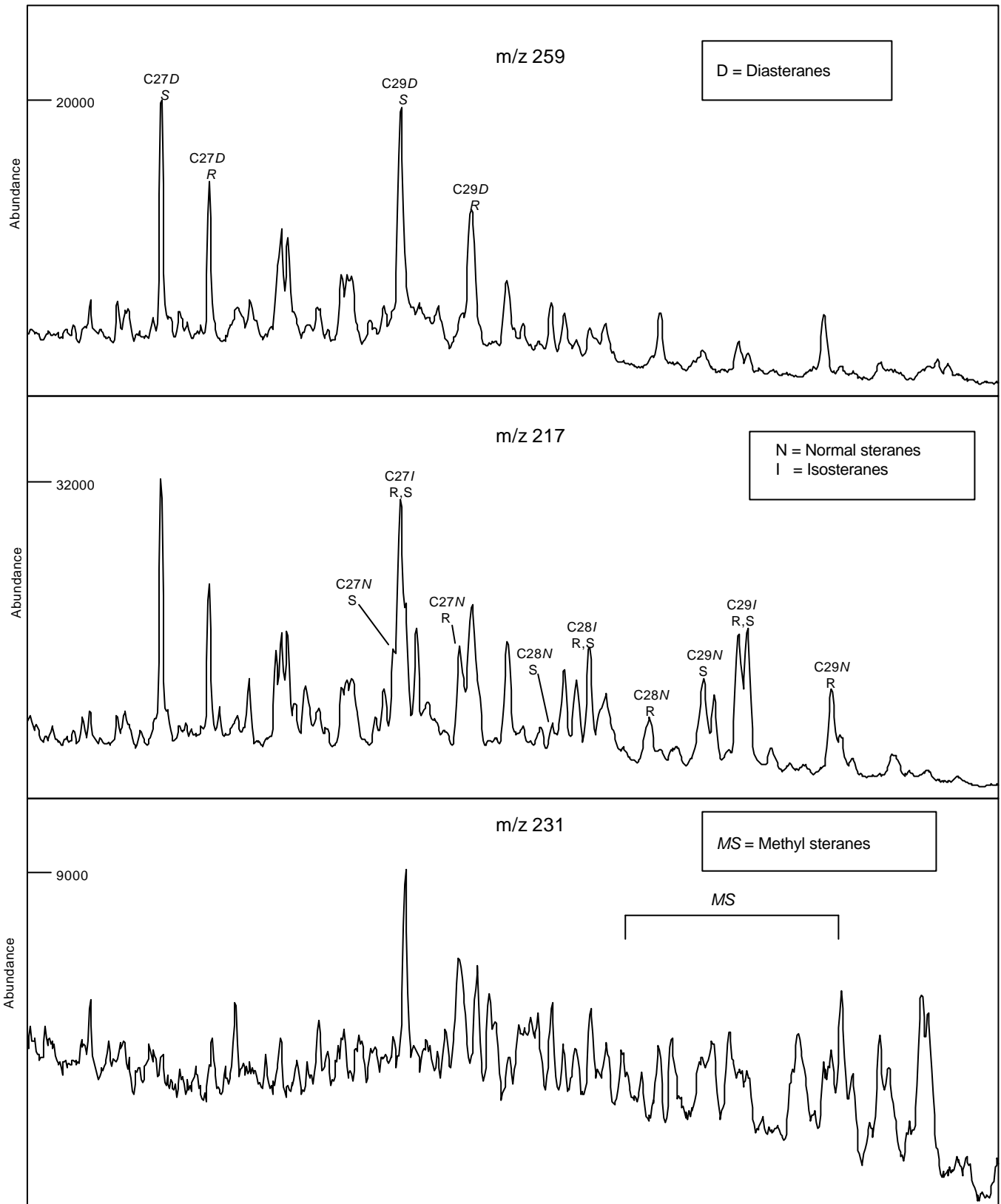


FIGURE 17F-3

Sample : MOBY-1, 588.5m, Test # 37, Crude Oil

File ID : 345808B



## **APPENDIX B**

### **THEORY AND METHODS**

## **PETROLEUM GEOCHEMISTRY**

### **1.0 INTRODUCTION**

Petroleum geochemistry is primarily concerned with the application of organic chemistry to samples of geological interest in hydrocarbon exploration.

Analyses can be carried out on cuttings, sidewall cores, conventional cores, relatively unweathered outcrop samples and fluid hydrocarbons (oil, condensate, gas).

Source rock evaluation is best performed on sidewall cores, since cuttings are more susceptible to contamination from both cavings and organic additives in the mud system. In petroleum geochemical studies it is vitally important for the geochemist/geologist to be aware of the type of mud additives used and the stage at which they are used during the drilling program. Any anomalous results must be carefully considered in conjunction with mud system records.

Petroleum geochemistry in exploration is applied for three major purposes:

1. Identification of richness, maturity and type of kerogen in (a large number of) whole rock samples by screening analyses.
2. Semi-detailed characterisation of kerogen in sediments from selected source intervals, to determine maturity, source type and genetic potential.
3. Detailed characterisation of petroleum fluids (extracts, oils and condensates) by assessment of thermal maturity, source type and depositional environment to enable oil-to-oil and oil-to-source rock correlation studies.

## 2.0 THEORY & METHODS

Samples are analysed according to the scheme illustrated in Figure 1 which shows the order and type of analysis for both screening and detailed tests.

### 2.1 Screening Analyses of Whole Rock Samples

#### 2.1.1 Headspace/Cuttings Gas Analysis

The headspace sample is usually provided in a sealed tin can which holds both cuttings and water to approximately three quarters capacity. This allows the volatile hydrocarbons to diffuse easily into an appreciable headspace.

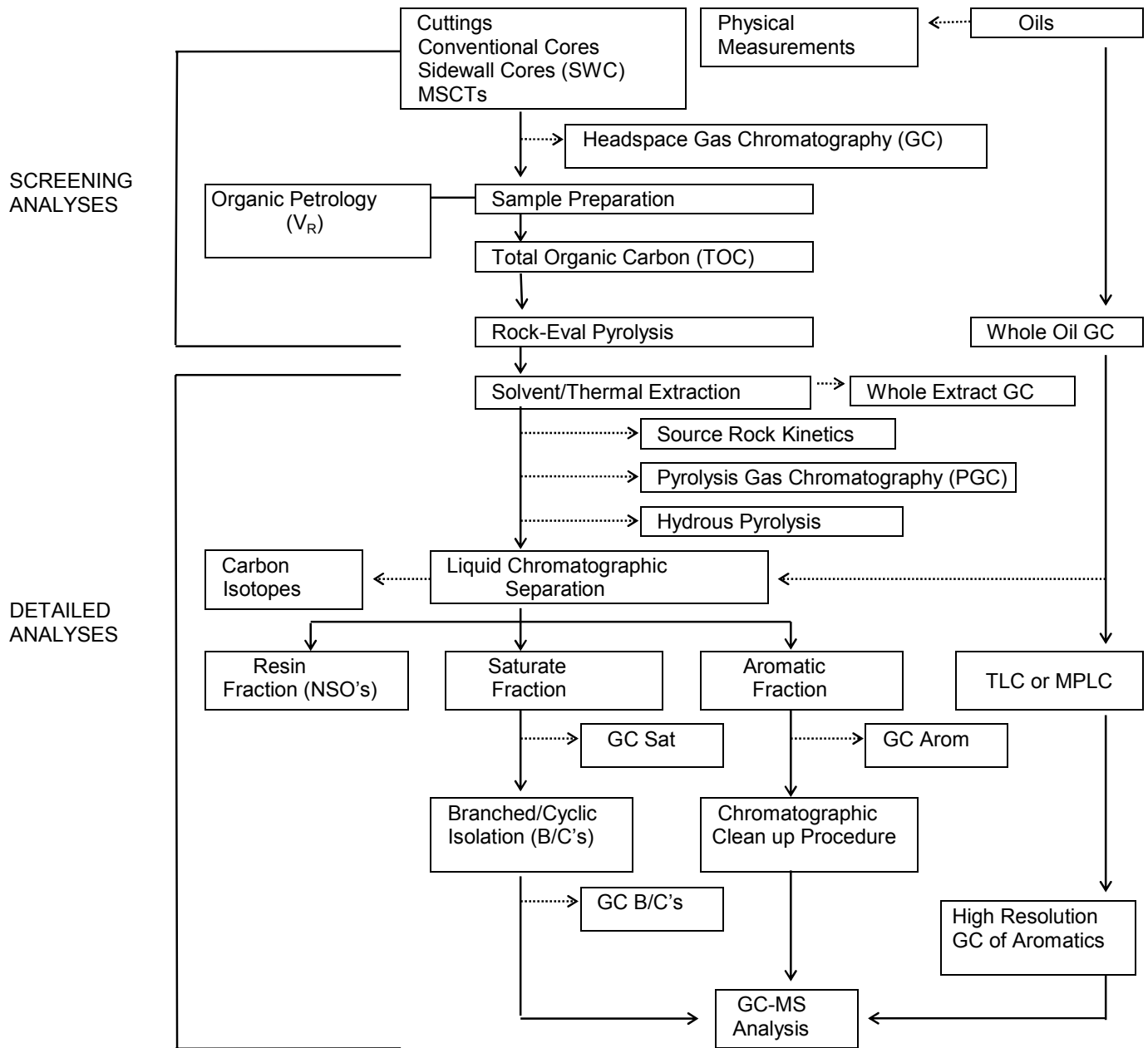
The gas is taken into a syringe through a silicone seal on the lid of the container and analysed by packed column gas chromatography using the following conditions:

Instrument:	Shimadzu GC-8APF
Column:	6'x 1/8" Chromosorb 102
Injector/Detector Temperature:	120°C
Column Temperature:	110°C
Carrier Gas:	Nitrogen

Cuttings gas analysis is performed in the same manner but on samples which do not liberate volatile gases readily. These sediments are subjected to very vigorous agitation prior to sampling.

Values are given as volume of gas per million volumes of sediment (ppm) for each hydrocarbon (methane, ethane, propane, iso- and n-butane), as composite values including C<sub>5</sub>-C<sub>7</sub>, and as ratios.

FIGURE 1  
FLOW DIAGRAM FOR PETROLEUM GEOCHEMICAL ANALYSES



Headspace/cuttings gas analyses are used as a screening technique to identify zones of significant gas generation and out-of-place gas (Letran et al, 1974). The classification for gas content is listed below:

Total gas content (C <sub>1</sub> ;C <sub>2</sub> -C <sub>4</sub> ; or C <sub>5</sub> -C <sub>7</sub> )	Description
10 -100ppm	very lean - lean
100-1,000	lean - moderate
1,000-10,000	moderate - rich
10,000-100,000	rich - very rich

The abundance of C<sub>2</sub>-C<sub>4</sub> components (wet gas) is used to locate the zone of oil generation, since wet gas is commonly associated with petroleum (Fuex, 1977).

It is important to ensure that the gases analysed are not of a biogenic origin, so an anti-bacterial agent must be added to the cuttings when they are stored in water.

### 2.1.2 Sample Preparation

Depending on drilling mud content, cuttings samples may be water washed before they are air dried, picked free of contaminants and cavings, and then crushed to 0.1mm using a ring pulveriser.

Sidewall cores are freed of mud cake and other visible contaminants, sampled according to homogeneity, air dried and hand crushed to 0.1mm grain size.

Conventional core and outcrop samples are inspected for visible contaminants and crushed to 1/8" chips using a jaw crusher. After air drying, the chips are crushed with a ring pulveriser to small particle size (0.1mm).

Petroleum aqueous mixtures are separated into oil and water/mud fractions by decanting off the oil layer and producing a clean separation by gently centrifuging the oil. If separation by this method is not effective, the petroleum is solvent extracted.

### 2.1.3 Total Organic Carbon(TOC)

The TOC value is determined on crushed sediment. The minimum sample requirement is one gram, however, results may be obtained from as little as 0.2mg in very rich samples. Carbonate minerals are first removed by acid digest (HCl) and the remaining sample heated to 1700°C (Leco Induction Furnace) in an atmosphere of pure oxygen. The CO<sub>2</sub> produced is measured with an infra-red detector, and values calculated according to standard calibration.

TOC is expressed as % of rock and is used as a screening procedure to classify source rock richness:

<b>Classification</b>	<b>Clastics</b>	<b>Carbonates</b>
Poor	0.00 - 0.50	0.00 - 0.25
Fair	0.50 - 1.00	0.25 - 0.50
Good	1.00 - 2.00	0.50 - 1.00
Very Good	2.00 - 4.00	1.00 - 2.00
Excellent	> 4.00	> 2.00

### 2.1.4 Rock-Eval Pyrolysis

Although a preliminary source rock classification is made using TOC data, a more accurate assessment of organic source type and maturity is possible by Rock-Eval pyrolysis. Two types of Rock-Eval analyses are offered: "one run" which involves pyrolysis of the crushed but otherwise untreated sediment and "two run" which involves pyrolysis of both the crushed, untreated sediment and the decarbonated sediment. The "two run" method provides more accurate S<sub>3</sub> values than the "one run" method. S<sub>1</sub> and S<sub>2</sub> values are of the same accuracy in both methods.

The method requires 0.4g of sample material, although reliable results can often be obtained from smaller amounts.

The crushed sediment is heated in an inert atmosphere of helium over a programmed temperature range.

Hydrocarbons present in the free or adsorbed state (S<sub>1</sub>) are thermally distilled at 300°C and measured by a flame ionisation detector (FID). Hydrocarbons are then cracked from the kerogen (S<sub>2</sub>) during a temperature ramp from 300° to 550°C and also measured by FID. CO<sub>2</sub> released during the kerogen cracking process (S<sub>3</sub>) is trapped and subsequently measured by a thermal conductivity detector.

The amount of free hydrocarbons in the sediment ( $S_1$ ) represents milligrams of hydrocarbons distilled from one gram of rock and is a measure of both in situ and out-of-place petroleum.

Free hydrocarbon richness is described by the following:

$S_1$ (mg/g)	Characterisation
0.20 - 0.40	fair
0.40 - 0.80	good
0.80 - 1.60	very good
> 1.60	excellent

The total amount of hydrocarbons present in the free state and as kerogen is a measure of the potential yield (genetic potential) of the sample ( $S_1 + S_2$ ) and is expressed as mg/g of rock.

Source rocks are classified accordingly:

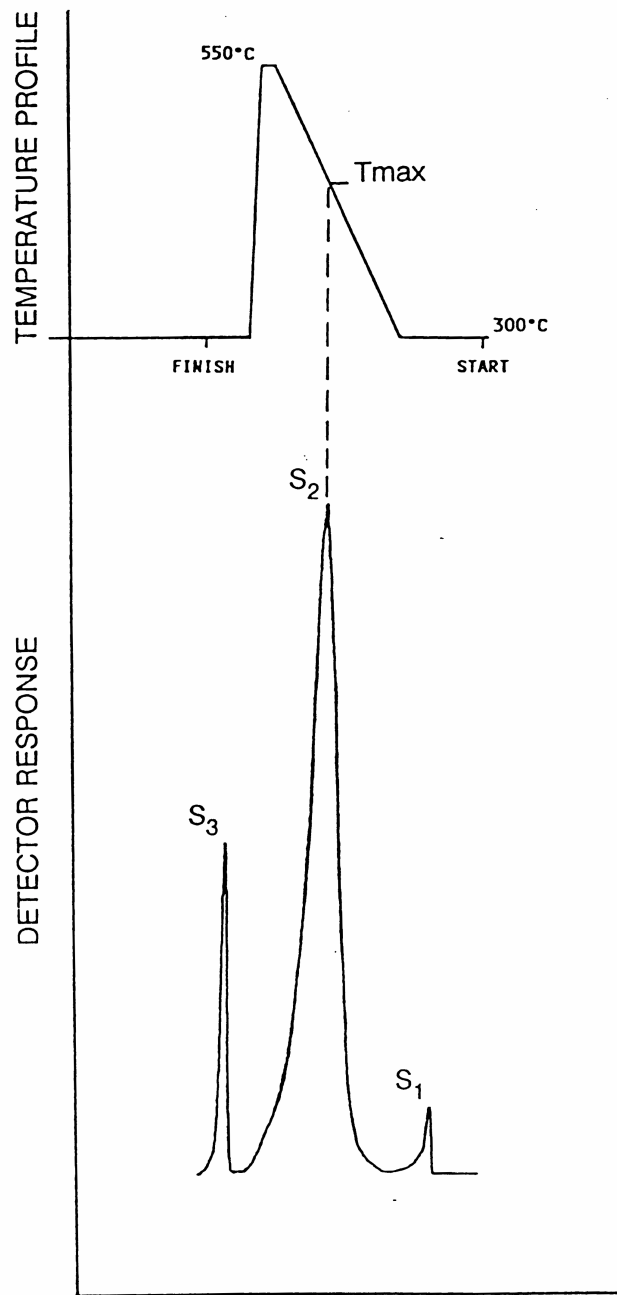
$S_1 + S_2$ (mg/g)	Source Rock Quality
0.00 - 1.00	poor
1.00 - 2.00	marginal
2.00 - 6.00	moderate
6.00 - 10.00	good
10.00 - 20.00	very good
> 20.00	excellent

The Production Index (PI) represents the amount of petroleum generated relative to the total amount of hydrocarbons present ( $S_1/S_1 + S_2$ ). It is a measure of the level of maturity of the sample. For oil prone sediments PI ranges from 0.1 at the onset of oil generation to 0.4 at peak oil generation. For gas prone sediments, PI shows only a small change with increasing maturity.

The temperature at which the maximum amount of  $S_2$  hydrocarbons is generated is called  $T_{MAX}$ . This temperature increases with the increasing maturity of sediments.

FIGURE 2

SCHEMATIC PYROGRAM OF ROCK-EVAL PYROLYSIS



The variation of  $T_{MAX}$  is summarised as

< 430°C	immature
430/435° – 460°C	mature (oil window)
> 460°C	overmature

Hydrogen Index ( $HI = S_2 \times 100/TOC$ ) and Oxygen Index ( $OI = S_3 \times 100/TOC$ ), when plotted against one another, provide information about the type of kerogen and the maturity of the sample. Both parameters decrease in value with increasing maturity. Samples with high HI and low OI are dominantly oil prone and samples with low HI and high OI are gas prone.

## 2.2 Analysis of Kerogen

### 2.2.1 Organic Petrology - Vitrinite Reflectance

Vitrinite is a coal maceral which responds to increasing levels of thermal maturity. This response is measured microscopically by the percent of light reflected off the polished surface of a vitrinite particle immersed in oil.

Measurement of vitrinite reflectance can be carried out on uncrushed, washed and dried cuttings (10-50gms of sample material required), sidewall cores (2-10gms), conventional cores (2-10 gms) or outcrop samples (2-10gms).

The values given are for standard lower size limits. In special cases, however, useful data may be obtained from as little as 0.1gm.

For each sample a minimum of 25 fields is measured in order to establish a range and mean for reflectance values.

Maturity classifications according to vitrinite reflectance values are:

% $V_R$ (approx)	Maturity
0.2 - 0.55	immature
0.55 - 1.2	mature
1.2 - 1.8	overmature
> 1.8	severely altered

Following vitrinite reflectance measurements, microscopic examination in fluorescence mode allows the description of liptinite macerals and an estimate of their abundances. The amount of dispersed organic matter is reported and its composition described.

Vitrinite reflectance results and maceral descriptions are best obtained from coals or rocks deposited in environments which received large influxes of terrestrially derived organic matter. Vitrinite reflectance cannot be measured in rocks older than Devonian age, since land plants had not evolved prior to this time.

### 2.2.2 Pyrolysis Gas Chromatography

Pyrolysis gas chromatography (PGC) is performed on solvent extracted source rocks or isolated kerogens. The sample is pyrolysed by an SGE pyrojector which is coupled directly to a Hewlett Packard 5890 gas chromatograph. The operating conditions are:

Pyrolysis temperature:	600°C
Column:	25m x 0.22mm ID BP-1 (SGE)
Carrier gas:	helium
Oven conditions:	-20° to 280°C @ 4°/min

Data are collected and recovered using DAPA scientific software.

Pyrolysis GC allows the examination of kerogen on the molecular level and thereby a better classification of source rocks with regard to source type and generative capacity than conventional bulk pyrolysis (ie. Rock-Eval). The analytical procedure is semi quantitative (with yield related to S<sub>2</sub> of Rock-Eval).

Samples are characterised according to the amounts of aliphatic, aromatic and phenolic components in the kerogen. The aliphatic carbon content of a kerogen is the critical factor in determining catagenic hydrocarbon yields in the earth's crust, while the gas/oil ratio is dictated by the distribution of the various structural elements in the kerogen (Larter, 1985). Using pyrogram fingerprint data, it is possible to distinguish substantial variations between kerogens, even those of the same bulk chemical type.

A major strength of pyrolysis methods is that, while quantitative yields of kerogens are maturity related, the qualitative pyrogram fingerprints obtained are relatively rank independent over much of the oil window (Espitalie et al, 1977; Van Graas et al, 1980; Larter, 1985). At high maturities (>1.2% V<sub>R</sub>) characteristics for all kerogen types tend to converge (Horstfield, 1984).

Data are presented by percentage and mg/g of individual substances as well as groups of compounds.

Significant parameters are:

$(C_1 - C_5)/C_6$  + abundance                      gas/oil ratio

$C_9 - C_{31}$  (alkenes + alkanes)                      oil yield

Type Index R:    aromaticity

(Larter & Douglas 1979, Larter and Senftle, 1985).

## 2.3 Detailed Analyses of Petroleum Fluids

### 2.3.1 Solvent Extraction of Sediment

The finely crushed sample (up to 100g) is extracted with dichloromethane (300mL) using sonic vibration. After Buchner flask filtration, the filtrate is re-vibrated with activated copper powder (1g) to remove elemental sulphur. The extractable organic matter (EOM) is afforded by further filtration and fractional distillation of the solvent.

Source rock richness based upon EOM is classified accordingly:

Yield	ppm
Poor	< 500
Fair/Good	500 - 2000
Very Good	2000 - 4000
Excellent	>4000

### 2.3.2 Liquid Chromatographic Separation

Sediment extracts, crude oil and condensate samples are separated into fractions corresponding to three structural types:

saturated hydrocarbons	(SAT)
aromatic hydrocarbons	(AROM)
resins plus asphaltenes	(NSO)

This separation is achieved by liquid column chromatography using activated silicic acid adsorbent and eluting solvents of varying polarity. Saturated, aromatic and NSO concentrates are recovered by fractional distillation/evaporation of the solvent and quantitative transfer to a small vial.

The amount of hydrocarbons (SAT plus AROM) can be used to classify source rock richness and the amount of saturates to classify oil source potential, according to the following criteria:

<b>Classification</b>	<b>ppm HC</b>	<b>ppm SAT</b>
Poor	0 - 300	0 - 200
Fair	300 - 600	200 - 400
Good	600 - 1200	400 - 800
Very Good	1200 - 2400	800 - 1600
Excellent	>2400	>1600

The composition of the extracts can also provide information about their levels of maturity and/or source type (LeTran et. al., 1974; Philippi, 1974). Generally, marine extracts have relatively low concentrations of saturated and NSO compounds at low levels of maturity, but these concentrations increase with increasing maturation. Terrestrially derived organic matter often has a low level of saturates and large amount of aromatic and NSO compounds, irrespective of the level of maturity.

Specific ratios are measured from solvent extraction and liquid chromatography data which give an indication of source type and maturity. EOM (mg)/TOC(g) can be used as a maturation indicator when plotted against depth for a given sedimentary sequence. Generally an EOM/TOC value of >100 indicates high maturity. If such a sample has a SAT (mg)/TOC(g) ratio <20, it is likely that the organic matter is gas prone. A value for SAT (mg)/TOC (g) >40 suggests an oil prone source type.

### 2.3.3 Capillary Gas Chromatography (GC)

C<sub>12+</sub> gas chromatography is most commonly carried out on saturate fractions, but in certain instances it is used to examine whole extracts/oils, aromatic or branched/cyclic fractions. It is also used as a tool to identify contamination. The analyses are performed under the following conditions:

Instruments:	Hewlett Packard 5890 Gas Chromatography
Injector:	SGE OCI-3 on column
Column:	25m x 0.2mm ID BP-1
Injector Temp:	280°C
Detector Temp:	320°C
Column Temp:	45°C to 280°C at 4°/min
Carrier Gas:	Hydrogen

Data are collected using an IBM compatible PC and DAPA scientific software.

#### 2.3.3.1 C<sub>12+</sub> Saturate Gas Chromatography

Saturate GC results provide information pertaining to source type, maturity and depositional environment.

The n-alkane distribution from n-C<sub>12</sub> to n-C<sub>31</sub> is determined from the area under the peaks representing each of these n-alkanes. The profile can yield information about maturity and source type and is quantified in the C<sub>21</sub> + C<sub>22</sub>/C<sub>28</sub> + C<sub>29</sub> ratio and Carbon Preference Indices (CPI 1 and 2).

$$\text{CPI(1)} = \frac{(\text{C}_{23} + \text{C}_{25} + \text{C}_{27} + \text{C}_{29}) \text{ wt}\% + (\text{C}_{25} + \text{C}_{27} + \text{C}_{29} + \text{C}_{31}) \text{ wt}\%}{2 \times (\text{C}_{24} + \text{C}_{26} + \text{C}_{28} + \text{C}_{30}) \text{ wt}\%}$$

$$\text{CPI(2)} = \frac{(\text{C}_{23} + \text{C}_{25} + \text{C}_{27}) \text{ wt}\% + (\text{C}_{25} + \text{C}_{27} + \text{C}_{29}) \text{ wt}\%}{2 \times (\text{C}_{24} + \text{C}_{26} + \text{C}_{28}) \text{ wt}\%}$$

Carbon preference indices:

- are approximately 1 for marine samples, regardless of maturity
- decrease from 20--> 1 for terrestrial samples as maturity increases

The C<sub>21</sub> + C<sub>22</sub>/C<sub>28</sub> + C<sub>29</sub> ratio is generally >1.5 for aquatic source material and <1.2 for terrestrial organic matter, however, the values increase with maturity.

Pristane/phytane (Pr/Ph) ratios can indicate depositional environments:

- . <3.0 - relatively reducing depositional environments;
- . 3.0-4.5 - mixed (reducing/oxidising) environments;
- . >4.5 - relatively oxidising depositional environments.

### 2.3.3.2 C<sub>1</sub> – C<sub>31</sub> Whole Oil Gas Chromatography

This analytical method is applied to oil and condensate samples. It provides a picture of the whole oil up to n-C<sub>31</sub> and allows quantitation of components with more than 4 carbon atoms. Several parameters are measured which illustrate changes in the degree of biodegradation and water washing in the reservoir. Because these measurements are performed on very volatile components in the oil, care should be taken during sampling, transportation and storage of the fluid to minimise evaporation.

Whole oil analytical conditions are listed below:

Instrument:	Shimadzu GC-9A
Column:	25m x 0.2mm ID BP-1
Injector/Detector Temperature:	290°C
Column Temperature:	-20°C to 280°C at 4°/min
Carrier Gas:	hydrogen

### 2.3.4 Carbon Isotope Analysis

This measurement is normally carried out on one or more of the following mixtures: topped oil, saturate fraction, aromatic fraction, NSO fraction. The organic matter is combusted in oxygen to produce carbon dioxide which is purified and transferred to an isotope mass spectrometer. The carbon isotope ratio ( $\delta C_{13}/\delta C_{12}$ ) is measured and compared to an international standard (the Peedee Belemnite Limestone - PDB).

Carbon isotope analysis is most commonly used to identify the source of methane according to the following criteria (Fuex 1977):

$\delta^{13}C$ ‰ PDB	Source
-75 to -55	Biogenic methane
-58 to -40	Methane associated with oil
-40 to -25	Thermal methane

Source rock-crude oil correlations have been attempted by observing the change in  $\delta^{13}\text{C}$  values of components of oils and rocks (Stahl 1977). Source rock extracts are usually isotopically heavier than the corresponding crude oil but are lighter than the asphaltenes of the oil and the kerogen of the rock (Hunt 1979). It has also been observed that marine organic carbon is generally isotopically heavier than contemporaneous terrestrial organic carbon (Tissot & Welte 1978). However, it should be noted that increasing maturity and biodegradation produce a shift toward heavier isotope values.

### 2.3.5 Gas Chromatography - Mass Spectrometry (GC/MS)

GC/MS analysis is normally performed on the branched and cyclic alkane fraction and/or the aromatic fraction of oils, condensates and sediment extracts. The specific fraction is first isolated and then injected into a gas chromatograph which is linked in series with a mass spectrometer. As compounds are eluted from the chromatography column they are bombarded with high energy electrons. This causes them to fragment into a number of ions each with a molecular weight less than that of the parent molecule. Individual compounds give a characteristic fragmentation pattern (mass spectrum), the major ions of which are presented in a series of mass fragmentograms [ie. plots of ion concentration against GC retention time].

GC/MS analysis can be carried out using one of the following modes of operation:

- (i) Acquire mode - in which all ions (within a broad range) in each mass spectrum are memorised by the data system.
- (ii) Selective Ion Monitoring (SIM) mode - in which only selected ions of interest are memorised by the data system.

#### 2.3.5.1 GC/MS Analysis of Branched/Cyclic Alkanes

The group of compounds to be analysed is first isolated from the saturate fraction by refluxing the sample with activated 5Å molecular sieves in cyclohexane for 24 hours. Branched/ cyclic alkanes, including alkylcyclohexanes, are recovered from the solvent by fractional distillation.

For condensates, and samples where information about alkylcyclohexanes is not required, the saturate fraction is passed through a small column packed with silicalite adsorbent. The branched/cyclic alkanes are recovered from the eluting solvent by fractional distillation.

Analysis is carried out in the SIM mode with a total of 33 ions being recorded over different time spans.

Operating conditions are:

Instrument:	5987HP GC mass spec data system
Column:	60m x 0.25mm ID cross linked methyl-silicone DB-1 (J&W) column of 0.25 micron film thickness connected directly to the ion source
Injector:	OCI-3(SGE)
Carrier gas:	hydrogen
Oven Conditions:	50° to 274°C at 8° /min 274° to 280°C at 1° /min
EM Voltage:	2,000 - 2,300V
Electron Energy:	70eV
Source temperature:	250°C

GC/MS mass fragmentograms are examined for particular 'biomarker' compounds which can be related to biological precursors. These allow the characterisation of petroleum with regard to thermal maturity, source, depositional environment and biodegradation.

The significance of selected parameters from branched/cyclic GC/MS analysis is outlined over the page.

#### 1. **18 $\alpha$ (H)-hopane/17 $\alpha$ (H)-hopane (Ts/Tm)**

Maturity indicator. The ratio of 18 $\alpha$  (H) trisnorhopane to 17 $\alpha$  (H) trisnorhopane increases exponentially with increasing maturity from approximately 0.2 at the onset to approximately 1.0 at the peak of oil generation, ie. Tm decreases with maturity. This parameter is not reliable in very immature samples.

#### 2. **C<sub>30</sub> hopane/C<sub>30</sub> moretane**

Maturity indicator. The conversion of C<sub>30</sub> 17 $\beta$ , 21 $\beta$  hopane to 17 $\beta$ , 21 $\alpha$  moretane is maturity dependent. Values increase from approximately 2.5 at the onset of oil generation to approximately 10. Once the hopane/moretane ratio has reached 10, no further changes occur. A value of 10 is believed to represent a maturity stage just after the onset of oil generation and hopane/moretane ratios are therefore useful mainly as indicators of immaturity in a qualitative sense.

**3&4. C<sub>31</sub> and C<sub>32</sub> 22S/22R hopanes**

Maturity indicator. An equilibrium between the biological R- and the geological S-configuration occurs on mild thermal maturation. A ratio of S:R = 60:40, ie, a value of 1.5, characterises this equilibrium which occurs before the onset of oil generation. The C<sub>32</sub> hopane pair is often more reliable for this purpose since co-elution sometimes affects the C<sub>31</sub> ratio.

**5. C<sub>29</sub>20S ααα/C<sub>29</sub>20Rααα steranes**

Maturity indicator. Upon maturation, the biologically produced 20R stereoisomer is diminished relative to the 20S form and a stabilisation is reached at approximately 55% 20R and 45% 20S compounds. V<sub>R</sub> equivalents are approximately 0.45% for a 20S/20R value of 0.2 and 0.8% for a 20S/20R value of 0.75. This parameter is most useful between maturity ranges equivalent to 0.4% to 1.0 V<sub>R</sub>.

**6. C<sub>29</sub>20S αααα /C<sub>29</sub>20R ααα + C<sub>29</sub>20S ααα steranes**

Maturity indicator. This ratio is a different way of expressing the relative abundance of the biological 20R to the geological 20S normal sterane (see parameter 5). Expressed as a percentage, a value of about 25% indicates the onset of oil generation, and of about 50% the peak of oil generation.

**7. C<sub>29</sub> αββ /C<sub>29</sub> ααα + C<sub>29</sub> αββ steranes**

Maturity indicator. The αα form is produced biologically. Its abundance diminishes upon maturation until a mixture of 65% ββ(iso) steranes and 35% αα (normal) steranes is reached, which is equivalent to approximately 0.9% V<sub>R</sub>.

**8&9. C<sub>27</sub>/C<sub>29</sub> diasteranes and steranes**

Source indicator. It has been suggested that marine phytoplankton is characterised by a dominance of C<sub>27</sub> steranes and diasteranes whereas a preponderance of C<sub>29</sub> compounds indicates strong terrestrial contributions. Values smaller than 0.85 for C<sub>27</sub>/C<sub>29</sub> diasterane and sterane ratios are believed to be indicative for terrestrial organic matter, values between 0.85 and 1.43 for mixed organic material, and values greater than 1.43 for an input of predominantly marine organic matter.

It has been suggested, however, that marine sediments can also contain a predominance of  $C_{29}$  steranes, so the above rules have to be applied with caution. Any simplistic interpretation of  $C_{27}/C_{29}$  steranes and diasteranes can be dangerous and the interpretation of these data should be consistent with other geological evidence.

**10.  $18\alpha$  (H) - oleanane/ $C_{30}$  hopane**

Source indicator. Oleanane is a triterpenoid compound which has often been reported from deltaic sediments of Late Cretaceous to Tertiary age. It is thought to be derived from certain angiosperms which developed in the late Cretaceous. If the  $18\alpha$  (H) - oleanane/ $C_{30}$  hopane ratio is below 10, no significant proportions of oleanane are present. At higher values, it can be used as indicator for a reducing environment during deposition of land plant-derived organic matter.

**11.  $C_{29}$  diasteranes/ $C_{29}$   $\alpha\alpha\alpha$  steranes +  $C_{29}$   $\alpha\beta$  steranes**

Source indicator. This parameter is used to characterise the oxidicity of depositional environments. High values (up to 10) indicate oxic conditions, low values (down to 0.1) indicate reducing environments.

**12.  $C_{30}$  (hopanes + moretanes)/ $C_{29}$  (steranes + diasteranes)**

Source indicator. Triterpanes are believed to be of prokariotic (bacterial) origin, whereas steranes are derived from eukariotic organisms. This ratio reflects the preservation of primary organic matter derived from eukariots, relative to growth and preservation of bacteria in the sediment after deposition.

**13.  $C_{15}$  drimane/ $C_{16}$  homodrimane**

Drimanes and homodrimanes are ubiquitous compounds most likely derived from microbial activity in sediments. The  $C_{15}$  drimane/ $C_{16}$  homodrimane ratio is a useful parameter for correlation purposes in the low molecular weight region, especially for condensates which lack most conventional biomarkers. Drimanes are also useful to assess the degree of biodegradation as the removal of  $C_{15}$  to  $C_{16}$  bicyclics characterises an extensive level of biodegradation.

#### 14. Rearranged/normal drimanes

Like parameter 13, this ratio can be used for correlation purposes in samples without conventional biomarkers, and to assess levels of biodegradation.

#### 2.3.5.2 GC/MS Analysis of Aromatics

The aromatic fraction or the oil to be analysed is first subjected to thin layer chromatography (TLC) or medium pressure liquid chromatography (MPLC), depending upon the analytical requirements.

1. Di- and tri- nuclear aromatic compounds are isolated by TLC. To effect this separation, the sample is applied to an alumina coated glass plate (0.6mm thickness). The plate is developed with hexane and the required band located using short wavelength UV light. The fraction is recovered by extraction and fractional distillation.

This aromatic fraction may be analysed by GC-FID, but GC/MS is recommended because of possible co-elution problems during GC.

Samples are analysed by GC/MS in the acquire mode scanning from 50 to 450 atomic mass units (amu).

Analytical conditions are:

Instrument:	HP5970 MSD
Column:	60m x 0.25mm ID, 0.25 micron film thickness, 5% phenylmethyl silicone column DB-5 (J&W) connected directly to the ion source
Injector:	automatic on-column
Carrier Gas:	helium
Oven Conditions:	70°C for 1 min 70°C --> 300°C at 3°/min
Data collection commences at 10 mins	
Mass spectrometry	
Em Voltage	1500 - 1800V
Electron Energy	70eV

Mass fragmentograms are presented for alkylbiphenyls, alkylnaphthalenes, alkylfluorenes and alkylphenanthrenes from a comprehensive data base. Aromatic compounds provide valuable information concerning thermal maturity since they can be applied outside the dynamic range

of saturate biomarker indicators and are particularly useful when conventional biomarkers are present in low amounts (Radke & Welte, 1983; Alexander et al, 1985). Maturity ratios are tabled below over the page.

### Aromatic Maturity Indicators

Abbrev.	Definition	oil onset	Range Wet gas
DNR 1	$(2,6\text{DMN} + 2,7\text{DMN})/1,5\text{DMN}$	1.5	10
DNR 2	$2,7\text{DMN}/1,8\text{DMN}$	50	2500
DNR 5	$1,6\text{DMN}/1,8\text{DMN}$	50	>3000
DNR 6	$(2,6\text{DMN} + 2,7\text{DMN})/(1,4\text{DMN} + 2,3\text{DMN})$	0.8	2
TNR 1	$2,3,6\text{TMN}/(1,4,6\text{TMN} + 1,3,5\text{TMN})$	0.5	4
MPR 1	$(2\text{MP} + 3\text{MP})/1\text{MP}$	1.5	3
MPI 1	$1.5 \times (2\text{MP} + 3\text{MP})/(\text{PH} + 1\text{MP} + 9\text{MP})$	0.3	1
MPI 2	$(3 \times 2\text{MP})/(\text{PH} + 1\text{MP} + 9\text{MP})$	0.3	2
Rc(a)	$0.6(\text{MPI}-1) + 0.4$ (for % Rm <1.35)		
Rc(b)	$-0.6(\text{MPI}-1) + 2.3$ (for % Rm >1.35)		

(from Radke et al, 1982; Radke & Welte, 1983; Alexander et al, 1985)

Some aromatic marker compounds have specific natural product precursors and can be used as signatures for sediments of a particular source, depositional environment or geological age:

TNR 5	$1,2,5\text{TMN}/1,3,6\text{TMN}$	
TNR 6	$1,2,7\text{TMN}/1,3,7\text{TMN}$	(Strachen et al, 1988)
1,7/X	$1,7\text{DMP}/(1,3 + 3,9 + 2,10 + 3,10\text{DMP})$	
Retene/9MP		
1MP/9MP		(Alexander et al, 1988)

2. Mono- and triaromatic steranes are analysed by GC/MS under the same analytical conditions as used for di- and tri-nuclear aromatics. However, isolation of this fraction is performed by MPLC. To achieve this, the saturate plus aromatic mixture is injected onto a Merck Si60 column. The separation is monitored with a refractive index detector for saturates and a UV absorbance detector for aromatics.

As aromatic steranes are generally present in low abundances, especially in oils, samples are analysed in the SIM mode and 16 ions are recorded.

The conversion of monoaromatic steranes to triaromatic steranes and the dimethylation of triaromatic steranes in sediments are considered to be maturity dependent (Mackenzie et al, 1981; Mackenzie, 1984). The triaromatic sterane maturity indicator should, however, not be applied to crude oils because migration effects appear to selectively deplete the triaromatic steranes.

# ENCLOSURES



# Petrophysical Analysis of: MOBY-1

COMPANY: BASS STRAIT OIL COMPANY LTD  
 LOCATION: VIC/P47  
 LATITUDE: 38° 01' 44" S  
 LONGITUDE: 148° 30' 27" E  
 X COORDINATE: 632316.41  
 Y COORDINATE: 5789884.86  
 HORIZONTAL UNITS: METRES  
 DATE PLOTTED: 19-Jan-2005

DATUM FOR ELEVATION: MSL  
 WATER DEPTH: 53.00  
 MEASUREMENT REF.: RT  
 ELEVATION MEAS. REF.: 21.50  
 DRILLED DEPTH: 660.00  
 VERTICAL UNITS: METRES  
 DATE LOGGED: 12-OCT-2004  
 VERTICAL SCALE: 1:200

Bit Size: 8.5 in  
 Mud Type: KCL/PHPA  
 DFD: 10.0003  
 BHT: 42.7 C

Rm 0.104 @ 21.680C  
 Rrf: 0.086 @ 21.700C  
 Rrc: 0.149 @ 21.810C  
 KCl: 6%

